Proceedings of the 6th International Conference on Heap Leach Solutions 2025

October 19–21, 2025, Sparks, USA

HEAP LEACH SOLUTIONS 2025

October 19-21, 2025 | Sparks, Nevada

Editor
Joe Goodwill, Vancouver, BC, Canada

ORGANIZED BY:

C3 Alliance

Disclaimer

Any views and opinions expressed in the articles published in these proceedings are solely those of the authors and do not necessarily represent those of C3 Alliance Corp. (C3) or of the panel of editors. The authors take full and exclusive responsibility for technical content and accuracy of the information published herein. This information is not intended nor implied to be a substitute for professional advice. C3 and the panel of editors are not responsible for any damage to property or persons that may occur as a result of the use of the information contained in this volume.

CONTENTS

ORGANIZER

C3 Alliance Corp.

Our mission at C3 Alliance Corp. is to create stronger communities through innovative and inclusive solutions for resource development. C3 has a well-established reputation based on success in delivering strategic advice, expert knowledge, and inclusive solutions to clients across Canada. We work with communities, industry leaders, and governments to build the relationships needed for the success of a project.

At C3, we understand how community members, business people, and government representatives can all benefit from meeting to share stories and knowledge. C3 employs an expert team of event planners who specialize in conferences and networking opportunities. We benefit from a vast network of professional contacts to organize exciting events that connect people and knowledge across resource sectors, communities and government.

For more information, visit the website at https://www.c3alliance.ca/

COMMITTEES

Conference Secretariat

Michaela Bubb
Melissa McRitchie
Meryl Nelson
Missy Preston
Sarah Weber

Organizing Committee

Jeff Parshley (Co-Chair), Corporate Consultant, SRK Consulting (US) Inc.
Dirk van Zyl (Co-Chair), Professor Emeritus, UBC
Francisco Barrios, P.E., Tierra Group International
Steve Boyce, Partner, ERM
Todd Minard, Principal Geotechnical/Civil Engineer – Mining Division, US West Water AECOM
Denys Parra, Executive Director, Anddes
Cristian Caro, Leaching Innovation Manager, Freeport-McMoRan
Daniel Kappes, President & CEO, Kappes, Cassiday & Associates
Jack McPartland, Metallurgist/President, McClelland Laboratories, Inc.
Michael Milczarek, President, GeoSystems Analysis Inc.
Thom Seal, Professor Emeritus, University of Nevada, Reno
Nick Rauh, Technical Mining Representative, Agru America, Inc.
Nick Gow, Senior Study Manager, Paterson & Cooke USA, Ltd
Bassam El Husseini, Director, Geotechnical, Technical & Heap Leach, Barrick Gold Corp.

Conference Chairs

Jeff Parshley, Corporate Consultant, SRK Consulting (US) Inc.
Dirk van Zyl, Professor Emeritus, UBC

Technical and Review Committee

The Organizing Committee expresses its appreciation and sincere gratitude to the following reviewers of the technical content, who helped to ensure the high quality of this publication.

Francisco Barrios, Tierra Group
Steve Boyce, ERM
Cristian Caro, Freeport-McMoRan
Nick Gow, Paterson & Cooke
John Lupo, Mayhem Creek LLC
Terry Mandziak, SLR International Corp.
Jack McPartland, McClelland Laboratories, Inc.
Jared Olson, McClelland Laboratories, Inc.
Denys Parra, Anddes
John Quaranta, West Virginia University, Civil & Environmental Engineering
Nick Rauh, Agru America, Inc.
David Romo, NewFields Mining Design & Technical Services
Michael Shelbourn, Newmont Corporation
Mark Smith, Piteau Associates USA Ltd
Robert Swan, Drexel University
Bryan Ulrich, Bryan Ulrich LLC
Vaibhav Srivastava, Freeport McMoRan Inc.
Daniel Zúñiga Rodríguez, Axios Engineering
Guillermo Torres, Geotechnos
Marvin Silva, AECOM
Huseyin Tekin, ENCON
Pelin Usta Ozkayhan, Centerra Gold
Nicolás Villanueva, Nava
Tancredi Botto, Muon Vision
Richard Wagner, ERM Canada
Nathan Toohey,
Ardy Sharifabadi, Arizona Department of Environmental Quality
Chris MacMahon, WSP USA Inc.
Krishna Sinha, KPS Consultants
Percy Mayta, PM&H Consulting SAC
Michael Etezad, WSP
Uddav Ghimire,
Josh Moncrieff, BMC Minerals Ltd.
Alhaji Safiwu, Henan Polytechnic University
Mathan Manmatharajan, WSP Canada Inc
Mohsen Rabbani, University of Nevada Reno
Clara Gomez, Coanda
Phil Dalke, Dalke LLC
Reza JafariRaviz, Sangbori Negin Aqiq Sabz Mehriz Inc
Rodrigo Arellano, Rio Tinto
Aaron Young, University of Utah

ACKNOWLEDGEMENTS

The Organizing Committee acknowledges with gratitude the authors' contributions of high-quality, detailed and innovative papers. Their papers reflect innovative and proactive solutions to challenging mining conditions around the world.

We would also like to thank the technical reviewers and all those involved in the organization of this conference and the preparation and production of these proceedings. The support of the committees is greatly appreciated.

The Organizing Committee also wishes to thank all of our exhibitors, sponsors, institutional partners and media partners.

Finally, we would like to thank all the delegates who attended the conference to exchange their valuable knowledge and expertise, thus contributing to the great success of the Fifth International Heap Leach Solutions Conference. We look forward to seeing you all again at the next conference in this series.

Organizing Committee
Heap Leach Solutions 2025

THE ORGANIZERS PROUDLY ACKNOWLEDGE THE FOLLOWING CONFERENCE SPONSORS AND EXHIBITORS:

SPONSORS

PLATINUM

Kapper TECH

GOLD

FORTE DYNAMICS

FREEPORT-McMoRan

srk consulting

SILVER

Anddes

BRONZE

AECOM

Agilent

ARS - Aqua Royal Spring Heap Leaching Technology

CONETEC

GSA GeoSystems Analysis, Inc. Innovations in Hydrology

METSIM INTERNATIONAL

BREAKFAST

KCA Kappes, Cassiday & Associates

LUNCH BREAK

wsp

EDUCATIONAL PARTNER

University of Nevada, Reno The Mackay School of Earth Sciences and Engineering

EXHIBITORS

AECOM
Agilent
Agru America
Anddes
AquaRoyalSpring
Barr
CETCO
ConeTec
EC Applications
Forte Dynamics
GeoSystems Analysis
hydroGEOPHYSICS
Jex Technologies
Kapper-Tech
Kappes, Cassiday & Associates
Mackay School of Mines
Muonvision
Orica Digital Solutions
PhotoSat
Solmax
SRK
Superior Industries
Tre Altmira
Victaulic
WSP

Chapter One

Gold, Copper, Nickel, Uranium and Other Metal Leaching

HEAP LEACH
SOLUTIONS 2025

Optimizing Gold Heap Leaching Performance: A Field Trial Using Ionquest 479

Jeremy Rodefer, Italmatch USA Corporation, USA
Chiara Carrozza, Italmatch Chemicals SpA, ITA
Daniele Ciferri, Italmatch Chemicals SpA, ITA
Robert Delgado, Italmatch USA Corporation, USA
Filip Dutoy, Italmatch Belgium Srl, BELGIUM

Abstract

Gold heap leaching is a widely used method for extracting gold from low-grade ores by percolating a cyanide solution through crushed ore under oxidizing and alkaline conditions. However, these conditions often lead to the formation of mineral scales—particularly calcium sulfate and carbonate—which can foul equipment, reduce gold recovery, and increase maintenance and water consumption.

To address these challenges, a field trial was conducted to evaluate Ionquest 479, a scale inhibitor designed for harsh leaching environments. Ionquest 479 demonstrated strong performance under high pH and long residence times, combining scale inhibition with dispersant action. It effectively prevented scale formation in critical system components, including pipes, pumps, and spray systems, thus supporting improved gold adsorption on activated carbon.

During the trial, Ionquest 479 was dosed at a gold mine where water chemistry indicated a high risk of calcium sulfate scaling. Laboratory tests showed 90% scale inhibition at 10 ppm and complete inhibition at 30 ppm. Field results confirmed a 34% reduction in monthly scale inhibitor consumption, with the main barren solution pipe remaining scale-free—unlike under the previous treatment. Additionally, dripper replacement rates dropped from 11 to 4 per week, a 64% improvement, enhancing solution distribution and reducing downtime.

Overall, Ionquest 479 provided effective scale control, operational reliability, and significant cost savings. These results highlight its potential as a superior alternative in gold heap leaching operations. Further trials are recommended to refine dosage strategies and maximize economic and operational benefits.

Introduction

Gold heap leaching is one of the most economically viable and widely applied hydrometallurgical processes

for extracting gold from low-grade ore deposits. Its use has grown substantially over the past few decades due to its low capital and operating costs, ease of implementation, and suitability for large-scale operations in remote and arid regions. The method involves stacking crushed ore onto large pads and irrigating it with a dilute cyanide solution that percolates through the heap, dissolving gold as a soluble cyanide complex ($Au(CN)_2^-$). The gold-laden solution, or "pregnant solution," is collected at the base and sent to recovery circuits such as carbon adsorption (Fig.1).

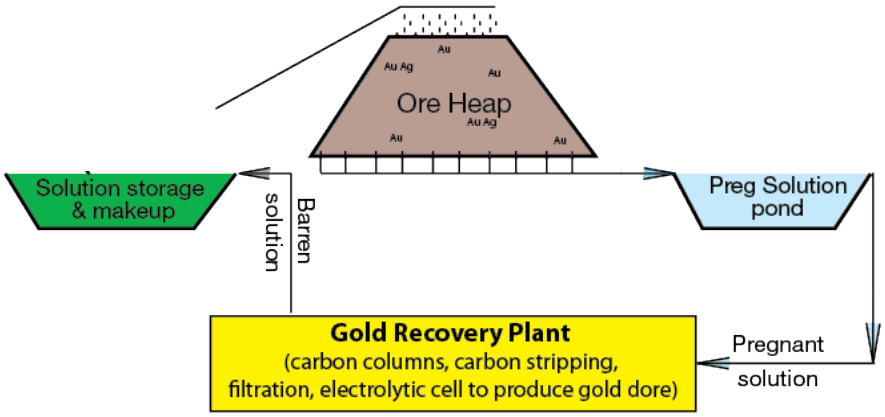

Figure 1: Gold heap leaching schematic process

To optimize the cyanidation reaction and maximize gold recovery, it is critical to maintain alkaline and oxidizing conditions throughout the leaching process. This is typically achieved by adding lime (CaO or $Ca(OH)_2$) or sodium hydroxide (NaOH) to maintain a pH above 9.5, which prevents the volatilization of toxic hydrogen cyanide (HCN) gas and enhances gold dissolution. However, these chemical conditions also promote the precipitation of sparingly soluble mineral salts, particularly calcium sulfate ($CaSO_4$), calcium carbonate ($CaCO_3$), and strontium sulfate ($SrSO_4$), leading to the formation of scale on process equipment, pipes, drippers, pumps, and spray systems.

Scaling in heap leaching operations presents a significant challenge to both productivity and operational efficiency. Scale buildup can lead to restricted flow, uneven lixiviant distribution, reduced percolation rates, and ultimately lower gold recovery. Additionally, frequent equipment maintenance, cleaning, and replacement contribute to increased downtime, labor costs, and water use—particularly in water-scarce environments.

To mitigate these issues, scale inhibitors have become an integral part of heap leach process water management. Scale inhibitors, such as phosphonates and carboxylic-based polymers, offer dual functionality by both inhibiting precipitation and dispersing suspended solids, maintaining the flow and effectiveness of the leaching solution.

One advanced product is Ionquest 479, a proprietary antiscalant designed to operate effectively under the high-pH and long residence time conditions typical of gold heap leaching. This product has been shown

to prevent the formation of complex scale deposits, reduce chemical consumption, extend equipment life, and improve overall process reliability. Given the economic and environmental implications of scaling, it is essential to continuously evaluate and optimize scale control strategies. This includes selecting effective inhibitors, determining optimal dosing strategies, and understanding site-specific water chemistries. The integration of advanced scale inhibitors like Ionquest 479 offers a pathway to enhanced gold recovery, lower operating costs, and more sustainable heap leach operations.

Methodology

Ionquest 479, as well as other scale inhibitors here referred to as Product 1 and Product 2, were tested in static jar tests. Synthetic water was used, targeting the composition of the field operation (Table 1). The tests were conducted at different dosing rates for 4 and 24 hours at pH 11 and a temperature equal to 55°C.

Table 1: Water Analysis

Total Dissolved Solid (ppm)		**pH**	
41540		11	
Cations (ppm)		**Anions (ppm)**	
Ca^{2+}	1,900	Cl^-	3,400.9
Na^+	2,651.3	SO_4^{2-}	5,200
Sr^{2+}	35	CO_3^{2-}	208

To determine the main components of scale, an X-ray fluorescence spectrometer (XRF) and an X-ray diffraction (XRD) were used to analyze the content of major elements. The results are shown in Table 2.

Table 2: XRF Analysis of the Scale Found in the Dripper Lines

Component	**Content %**
Calcium (CaO)	29.7
Sodium (Na_2O)	1
Magnesium (MgO)	0.02
Strontium	0.57
Iron (Fe_2O_3)	0.12
Sulfur (SO_4^{2-})	10.4
Chloride	2.3

Result and Discussion

Scale Inhibition Performance Test under Static Conditions

Using the water analysis reported in Table 1, with a pH of 11 and a temperature of 55°C, the effect of different concentrations of scale inhibitors was investigated (from 2.5 to 50 ppm). The experimental results are shown in Figure 2.

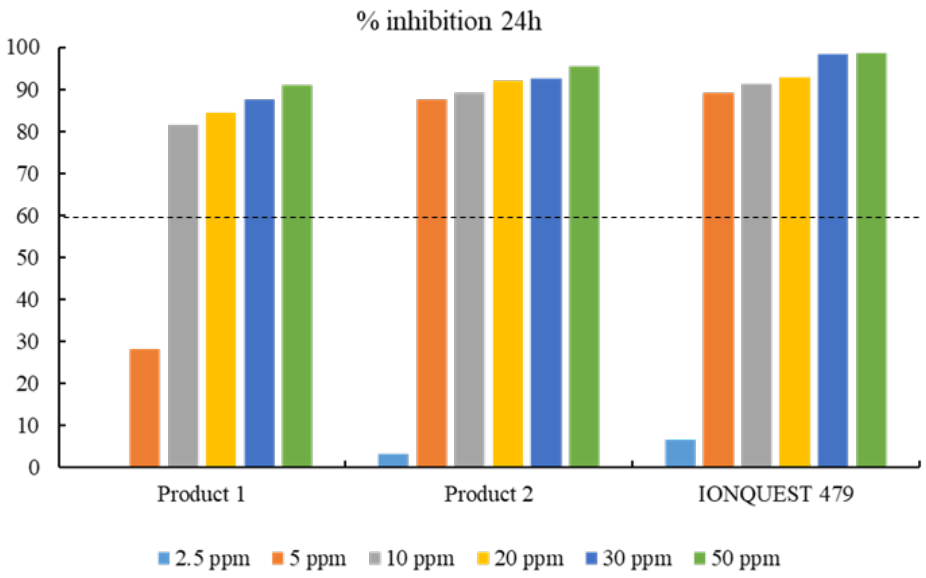

Figure 2: Jar test results at scale inhibitor dosage.
The dotted line indicates the scale precipitation without scale inhibitor addition

At a concentration of 10 ppm, Ionquest 479 effectively inhibited scale formation by 90%, while at 30 ppm, it completely inhibited scale formation. Product 1 has overall the worst conditions. Product 2 behaves well, although at 30 ppm, inhibition is slightly below 90%. Ionquest 479 shows the best inhibition efficiency in the whole dosage range tested. These results indicated that the product was highly effective in preventing the formation of calcium sulfate in an environment similar to that of the field.

Plant Design and On-Site Trial

The gold mine site consisted of 11 heaps and one recovery plant; Heap Numbers 9-11 have been selected to carry out the on-site trial. The Barren Leach Solution that flows to the Heap Leach Pad is diluted sodium cyanide at pH = 11.10 and ambient temperature (around 20°C in winter and 40°C in summer), with a flow rate up to 350 m^3/h. A solenoid metering pump was used to dose the scale inhibitor chemical at 20% stroke. Figure 3 shows a schematic plant design as well as the designated dosage point for Ionquest 479. 30 ppm was the selected dosage based on the static test.

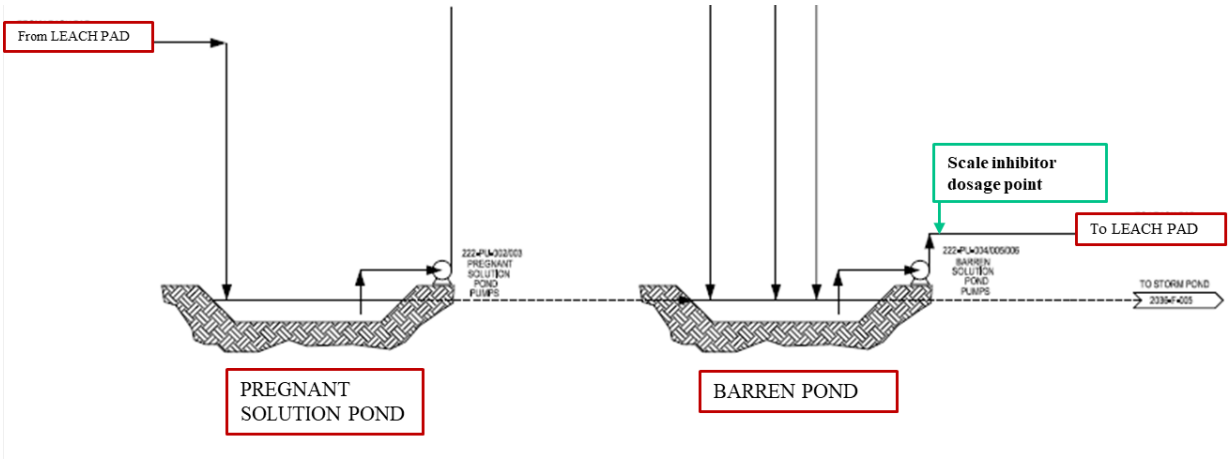

Figure 3: Plant design and scale inhibition dosage point

Scale inhibitor performances were evaluated in a 3-month on-site trial with the objectives of:

- Controlling the scale formation potential in the dripper emitter.
- Reducing the current dripper lines replacement rate (30 to 40% replaced every two weeks).
- Increasing the dripper emitters' online service, with lowering operational workloads.
- Improving the current product performance.

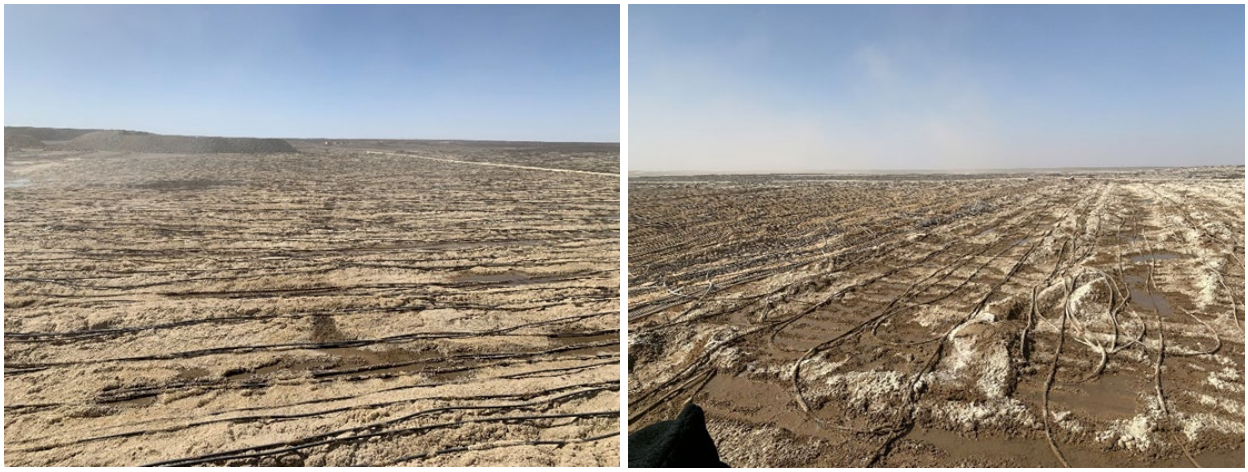

Figure 4: Images of the gold heap leaching site

Ionquest 479 performance during the trial

Different sampling points were strategically selected to evaluate the actual concentration of Ionquest 479 throughout the process and its direct impact on two critical areas: the heap leach dripper emitters and the carbon adsorption column in the recovery system. Scale inhibitor concentrations were analyzed using a

spectrophotometer to ensure consistent and accurate measurement. Table 3 demonstrates that the Ionquest 479 was dosed consistently throughout the trial.

Table 3: Ionquest 479 Concentration at each Sampling Point

	1 Feb.	27 Feb.	20 April
Barren Solution Stream	31.5	31.1	30.8
Pregnant Solution Stream	5.5	7.2	6.2
Carbon Column Feed	5.0	5.7	3.4
Carbon Column Tails	4.2	5.5	2.8

The three recorded dosage measurements revealed a strong effect in reducing scale formation across the system. Up to 80% of the scale inhibitor was consumed between the dripper emitter and the pregnant solution, indicating significant scale inhibition activity within the heap. A further average 34% reduction in active concentration was observed from the pregnant solution to the carbon column tailings, highlighting the continued Ionquest 479 activity through the recovery circuit. These results confirm the effective distribution and utilization of the Ionquest 479 across key process points.

Figure 5 illustrates that the barren solution flow rate was consistently maintained at its maximum level immediately following the introduction of the Ionquest 479. This stability was critical to ensuring a consistent scale inhibitor concentration throughout the trial period. Fluctuations in the barren solution flow rate—either increases or decreases—would result in dilution or concentration of the scale inhibitor, respectively. A higher-than-required concentration can lead to unnecessary overconsumption of the chemical, increasing operational costs. In contrast, a lower concentration may be insufficient to prevent scale formation, compromising system performance and increasing the risk of fouling.

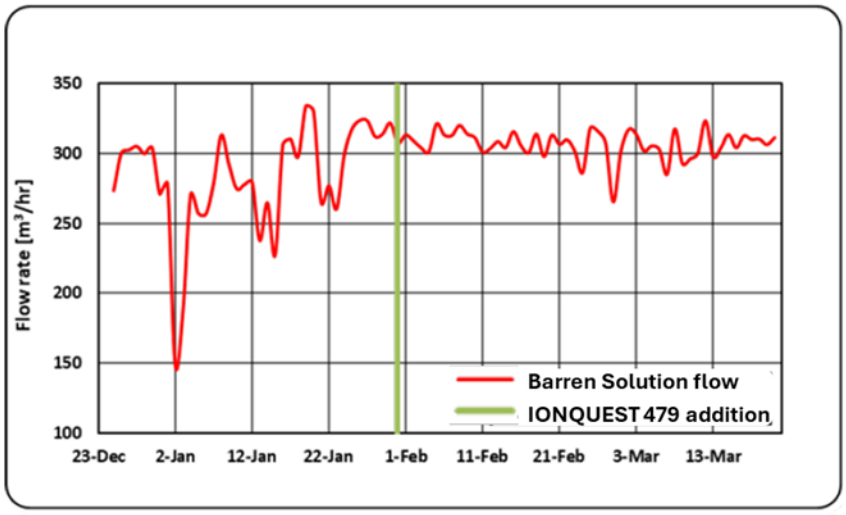

Figure 5: Plant design and scale inhibition dosage point

With the addition of Ionquest 479 into the barren solution stream feeding the heap leach pad, a significant improvement was observed in the performance of the dripper emitters and distribution tubing. Scale formation was effectively minimized, resulting in extended operational uptime along with a notable reduction in both cleaning frequency and equipment replacement. The replacement rate for distribution hose pipes dropped from 11 per week to just 2.5 per week (a reduction from 22 hose replacements every two weeks to 10 per month). Additionally, the main distribution line—delivering barren solution to the emitters and tubing—remained free of significant scale buildup, maintaining efficient and uninterrupted flow throughout the trial period. The use of the Ionquest 479 also demonstrated greater efficiency in chemical consumption compared to the previously used product.

During the trial, the average daily consumption of the Ionquest 479 was 146 kg/day, compared to 215 kg/day with the previous scale inhibitor—a reduction of approximately 32%. This enhanced performance not only reduced chemical usage but also translated to operational savings equivalent to an average of three days of chemical use saved per week. The minimized scale formation contributed to fewer emitter replacements and eliminated the need for cleaning the main distribution line. These performance gains are summarized in Table 4.

Table 4: Comparison between the Previous Scale Inhibitor and Ionquest 479 on the Heap Dripper Emitter Conditions

	Ionquest 479	Existing Used Antiscalant
Cleaning or flushing requirements	No cleaning and flushing required	Flushing required
Emitter tube replacement rate (tubes/weeks)	$\frac{10 \text{ tubes}}{4 \text{ weeks}}$	$\frac{22 \text{ tubes}}{2 \text{ weeks}}$
Scale inhibitor consumption (kg/month)	4380	6450

Conclusion

The performance of the Ionquest 479 was highly satisfactory over the trial period. Both the heap leach dripper emitters and the carbon columns at the recovery plant operated under improved conditions, with minimal scale formation observed. As illustrated in Figure 3, the scale inhibitor was injected into the barren solution stream and proved effective across the entire process, from heap irrigation to gold recovery.

In the heap leach system, barren solution distribution was uninterrupted, with no significant blockages or flow reductions observed. The trial was conducted under the following operating parameters: Ionquest 479 at 30 ppm dosage, barren solution flow rate up to 350 m^3/h, pH maintained at 11.10, and ambient temperature conditions. As a result, the trial achieved up to 77% reduction in dripper emitter tube replacements and 32%

savings in scale inhibitor consumption, compared to the previously employed product. Additionally, no scale formation was reported in the carbon adsorption columns during the trial—an area typically prone to fouling. The overall heap leach process became more stable and efficient throughout the trial. Increased dripper emitter uptime, reduced maintenance frequency, fewer replacements, and rare occurrences of dosing pump shocks contributed to smoother plant operations and lower operational workloads.

Based on these performance indicators, Ionquest 479 demonstrated effective scale control and operational reliability. Its use is considered successful, and it is recommended for implementation at other similar gold heap leaching sites.

Extraction of Rare Earth Elements from Appalachian Coarse Coal Refuse through Heap Leaching

Zainab S. Jawad, West Virginia University, USA
Nathan C. DePriest, West Virginia University, USA
Leslie C. Hopkinson, West Virginia University, USA
John D. Quaranta, West Virginia University, USA
Rachel Spirnak, West Virginia University, USA
Paul F. Ziemkiewicz, West Virginia University, USA

Abstract

Coal and coal byproducts have been identified as potential sources of rare earth elements (REE). Most REE associated with coal preparation plants have been identified in mine refuse, which is enriched in pyritic sulfur. The weathering of refuse results in the oxidation of its pyritic shale and, thus, the formation of acidic leachates that are enriched in REE. Acid mine drainage (AMD) discharges in the Northern and Central Appalachian coal basins have the potential to produce approximately 1,000 tons per year of REE oxides. This represents approximately 5% of the total U.S. Department of Defense needs.

This research aimed to determine whether existing surface deposits of coarse coal refuse (CCR), in their current sitting conditions, can be managed as an REE feedstock while controlling CCR's long-term AMD liability. This study evaluated the mechanics of heap leaching CCR to extract REE through bench-scale leaching experiments. Two CRR feedstocks were evaluated: "fresh" (subsurface, or new pile source) and "weathered" (older pile source). CCR types were tested in their current stockpiled condition. Three leaching solutions (deionized water, AMD, and AMD plus hydrogen peroxide) were evaluated. Column leaching tests were employed as the most appropriate bench-scale representation of heap leaching. The novelty of this study lay in the use of the AMD produced from the CCR itself as a leachant in the heap leach process to produce an REE-enriched leachate.

Results revealed that REE concentrations in AMD increased by 116 to 252% in unsaturated column leaching tests of CCR. Leaching primarily occurred in the first leaching cycle, removing the REE compounds made readily available by weathering. The highest leaching efficiencies were observed in weathered CCR with AMD as the leachant.

Introduction

Prior to delivery to power plants, coal must undergo preparation to remove impurities and to size for combustion. Preparation plants separate material into products (coal) and reject streams (coal refuse). Currently, coal refuse is managed by practices such as onsite treatment and tailing impoundments. The current piecemeal and linear approach has resulted in issues such as acidification and elevated total dissolved solids in receiving waters, toxic chemicals leaching, and structural failures, posing threats to the environment and public health (Wang et al., 2019; Hudson-Edwards et al., 2024). Recently, there has been increased interest in the use of coal mine tailings as a potential feedstock to extract valuable elements, especially heavy and light rare earth elements (REE) (Lin et al., 2017; Honaker et al., 2018; Yang, 2019).

REEs are 17 elements divided into two groups based on their atomic weights. REEs are critical to modern technologies (e.g., electronic displays, health care, green energy; Lin et al. 2017). Over the next two decades, Nd and Dy demand is expected to increase by more than 700% and 2,600%, respectively (Honaker et al., 2018). The United States Department of Energy (USDOE) identified Nd and Dy as essential for future supply, along with Y, Tb, and Eu. (USDOE, 2011; Honaker et al., 2018).

Most REEs associated with coal preparation plants have been identified in mine refuse (Lin et al., 2017; Honaker et al., 2018). The exposure of refuse to weathering conditions results in the oxidation of its pyritic shale and the formation of acidic liquid discharge (leachate) that is enriched in REEs. Honaker et al. (2018) analyzed leachates generated from CCR and found that the REEs are concentrated in the leachate samples (>300 ppm). The research team at West Virginia University's (WVU) West Virginia Water Research Institute (WVWRI) has also identified acid mine drainage (AMD) as a promising source for REEs (Ziemkiewicz et al., 2016; Ziemkiewicz et al., 2018). Ziemkiewicz et al. (2018) indicated that AMD discharges in the Northern and Central Appalachian coal basins have the potential to produce about 1,000 tons per year of REE oxides. This value represents approximately 5% of the total US demand and would satisfy the United States Department of Defense (USDOD) needs. The elevated concentration of REEs in the leachate generated by CCR (i.e., AMD) is evidence of its ability to extract these valuable elements from coal refuse (Honaker et al., 2018; Zhang and Honaker, 2018). In addition to using loose coal mine refuse as an alternative ore, leaching with acids naturally produced from coal refuse has the potential to be an economical method of extracting REEs. Consequently, the hypothesis that underlies this project is that pyrite oxidation can be accelerated, and REE extraction can be enhanced through the recirculation of AMD.

Heap leaching is a widely used metallurgical method that can process a variety of low-grade ores through selective removal. This technology was developed to recover metals such as copper (Cu), uranium (U), nickel (Ni), silver (Ag), and gold (Au) (Ghorbani et al., 2016). Metal-bearing ore is stacked into a heap

on an impermeable pad and irrigated for an extended period (weeks to years) with a chemical leaching solution (leachant) to dissolve the metals. The metal-rich leachate is collected for further processing. Heap leaching has been employed for hundreds of years, but according to the authors' knowledge, no heap leaching has been applied to coal mine refuse for REE extraction purposes. The need is imperative, as the pyritic sulfur in CCR makes the material a promising feedstock for metal extraction.

The work discussed herein evaluated the use of CCR as a REE feedstock. This otherwise unused resource may present a viable commercial opportunity to furnish a secure REE supply chain in Appalachia. To identify and experimentally quantify the REE source amount and the extraction potential of two CCR processing streams, column leaching tests were conducted. These tests were employed as the most appropriate bench-scale representation of heap leaching in the field. Specific objectives were as follows: i) identify whether CCR could serve as a potential feedstock to extract REEs via heap leaching with no additional processes, and ii) identify key management and control variables in the process.

Methodology

Study Area and Sample Collection

The study area was the Monongalia County Mine, formerly known as the Blacksville #2 Coal Mine, located in Monongalia County, WV, USA. The Hughes Hollow coal refuse impoundment (located at 39° 43' 22.89" N, 80° 17' 33.53" W), was backfilled with CCR and is actively being reclaimed (Fig. 1 adapted from Google Earth Pro, 2020]. Two types of CCR were collected from the impoundment area (hereafter referred to as "weathered CCR" and "fresh CCR"). Older tailings were chosen as the source for the weathered samples, whereas newer tailings were the source for the fresh samples. The fresh sample was approximately two years old; the weathered sample had been on site for approximately five years and was thereby exposed to weathering conditions for a longer time. The Crest Pond at the site was the source for AMD due to its low pH value (2.4 to 2.8) and high total REE (TREE) concentration (1,650 ug/L). Other characteristics and composition of the AMD include acidity (4,783.3 mg/L), electrical conductivity (4,060 uS/cm), and total major metals (TMM) (1,580 mg/L).

Geotechnical Laboratory Analysis

Bench-scale geotechnical laboratory testing was performed to determine CCR grain size distribution (GSD), moisture content (ω), specific gravity (G_s), and other properties. The baseline parameters of the two types of CCR were determined in triplicate as received from the field in accordance with the American Society of Testing Materials (ASTM) protocols (D-2216 for ω determination, D-854 for G_s, D-422 test procedure of dry sieving for GSD, D-2487 for classification, and D-698 for standard compaction).

Column Leaching Tests

Bench-scale leaching tests in columns are considered an excellent representation of heap leaching (Larrabure et al., 2024) and can provide valuable information regarding heavy metal transport in mine tailings (Wang et al., 2019). The same mechanism applies to REEs, as they are reported to the AMD stream along with heavy metals. Column leaching tests have been used to leach different metals, such as Ni and U, from a variety of ores (Wang et al., 2019; Nagar et al., 2020). In the present study, leaching experiments were conducted using PVC columns (internal diameter of 10 cm [4 inches] and a length of 91 cm [3 ft]). The columns provided a diameter-to-particle size ratio of 5, which satisfies the ratio specified in the literature and considered a rule of thumb (Iasillo et al., 2013; Van Staden and Petersen, 2018).

The column leaching tests were performed with fresh and weathered CCR samples. Each type of CCR was placed in three columns (Figs. 2 and 3). Approximately 7 kg (16 lb) of CCR was placed in each column. Three different leachants were used in the process: AMD, AMD plus hydrogen peroxide (H_2O_2), and deionized water (DI water). AMD leachant was chosen to represent the onsite AMD pond source as it currently exists. H_2O_2 was added to AMD to simulate the additional oxidizing agent used in previous REE leaching studies with different ores (Atia et al., 2021). DI water simulated non-AMD infiltration via rainfall. Each leaching cycle was carried out with a volume of 1.0 Liter (L) of leachant; leachant volume was estimated as a percentage of CCR volume based on scaling up to future field demonstration. For columns using AMD+ H_2O_2, approximately 100 milliliters (mL) of H_2O_2 was added to the AMD each leaching cycle. AMD and AMD+ H_2O_2 leachates were recirculated each cycle; the collected leachate in a particular week was used as the leachant in the following week (e.g., leachate from week 1 was used as the leachant in week 2). The collected leachate was supplemented whenever needed with raw AMD to achieve a 1.0 L leachant volume during each leaching cycle. REE concentrations in leachate collected from columns AMD-W, AMD-F, H_2O_2-W, and H_2O_2-F were calculated by subtracting the REE concentrations already available in leachant from what was determined by the analytical results after each leaching cycle. DI water was not recirculated. The application flow rate was 50 mL/min for all tests. The outflow rate was monitored during the testing period by documenting the volume of leachate collected over time.

The leaching tests lasted six weeks, with a one-week break after the third leaching cycle to allow for analytical data processing. During the first three weeks, one leaching cycle followed by leachate collection for analytical testing was completed per week. Each leaching cycle was conducted over an approximately two-hour period. Two leaching cycles were performed each week during the last two weeks (weeks 5 and 6), and leachate collection was done after the end of the second cycle in week 6 (leaching cycle # 7). Leachant blend volumes of raw and recirculated AMD were used to estimate TREE concentration in the leachant used each cycle during weeks 1 through 6. pH readings of the leachants and collected leachate were taken using a pH probe before and after each leaching cycle. Collected leachates (350 mL for each

column) were sent to the West Virginia University Institute for Sustainability and Energy Research (WISER) Analytical Laboratory for REE concentrations (EPA 200.8). pH readings of the collected leachate were also taken at the analytical laboratory.

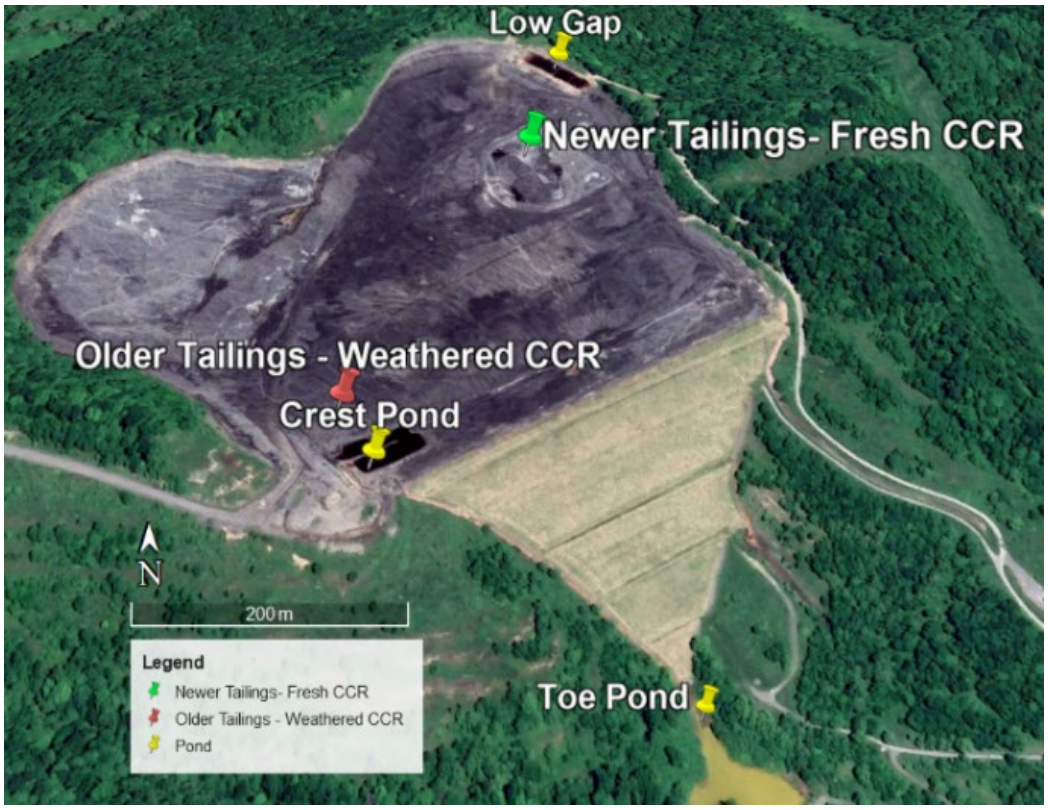

Figure 1: Hughes Hollow coal refuse impoundment at Monongalia County Mine (Google Earth Pro 2020)

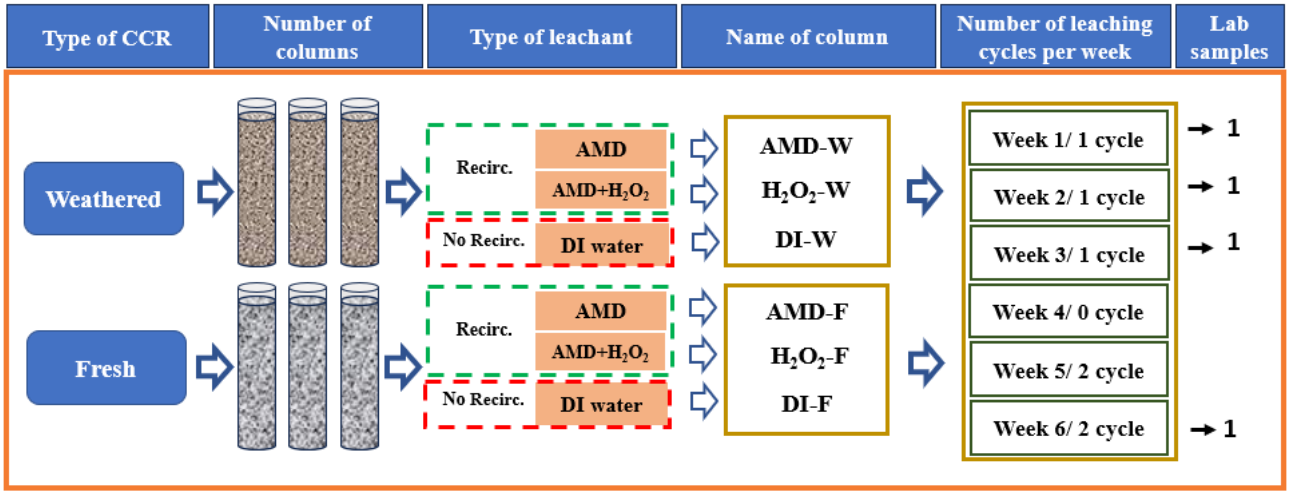

Figure 2: Column leaching test plan

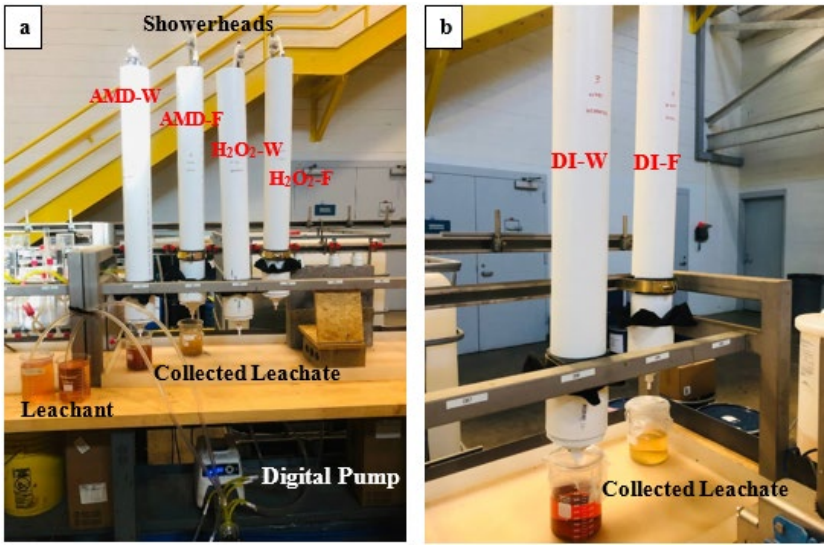

Figure 3: Bench-scale column leaching tests for fresh and weathered CCR: a) AMD and AMD+H_2O_2 as the leachant, b) DI water as the leachant

Results

Geotechnical Properties

Geotechnical properties for fresh and weather CCR are summarized in Table 1.

Table 1: Summary of CCR Mean Geotechnical Physical Properties

Geotechnical properties	CCR	
	Fresh	Weathered
Initial moisture content, ω_{oven} (%) - oven dried	14	18
Initial moisture content, ω_{air} (%) - air dried	11	13
Specific gravity, *Gs*	2.30	1.99
D10 (mm)	0.7	0.7
D30 (mm)	3.0	2.5
D50 (mm)	6.0	4.8
D60 (mm)	8.1	6.0
Uniformity coefficient, *Cu*	11.6	8.6
Coefficient of curvature, Cc	1.6	1.5
Group symbol	GW	GW
Dry unit weight, γ_d (kN/m^3) -Standard Compaction	15.5	15.4
Initial Void Ratio, e_o	0.44	0.27
Porosity, *n*	0.31	0.21
Degree of saturation, *S*	58.2	97.4

Weathered CCR had a higher initial moisture content (18%). Both sample moisture contents were lower when air dried. Values of Gs were within the most common values defined by the Mine Safety and Health Administration (MSHA) (D'Appolonia, 2009) and reported in literature (Quaranta and Tolikonda, 2011). The weathered CCR had the lowest Gs (1.99). Both types of CCR were identified as well-graded gravel with sand (GW). The weathered refuse had the highest degree of saturation calculated using air-dried moisture content (13%) and dry density (15.4 kN/m3) (Table 1).

Column Leaching Tests

The increase in TREE concentrations was always higher in leachate collected from weathered CCR columns as compared to fresh CCR, regardless of leachant type (Fig. 4a). The majority of REE leaching occurred in the first leaching cycle. The first leaching cycle resulted in an increase in TREE concentration of 252%, 178%, 229%, and 116% in leachate collected from columns AMD-W, AMD-F, H_2O_2-W, and H_2O_2-F, respectively. TREE concentration in leachate collected from the same columns either remained constant or slightly decreased after the first leaching cycle. Beyond the first leaching cycle, the percentage increase of TREE concentration in collected leachate ranged from 13% to 50%. Columns DI-W and DI-F showed a constant decrease in leachate TREE concentration after the first leaching cycle. Multiple leaching cycles conducted in weeks 5 and 6 had no substantial effect compared to a single leaching cycle (Fig. 4).

Recirculated AMD and recirculated AMD+H_2O_2 leached more TREE than DI water. During the first three leaching cycles (weeks 1 through 3), recirculated AMD had the highest cumulative percentage of leached TREE from the solid. However, recirculated AMD+H_2O_2 had the highest percent of leached TREE from the solid after four additional leaching cycles (Fig. 4b). Column DI-F, which had the highest outflow rate, yielded the lowest cumulative percentage leached from the solid.

Weathered refuse columns had a lower outflow rate than those filled with fresh refuse. The outflow rate did not follow a specific trend. Columns AMD-W and DI-W had an increase in outflow rate after the first leaching cycle, while column H_2O_2-W had a decrease in flow rate. Column H_2O_2-F had an increase in outflow rate after the first leaching cycle; flow rate decreased again after the third leaching cycle. Column AMD-F showed a relatively constant outflow rate, and column DI-F showed a constant high outflow rate ranging between 150 and 270 mL/min throughout the testing period. Columns DI-W and H_2O_2-W showed a unique behavior of flow rate slowing down and water ponding during the second cycles of leaching performed in weeks 5 and 6 (Fig. 5).

Based on the percent TREE increase in leachate collected during the first leaching cycle, it was concluded that pH of DI water (approximately 5) did not adversely affect the performance of leaching tests conducted with DI water as the leachant. Leachate pH values decreased after the first leaching cycle. The pH readings of leachate collected from all columns showed a decrease (minimum value of 1.72 and

maximum value of 2.36). Leachate pH remained relatively constant for all tests after the first cycle. Cerium (Ce), neodymium (Nd), and lanthanum (La) were the most abundant REEs in both weathered and fresh CCR. Meanwhile, scandium (Sc) and yttrium (Y) were abundant only in weathered coal refuse (Figure 6).

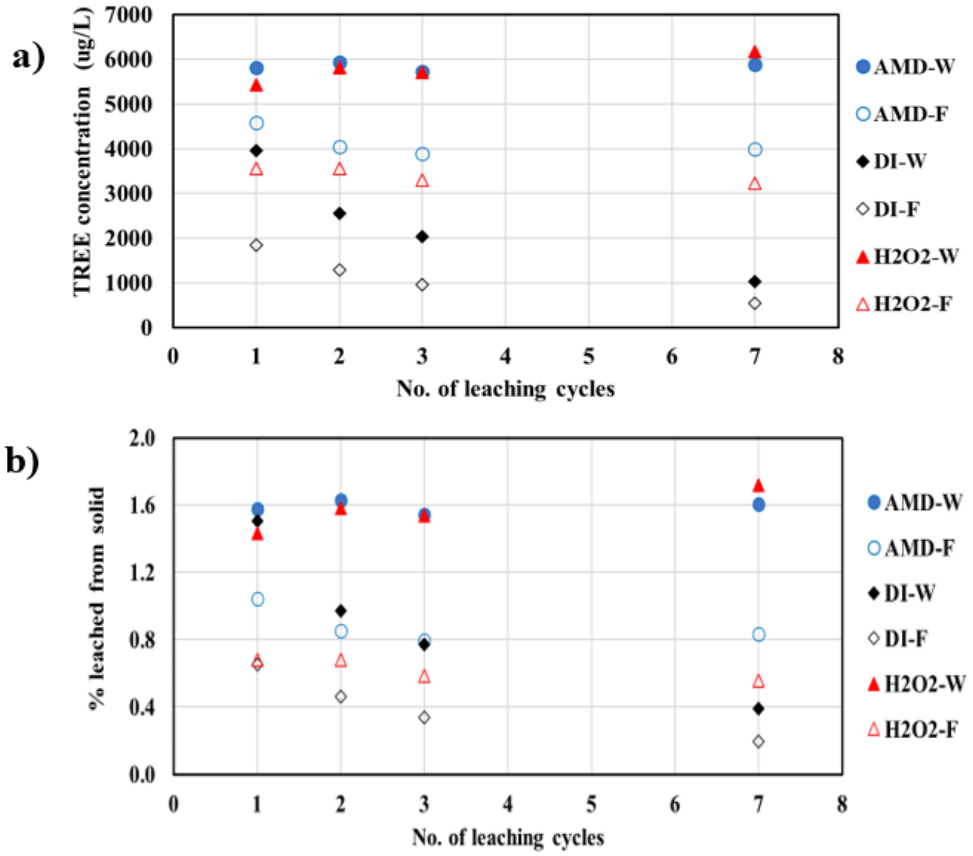

Figure 4: Leaching results: a) TREE concentration in leachate, b) percent leached from solid (b)

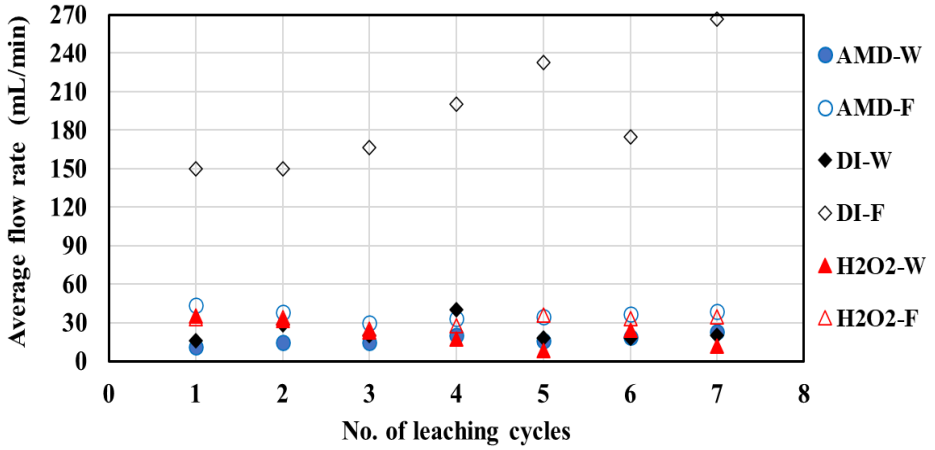

Figure 5: Average outflow rate of leachant in six columns

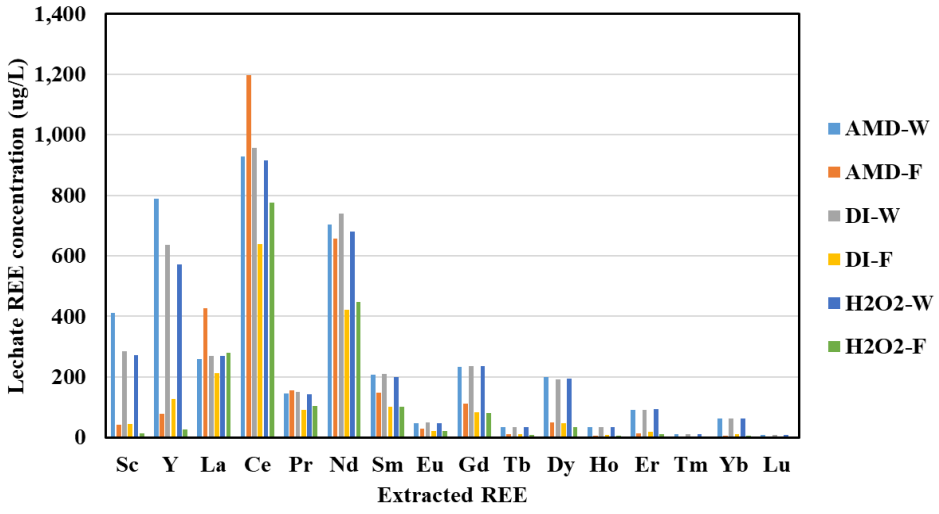

Figure 6: Individual REE concentration in leachate collected from six columns after the first leaching cycle

Discussion

Results indicated that the more weathering promoted more REE extraction. The best REE leaching results were associated with the weathered refuse, which had been on site for at least five years. The first key factor that can explain the high leaching potential is the smaller particle size associated with weathered CCR. Previous studies indicated that as coal mine waste is subject to environmental factors (rainwater and oxygen), its physical characteristics change, such as increasing brittleness and decreasing fragment size (Eppes, 2022; Fabiańska et al., 2024). The change in pressure and stress leads to cracking and eventually breaking down into smaller particles via fragmentation and slaking (D'Appolonia, 2009). Stresses produced by mechanical weathering break molecular bonds in rocks along a defined plane without modifying their chemical composition (Eppes, 2022). When overburdened material is fragmented, the weatherable surface area of minerals is increased (Jain et al., 2021). Leaching characteristics and particle liberation within a given sample are known to be impacted by particle size (Zhang & Honaker, 2018; Yang, 2019; Yang and Honaker, 2020). The smaller the particle size, the more surface area is available for leachant contact and REE liberation (Yang and Honaker, 2020). It should be noted that the main goal was not to test the particle size effect but rather to test the potential of leaching CCR under its current sitting conditions. Thus, it was concluded that weathered refuse had the highest potential for heap leaching without additional mechanical processes (e.g., grinding or crushing), as it had the smallest particle size range due to weathering.

Smaller particle size in weathered CCR also distributed fines that clogged pores between large CCR particles, resulting in a decrease in the movement of the solution going through the solids. This difference in particle size distribution was illustrated by the difference in outflow rates among the columns. Columns filled with the weathered CRR had a lower outflow rate compared to columns filled with fresh CRR.

In addition to a decrease in particle size, spoil slaking has adverse effects, such as a decrease in material strength and an increase in moisture content (D'Appolonia, 2009). The weathered CCR had a higher initial moisture content (18%) compared to the fresh CCR (14%). A higher moisture content helps to ensure oxidation. Another important factor that may have had a substantial impact on results is that pyrite oxidation had already taken place at least within the outer layer of weathered refuse, and oxidation products, such as REE oxides, had already become available on the surface. Introducing an acid enriched with hydrogen ions (H+) (i.e., AMD) broke down those compounds and released the REE into the leachate. This quick reaction was evident through the first leaching cycle that resulted in the highest percentage increase in TREE concentration, as the H+ had quick reaction kinetics with REE-bearing compounds available at the surface of the solid particles. This resulted in the release of the "easy-to-leach" REEs.

Refuse that has been exposed to weathering conditions has what is known as existing or stored acidity that is readily available for transport to the receiving environment. The stored acidity can be found in the form of soluble acidic components, including hydrogen ions or soluble sulfate salts. Generally, sulfate salts are water-soluble and build up on coal waste during dry periods due to surface evaporation (Daniels et al., 2018), then release acidity and metals during rainfall events (Pope et al., 2003). When DI water with a pH value of approximately 5 was used as the leachant, the stored acidity contributed greatly to reducing the pH value and releasing the REE along with other major metals. Therefore, there was no substantial difference between the performance of the three different leachants (AMD, AMD+H_2O_2, and DI water), even though they had different pH values.

Multiple leaching cycles did not promote REE extraction. It is believed that those cycles were actually flushing cycles rather than leaching. These cycles provided sufficient wetting periods and elongated drying periods when testing the weathered and fresh refuse. In the absence of sufficient oxygen and aeration, pyrite oxidation and weathering will be prevented, and AMD production will be limited (Hornberger and Brady, 2009). The current study has proven that pyrite oxidation is a time-dependent process that should be promoted by providing the factors needed (e.g., humidified air and reduced particle size ore) for the process to take place between flushing cycles. This finding is consistent with previous studies (Geidel, 1979; Jain et al., 2021). It is important to note that the required factors for a successful leaching process may vary depending on the goal of the project (e.g., targeting pyrite oxidation or REE-bearing compounds).

Conclusion

Heap leaching of REEs from low-grade CCR ores was investigated through column leaching tests. Three leachants (AMD, AMD+H_2O_2, DI water) and two types of CCR (fresh, weathered) were evaluated. The results showed that the combination of AMD and weathered CCR offered the best opportunity for leaching REEs within the first leaching cycle. Improved leaching potential may be possible through additional

engineering controls. Decreasing the grain size distribution, humidified air application, and studying time intervals between flushing cycles could be investigated in the future.

Acknowledgements

The work described in this publication was supported by Grant/Cooperative Agreement Number S23AC00063 from the US Department of the Interior, Office of Surface Mining, Reclamation, and Enforcement (OSMRE), Applied Sciences Program, project technical reviewer Steve Ball, Technical Support Division, Physical & Biological Sciences Branch, Pittsburgh, PA. The work also received in-kind support from Monongalia County Coal Resources, Inc. (MCCR), a subsidiary of American Consolidated Natural Resources, Inc. (ACNR). ACNR's contact for the study was Kim Betcher, Director of Environmental Regulatory Affairs. Its contents are solely the responsibility of the authors and do not necessarily represent the official views of the OSMRE and ACNR.

References

Atia, T. A., Wouters, W., Monforte, G., & Spooren, J. (2021). Microwave chloride leaching of valuable elements from spent automotive catalysts: Understanding the role of hydrogen peroxide. *Resources, Conservation and Recycling, 166,* 105349.

Daniels, W. L., Stewart, B. R., & Zipper, C. E. (2018). Reclamation of coal refuse disposal areas.

D'Appolonia. (2009). *Engineering and design manual: Coal refuse disposal facilities.* US Department of the Interior, Mining Enforcement and Safety Administration.

Eppes, M.-C. M. (2022). Mechanical weathering: A conceptual overview. In *Treatise on geomorphology* (3, pp. 30–45). Elsevier Academic Press.

Fabiańska, M., Ciesielczuk, J., Szczerba, M., Misz-Kennan, M., Więcław, D., Szram, E., Nádudvari, Á., & Ciesielska, Z. (2024). Weathering alterations of coal mining wastes geochemistry, petrography, and mineralogy: A case study from the Janina and Marcel coal mines, Upper Silesian Coal Basin (Poland). *International Journal of Coal Geology, 281,* 104407.

Geidel, G. (1979). Alkaline and acid production potentials of overburden material: The rate of release. *Reclamation Review, 2*(3–4).

Ghorbani, Y., Franzidis, J.-P., & Petersen, J. (2016). Heap leaching technology—Current state, innovations, and future directions: A review. *Mineral Processing and Extractive Metallurgy Review, 37*(2), 73–119.

Google Earth Pro. (2020). Data SIO, NOAA, U.S. Navy, NGA, GEBCO.

Honaker, R., Zhang, W., Yang, X., & Rezaee, M. (2018). Conception of an integrated flowsheet for rare earth elements recovery from coal coarse refuse. *Minerals Engineering, 122,* 233–240.

Hornberger, R., & Brady, K. (2009). The development and interpretation of the ADTI-WP2 leaching column method (kinetic test procedure for the prediction of coal mine drainage quality) EPA method 1627. PA Department of Environmental Protection, Pennsylvania State University, CSC Dyncorp, U.S. Office of Surface Mining Reclamation and Enforcement, U.S. EPA, U.S. Geological Survey.

Hudson-Edwards, K. A., Kemp, D., Torres-Cruz, L. A., Macklin, M. G., Brewer, P. A., Owen, J. R., Franks, D. M., Marquis, E., & Thomas, C. J. (2024). Tailings storage facilities, failures and disaster risk. *Nature Reviews Earth & Environment, 5*(9), 612–630.

Iasillo, E., Rempel, C., & Holtzapple, A. (2013). Development of accurate metal production forecasts for a heap leach project using METSIM® dynamic simulation and defensible column leach testing data. *Heap Leach Solutions 2013,* 22–25.

Jain, K. R., Edraki, M., & McIntyre, N. (2021). Controls of wetting and drying cycles on salt leaching from coal mine spoils. *Water, Air, & Soil Pollution, 232*(11), 472.

Larrabure, G., Salinas-Farran, L., Neethling, J., & Brito-Parada, R. (2024). A review on strategies to assess the spatiotemporal heterogeneity of column leaching experiments for heap leaching upscaling. *Minerals Engineering, 216,* 108892.

Lin, R., Howard, H., Roth, A., Bank, L., Granite, J., & Soong, Y. (2017). Enrichment of rare earth elements from coal and coal by-products by physical separations. *Fuel, 200,* 506–520.

Nagar, S. M., El-Sayed, F. A., Morsy, W. M., Mady, A. H., Mohamed, A. M., & Mahmoud, K. F. (2020). Capability of uranium heap leaching from Gattar and El Missikat area, Eastern Desert, Egypt: A kinetic approach. *Journal of Engineering and Applied Sciences Technology, 2*(4), 1–7.

Pope, J., Bayless, E., Olyphant, G., & Branam, T. (2003). The role of efflorescent sulfate salts in Indiana's mine water quality. In *Effects of abandoned mine land reclamation on ground and surface water quality: Research and case histories from Indiana* (pp. 259–279).

Quaranta, J. D., & Tolikonda, R. (2011). Design of non-woven geotextiles for coal refuse filtration. *Geotextiles and Geomembranes, 29*(6), 557–566.

U.S. Department of Energy. (2011). *Critical materials strategy* (Technical Report, OSTI ID 1000846).

Van Staden, P., & Petersen, J. (2018). The effects of simulated stacking phenomena on the percolation leaching of crushed ore, Part 1: Segregation. *Minerals Engineering, 128,* 202–214.

Wang, P., Sun, Z., Hu, Y., & Cheng, H. (2019). Leaching of heavy metals from abandoned mine tailings brought by precipitation and the associated environmental impact. *Science of the Total Environment, 695,* 133893.

Yang, X. (2019). Leaching characteristics of rare earth elements from bituminous coal-based sources.

Yang, X., & Honaker, Q. (2020). Leaching kinetics of rare earth elements from fire clay seam coal. *Minerals, 10*(6), 491.

Zhang, W., & Honaker, Q. (2018). Rare earth elements recovery using staged precipitation from a leachate generated from coarse coal refuse. *International Journal of Coal Geology, 195,* 189–199.

Ziemkiewicz, P., He, T., & Noble, A. (2016). Recovery of rare earth elements (REEs) from coal mine drainage.

Ziemkiewicz, P., Liu, X., & Noble, A. (2018). REE identification and characterization of coal and coal by-products containing high rare earth element concentrations (Final Report, U.S. Department of Energy, FE0026444-Final-Report-092618).

Eco-Efficient Nickel: Heap Leaching as a Game-Changer for Indonesia's Nickel Industry

Achmad Fauzi Trinanda, Terramet Metallurgy Solution, Indonesia
Ridho Lestari, Terramet Metallurgy Solution, Indonesia
Muhamad Ichlas Juliansyah, Terramet Metallurgy Solution, Indonesia
Rizky Aisyah Septi Maharani, Terramet Metallurgy Solution, Indonesia
Natasha Kisti Anugrah, Terramet Metallurgy Solution, Indonesia

Abstract

Indonesia, home to the world's largest nickel laterite reserves, plays a critical role in the global stainless steel and electric vehicle (EV) battery supply chains. The country's nickel industry has long been dominated by pyrometallurgical processes, including Rotary Kiln-Electric Furnace (RKEF) and Blast Furnace (BF) technologies. In response to the emerging EV battery market, hydrometallurgical technology—specifically High-Pressure Acid Leaching (HPAL)—has been introduced over the past three to four years. However, both approaches are capital-intensive, highly energy-consuming, and environmentally burdensome, contributing to the perception of Indonesia as a producer of "dirty nickel." Moreover, their application has resulted in a significant portion of nickel laterite reserves remaining unutilized. Heap leaching presents a promising alternative: a low-cost, eco-efficient, and scalable hydrometallurgical process particularly suited to Indonesia's tropical laterite profiles and low-grade ores.

This paper explores heap leaching as a transformative solution for the Indonesian nickel industry, emphasizing its potential to reduce greenhouse gas emissions, lower capital and operational expenditures, and improve ore utilization efficiency. Importantly, heap leaching produces a more stable form of tailings (spent ore), which can be rehabilitated or repurposed as plantation media—minimizing long-term environmental impacts and creating opportunities for post-mining land use. Additionally, the process enables the recovery of valuable by-products, particularly magnesium sulfate, from effluent streams—opening new revenue sources and supporting circular economy principles. Its operational flexibility allows for the production of various nickel products, serving both stainless steel and battery-grade markets. This study highlights heap leaching's advantages over conventional methods in terms of life-cycle emissions, water consumption, waste management, economic performance, and the broader transferability of operational knowledge to local stakeholders. By adopting heap leach technology, Indonesia has the

opportunity not only to enhance the sustainability of its nickel sector but also to shed its "dirty nickel" label—positioning itself as a global leader in clean and responsible mineral extraction.

Introduction

Indonesia holds the world's largest reserves of nickel laterite, making it a key player in the global supply chains for stainless steel and electric vehicle (EV) batteries. Over the past two decades, the country's nickel industry has been driven primarily by pyrometallurgical processes—such as Rotary Kiln-Electric Furnace (RKEF) and Blast Furnace (BF)—which produce ferronickel and nickel pig iron for stainless steel production. More recently, growing demand for EV batteries has led to the introduction of High-Pressure Acid Leaching (HPAL) technology to produce battery-grade nickel.

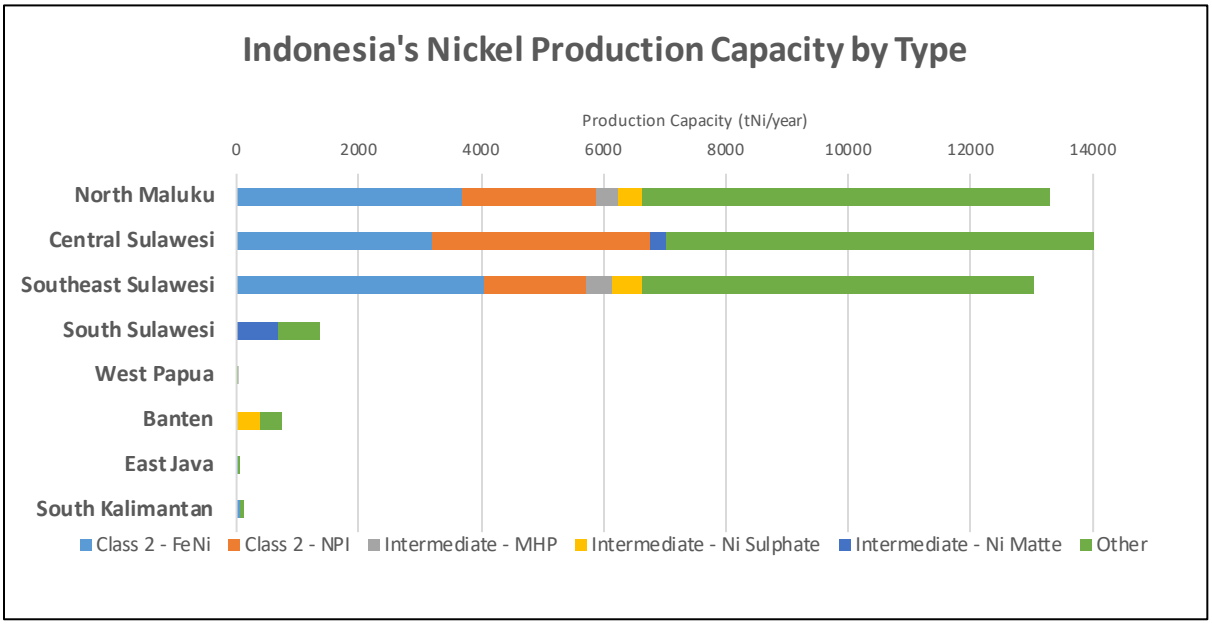

Figure 1: Indonesia's nickel production capacity by type (CREA, 2024)

While both pyrometallurgy and HPAL have enabled Indonesia to industrialize its nickel resources, they come with significant environmental and economic costs. These methods are capital-intensive, energy-consuming, and produce high volumes of carbon emissions and hazardous tailings. Consequently, Indonesia's nickel has increasingly been labeled as "dirty nickel," a perception that threatens the industry's long-term competitiveness. This reputation is beginning to influence global trade dynamics, with environmentally conscious markets—particularly in Europe and North America—scrutinizing the carbon footprint and sustainability of raw material imports. Some buyers have already started prioritizing "green nickel" from jurisdictions with lower environmental impacts, potentially marginalizing Indonesia's market position and limiting its access to premium pricing or strategic partnerships.

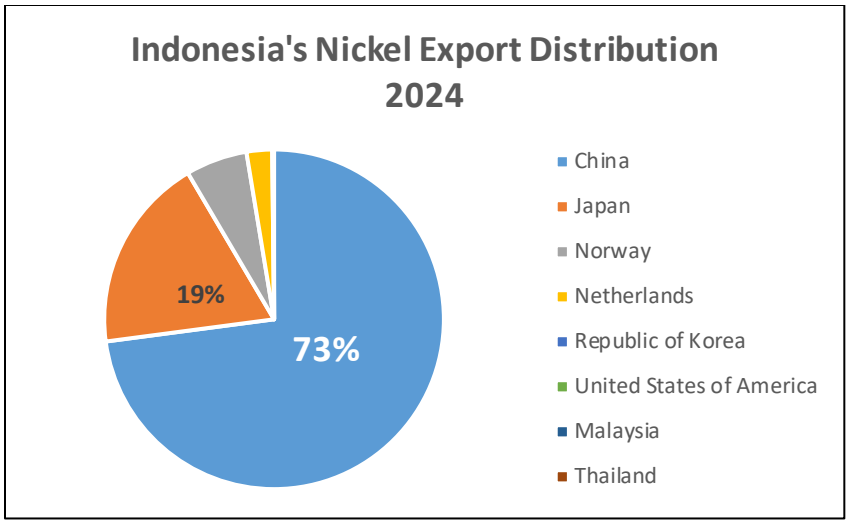

Figure 2: Indonesia's nickel production capacity by type (Trademap, 2024)

Moreover, these extraction technologies are selective in the types of ore they can process efficiently, leaving significant portions of low-grade laterite resources underutilized or discarded. This not only reduces overall resource efficiency but also increases the environmental footprint per ton of nickel produced.

In this context, heap leaching has emerged as a compelling alternative. It is a low-cost, environmentally friendly, and scalable hydrometallurgical method well-suited to Indonesia's tropical climate and laterite ore profiles. Unlike conventional methods, heap leaching offers improved ore utilization, lower greenhouse gas emissions, and the ability to produce more stable tailings that can be rehabilitated or repurposed for sustainable land use. The technology also provides opportunities to recover valuable by-products, such as magnesium sulfate, supporting a more circular and resource-efficient mining model.

This paper examines the potential of heap leaching to transform Indonesia's nickel sector into a cleaner, more inclusive, and sustainable industry. It evaluates the environmental, economic, and social benefits of heap leaching, compares its performance with existing technologies, and discusses its role in helping Indonesia transition from "dirty nickel" toward a greener and more resilient mining future.

Method

To achieve the study's objectives, several methods were employed, including a literature review and a comparative study. These methods focused on collecting and analyzing information and data related to nickel production and Heap Leach technology.

The opportunities for developing Heap Leach in Indonesia, as well as its applications worldwide, are discussed and presented.

Results and Discussions

Indonesia's Current Industry

The downstream development of natural resources has become a key priority in Indonesia's national agenda to drive and sustain economic growth, which is crucial for achieving the Golden Indonesia 2045 Vision. As the country approaches its centennial celebration of independence, the government has launched strategic initiatives aimed at transforming Indonesia into a developed nation by 2045 and escaping the middle-income trap (Kominfo, 2023).

Among these initiatives, the nickel sector has received significant attention due to its rapid export growth. Global demand for nickel has surged by approximately 10% annually over the past five years, increasing from 2.44 million tons in 2019 to 3.61 million tons in 2023 (Statista, 2022). In response, Indonesia has substantially increased its nickel production, raising output from 0.2 million tons in 2016 to 0.76 million tons in 2020, which accounts for nearly 30% of global production (MEMR, 2021). Figure 3 illustrates the distribution of major nickel reserves and the locations of smelting and refining facilities across Sulawesi, the Maluku Islands, and Papua.

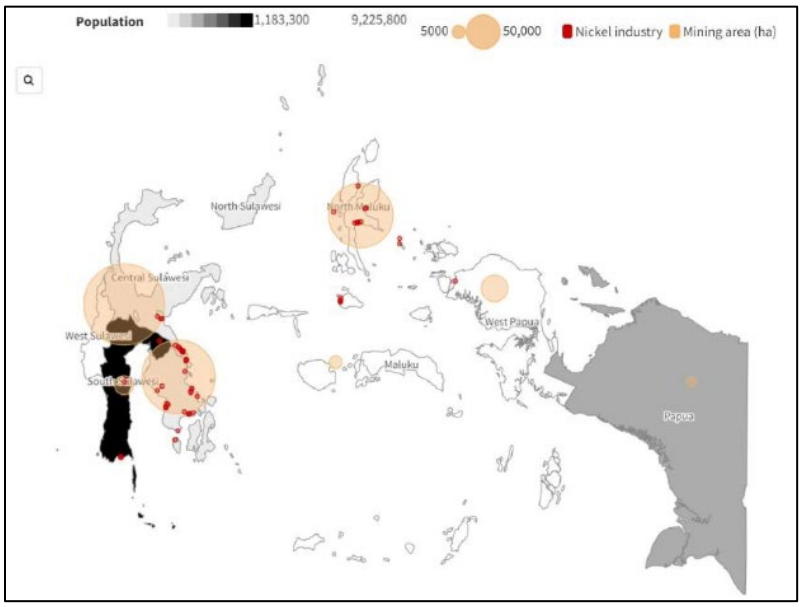

Figure 3: Distribution map of Indonesia's current nickel industry across Eastern Indonesia

Indonesia's most substantial nickel reserves are located in the eastern region of the country, with total nickel ore and metal resources estimated at 143 million tons and 49 million tons, respectively. By June 2021, the government had issued 338 active mining licenses for nickel operations (MEMR, 2021). The expansion of nickel smelting and refining facilities has accelerated rapidly, particularly in Southeast

Sulawesi, Central Sulawesi, and North Maluku, with further growth expected through 2025 and likely continuing to 2030.

The country's nickel deposits are primarily laterite ores, categorized into two types: limonite ores, which contain 0.8–1.5% nickel and high iron content, and saprolite ores, which contain 1.5–3% nickel and 0.1–0.2% cobalt, recoverable through chemical processes (Anderson, 2023). Based on current extraction rates, the Geological Agency under MEMR estimates the remaining lifespan of limonite reserves at 34 years and saprolite reserves at 15 years (Handayani, 2023).

Historically, Indonesia's nickel sector has focused on producing Class 2 nickel products, such as Ferronickel (FeNi) and Nickel Pig Iron (NPI), both of which are essential for stainless steel manufacturing. These products are predominantly derived from saprolite ores, processed via pyrometallurgical methods using Blast Furnace (BF) and Rotary Kiln Electric Furnace (RKEF) technologies. The government's ban on raw nickel ore exports has been a key policy to promote domestic downstream processing and increase value addition within Indonesia. As a result, the use of Class 2 nickel products has grown for stainless steel production and as feedstock for refining into high-purity Class 1 nickel products and intermediates required for electric vehicle (EV) batteries, renewable energy applications, and superalloys (MEMR, 2021; Huber, 2021).

Limonite ores serve as feedstock for hydrometallurgical processes, particularly High-Pressure Acid Leach (HPAL), which produces nickel and cobalt intermediates such as Mixed Hydroxide Precipitate (MHP) and Mixed Sulfide Precipitate (MSP). Further processing of MHP or MSP can yield Nickel Sulfate (21% Ni) and Nickel Hydroxide (40% Ni), while Nickel Matte (80% Ni) is obtained from FeNi or NPI via RKEF routes. These materials are integral components in the production of battery cells.

As highlighted by the International Energy Agency (IEA), Indonesia has become the world's largest center for nickel mining and refining, positioning itself as a crucial supplier for stainless steel production and the global battery supply chain, particularly through commodities such as FeNi, NPI, MHP/MSP, Nickel Sulfate, Nickel Hydroxide, and Nickel Matte (IEA, 2023; Melvin, 2023). At the Asia-Pacific Economic Cooperation (APEC) Summit in November 2023, President Joko Widodo announced Indonesia's plan to commence domestic EV production in 2024, targeting an output of 600,000 units annually by 2030. He also reaffirmed Indonesia's commitment to renewable energy development, including plans for a 30,000-hectare green industrial zone (Setkab, 2030).

Opportunities and Challenges

The extractive industry is inherently energy-intensive and generates substantial emissions, with one of the most pressing concerns being Indonesia's heavy reliance on coal to support downstream operations. Approximately 76% of the country's total captive coal power capacity—equivalent to 8.2 GW of 10.8

GW—is allocated to metal processing activities (CREA, 2023). Despite this, captive coal power remains largely excluded from Indonesia's national energy strategies and climate mitigation plans.

The Comprehensive Investment and Policy Plan (CIPP) under the Just Energy Transition Partnership (JETP), completed in November 2023, confirms that off-grid captive coal power plants are currently not included within the initiative's scope. Given the existing captive power landscape, achieving the targeted peak emissions of 290 million tons of CO2 by 2030 is considered highly challenging (JETP Secretariat, 2023). Decarbonizing Indonesia's metal sector is further complicated by competing economic priorities, limited availability of affordable alternative energy options, and an unreliable national power grid (Zhu et al., 2023).

China has emerged as the dominant investor in Indonesia's captive coal sector, holding over 70% ownership across 14 state-owned and private companies involved in mining and metals processing. International stakeholders could support Indonesia's decarbonization by enforcing stricter emissions standards aligned with global best practices or China's more stringent domestic regulations (Zhu et al., 2023; Wang, 2022).

Despite regulations intended to control emissions in the mining sector, the rapid expansion of nickel mining and processing has triggered numerous environmental issues in recent years. Documented incidents include seawater discoloration caused by effluent discharge near Obi Island; heavy metal contamination in Weda Bay and Buli Bay (Halmahera); offshore wastewater disposal by the Indonesia Morowali Industrial Park; extensive land degradation in North Konawe following mining operations; and air pollution from coal transport and coal-fired plants affecting communities around the Konawe Industrial Park (Mongabay Environmental News, 2022; Kompas, 2023; Ginting & Moore, 2021; Barus et al., 2022).

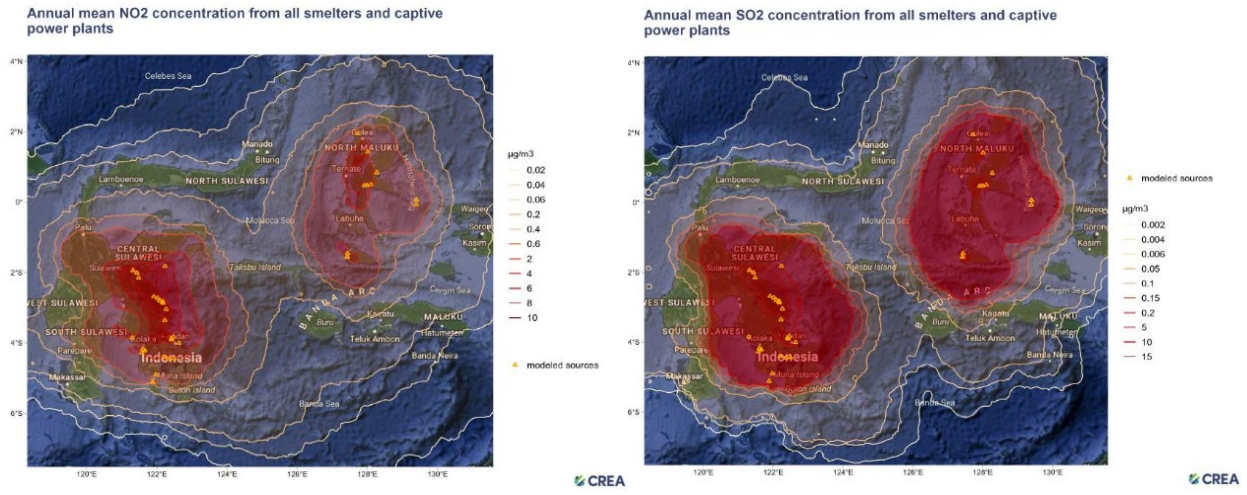

Figure 4: Annual average concentration of SOx and NOx from the three provinces' metal smelting facilities and captive power plants (CREA, 2024)

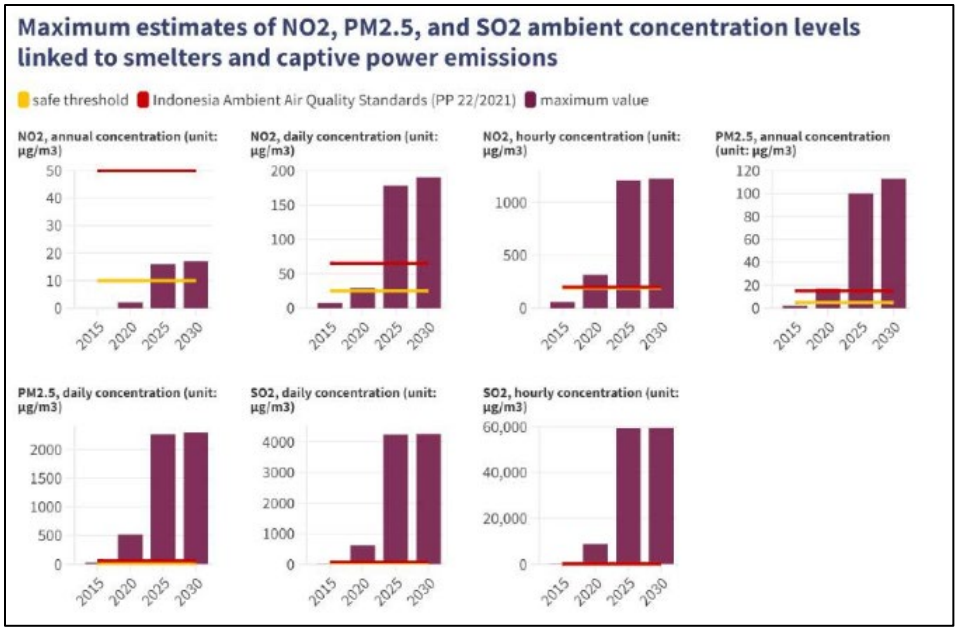

Figure 5: Maximum estimates of NO2, PM2.5, and SO2 ambient concentration levels linked to emissions from three provinces' metal smelting facilities and captive power plants, from 2015 to 2030 (CREA, 2024)

The Coral Triangle, which hosts approximately 76% of the world's shallow-water coral species, faces significant environmental threats as Indonesia's nickel mining and processing industries rapidly expand (CTI-CFF, 2009). Environmental organizations and members of Indonesia's House of Representatives have raised concerns that this accelerated industrial growth could increase pressure to loosen or bypass regulations on deep-sea tailings disposal, potentially heightening the risk of illegal waste dumping. In response, Indonesia's Coordinating Minister for Maritime Affairs and Investment, Luhut Binsar Pandjaitan, emphasized in July 2023 that waste disposal is only permitted through approved facilities, such as engineered containment structures, dry stacking, or a combination of both (Setiawan, 2023).

Simultaneously, the expansion of nickel mining has contributed to substantial deforestation and biodiversity loss, particularly in Sulawesi and North Maluku. Reports indicate that over 500,000 hectares of forest in Central and Southeast Sulawesi have been cleared, not only through legal concessions but also through suspected illegal practices (Hidayat & Hermawan, 2022). As of 2022, government-issued mining concessions exceeded one million hectares, with more than 75% of that area consisting of forested land, according to data from WALHI, Indonesia's environmental watchdog (Wicaksono, 2023).

Social and governance challenges have also become increasingly visible, especially regarding the rights and safety of workers and local communities in nickel-producing regions. Between 2019 and 2023, at least 32 community members were criminally charged in disputes with nickel mining companies, with reports of two arrests and 14 individuals experiencing abuse by law enforcement (Bhawono, 2023).

Furthermore, revisions to Article 162 of Law No. 3/2020 on Mineral and Coal Mining have been criticized by activists and community groups as a tool to suppress environmental defenders and local advocates (Constitutional Court of Indonesia, 2022).

Worker safety remains a pressing concern, highlighted by the tragic smelter explosion on December 24, 2023, at facilities operated by PT Indonesia Tsingshan Stainless Steel and PT Gunbuster Nickel Industry, which resulted in 21 fatalities (Tenggara Strategics, 2024). Unfortunately, this incident is not an isolated case. Trend Asia recorded at least 65 fires and explosions at smelter sites between 2015 and 2023, with 53 worker deaths reported from 2015 to 2022, including both Indonesian and Chinese nationals (Handayani, 2024).

The recurrence of these fatal incidents suggests systemic shortcomings in occupational health and safety practices, including inadequate audits and enforcement of safety protocols. The December 2023 explosion further underscores the urgent need for stricter regulations and improved oversight within the sector (Tenggara Strategics, 2024).

Indonesia faces a critical need to reform its metal industry to ensure both worker safety and environmental protection. A responsible and sustainable approach to sourcing critical minerals is essential for achieving a fair energy transition, requiring collaboration and accountability from all stakeholders in the nickel supply chain.

The Development of Nickel Heap Leach

The development of nickel heap leach technology has followed a systematic progression, from laboratory experiments to larger-scale validation programs. Initial investigations were conducted at the laboratory scale, where controlled leaching tests were performed on representative samples of the ore. These trials provided early confirmation of the leachability of nickel laterites under heap leach conditions, yielding baseline data on nickel extraction efficiency, acid requirements, and leach kinetics. The laboratory results established technical confidence in the process and served as the foundation for subsequent studies.

Figure 6: The development test of Nickel Heap Leach

To better replicate field-scale behavior, column leach tests were subsequently conducted. These tests provided a more realistic simulation of heap conditions, including percolation characteristics, solution flow, and leach cycle duration. The column experiments demonstrated the potential for significant nickel recoveries while also highlighting operational challenges, particularly in maintaining uniform percolation and controlling the excessive dissolution of impurities such as iron. The findings from this stage offered essential insights into scaling issues and process optimization.

Pilot-scale programs represented the next step in the testwork sequence. In these trials, larger ore volumes were stacked and irrigated under conditions designed to approximate commercial operations. The pilot heaps generated critical engineering and metallurgical data, including recovery performance over extended cycles, acid consumption trends, and solution management strategies. These results validated the technical feasibility of nickel heap leaching on a larger scale and emphasized the importance of proper agglomeration, acid distribution, and heap stability in ensuring consistent performance.

Table 1: The Extraction Performance of Laboratory Scale and Pilot Tests

Parameter	Unit	CRIB C	CRIB B	CRIB D	CRIB E	CRIB F	Column C	Column B	Column D	Column E	Column F
Ore Type		MGSO	MGSO	MGSO	MGSO	HGSO	MGSO	MGSO	MGSO	MGSO	HGSO
Leaching Method		Single Pass	CCHL	CCHL	CCHL	CCHL	Single Pass	CCHL	CCHL	CCHL	CCHL
Fe conc. in lixiviant	gpl	N/A	< 10	> 10	> 10	> 10	N/A	< 10	> 10	> 10	> 10
Heap Height	m	3.5	3.0	3.0	3.5	3.0	3.5	3.0	3.0	3.5	3.0
Estimated True SG	t/m3	2.5	2.6	2.7	2.7	2.3	2.5	2.6	2.7	2.7	2.3
Ore dry weight	kg	26,750	21,926	22,467	27,026	17,085	82.0	74.7	62.7	68.8	47.8
Average flux rate	L/h.m2	8.4	6.9	9.0	8.7	8.7	8.3	8.8	9.3	7.3	8.2
Reconciled feed grade:											
Al	%	1.51	1.58	1.48	1.57	0.32	1.51	1.59	1.50	1.58	0.32
Co	%	0.04	0.04	0.04	0.04	0.04	0.04	0.04	0.04	0.04	0.04
Cr	%	0.87	0.93	0.88	0.91	0.76	0.87	0.87	0.89	0.91	0.75
Cu	ppm	0.37	0.43	0.39	0.44	0.10	0.37	0.37	0.40	0.44	0.07
Fe	*%*	*17.77*	*19.04*	*17.51*	*17.98*	*14.86*	*17.79*	*17.79*	*17.70*	*18.00*	*14.71*
Mg	*%*	*12.21*	*11.10*	*11.98*	*12.01*	*13.57*	*12.23*	*12.23*	*12.10*	*12.00*	*13.60*
Mn	%	0.29	0.31	0.29	0.30	0.24	0.29	0.29	0.29	0.30	0.24
Ni	*%*	*1.50*	*1.63*	*1.56*	*1.54*	*1.83*	*1.50*	*1.65*	*1.58*	*1.53*	*1.81*
Si	%	17.77	17.28	18.16	17.84	18.84	17.75	17.43	17.97	17.86	18.97
Fe/Mg		*1.45*	*1.72*	*1.46*	*1.50*	*1.10*	*1.45*	*1.45*	*1.46*	*1.50*	*1.08*
At 75% Ni Extraction											
Leaching duration	days	150	134	139	166	122	143	151	134	188	124
S/O Ratio	m3/t ore	9.97	11.25	11.33	11.12	11.99	9.96	11.05	12.24	11.29	14.12
Metal Extraction:											
Al	%	31.5	31.8	27.0	34.9	14.7	34.6	47.3	36.3	37.5	24.3
Co	%	78.7	79.3	53.5	89.0	76.5	83.3	81.6	82.3	90.5	77.9
Cr	%	22.1	17.4	15.3	14.9	0.8	16.4	19.4	17.5	19.6	3.5
Cu	%	49.6	35.3	46.7	44.7	-2.1	54.7	56.2	51.6	48.1	-9.2
Fe	*%*	*39.2*	*32.8*	*42.5*	*21.0*	*-2.6*	*38.2*	*37.7*	*24.2*	*32.9*	*8.8*
Mg	*%*	*54.7*	*49.0*	*38.7*	*56.2*	*64.2*	*56.8*	*52.2*	*56.1*	*55.7*	*70.3*
Mn	%	74.5	78.5	51.9	85.7	73.7	84.2	77.9	83.4	86.6	82.8
Ni	%	75.0	75.0	75.0	75.0	75.1	75.0	75.2	75.3	75.0	75.0
Acid Consumption	*kg/t ore*	*522*	*525*	*472*	*465*	*457*	*539*	*542*	*548*	*500*	*538*
	kg/kg Ni Ext.	*49*	*50*	*44*	*43*	*34*	*52*	*50*	*50*	*45*	*37*

The cumulative progression of these investigations has provided a comprehensive understanding of the nickel heap leach process. Laboratory studies confirmed the process's viability, column tests defined operational parameters, and pilot programs validated performance under semi-commercial conditions.

Together, these results establish a strong technical foundation for evaluating commercial-scale heap leaching of nickel laterites while also identifying key areas for optimization in future developments.

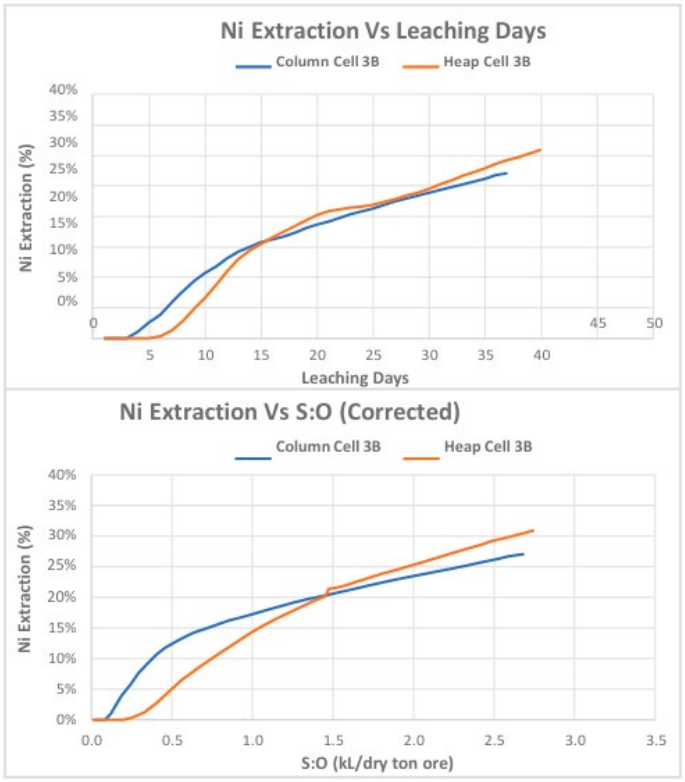

Figure 7: The extraction kinetics of the demonstration leach trial are identical to the extraction kinetics of the reference column

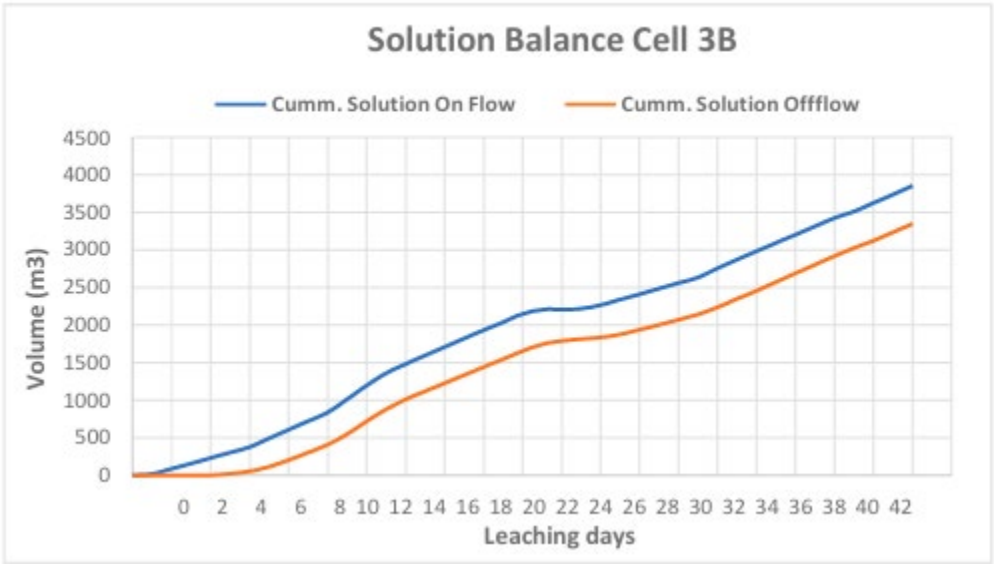

Figure 8: The water balance in and out of the heap is stable, and there is no ponding on the surface of the heap

At the demoplant or semi-commercial scale, utilizing 5,000 tons of nickel laterite ore—equivalent to one barge—the results remain consistent with those observed in previous testing stages. These findings provide strong evidence supporting the feasibility of heap leaching at the commercial scale. The data serve as the basis for designing a nickel heap leach plant. With the current dynamic heap scheme, the total footprint required to produce 10,000 tNi/year is approximately 53 hectares, which is comparable to the land requirement of RKEF processing plants, typically around 50 hectares.

Figure 9: Upstream plant facility

Figure 10: Commercial trial documentation

Heap Leach Technology as the Game Changer

Heap leaching is a hydrometallurgical process that involves stacking crushed ore onto a lined pad and applying a leaching solution (typically sulfuric acid) to dissolve nickel and cobalt. The resulting pregnant

leach solution (PLS) is then collected and processed to recover these metals.

Heap leaching has been successfully employed for the extraction of gold, silver, and copper (Johnson & Lee, 2019). Its adaptation for nickel laterites presents an opportunity to overcome the challenges associated with conventional methods. In this process, crushed ore is stacked onto a lined pad, and a leaching solution is applied to dissolve nickel and cobalt, which are subsequently recovered from the solution. Heap leaching offers several distinct advantages:

Proven and Low-Risk Technology

Figure 11: Heap leach commercial plants around the world; A) Brazilian Nickel (Brazil), B) Hellenic Minerals (Cyprus), C) Bukit Makmur Resources (Indonesia)

Extensively used in the extraction of various metals, heap leaching requires lower operational complexity and eliminates the need for high-temperature or high-pressure systems. This technique has been successfully implemented in numerous mining operations worldwide, such as Brazilian Nickel in Brazil and Hellenic Minerals in Cyprus. Its simplicity in operation, combined with lower capital and operational expenditures, makes heap leaching an attractive option for Indonesia's mining industry.

Heap leaching operates at ambient temperature and pressure, which inherently enhances safety and simplifies process control (Anna et al., 2019). In contrast, the Rotary Kiln-Electric Furnace (RKEF) method operates at extremely high temperatures, posing significant explosion risks. In contrast, High-Pressure Acid Leaching (HPAL) operates at around 220°C under high pressure, which increases the likelihood of mechanical failures and pressure-release incidents (Phillips, 2010). This stark difference in operational conditions highlights heap leaching's advantages in both safety and ease of implementation.

Lower Carbon and Energy Footprint

As previously mentioned, numerous nickel projects in Indonesia have primarily focused on pyrometallurgical technologies, such as Rotary Kiln Electric Furnaces (RKEF), which produce ferronickel (FeNi) and nickel pig iron (NPI) mainly for stainless steel production. While these methods are effective for processing high-grade ores, they are highly energy-intensive and contribute substantially to carbon emissions.

Figure 12 illustrates the significant difference in energy consumption and carbon emissions between traditional pyrometallurgical methods and heap leaching. For instance, HPAL and RKEF processes consume approximately 25–30 MWh per ton of nickel and emit 40–50 tCO_2 per ton of nickel. In contrast, heap leaching requires only about 5.5 MWh/tNi and produces just 16 tCO_2/tNi (World Bank, 2021). These data highlight the promising potential of heap leaching as a more sustainable, low-carbon alternative for nickel extraction.

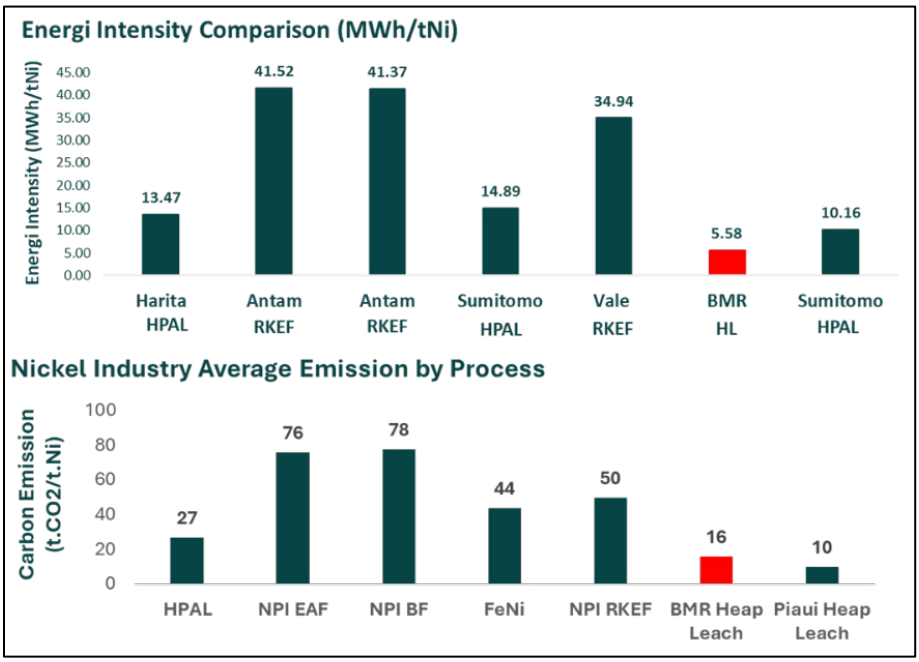

Figure 12: Energy intensity and emission of various nickel projects' efficient resource utilization

Heap leaching consumes significantly less energy than conventional methods such as Rotary Kiln-Electric Furnace (RKEF) and High-Pressure Acid Leaching (HPAL), requiring as little as 5.5 MWh per ton of nickel and generating only 16 tCO_2 per ton of nickel (World Bank, 2021). This low-energy, low-emission profile makes heap leaching an increasingly attractive option, aligning with global initiatives to reduce the carbon footprint of mining operations and promote more sustainable extraction practices.

Efficient Resource Utilization

The development of nickel smelter projects in Indonesia in recent years has been predominantly driven by Rotary Kiln-Electric Furnace (RKEF) technology. These smelters utilize high-grade nickel ore as feedstock to produce Nickel Pig Iron (NPI) and Ferronickel (FeNi). The rapid proliferation of RKEF smelters in Indonesia has led to a significant influx of nickel into the global market, creating an oversupply that contributed to the decline in nickel prices in 2024. Furthermore, the widespread expansion of RKEF smelters has raised concerns about the depletion of high-grade nickel ore reserves, which are projected to

last only the next ten years (Figure 13) due to the substantial growth of RKEF-based smelting capacity in recent years.

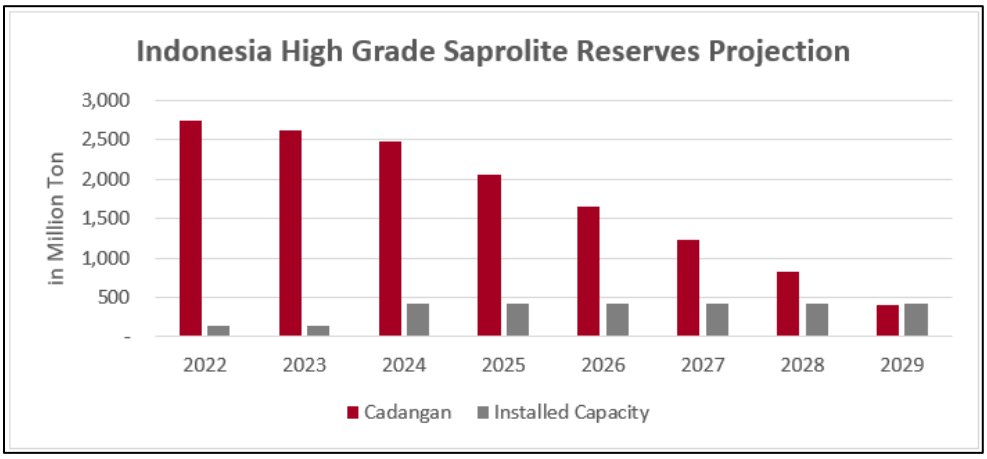

Figure 13: High-grade nickel ore reserves projection (MEMR, 2022)

Heap leaching enables the processing of low-grade saprolite and ferruginous ores that are unsuitable for the RKEF and HPAL, maximizing resource utilization and extending the lifespan of nickel reserves.

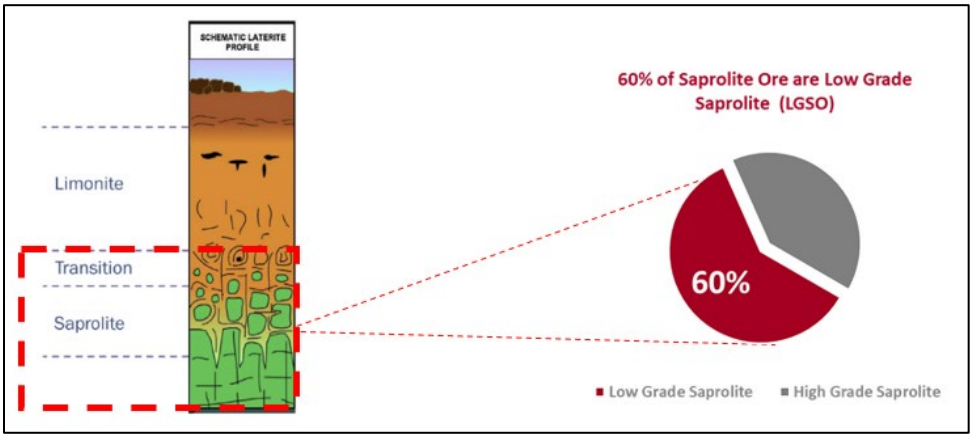

Figure 14: Ore type processed in heap leach and its typical proportion in mine (Brand et al, 1998)

Environmentally Friendly

The residue resulting from the heap leach process is referred to as spent ore. Once the extraction process reaches its target, the spent ore is thoroughly rinsed to remove any remaining heavy metals from the solid material. After rinsing, the spent ore is drained for 2–5 days. This wet spent ore is then treated with limestone, which serves to neutralize residual metal ions released during extraction and to counteract any remaining acidity in the residue. The costs associated with rinsing and neutralization are already included

in the operational expenditures (OPEX). The only additional expense is the dismantling of the processing facility, which varies depending on the specific downstream plant configuration.

The treated spent ore from the heap leach process is stable and non-hazardous, significantly minimizing environmental risks. Table 2 presents the results of the Toxicity Characteristic Leaching Procedure (TCLP) for the heap leach residue.

Table 2: Toxicity Characteristic Leaching Procedure (TCLP) Test Result of Bukit Makmur Resources Heap Leach Residue

No.	Description	Unit	Result	TCLP-A	TCLP-B	TCLP-C
TCLP Anions						
1	Chloride, Cl-	mg/L	147	75,000	12,500	5,000
2	Cyanide (Total), CN-	mg/L	<0,005	21	4	1,4
3	Fluoride	mg/L	0,06	450	75	30
4	Nitrate, NO3 _N	mg/L	0,042	40	5	1,000
5	Nitrite, NO2-N	mg/L	<0,001	900	150	60
TCLP Inorganic						
1	Antimony, Sb	mg/L	<0,0005	6	1	0,4
2	Arsenic, As	mg/L	<0,0005	3	0,5	0,2
3	Barium, Ba	mg/L	<0,1	210	35	14
4	Beryllium, Be	mg/L	<0,01	4	0,5	0,2
5	Boron, B	mg/L	<0,1	150	25	10
6	Cadmium, Cd	mg/L	<0,005	0,9	0,15	0,06
7	Chromium Hexavalent, Cr6+	mg/L	<0,002	15	2,5	1
8	Copper, Cu	mg/L	<0,01	60	10	4
9	Iodide,	mg/L	<0,01	40	5	2
10	Lead, Pb	mg/L	<0,05	3	0,5	0,2
11	Mercury, Hg	mg/L	<0,00005	0,3	0,05	0,02
12	Molybdenum, MO	mg/L	<0, 1	21	3,5	1,4
13	Nickel, Ni	mg/L	0,26	21	3,5	1,4
14	Selenium, Se	mg/L	<0,0005	3	0,5	0,2
15	Silver, Ag	mg/L	<0,02	40	5	2
16	Tributyl Tin Oxide (as Organotins) **	mg Sn/L	<0,005	0,4	0,05	0,02
17	Zinc, Zn	mg/L	0,064	300	50	20

Figure 15: Plantation trial on Bukit Makmur Resources heap leach residue

All measured parameters, including Chloride (147 mg/L), Cyanide (<0.005 mg/L), Fluoride (0.21 mg/L), Nitrate (0.042 mg/L), Nitrite (<0.001 mg/L), and heavy metals like Arsenic (<0.0005 mg/L), Cadmium (<0.001 mg/L), Chromium (<0.005 mg/L), Nickel (<0.005 mg/L), and Zinc (0.064 mg/L), fall significantly below the regulatory limits for TCLP-A, TCLP-B, and TCLP-C standards. This indicates that the residue does not leach hazardous levels of contaminants and is classified as non-hazardous, compliant for standard waste disposal without special hazardous waste treatment requirements.

Cost-Effective

Heap leaching eliminates the need for expensive infrastructure like rotary kilns and electrical furnaces in RKEF or autoclaves and high-pressure systems in HPAL, thereby reducing capital and operational costs. The table shows the CAPEX of some heap leach projects worldwide.

Table 3: Heap Leach Project List (Oxley et al., 2016)

Project	Country	Owner	Estimated CAPEX (US$ Million)	Planned Capacity (t.Ni/year)	CAPEX Intensity (US$/t.Ni)
Piaui	Brazil	BRN	450	22,000	20,455
NiWest	Australia	GME	400	14,000	28,571
Cerro Matoso	Colombia	BHPB	750	20,000	37,500
Caldag	Turkey	ENK	450	20,000	22,500
	Guatemala	BHPB	2550	79,500	32,075
Pearl	Indonesia	BHPB	800	32,000	25,000
Gag Island	Indonesia	BHPB	800	27,300	29,304
Cleopatra	USA	RFN	475	21,500	22,093
Acoje	Philippines	ENK	498	24,500	20,327
Kabaena	Indonesia	BMR	260	10,000	26,000

Table 4: CAPEX Intensity of Nickel Processing Projects (Oxley et al., 2016)

Process Technology	Typical Capacity (kt.Ni/year)	CAPEX Intensity (US$/t.Ni Capacity)	OPEX Intensity (US$/t.Ni)
Smelting	18–60	48,000-90,000	4,400–8,000
HPAL/AL	10–60	42,000–140,000+	5,400–22,000
Heap Leach	10–60	18,000–30,000	4,400–6,000

Heap leach is not as mature as HPAL in nickel hydrometallurgy, which has been developed over the past 50 years. However, the CAPEX of heap leach projects at this stage can be considered low compared to HPAL projects during their early development phases. There are still many efficiency opportunities that can be pursued if heap leaching is later operated on a commercial scale.

Conclusion

Heap leaching presents a transformative opportunity for Indonesia's nickel industry. By utilizing low-grade saprolite and transition ores, the process addresses critical resource conservation needs while meeting the growing demand for "green nickel." Its low carbon footprint, minimal environmental impact, and adaptability to Indonesian ore conditions make it a compelling alternative to conventional methods.

Acknowledgements

The authors would like to express their heartfelt appreciation to all employees of BMR whose dedication, hard work, and contributions have been instrumental in helping us reach this significant milestone. Although current financial and market conditions have separated us from working together side by side, we believe that the seeds we have planted—much like those that germinate in our spent ore—will grow, and together we will harvest the results in the future.

References

Anderson, J. (2023, November 4). Are days numbered for Indonesia's kilns? *Skarn Associates*. https://www.skarnassociates.com/insights/indonesia

Anna, X., Smith, Y., & Lee, Z. (2019). Comparison of methods of processing the gold-containing refractory concentrates. *International Journal of Mechanical and Production Engineering Research and Development, 9*(3), 179–185.

Barus, B., Tarigan, S. D., Tejo, R. K., & Stanny, Y. A. (2022). Development of a land stability index for land damage assessment: The case of a nickel mine, North Konawe, Indonesia. *Journal of Degraded and Mining Lands Management, 9*(4), 3695–3704. https://doi.org/10.15243/jdmlm.2022.094.3695

Bhawono, A. (2023, October 10). Sulawesi kian hancur oleh over eksploitasi nikel. *Betahita.id*. https://betahita.id/news/detail/9346/sulawesi-kian-hancur-oleh-over-eksploitasi-nikel.html?v=1700262676

Brand, N. W., Butt, C. R. M., & Elias, M. (1998). Nickel laterites: Classification and features. *AGSO Journal of Australian Geology & Geophysics, 17*(4), 81–88.

Cabinet Secretariat of the Republic of Indonesia (Setkab). (2023, November 17). APEC summit: President Jokowi unveils Indonesia's investment priority sectors. https://setkab.go.id/en/apec-summit-president-jokowi-unveils-indonesias-investment-priority-sectors/

Centre for Research on Energy and Clean Air (CREA). (2023, October 19). Emerging captive coal power: Dark clouds on Indonesia's clean energy horizon. https://energyandcleanair.org/publication/emerging-captive-coal-power-in-indonesia/

Centre for Research on Energy and Clean Air (CREA), & CELIOS. (2024, February). *Indonesia's nickel development: Balancing growth, environment, and the global energy transition*.

Constitutional Court of Indonesia (Mahkamah Konstitusi Republik Indonesia). (2022, January 19). Ahli: UU Minerba kriminalisasi pembela HAM.

Coral Triangle Initiative on Coral Reefs, Fisheries and Food Security (CTI-CFF). (2009, May 15). *CTI-CFF leader's declaration*. https://www.coraltriangleinitiative.org/library/cti-cff-leaders-declaration

Ginting, P., & Moore, E. (2021, November 25). Indonesia Morowali Industrial Park (IMIP). *The People's Map of Global China*. https://thepeoplesmap.net/project/indonesia-morowali-industrial-park-imip/

Handayani, L. (2023, November 10). Kementerian ESDM menampik anggapan cadangan nikel habis 6 tahun lagi. *Media Nikel Indonesia*. https://nikel.co.id/2023/11/07/kementerian-esdm-menampik-anggapan-cadangan-nikel-habis-6-tahun-lagi/

Handayani, L. (2024, January 11). Insiden kebakaran smelter terjadi berulang, berikut daftar nama perusahaannya. *Media Nikel Indonesia*.

Hidayat, B., & Hermawan, E. (2022, February 3). Tentacles of the nickel mines. *Pulitzer Center*. https://pulitzercenter.org/stories/tentacles-nickel-mines

Huber, I. (2021, December 8). Indonesia's nickel industrial strategy. *Center for Strategic and International Studies (CSIS)*. https://www.csis.org/analysis/indonesias-nickel-industrial-strategy

Indonesian Ministry of Energy and Mineral Resources. (2022). *Nickel production and sustainability in Indonesia*. Government Press.

International Energy Agency (IEA). (2023, July). *Critical minerals market review 2023*. https://www.iea.org/reports/critical-minerals-market-review-2023

International Trade Centre. (2025, May 23). *Trade Map—Trade statistics for international business development*. https://www.trademap.org/

Johnson, L., & Lee, K. (2019). Heap leaching of nickel laterites: A review. *Hydrometallurgy, 45*(3), 123–135.

Just Energy Transition Partnership Indonesia Secretariat (JETP Secretariat). (2023, November 21). *Comprehensive investment and policy plan 2023*. https://jetp-id.org/cipp

Kompas. (2023, November 7). Perairan Halmahera tercemar logam berat. https://www.kompas.id/baca/nusantara/2023/11/06/perairan-halmahera-tercemar-logam-berat

Melvin, T. (2023, May 26). Nikel 101: Perbedaan produk akhir NCKL, MBMA, INCO, dan ANTM. *Stockbit Snips*. https://snips.stockbit.com/unboxing/nikel-101-perbedaan-produk-akhir-nckl-mbma-inco-dan-antm

Ministry of Communication and Information (Kominfo). (2023, July 8). Indonesia.go.id—Nilai ekspor hilirisasi nikel melonjak 745%. https://indonesia.go.id/kategori/editorial/7255/nilai-ekspor-hilirisasi-nikel-melonjak-745?lang=1

Ministry of Energy and Mineral Resources (MEMR)—KESDM. (2021, December 5). *Grand strategy mineral dan batubara, arah pengembangan hulu hilir mineral utama dan batubara menuju Indonesia maju; Grand strategy for minerals and coal, upstream and downstream development directions main minerals and coal towards advanced Indonesia*. https://www.esdm.go.id/assets/media/content/content-buku-grand-strategy-komoditas-minerba.pdf

Mongabay Environmental News. (2022, February 16). Red seas and no fish: Nickel mining takes its toll on Indonesia's Spice Islands. https://news.mongabay.com/2022/02/red-seas-and-no-fish-nickel-mining-takes-its-toll-on-indonesias-spice-islands/

Oxley, A., Smith, M. E., & Caceres, O. (2016). Why heap leach nickel laterites? *Minerals Engineering, 88*, 53–60. https://doi.org/10.1016/j.mineng.2015.09.018

Setiawan, V. N. (2023, July 25). Tegas! Luhut: Limbah nikel tidak diizinkan dibuang ke laut. *CNBC Indonesia*. https://www.cnbcindonesia.com/news/20230725142816-4-457139/tegas-luhut-limbah-nikel-tidak-diizinkan-dibuang-ke-laut

Statista. (2022, May 31). Demand for nickel worldwide 2019–2023. https://www.statista.com/statistics/273653/global-nickel-demand/

Tenggara Strategics (The Jakarta Post). (2024, January 10). Analysis: Safety standards under scrutiny after explosion in Morowali. *The Jakarta Post*.

Wang, C. (2022, January 18). Interpretation of the 2022 "Guidelines for ecological environmental protection of foreign investment cooperation and construction projects." *Green Finance & Development Center*. https://greenfdc.org/interpretation-2022-guidelines-ecological-environmental-protection-of-foreign-investment-cooperation-and-construction-projects/

Wicaksono, R. A. (2023, May 22). Kawasan hutan seluas 765 ribu hektare jadi konsesi tambang nikel. *Betahita.id*. https://betahita.id/news/detail/8792/kawasan-hutan-seluas-765-ribu-hektare-jadi-konsesi-tambang-nikel.html?v=1684714832

World Bank. (2021). *The role of nickel in the global energy transition*.

Zhu, M., Lou, Z., Cui, R. Y., Cheng, X., Li, S., Li, D., Tumiwa, F., Arinaldo, D., Li, W., & Hultman, N. (2023, October 6). *Decarbonizing captive coal power plants in Indonesia and implications for Chinese stakeholders: Trends, challenges and opportunities*. Center for Global Sustainability, University of Maryland. https://cgs.umd.edu/research-impact/publications/decarbonizing-captive-coal-power-plants-indonesia-and-implications

Closure and Post-Closure Case Study: San Manuel Heap Leach Facility, Arizona, USA

Terry Braun, SRK Consulting (U.S.), USA
David Ludwick, SRK Consulting (U.S.), USA
Clara Balasko, BHP, USA

Abstract

This paper presents a case study of the active closure and post-closure monitoring period for the San Manuel Heap Leach Facility (HLF) at the BHP San Manuel copper mine in Pinal County, Arizona, USA. Prior to closure, this HLF contained approximately 90 million tons of oxide ore and covered a 237-acre HDPE-lined footprint adjacent to the northeastern extent of the open pit and in-situ recovery wellfield. Operations at the HLF started in 1985 and ended in 2002. With the formal suspension of mining operations at the San Manuel Mine Site in June 1999, BHP started the formal process of closure of the mine site and HLF.

Site-specific challenges to closure of this copper HLF included short-term management of the acidic solution inventory circulating through the HLF, design of a regrade surface that achieves physical mass and erosional stability, installation of a surface water control system to contain contact water, and long-term management of residual draindown from the HLF

In 2004, the project received owner funding to commence detailed engineering and construction for permanent closure. Final closure of the HLF included expansion of the HDPE-lined footprint to accommodate the proposed regrade design, management of residual solution drain down, incorporation of landform elements, and selection of a final cover system. During the active closure period, the original cover system design failed to perform as designed, and the project team re-designed the system prior to completion of construction activities in 2008. BHP completed construction activities in 2008.

Post-closure monitoring and inspection results include cover stability, recording long-term draindown rates, stormwater runoff volumes, and maintenance activity. The long-term erosional performance of the final regrade and rock armor cover system informs future engineering trade-off studies for alternative cover systems at other sites.

Introduction

Magma Copper Company (predecessor company to BHP) developed the San Manuel Mine and Plant sites as an integrated copper mining, milling, smelting, and refining complex. Magma also built the company town of San Manuel, approximately 50 miles north of Tucson and 130 miles east of Phoenix (Figure 1).

Figure 1: Site location

Site History

Production from the underground block cave operation started in 1953. A dedicated 6-mile-long railroad hauled ore from the mine site to the mill facility at the Plant site near the town of San Manuel. Concentrate from the mill entered the smelter and refinery process. A COMEX warehouse stored the refined product before off-site shipping.

Development of the open pit to access the oxide resource and construction of the HLF started in the mid-1980s. Development of the in-situ leach operation within the open pit started in 1986 and continued through 1999. At the time of closure, the in-situ leach (ISL) produced approximately 18,000 tonnes of copper annually (Sutton, 2019). Figure 2 shows the position of the HLF and adjacent ISL with respect to the open pit and underground and surface infrastructure, overburden stockpiles, and process facilities (solvent extraction/electro-wining or SX/EW plant).

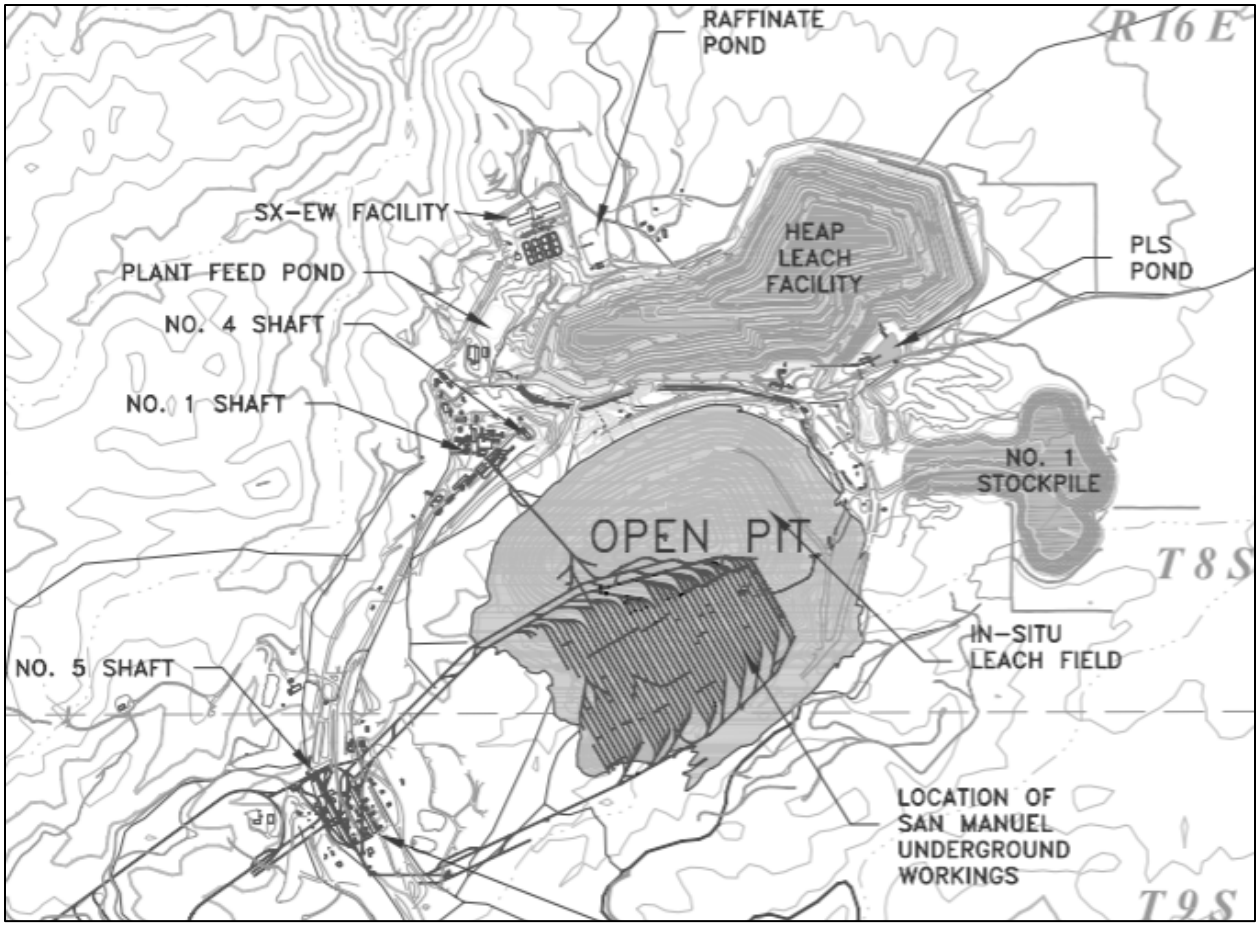

Figure 2: Site layout of the San Manuel Mine Site, Arizona

Site and Facility Overview

Climate

The regional climate setting is a semi-arid environment, and the site experiences average daily temperatures ranging from 52°F in winter to 79°F in summer. Annual precipitation and evaporation average approximately 9.1 inches and 63.4 inches, respectively. Rainfall patterns in southern Arizona are characterized by long-duration, low-intensity frontal storms during the winter and short-duration, high-intensity summer monsoons.

Geological Background and Ore Characteristics

Initial geological reserve estimates determined the oxide deposit contained approximately 286.5 million tons of ore at an average grade of 0.60% total copper and 0.39% acid-soluble copper. Chrysocolla is the primary copper-bearing mineral in the deposit. Within this reserve, roughly 21 million tons were designated as minable by open-pit methods. Ultimately, the pit operated for 10 years, from 1985 to 1995, and supplied 90 million tons of ore to the facility.

Facility Design and Operation

The San Manuel Heap Leach Facility was one of the first copper heap leach projects in Arizona to include a lined leach pad. Construction of the HLF liner pad commenced in 1986 and extended over six phases through 1992. The final HDPE liner footprint covered an area of approximately 237 acres prior to reclamation. The base of the heap was constructed at an elevation of approximately 3,110 feet above mean sea level (amsl). In comparison, the maximum HLF height reached approximately 3,460 feet amsl—an elevation gain of 350 to 420 feet depending on the section of the facility.

The leach pad consisted of an 80 mil HDPE liner placed over a compacted San Manuel Formation sub-base. An 18-inch sand layer overlays the HDPE and contains a 12-inch perforated HDPE collection pipe network for solution recovery. The base slope of the liner ranged from 1% to 8%, directing gravity flow toward the pregnant leach solution (PLS) collection pond.

During the early operating period, the HLF received sequential lifts of truck-hauled run-of-mine oxide ore at a rate of 30,000 to 40,000 short tons per day. Each leach cycle lasted for approximately 45 to 60 days with an average application rate of raffinate solution of 0.008 gallons per minute (gpm) per square foot. Applied raffinate exhibited a pH of 1.6 units, containing 1.8 grams per liter (g/L) of iron, 0.20 g/L copper, and 15 g/L sulfuric acid. During steady-state operations, approximately 7,000 gpm of raffinate circulated through the HLF.

Subsequent lifts were added by stripping and ripping the surface of the previous lift to optimize acid flow and recovery. The HDPE-lined perimeter channel collected the Pregnant Leach Solution from the internal drainage system and conveyed PLS to the Heap PLS pond. Pump systems at PLS pond transferred the PLS to the Plant Feed Pond prior to processing in the SX-EW Plant. The estimated overall copper recovery from the HLF was 88.3%, equivalent to 690.6 million pounds of high-purity cathode copper over the facility's operational life.

Closure Engineering Phase

In the low copper price environment of the late 1990s, BHP suspended mining operations at the San Manuel Mine and Plant Sites in June 1999. Sulfide ore mining and milling activities ceased while oxide leach operations idled and re-circulated existing process solution inventory in the HLF and ISL. BHP maintained the underground mine dewatering systems and underground access. Dewatering continued until BHP completed technical studies regarding PLS solution containment of the in-situ leach operation within the pit. In February 2002, BHP stopped dewatering the underground mine and circulating solutions in the ISL.

BHP formed an owner's team to manage the development of conceptual to detailed engineering deliverables. External consultants provided subject matter expertise as well as institutional knowledge about

the mine site. BHP integrated and maintained site data, including historical operating records, as-built documentation, and monitoring data.

Design Criteria

Design criteria for closure of the San Manuel HLF included the regulatory framework for the state of Arizona and internal governance related to responsible closure. Table 1 summarizes the principal regulatory framework for mine closure in the state of Arizona.

Table 1: Principal Regulatory Framework for Mine Closure in Arizona, USA

Program and Lead Agency	Mine Closure Elements
Aquifer Protection Program, Groundwater Protection Program of the Water Quality Division of ADEQ	Groundwater quality protection at designated points of compliance; BADCT engineering guidelines related to closure design
Surface Water Protection Program, Surface Water Quality Improvement Section of ADEQ	Point source and non-point source of pollutants resulting in a discharge to the water of the US
Mined Land Reclamation Plan, Reclamation Division of the Arizona State Mine Inspector	Mitigate public safety hazards and maintain the closed site in a safe manner

Regulatory

Closure and post-closure requirements for mining facilities in the state of Arizona are governed by the Aquifer Protection Permit (APP) program for groundwater, the Arizona Storm Water Pollution Protection Plan (SWPPP) for surface water, and the Mined Land Reclamation Plan for surface reclamation.

The APP program authorizes new operations, existing operations, and mine closure. For the San Manuel HLF, the operator filed a full APP application for final closure. This closure-based application included assessment of engineering controls to reduce the potential discharge of pollutants to groundwater (informed by Best Available Demonstrated Control Technology or BADCT), characterization of existing groundwater conditions, prediction of future groundwater quality and gradients, and demonstration of compliance with aquifer quality standards at one or more designated points of compliance.

Table 2 presents the closure-related elements of BADCT guidelines. The purpose of BADCT is to employ engineering controls, processes, operating methods, or other alternatives, including site-specific characteristics (i.e., the local subsurface geology), to reduce discharge of pollutants to the greatest degree achievable before they reach the aquifer. Prescriptive closure BADCT for HLF requires the operator to prevent, contain, or control discharges after closure.

Table 2: Prescriptive BADCT Guidelines for HLF Closure in Arizona, USA

Element	Prescriptive Criteria
Groundwater	Eliminate, to the greatest extent practicable, any reasonable probability of further discharges and of exceeding Aquifer Water Quality Standards at the point of compliance
Solution Management	Neutralize or rinse all spent ore and waste residues; Eliminate free liquids; Recontour the HLF as necessary to eliminate ponding
Physical Stability	Demonstrate long-term stability of HLF materials

Internal Governance

BHP governance included risk assessment methodologies, capital project processes such as stage-gate reviews of conceptual to detailed engineering packages, and decision-support models. Inherent in these processes, BHP and the technical team conducted trade-off studies of economics, risk profiles, and additional site characterization to address meaningful data gaps.

Criteria

Based on the regulatory framework and internal governance, the project team adopted the closure objectives of physical stabilization and chemical stabilization. Physical stabilization considered both slope stability and cover stability, and control technologies were established with both surface regrading to enhance runoff and an engineered cover system to reduce infiltration to the maximum extent practicable through the HLF. To resist water and wind erosion, permanent surface water run-on controls were installed with riprap or an alternative erosion protection where flow concentration occurs.

From these closure objectives, the engineering team identified engineering design criteria (SRK, 2004) for the 2004 design of the HLF closure (Table 3).

Table 3: 2004 Select Design Criteria for HLF Closure

Item	Sub-Item	Value	Comment
Foundation	Limits of Expansion	Expand only as much as required to achieve nominal 3H:1V slopes without removing spent ore from the lined pad	Maintain current distance from the edge of pit
	Minimum slope of the Heap Liner subgrade	2%	BADCT
	Rough Grade Surface	Compact random fill of the excavation surface	
	Overall Heap Slope	3H:1V nominal	
Composite Liner System	Prepare subgrade thickness	12-inch minimum	Low-permeability compacted soil liner (BADCT)
	HDPE Membrane Liner	60 mil minimum	Subject to compatibility analysis with the overliner

Item	Sub-Item	Value	Comment
	Protective/Overliner thickness	18 inch	Minus ¾" particle size, non-calcareous, free-draining
Soil Cover	Cover thickness	24-inch minimum	
	Surface treatment	Cross-rip along contour	Roughening reduces sheet flow, aids revegetation
	Surface Water Management	Lateral channel down-slope spacing at 150 feet	Limit slope length and catchment area
	Lateral Channel Capacity	5 to 10 cubic feet per second	100-year/1-hour flow from approximately 1acre at 3H:1V
	Revegetation	Seed with native grasses, hydromulch and tackifier	Consider the grain-size, slope, and chemistry aspects of the area to be revegetated

Solution Management

BHP operated the HLF as a closed-loop system. During the interim period between cessation of leach operations (early 2002) and final closure of the HLF (2004), BHP re-circulated raffinate solution through the HLF. Recorded HLF draindown in March 2002 at the time of suspended leach operations, the approximate flow rate was 2,500 gpm. Recorded flow data indicate an 85% reduction in draindown rate between March 2002 and July 2002.

BHP conducted studies of the groundwater containment and geochemistry of the decommissioned ISL/underground facilities. The studies demonstrated that the decommissioned ISL/underground facilities were within hydraulic containment and of similar chemical composition. With regulatory approval of the proposed action and implementation of a monitoring program, BHP diverted the initial HLF draindown into the ISL/underground.

The final closure design included construction of a gravity-fed diversion channel that conveyed long-term HLF draindown into the former ISL/underground. Surface water runoff from the closed HLF also discharges to the open pit.

Heap Leach Regrade

With early community input collected by BHP, the 2004 regrade plan incorporated some elements of what is defined today as landform design.

Base Liner Expansion

The closure grading plan flattened slopes to 3H:1V. Slope regrading of the San Manuel HLF required two liner extension zones to create enough lined foundation area. The North Liner Extension covered an area of 638,602 ft^2 (14.7 acres) and received spent ore from the east slope of the HLF. The South Liner Extension

covered an area of 308,326 ft^2 (7.1 acres) and received spent ore from the south slope, as well as covered the reclaimed and buried PLS Pond. The as-built pad extension liner consisted of:

- Liner bedding layer of 12” screened from No. 1 Stockpile
- 60-mil HDPE geomembrane
- 18" overliner crushed and screened from Tiger Flux Pit

Spatial constraints (e.g., eastern property boundary and the open pit to the south) and the topography limited the footprint expansion areas and associated regrade plans.

Geotechnical Stability

The slope stability analysis for the existing and future HLF layout was conducted using static and pseudostatic (0.1g seismic load) analysis versus the BADCT criteria. The analysis assumed unsaturated and drained conditions within the heap. The project team selected a 3H:1V overall slope based on the geotechnical stability analysis and to promote vegetation and eliminate flat spots.

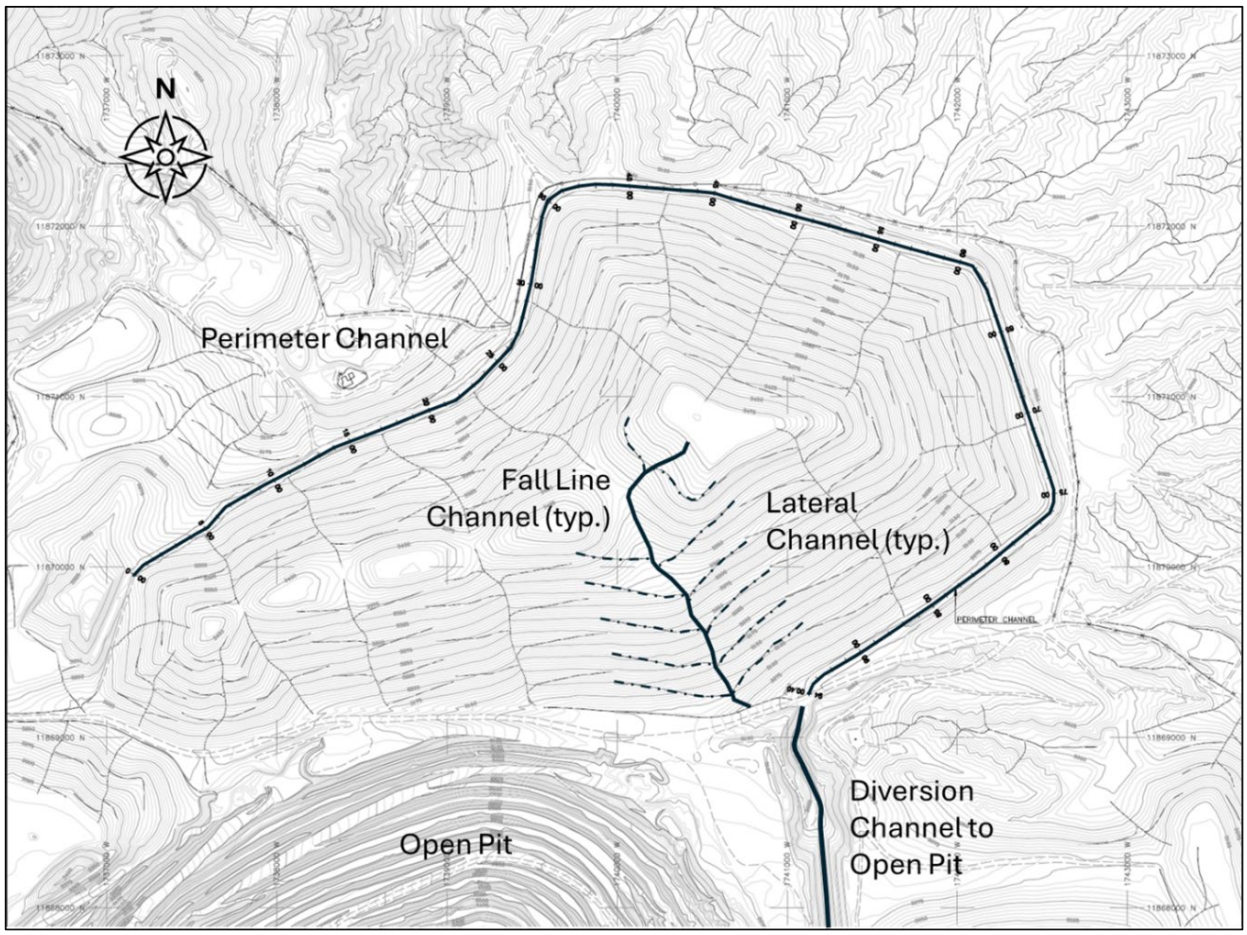

Figure 3: 2006 Closure design of the HLF

Surface Water Management

The regrade design incorporated a lateral and fall line surface water management system. Figure 3 illustrates the lateral channels that collect surface water runoff from sub-basins and convey the runoff to a larger fall line channel designed to discharge into the HDPE-lined perimeter channel.

Rinsing

Arizona prescriptive BADCT calls for rinsing of heap leach pads for closure; however, the requirement is not specific to copper mining, which is leached with acid rather than cyanide. The designers cite a statement from ADEQ (1998) stating that little research has been done to demonstrate the effectiveness of rinsing and detoxification to remove acidity; therefore, rinsing was not performed (SRK 2004).

2004 Cover Concept

Cover modeling estimated negligible infiltration with a cover thickness greater than 1 ft using the local borrow. The design specified a minimum 2-ft thick run of borrow soil cover. Surface water runoff management for the cover system was a lateral and fall line channel concept. The 2004 design included re-vegetation of the cover to provide the estimated shear strength to resist erosive forces on the cover.

Construction Phase

Between 2001 and 2004, BHP and external project teams conducted internal technical studies to support the development of the integrated mine closure plan and to support the permitting requirements for closure. This period included active dialog with regulatory representatives and engagement with the local community. In 2004, BHP applied for permanent closure of the San Manuel Mine Site. This application included the designs and supporting technical studies for the closure of the HLF. Construction activity at the HLF started in early 2005.

2005 and 2006 Construction

The leach pad closure and cover construction process consisted of:

- Decommissioning of underdrain pipes used for the leaching process through in-place burial, removal of pipes and pumps above grade around the perimeter, and demolition/removal of concrete structures.
- Construction of an internal toe drain system to separate residual draindown solutions from storm water runoff.
- Placement of up to 2.5 feet of mixed San Manuel Formation and inert leach cap from local borrow.

- Construction of the lateral channels and connected fall line channels to convey surface water runoff to containment in the perimeter drainage channel.
- Revegetation of growth material using conventional hydroseeding technology during the summer monsoon period in 2006.

2006 Cover Failure

In July 2006, the contractor completed installation of the lateral and fall line channels and started hydroseeding of the soil cover. The timing of the hydroseeding coincided with the summer monsoon season. According to NOAA data, the region recorded its wettest monsoon season on record, with 12.2 inches of rainfall, representing a 33-year recurrence event. Over a span of five days in early August 2006, the site received 10.12 inches of rain, approximately half its average annual precipitation. The daily average precipitation over this period was less than the design storm event.

Erosion from the monsoon event resulted in sediment infilling and rill erosion between the lateral channels, which caused the channels to accumulate sediment, become blocked, and subsequently overtop. Failure in one lateral channel resulted in a "cascading" overtopping failure of the downstream lateral channels. The perimeter diversion channel, designed to control runoff, was also breached in one location, leading to off-site discharges of sediment-laden water. Figure 4 presents post-event damage to the HLF.

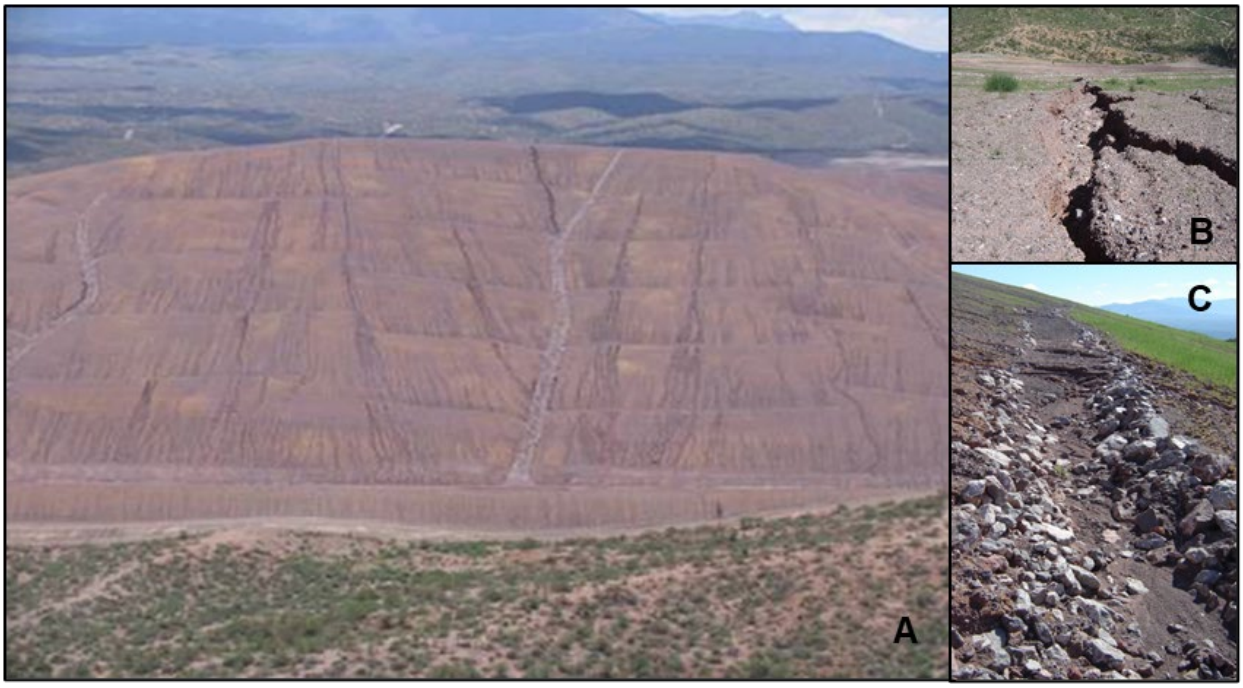

Figure 4: Post-storm event damage, San Manuel HLP (August 2006)

Contributing factors to the August 2006 cover failure include:

- Inadequate structural best management practices (e.g., silt fence) for stormwater control post-hydroseeding (Inset A, Figure 4)
- Lack of surface water engineering controls (e.g., increased capacity of downstream lateral channels) to prevent a cascading overtopping failure (Inset B, Figure 4)
- Inadequate sediment storage capacity in the lateral channel design (Inset C, Figure 4)

2007 Cover Redesign

Within days of the cover failure, BHP reconvened the design team and retained additional subject matter expertise to assess the scope and cause of the cover system failure. This assessment led to a new design concept that minimized flow concentration by eliminating the lateral channels and improved the erosional resistance through the installation of a rock armor top cover. The tallest portions of the HLF facility have 3H:1V slopes with slope lengths up to 1,300 ft. Figure 5 presents the revised cover and regrade design.

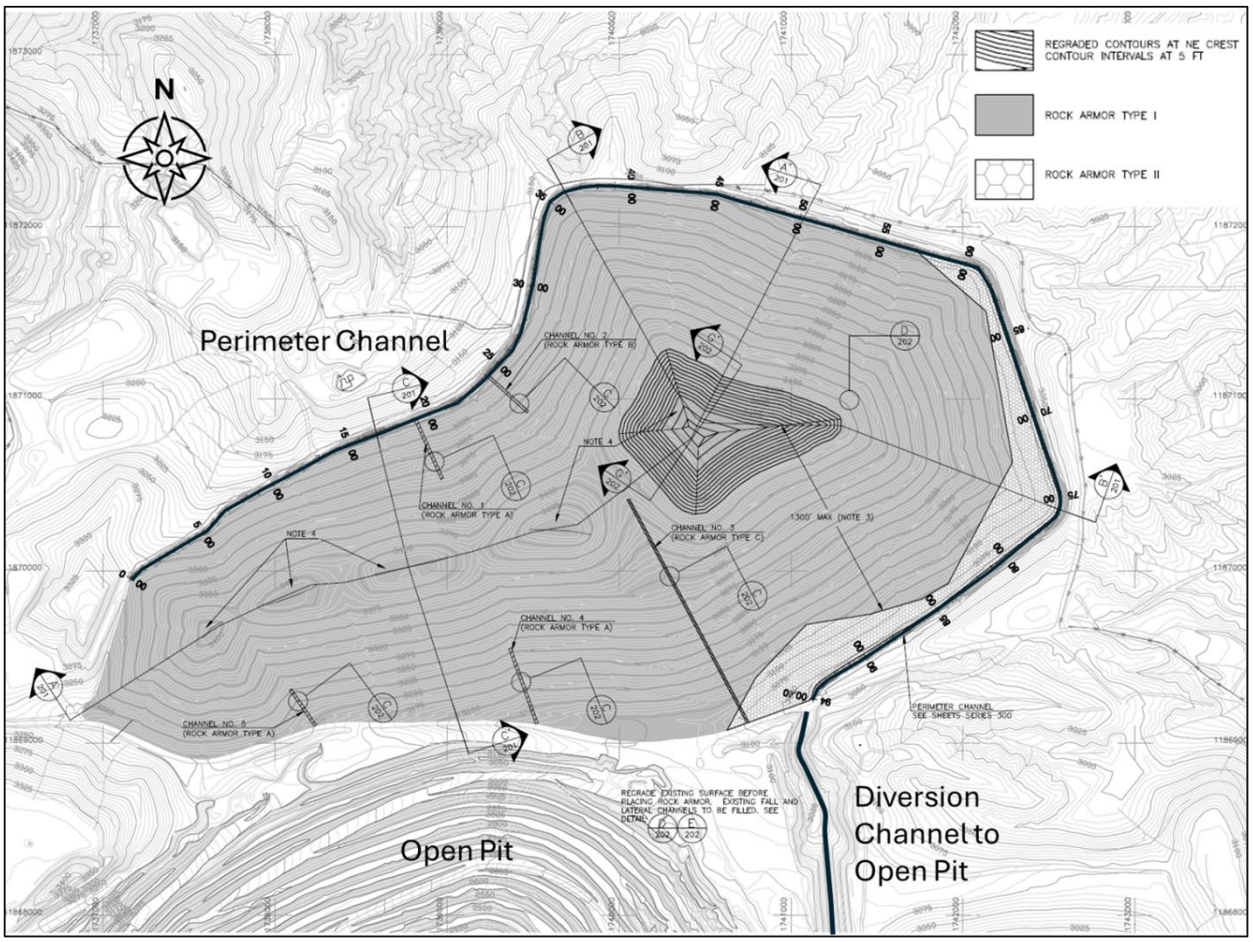

Figure 5: 2008 Closure design of the HLF

2007 and 2008 Construction

The timing of the 2006 failure of the 2004 cover design and surface water management system proved

valuable in that the primary earthwork contractor was conducting closure at the Plant Site. The construction-related infrastructure (stockpiles, equipment, and laydown yards) and BHP-owned quarries and borrow sources were active. As BHP and the project team assessed the root cause of the cover failure, the remedial options included cost-effective construction options for earthwork and borrow materials.

In July 2007, the contractor filled existing erosion gullies and depressions and removed the lateral and fall line channel system. In addition, the contractor regraded the five topographic highs of the HLF to improve stormwater drainage and reduce the risk of ponding. The contractor placed erosion-resistant rock armor (D_{max} of 8 inches) on the slopes and larger rock armor (D_{max} of 9 inches) in areas susceptible to concentrated flow. Construction finished in January 2008.

Post-Closure Phase

BHP maintains ownership of the San Manual HLF and mine site. The post-mining land use is private range land. Signage, perimeter fencing, and routine site inspection discourage public access to the former mining site. The closed HLF remains visible from Highway 77 and from the town of Mammoth, Arizona.

Long-Term Draindown

BHP maintains instrumentation to record long-term draindown rates, surface water runoff rates, and local precipitation. Measured draindown rates for the uncovered HLF dropped from 2,500 gpm in March 2002 to approximately 50 gpm in September 2003. Following installation of the original HLF cover in September 2006, measured draindown rates dropped to less than 10 gpm. Draindown steadily declined to less than 3 gpm at the present day (2025).

Figure 6: HLF Draindown vs. precipitation 2018—April 2025

Figure 6 compares the HLF draindown and daily precipitation data from January 2018 to April 2025. The comparison shows seasonal fluctuations in flow rate in response to specific rain events or winter wet seasons. For example, the winter monsoon periods of 2019 and 2020 increased recorded draindown by a factor of 3 times the average (~3gpm vs. 1 gpm). The summer/early fall and winter monsoon periods of 2022 were followed by an increase in draindown response over the following 6 months.

Observations at multiple legacy sites in the arid southwest suggest maximum infiltration typically occurs during low-intensity, long-duration winter storms and when seasonal evaporation is low. The San Manuel HLF monitoring data show "breakthrough" of the soil cover during extreme monsoon events, such as the storms in July of 2021 and 2022, where the storage capacity of the soil cover is depleted (i.e., saturation = 100%), followed by peak seepage shortly after.

Erosion Performance

BHP manages several closed legacy mine sites in southern Arizona, USA. Applied reclamation techniques at these sites are generally characterized by continuous slopes with a rock armor veneer to resist erosion. Some reclaimed legacy sites have performed well, while others experience repeated rilling and gullying during storm events, requiring extensive maintenance. In 2019, BHP initiated a multi-year erosion research study with the University of Arizona. Published technical reports from this program include evaluation of existing erosion models and the need for a new model (Abramson, et al., 2022), documenting the development of a new erosion model, Rillgen2D (Pelletier, et al., 2024), and the application of landform modeling inputs to engineering design using common engineering tools like AutoCAD (Buechler, et al., 2023).

Summary findings from the research program include:

- Erosion resistance in dryland regions relies on the shear strength of the soil particles rather than vegetation. Erosion performance can be improved by increasing the particle size (i.e., adding rock armor) and predicted using the tools developed by Pelletier and Abramson and research datasets developed by Abt et al. (2013).
- Variations in surface topography due to consolidation, variations in grading, etc., lead to "microtopography" that significantly increases the runoff contributing area beyond design assumptions. This converging pattern of flow is often substantially different than the idealized planar surfaces designed with tools like AutoCAD.

Generally, the rock cover and limited flow concentration design of the San Manuel HLF has performed well, with minor rilling observed. (Figure 7). The HLF has been nearly maintenance-free since the addition of the rock armor cover. Vegetation of the rock cover is opportunistic and a residual result of the 2006 hydroseed applications to the underlying soil cover system.

Figure 7: San Manuel HLF rock armor cover, present day

Conclusion

The case study of the closure of the San Manuel HLF starts with the operating decisions to construct the facility as part of an integrated mining complex of deep underground mining, HLF operation, and the ISL in the open pit. The operational knowledge base provided a strong basis for closure-related strategy, taking advantage of the integrated water budget, hydraulic containment, and surface water management. This knowledge base expanded as additional site characterization activities addressed substantive data gaps related to long-term closure risks.

The integrated knowledge base includes design and as-built documentation, site characterization work, monitoring and maintenance activities, and data logging instrumentation. The closure permit for the San Manuel Mine site requires 5-year reviews of original mine flooding models and forecasts, and recalibration of the predicted evolution of hydraulic containment.

Acknowledgements

The authors acknowledge the contribution of the BHP Copper Legacy Assets team, including the site staff who monitor and maintain the site. These efforts lead to the high-value time-series data sets that continue to offer useful benchmarks and insights to inform future closure designs.

References

Abramson, N., Pelletier, J. D., Ananthanarayan, S., Chataut, S., & Ludwick, D. (2022). Assessment and development of erosion models for landform design at BHP legacy tailings storage facilities in Arizona,

USA. In A. B. Fourie & G. Boggs (Eds.), *Mine Closure 2022: Proceedings of the 15th International Conference on Mine Closure* (pp. 1037–1046). Australian Centre for Geomechanics. https://doi.org/10.36487/ACG_repo/2215_76

Abt, S. R., Thornton, C. I., Scholl, B. A., & Bender, T. R. (2013). Evaluation of overtopping riprap design relationships. *Journal of the American Water Resources Association, 49*(4), 923–937. https://doi.org/10.1111/jawr.12074

Arizona Department of Environmental Quality. (1998). *Arizona mining guidance manual, aquifer protection program*. Water Quality Division, Water Permits Section.

Buechler, C., Ludwick, D., Pelletier, J. D., Abramson, N., & Chataut, S. (2023). Repurposing Autodesk Civil 3D grading tools for natural landform closure design. In B. Abbasi, J. Parshley, A. Fourie, & M. Tibbett (Eds.), *Mine Closure 2023: Proceedings of the 16th International Conference on Mine Closure*. Australian Centre for Geomechanics. https://doi.org/10.36487/ACG_repo/2315_043

Pelletier, J. D., Abramson, N., Chataut, S., Ananthanarayan, S., Ludwick, D., & Roddy, B. P. (2024). New model for predicting the erosional performance of rehabilitated mine sites. *Mining Engineering, 76*(3), 23–28.

SRK Consulting. (2004). *Design report no. 1, BHP San Manuel mine site*. Prepared for BHP Copper Inc.

SRK Consulting. (2006). *As-built report for the closure of the heap leach facility and diversion structure, BHP Copper San Manuel mine site*. Prepared for BHP Copper Inc.

Sutton, G. A. (2019). Reconciling mineral reserves at the well-to-well in-situ copper leaching operation at San Manuel Mine, Arizona, USA. *CIM Journal, 10*(3).

Two-Level Solution Collection System: A Case History

Marvin Silva, AECOM, USA
Todd Minard, AECOM, USA
Bibhuti Panda, AECOM, USA

Abstract

Expanding leach pads is a common practice in which the liner system is extended, and ore is stacked against the existing heap. This case history presents an approach to overcoming unfavorable ground conditions by creating a two-level solution collection system and using a numerical seepage model to evaluate its performance. A heap leach pad expansion adjacent to an existing heap leach facility (HLF) was identified as the preferred site, with ore stacked in the expansion area and extending over the existing heap, with pregnant solution collected and conveyed through the existing infrastructure. The expansion site incorporated an independent solution collection system in the newly lined pad area to improve solution recovery. The existing HLF was constructed in multiple phases, with each expansion built upgradient, allowing leachate to be collected and transported via gravity to the existing pregnant leach solution (PLS) pond. The expansion site was located next to the most recent phase. The initial grading plan directed PLS to a proposed new PLS pond to accelerate mineral recovery, rather than relying on the longer existing collection system, which posed risks of prolonged travel time and potential losses through perforated pipes.

The topography of the expansion pad area presented a challenge, as a portion of the site was in a depression sloping toward the existing pad, making independent solution collection difficult. One option considered was placing borrow material in the depression to modify the flow direction before placing the composite liner system. However, this approach had high capital costs and would reduce ore capacity by approximately 232,000 tonnes. To maximize ore stacking capacity while ensuring effective solution collection, a two-level solution collection system was designed and implemented. The lower-level system ensures environmental compliance and conveys the solution to existing infrastructure, while the upper-level system is installed once the ore reaches a suitable elevation. The second-level collection system, placed directly on the prepared ore surface, consists only of perforated solution collection pipes without a geomembrane. It captures most of the leachate from additional ore lifts placed above it, with the remaining solution collected by the lower-level system.

A numerical model, calibrated using both transient and steady-state flow conditions, was developed to evaluate system performance. When field-measured ore and overliner parameters were used, results showed a strong correlation with actual measured solution flow rates. Field data confirmed that 90.9% of the solution is captured by the second-level system and conveyed directly to the expansion PLS pond, reaching it within 12 days from the start of irrigation. The remaining 9.1% is captured by the lower-level system.

This case history illustrates that a set of solution collection pipes installed in an upper-level lift, without a geomembrane, can effectively collect most of the leachate solutions. This approach mitigates unfavorable grading conditions without requiring extensive earthworks. The two-level solution collection system has performed as intended, accelerating mineral recovery and providing an efficient alternative to traditional heap leach pad designs.

Introduction

Heap leach facilities (HLFs) are commonly expanded by stacking ore against existing lined pads, extending the liner system, and integrating solution collection infrastructure. However, site topography and ground conditions may present design challenges, especially when independent solution collection is required for quicker recovery and enhanced environmental performance. This paper presents a case history where an unfavorable topographic condition was addressed using a two-level solution collection system. The objective was to avoid extensive borrow material placement, maximize ore capacity, and ensure efficient leachate collection. Numerical modeling was used to evaluate performance and was validated against field flow rates.

Brief Literature Context

Prior studies highlight that heap instabilities typically arise from multiple interacting hydraulic–geotechnical factors rather than a single trigger, including pore-pressure buildup, injection spacing, and lift construction effects. Recent work emphasizes the value of unsaturated flow modeling, especially for low-permeability ores, to predict breakthrough times and head distributions that influence operational performance and slope stability. Other investigations show that hydraulic properties vary with rock type, construction method, and consolidation under increasing lift height. These insights motivate the two-level drainage configuration and the combined transient/steady-state modeling adopted here (e.g., Breitenbach & Dolezal, 2015; Breckenridge & Todd, 2023; Dompier et al., 2023; Milczarek & Keller, 2022).

Conceptual Plan View

The expansion pad was adjacent to a previously constructed HLF. A significant portion of the expansion area lay in a topographic depression that sloped toward the existing pad, as shown in Figures 1, 2, and 3. The initial design was intended to direct pregnant solution from the expansion area to a new PLS pond, thereby reducing travel time and losses. To avoid costly borrow material placement and ore displacement, a revised design was selected that incorporated a two-level solution collection approach:

- Lower-Level System: Composite liner installed at the base of the expansion, connecting to the existing collection system, as shown in Figure 2.
- Upper-Level System: Installed without a geomembrane directly on the graded ore surface of the placed ore lift, after ore stacking reaches a suitable elevation. It serves to intercept leachate from the upper lifts and convey the pregnant leach solution (PLS) to the upper-level collection system, as shown in Figure 3.

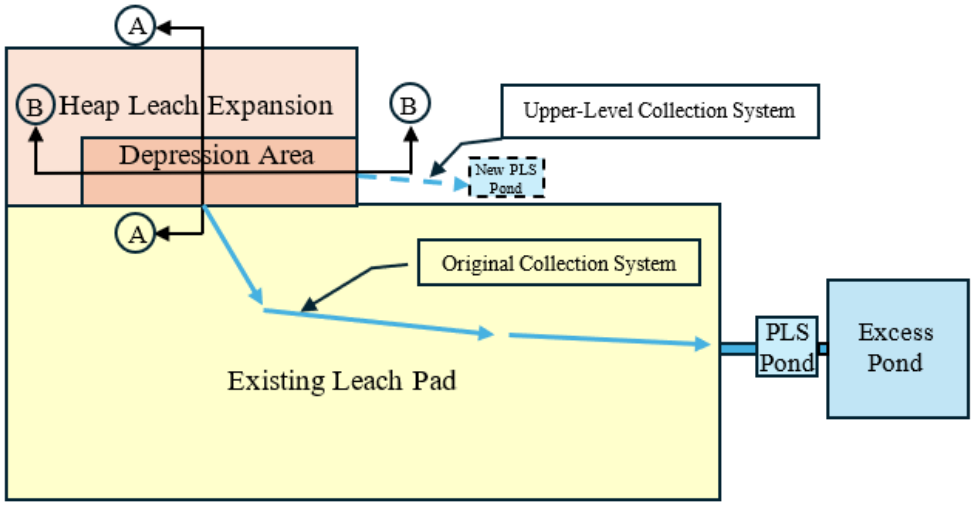

Figure 1: Plan view of existing leach pad and heap leach expansion

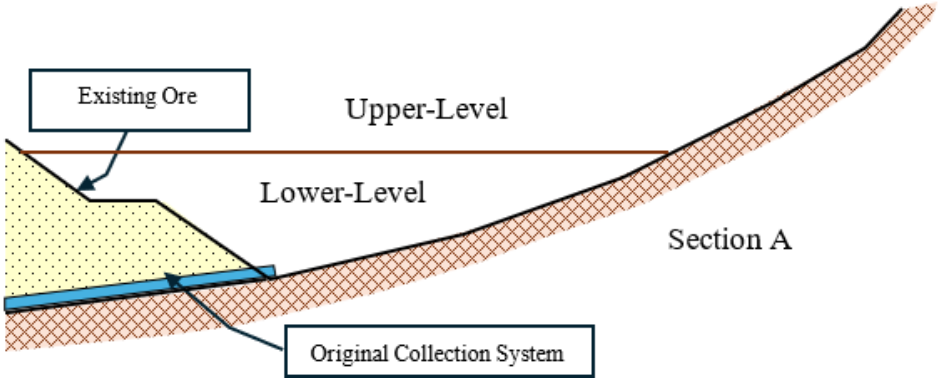

Figure 2: Cross-section A showing the upper-level and lower-level systems

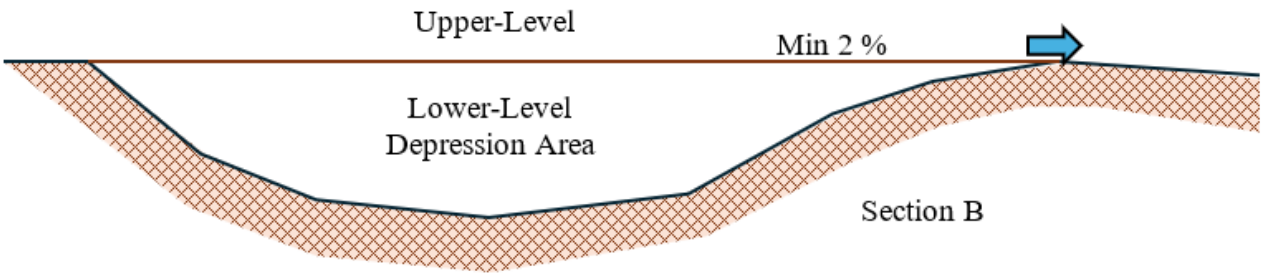

Figure 3: Cross-section B showing the PLS flow from the upper-level system

This upper-level system comprises perforated HDPE pipes and a coarse overliner placed directly on the graded surface of the freshly placed ore lift, without the use of a geomembrane. Its primary function is to intercept the bulk of the leachate generated by successive ore lifts and route it to the new PLS pond through a dedicated, much shorter piping run. Field data collected while the third 8-m lift was under irrigation show that pregnant solution reached the new PLS pond in as little as 12 days. In contrast, flow through the exiting pad and its longer collection network is expected to take significantly more time, although the exact breakthrough duration was not measured. While solution travel time will naturally increase as additional lifts are stacked above the upper-level system, this design has already demonstrated a substantial reduction in solution residence time and a corresponding decrease in the risk of solution losses and operational delays.

Methodology

A series of two-dimensional numerical seepage models was developed using the finite element method to evaluate the performance of the two-level solution collection system. Both steady-state and transient flow conditions were simulated to assess the behavior of leachate flow through stacked ore lifts and to quantify solution collection efficiency.

The modeling began with a steady-state simulation of the first ore lift, 8 meters in height, with solution collection pipes spaced 7 meters apart, as shown in Figure 4. The hydraulic head between adjacent pipes was estimated using the Hooghoudt (1940) equation for subsurface drainage, and this value was verified against the numerical model output. The calculated flow rates in the collection pipes and the head distribution served as a baseline for subsequent evaluations.

Transient flow conditions were then modeled to estimate the time required for the solution to migrate from the top surface of the lift to the collection pipes. The simulation allowed tracking of the advancing wetting front through the ore profile and confirmed the transition to near steady-state infiltration conditions. The modeled flow rate and head under transient conditions were compared to the steady-state results to confirm convergence.

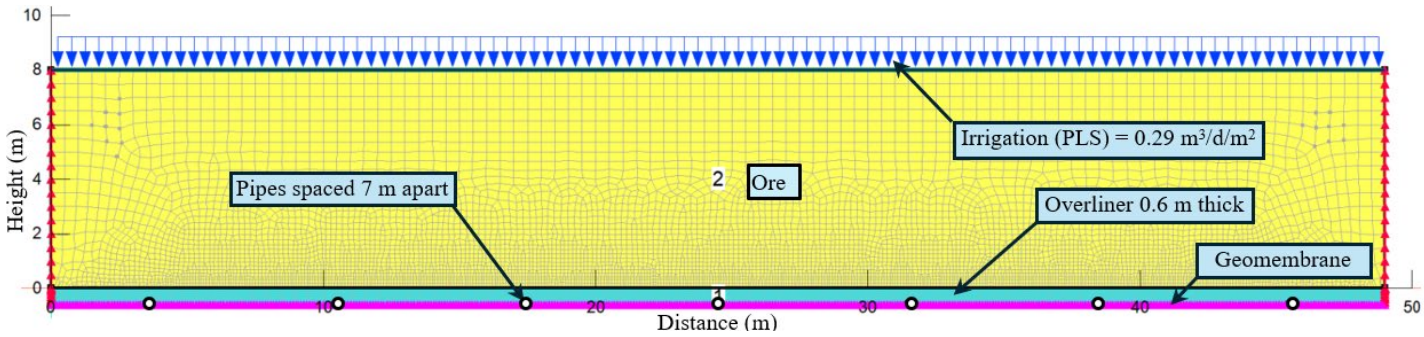

Figure 4: Configuration of initial ore lift under steady-state conditions

The same modeling approach was applied sequentially to the second and third ore lifts. Each lift was assigned distinct hydraulic properties to reflect material variability and the effects of consolidation from overlying ore. For the second lift, the underlying first-lift ore exhibits lower permeability than the newly placed second lift due to cumulative loading effects. For the third lift, the underlying base lift exhibited the lowest permeability among the lifts modeled at that time, consistent with increased consolidation and reduced pore connectivity at greater depth.

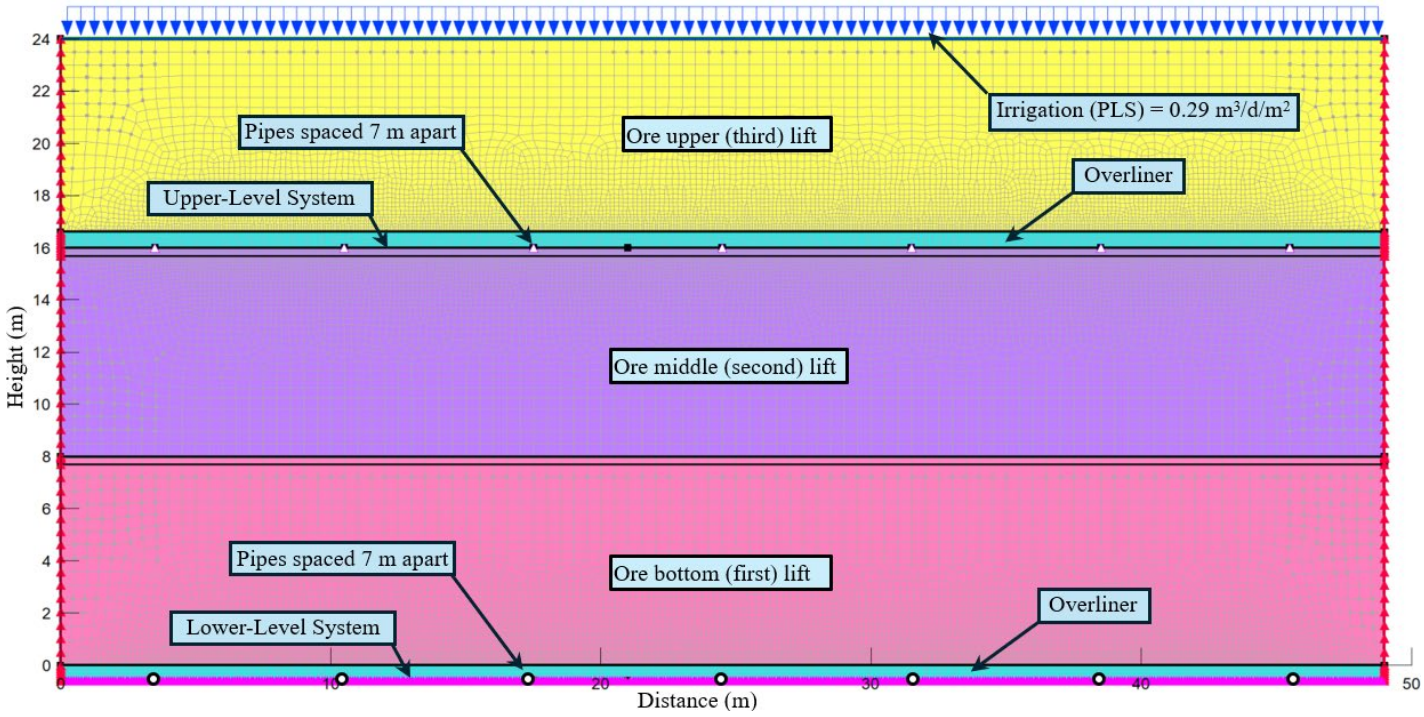

Figure 5: Configuration of three ore lifts under steady-state conditions

A model was then developed incorporating three ore lifts, with a solution collection system and overliner placed above the second lift of ore to simulate the upper-level system drainage configuration, as shown in Figure 5. This setup allowed analysis of solution distribution between the upper and lower

collection systems. Both steady-state and transient flow conditions were modeled, confirming that the transient regime gradually transitioned to a steady-state profile, with some solutions reaching the lower pipes prior to full stabilization of flow conditions.

Each lift undergoes a 90-day irrigation cycle. For the second and third lifts, it was assumed that the underlying ore had previously drained and returned to its natural specific retention moisture content. This assumption mirrors field practice, in which ore is allowed to gravity-drain and desaturate between irrigation phases. The purpose of running both transient and steady-state simulations was to confirm that flow behavior during active irrigation converges toward steady-state conditions over the cycle.

Seepage Model Setup

The numerical seepage model was built in SEEP/W (Seequent, 2023) to capture coupled saturated–unsaturated flow through the stacked ore lifts and overliner, using a two-dimensional, finite-element mesh that represents the geometry of three sequential ore lifts and overliner layers. Soil–water characteristic curves (SWCC) and unsaturated hydraulic conductivity functions were implemented via van Genuchten (1980) parameterizations. The following subsections describe the assignment of hydraulic properties and the imposed boundary conditions.

Geotechnical Parameters

Hydraulic properties for each ore lift and the overliner were obtained from laboratory tests, grain-size analyses, and field measurements. Table 1 summarizes the saturated conductivity, porosity, and key unsaturated parameters used in the model. Activation PWP is the pore water pressure at which unsaturated flow initiates. Retention and conductivity functions for the top-lift ore and overliner are shown in Figures 6 and 7.

Table 1: Hydraulic Parameters for Ore Lifts and Overliner

Material	Layer	Ksat (m/d)	θsat (-)	θres (-)	Activation PWP (kPa)
Ore	Top lift	3.00	0.38	0.05	-1.10
	Middle lift	0.15	0.34	0.05	-1.10
	Bottom lift	0.015	0.33	0.05	-1.10
Overliner	Overliner	8.64	0.30	0.10	-0.13

Note: (-) dimensionless

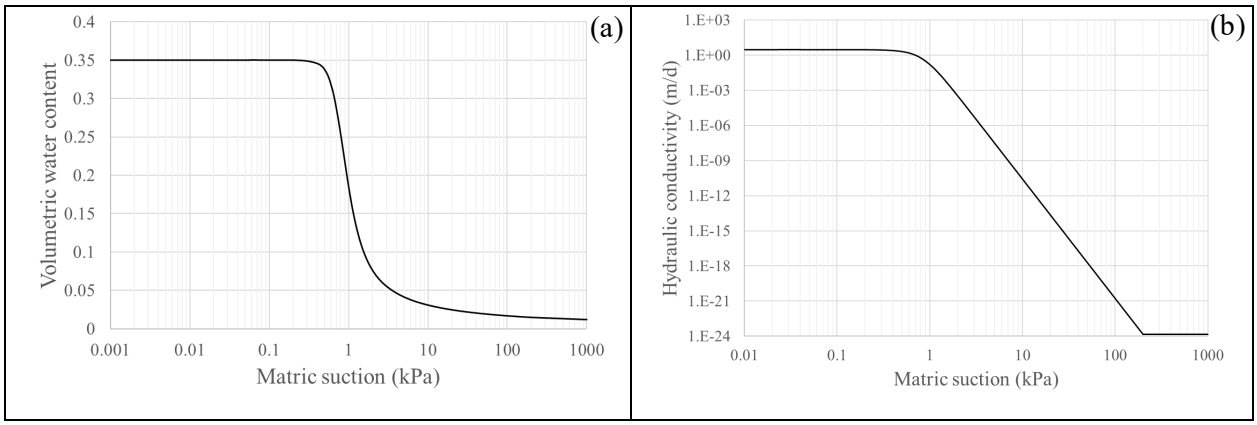

Figure 6: Ore SWCC (a) and hydraulic conductivity curve (b)

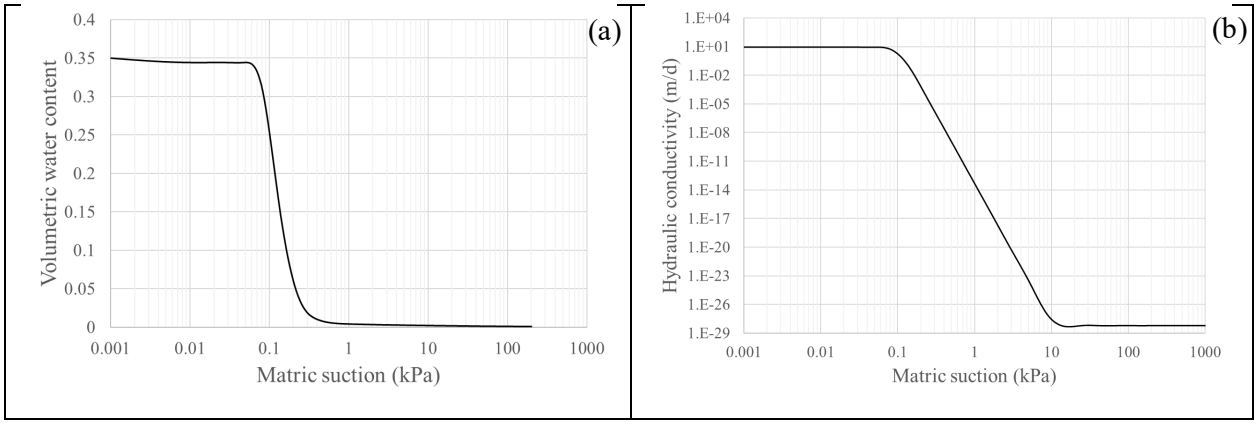

Figure 7: Overliner SWCC (a) and hydraulic conductivity curve (b)

Boundary Conditions

The model boundary conditions reproduce field operating conditions, including application of irrigation flux, impermeable boundaries, and solution collection. Table 2 details the prescribed flux and head conditions used to drive flow through the domain.

Table 2: Model Boundary Conditions

Boundary	Condition Type	Value	Location
Irrigation (PLS)	Flux	0.29 $m^3/d/m^2$	Ore surface (top)
Lateral no-flow	Flux = 0	0 m^3/d	Both vertical ends of the mesh
Bottom liner no-flow	Flux = 0	0 m^3/d	Base of the bottom liner
Bottom collection pipes	Pressure head	0 m	Along the collection pipe nodes at the base
Upper lift drain pipes	Face Review—Specified extraction flux	25 m^3/d	Along the pipe face above the second lift

Model Results

This section presents the key outputs from the numerical seepage simulations for single-, two- and three-lift configurations, under both steady-state and transient flow regimes. Steady-state analyses quantify equilibrium flow rates and inter-pipe hydraulic heads; while transient simulations determine breakthrough times and the convergence toward steady-state conditions. The results are used to evaluate drain performance, flow rates per pipe, maximum head differentials, and the distribution of leachate capture between upper- and lower-level collection systems, thereby demonstrating the efficacy of the two-level design.

Single-Lift Performance

Under steady-state conditions, the model predicts a flow rate of 2.0 m³/d per pipe for a single 8 m lift. The maximum hydraulic head between adjacent pipes is less than 0.6 m (Figure 8), matching the design head calculated via the Hooghoudt (1940) equation. In transient simulations, the irrigation front reaches the collection drains in 4 days, at which point flow rates converge to the steady-state value of 2.0 m³/d per pipe.

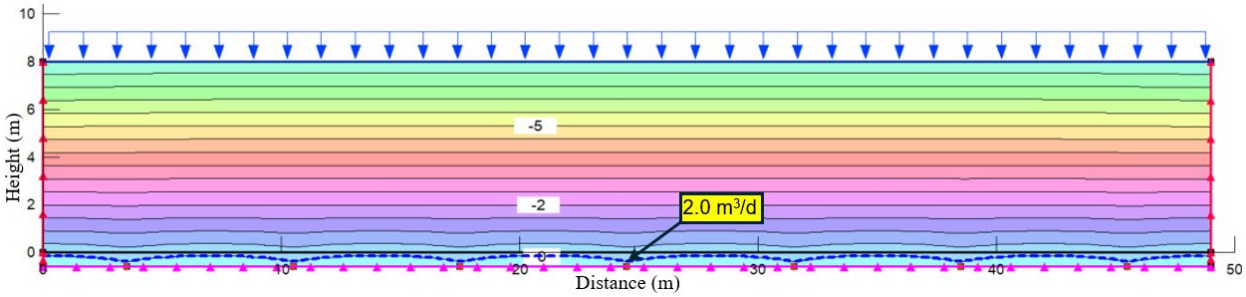

Figure 8: Steady-state results for a single-lift

Two-Lift Performance

With two stacked lifts, the reduced permeability of the bottom lift, due to the overlying load, delays breakthrough. The transient model shows that solution arrival at the base drains occurs in 34 days, after which the system transitions to steady state. Prior to breakthrough, unsaturated flow yields lower pipe flow rates. Once steady state is attained, each pipe again conveys 2.0 m³/d.

Three-Lift Performance with Collection Pipes and Overliner above the Second Lift

In the three-lift scenario incorporating an overliner and upper-level collection pipes above the second lift, steady-state flow rates divide between levels:

- Upper-level pipes: 1.8 m³/d each
- Lower-level pipes: 0.2 m³/d each

Transient behavior stabilizes after approximately 50 days of irrigation, with flow conditions remaining in steady-state for the remaining 40 days of the 90-day cycle. The majority of the solution is intercepted by the upper drains, where the modeled flow rate reaches 1.8 m^3/d and the maximum hydraulic head remains below 0.6 m. At the lower drains, flow is minimal, approximately 0.2 m^3/d, and the modeled pressure head approaches zero, indicating minimal or no ponding above the liner. This outcome is favorable from an environmental standpoint, as lower head reduces the potential for fugitive losses through the liner system. The model result for the steady-state condition is shown in Figure 9.

The apparent discrepancy in hydraulic head at the bottom drains arises from the local flow conditions. In steady-state unsaturated flow, pressure head near well-draining collection pipes can be near zero or slightly negative (tension), even with continuous percolation. This aligns with analytical drainage models such as Hooghoudt (1940), which predict negligible head under low application rates and effective pipe spacing.

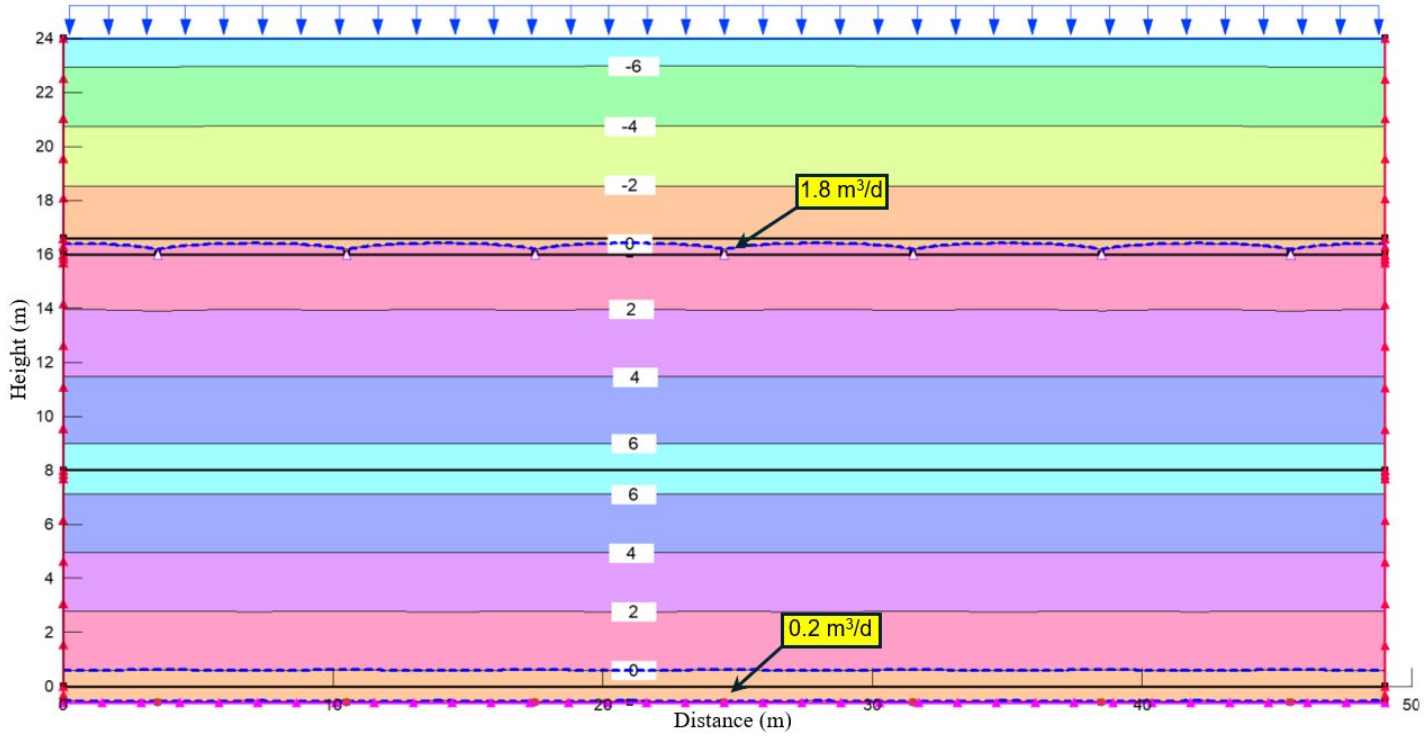

Figure 9: Steady-state results for three lifts with upper-level collection system and overliner

Overall Capture Efficiency

Across all scenarios, the model indicates that roughly 90% of the leachate is intercepted by the upper-level system, with the remaining 10% percolating downward and captured by the lower-level system. These results confirm that the two-level configuration effectively accelerates PLS recovery while minimizing reliance on the existing buried collection network.

Comparison with Measured Values

During construction of the heap leach expansion, instrumentation was installed to measure flow rates from the upper- and lower-level systems. Flow meters on the upper-level recorded that 90.9% of the irrigated solution was intercepted by the upper-level system and delivered to the new PLS pond within 12 days of irrigation start. The flow meter on the lower level recorded that the remaining 9.1% percolated downward and was captured by the lower-level system. These field observations closely match the numerical model's prediction of a 90/10 split and the measured transit time to the PLS pond. The close agreement validates the calibrated hydraulic parameters and confirms that the model reliably reproduces both the distribution of flow between drain levels and the solution breakthrough rate under operational conditions.

Conclusion and Industry Implications

This case history confirms that a two-level solution collection system provides a robust, cost-effective alternative for heap leach expansions in challenging topography. By installing an upper-level drain network above a conventional underdrain system, without the need for engineered borrow material or a continuous geomembrane in the upper lifts, operators can achieve rapid and reliable recovery of PLS.

Key Findings

- Optimized ore stacking: Low-lying or depressed areas can be fully utilized for leaching without displacing ore for borrow material, preserving valuable tonnage and reducing earthwork costs.
- Effective dual-level drainage: Upper-level pipe networks capture approximately 90% of PLS and convey it directly to the new PLS pond within days, while the base system intercepts the remainder, eliminating reliance on long, buried collection runs.
- Predictive numerical modeling: Finite-element analyses calibrated with field-measured parameters accurately predicted flow rates, hydraulic heads, and breakthrough times, supporting confident design and scale-up.

Benefits to the Mining Industry

- Reduced borrow material and liner quantities: Compared with the baseline option of placing a thick structural fill across the depression and then lining that surface, the two-level concept eliminates the bulk-fill requirement and limits new geomembrane installation to a localized inter-lift zone. Although an inter-lift drain package (pipes + over-liner) is still required, avoiding import of thousands of cubic meters of borrow and the associated liner area delivers demonstrable capital-cost and schedule savings.

- Quantifiable inner-lift liner performance: Many heap leach facilities install thin geomembranes between lifts to manage pH or segregate reagent fronts. The transient/steady-state modeling and calibration workflow described in this case history can be applied directly to evaluate the hydraulic effectiveness of such inner-lift liners (e.g., alternative materials, spacing, or thickness), providing a defensible design tool for other operations.
- Operational flexibility during pad build-out: Because the inter-lift drain layer is installed lift-by-lift, operators can expand the pad footprint or adjust stacking plans incrementally, without committing to full final height or large, one-time earthworks.
- Lower head on the basal liner and reduced seepage risk: Intercepting most pregnant solution in the upper drain horizon shortens vertical flow paths and limits ponding above the basal liner. Steady-state modeling shows pressure heads less than 0.6 m at the upper drains and head is approximately zero at the lower drains under the operating irrigation rate, minimizing the driving force for fugitive losses through geomembrane defects.
- Applicability to challenging topography: The two-level drainage concept is readily adapted to either greenfield or brownfield HLFs where uneven terrain or subsidence make wholesale backfilling unattractive, providing a lower-risk and more economical alternative to full backfill-and-line approaches.

Future heap leach projects facing similar geotechnical or topographic constraints should consider a two-level drainage scheme in conjunction with calibrated seepage modeling. The approach offers a clear pathway to improved hydraulic performance, measurable reductions in earthworks and liner quantities, and enhanced environmental stewardship.

These findings align with published observations on the role of unsaturated flow behavior, pore-pressure management, and lift-dependent hydraulic properties in heap performance and risk management.

Acknowledgements

The authors gratefully acknowledge AECOM for its support in the research, development, and preparation of this paper.

References

Breckenridge, L., & Todd, H. (2023). Modeling heap leach solution to optimize safety and revenue. *Proceedings of the International Mine Water Association Conference*, Newport, Wales, UK.

Breitenbach, A. J., & Dolezal, A. L. (2015). Impact of shallow and deep injection well leach solutions with respect to ore heap slope stability. *Proceedings of Heap Leach Solutions 2015*, September 14–16, Reno, Nevada, USA.

Dompier, K., Castonguay, V., & Kellen, C. (2023). 3D seepage and slope stability assessment of a heap leach pad. *Proceedings of the 76th Canadian Geotechnical Conference*, Saskatoon, Canada, October.

Hooghoudt, S. B. (1940). General consideration of the problem of field drainage by parallel drains, ditches, watercourses, and channels. *Publication No. 7 in Contribution to the Knowledge of Some Physical Parameters of the Soil* (translated from Dutch). Bodemkundig Instituut, Groningen, The Netherlands.

Milczarek, M., & Keller, J. (2022). Flow and transport characteristics of waste rock and heap leach facilities. *Proceedings of the 12th International Conference on Acid Rock Drainage*, September 18–24.

Seequent. (2023). *SEEP/W: Seepage modeling with GeoStudio*. Christchurch, New Zealand: Seequent Ltd.

van Genuchten, M. Th. (1980). A closed-form equation for predicting the hydraulic conductivity of unsaturated soils. *Soil Science Society of America Journal, 44*(5), 892–898.

Catalyzing Change: Is it Time for a Paradigm Shift in Sulfide Leaching?

Aleksandr Milshteyn, Transition Biomining, Inc., USA
Diana Bojanova, Transition Biomining, Inc., USA
Suzan Yilmaz, Transition Biomining, Inc., USA
Jeremy H. Wei, Transition Biomining, Inc., USA
Alexandra Shiluk, Transition Biomining, Inc., USA

Abstract

While regularly achieving copper recoveries approaching 100% for oxide ores, the traditional acid heap leaching process leaves as much as 90% of copper in sulfide mineralogies unextracted. This performance gap is critical because sulfide ores represent 70-80% of remaining copper reserves, while declining grades and complex mineralogies are making pyrometallurgical processing increasingly uneconomical.

Unlike oxides, leaching from sulfides requires microorganisms to catalyze iron and sulfur oxidation. Since the discovery of *Acidithiobacillus ferrooxidans* in 1947, the dominant approach to enhance copper recovery from sulfides has been the introduction of laboratory-cultivated microbes, like A. ferrooxidans, to the heap. However, such past and current strategies have largely failed to address two critical points: (1) efficient copper dissolution requires coordinated reactions between multiple microbial types—iron oxidizers, sulfur processors, and acid producers working together, not individual strains acting alone; and (2) like all natural environments, leach heaps contain resilient microbial communities, well adapted to site-specific mineralogy, pH conditions, and nutrient availability, which the introduced microbes have to outcompete and may disrupt. This has led to inconsistent results, typically failing to translate from controlled laboratory environments to real-world heaps at considerable time and financial expense.

Here, we propose a new paradigm for optimizing sulfide heap leaching efficiency by supporting biological processes already occurring in the heap. Drawing on the modern scientific understanding of microbial ecology in the human gut and other environments, we propose that improvements in sulfide leaching can be achieved through what effectively amounts to a prebiotic approach. By delivering targeted chemical additives that support beneficial microbes in existing communities rather than attempting to replace them, natural community resilience can be leveraged to unlock significant improvements in metal recovery, cycle time, and acid consumption. Moreover, this approach requires no flowsheet change and no

additional capital expenditure. By enabling heaps to function as efficient bioreactors, this method increases copper recovery while reducing operating costs and environmental liabilities—offering a sustainable pathway for processing low-grade sulfide ores.

Introduction

The mining industry stands at a critical juncture. While acid heap leaching has achieved remarkable success in extracting copper from oxide ores, with recoveries often approaching 100%, this success does not translate to sulfide ores, which constitute 70-80% of remaining copper reserves. Traditional heap leaching methods leave as much as 90% of the copper in sulfide mineralogies unextracted, creating a significant challenge for an industry facing unprecedented copper demand driven by global electrification and decarbonization efforts, as well as added pressure from AI power demands in recent years.

The magnitude of this challenge is compounded by declining ore grades across the global copper industry. Average copper ore grades have declined from over 1% in 2000 to less than 0.6% today, with some analyses showing declines of 25-40% over the past two decades (Craig, 2024). This decline means that substantially more ore must be processed and, accordingly, capital expended to meet existing metal requirements, let alone satisfy future needs. According to McKinsey analysis, the volume of ore sent to concentrators has risen by 44% to 1.1 billion metric tons over the past ten years, and this volume would need to increase by another 44% by 2031 to produce enough copper necessary for the global energy transition (Crooks et al., 2023).

Unlike oxide ores, sulfide leaching requires microorganisms to catalyze critical iron and sulfur oxidation reactions. Without microbial activity, the leaching kinetics are too slow and recoveries too low for economic viability (Saldaña et al., 2023; Vera et al., 2022). While miners have been unknowingly using microbes to aid copper extraction as far back as the 6th or 7th century BC, the discovery and isolation of Acidithiobacillus ferrooxidans in 1947 enabled targeted biological applications in industrial processes (Colmer et al., 1950; Johnson and Roberto, 2023). However, despite decades of research and development, the industry has struggled to achieve consistent, reliable performance from biological solutions at commercial scale.

The current state of sulfide leaching presents a contradiction: while the biological processes underlying metal extraction are seemingly well understood and the economic incentives for improved recovery are compelling, the industry continues to struggle with implementing effective biological solutions. Here, we submit that the challenges facing sulfide leaching stem not from limitations in our understanding of individual microorganisms, but from a fundamental lack of attention to the ecological realities of microbial community function.

Historical Mining Industry Approaches to Biology and Their Limitations

First Wave: The Probiotic Approach (1950s to 2010s)

The first systematic attempts to biologically enhance heap leaching emerged from the discovery of key microorganisms and focused on what can be characterized as "microbial inoculation" strategies. These consist of culturing and isolating microorganisms that can catalyze the two strictly required redox reactions.

1. Iron oxidation: $4Fe^{2+} + O_2 + 4H^+ \rightarrow 4Fe^{3+} + 2H_2O$

which generates ferric iron as a powerful oxidizing agent (Bosecker, 1997).

2. Sulfur oxidation: $4S^0 + 6O_2 + 4H_2O \rightarrow 4SO_4^{2-} + 8H^+$

produces sulfuric acid that maintains the acidic conditions necessary for metal dissolution (Bosecker, 1997).

The underlying philosophy was straightforward: if specific microorganisms could be identified that accelerated metal extraction under laboratory conditions, then adding these organisms to heap leaching operations should improve performance (Gericke et al., 2009).

To implement this approach, bioreactor-based systems were developed where *A. ferrooxidans* and other well-known acidophilic bacteria were cultured in controlled environments and then introduced into heap leaching operations. Companies pursuing this strategy invested heavily in bioreactor infrastructure, quality control systems, and microbial cultivation protocols. However, the controlled conditions that enabled robust microbial growth in bioreactors bore little resemblance to the heterogeneous, dynamic conditions of industrial heaps, and these approaches encountered consistent challenges in translating laboratory successes to field-scale operations.

While early research focused primarily on *A. ferrooxidans*, comprehensive studies of operating heaps have revealed complex, native microbial communities composed of *Leptospirillum ferriphilum*, *Sulfobacillus thermosulfidooxidans*, *Ferroplasma acidiphilum*, and various other bacterial and archaeal species (Hu et al., 2015; Zhang, et al., 2016). Introduced microorganisms often failed to establish sustainable populations or compete effectively with the established indigenous microbial communities already well adapted to site-specific conditions. Moreover, it can be inferred from probiotic-based gut microbiome studies that the addition of singular monocultures does not have a significant impact on the existing community structure (Mörschbächer et al., 2023). Even when microbial inoculation showed initial promise, performance was typically inconsistent and difficult to sustain over extended operational periods and was not transferable to a different ore feedstock.

Second Wave: The Advanced Probiotic Approach (Late 2010s to Present)

The limitations of First Wave bioleaching drove the development of what can be termed Second Wave bioleaching strategies, characterized by more sophisticated genetic engineering and microbial optimization techniques. These approaches leveraged advances in synthetic biology, such as CRISPR gene editing and adaptive laboratory evolution (ALE), to develop enhanced microorganisms that could theoretically outperform their natural counterparts. Enhanced copper resistance, increased iron oxidation rates, and improved biofilm formation were among the targeted improvements (Carr et al., 2025; Liu et al., 2019).

A parallel Second Wave strategy involves cultivating naturally occurring microbial communities from a well-performing heap, adapting these communities to the ore compositions of underperforming or new heaps, and using these adapted cultures to inoculate them. This community-based tactic is predicated on the assumption that multi-species consortia would provide greater robustness and functional redundancy compared to single-organism solutions. However, community cultivation introduces distinct technical challenges that proved equally problematic. The transfer of native communities from their natural heap environments to controlled bioreactor systems fundamentally altered community composition and dynamics, with liquid media conditions typically favoring rapid expansion of one or two dominant species at the expense of community diversity (Hao et al., 2024; Prieto-Fernández et al., 2024).

Despite their different technical approaches, both genetic engineering, ALE, and community cultivation strategies within the Second Wave have encountered similar fundamental limitations. Genetically modified organisms struggle to compete with indigenous communities in complex heap environments, while cultivated natural communities lose their diversity and functional capabilities when removed from their native contexts. Additionally, regulatory constraints around genetically modified organisms have limited deployment opportunities for engineered solutions in many jurisdictions, including total bans in countries like Peru, while community cultivation approaches face practical scalability limitations that have prevented widespread commercial adoption.

Systemic Scaling Challenges

The persistent failure of both First and Second Wave strategies to achieve consistent commercial success reflects the fundamental lack of consideration for the ecological dynamics of heap leaching systems. Traditional approaches treat heap leaching as an engineering problem where microbial communities can be optimized through brute force external intervention. In reality, heap environments represent complex ecosystems where community structure, function, and stability emerge from intricate interactions between microorganisms, geochemical conditions, and environmental variables (Niu et al., 2016; Saldaña et al., 2023). Introduction of foreign microorganisms, whether natural or engineered, can disrupt these established ecological relationships.

Furthermore, focus on individual microorganisms ignores the community-level properties that drive effective metal extraction. Heap leaching performance under real world conditions depends on the coordinated function of diverse microbial populations, each contributing specialized capabilities to the overall process. This ecological complexity cannot be effectively replicated through the introduction of single species or even defined consortia, regardless of their individual capabilities.

Native Microbial Communities and Systems Biology

Microorganisms are ubiquitously present in every natural environment, where they drive major geochemical transformations (Falkowski et al., 2008). The immense microbial diversity extends to the extreme conditions associated with mining operations, where acidophilic, metal-tolerant microorganisms have adapted to thrive under chemical and physical conditions that would be lethal to most life.

The effectiveness of bioleaching depends on the tightly interconnected structure of these microbial communities, where the coordinated function of the entire ecosystem outweighs the function of any individual species. Iron-oxidizing bacteria regenerate ferric iron from ferrous iron, maintaining the oxidizing potential necessary for mineral dissolution, while sulfur-oxidizing bacteria convert intermediate sulfur compounds to sulfuric acid, preventing the accumulation of a passivating sulfur layer while maintaining optimal pH conditions (Bosecker, 1997). An entire cast of lesser-known acidophilic microbes provides supporting functions like nitrogen and carbon fixation, biofilm formation, detoxification, and degradation of complex molecules that can be more efficiently utilized by leaching species.

The community composition tends to follow predictable geochemical and temporal patterns. This has been demonstrated with the canonical bioleaching microorganisms. Populations of microbes like *A. ferrooxidans* typically achieve their highest abundance when pH values exceed 2.0 and ferric iron concentrations remain below 1 g/L, establishing initial oxidizing conditions. Whereas, species like *Leptospirillum* and *Ferroplasma* dominate when pH drops below 2.0 and high ferric iron concentrations prevail as the heaps mature and conditions become more extreme (Demergasso et al., 2010). This natural succession ensures optimal microbial activity throughout the operational life of heap leaching systems.

Native microbial communities in heap leaching environments demonstrate sophisticated organizational structures that optimize both individual species survival and overall ecosystem function through functional redundancy, where multiple species can perform similar metabolic functions under different limiting conditions, providing resilience against environmental perturbations (Allison & Martiny, 2008; Gericke et al., 2009; Puente-Sánchez et al., 2024). This redundancy ensures that critical processes like iron oxidation and sulfur metabolism continue even when individual species populations fluctuate.

Bacteria have historically been the focal point of bioleaching operations, overlooking *Ferroplasma* and other archaea which are key players in heap leaching communities. These evolutionary intermediates

between bacteria and eukaryotes possess unique metabolic and homeostatic capabilities that make them exceptionally well-suited for extreme environment applications, demonstrating remarkable tolerance to high temperatures, low pH, and elevated metal concentrations. Their metabolic versatility enables function across wide geochemical ranges through utilization of multiple electron acceptors and donors, making them particularly valuable for improving metal extraction from complex ore compositions with multiple mineral phases. Most archaea depend on symbiotic relationships with bacteria and, therefore, are even more challenging to culture in a laboratory setting.

Traditional culturing techniques identified dozens of species associated with metal extraction. However, culturing efforts are victim to what is known as the Great Plate Count Anomaly, which refers to the fact that close to 99% of naturally occurring microorganisms observed in a given environment cannot be isolated in cultures (Stanley & Konopka, 1985; Connon & Giovannoni, 2002). In fact, modern molecular analysis techniques reveal that operating heaps actually harbor hundreds of distinct microbial taxa, the vast majority of which remain unculturable, and many cannot be taxonomically identified with current databases (Hu et al., 2015; Remonsellez et al., 2009). To understand their role in the heap leach community, advanced deep sequencing techniques, which can reveal metabolic capabilities as well as taxonomy, are required.

Understanding these communities as integrated functional ecosystems that exhibit predictable responses to environmental changes provides the foundation for metal extraction optimization strategies that leverage rather than disrupt natural ecological relationships.

Prebiotic Paradigm from Human Health: A Model for Microbial Community Optimization

The human gut microbiome represents one of the most extensively studied microbial ecosystems and provides valuable insights into optimizing the less complex but also much less studied leaching microbiome. One of the most important insights from microbiome research is the critical role of community stability in maintaining functional performance. This resilience emerges from complex ecological interactions between approximately 1,000 distinct microbial species that collectively perform essential functions including nutrient metabolism, immune system regulation, and pathogen resistance (Jovel et al., 2016). Upon disruption of this community stability through nutrient deficiencies, foreign microbial intrusion, or other events, the aforementioned functions break down, and the health of the host can be severely affected.

The gut microbiome field has made significant advances in combating community instability and re-establishing desired functions through probiotic and prebiotic treatments. The distinction between these approaches represents a fundamental philosophical difference in microbial community intervention strategies. Probiotic approaches focus on introducing specific microorganisms to achieve desired functional outcomes by providing functionality that may be missing in the unbalanced microbiome or by competing

out pathogenic bacteria. However, the diversity and complexity of gut microbial communities far exceed what can be achieved through probiotic supplementation alone, leading modern approaches to evolve toward strategies that work with native microbial communities. Rather than attempting to establish foreign microorganisms in complex ecosystems, successful interventions focus on creating conditions that favor the growth and function of beneficial native species, usually by providing targeted bioavailable nutrients, or prebiotics. Clinical evidence increasingly supports the superiority of prebiotic approaches for achieving sustainable improvements in microbial community function (Yassine et al, 2025). The heap leach microbiome is less diverse than the gut microbiome. It is not tied to supporting the health of a host, simplifying the ability to use prebiotics to drive the community towards functions that would benefit bioleaching.

Prebiotic philosophy directly addresses the fundamental limitations that have constrained traditional bioleaching approaches. It provides significant advantages for industrial applications where environmental conditions are inherently variable: temperature fluctuations, pH variations, changing metal concentrations, and other dynamic conditions that would challenge artificially assembled communities. Rather than introducing foreign microorganisms that must compete with established communities, prebiotic strategies optimize the function of native microorganisms already adapted to site-specific conditions. This approach eliminates many of the challenges of microbial inoculation: cost and complexity of infrastructure required for culturing and inoculating microbes at mining scales; functional challenges for cultured microbes when introduced to fluctuating environmental conditions outside of bioreactors; competition with a resilient native microbiome; and the ability to establish a population in the heap. At the same time, it leverages the inherent stability and resilience of the native communities.

The parallels between gut microbiome optimization and heap leaching are striking: both systems involve complex microbial communities with predefined essential functions, both exhibit spatial and temporal heterogeneity, and both demonstrate resistance to colonization by foreign microorganisms. The successful translation of microbiome science to clinical applications provides a compelling model for reimagining biological approaches to mining applications, particularly through the lens of prebiotic versus probiotic intervention philosophies.

Third Wave: the Prebiotic Approach

The Third Wave approach to heap leaching optimization represents a fundamental paradigm shift from organism-centric to ecosystem-centric thinking. This approach recognizes that heap leaching performance depends not on individual microorganisms but on the coordinated function of entire microbial communities operating within complex and variable biogeochemical systems. Rather than attempting to engineer or introduce superior organisms, Third Wave strategies focus on understanding and optimizing the ecological

processes that drive effective metal extraction through addition of targeted prebiotics.

This systems-focused perspective integrates knowledge from multiple disciplines including microbiology, geochemistry, ecology, and process engineering, recognizing that optimal performance requires understanding of the interactions between microbial communities, mineral surfaces, solution chemistry, and mass transfer processes. This type of holistic understanding enables the design of interventions that work with natural biogeochemical processes rather than against them. It also emphasizes the importance of tailoring biological optimization to the unique combinations of ore composition, microbes, climate conditions, and operational practices at each individual leach leaching operation. This contrasts with traditional approaches that primarily sought universal solutions applicable across diverse operational contexts.

The practical implementation of such an approach is not without challenges and requires a set of capabilities not commonly found together in either biology or metallurgy laboratories. The design of effective non-microbial additives requires a detailed understanding of ore mineralogy, the native microbial community, and how the two interact under leaching conditions. Mining samples are some of the most challenging environmental samples to successfully extract nucleic acids (DNA, RNA, etc.) required for modern genomics analyses. In addition, sophisticated analytical and computational capabilities, as well as high-throughput screening systems that combine biological and chemical measurements, are required to enable rapid optimization protocols.

Unlike strain or mixed culture engineering or adaptation, which can take years, the entire fully custom solution development process can already be done in our laboratory in under 4 months. In proof-of-concept studies, our process delivered a ~30% uplift in total copper recovery, relative to unsupplemented control, from a primary sulfide ore and up to 3X higher metal concentration in solution, across the periodic table, in batch tests of tailings samples. Importantly, no microbes were added or externally enriched in any of the experiments, and improvements in the metals extraction into solution correlated with the microbial community changes. As our predictive abilities improve with increasing volume of data, we anticipate being able to reduce the time for delivering custom formulations by half. Moreover, this approach enables adaptive management strategies that allow interventions to evolve in response to changing heap chemistry, community composition, and environmental conditions, ensuring that biological optimization remains effective throughout the operational life of heap leaching systems.

While the upfront complexity of this approach may seem daunting, it produces an elegant and simple solution: a chemical additive that can be formulated and delivered by any major chemical supplier to be applied directly in the leaching solution, providing a substantial improvement in metal leaching rate and total recovery.

Conclusion

Bioleaching of copper sulfides has experienced numerous setbacks over the past decades, leaving some in the industry rightfully skeptical of biological approaches. We argue that the solution to overcoming the setbacks is a fundamental paradigm shift in how we apply biology in heap leaching. Attempts to introduce foreign microorganisms have repeatedly failed to achieve reliable commercial success, despite decades of development and substantial investment. However, these failures stem not from limitations of individual microbial abilities but from fundamental misalignment between solutions and the ecological dynamics of these systems.

Modern understanding of biological systems, as well as major advances in experimental and computational methods, set the stage for a new, holistic approach to improving the function of native microbial communities that are pre-adapted to the unique conditions of each heap. This "Third Wave" paradigm offers a compelling alternative that addresses the systemic limitations of previous strategies by leveraging the inherent stability, resilience, and functional optimization that exist in the heap microbiome. The prebiotic approach, successfully demonstrated in human health applications, provides a framework for achieving sustainable improvements in microbial community bioleaching capabilities.

The industry implications of this paradigm shift are profound. Rather than requiring years of development, substantial capital investment, and added operational complexity such solutions can be implemented rapidly and inexpensively using existing infrastructure. Moreover, this strategy avoids added regulatory burden associated with genetically modified organisms or introduction of non-native microbes into the environment while providing site-specific optimization necessary for effective performance. Most importantly, our approach offers a low-risk path to achieving high copper recovery and accelerated leach cycles that can unlock massive economic value from existing mining operations, all while reducing environmental impact through reduced water and acid consumption and reducing downstream ARD liabilities.

Sulfide leaching can be transformed from a challenging technical problem to a competitive advantage. However, this will require shifting from treating native biology as an uncontrollable variable to managing it as an optimizable process, while embracing the full ecological complexity of these communities rather than attempting to simplify it.

References

Allison, S. D., & Martiny, J. B. H. (2008). Resistance, resilience, and redundancy in microbial communities. *Proceedings of the National Academy of Sciences of the United States of America, 105*(supplement_1), 11512–11519. https://doi.org/10.1073/pnas.0801925105

Bosecker, K. (1997). Bioleaching: Metal solubilization by microorganisms. *FEMS Microbiology Reviews, 20*(3–4), 591–604.

Carr, C. M., Harkova, L. G., & McCarthy, R. R. (2025). Engineering biology approaches to modulate bacterial biofilms. *Trends in Biotechnology, 43*(7), 1525–1527.

Colmer, A. R., Temple, K. L., & Hinkle, M. E. (1950). An iron-oxidizing bacterium from the acid drainage of some bituminous coal mines. *Journal of Bacteriology, 59*(3), 317–328. https://doi.org/10.1128/jb.59.3.317-328.1950

Connon, S. A., & Giovannoni, S. J. (2002). High-throughput methods for culturing microorganisms in very-low-nutrient media yield diverse new marine isolates. *Applied and Environmental Microbiology, 68*(8), 3878–3885. https://doi.org/10.1128/aem.68.8.3878-3885.2002

Craig, B. (2024). BHP 2024 Chilean copper site tour. BHP. https://www.bhp.com/-/media/documents/media/reports-and-presentations/2024/241118_chilecoppersitetour_presentation.pdf

Crooks, S., Lindley, J., Sellschop, R., Lipus, D., Smit, E., & van Zyl, S. (2023). Bridging the copper supply gap. *McKinsey & Company*. https://www.mckinsey.com/industries/metals-and-mining/our-insights/bridging-the-copper-supply-gap

Demergasso, C., Galleguillos, F., Soto, P., Serón, M., & Iturriaga, V. (2010). Microbial succession during a heap bioleaching cycle of low grade copper sulfides. *Hydrometallurgy, 104*(3–4), 382–390.

Falkowski, P. G., Fenchel, T., & Delong, E. F. (2008). The microbial engines that drive Earth's biogeochemical cycles. *Science, 320*(5879), 1034–1039. https://doi.org/10.1126/science.1153213

Gericke, M., Neale, J., & van Staden, P. (2009). A Mintek perspective of the past 25 years in minerals bioleaching. *The Journal of the Southern African Institute of Mining and Metallurgy, 109*, 567–585.

Hao, X., Zhu, P., Liu, X., Jiang, L., Jiang, H., Liu, H., & Chen, Z. (2024). Bioreactor expansion affects microbial succession of mixotrophic acidophiles and bioremediation of cadmium-contaminated soils. *Toxics, 12*(5), 362. https://doi.org/10.3390/toxics12050362

Hu, Q., Guo, X., Liang, Y., Hao, X., Ma, L., Yin, H., & Liu, X. (2015). Comparative metagenomics reveals microbial community differentiation in a biological heap leaching system. *Research in Microbiology, 166*(6), 525–534.

Johnson, D. B., & Roberto, F. F. (2023). Evolution and current status of mineral bioprocessing technologies. In D. B. Johnson, C. G. Bryan, M. Schlömann, & F. F. Roberto (Eds.), *Biomining technologies* (pp. 1–13). Springer International Publishing.

Jovel, J., Patterson, J., Wang, W., Hotte, N., O'Keefe, S., Mitchel, T., Perry, T., Kao, D., Mason, A. L., Madsen, K. L., & Wong, G. K.-S. (2016). Characterization of the gut microbiome using 16S or shotgun metagenomics. *Frontiers in Microbiology, 7*, 459. https://doi.org/10.3389/fmicb.2016.00459

Liu, R., Chen, Y., Tian, Z., Mao, Z., Cheng, H., Zhou, H., & Wang, W. (2019). Enhancing microbial community performance on acid resistance by modified adaptive laboratory evolution. *Bioresource Technology, 287*, 121416. https://doi.org/10.1016/j.biortech.2019.121416

Mörschbächer, A. P., Pappen, E., Henriques, J. A. P., & Granada, C. E. (2023). Effects of probiotic supplementation on the gut microbiota composition of adults: A systematic review of randomized clinical trials. *Anais da Academia Brasileira de Ciências, 95*(3), e20230037. https://doi.org/10.1590/0001-3765202320230037

Niu, J., Deng, J., Xiao, Y., He, Z., Zhang, X., Van Nostrand, J. D., Liang, Y., Deng, Y., Liu, X., & Yin, H. (2016). The shift of microbial communities and their roles in sulfur and iron cycling in a copper ore bioleaching system. *Scientific Reports, 6*(1), 34744. https://doi.org/10.1038/srep34744

Prieto-Fernández, F., Lambert, S., & Kujala, K. (2024). Assessment of microbial communities from cold mine environments and subsequent enrichment, isolation and characterization of putative antimony- or copper-metabolizing microorganisms. *Frontiers in Microbiology, 15*, 1386120. https://doi.org/10.3389/fmicb.2024.1386120

Puente-Sánchez, F., Pascual-García, A., Bastolla, U., Pedrós-Alió, C., & Tamames, J. (2024). Cross-biome microbial networks reveal functional redundancy and suggest genome reduction through functional complementarity. *Communications Biology, 7*(1), 1046.

Remonsellez, F., Galleguillos, F., Moreno-Paz, M., Parro, V., Acosta, M., & Demergasso, C. (2009). Dynamics of active microorganisms inhabiting a bioleaching industrial heap of low-grade copper sulfide ore monitored by real-time PCR and oligonucleotide prokaryotic acidophile microarray. *Microbial Biotechnology, 2*(6), 613–624.

Saldaña, M., Jeldres, M., Galleguillos Madrid, F. M., Gallegos, S., Salazar, I., Robles, P., & Toro, N. (2023). Bioleaching modeling—a review. *Materials, 16*(10), 3812. https://doi.org/10.3390/ma16103812

Staley, J. T., & Konopka, A. (1985). Measurement of in situ activities of nonphotosynthetic microorganisms in aquatic and terrestrial habitats. *Annual Review of Microbiology, 39*(1), 321–346. https://doi.org/10.1146/annurev.mi.39.100185.001541

Vera, M., Schippers, A., Hedrich, S., & Sand, W. (2022). Progress in bioleaching: Fundamentals and mechanisms of microbial metal sulfide oxidation—Part A. *Applied Microbiology and Biotechnology, 106*(21), 6933–6952.

Yassine, F., Najm, A., & Bilen, M. (2025). The role of probiotics, prebiotics, and synbiotics in the treatment of inflammatory bowel diseases: An overview of recent clinical trials. *Frontiers in Systems Biology, 5*, 1561047. https://doi.org/10.3389/fsysb.2025.1561047

Zhang, X., Niu, J., Liang, Y., Liu, X., & Yin, H. (2016). Metagenome-scale analysis yields insights into the structure and function of microbial communities in a copper bioleaching heap. *BMC Genomics, 17*(1), 21.

Heap Leach Closure Strategies in Semi-Arid Conditions: A Data-Driven Approach at the Öksüt Gold Mine

Richard Wagner, ERM, Canada
Mertcan Ozbakir, ERM, United Kingdom
Tom Petry, ERM, United Kingdom
Paul Hesketh, ERM, United Kingdom
Pelin Neriman Usta Ozkayhan, Centerra Gold, Türkiye
David Bickford, Centerra Gold, Türkiye

Abstract

Considering the heap leach facilities operating in semi-arid climates globally, the mining industry faces an increasing need to develop long-term closure strategies that effectively mitigate environmental risks in this climate setting. This paper presents a case study on the testing approaches taken to develop a closure plan for the Heap Leach Facility at the Öksüt Gold Mine, operated by Centerra Gold located in south-central Türkiye (Kayseri Province). A suite of technical investigations has been initiated to support sustainable closure strategies that rely on the use of locally available materials and natural attenuation processes, with the aim of minimizing long-term environmental liabilities and reducing closure costs.

The study evaluates key site characteristics including hydrometeorology, hydrogeology, environmental geochemistry as well as the availability of suitable cover materials and project's proximity to nearby communities. The semi-arid climate, with low annual precipitation and high evaporation rates, is a critical factor influencing both the leachate generation potential and the selection of suitable closure techniques.

Initial investigations have focused on characterizing the quality of the leachates generated from the heap residue, with the goal of identifying appropriate management strategies such as biological or chemical treatment, soil attenuation, evaporation, or the application of covers.

The paper details the characterization strategy, including drilling and collection of representative samples, and describes the rationale for conducting laboratory-based column humidity cell tests. These tests are designed as part of a phased analysis to simulate long-term leaching behavior under site-specific conditions and provide critical data to support the selection and design of effective closure measures. The case study highlights the practical benefits of these investigations and their role in guiding the site's proactive closure planning process, and also offers scalable strategies for heap leach closure in other semi-

arid regions, contributing to future research and sustainable mining practices. This initial testing and analysis will set a foundation for critical pilot-scale evaluations to further isolate key closure opportunities and optimize costs and risk.

Introduction

The closure of gold heap leach facilities is a critical and complex component of the mine life cycle, with direct implications for long-term environmental sustainability and regulatory compliance. One widely considered approach is rinsing, which involves the controlled flushing of the heap with water or treated solutions to remove remaining solutes from pore spaces. However, rinsing is not universally applicable; its effectiveness and long-term benefits are highly site-specific, depending on the geochemical and hydraulic characteristics of the heap material, as well as the heap's overall geotechnical performance. For example, in finer-grained leach ores, slower drain-down to field capacity can prolong elevated moisture contents, potentially increasing susceptibility to undrained behavior and associated stability risks.

Best practice guidance from the International Council on Mining and Metals (ICMM) emphasizes that mine closure should aim to achieve physically and chemically stable landforms that pose minimal long-term risk to the environment (ICMM, 2025). Closure strategies should be integrated into the early stages of mine planning and should reflect a comprehensive understanding of the geochemical and hydrological context of the site. The Global Acid Rock Drainage (GARD) Guide also highlights that rinsing may be an effective tool under certain conditions, but it requires careful evaluation to determine whether it will improve water quality or simply redistribute contaminants (INAP, 2014). Understanding when rinsing is beneficial is, therefore, essential for sound closure decision-making.

Early closure investigations undertaken at the Öksüt Gold Mine suggest that rinsing in isolation may not achieve the desired long-term stability, particularly due to site-specific mineralogy and water limitations. This paper highlights current investigations undertaken to better understand the geochemical behavior of the heap material and the quality of the leachates generated from the heap residue of the Öksüt Gold Mine, with the goal of identifying appropriate management strategies such as biological or chemical treatment, soil attenuation, evaporation, or the application of covers.

The initial investigations focused on:

- Performing humidity cell testing for Acid Rock Drainage (ARD) and Metal Leaching (ML) potential;
- Assessing if rinsing would be beneficial or feasible;
- Identifying alternative closure approaches that are both technically viable and cost-effective; and;
- Using data-driven evaluations to inform long-term closure planning.

This paper presents the approach to characterize the heap material at Öksüt, evaluates the potential of rinsing in the closure strategy, and outlines the technical basis for future decision-making. The outcomes of these investigations will support the design of a closure plan that is both technically robust and environmentally responsible.

Closure Challenges for Heap Leach Facilities in Semi-Arid Environments

The closure of heap leach facilities in semi-arid environments presents a complex interaction of environmental, engineering, and regulatory challenges. Characterized by low annual precipitation and high evaporation rates, these regions are often characterized by constraints on water availability, which is an essential factor for both the operation and closure of heap leach facilities. Closure planning of these facilities should be embedded early with a tailored approach that considers options for managing residual contaminants, including the potential use of cover systems alongside other measures, while also meeting evolving regulatory expectations and international best practice.

Water Availability and Rinsing Effectiveness

The scarcity of water in semi-arid environments directly impacts the effectiveness of rinsing – the process used to flush residual cyanide, salts, and dissolved metals from the heap. Rinsing serves dual purposes, both reducing the environmental risk posed by residual contaminants and, in some cases, facilitating the recovery of additional gold. However, in these climates, the limited availability of water presents economic and logistical difficulties, wherein the benefits of further rinsing must be weighed against the environmental implications of using scarce water resources. In addition, rinsing effectiveness is also constrained by the physical characteristics of the heap itself, wherein older or poorly constructed heaps may have low permeability, which limits the penetration of rinse water and retains pockets of contamination that could pose long-term risks. Such conditions can also prolong elevated moisture levels in some areas of the heap, which in turn may have implications for its geotechnical performance, including a greater potential for undrained response under loading. In some heaps with more sulfidic ores, rinsing may reduce the added alkalinity of the heap and trigger acid-generating conditions. Despite these challenges, preliminary cost-benefit analysis and risk ranking indicate that rinsing offers more reliable control of residual cyanide, metal release, and long-term contaminant mobility at Öksüt, and was prioritized over alternatives such as in-situ stabilization, soil attenuation, and engineered passive barriers.

Long-Term Leachate Management

Even after rinsing, heap leach facilities can retain contaminants which pose a challenge if not managed adequately, and while the overall volume of leachate may be lower due to limited rainfall in semi-arid climates, the seasonal nature of precipitation can lead to unpredictable leachate pulses. This necessitates

the implementation of robust containment and treatment systems, such as low-permeability cover systems, engineered drainage systems, and, if feasible, passive treatment technologies.

Regulatory Expectations

The regulatory landscape further shapes closure strategies, with significant variation between national and international frameworks. In Türkiye, the regulatory framework for mine closure has evolved considerably over the past two decades, with the introduction of the "Reclamation of Lands Disturbed by Mining Activities" regulation in 2007 and its subsequent revisions marking a shift toward more structured closure planning. The 2015 "Mine Waste Management Regulation," which aligns more closely with European Union directives, introduced more rigorous requirements for waste classification and geochemical risk assessment.

These frameworks also mandate long-term environmental monitoring and adaptive management strategies, recognizing that the environmental risks associated with heap leach facilities can persist for decades. The International Cyanide Management Code (ICMC) further provides industry-specific guidance on the safe handling and detoxification of cyanide, which is particularly relevant for gold heap leach operations.

Being one of the first proactive and data-driven heap closure initiatives under Türkiye's evolving regulatory framework, the closure strategy outlined in this paper has been designed to align not only with current national requirements, but also with international best practices—particularly in areas such as rinsing effectiveness, long-term monitoring, and financial planning. This approach aims to support regulatory advancements and could help establish a practical precedent for future closure planning in similar semi-arid heap leach contexts.

Site Description

The Öksüt Gold Mine, located in the Öksüt neighborhood of the Develi district within Kayseri Province in central Türkiye, involves conventional open-pit gold mining operations and commenced production in 2019.

The project site is situated within a topographically varied landscape, with elevations ranging between 1,500 and 2,075 meters above sea level. Seasonal watercourses, with no permanent streams present within the project boundaries, characterize the area. These ephemeral channels typically convey flow during spring snowmelt and intense rainfall events, while remaining dry throughout much of the arid summer season.

Hydrologically, the project area is largely influenced by direct precipitation and snowmelt. Surface water runoff is dominated by intermittent stream flows, which generally diminish during the dry season. The most significant water body in the broader hydrological context is the Zamantı River, located to the

south and east of a nearby wetland system. This river supports multiple irrigation dams and hydropower reservoirs in the region.

The regional climate is defined by hot, dry summers and cold, snowy winters. According to the Thornthwaite climate classification, Kayseri Province is classified as semi-arid, first-degree mesothermal, with a moderate water surplus occurring primarily in the winter months. These climatic conditions influence the hydrogeological behavior of the site, particularly the infiltration potential, long-term leachate mobility, and the overall availability and movement of water within the heap leach facility and surrounding catchment, which make water retention and evaporation key considerations in the context of closure planning.

Öksüt Gold Mine Heap Leach Facility is located within a third-degree earthquake zone according to the Turkey Earthquake Zones Map (General Directorate of Disaster Affairs, 2007). While this represents a moderate seismic hazard, it may influence certain aspects of closure planning, such as cover design and overall structural integrity considerations.

Methodology

Sampling and Sample Preparation

The sampling and testing program was designed to evaluate the leachate quality from residual heap material and to determine whether rinsing can be a viable and beneficial closure strategy for the Öksüt Gold Mine. The approach combines static and kinetic testing methods to assess the leaching behavior of spent ore under simulated closure conditions.

A total of 17 sampling locations were selected across the heap leach facility on different benches to ensure spatial and vertical representation. From each location, material was collected at appropriate depths to capture both surface and internal geochemical conditions. Among the collected samples, approximately 7 kg of material was taken from each drill hole sample, resulting in a total of 119 kg of solid material, which was used to create a master composite sample. This master composite was homogenized using riffle splitting and coning and quartering techniques to ensure representative mixing and to ascertain the average geochemical behavior across the heap, enabling a more efficient assessment of rinsing viability under controlled laboratory conditions.

Sample handling protocols included immediate crushing of the composite material to a particle size suitable for standard humidity cell testing (ASTM D5744-18). All samples were stored under refrigerated conditions to minimize oxidation until testing.

Static Testing

Prior to initiating column leach tests, a suite of static tests was conducted on each of the 17 solid samples and the master composite to evaluate the Acid Rock Drainage and Metal Leaching (ARD-ML) potential and baseline geochemical conditions. These tests included:

- Total Sulfur (S), Sulfate-S, and Sulfide-S.
- Total Inorganic Carbon (TIC).
- Modified Acid Base Accounting (ABA).
- Paste pH and Electrical Conductivity (EC).
- Net Acid Generation (NAG) Test.

These tests helped characterize the geochemical behavior of the heap material and supported the selection of samples for the humidity cell column test scenarios.

Two-Stage Column Testing to Track Contaminant Mobility

To simulate heap rinsing processes and track contaminant mobilization, a two-stage column testing program was implemented, consisting of small bench-scale columns and larger pilot-scale columns.

Small Column (Bench-Scale) Tests

Five small high-density polyethylene (HDPE) columns were constructed using the master composite (17 kg per column, of one kg per each of 17 drill holes). HDPE was selected as the column material due to its resistance to anticipated thermal increases from the bacterial activity in the column, acidic solutions, and alkaline cyanide solutions.

The five columns represented the following rinsing scenarios:

- Columns 1–3: Rinsing solutions at pH 7.5, 8.5, and 9.5 to evaluate the influence of pH on Hydrogen Cyanide (HCN) formation and contaminant mobility.
- Column 4: Barren Adsorption, Desorption, and Recovery (ADR) pond water to simulate in-situ rinsing conditions by recycling the Heap Leach process plant barren solution to the heap residue.
- Column 5: Synthetic solution with 50 ppm cyanide to simulate partial cyanide degradation rinse down conditions for comparison purposes.

A solid-to-liquid ratio of 1:1 was maintained in each column. Weekly leachate was collected and analyzed for a suite of physical parameters, analytes and dissolved metals, including:

- Physical parameters: pH, oxidation reduction potential (ORP), EC, acidity, alkalinity
- Cyanide species: Total cyanide (CN), weak acid dissociable (WAD) CN, thiocyanate, cyanate, cyanogen

- Sulfur species: Total S, sulfate, thiosalts
- Nitrogen species: Ammonia, ammonium, nitrate, nitrite, total Kjeldahl nitrogen (TKN)
- Metals: Gold, silver, and monthly inductively coupled plasma mass spectrometry (ICP-MS) screening
- Others: Chloride, fluoride, total dissolved solids, dissolved organic carbon (DOC), bacterial deoxyribonucleic acid (DNA), (e.g., Thiobacillus ferrooxidans)

As of 13 June 2025, the small column tests had reached Week 23 of the testing cycle, allowing some preliminary trends to be observed.

Pilot Column Tests

Building on the findings from the bench-scale tests, two pilot-scale column tests were initiated to better replicate field-scale rinsing conditions and assess scalability. Each HDPE pilot column was filled with 80 kg of crushed and homogenized heap material derived from the master composite (170 kg total), prepared and homogenized using standardized splitting and coning techniques. Similarly to the small columns, HDPE was selected as the pilot column material due to its resistance to anticipated thermal increases from the bacterial activity in the column, acidic solutions, and alkaline cyanide solutions.

As of 13 June 2025, the pilot column tests had reached Week 3 of the column test cycle. The column setup, rinsing procedures, and leachate collection protocols have been implemented, and baseline data collection has commenced. While it is difficult to draw trends at this stage, these early data will primarily inform the refinement of rinsing protocols and sample handling procedures. However, once the columns reach steady-state leaching conditions, the future data will be more representative, allowing evaluation of rinsing effectiveness, contaminant mobility, and potential water treatment needs. These data will be used to develop a decision matrix to determine the feasibility and extent of rinsing under different site conditions.

Test Scenarios

Two pilot column test scenarios were designed to simulate site-relevant rinsing conditions. The first column was rinsed using barren solution from the ADR pond, with the aim of maximizing resource efficiency by reusing on-site water and reducing the need to source additional rinsing water from groundwater or surface water resources. While the barren solution may still contain trace amounts of cyanide, gold, and other contaminants, it represents a practical and sustainable option based on site operational conditions. The second column was treated with a synthetic solution containing 50 ppm cyanide, simulating partial rinse-down conditions for comparison purposes.

Test Setup

The test setup included two pilot-scale columns, each approximately 2 meters in height and 30 centimeters in diameter. Both columns were operated outdoors under direct sunlight and precipitation to replicate local

environmental conditions and promote photodegradation of cyanide compounds. This serves as a seasonal comparison, with the small column tests being indoors to simulate winter conditions, and the pilot column tests simulating spring, summer, and fall conditions. A weekly wet-dry cycle was applied, consistent with the methodology used in kinetic humidity cell tests. During each cycle, a 1:1 solid-to-liquid ratio was maintained to ensure adequate contact between the rinsing solution and the heap material.

Leachate Analysis

Pilot Column Leachate collected weekly from drain containers may be analyzed for:

- Physical parameters: pH, ORP, EC, acidity, alkalinity
- Sulfur species: Total S, sulfate (SO_4), thiosalts
- Cyanide species: Total CN, WAD CN, thiocyanate (CNS^-), cyanate (CNO^-), cyanogen
- Nitrogen species: Ammonia, ammonium, nitrate, nitrite, TKN
- Other analytes: Chloride, fluoride, total dissolved solids, gold (Au), silver (Ag)

Monthly analyses included:

- ICP-MS metal suite
- DOC
- Microbial DNA and Thiobacillus ferrooxidans

The above list of analyses is a dynamic list that will be revised as test results become available.

Quality Assurance

To ensure data quality and analytical consistency, duplicate leachate samples are collected once per month and submitted to an accredited external laboratory for independent quality assurance and quality control (QA/QC) analysis. Special care is taken during rinsing operations to minimize splashing and physical disturbance, which affect measurements—particularly those sensitive to redox conditions, such as oxidation-reduction potential (Eh). Leachate samples not required for immediate analysis are stored in clearly labelled Intermediate Bulk Containers (IBCs) positioned outdoors and exposed to direct sunlight. This approach maintains consistency with the test conditions and supports potential follow-up analyses or water treatment after site-specific environmental weathering exposures.

Preliminary Results

Static Testing

From the 17 samples tested, the following key results were obtained:

- The average Acid Potential (AP) was 51 eq.kg (CaCO3)/t, with a maximum and minimum of 112 and 20, respectively.

- The average Neutralizing Potential (NP) was 37 eq.kg (CaCO3)/t, with maximum and minimum being 65 and 13, respectively.
- The resultant Neutralizing Potential Ratios (NPR) ranged between 3.31 and 0.28, with an average of 0.94 (Fig. 1)
- The resultant Net Acid Generation (NAG) pH ranged between 7.02 and 3.12, with an average of 5.28 (Fig. 2).

The static testing data results are plotted in Figures 1 and 2.

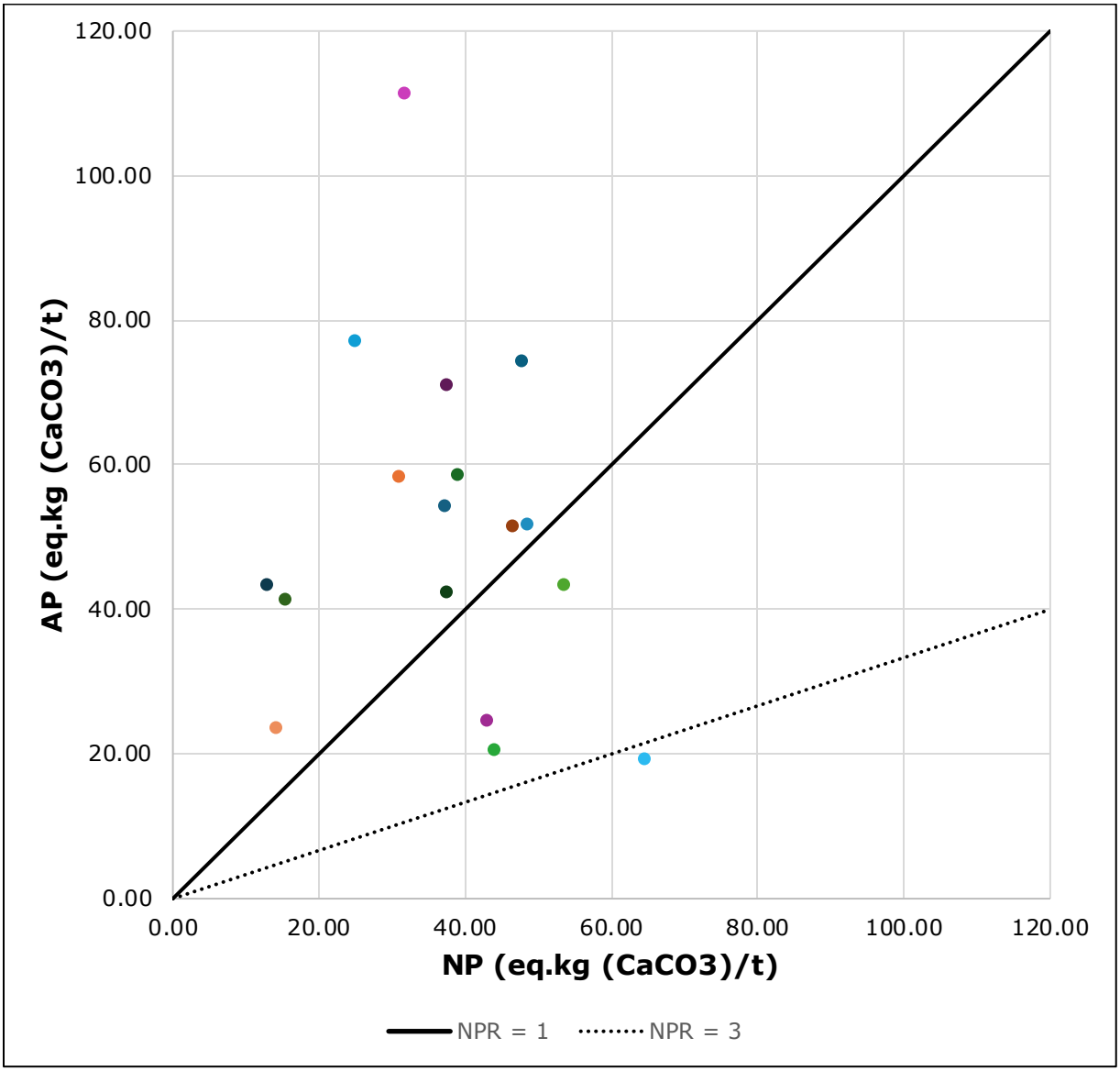

Figure 1: NPR results

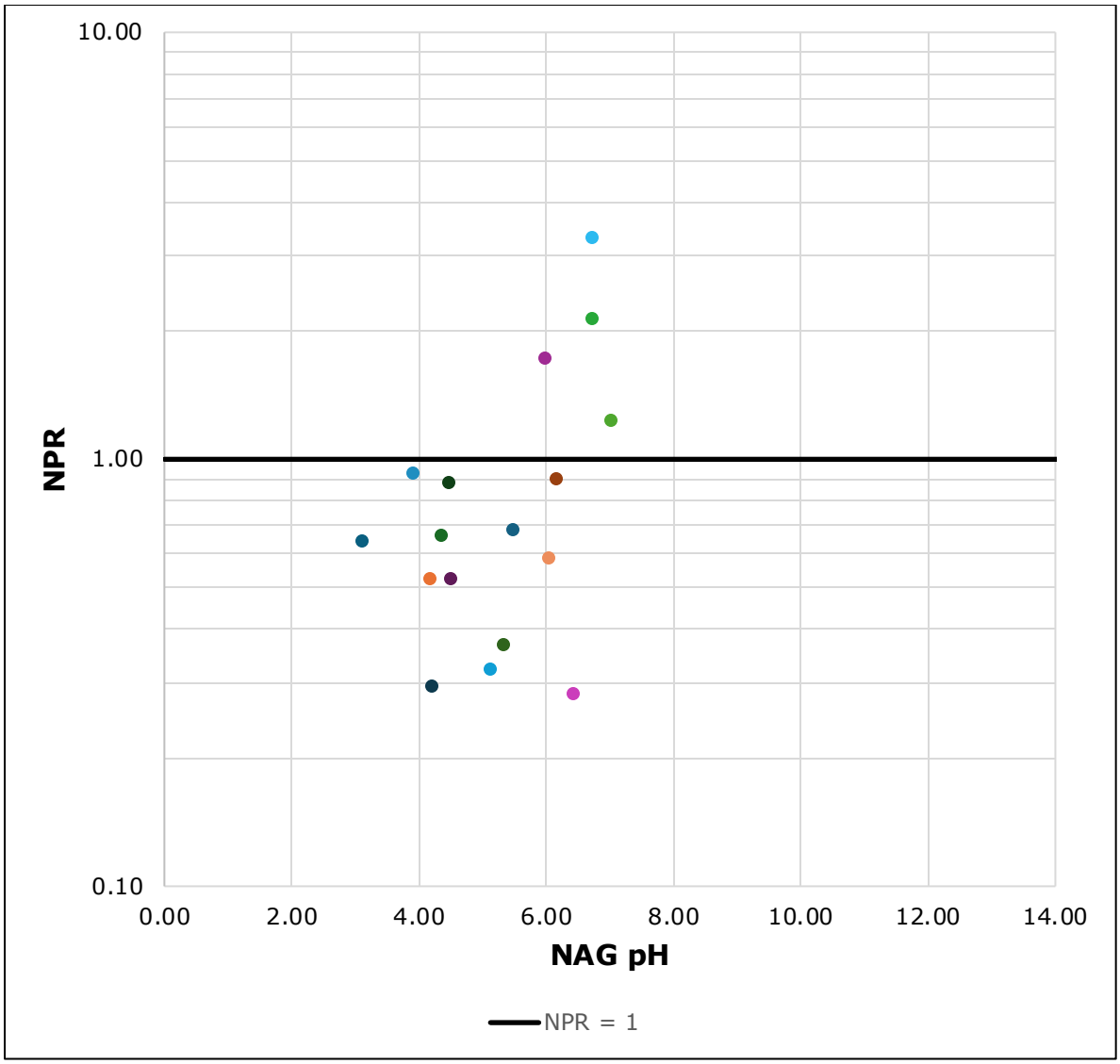

Figure 2: NAH pH vs. NPR

Column Testing

General Parameters

pH

The pH trends observed across all column tests (Fig. 3) indicate a generally stable to strongly alkaline pH profile over time. Columns SC-01 to SC-03, which were rinsed with groundwater adjusted to pH 7.5, 8.5, and 9.5, respectively, maintained pH values in the neutral to mildly alkaline range, and SC-04, which was rinsed with ADR barren solution, consistently exhibited the greatest pH values, often exceeding 10. After 23 weeks, all measured solution pHs were equal to or greater than pH 9.5.

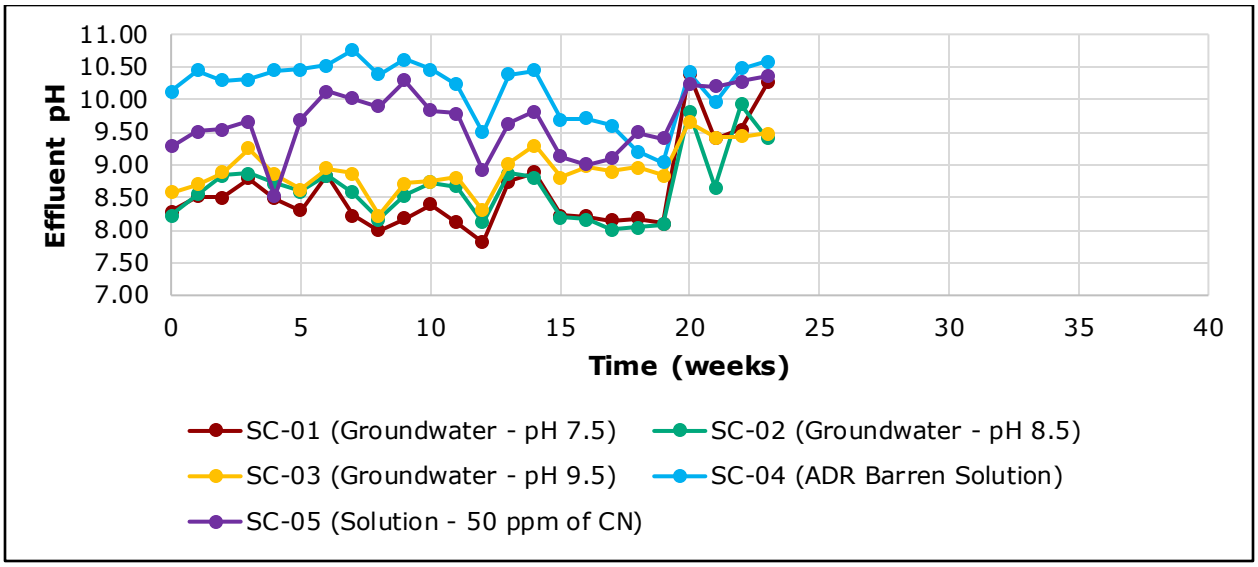

Figure 3: PH trends

Alkalinity

In SC-01 to SC-05, alkalinity showed increased trend over time (Fig. 4), with SC-04 maintaining the greatest alkalinity throughout the test period. It should be noted that results for SC-01 at weeks 5 and 16 are showing fluctuations, indicating potential consumption by contaminants, but generally, the alkalinity for all samples is increasing slightly with time, suggesting alkalinity is leaching from the heap residue solids.

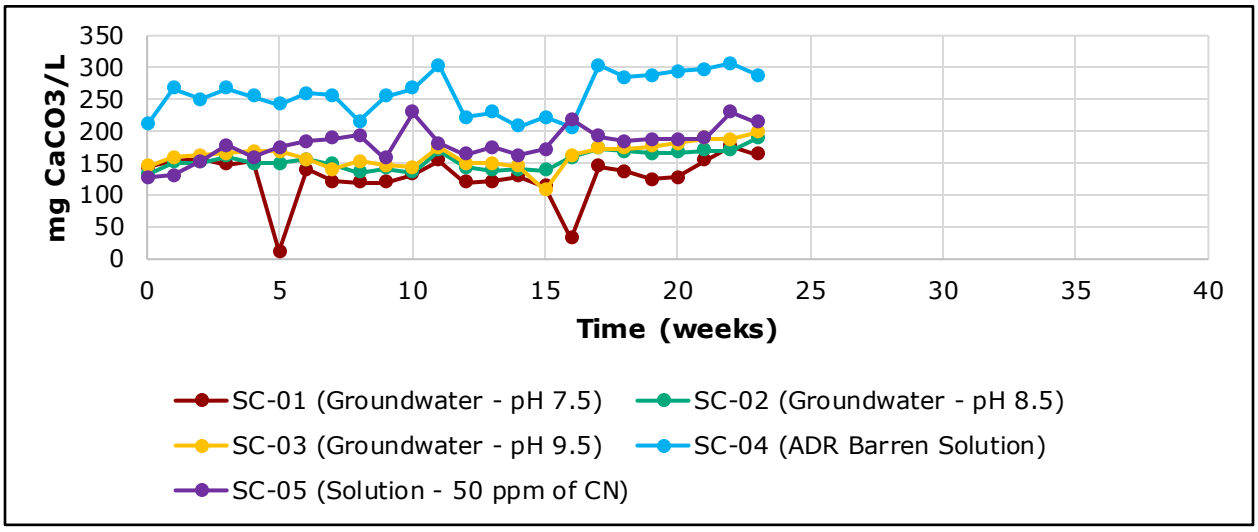

Figure 4: Alkalinity trends

Electrical Conductivity (EC)

In SC-01 to SC-05, EC values have some fluctuations, but generally all leachates are showing a declining trend over time in Figure 5. This may indicate that rinsing is effective in removing sulfate and other soluble

salt constituents from the heap material. SC-04 began with much greater EC values, reflecting the greater initial solute concentrations in the rinsing solution.

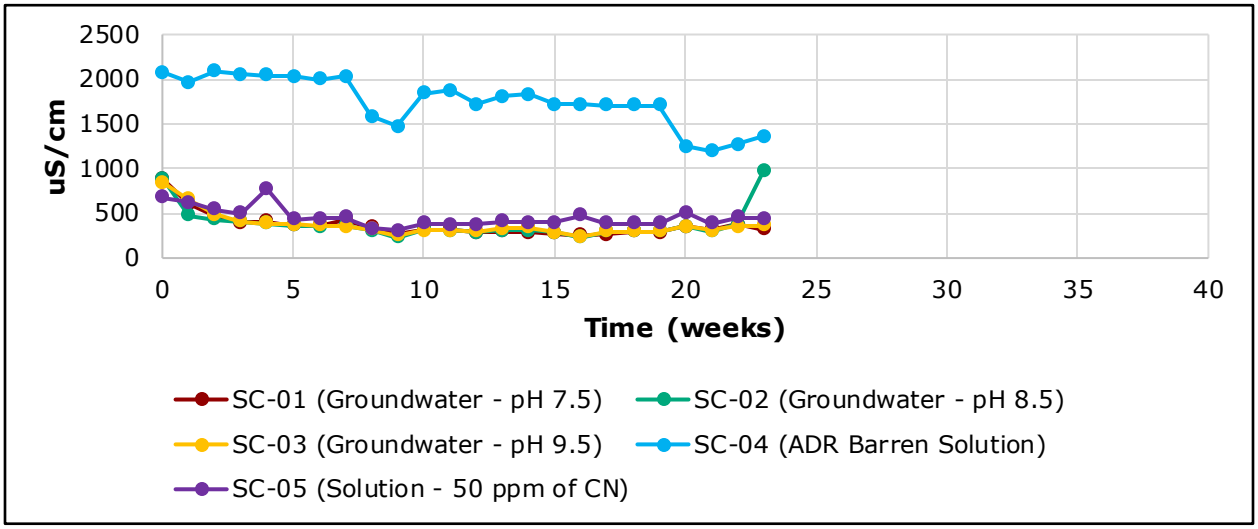

Figure 5: EC trends

Redox Potential

Redox potential measurements shown in Figure 6 revealed that SC-01 to SC-03 showed fluctuating oxidizing conditions, with SC-04 showing more reducing conditions initially. Applying a gentler water application (less splashing) at approximately week 12 also resulted in less oxygen addition for all solutions, with more consistent results, and fewer fluctuations in Redox potential.

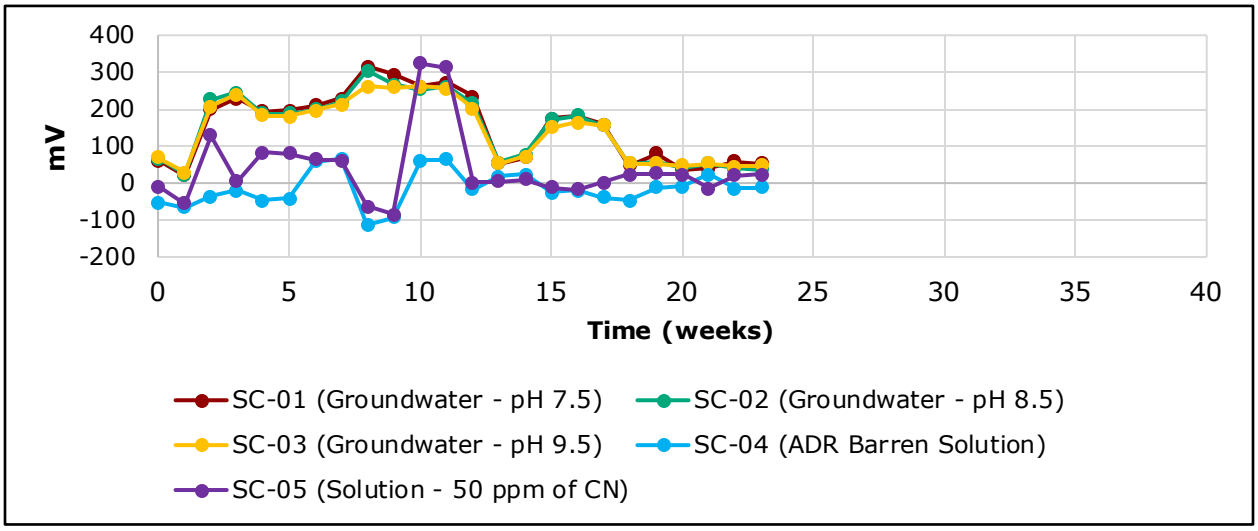

Figure 6: Redox potential trends

Sulfur Species

For sulfur species, both total sulfur and sulfite have remained under detection limits, with sulfate and

thiosalts being detectable. In SC-01 to SC-03, sulfate levels declined steadily, while SC-04 exhibited greater and more variable sulfate concentrations, likely due to the initial composition of the barren solution. Thiosalts remained low and stable in SC-01 to SC-03 but were elevated in SC-04.

Cyanide Species

For cyanide species, both thiocyanate and cyanogen have remained under detection limits, with total cyanide, Weak Acid Dissociable (WAD) cyanide, thiosulfate, and cyanate all being detected. Cyanide species, particularly total and weak acid dissociable (WAD) cyanide, showed rapid declines in SC-01 to SC-03, passing under detection limits within a few weeks. SC-04 and SC-05 started with more elevated cyanide concentrations but also demonstrated consistent degradation over time.

Key Contaminant Metals

Of the contaminant metals, chromium, copper, iron, mercury, zinc, arsenic, and nickel are of interest due to their environmental relevance and mobility under varying geochemical conditions. In general, concentrations of these metals were low in the early weeks of testing, with many values near or below detection limits, especially in the columns rinsed with groundwater (SC-01 to SC-03). However, in SC-04 and SC-05, some metals, particularly copper and arsenic, were detected at greater concentrations during the initial weeks.

It should be noted that lead was also a contaminant of concern; however, it has registered under detection limits for all samples to date.

Gold Recovery

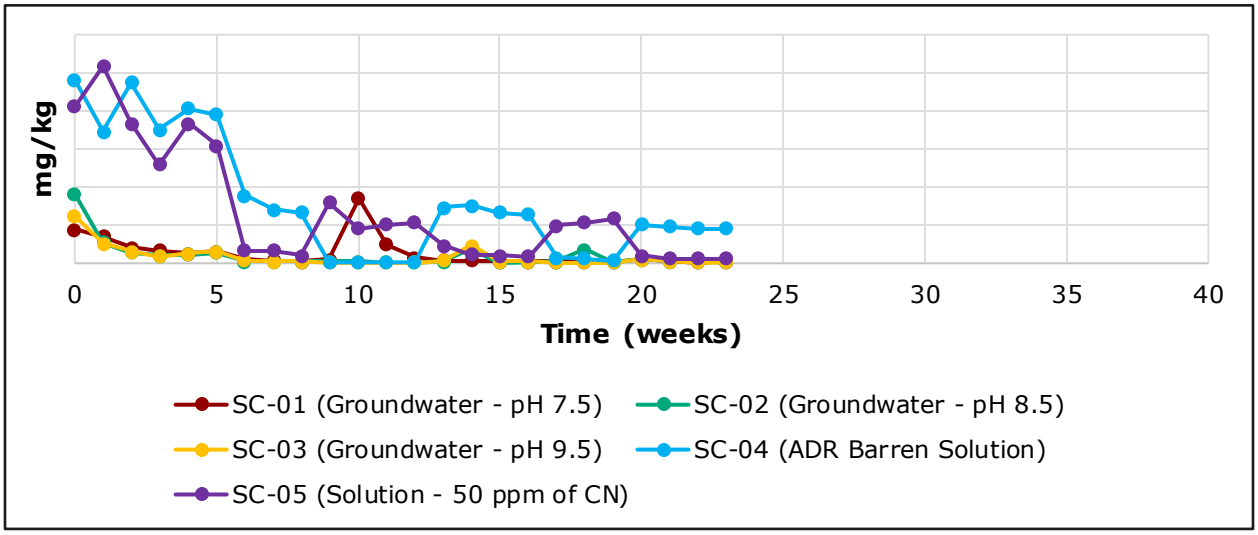

Figure 7: Gold trends

As shown in Figure 7, gold recovery trends indicate that some residual gold was mobilized during the early weeks of rinsing, particularly when using the barren solutions of SC-04 and SC-05.

Conclusion

Static Testing

Static testing revealed significant results pertaining to the ARD-ML potential and baseline geochemical conditions of the ore, key among these being:

- Average Acid Potential (AP) values were 51 eq.kg (CaCO3)/t, with a maximum and minimum of 112 and 20, respectively, across the samples, while Neutralizing Potential (NP) was often insufficient, resulting in Neutralizing Potential Ratios (NPR) below 1 for most samples. This indicates potential for acid generation.
- NAG pH values supported the ABA results, with lower pH values observed in samples with high AP and low NP.
- Only one sample exhibited strong buffering capacity (NPR>3), while the majority are potentially acid-generating or have uncertain acid generation potential.
- The wide variability in AP and NP values suggests significant geochemical heterogeneity within the heap leach residue. This heterogeneity is significant and could influence future zoning strategies and cover optimization.

These results underscore the importance of kinetic testing to simulate long-term leaching behavior. The static test data served as a foundation for designing the column testing program, particularly in identifying the need to evaluate rinsing effectiveness and the potential for acid generation under closure conditions.

Column Testing

General Parameters

Across all five column tests, pH remained above neutral to strongly alkaline. Groundwater-rinsed columns (SC-01 to SC-03) stabilized to 9.5, while those treated with ADR barren (SC-04) and synthetic cyanide (SC-05) exceeded pH 10, potentially due to residual alkaline (hydrated lime) reagents. This elevated pH is advantageous for closure, as it reduces metal solubility and stabilizes cyanide, however, it could also introduce other risks such as scaling and ammonia formation.

Alkalinity trends aligned with pH behavior. Groundwater-rinsed columns showed a gradual increase in alkalinity to 23 weeks, indicating depletion of long-term neutralization capacity. In contrast, SC-04 maintained elevated alkalinity, highlighting the buffering effect of the ADR barren solution. This sustained

buffering is advantageous for long-term stability, particularly in preventing acid generation and maintaining favorable conditions for passive treatment.

SC-01 to SC-03 showed steady EC decline, indicating that rinsing is effectively removing soluble contaminants and is therefore a viable closure strategy for reducing long-term leachate contamination. SC-04, despite starting with elevated EC, also trended downward, demonstrating that even high-strength solutions can be decreased over time, which is key for reducing contaminant loads during closure.

Redox potential initially fluctuated due to water addition methods, but stabilized with gentler (less splashing, less dissolved oxygen entrainment) application. Groundwater-rinsed columns maintained oxidizing conditions favorable for cyanide and sulfur breakdown, while SC-04 showed early reducing conditions, likely from residual process chemicals. It should be noted that as the columns are moved and exposed to direct sunlight, redox conditions would also change to become more oxidative.

Together, these parameters reveal that while the heap has some natural buffering and flushing capacity, rinse solution choice critically shapes geochemical outcomes. These insights will guide pilot-scale testing and inform sustainable closure strategies.

Sulfur Species

Sulfate concentrations declined in groundwater-rinsed columns, stabilizing near detection limits after five weeks, indicating successful flushing of these constituents. ADR barren solution columns showed fluctuating sulfate levels, likely due to oxidation of thiosalts. Thiosalts and thiosulfate were undetectable in groundwater-rinsed columns, while ADR barren columns initially contained thiosalts and thiosulfate of low concentrations that degraded over time. This suggests that the source of the thiosalts and thiosulfate was the rinse solution itself, and that thiosalts were not rinsed from the heap residues when using the groundwater as a rinse solution.

Cyanide Species

Total and WAD cyanide concentrations in groundwater-rinsed columns were consistently below detection limits, implying that natural attenuation processes (e.g., sunlight, microbial activity) may have already reduced cyanide levels in the heap. This indicates that passive treatment methods such as wetlands or surface photodegradation systems could be effective closure strategies. In contrast, columns rinsed with ADR barren and synthetic cyanide solutions exhibited persistent cyanide concentrations, with minimal degradation observed under indoor lab (no natural sunlight) conditions. This highlights the importance of sunlight exposure for passive cyanide degradation and supports the decision to move pilot columns outdoors to simulate seasonal variations.

Key Contaminant Metals

Dissolved metal concentrations were generally low across all columns, suggesting that under near-neutral to mildly alkaline conditions, metal solubility is limited, which is consistent with the observed pH and redox trends. Arsenic and copper were more prominent in ADR barren and synthetic cyanide columns, likely due to higher ionic strength and complexing agents in these solutions. Arsenic, a redox-sensitive element, also showed elevated levels in SC-04, which may be linked to the more reducing conditions observed in this column during the early stages of testing.

These findings underscore the need for continued monitoring of potential leachates from process solution rinsing.

Gold Recovery

Gold concentrations in leachates peaked within the first five weeks of rinsing, particularly in columns treated with ADR barren solution. Most of the additional gold recovery occurred early in the first five weeks of the barren rinsing process. The barren solution, containing WAD cyanide concentrations between 25–200 ppm, was significantly more effective at mobilizing residual gold than pH-adjusted groundwater. These findings suggest that early-stage rinsing of five weeks with barren process water will enhance gold recovery while informing closure cost-benefit analyses.

Limitations

The initial laboratory column humidity cell tests on the heap leach residues are samples that were drilled from the heap and crushed for testing; however, they may not be spatially representative and are finer in particle size, making them more leachable for gold, alkalinity and other contaminants than in-situ conditions.

References

General Directorate of Disaster Affairs. (2007). *Turkey earthquake zones map*. Ministry of Public Works and Settlement, Ankara, Turkey.

International Cyanide Management Institute (ICMI). (2021). *The international cyanide management code for the manufacture, transport, and use of cyanide in the production of gold*. Washington, DC: International Cyanide Management Institute.

International Council on Mining and Metals (ICMM). (2025). *Integrated mine closure: Good practice guide* (3rd ed.). London: International Council on Mining and Metals.

International Network for Acid Prevention (INAP). (2014). *The global acid rock drainage (GARD) guide* (Version 1.0). Vancouver: International Network for Acid Prevention.

Geotechnical Monitoring and Evaluation of Liquefaction Potential of a Heap Leach Facility in Turkey

Hülya Salihoglu Ertürk, WSP USA Inc., USA
Longde Jin, WSP USA Inc., USA
Volkan Boğazlıyanlıoğlu, WSP USA Inc., USA
Panos Kiousis, WSP USA Inc., USA
Ali Burak Aktaş, Tümad Madencilik A.Ş., Turkey
Alper Aruer, Tümad Madencilik A.Ş., Turkey

Abstract

A monitoring program was prepared for a 120-meter (m) thick gold ore heap during the design of Ivrindi heap leach facility (HLF) located in western Turkey, to evaluate whether the initial design assumptions were met through the construction and operation of the facility. Flow behavior and saturation levels throughout the ore were evaluated using HYDRUS-1D unsaturated flow modelling based on soil-water characteristic curves and load/percolation testing performed on agglomerated ore samples. The modelling predicts an increase in the degree of saturation with depth, within the ore, to levels which increase the risk of static and seismic liquefaction. For mitigation, an interlift drain system was designed to limit the saturation of the ore and to decrease gold recovery time for fresh ore.

The HLF was characterized using standard penetration test (SPT), intact sampling through boreholes, test pits, a cone penetration test (CPT) program, and a comprehensive laboratory testing program. CPT response was used to identify the ore zones that may be susceptible to liquefaction. A three-dimensional (3D) geological model based on the ore layers identified through the CPT program was developed using LeapFrog 3D modelling software to generate cross-sections for use in slope stability evaluations. Slope stability of the heap was assessed by performing static and post-liquefaction loading scenarios based on the outcomes of field and laboratory studies and existing monitoring data. A one-dimensional site response analysis was also performed to assess the response of the ore to seismic events and estimate the displacements for the design earthquake event. The existing monitoring system was updated to consider these results.

Introduction

Implementation of an instrumentation monitoring system (IMS) plan for a heap leach facility (HLF) is critical to evaluate the short-term and long-term effects of solution application and the environmental conditions on the HLF. The plan provides early warnings of conditions that could lead to geotechnical risks, particularly important for fine ores (particle sizes between 1 and 10 mm). As ore stacking continues, the fines may densify, resulting in low permeability. Such a reduction in permeability can result in uneven solution distribution, which reduces gold recovery and also elevates saturation levels that can cause seeps to appear on the ore side slopes, leading to erosion and raising concerns about slope stability. Loosely dumped ore in saturated or near-saturation conditions (saturation >80%) is prone to liquefaction when subjected to static or dynamic loads. IMS helps optimize the leaching process by adjusting the solution application strategy, ensuring the stability of the heap. Data collection methods, including sample collection and laboratory testing, pore pressure monitoring through piezometers, deformation monitoring, and visual inspections, are recommended for an instrumentation monitoring system to be performed on a regular schedule (Grass et al., 2022).

In this paper, material characterization of the ore at Ivrindi HLF was presented using the data collected from the geotechnical exploration program, which consists of geophysical survey, cone penetration testing (CPT), borehole drilling, test pits, and laboratory testing program. Material characterization is performed to evaluate the changes in ore characteristics since the design, and reevaluate the stability of the heap with the updated ore characteristics. An overview of the unsaturated flow model and interlift drain system design executed during the design phase was also provided for comparison with the existing conditions. Unsaturated flow modelling was performed to predict the degree of saturation within the ore, considering the ultimate ore stack height. To reduce the saturation levels in the heap, interlift drains were integrated into the design. An instrumentation and monitoring plan was developed, which included monitoring the installed vibrating wire piezometers, survey prisms, and moisture sensors within the heap. This monitoring plan is continually revisited through additional geotechnical studies, including CPT, borehole drilling, and the installation of additional instrumentation, all supported by engineering analyses throughout the operations. This paper presents an overview of the geotechnical studies completed to date and the current status of the heap at Ivrindi HLF, along with the updated instrumentation monitoring system plan.

Design Overview

Ivrindi HLF project includes mining 69.4 million tonnes (Mt) of gold ore over an approximately 10-year mine-life. The ore is produced at approximately 20,000 tonnes/day nominal rate. The ore removed from the pit is crushed to 6.3 mm P80 ore crush size (i.e., 80% of the ore material passes through a screen size of 6.3

mm) via a three-stage crushing process: primary, secondary, and high-pressure grinding rolls (HPGR). Crushing is followed by drum agglomeration. The crushed ore is belted to the heap leach pad and stacked in lifts using a radial stacker and conveyor system. The ore is then irrigated with cyanide leach solution to extract the gold.

The design of the facility includes a maximum allowable ore stacking height of 120 m, which is placed in 10 m lifts. Ore is leached in an approximately 155-day leach cycle with a solution application rate of 10 l/h/m^2. Containment of the ore and leach solutions is maintained with two different liner systems (geomembrane-geosynthetic clay liner, and geomembrane-clay liner) and a solution collection system. Above the liner system, a minimum 0.6 m-thick drain-cover fill material with solution collection pipes is placed to drain the leach solution by gravity toward a double-lined pregnant leach solution (PLS) pond. An excess water (EW) pond is designed with a capacity with 95% probability of non-exceedance in water balance, plus a 1 m freeboard. Due to the fine particle size of the ore, the design included unsaturated flow modelling to understand the expected saturation levels within the ore. Consequently, an interlift drain system was added to the design to reduce these saturation levels throughout the operations.

Unsaturated Flow Modelling

A one-dimensional finite element modelling software for water and solute flow in porous media, HYDRUS-1D, Version 4.17 (Simunek et al., 2013), is used to model the flow behavior and saturation within the ore, assuming no interlift drains or other engineering solutions are implemented. A 120 m-thick single profile of ore was evaluated for the 1D flow model, considering varying material properties along the profile with increasing depth. A 120 m-thick profile represents the worst-case scenario where the ore heap reaches a maximum height, and the saturated hydraulic conductivity of the lower layers decreases due to the increasing height of the heap with the addition of each new lift. Similarly, the soil water characteristic curve used in the model changes with depth. Climate data and leach application rate of 10 l/h/m^2, along with a leach cycle of 155 days, are used in the simulations. Based on laboratory test results, the retention characteristic of the ore is calculated using bimodal fitting parameters (Durner, 1994). A volumetric water content of 21% is applied as the initial condition in the flow models. At the bottom of the ore, free-draining conditions are assumed. At the top of the ore, time-dependent atmospheric conditions with precipitation (including leaching), evaporation, and surface runoff are defined.

Three scenarios are considered to determine the time to achieve steady state conditions:

- Scenario 1: Model runs with saturated hydraulic conductivity data based on laboratory testing.
- Scenario 2: Model runs with one order of magnitude lower saturated hydraulic conductivity data than those obtained by laboratory testing.

- Scenario 3: Model runs with half an order of magnitude lower saturated hydraulic conductivity data than those obtained by laboratory testing.

Based on the model results for scenario 1, significant portions of the ore are predicted to reach saturation above 85% with the applied leaching cycle. The top 60 m of the ore is predicted to have saturation less than 80%. If the field permeability is similar to laboratory measurements, the model does not predict issues of high saturation in these zones. However, it is expected that the field hydraulic conductivity is less than laboratory data due to the internal soil structure of the intact sample, scaling factors, and idealized boundary conditions used in the model. Therefore, lower hydraulic conductivity scenarios (Scenario 2 and Scenario 3) are also run. In these cases, the time to reach steady state is longer than the base case scenario (39 days), which uses the values obtained in laboratory tests, and saturation levels are greater than 80% below the 20 m-ore depth.

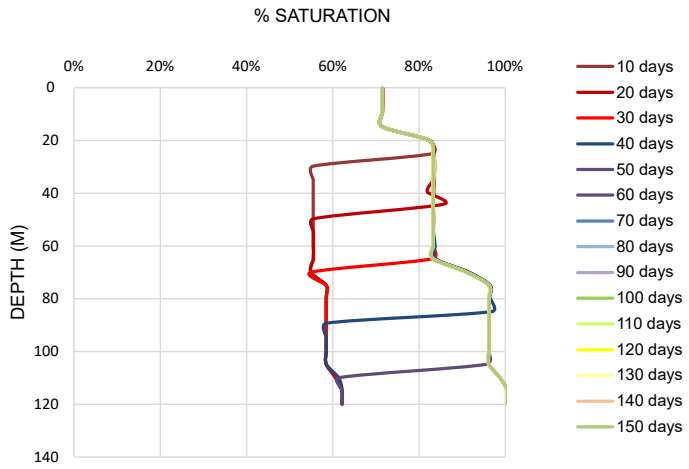

Figure 1: Saturation levels within the ore as predicted from HYDRUS-1D model using half an order of magnitude less permeability than the laboratory hydraulic conductivity data (saturation plots after 60 days are overlapped)

The "stepped" appearance in Figure 1 is an artifact of the simplified model where four zones of constant permeability are considered. If the percent saturation curve shown in Figure 1 is smoothened to account for the expectation of more gradual changes with depth, the model would estimate that ore will exceed the nominal 80 to 85% saturation levels at a depth of approximately 40 to 60 m. Therefore, an interlift drain system at every 40 m vertical height is integrated into the design.

Interlift Drain System Design

The designed interlift drain system consists of a series of corrugated perforated pipes embedded in a gravel layer and placed on top of the ore at 40 m vertical intervals. The top of the ore is sloped prior to interlift

drain construction, smoothed, and slightly compacted to produce a lower permeability zone at the surface to reduce vertical downward flow of leach solutions through the base of the interlift drain system. The ore area where the interlift drain system is installed is divided into smaller areas in the north-south direction, which is called the finger system. Each finger operates independently and has corrugated perforated pipes embedded in drain gravel sloping towards a geomembrane-lined header channel on either the east or west side of the finger. The header channels divert the solution to either the solution collection pipe network at the bottom of the HLF or the transfer pipes over the ore benches towards the pond area. The flow capacity of the pipes within the interlift drain system, as well as the solution collection pipes receiving flow from the interlift drain system, is evaluated considering the leach application rate and climate impacts. Such a system allows the flow to bypass the lower layers of the ore, decreases the saturation at lower levels, improves stability, and increases the gold recovery.

The implementation of the interlift drains system is also evaluated with 2D seepage analysis in Slide v.7.0. The results show that while drains at 60 m spacing prevent positive pore pressure from developing (i.e., saturation), there appears to be a "bulb" or concentration of material with increased saturation near the center of the heap. The model with drains at 40 m spacing shows no such bulb.

Evaluation of Existing Conditions within the Heap

Geotechnical Site Studies

Geotechnical site studies were completed at the Ivrindi Site in 2021 before the placement of the initial interlift drain system and in 2024 prior to the placement of the second interlift drain system. These studies included geophysical surveying, CPT soundings, SPT, and sampling through borehole drilling, test pitting, and instrumentation installation within the ore, as well as the laboratory testing of disturbed and undisturbed samples collected from the boreholes. This paper focuses on the geotechnical studies completed in 2024 and integrates test results and interpretations from the 2021 program.

The geotechnical site studies in 2024 were conducted to evaluate current conditions within the ore. Electrical resistivity survey profiles in north-south and east-west directions were conducted. Based on the collected geophysical data, CPT sounding locations were identified. Among these CPTs, some locations were tested with seismic CPT to measure shear wave velocity, and other locations were tested with either CPT or resistivity CPT. Based on the CPT results, borehole locations were drilled to collect intact samples and perform SPT within the ore. Test pits were excavated to evaluate water content at different time intervals following cessation of leaching. The SPT data from the boreholes are used along with the CPT data for classification of the ore.

Based on the CPT sounding, dynamic pore pressure response was observed within the ore, locally indicating the saturation of the ore. These pore pressures are found in the deeper parts of the ore and are

generally not encountered closer to the surface. The upper parts of the ore showed rapid changes due to leaching operations and rainfall. The observation of dynamic pore pressures in the deeper sections, especially within the lift transition zones, suggests that the ore may compress with depth over time because of additional loadings from more lifts or due to trafficking and compaction at the top surface of the lift.

Laboratory Tests

The laboratory testing program is divided into two phases. Phase 1 included the index tests such as moisture content determination (ASTM D2216), sieve and hydrometer analysis (ASTM D422), and Atterberg limits (ASTM D4318) on disturbed samples obtained from standard penetration tests (SPTs) and conducted in a local university laboratory in Turkey. Phase 2 tests included more advanced testing such as consolidated drained and consolidated undrained triaxial testing (ASTM D7181 and ASTM D4767, respectively), one dimensional consolidation testing (ASTM D4186), soil water characteristics curve (SWCC) testing (ASTM D6836), cyclic direct simple shear (CDSS) test (ASTM D8296) with post cyclic monotonic simple shear, and critical state line (CSL) testing (ASTM D7181) at laboratories in the United States. Some of the advance tests on intact samples that are obtained through Shelby tubes were also conducted in a local laboratory in Turkey to determine shear strength, compressibility, and permeability of the ore material and compare the test results from both laboratories.

The classification of the ore based on Unified Soil Classification System (USCS) from the 2021 and 2024 studies ranges from Silty Sand (SM) to Clayey Sand (SC) to Gravelly Sand. The grain size distribution of the intact samples from the boreholes was finer than the ore gradation used during the design, as shown in Figure 2.

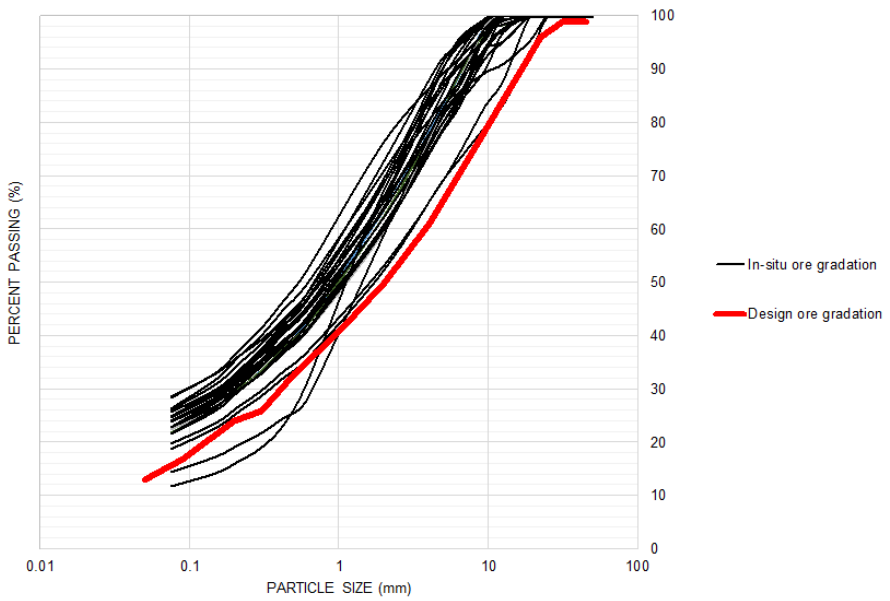

Figure 2: Comparison of grain size distribution of in-situ ore and the ore used during the design

The SWCC wetting curve generated from in-situ ore testing in 2021 and 2024 at similar density used in the design was shifted to the right as compared to the curve used in the design (Fig. 3). This behavior indicates that the in-situ ore has finer particles, enabling it to hold more water at low (<100 kPa) and intermediate suction (between 100 and 10,000 kPa). At high suctions, the in-situ ore and the ore tested during the design converge, meaning that both materials have similar residual water content, implying they behave similarly under very dry conditions.

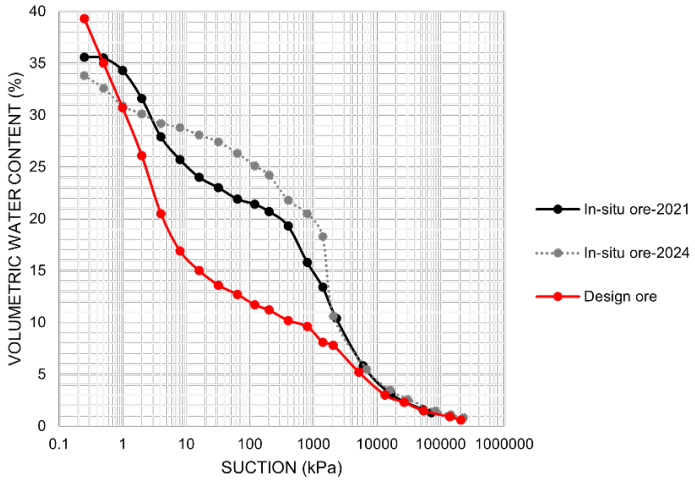

Figure 3: Comparison of SWCC test results from 2021 and 2024 studies and test results used during the design

Stress-controlled cyclic direct simple shear test with a cyclic loading frequency of 0.1 Hertz was performed on the ore sample for cyclic stress ratios of 0.10, 0.23, and 0.26 (one test per cyclic stress ratio) along with a normal stress of 400 kPa. This normal stress is selected as representative of 20 to 30 meters of ore depth, which has more liquefaction potential than deeper parts of the ore due to confinement effects. With CSR of 0.1, the sample did not liquefy in more than 500 cycles. For the CSRs of 0.23 and 0.26, the ore samples liquefied at 65 and 5 cycles, respectively.

Based on the ore properties, maximum design earthquake peak ground acceleration, and the assumed liquefaction depth of 20 to 30 m of soil, the expected CSR for the site is calculated by dividing the average cyclic shear stress induced by the design earthquake by the effective vertical overburden stress as 0.228. The number of cycles to failure for the site is likely less than 65 but more than 10. If an earthquake generates more than 10 cycles, which is usually expected from an earthquake with a magnitude of 7 and above (Idriss, 1999), saturated ore could liquefy.

Screening Level Liquefaction Assessment and Classification of Ore Based on CPT

The screening-level static liquefaction potential of the ore is evaluated using the state-parameter (ψ)-based

method developed by Jeffries and Been (Jeffries & Been, 2016). The linear slope of the critical state line (λ_{10}) from the laboratory critical state locus testing is used to estimate the inverse parameters $\bar{k}$ and $\bar{m}$, using the empirical correlation suggested by the authors. Each CPT output was evaluated individually to identify stratigraphic layers within the ore based on key parameters: state parameter (ψ), soil behavior type index (Ic) (Robertson, 1998), normalized excess-pore pressure response (Bq), and residual strength ratio (s_r/σ'_{vo}). Four layers were identified within the ore:

- Ore-Dilative: characterized by $\psi < -0.05$, $Ic < 2.95$, and minimal Bq response, indicating a predominantly coarse-grained, dilative material with limited excess pore pressure response
- Fine Ore-Clay: characterized by $\psi < -0.05$ with $Ic > 2.95$ and a notable Bq response, suggesting a finer-grained material with higher clay content.
- Ore-Transitional: characterized by $\psi \approx -0.05$, $Ic < 2.95$, and negligible Bq response, near the boundary between dilative and contractive behavior.
- Ore-Contractive: characterized by $\psi > -0.05$, $Ic < 2.95$, and negligible Bq response, significantly more contractive and thus more susceptible to liquefaction.

Screening-level cyclic liquefaction assessment using the Youd et al. (2001) method shows that layers identified as ore-contractive and ore-transitional are susceptible to seismic liquefaction if saturated, which is consistent with the observation from the static liquefaction assessment as stated above.

Instrumentation and Monitoring

An instrumentation and monitoring plan was prepared for the Ivrindi HLF Site during the design stage, which included monitoring requirements, frequency of data collection, responsible parties, monitoring protocol, and quality control methods. Triggering levels were set based on initial stability models developed for the facility. This plan was updated with additional site studies in 2021, with new trigger levels as more piezometers were installed within the ore, and the ore is characterized by CPT. Geotechnical site studies and laboratory test results completed in 2024 indicate that the ore became finer over time with the addition of each ore lift, which increases the liquefaction susceptibility of the ore as it becomes saturated.

To date, a total of seventy-five vibrating wire piezometers (VWP) have been installed at the site. Among these, thirty-eight VWPs were within the ore at varying depths, thirty VWPs were below and above the interlift drain system, two were within the underdrains beneath the geomembrane liner, and five were within the overdrain system above the geomembrane liner. No significant pore pressures were observed in the piezometers installed within the underdrain and overdrain system since the beginning of the operations, which suggests that the drain system at the base of the heap leach pad is operating as intended. The majority of the VWPs within the ore do not indicate pore pressures more than 5 kPa, except for two locations at which pore pressures up to 30 kPa are encountered during the leaching. When these two locations became

inactive leaching zones, the pore pressures dissipated. VWPs within the interlift drain system show a typical fluctuating response to each leaching cycle with distinct peaks (Fig. 4).

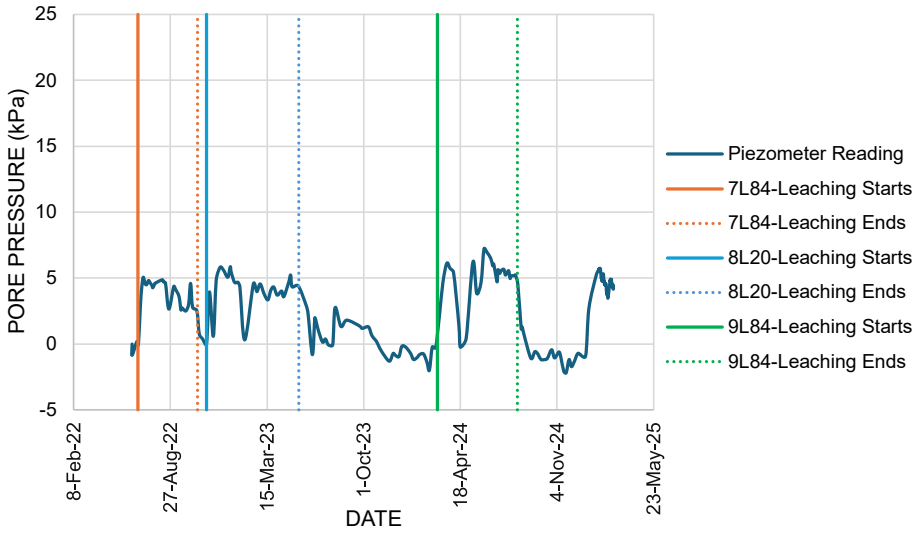

Figure 4: Response of a piezometer within the interlift drain system

Pressure rises during the active irrigation period when the solution is applied and quickly reaches the piezometer within the drain layer. The pressure dissipates rapidly as the solution percolates and drains away due to efficient drainage within the interlift drain layer. Sharp rises and falls indicate that the interlift drain system functions as intended and provides drainage. The initial response of piezometers within the ore to leaching is usually slower due to its lower permeability as compared to the interlift drain layer. Slow decline or retention of pressure for longer is expected after the leach cycle ends.

A total of twenty-four prisms are installed over the ore benches and within the pond areas of the HLF. Raw data collected with the total station instrument is processed, and inverse average velocity plots for potential failure prediction are generated monthly. If the inverse velocity plot shows a decreasing trend, that is, a linear trend towards zero indicating an impending failure, with the x-axis representing the predicted failure time. Since the beginning of operations, the inverse velocity plots of the survey prisms indicate a positive trend. No notable movement has been recorded to date.

A total of thirteen moisture sensors have been installed to date within the ore. The volumetric water content vs time data from moisture sensors generally indicates an increasing trend with leaching. When the leaching operations end, the volumetric water content and, consequently, the saturation levels are reduced.

Static and Post-Liquefaction Limit Equilibrium Slope Stability

The data collected from instrumentation over time, ore layering identified from CPT data, and existing ore geometry, as well as expected future ore geometry, are used to reevaluate the slope stability along the critical

sections to check whether an acceptable factor of safety is maintained.

Ore material characteristics are developed from the field and laboratory studies. Strength of the ore is identified through the interpretation of triaxial test data of in situ samples obtained from the borehole drilling through the ore. Post-liquefaction strength determined from the CPT evaluations and cyclic direct simple shear test, with post-cyclic monotonic simple shear results, was comparable.

Ore layers identified from each CPT data processing and subsequent statistical analyses of the data were modelled in LeapFrog Geo (Seequent, 2023). Critical sections were cut through the LeapFrog geological model and imported into Slide 2 (Rocscience, 2023) for stability runs. For static conditions, undrained shear strength is assigned to the layers identified as fine ore-clay from the CPT interpretations and to the ore material remaining below the interpreted piezometric line at the base of the ore based in instrumentation data. Post-liquefaction strengths that are interpreted from CPT data and CDSS test results were applied to each respected ore layer exported from the LeapFrog model for the selected cross-sections. For the critical sections analyzed, the static and post-earthquake factor of safety met or exceeded the minimum acceptable factor of safety identified in the project design criteria. Along with the stability analyses, trigger levels were set by offsetting the interpreted piezometric line at the base of ore in the stability sections to meet the design requirements. For areas where piezometer data do not exist, the closest CPT information to the critical section or geophysics results was used. For future studies, installation of additional piezometers along the benches of the ore is planned to improve data interpretation.

A computational tool has been developed using Embarcadero's Delphi programming language to estimate the permanent deformations using simulated time histories, produced from design earthquake frequency response data for the site. A simple model is developed where the ore is discretized into a number of layers. Each discretized layer has its own mass. Neighboring masses are connected with springs representing the shear stiffness of each layer. When subjected to a seismic load, the damped forced vibration equation of $\mathbf{M}\ddot{\mathbf{x}} + \mathbf{C}\dot{\mathbf{x}} + \mathbf{K}\mathbf{x} = -\mathbf{m}a_g$ is solved numerically to estimate the displacements. $\mathbf{M}$, $\mathbf{C}$, and $\mathbf{K}$ are the mass, damping, and stiffness matrices, respectively. $\ddot{\mathbf{x}}$, $\dot{\mathbf{x}}$, and $\mathbf{x}$ are the relative to the ground motion acceleration, velocity, and displacement, respectively, of each layer, $\mathbf{m}$ is the mass vector and a_g is the ground acceleration. Density and shear wave velocity used in the tool are identified through the in-situ testing of the ore samples. Shear wave velocities ranged from 200 m/s at approximately 3 m depth to 500 m/s at approximately 70 m depth based on the SCPT measurements. Ore strength is defined in the tool for drained and undrained behavior. The analyses estimate that deformations up to approximately 30 cm with residual deformations of approximately 20 cm may be expected as a result of the design earthquake event at the top layer, which meets the design criteria. At the same time, the bottom layers of the ore may be subject to deformations of less than 5 cm (Fig. 5).

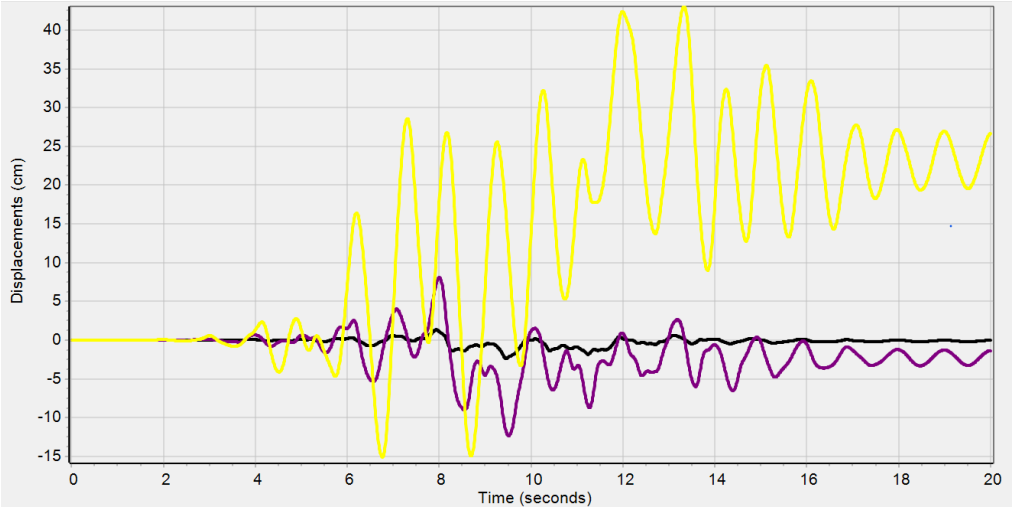

Figure 5: Displacement of ore layers assuming undrained response (yellow: top layer, black: bottom layer, purple: middle layer)

Conclusion

Geotechnical site studies and laboratory testing completed to date at the site indicate that the ore characteristics and material properties differ from the design assumptions, which has implications for the hydraulic performance of the ore. Evaluation of the existing conditions within the ore indicates that the ore is susceptible to liquefaction if saturated. There may also be localized zones of low permeability within the ore that may cause localized increased pore pressures and decreased metal recovery efficiency. Saturated zones can develop above these low-permeable layers and compromise the stability of the ore for both static and post-liquefaction conditions. Vibrating wire piezometers show that the drainage of the ore improves with the installation of interlift drains, which enable bypassing of the lower ore layers that are being depleted. The response of the piezometers within the interlift drain system indicates that the drainage system is operating as intended. Stability analyses that integrate available piezometer data, four ore layers identified through the CPT program, and future ore geometry showed that the minimum acceptable factor of safety is achieved with the current conditions. However, the stability analyses are sensitive to the piezometric levels at the base of the ore deposit. To manage these geotechnical risks effectively and improve the data interpretation, the owner intends to install additional piezometers along the ore benches. Additionally, InSAR-based deformation monitoring is currently carried out by the owner on-site, allowing for real-time performance tracking. Pore pressure and deformation trends are analyzed continuously, with stability assessments updated based on the most recent instrumentation and as-built data. These actions aim to support operational safety, improve regulatory compliance, and strengthen long-term corporate credibility.

Acknowledgements

The author would like to acknowledge Yasin Akçay, Umur Keskin, and Adrian Garcia for their work in processing the field CPT data and the support of Tümad Madencilik San. ve Tic. A.S in developing this paper.

References

Durner, W. (1994). Hydraulic conductivity estimation for soils with heterogeneous pore structure. *Water Resources Research*, *30*(6), 211–223. https://doi.org/10.1029/93WR02676

Grass, M., Nketia, P., & Jester, C. (2022). Geotechnical engineering: The observational method applied to monitoring of slopes during operational activities for heap leach pad facilities. In *Proceedings of Heap Leach Solutions 2022 Conference* (pp. 117–128). Sparks, USA. Retrieved from https://www.heapleachsolutions.ca/WPwebsite/wp-content/uploads/2024/10/12.-Geotechnical-Engineering-The-Observational-Method.pdf

Idriss, I. M. (1999). An update to the Seed-Idriss simplified procedure for evaluating liquefaction potential. In *Proceedings of TRB Workshop on New Approaches to Liquefaction* (Publication No. FHWA-RD-99-165). Federal Highway Administration. Retrieved from https://www.scirp.org/reference/ReferencesPapers.aspx?ReferenceID=1301021

Jefferies, M., & Been, K. (2016). *Soil liquefaction: A critical state approach* (2nd ed.). CRC Press. https://doi.org/10.1201/b19114

Robertson, P. K. (1998). Interpretation of cone penetration tests – A unified approach. *Canadian Geotechnical Journal*, *35*(3), 449–460. https://doi.org/10.1139/t98-029

Rocscience Inc. (2023). *Slide2* (Version 9.0). Retrieved from https://www.rocscience.com

Seequent. (2023). *Leapfrog Geo* (Version 4.3). Retrieved from https://www.seequent.com

Šimůnek, J., Šejna, M., Saito, H., & van Genuchten, M. Th. (2013). *The HYDRUS-1D software package for simulating the one-dimensional movement of water, heat and multiple solutes in variably-saturated media* (Version 4.17). Department of Environmental Sciences, University of California Riverside. Retrieved from https://www.ars.usda.gov/arsuserfiles/20360500/pdf_pubs/P2119.pdf

Youd, T. L., Idriss, I. M., Andrus, R. D., Arango, I., Castro, G., Christian, J. T., Dobry, R., Finn, W. D. L., Harder Jr, L. F., Hynes, M. E., Ishihara, K., Koester, J. P., Liao, S. S. C., Marcuson III, W. F., Martin, G. R., Mitchell, J. K., Robertson, P. K., Seed, R. B., & Stokoe II, K. H. (2001). Liquefaction resistance of soils: Summary report from the 1996 NCEER and 1998 NCEER/NSF workshops on evaluation of liquefaction resistance of soils. *Journal of Geotechnical and Geoenvironmental Engineering*, *127*(10), 817–833. https://doi.org/10.1061/(ASCE)1090-0241(2001)127:10(817)

16S Microbial Profiling of Two Heaps in Southern Arizona Reveals Depth-Based Differences in Genus Distribution

Sydney Cunningham, Freeport-McMoRan, USA
Stephan Christel, Endolith Inc, USA
Parker Cline, Endolith Inc, USA
Christy Green, Endolith Inc, USA
Lynnsey Goyarts, Freeport-McMoRan, USA
Mitchell Catling, Freeport-McMoRan, USA

Abstract

Microbes colonizing mineral surfaces in leach systems can drive oxidation and reduction (redox) reactions with the potential to either catalyze or impede leach chemistry according to environmental and electrochemical contexts. Leach pads comprise complex ecosystems of microbes with dimensional differences in temperature, irrigation, oxygen saturation, and nutrient or metal dissolution. These multidimensional environmental factors differentially impact the growth of certain microbes, which can, in turn, change microenvironments and ultimately impact leaching kinetics. Therefore, surveying dimensional differences in native ore microbiomes is critical for optimizing hydrometallurgical operations.

This study used 16S sequencing to survey 106 samples ranging from 30–700 feet (ft) from 13 boreholes in two Southern Arizona sites: Site (A) and Site (B). This study identified depth-based differences in taxonomy and microbial substrate utilization with hydrometallurgical implications in both heaps. Shallow intervals (<300 ft) contained greater biodiversity of bioleaching-relevant genera. These depths were enriched in mesophilic and acidophilic iron-oxidizing genera, including highly abundant *Leptospirillum* and smaller populations of *Acidithiobacillus*, *Ferroplasma,* and *Sulfobacillus*. Deeper samples (>300 ft deep) contained thermophilic genera *Geobacillus* and *Thermus*. In both sites A and B, obligately aerobic microbes were identified in samples at depths ranging from 0 to 635 ft. Obligately aerobic microbes were absent from samples derived from intervals 640–700 ft deep. Anaerobic microbes were present in samples as shallow as ~275 ft deep in A. These depth-based differences in oxygen consumption may reflect localized microenvironments in the heap with less oxygen saturation. In A and B, samples across all depths contained ecosystems with diverse substrate utilization featuring interspersed autotrophic,

mixotrophic, and heterotrophic communities. Tolerance for higher temperatures increased with depth, with mesophilic microbes more abundant above 200 feet deep and thermophiles more abundant below 200 feet deep.

Introduction

Copper is a critical mineral prized as a strategic commodity for its conductive properties, which are necessary for the global energy transition towards renewable energies. Additionally, copper is crucial for various market sectors, including construction, national defence, transportation, medical devices, and electronics (UNCTAD, 2025). The global trend towards increasingly renewable and digital economies projects that the demand for copper will rise by over 40% in the next 15 years (UNCTAD, 2025). Declining copper ore grades and increasing global demand highlight an urgent need to invest in novel hydrometallurgical applications for processing of more abundant, lower-grade sulfidic ore types. Metal sulfides are amenable to microbially catalyzed dissolution, a process called "bioleaching," which could contribute to novel copper recovery methods from refractory ore types.

Microbes have an ancient evolutionary history inextricably linking them to iron and sulfur cycling systems and have evolved to use sulfur and iron as energy sources, a process called chemolithotrophy (Zhou et al., 2024; Kappler et al., 2021). A vast diversity of bacteria and archaea evolved to oxidize sulfides, elemental sulfur, thiosulfates, and sulfites for their own energy and bio-assimilation or reduce sulfur compounds for their energetic needs (Zhou et al., 2024). For example, bacteria in the genus *Acidithiobacillus* can fix carbon from CO_2, oxidize sulfur, and some species can also oxidize iron (Moya-Beltrán et al., 2021). In contexts of bioleaching copper-sulfides, *Acidithiobacillus* can aid in copper dissolution by removing passivating layers of solid elementary sulfur on the ore's surface (Mangold et al., 2011). Another dominant microbe in many heap-leach ecosystems includes the iron-oxidizing *Leptospirillum* genus. These bacteria have been shown to tolerate oxidative stress, likely conferring a competitive advantage over other microbes such as *Acidithiobacillus* in the heap (Vera et al., 2022; Farías et al., 2021). Cited as one of the most important iron oxidizers in heap-leach contexts, *Leptospirillum* species excel at attaching to mineral surfaces and forming biofilms and are especially well-adapted to low pH levels (Christel et al., 2018; Zhang et al., 2015). Iron-oxidizing microbes such as those in the genus *Leptospirillum* are crucial for the regeneration of the oxidizing agent Fe^{3+} (Vardanyan et al., 2023), which is central to the leaching chemistry of sulfidic ore bodies.

Beyond bacteria, other microbes called archaea are emerging in the literature as key microbes for bioleaching, although relatively less is known about these recently discovered microbes. Many of these archaea are attractive for bioleaching applications because of their ability to withstand high temperatures, low pH, and demonstrate trophic versatility, using organic carbon and iron oxidation or sulfur oxidation for

growth and energy. For example, *Ferroplasma* are extreme acidophiles that use iron oxidation as an energy conservation process, and some species identified thus far can withstand high temperatures (Hawkes et al., 2006). As another example, *Desulfurolobus* are sulfur-dependent, extremely thermophilic and acidophilic, whereas *Cuniculiplasma* in the order *Thermoplasmatales* have been shown to be mesophilic with heterotrophic abilities (Golyshina et al., 2016). Although incompletely understood, archaea are emerging as biomining-relevant species due to their ability to thrive at higher temperatures, lower pHs and trophic versatility.

Taken together, diverse ecosystems of microbes govern different biochemical pathways of sulfur or iron oxidation, carbon fixation, and oxygen consumption. Specific microbes may also apply selective pressure across communities as they either compete with or synergize with neighboring microbes to survive. Within heap leach ecosystems, heat, pH, O_2 saturation, salinity, aridity, and substrate availability within minerals all converge to apply selective pressure on the available microbial diversity. Therefore, the surveillance and optimization of microbial communities native to a heap can be critical to the success of leaching operations of low-grade ore bodies. This investigation primarily focuses on surveying the taxonomic distribution, substrate utilization, and oxygen requirement profiles of microbes colonizing ore stockpiles in Heaps A and B in the Southern Arizona mine.

Methodology

Conducted analyses focus on comparing the native microbiome distributed within two Southern Arizona heaps: “Heap A” and “Heap B”. Heaps in copper mines can contain porphyry copper deposits containing oxides, secondary sulfides including chalcocite, and primary sulfides such as chalcopyrite. Drilling and sampling methods inherent to the district include diamond drill core techniques, wherein most drill holes are conducted vertically. Drill core samples of heaps are collected in 10-foot intervals, wherein the present study began sampling from Heaps A and B at 30 feet.

Drill core samples are typically hydraulically split for downstream internal and third-party laboratory assays. Thirteen boreholes from either Heap A or Heap B were collected. Their corresponding 106 drill core samples of varying depths were shipped to Endolith, Inc., for further processing and analysis (see Figure 1).

Endolith identified microbes present in the obtained ore samples by isolating and analyzing the sequences of the hypervariable V4 region of the 16S ribosomal subunit; a technique called 16S amplicon sequencing (16S-SEQ). By sequencing the DNA that encodes for the V4 region of the 16S ribosomal subunit, 16S-SEQ studies can confidently resolve bacterial phylogeny (Yang et al., 2016).

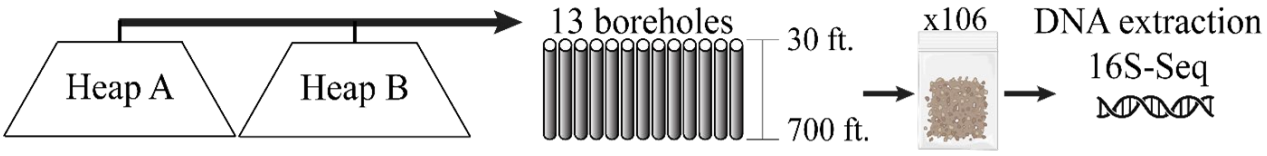

Figure 1: Experimental overview

The resulting data contain the relative abundances of microbes in each sample. Using internal, proprietary processes and databases, the Endolith team functionally annotated aerobic respiration and substrate utilization at the highest available taxonomic resolution as a function of heap depth, following an internal proprietary process. Exclusion criteria mandated the removal of contaminants, microbes incapable of surviving in acidic environments. Furthermore, organisms with relative abundances of less than 1% were excluded from the analyses. All samples yielded more than 100,000 sequencing reads.

Results

Profiling the Taxonomic Distributions of Microbes Colonizing Heap A and Heap B with Depth

Unique DNA sequence variants identified within ore samples represent microbes that were subsequently annotated by their metabolic association with metal sulfides across the samples. Most identified microbes were known to be metal sulfide-associated in Heaps A and B (Fig. 2). Amplified DNA concentrations and resulting sequencing depth were plotted for each heap (see Figs. A1 and A2 in Appendix), indicating higher biomass in shallow samples.

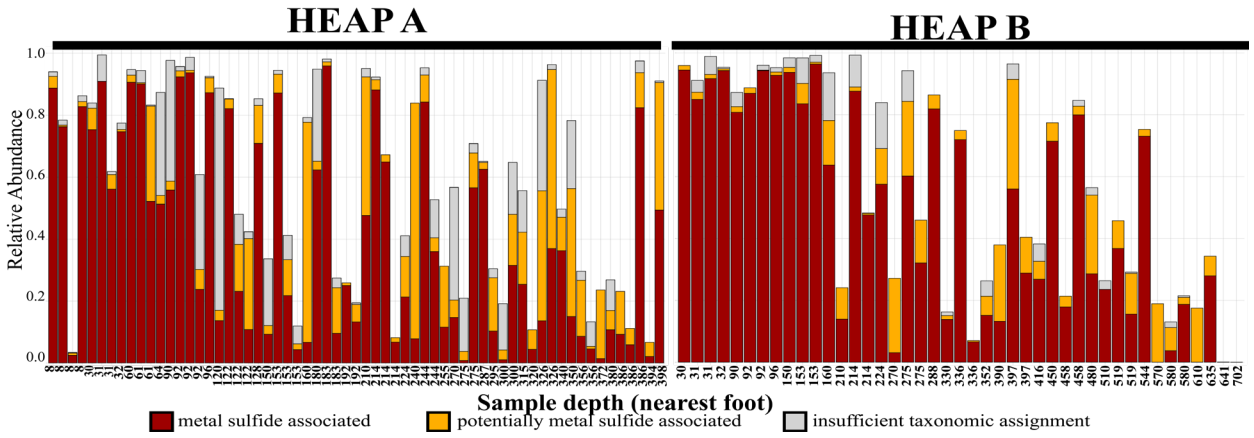

Figure 2: Most of the microbes in Heap A and Heap B are associated with metal sulfides

After validating the bioleaching-relevance of microbes across the datasets, genus- and species-level taxonomy assignments were analyzed in samples derived from Heaps A (Fig. 3a) and B (Fig. 3b). Across both heaps, depth drives differentiation in microbial community profiles. The predominant genus in both heaps belongs to the iron-oxidizing *Leptospirillum* genus, where Fe^{2+} is necessary for energy (Christel et

al., 2018; Coram & Rowlings, 2002). Both heaps have a high prevalence of iron-oxidizing archaea, including A-Plasma, Acidiplasma, and Ferroplasma in more shallow samples, less than 200 feet deep (Johnson et al., 2012). Of the four identified isolated species of *Ferroplasma,* all have been published to be facultatively anaerobic, capable of oxidizing iron, and versatile heterotrophs that can utilize organic carbon (Batrakov et al., 2002; Castelle et al., 2015; Zhou et al., 2008; Hawkes et al., 2006). With increasing depth beyond 300 feet, thermophilic microbes of the genera *Geobacillus* and *Thermus* prevail (Hussein et al., 2015; Cava et al., 2009).

In addition to iron-oxidizing microbes, there appeared to be a smaller but considerable community of microbes capable of utilizing sulfur, including but not limited to those in the genus *Acidianus, Acidithiobacillus,* and *Sulfobacillus* (Hart & Gorman-Lewis, 2025; Sarkodie et al., 2022).

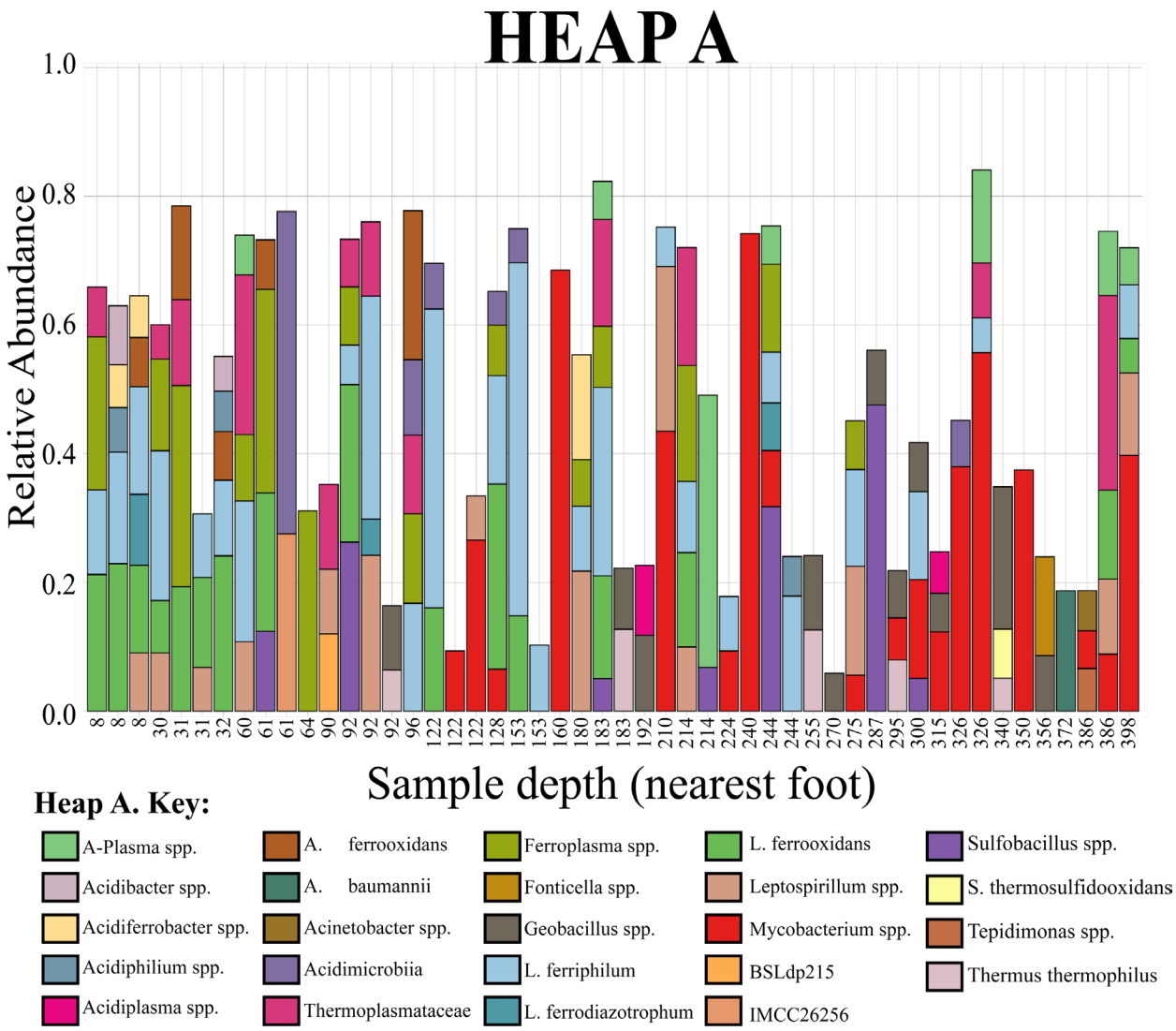

Figure 3a: Taxonomic diversity across depths from Heap A

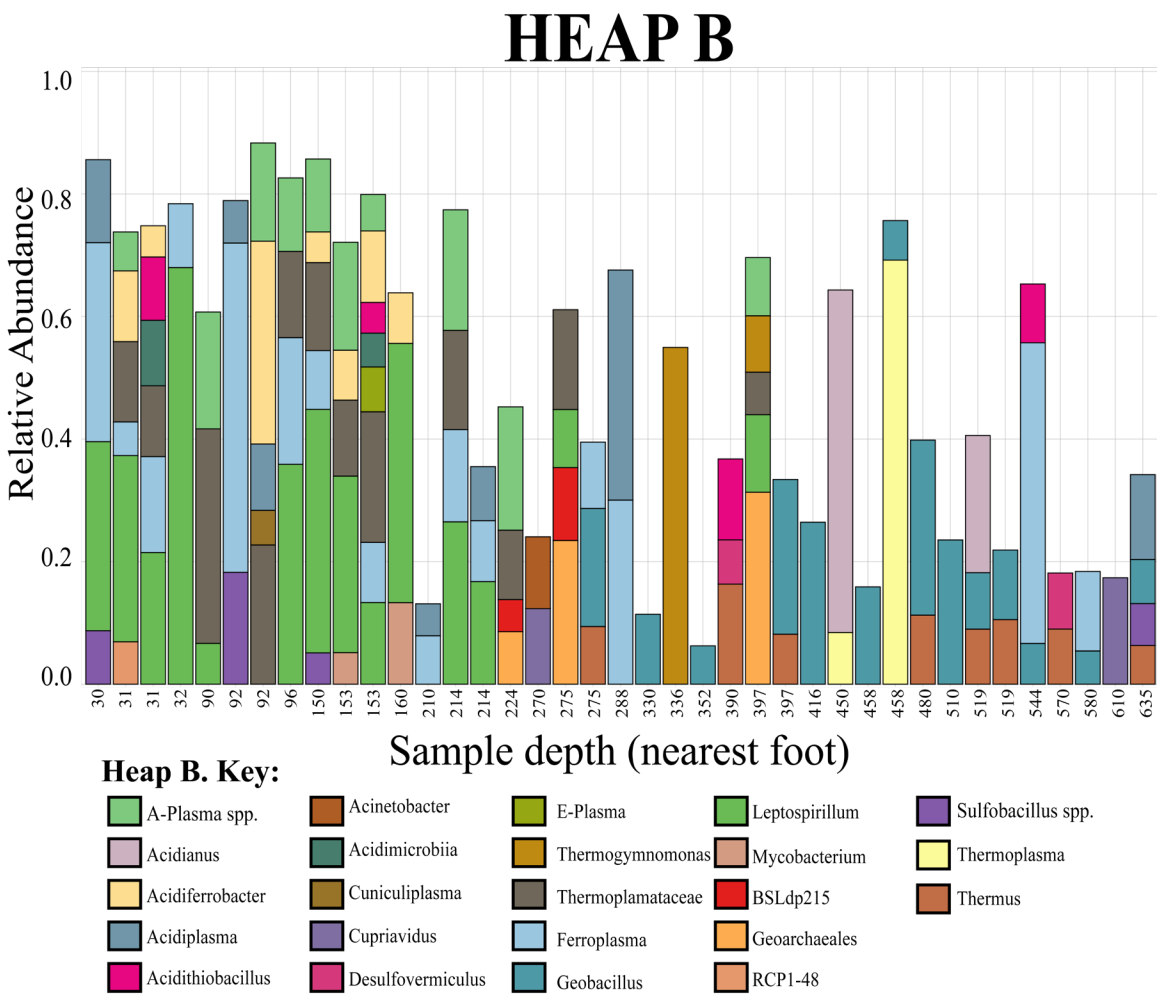

Figure 3b: Taxonomic diversity across depths from Heap B

In summary, both heap leach ecosystems contained a majority of metal-sulfide-associated microbes. Interestingly, iron-oxidizing microbes thrived in both heap environments with a prevalence of archaea with no cell walls (e.g., *Ferroplasma*). Canonical leaching genera, including Acidithiobacillus (Fig. 3a and 3b), including species Acithiobacillus ferrooxidans (Fig. 3a) and Leptospirillum (Fig. 3a and 3b), were detected in both heaps, with a dominant prevalence of iron-oxidizing microbes and a dearth of sulfide-oxidizing communities. Community profiles changed as a function of stockpile depth, with thermophilic microbes being more prevalent beyond 300 feet in depth.

Analyzing the Substrate Utilization of Microbes Colonizing Heap A and Heap B with Depth

The preceding analyses annotated the data based on metabolic distributions of the microbes identified in the heap leach ecosystems (Fig. 4a and Fig. 4b). In Heap A, iron-oxidizing microbes are found throughout all depths. In contrast, sulfur-oxidizing microbes are more prevalent below 150 feet deep (Fig. 4a).

Heterotophic microbes using organic carbon as well as mixotrophs using combinations of iron, sulfur, and organic carbon were present in minority abundances throughout the stockpile in Heap A (Fig. 4a). For some microbes identified in the leach heap, there are few publications describing their metabolism, but some evidence indicates a capacity for a certain metabolic profile. For example, if a microbe contains a gene that encodes for an enzyme capable of oxidizing sulfur, this is necessary but insufficient evidence of a microbe's metabolic capacity without direct functional studies. These microbes are assigned as "putative" metabolizers, where the metabolic assignment published in this report may change with a refined understanding of the metabolic capabilities of novel microbes.

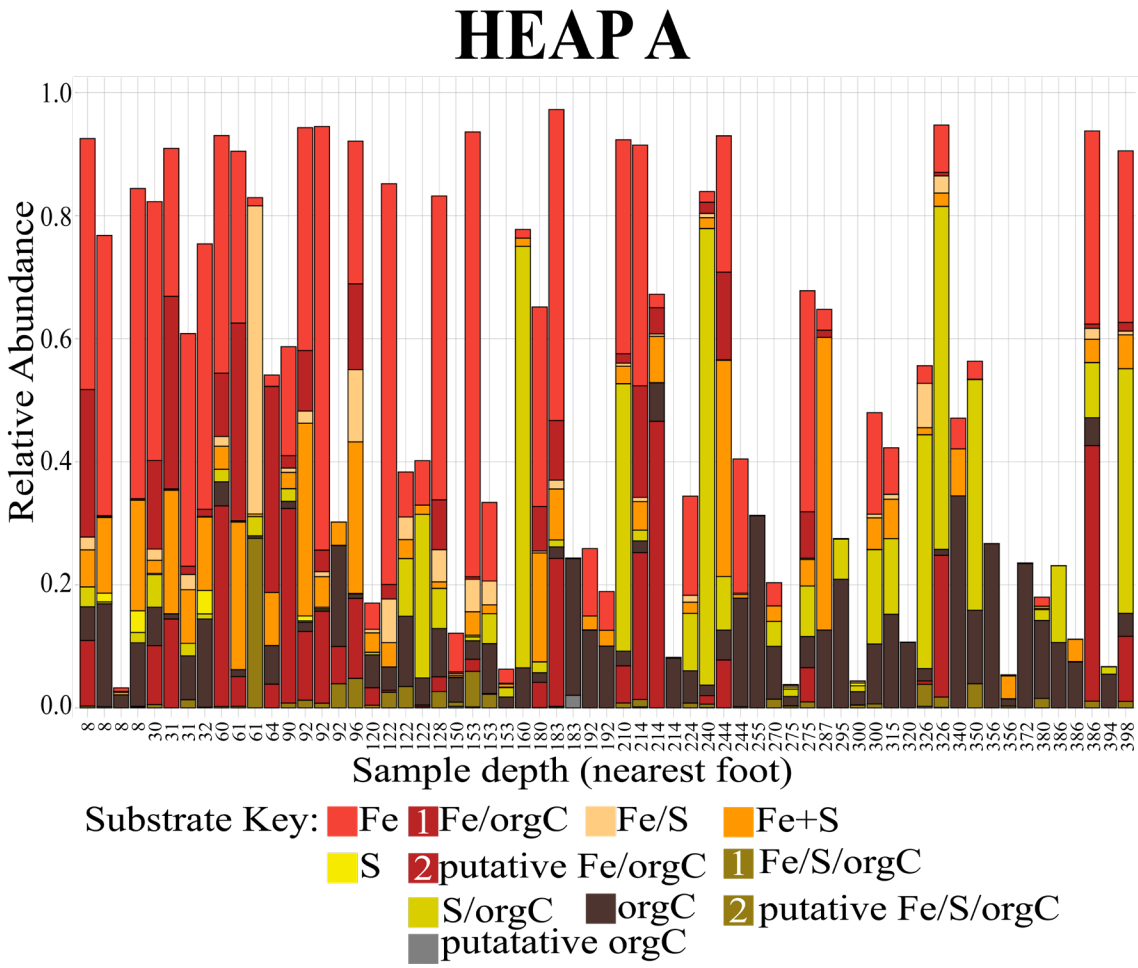

Figure 4A: Genus-level substrate utilization by depth for Heap A

In Heap B, there is a stark change in metabolic profiling in shallow (above 300 feet) and deep (below 300 feet) drill core samples. Iron-oxidizing microbes prevail above 200 feet (Fig. 4b). Heterotrophic thermophilic microbes are highly represented by archaea, including *Thermoplasma* and *Ferroplasma*. Heap B contained relatively few sulfur oxidizers.

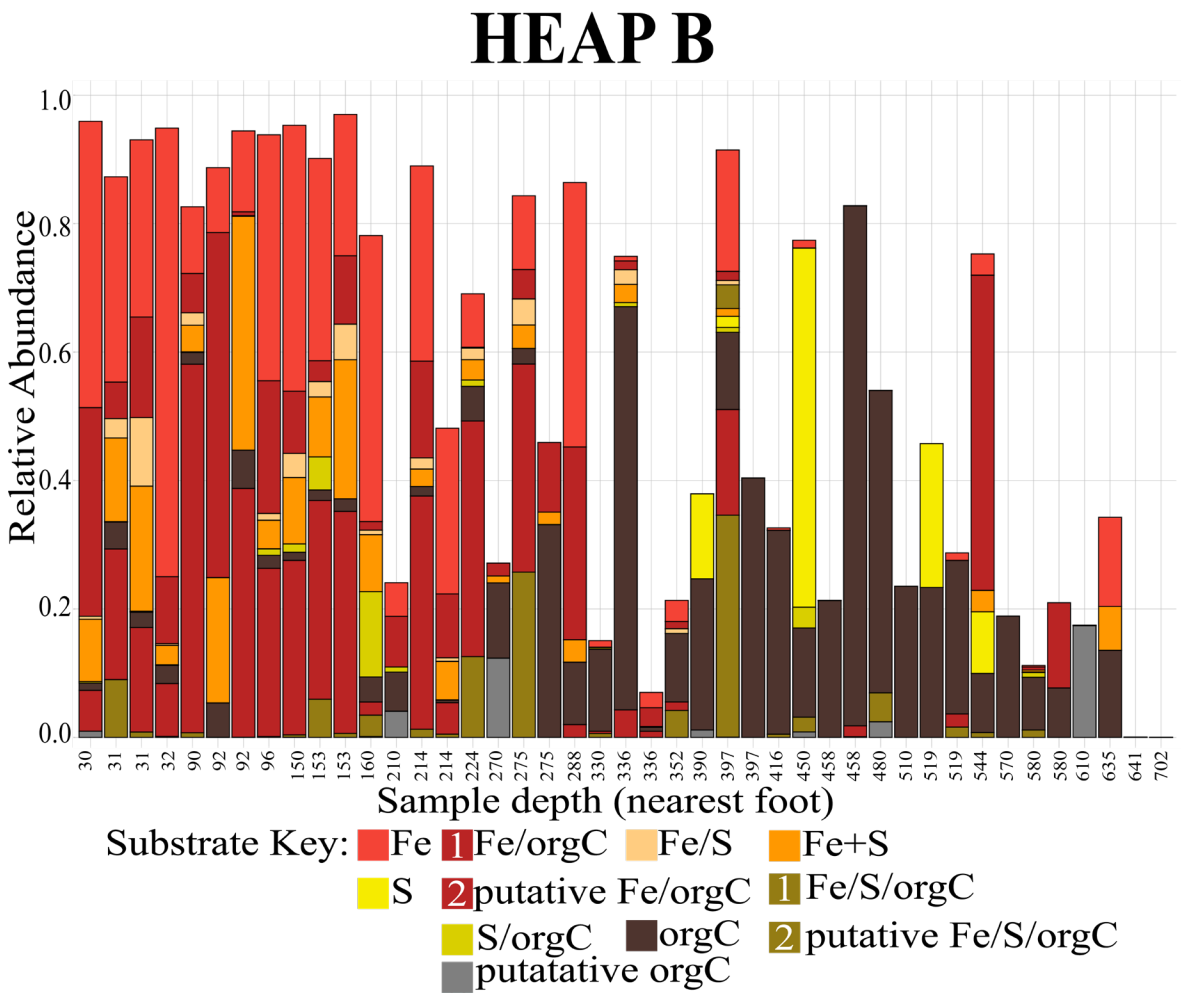

Figure 4B: Genus-level substrate utilization by depth for Heap B

The differing metabolic profiles of microbes colonizing ore samples between Heaps A and B may reflect differences in ore mineralogy and placements with depth. Differences in metabolic profiles with depth may reflect a prevalence of heterotrophic and thermophilic archaea capable of thriving deep within the stockpile as facultative anaerobes.

Comparing the Cellular Respiration Demands of Microbes Colonizing Heap A and Heap B with Depth

This analysis tests the hypothesis that aerobic microbes prevail in shallow regions of a heap leach, whereas anaerobic microbes would dominate deeper regions. Interestingly, strictly anaerobic microbes, including *Fonticella,* rarely appeared in the dataset in deeper drill core samples; 356 feet deep in Heap A or 580 feet deep in Heap B. Instead, facultative anaerobes capable of existing in environments with and without oxygen prevail throughout all depths in both heap ecosystems (Fig. 5).

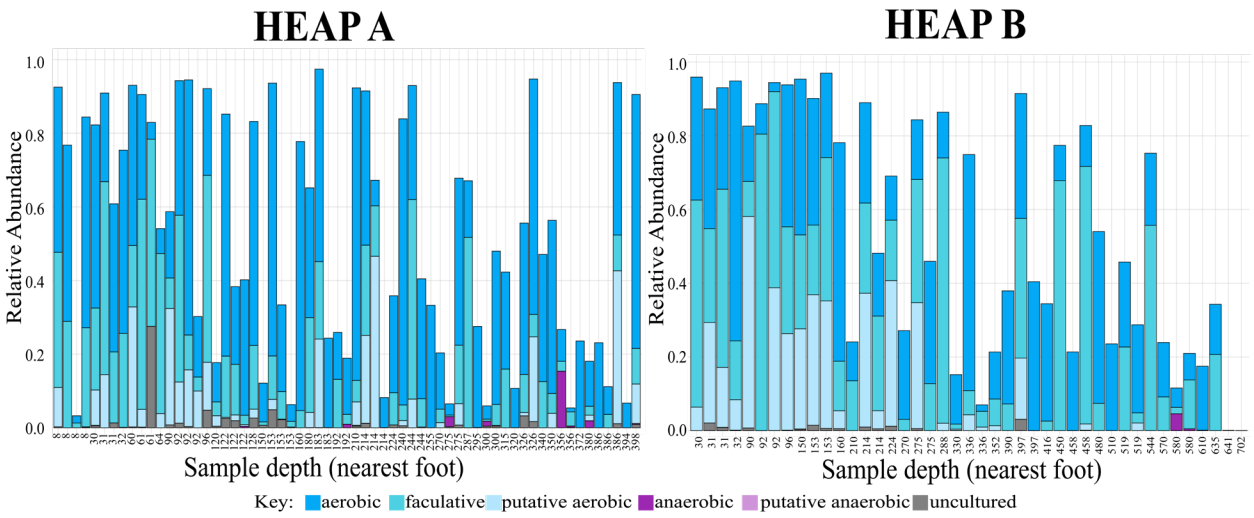

Figure 5: Oxygen requirement for cellular respiration by depth in Heap A

Finally, the prevalence of strictly aerobic microbes is high throughout both heaps across virtually all depths. This finding may reflect sufficient oxygenation without engineered air injection strategies, or at least the periodic availability of oxygen throughout the stockpile capable of supporting aerobic microorganisms.

Conclusion

This study profiles native microorganisms living in Heap A and Heap B as a function of depth. Sufficient sequencing depth across samples enabled in-depth analyses of bioleaching-relevant species and the functional annotation of taxonomy, leach-relevant metabolism, and cellular respiration. From these analyses, several clear insights emerge. Importantly, both stockpiles prevailed in iron-oxidizing microbes and contained a relative dearth of sulfur-oxidizing microbes. A diversity of microbes was observed at shallow depths, with a prevalence of *Leptospirillum* and several archaea.

Profiling the native microbiome in two heap leach ecosystems in the mine enables strategic optimization of leach chemistry. Process modifications may aim to supplement the predominantly iron-oxidizing profile with supplementations to restore a metabolic synergy throughout the stockpiles.

References

Arnulf, K. (1993). Sulfur oxidation and reduction in archaea: Sulfur oxygenase/-reductase and hydrogenases from the extremely thermophilic and facultatively anaerobic archaeon *Desulfurolobus ambivalens*. *Systematic and Applied Microbiology*, *16*(1), 16–22.

Batrakov, S. G., Pivovarova, T. A., Esipov, S. E., Sheichenko, V. I., & Karavaiko, G. I. (2002). β-D-glucopyranosyl caldarchaetidylglycerol is the main lipid of the acidophilic, mesophilic, ferrous iron-oxidizing archaeon *Ferroplasma acidiphilum*. *Biochimica et Biophysica Acta (BBA)—Molecular and Cell Biology of Lipids*, *1581*(1–2), 29–35. https://doi.org/10.1016/S1388-1981(01)00199-8

Castelle, C. J., Roger, M., Bauzan, M., Brugna, M., Lignon, S., Nimtz, M., Golyshina, O. V., Giudici-Orticoni, M.-T., & Guiral, M. (2015). The aerobic respiratory chain of the acidophilic archaeon *Ferroplasma acidiphilum*: A membrane-bound complex oxidizing ferrous iron. *Biochimica et Biophysica Acta (BBA)—Bioenergetics*, *1847*(8), 717–728.

Cava, F., Hidalgo, A., & Berenguer, J. (2009). Extremophiles, *13*(2), 213–231.

Christel, S., Herold, M., Bellenberg, S., El Hajjami, M., Buetti-Dinh, A., Pivkin, I. V., Sand, W., Wilmes, P., Poetsch, A., & Dopson, M. (2018). Multi-omics reveals the lifestyle of the acidophilic, mineral-oxidizing model species *Leptospirillum ferriphilum* T. *Applied and Environmental Microbiology*, *84*(e02091-17). https://doi.org/10.1128/AEM.02091-17Dialnet

Coram, N. J., & Rawlings, D. E. (2002). Molecular relationship between two groups of the genus *Leptospirillum* and the finding that *Leptospirillum ferriphilum* sp. nov. dominates South African commercial biooxidation tanks that operate at 40°C. *Applied and Environmental Microbiology*, *68*(2), 838–845. https://doi.org/10.1128/AEM.68.2.838-845.2002CNIB+2SpringerLink+2

Farías, R., Norambuena, J., Ferrer, A., Camejo, P., Zapata, C., Chávez, R., Orellana, O., & Levicán, G. (2021). Redox stress response and UV tolerance in the acidophilic iron-oxidizing bacteria *Leptospirillum ferriphilum* and *Acidithiobacillus ferrooxidans*. *Research in Microbiology*, *172*(3), 103833. https://doi.org/10.1016/j.resmic.2021.103833

Golyshina, O. V., Lünsdorf, H., Kublanov, I. V., Goldenstein, N. I., Hinrichs, K. U., & Golyshin, P. N. (2016). The novel extremely acidophilic, cell-wall-deficient archaeon *Cuniculiplasma divulgatum* gen. nov., sp. nov. represents a new family, *Cuniculiplasmataceae* fam. nov., of the order *Thermoplasmatales*. *International Journal of Systematic and Evolutionary Microbiology*, *66*(1), 332–340. https://doi.org/10.1099/ijsem.0.000725Bangor University

Hart, C. E., & Gorman-Lewis, D. (2025). Energetic investigations of *Acidianus ambivalens* metabolism during anaerobic sulfur reduction and comparisons to aerobic sulfur oxidation. *Extremophiles*, *29*, 19. https://doi.org/10.1007/s00792-025-01385-3SpringerLink+2CoLab+2

Hawkes, R. B., Franzmann, P. D., & Plumb, J. J. (2006). Moderate thermophiles including "*Ferroplasma cupricumulans*" sp. nov. dominate an industrial-scale chalcocite heap bioleach operation. *Hydrometallurgy*, *83*(1–4), 229–236.

Hussein, A. H., Lisowska, B. K., & Leak, D. J. (2015). Advances in applied microbiology. Elsevier.

Johnson, D. B., Kanao, T., & Hedrich, S. (2012). Redox transformations of iron at extremely low pH. *Frontiers in Microbiology*, *3*, 96. https://doi.org/10.3389/fmicb.2012.00096

Kappler, A., Bryce, C., Mansor, M., et al. (2021). An evolving view on biogeochemical cycling of iron. *Nature Reviews Microbiology*, *19*, 360–374.

Konhauser, K., & Alessi, D. (2024). Geomicrobiology: Present approaches and future directions. In L. C. Staicu & L. L. Barton (Eds.), *Geomicrobiology: Natural and Anthropogenic Settings* (pp. 1–19). Springer.

Mangold, S., Valdés, J., Holmes, D. S., & Dopson, M. (2011). Sulfur metabolism in the extreme acidophile *Acidithiobacillus caldus*. *Frontiers in Microbiology*, *2*, 17. https://doi.org/10.3389/fmicb.2011.00017

Moya-Beltrán, A., Beard, S., Rojas-Villalobos, C., Issotta, F., Gallardo, Y., Ulloa, R., Giaveno, A., Degli Esposti, M., Johnson, D. B., & Quatrini, R. (2021). Genomic evolution of the class *Acidithiobacillia*: Deep-branching Proteobacteria living in extreme acidic conditions. *The ISME Journal*, *15*(11), 3221–3238.

Sarkodie, E. K., Jiang, L., Li, K., Yang, J., Guo, Z., Shi, J., Deng, Y., Liu, H., Jiang, H., Liang, Y., Yin, H., & Liu, X. (2022). A review on the bioleaching of toxic metal(loid)s from contaminated soil and sediments by microorganisms. *Frontiers in Microbiology*, *13*, 1049277. https://doi.org/10.3389/fmicb.2022.1049277

Staicu, L. C., & Barton, L. L. (Eds.). (2024). *Geomicrobiology: Natural and anthropogenic settings*. Springer.

United Nations Conference on Trade and Development [UNCTAD]. (2025). *Global trade update (May 2025): Focus on critical minerals – Copper in the new green and digital economy*. Geneva: UNCTAD. https://unctad.org/webflyer/global-trade-update-may-2025

Vardanyan, A., Khachatryan, A., Castro, L., Willscher, S., Gaydardzhiev, S., Zhang, R., & Vardanyan, N. (2023). Bioleaching of sulfide minerals by *Leptospirillum ferriphilum* CC from polymetallic mine (Armenia). *Minerals*, *13*(243). https://doi.org/10.3390/min13020243

Vera, M., Schippers, A., Hedrich, S., & Sand, W. (2022). Progress in bioleaching: Fundamentals and mechanisms of microbial metal sulfide oxidation – Part A. *Applied Microbiology and Biotechnology*, *106*(21), 6933–6952.

Yang, B., Wang, Y., & Qian, P. Y. (2016). Sensitivity and correlation of hypervariable regions in 16S rRNA genes in phylogenetic analysis. *BMC Bioinformatics*, *17*, 135. https://doi.org/10.1186/s12859-016-0992-yPaperity+1

Zhang, L., Zhou, W., Li, K., Mao, F., Wan, L., Chen, X., Zhou, H., & Qiu, G. (2015). Synergetic effects of *Ferroplasma thermophilum* in enhancement of copper concentrate bioleaching by *Acidithiobacillus caldus* and *Leptospirillum ferriphil*. *Biochemical Engineering Journal*, 142–150.

Zhou, H., Zhang, R., Hu, P., Zeng, W., Xie, Y., Wu, C., & Qiu, G. (2008). Isolation and characterization of Ferroplasma thermophilum sp. nov., a novel extremely acidophilic, moderately thermophilic archaeon and its role in bioleaching of chalcopyrite. *Journal of Applied Microbiology*, *105*(2), 591–601. https://doi.org/10.1111/j.1365-2672.2008.03807.x

Zhou, Z., Tran, P. Q., Cowley, E. S., Trembath-Reichert, E., & Anantharaman, K. (2024). Diversity and ecology of microbial sulfur metabolism. *Nature Reviews Microbiology*, *23*(2), 122–140. https://doi.org/10.1038/s41579-024-01104-3

Appendix

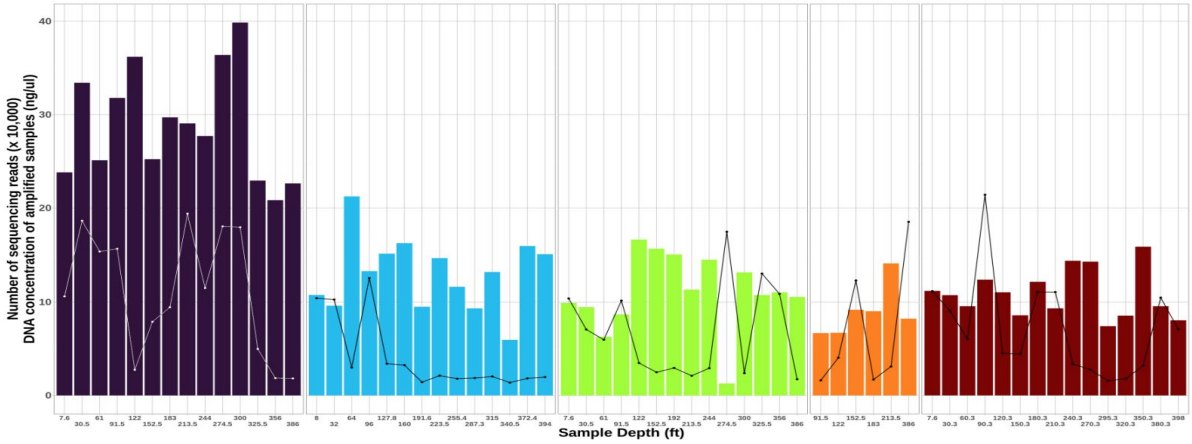

Figure A1: Amplified DNA concentration (line plot) and sequencing depth (bar plot) of samples across Heap A

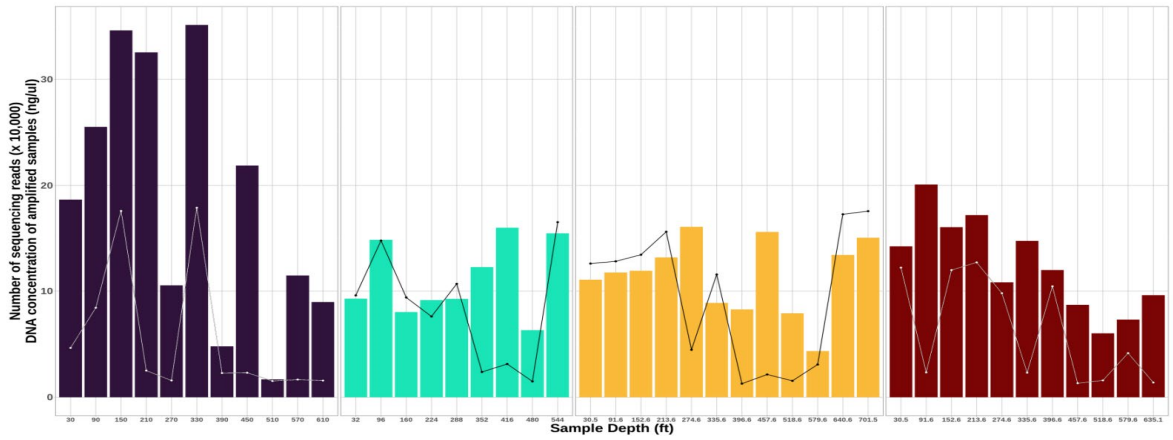

Figure A2: Amplified DNA concentration (line plot) and sequencing depth (bar plot) of samples across Heap B

Reinforcement and Stabilization of Ripios Dumps Platforms Using Leached Ripios Fill and Geocells

Sergio Pinos, Geotechnos, Chile
Guillermo Torres, Geotechnos, Chile
Sebastián Moffat, Geotechnos, Chile

Abstract

In large-scale mining operations, ensuring the stability of roads and working platforms is a major challenge due to the mechanical behavior of leaching ripios, which is often used as a construction material. This study presents the application of geocells as a reinforcement solution to enhance the load-bearing capacity and stability of infrastructure built over leaching ripios. The proposed methodology offers a cost-effective and technically feasible alternative to traditional soil stabilization methods, reducing resource consumption and execution time.

Geocells have proven to be highly effective in geotechnical engineering by confining granular materials and improving their mechanical properties. Originally developed by the US Army Corps of Engineers in the 1980s, geocells provide structural integrity by increasing shear resistance, reducing lateral displacement, and distributing loads more efficiently. The implementation of this technology aims to address the limitations of leaching ripios, which exhibit high moisture content, fine particle fractions, and low undrained shear strength.

The research involved the execution of a field trial where geocells were deployed over leaching ripios, filled with material, and compacted to form stable working platforms. Instrumentation, including pressure cells and laser displacement measurement, was used to monitor stress distribution and deformation behavior. The construction process consisted of geocell installation, filling, compaction, and load verification using a Bulldozer D9 to assess bearing capacity under operational conditions.

Results demonstrate that geocell reinforcement significantly enhances the performance of leaching ripios by reducing settlement and increasing structural stability. Saturated and highly deformable areas adjacent to the reinforced sections exhibited noticeable differences in load-bearing capacity, confirming the effectiveness of geocells in mitigating excessive deformation.

This study concludes that the use of geocells as a reinforcement system for leaching ripios is a practical and sustainable solution for mining infrastructure. The approach minimizes material replacement costs,

optimizes resource utilization, and enhances operational safety. Future research should focus on optimizing design parameters and expanding its application to other geotechnical challenges in the mining industry.

Introduction

In large-scale mining operations, roads and working platforms built over leached ripios dumps present significant challenges in terms of stability and bearing capacity. The use of geosynthetics for soil reinforcement and bearing capacity improvement has been successfully applied for several decades. In particular, the use of geocells—a three-dimensional confinement system—was initially developed by the US Army Corps of Engineers in the 1980s to improve soft subgrades for the construction of temporary roads for heavy military vehicles.

Based on the successful application of this technology in similar contexts, the use of geocell-reinforced soils is proposed to enable the passage of heavy equipment over highly deformable materials with low bearing capacity, such as those found in copper leaching ripios dumps.

This study presents a field case evaluating the use of geocells as direct reinforcement over leached ripios, with the objective of improving the stability and operational performance of working platforms subjected to heavy machinery traffic in a mining operation in northern Chile.

General

This document presents the technical aspects that support the application of geocells as a reinforcement system for soils composed of leaching ripios. It describes the functional principles of geosynthetics, with emphasis on geocells, along with the geotechnical characteristics of the ripios material and the conditions that led to the search for an alternative solution to the conventional material replacement method. Additionally, the instrumentation used, the construction procedure implemented during the field experience, and the results obtained are detailed, including a cost estimate for the solution.

Geosynthetics

Geosynthetics are materials manufactured from synthetic polymers, designed to fulfill specific functions within civil and geotechnical engineering projects. Their use has expanded significantly over the past decades due to their versatility, durability, and cost-effective technical performance. These properties have positioned them as effective solutions for erosion control, material separation, filtration, drainage, impermeabilization, and, in particular, soil reinforcement.

Since the 1960s and 1970s, geosynthetics have been employed as technical alternatives in projects where conventional methods proved costly or limited. Within this category, geocells stand out as one of the

most innovative and effective systems for improving the load-bearing capacity of soft soils, due to their ability to provide three-dimensional confinement of granular materials.

Geocells and Reinforcement Mechanisms

Geocells are three-dimensional structures composed of interconnected polymeric cells that expand to form a honeycomb-like matrix. This configuration enables the confinement of granular material within the cells, improving its mechanical performance under applied loads. Their use was initially developed by the United States Army Corps of Engineers during the 1980s, with the objective of stabilizing soft subgrades and constructing temporary roads for the passage of heavy military vehicles.

The improvement in the strength and the stiffness of the soil reinforced with the geocells has been studied using triaxial tests. Bathurst and Karpurapu (1993) carried out a series of large-scale triaxial tests on a 200 mm high isolated geocell specimen. Test results indicated a drastic improvement in the apparent cohesion with geocell reinforcement. Rajagopal et al. (1999) also performed triaxial compression tests on granular soil encased in single and multiple geocells. Both geocell reinforced and unreinforced samples exhibited the same frictional strength, but a significant increment in apparent cohesion (Cr) was observed in the reinforced case, as shown in Fig. 1. In the figure, the small circle refers to the Mohr circle of the unreinforced soil. Due to the provision of geocell reinforcement, the confining stress increases from $\sigma 3$ to $\sigma 3 + \Delta\sigma 3$. Due to which the ultimate normal stress increases to $\sigma 1$ from $\sigma 1u$.

The intermediate circle in the figure indicates the Mohr circle corresponding to this state. The same ultimate stress can also be represented with the larger Mohr circle, which has a confining pressure of $\sigma 3$ and an apparent cohesion of Cr. Researchers observed that the geocell reinforcement imparts apparent cohesive strength even to the cohesionless soil.

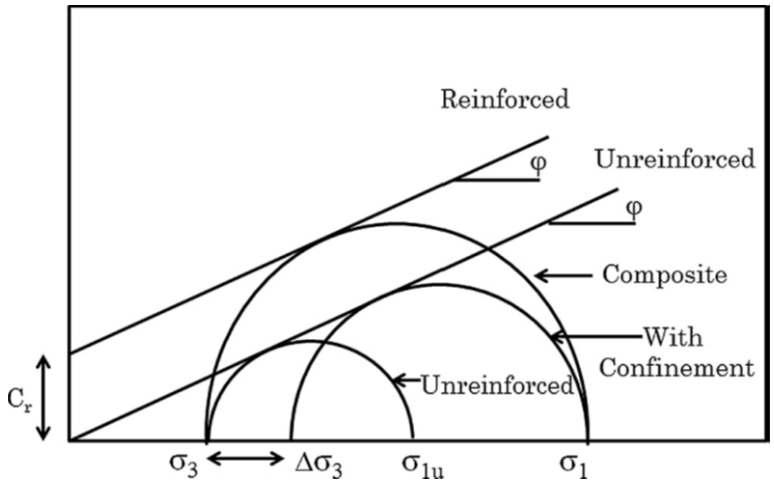

Figure 1: Mohr circle for the calculation of the apparent cohesion for geocell soil composite (source: Rajagopal et al., 1999)

The reinforcement provided by geocells is based on three main mechanisms:

1. Lateral Resistance Effect:

When a load is applied to the geocell panel, the confinement and stiffness of the infill material increase, generating a distribution of horizontal stresses between the infill and the geocell walls. The confinement effect contributes in two ways: it geotechnically enhances the infill material (in terms of strength and deformability), and it also provides better load distribution.

The passive resistance generated by the interaction between continuous cells induces a modification in the failure surface geometry, which, due to the lateral restriction of granular soil movement, tends to deepen an effect that favors the performance of the granular structure.

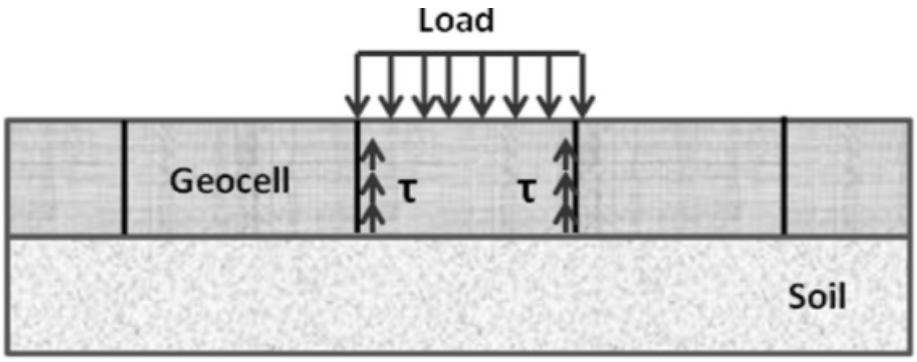

Figure 2: Lateral resistance effect (source: Hedge, 2017)

$$\Delta P_1 = 2\tau \quad (1)$$

$$\tau = P_r tan^2(45 - \varphi/2) \tan\delta \quad (2)$$

2. Vertical Stress Dispersion Effect:

Another important effect of geocells on the behavior of a pavement structure is load redistribution. By confining the granular material, an increase in the modulus and stiffness of the system is achieved, forming a semi-rigid beam or slab that absorbs stress and reduces settlements, as the load applied over a localized area is distributed over a larger area.

The load distribution area in a reinforced condition can increase up to three times compared to the initial condition of an unreinforced material. This load redistribution results in an increase in bearing capacity and a reduction in both total and differential settlements.

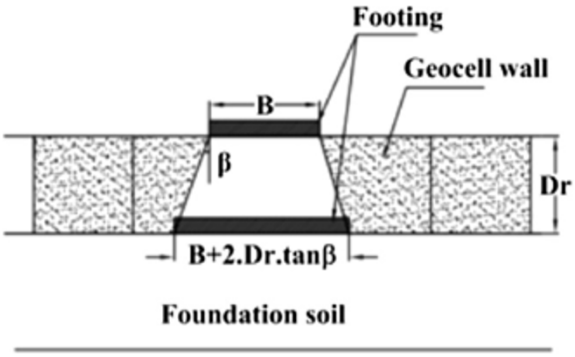

Figure 3: Vertical stress dispersion effect (source: Hedge, 2017)

$$\Delta P_2 = P_r \left(1 - \frac{B}{B+2D_r \tan \beta}\right) \quad (3)$$

3. Tensioned Membrane Effect:

The tensioned membrane effect, or beam effect, refers to the tensile force developed in the curved mattress reinforced with geocells to resist vertical loading (Rajagopal et al., 1999; Dash et al., 2004; Zhou & Wen, 2008). However, the tensioned membrane effect is mobilized when the pavement structure undergoes significant deformation (Giroud & Han, 2004a). For this reason, the reinforced section becomes stiffer than the surrounding soil, and the curved surface generates an upward reaction that helps reduce the net stress applied to the subgrade.

Although this tensioned membrane concept is typically associated with planar geosynthetics (such as geotextiles and geogrids), it also applies when geocells are installed over very soft soils. Under these conditions, it is usually necessary to include a woven geotextile to help distribute stresses more effectively.

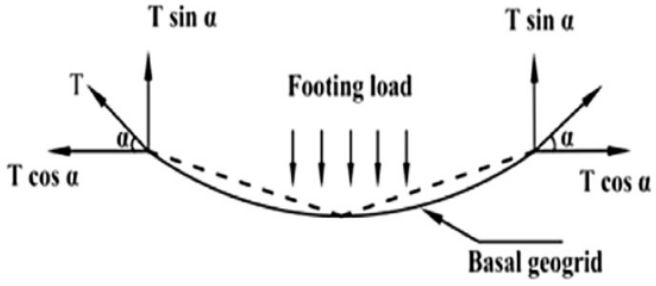

Figure 4: Tensioned membrane effect (source: Hedge, 2017)

$$\Delta P_3 = \frac{2T \sin \alpha}{B} \quad (4)$$

Use of Leaching Ripios as Fill Material

Leached ripios are the residual material remaining after the heap leaching process of minerals. When

disposed of in dumps, these materials exhibit geotechnical characteristics that differ significantly from the initial assumptions considered during the design stages. Studies conducted on deposited ripios have shown a fines content (material passing through ASTM #200 sieve) ranging from 27% to 49%, and gravimetric moisture contents fluctuating between 6.5% and 17.6%, with peak values reaching up to 22%.

These properties result in a "fluid paste" behavior during deposition, leading to gravity-driven flow downstream from the discharge point (Spreader), exceeding the flow distances considered for dump design. Consequently, the ripios exhibit low bearing capacity and high settlements, posing a risk to infrastructure installation or equipment traffic over these platforms' surfaces.

For geotechnical characterizations over these materials, exploration campaigns have been conducted using Cone Penetration Tests (CPTu), which allow the continuous profiling of strength, deformability, and stratigraphy profile. In the specific area where the field trial was conducted, CPT44 and CPT45 tests were available, describing a stratigraphy composed of a 0.5 m surface layer of very dense or stiff soil, followed by 4 to 5 meters of material predominantly composed of silts and sands. The estimated undrained shear strength (Su) for the first 5 meters ranges from 50 to 60 kPa.

Estimation of Bearing Capacity of Unreinforced Ripios

Considering that the ripios exhibit undrained behavior, the following expression has been used to estimate the ultimate bearing capacity (qf) within the first 5 meters:

$$qf = (2 + \pi)Su = 5{,}14 * Su \qquad (5)$$

with **Su**, the undrained shear strength of the ripios.

Given the criticality of the equipment and facilities for operational continuity, a Factor of Safety of 5 was considered for the allowable bearing capacity (qa), resulting in:

$$qa = \frac{qf}{5} = 51{,}4\ kPa \qquad (6)$$

Design

The reinforcement was designed to withstand the load imposed by the Spreader (90 kPa), which operates slowly and remains stationary for extended periods at different ripios deposition points. An approach analogous to the design of soil reinforcement beneath a footing was applied, following the recommendations of Hedge (2017) and Sitharam (2013), considering the contributions of both the soils and the geosynthetics to the overall bearing capacity. A satisfactory design was achieved by verifying that the vertical pressure exerted by the Spreader on the improved reinforced ripios layer does not exceed the bearing capacity of the unreinforced ripios at that depth.

Based on the above, a reinforcement scheme was defined consisting of two layers of geocells, each 30 cm in height.

Initial Conditions and Execution of Works

The location selected for the execution of the trial was defined by the mining company with the objective of representing unfavorable geotechnical conditions within the ripios dump. As an initial preparation, 1.5 meters were excavated, and the first 0.35 meters were backfilled with low moisture ripios.

This initial backfills allowed for the formation of a horizontal and sufficiently resistant surface to proceed with the assembly of the geocell system. This stage was key to ensure the proper performance of the reinforcement, facilitating both the construction process and the compaction of material in the upper layers.

Installation of Pressure Cells (Instrumentation)

To estimate the distribution of pressures generated by the load applied on the reinforced ripios layer, three Geosense pressure cells, model SGTPC-4020, with a measurement range of up to 700 kPa, were installed.

The installation of each cell involved a localized excavation in the ground, over which a layer of sand was placed to serve both as a bedding and cover for the cell, ensuring uniform contact and preventing stress concentrations.

Deployment, Filling, and Connection of the First Geocell Layer

Over the initial 0.35 m layer of low moisture ripios, the first geocell layer was installed. The geocells used in this layer were of the type PRS Neoloy 660-300-C-28PS. These are perforated, have a height of 30 cm, and a welding distance of 660 mm.

Once installed, the geocells were filled. The ripios used as fill material behaved as granular soils due to their moisture content. Three samples were taken directly from the material transported by trucks to the test site, which were subsequently tested.

The moisture content results obtained are presented below:

Table 1: Moisture Content Results of Ripios Used as Fill Material in Geocells

Sample	Moisture [%]
Sample 1	7,07
Sample 2	7,11
Sample 3	7,56

These results indicate an average moisture content of 7,2%.

In this first geocell layer, the reinforced ripios exhibited good performance, allowing the excavator to position itself directly on the filled cells and proceed with its movement until the entire panel was completed.

Compaction of Fill and Placement of Ripios Layer over the First Geocell Layer

The good performance of the reinforced ripios layer allowed the use of a 10.55-ton Caterpillar CS54B compactor roller. Six passes were carried out at each point, using high frequency in the central area and low frequency along the edges of the fill.

According to the reinforced ripios scheme, a 0.3 m layer of ripios was placed over the first geocell layer. This fill was successfully placed using a Caterpillar D8T bulldozer. After spreading the material, it was compacted with the same roller, operating at high frequency across the entire fill area.

Deployment, Filling, and Connection of the Second Geocell Layer

Over the 0.3 m ripios layer, the second geocell layer was installed. The geocells used in this layer were of the type PRS Neoloy 445-300-C-40PS. These are perforated, have a height of 30 cm, and a welding distance of 445 mm.

This geocell layer was filled with low moisture ripios using the Caterpillar D8T bulldozer. The process was quick and encountered no difficulties.

Compaction of Fill in the Second Geocell Layer

Before compacting the fill, a motor grader was used to trim the excess material.

For the compaction of the second geocell layer fill, a 10.55-ton Caterpillar CS54B compactor roller was used. Six passes were carried out at each point using high frequency.

Upon completion of the compaction, the surface appeared compacted and level. With this final activity, the reinforced ripios structure was ready for the 50-ton Caterpillar D9 bulldozer pass test and the corresponding measurements.

Results

Performance of the Solution

To technically evaluate the performance of the reinforced ripios, three pressure cells and a laser level were used. The pressure cells were intended to determine the load transmitted at depth and to assess the effect of the reinforced ripios system on vertical load transfer. The laser level was used to measure the displacements affecting the reinforced ripios system as a result of surface-applied loads.

It is worth noting that the good performance of the reinforced ripios system was already evident during the construction process.

Pressure Cell Results

Based on the pressure cell readings, a reduction of approximately 40% to 45% in the load applied by the Caterpillar D9 bulldozer at the surface (pressure cell SG00802) can be observed when compared to the

second pressure cell (SG00801). The third pressure cell did not register significant load changes, indicating that most of the load is absorbed by the reinforced ripios system, as shown in the following image.

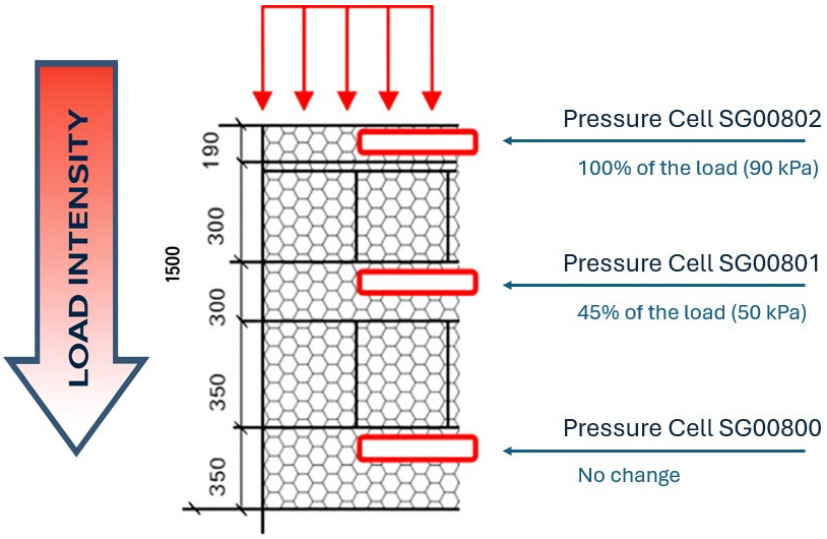

Figure 5: Reduction of load intensity with depth (source: author's own work)

The measurements obtained were compared with theoretical estimates of pressure reduction at depth due to the inclusion of geocells in the reinforcement system. The following figure presents this comparison graph.

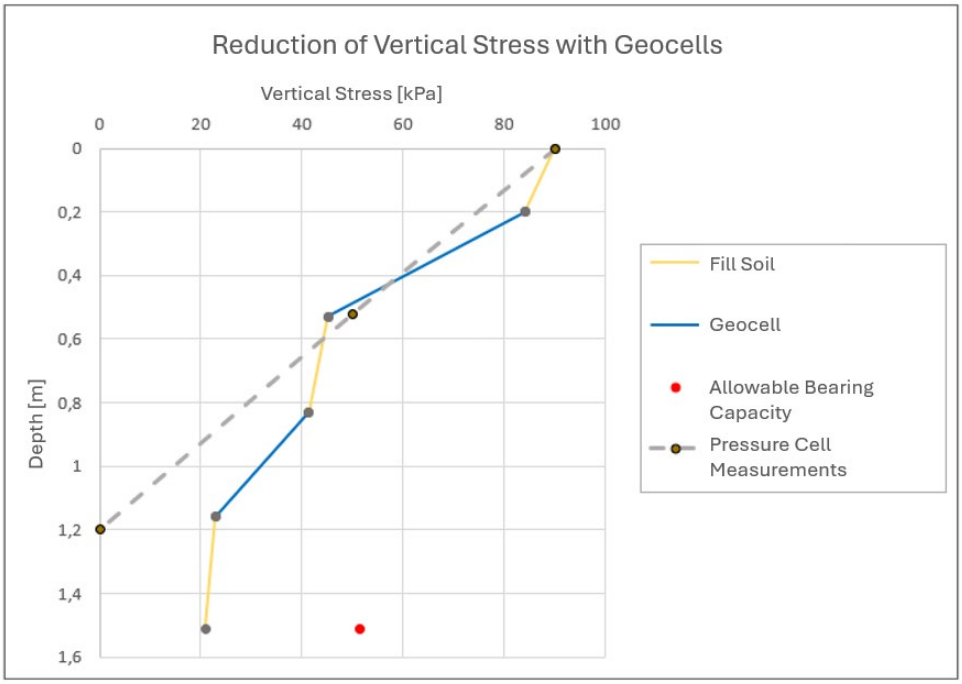

Figure 6: Comparison of vertical pressure measurements with theoretical estimation (source: author's own work)

In the previous figure, the reinforced ripios section was identified as “Fill Soil” (unreinforced ripios) and “Geocell” (ripios reinforced with geocells). The allowable bearing capacity at that depth is also included.

Based on the data, a Factor of Safety of 2 was obtained for the bearing capacity at the elevation corresponding to the start of the geocell-reinforced ripios.

Additionally, the theoretical estimates at the depths of the first two pressure cells align well with the measured results. The last and deepest pressure cell did not record any pressure change; however, a pressure of approximately 20 kPa was expected at that depth.

Displacement Measurement Results

To determine the potential settlements caused by the load applied to the surface of the reinforced ripios system, the vertical displacement of the D9 bulldozer was measured using a laser level with 0.5 mm precision and a measurement rod attached to the body of the machine.

More than 20 passes of the bulldozer were conducted, with the first measurement taken at the beginning and subsequent readings recorded every five passes. The results are shown in Table 2, where the effective vertical displacement recorded for the reinforced ripios system was 2 cm.

Table 2: Record of Vertical Displacement Measurements

Measurement	Settlement (cm)
Initial	–
5 passes	0,5
10 passes	1,0
15 passes	2,0
20 passes	2,0

As a reference, the mining company reported settlements exceeding 30 cm in the case of the traditional solution, which involves replacing ripios with mine waste. This comparison highlights a substantial improvement in deformation control through the geocell solution filled with low-moisture ripios.

Comparison between the Proposed Solution and the Current System Used by the Mining Company

Due to the high content of fines and moisture in the ripios, the material has low strength for supporting equipment movement and infrastructure installation. Therefore, to ensure bearing capacity in specific areas of the dump, a proceeding has been implemented involving the excavation of trenches 2.1 m deep and 10 m wide over the dump surface, replacing them with coarse, low-moisture mine waste. This activity is carried out over a total length of 5,000 m. The current road construction approach is highly resource and time-intensive.

The proposed solution, using geocells filled with the same ripios from the dump, increases bearing capacity while reducing execution time and the costs associated with transporting and placing large volumes of mine waste. In the proposed reinforcement solution, the excavation depth is reduced to 1.5 m instead of the 2.1 m currently excavated. Figure 7 compares the distribution of vertical stresses between the geocell-reinforced solution and the unreinforced condition.

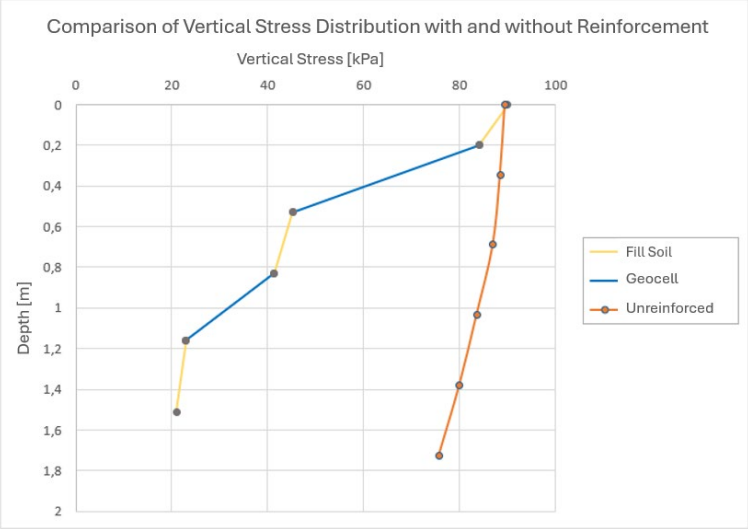

Figure 7: Comparison of vertical stress distribution with geocell-reinforced ripios ("geocell") and without reinforcement (source: author's own work)

In the previous figure, the reduction of stresses transmitted to the underlying ground is clearly observed, attributable to the confinement and redistribution effect provided by the geocell system.

Cost Estimation

The following section details the cost estimation for the two layers of geocells reinforced with ripios, including direct and indirect costs. The calculation is summarized in Table 3.

Table 3: Summary of Costs

Item	Unit	U.P.
Supply of Geocells (2 layers)	USD/m²	6,74
Supply of Geotextile	USD/m²	1,26
Transport of Geocells	USD/m²	0,42
Transport of Geotextile	USD/m²	0,28
Geocells Installation (labor)	USD/m²	2,70
Geotextile Installation (labor)	USD/m²	1,00
TOTAL	**USD/m²**	**12,39**

The total price for this solution is $12,39 USD/m².

Conclusion and Recommendations for Future Work

After performing the field tests and reviewing the results, the following conclusions were reached:

- The use of geocells filled with the same leaching ripios makes possible the transit of heavy equipment on saturated soils, highly deformable, and with low bearing capacity.
- The use of ripios with a lower moisture content than that of deposition moisture causes it to behave as a granular soil that allows the geocells to be filled without difficulty and allows a good level of compaction of the backfill to be achieved.
- The use of geocells implies considerable savings in the use of materials (selected soils) and transportation and machinery costs for their placement.
- The results obtained allow validation of the design and construction method of the proposed solution, achieving the objective of increasing the bearing capacity of the ripios for the loads tested, with minimum settlement and simple logistics.
- Cost estimate of the solution is in the order of 12,4 USD/m^2, which should be compared with the cost of conditioning the ripios dump surface with alternative solutions.
- For this test configuration, the highest cost is over geocells, so if reducing layers to a single one or proposing different geocells and geosynthetics combined configuration could significantly reduce the costs.

The results obtained from pressure cell measurements, displacement records, and field observations allow us to conclude that the solution using geocell-reinforced ripios satisfactorily meets the requirements for creating safe and stable operational roads and platforms, capable of supporting the movement of heavy equipment and the installation of mining infrastructure.

Regarding future work, the positive results allow for potential optimizations in the design of the reinforced ripios system, mainly focusing on modifying the configuration by combining a single geocell layer with a geogrid layer. Implementing this alternative would impact installation productivity as well as reduce construction costs and, subsequently, time saving.

References

Bathurst, R. J., & Karpurapu, R. (1993). Large scale triaxial compression testing of geocell reinforced granular soils. *Geotechnical Testing Journal.*

Dash, S. K., Rajagopal, K., & Krishnaswamy, N. R. (2004). Performance of different geosynthetic reinforcement materials in sand foundations.

Giroud, J. P., & Han, J. (2004a). Design method for geogrid-reinforced unpaved roads. I: Development of design method.

Hegde, A. (2017). Geocell reinforced foundation beds–past findings, present trends and future prospects: A state-of-the-art review.

Hegde, A., & Sitharam, T. G. (2013). Design and construction of geocell foundation to support embankment on settled red mud.

Rajagopal, K., Krishnaswamy, N. R., & Madhavi Latha, G. M. (1999). Behaviour of sand confined with single and multiple geocells.

Zhou, H., & Wen, X. (2008). Model studies on geogrid- or geocell-reinforced sand cushion on soft soil.

Recent Developments in the Heap Leaching of Chalcopyrite Ores

D.N. Nxumalo, Mintek, South Africa
S.W. Robertson, Mintek, South Africa

Abstract

The global copper industry is facing increasing pressure to develop economically viable and environmentally responsible methods for the extraction of copper from low-grade and refractory ores. This has led to a substantial growth in the number of heap leach operations over the past decades. However, chalcopyrite, an abundant copper source, is currently not amenable to heap leaching at ambient conditions due to passivation of the mineral surface. Several technologies have been developed to overcome this challenge. These include microbial-assisted heap leaching with internal heat generation or external heating. Additionally, heap leaching processes utilizing acidic chloride medium have also been developed for both secondary and primary copper sulfide ores. Despite these advancements, several challenges remain, limiting commercial application to date. This paper provides a brief review of existing processes and presents a new Mintek-developed process that integrates an acidic chloride medium with external heating. The innovative lean solution application approach overcomes obstacles commonly associated with chloride heap leaching processes, such as the high copper inventories and high heating costs. For example, whereas existing processes recycle 5 g/L Cu over the heaps, the new process only requires 0.5 g/L Cu. Also, the capital cost for heating can be reduced from USD 18 million to USD 1.5 million for a heap processing 2 million tons per annum.

Introduction

The rising global demand for copper has intensified the need to develop effective methods for extracting the metal from low-grade and refractory chalcopyrite ores, which are not amenable to traditional leaching methods. Major producers, including BHP Group, Antofagasta PLC, Rio Tinto (through its Nuton™ venture), and Freeport-McMoRan, are actively advancing sulfide leaching technologies to unlock these challenging and previously inaccessible copper resources. Among the various approaches under investigation, microbial-assisted and acidic chloride heap leaching have emerged as the most promising strategies to overcome the kinetic and passivation limitations associated with traditional leaching methods.

Microbial-Assisted Heap Leaching

Microbial-assisted leaching has been demonstrated to enhance copper recovery from chalcopyrite ores, particularly under thermophilic conditions. Operating at temperatures typically above 50°C and up to 85 °C has been shown to effectively overcome surface passivation, thereby enabling accelerated leach kinetics and higher copper recoveries (Dew et al., 2011). In heap configurations, the elevation of temperature is achieved and maintained through self-heating, driven by the exothermic oxidation of sulfide minerals within the ore body. The process relies on thermotolerant microbial consortia that catalyze sulfide mineral oxidation through two primary mechanisms:

1. The microbial regeneration of ferric iron (Fe(III)), which is the primary oxidant by the oxidation of ferrous iron (Fe(II)) in the ore, and
2. The direct oxidation of sulfur, which generates exothermic heat, further enhances the rate of mineral leaching.

Although the microbial self-heating process has been demonstrated on a pilot scale (Robertson et al., 2007; Dew et al., 2011), it was subject to a number of problems, including

- poor air permeability,
- long pH reduction periods (for high acid-consuming ores),
- the need for microbial succession,
- insufficient pyrite (the main sulfide source) in the ore, and
- the negative effect of high sulphate concentrations and other impurities such as chloride on the microbial activity.

As a result, this process has found limited commercial application.

Among recent advancements is Rio Tinto's Nuton™ technology (Gleeson, 2022b), which has been reported to achieve copper recoveries above 80% from chalcopyrite ores using a high-temperature, microbial-assisted heap leaching process. However, the specific operational conditions underpinning these results have not been publicly disclosed. Another notable development is Jetti Resources' proprietary catalytic technology, which was reportedly proven to disrupt the passivation layer on chalcopyrite surfaces at a commercial scale (Kuykendall, 2022).

Acidic Chloride Heap Leaching

Acidic chloride leaching has gained increasing attention as a promising alternative to conventional sulphate-based processes for the treatment of chalcopyrite ores. Chloride media offer several advantages, including enhanced solubility of metal-chloride complexes, improved oxidation kinetics, and the suppression of passivating surface layers that typically hinder leaching efficiency.

Notable acidic chloride heap leaching processes include BHP's SaL (Simple Approach to Leaching) process, which employs a single leach circuit and avoids the need to separate the chloride-rich oxide leach liquor from the cleaner process water typically required in microbial-assisted circuits (Rautenbach, 2015; Moore, 2023). In this approach, chloride concentrations are elevated to levels above 40 g/L, primarily due to the leaching of atacamite [$Cu_2Cl(OH)_3$] naturally present in the ore.

Another example is Antofagasta PLC's Cuprochlor® process, which uses a chloride-based leach environment at ambient conditions, suitable primarily for secondary copper minerals. A high-temperature variant, the Cuprochlor-T® process, operating at 30ºC to 70ºC, was also developed specifically to leach primary copper sulfides such as chalcopyrite. The Cuprochlor-T® process has been reported to achieve copper recoveries above 70% after 200 days in a 40,000-tonne test heap. Agglomeration is performed with calcium chloride ($CaCl_2$) and intermediate leach solution (ILS). A crush size of 80% passing 12 mm to 80% passing 3 mm is recommended (Gleeson, 2022a; Moore, 2022; Gutierrez & Cortes, 2017). High copper feed concentrations (typically 5 g/L) are employed in the Cuprochlor® and SaL processes and are achieved by recycling pregnant leach solution (PLS) or ILS over the heaps (Lopez, 2021; Rautenbach, 2015). Chloride-based systems also offer operational flexibility, as chloride-rich solutions can be sourced from seawater or industrial brines, supporting their applicability in arid regions where freshwater availability is limited. Ongoing research is focused on optimizing temperature, redox potential, and reagent management to further advance the industrial viability of chloride-based heap leaching.

Mintek has developed an innovative process that integrates an acidic chloride medium with external heating, effectively addressing challenges typically associated with existing chloride leaching processes, namely:

1. High copper inventories
2. High energy costs associated with external heating
3. High acid consumption associated with acid additions during cure and irrigation.

Mintek's Acidic Chloride Leach Process

Experimental

Test work was conducted to develop a process for heap leaching of low-grade refractory (chalcopyrite) copper ores. The concept was tested on a Southern African copper ore, with a head grade of 1.05% Cu, comprising primarily chalcopyrite (98.5%) in 1 m, 97 mm ID, water-jacketed columns.

The feed material was crushed to 100% passing 6.7 mm and agglomerated with 16 kg/t sodium chloride (NaCl) and 4 kg/t sulfuric acid (H_2SO_4), and synthetic raffinate solution, and cured for 30 days. The ore was irrigated with synthetic raffinate solution, simulating solutions from the barren pond, or process

water, brine (e.g., produced from reverse osmosis of seawater), or seawater, to which H2SO4 and a chloride salt (e.g., NaCl, MgCl2, KCl, or $AlCl_3$) are added. The adjusted feed solution (lixiviant) contains Cu (0.1-1 g/L), Cl^- (20-90 g/L), Fe (0-20 g/L), and H_2SO_4 (0-50 g/L). The copper concentrations are much lower than the typical levels used in the Cuprochlor® and SaL processes (5 g/L).

The process utilizes a lean solution application strategy, with external heating of the leach solution to achieve heap temperatures of 30°C to 50°C. External heating can be achieved through various methods, including solar heating and steam heating.

Figure 1: Mintek's 1 m column leach facility

Summary of Key Results

A summary of the key results is presented in Figures 2 to 4, highlighting copper dissolutions, PLS pH and redox, copper and iron concentrations, and acid consumption profiles under varying reagent and temperature conditions.

Figure 2 demonstrates a strong dependence of copper dissolution rates on temperature, with 87% copper dissolution achieved at 40°C after 575 days. Although the leach cycle is relatively prolonged, it is anticipated that lower head grades would correspond to shorter leach durations under comparable thermal conditions.

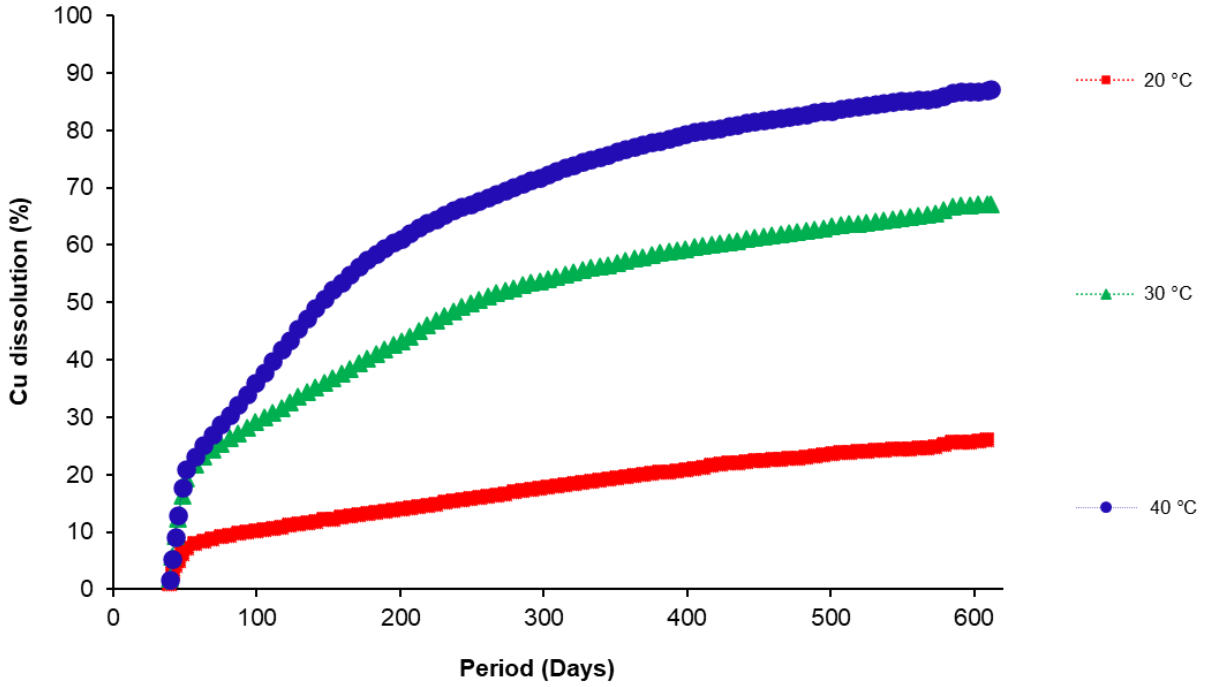

Figure 2: Effect of temperature (10 g/L H_2SO_4, 0.5 g/L Cu, 3 g/L Fe $^{3+}$, 7 g/L Fe $^{2+}$ and 90 g/L Cl^-)

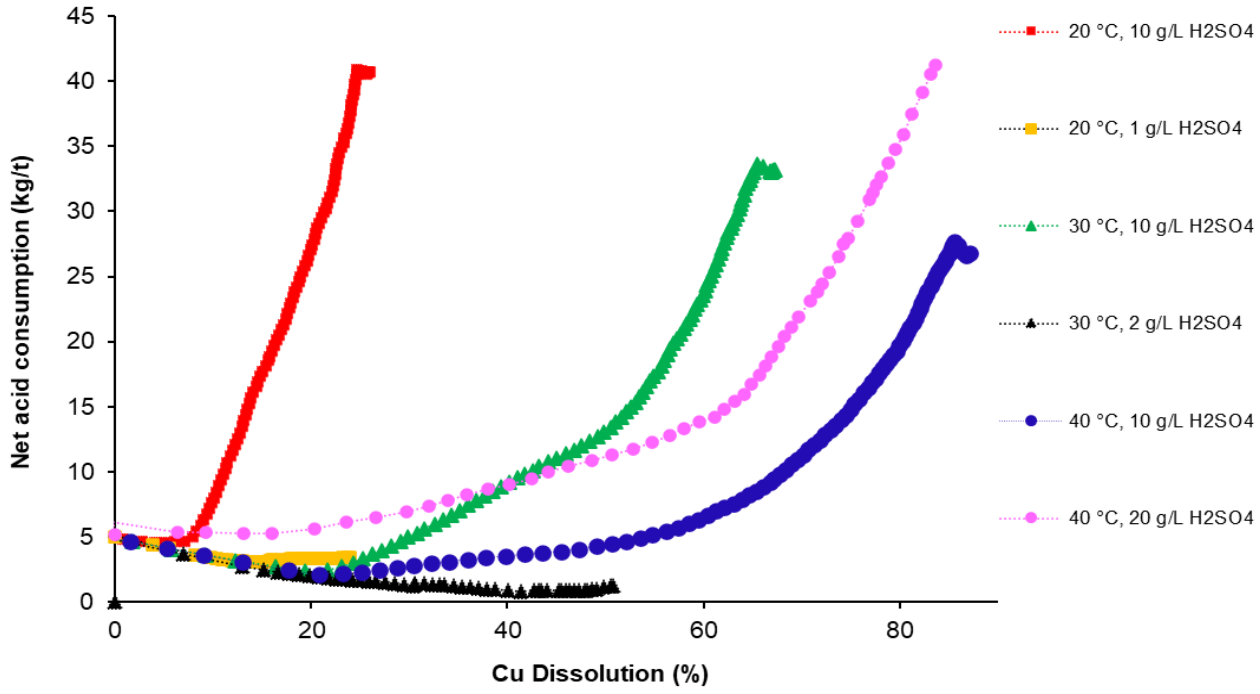

Figure 3: Net acid consumption profiles (0.5 g/L Cu, 3 g/L Fe $^{3+}$, 7 g/L Fe $^{2+}$ and 90 g/L Cl^-)

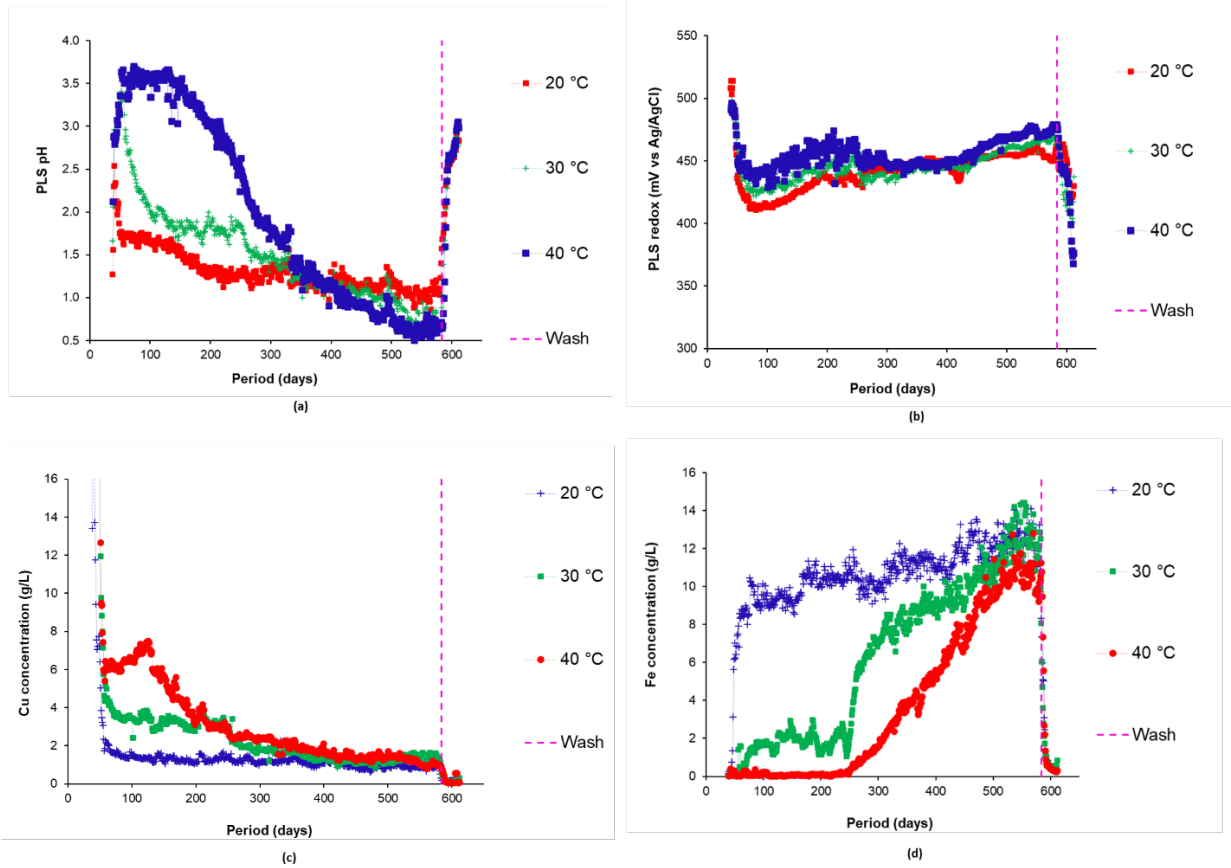

Figure 4: PLS (a) pH, (b) redox, (c) copper, and (d) iron concentration profiles (10 g/L H_2SO_4, 0.5 g/L Cu, 3 g/L Fe $^{3+}$, 7 g/L Fe $^{2+}$ and 90 g/L Cl^-)

The copper dissolution rates showed limited sensitivity to variations in feed acid concentration; however, lower acid concentrations led to a noticeable reduction in overall acid consumption, indicating potential for significant cost savings and improved reagent efficiency in large-scale operations.

In comparison to the SaL and Cuprochlor®-T processes, the lean solution application approach in the Mintek process results in substantial reductions in heating requirements and associated costs. For example, the heat load and capital cost of the solar plant can be reduced from USD 18 million to below USD 1.5 million for a plant treating 2 million tonnes per annum of ore.

Conclusion

Recent developments in the heap leaching of chalcopyrite ores have demonstrated significant progress in overcoming traditional limitations such as slow copper recovery rates. These developments reflect ongoing efforts across the mining sector to advance processing technologies. While challenges remain in optimizing long-term performance, the progress offers promising pathways for economically processing low-grade ores.

The results presented in this paper demonstrate the potential of the Mintek process, which is both robust and conceptually simple, offering advantages such as:

- Operating at higher pH levels (< 4) significantly reduces acid consumption compared to bioleaching.
- Substantially lower chloride concentrations than ambient-temperature processes such as BHP's SaL process.
- Lower operating temperatures compared to bioleaching (40°C vs. above 50°C).
- Significantly lower heating costs compared to other processes, from approximately USD 18 million to USD 1.5 million for a 20 Mtpa heap at 40°C.

Acknowledgments

The authors gratefully acknowledge Mintek for its financial support and for granting permission to publish the results presented in this paper. Appreciation is also extended to the Mintek Biometallurgy Division's operational support team for their high standard of technical work, and to Tshedza Mpfuni, Virginia Mathisa, Thokozani Gwala, and Neo Motlhake for their significant individual contributions throughout the study.

References

Dew, D. W., Rautenbach, G. F., van Hille, R. P., Davis-Belmar, C. S., Harvey, I. J., & Truelove, J. S. (2011). High temperature heap leaching of chalcopyrite: Method of evaluation and process model. In *Proceedings of the Percolation Leaching: The Status Globally and in Southern Africa Conference* (pp. 201–220). The Southern African Institute of Mining and Metallurgy.

Gleeson, D. (2022a, July 13). Antofagasta readies primary sulfide leaching technology options. *International Mining*. https://im-mining.com/2022/07/13/antofagasta-readies-primary-sulfide-leaching-technology-options/

Gleeson, D. (2022b, October 14). Rio Tinto's Nuton ready to leverage its leaching R&D legacy. *International Mining*. https://im-mining.com/2022/10/14/rio-tintos-nuton-ready-to-leverage-its-leaching-rd-legacy/

Gutiérrez, A. B., & Cortes, G. T. (2017). Process for the improvement of copper leaching processes using calcium chloride. US Patent No. US2017/0335428 A1.

Kuykendall, T. (2022, April 13). Holy grail of copper mining can unlock metal from waste stream – Jetti CEO. *S&P Global Market Intelligence*. https://www.spglobal.com/market-intelligence/en/news-insights/articles/2022/4/holy-grail-of-copper-mining-can-unlock-metal-from-waste-stream-8211-jetti-ceo-69761126

Lopez, M. J. (2021, July 17). *Proceso de lixiviación clorurada para sulfuros de cobre, carreras técnicas* [Video]. YouTube. https://www.youtube.com/watch?v=ZjDTVqobFYQ

Moore, P. (2023, August 22). BHP goes full steam ahead on full SaL leaching technology study at Escondida. *International Mining*. https://im-mining.com/2023/08/22/bhp-goes-full-steam-ahead-on-full-sal-leaching-technology-study-at-escondida/

Rautenbach, G. F. (2015). Heap leaching of copper. Patent WO2015059551 A1.

Robertson, S. W., van Staden, P. J., Vercuil, A., Glover, G., & Shaidaee, B. (2007). Heap bioleaching of low-grade chalcopyrite ore from the Darehzare deposit. In *Proceedings of the ALTA 2007 Conference*. Perth, Australia.

Chapter Two

Heap Leach Hydrology

X-Ray Tomography of Heap Leach Columns to Evaluate Pore Network Properties

Aaron Young, University of Utah, USA
Jiaqi Jin, University of Utah, USA
Rosalia Jaramillocherrez, University of Utah, USA
W. Pratt Rogers, University of Utah, USA

Abstract

Modeling run-of-mine (ROM) pore network properties within heap leach material is particularly difficult because of the challenge of validating and calibrating porosity models. This paper investigates a novel method for evaluating pore network properties from within a ROM heap leach pile. This method involves drilling and sampling composites from drill cuttings of a ROM leach pad, packing representative leach columns from the samples, compressing the samples using proprietary techniques to their corresponding interval pressures, and performing numerous analyses along each step of the process. In addition to sample characterization tests, particle size distribution (PSD) analysis and compression data, High-resolution X-ray Computed Tomography, image processing and analysis, and flow simulation using Lattice Boltzmann Method (LBM) were performed on the samples both before and after compressions. Decreases in void space and porosity were observed to increase at depth. Surprisingly, total compressive displacement of the samples was primarily dependent on the concentration of fines in the interval particle size distribution (PSD) instead of on the total force applied to the sample to simulate the interval depth. Future work will involve developing a diffusion model that matches the data observed.

Introduction

Field studies have demonstrated for decades that flows in heaps and dumps will concentrate into preferred pathways over time (Fala et al., 2005). Development of a diffusion model to match field observations is crucial for understanding and predicting these preferential flow patterns (Gerke, 2006). Traditional diffusion modeling of heap leach behavior often relies on assumed porosity distributions due to limited data on in-situ pore structures (Gbor & Jia, 2004), especially for run-of-mine (ROM) material where particle size is heterogeneous (van Staden & Petersen, 2021). Despite advances in evaluation techniques, directly measuring characteristic distributions of an operational heap is highly challenging. Therefore, laboratory

work is required to confirm, calibrate, and validate not only field measurements, but also backfill data in modeling efforts (Young & Rogers, 2022).

Laboratory XCT methods have been widely applied for heap leach material characterization, but a consistent challenge is balancing the field of view with spatial resolution (Miller & Lin, 2004; Erskine et al., 2024). In a study from over twenty years ago (Miller & Lin, 2004), the XCT voxel size used to scan a 6-inch diameter leach column was 0.624 mm, with a field of view of 160 mm. A more recent study scanned 6-inch leach columns with a 100 µm voxel size and 4-inch leach columns with a 68 µm voxel size (Erskine et al., 2024). The characteristics of the pore network, including porosity, pore size distribution, pore connectivity, and simulated permeability using the Lattice Boltzmann Method (LBM), have been quantitatively analyzed.

Additionally, to simulate in-situ conditions, several research groups have coupled XCT with loading systems. For example, miniature triaxial rigs have enabled real-time CT imaging of sands under shear and compression (Cheng & Wang, 2021), while high-pressure oedometer setups have been used to track particle crushing and void evolution up to 79 MPa (Al Mahbub & Haque, 2016; Zhao et al., 2019). In rock mechanics, synchrotron triaxial rigs such as HADES (Renard et al., 2016) and Mjölnir (Butler et al., 2020) have demonstrated that porosity, permeability, and other characteristics can be imaged continuously under simulated in-situ conditions. Building on these advances, this study applies an XCT-compression framework specifically to ROM heap leach materials, where the influence of fines on compressibility has not yet been investigated.

The objective of this study was to evaluate how pore networks evolve under stress from the conditions created due to compression in ROM heap leach material, and to test the hypothesis that fines concentration, rather than applied stress alone, is a key driver of compressive displacement and pore collapse.

Methodology

Figure 1 illustrates the methodology used in this study. Each step is also described in its corresponding subsection. The approach illustrated in Figure 1 provides a controlled environment for replicating and analyzing the complex conditions within a heap. By utilizing drill cuttings, compression testing, and advanced XCT imaging, this method enables a detailed examination of pore network evolution under varying depths and compression levels. This study aims to establish correlations between compressibility and porosity while validating the laboratory findings against observations from operational heaps and computer models.

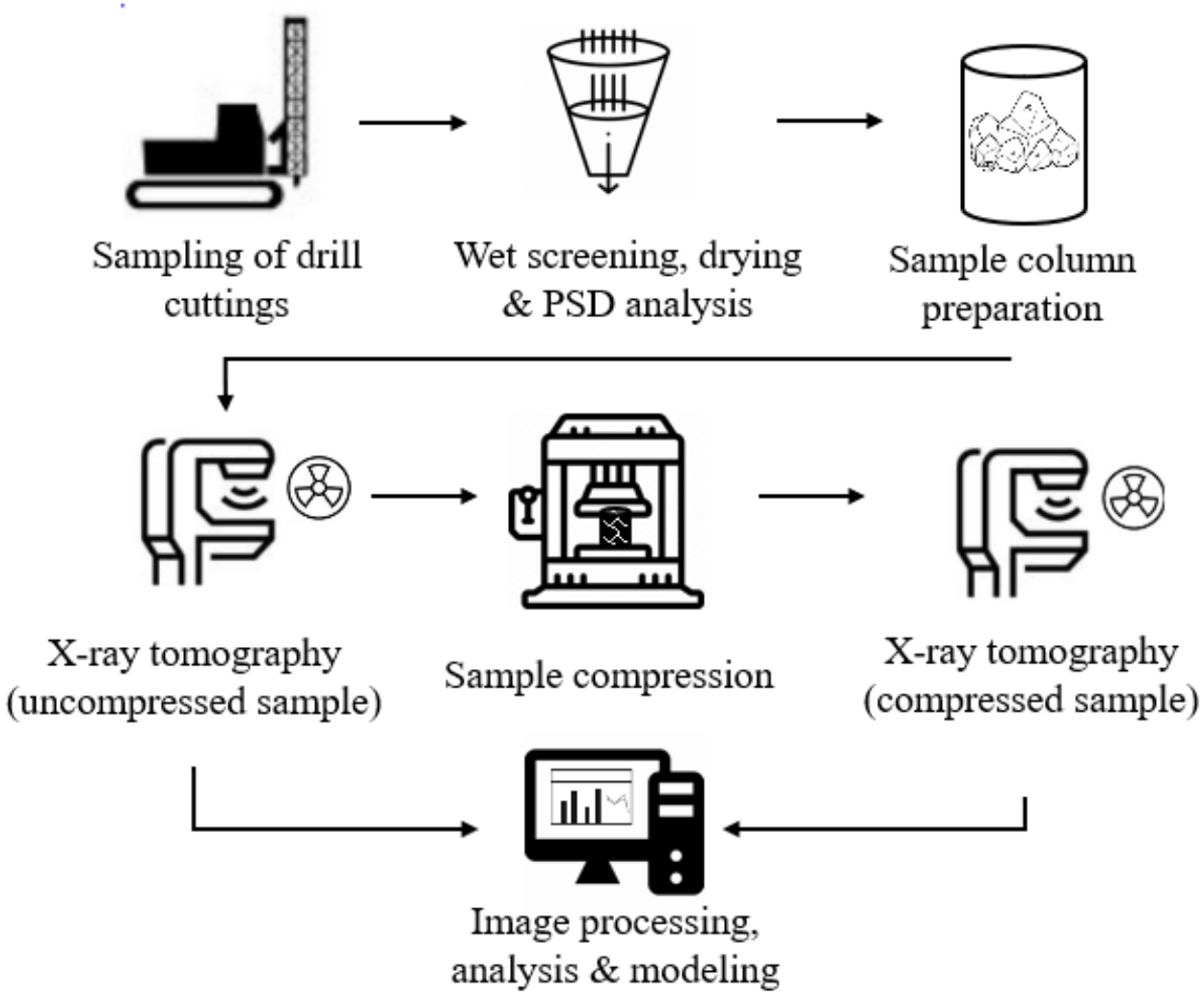

Figure 1: Schematic workflow of study method

Sampling and Compositing

Samples were collected from reverse circulation (RC) drilling of an operational ROM leach pad. RC methods can break coarse fragments into smaller sizes, potentially biasing fines content. To mitigate this, composite samples were compared against known PSD estimates from the ROM; similarities suggest the bulk distribution was largely preserved.

Drill cuttings were composited into depth intervals of 70 ft to create representative samples that reflect the PSD and lithological variation at each depth interval within the heap. For simplicity, the samples are named based on their depth interval, i.e., the sample named 0–70 represents material that is in the top 70 ft of the heap, sample 70–140 is material that is located at a depth of 70 ft to 140 ft below the surface of the heap, etc.

Screening, Drying, and Particle Size Analysis

Prior to compression, samples underwent comprehensive characterization, including wet screening at 100 mesh, filter pressing, drying overnight, and particle size analysis by dry screening. The composite samples were reconstructed into 4-inch-diameter laboratory-scale leach columns. The columns were made of Polyvinyl chloride (PVC) pipe, a PVC base endcap, and a 3.95 in steel disk.

Leach Column Reconstruction and Compression Testing

A custom compression apparatus applied vertical loads equivalent to estimated overburden pressures corresponding to heap depths. At this stage, detailed schematics and photographs of the proprietary compression rig are not provided. The focus of this paper is on demonstrating the novel experimental concept, with apparatus details to be reported in forthcoming methodological publications once the design is finalized. The system consisted of a rigid cylindrical housing that confined the column laterally, upper and lower platens to transmit load, and an actuator capable of maintaining constant stress over extended periods. The apparatus was designed to ensure uniform vertical loading and minimal lateral deformation, consistent in style with common oedometer test conditions.

Vertical loads applied by the custom apparatus were calculated to simulate overburden stresses using an assumed bulk unit weight of 22.6 kN/m³ and depth intervals of 70 ft. Overburden stress σv was estimated as $\sigma v = \gamma \times h$, where γ is the unit weight and h is the depth. Lateral stresses were neglected. Calibration of the load frame was performed against a certified load cell with ±2 % accuracy, and displacements were tracked continuously using an integrated displacement gauge.

High-Resolution X-Ray Computed Tomography (XCT)

Samples were scanned using XCT both before and after compression. The scanning protocol used a voxel size of 66.5 µm for the field of view of about 4 inches, allowing for detailed visualization of void spaces and solid particle configurations. Figure 3 (top) shows the sample setup inside the Zeiss Xradia 620. The yellow arrows represent the X-ray path, and the green box marks approximately the volume of the leach column imaged by XCT. Figure 2 (bottom left) is a project image of the column, and Figure 2 (bottom right) is the reconstructed 3D image for this section of the leach column.

Two sections per leach column were scanned to increase the volume of the leach column characterized by 3D imaging. These two sections have been named “upper” and “lower” for each column. Care was taken to mark each sample orientation before the initial scan and replicate the same orientation during scanning after compression to ensure the resulting scan data could be compared from approximately the same vantage point before and after compression.

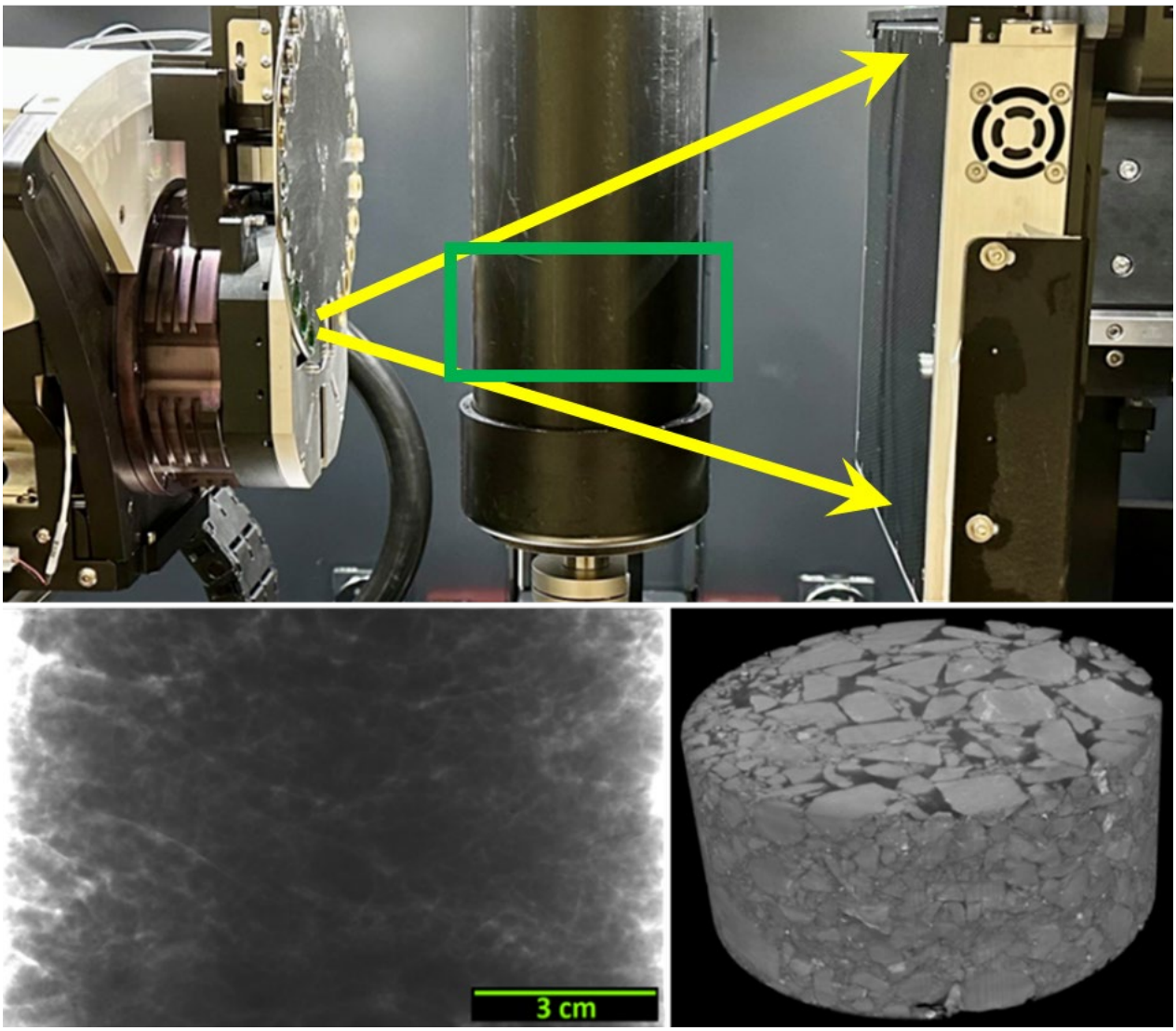

Figure 2: X-ray CT scanning using Zeiss Xradia 620

The image processing and analysis procedures have been discussed in a previous study (Erskine et al., 2024). A machine learning segmentation method was used in this study. The watershed thresholding and the machine learning segmentation methods were compared in the literature (Erskine et al., 2023). Quantitative results of pore networks include porosity of all pores and connected pores, pore size distribution, LBM simulated permeability, and flow velocity.

Results

Since RC drilling was used, returned cuttings may under-represent coarse fragments >4 inches. This limitation should be recognized when interpreting results, although the PSD analysis suggests overall coarseness remained consistent with expected ROM material. Table 1 summarizes the key results of each

of the analyses used in this study. Detailed results of each analysis are broken down in their corresponding subsequent subsections.

Table 1: Summary of Compression Displacement and Porosity Results by Depth Interval

Depth Interval (ft)	Fines (%)	Uniaxial Strain	Porosity (Mean % ± SD)	Permeability (Mean cm² ± SD)
0–70	7.8	0.0357	14 ± 2	$4.0 \times 10^{-6} \pm 0.2$
70–140	9.6	0.0464	15 ± 3	$5.1 \times 10^{-6} \pm 0.7$
140–210	10.6	0.0573	14 ± 3	$4.7 \times 10^{-6} \pm 0.5$
210–280	9.0	0.0769	10 ± 4	$4.2 \times 10^{-6} \pm 0.3$
280–350	7.0	0.0716	14 ± 2	$5.1 \times 10^{-6} \pm 0.3$

Particle Size Analysis

Figure 3 displays the results of the PSD analysis for each sample.

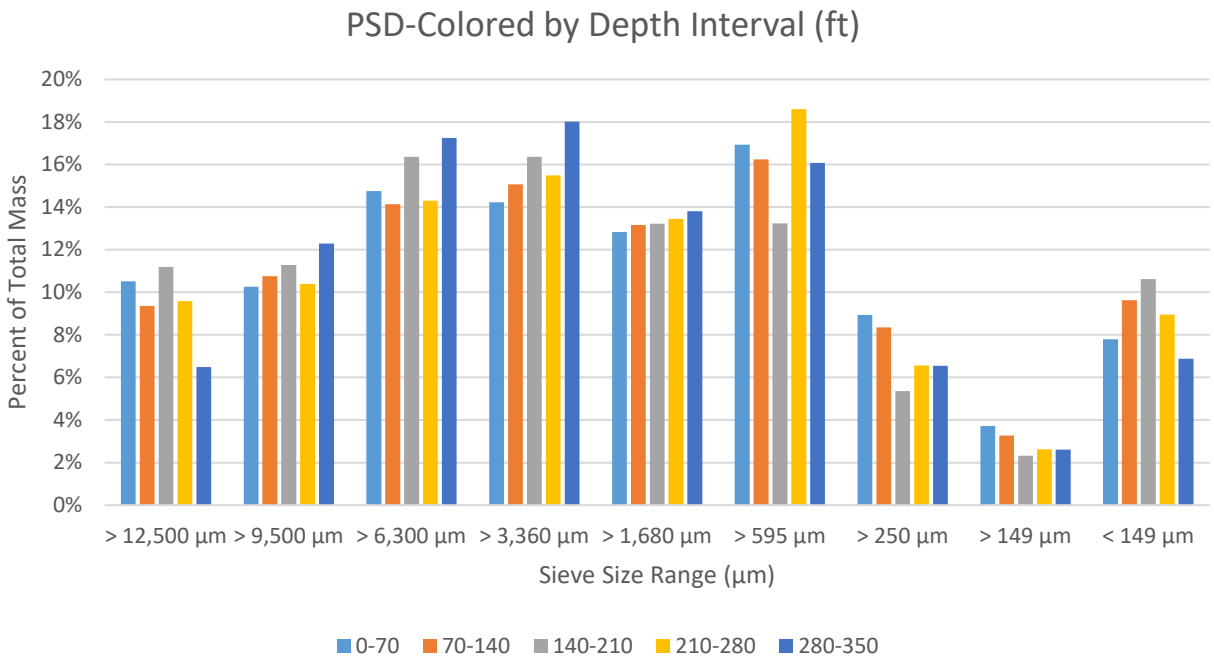

Figure 3: PSD Analysis by depth interval

The PSD curves for each depth are nearly parallel, which indicates similar and poor sorting through the heap profile. A quick examination of the data shown in Figure 2 is summarized in the table below.

Table 2: PSD Dominant Size Classes by Depth Interval

Depth Interval (ft from Surface)	Dominant Size Classes
0–70	>3.4 mm > 595 µm (45% of the mass)
70–140	Like the above, but more fines
140–210	Most uniform of all intervals
210–280	Peak between > 1,680 µm and > 595 µm
280–350	Coarsest of all intervals
All Intervals	Fines (< 149 µm) never exceed ~11 %

The PSD analysis reveals consistent particle size distribution patterns across different depth intervals, with slight variations in dominant size classes. The presence of coarser particles throughout the heap profile suggests limited size segregation during the heap construction process. These findings indicate that the material's physical characteristics remain relatively uniform with depth, which may have implications for heap leaching performance and fluid flow dynamics within the system.

Compression Test Observations

Compression testing showed that vertical displacement depends partly on material composition, not only on the load alone. Of the five samples investigated, the two depth intervals with the greatest fines content (≈ 9–11 %) were actually the stiffest and settled the least (only 0.09–0.11 strain) despite being compressed under the highest stresses. Conversely, the upper intervals, which contained the lowest fines percentages (≈ 7–8 %), compressed nearly five times as much under much smaller loads. Thus, within this heap, added fines appear to fill voids and lock the coarse skeleton, reducing pore collapse rather than promoting it; displacement is inversely, not directly, related to fines content.

The stress versus strain curves for the compressions are shown in Figure 4. The stress versus strain curves shown in Figure 4 suggest that overburden stress stiffens the heap until a threshold is reached where particle breakage dominates. In this material, the threshold lies somewhere near 200 psi vertical stress (≈ 250 ft depth). Below it, higher pre-stress means higher modulus; beyond it, mechanical degradation reverses the trend.

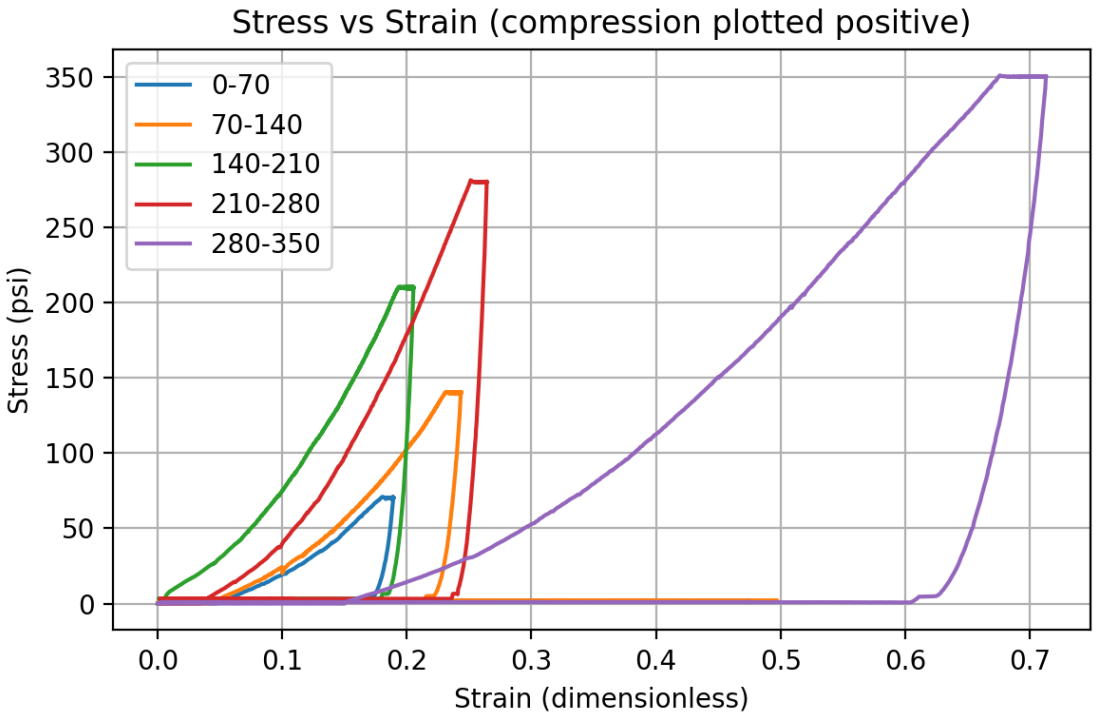

Figure 4: Stress versus strain curves of compression data

High-Resolution XCT Pore Network Analysis

High-resolution XCT imaging confirmed a reduction in void space with increasing compression up to approximately the same depth threshold as was observed in the compression testing. The 0–70 ft and 70–140 ft depth intervals have porosities of around 15% and permeabilities of 4–5 × 10^{-6} cm^2. In other words, the upper cap of the heap is still fairly open and drains easily. The 140–210 ft depth drops back to the same porosity as the top lift (14.3 %), yet its permeability is only middling. These voids may be finer-scaled or partly clogged by migrated fines, reducing flow paths without significantly changing total pore volume. The 210–280 ft depth interval is again the outlier. Its porosity plunges to 10%, making it the tightest fabric in the group, while its permeability slips to the lower end of the range (4.2 × 10^{-6} cm^2). That dovetails with the compression data, which shows this lift as the densest and stiffest. The 280–350 ft depth interval climbs back toward 14 % porosity but, interestingly, maintains the same permeability as the upper lifts. This suggests that new micro-voids created during deep particle breakage are well connected, restoring flow even as the skeleton remains comparatively stiff.

Results of the pore network analyses are shown in Figures 5 through 14.

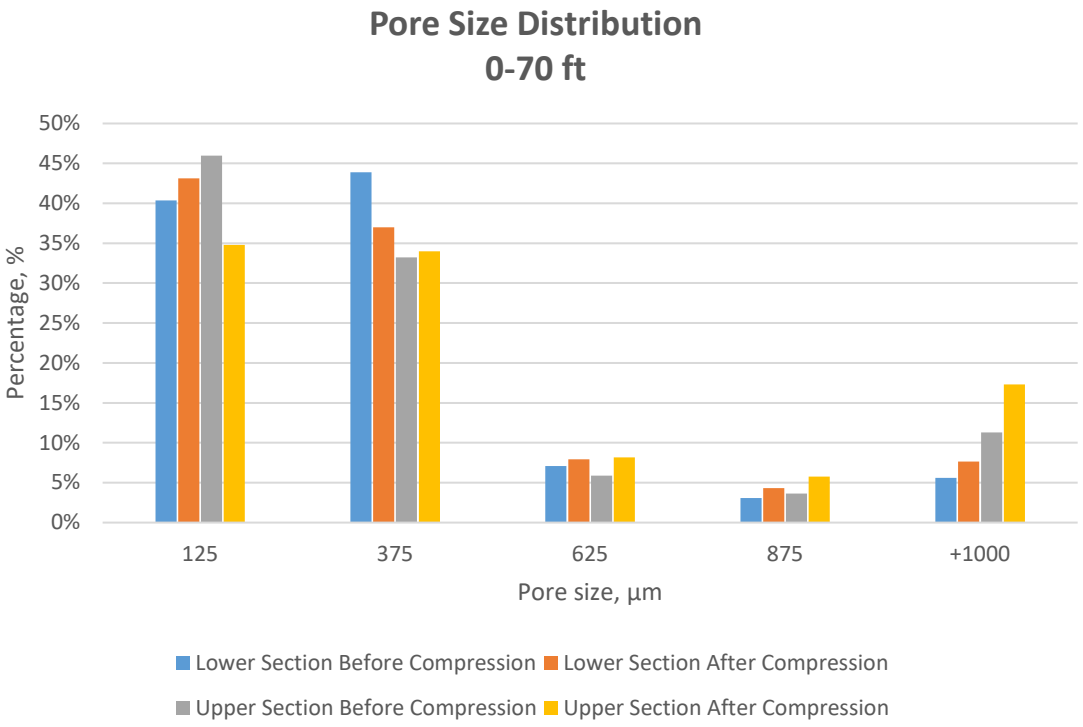

Figure 5: Pore size distribution 0–70 ft interval

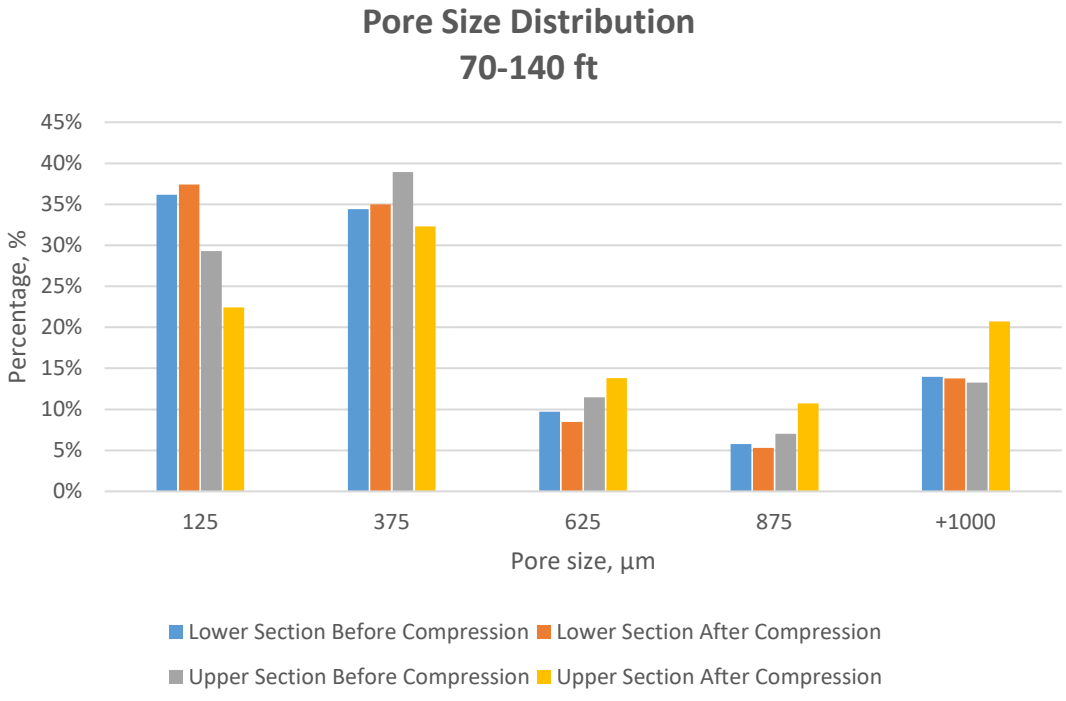

Figure 6: Pore size distribution 70–140 ft interval

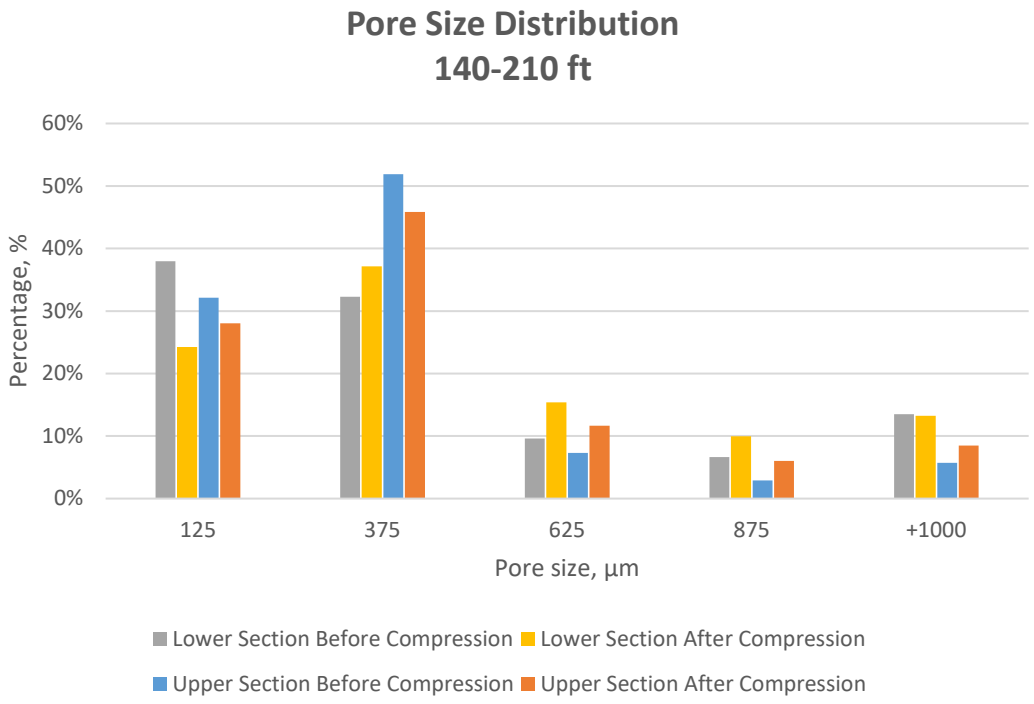

Figure 7: Pore size distribution 140–210 ft interval

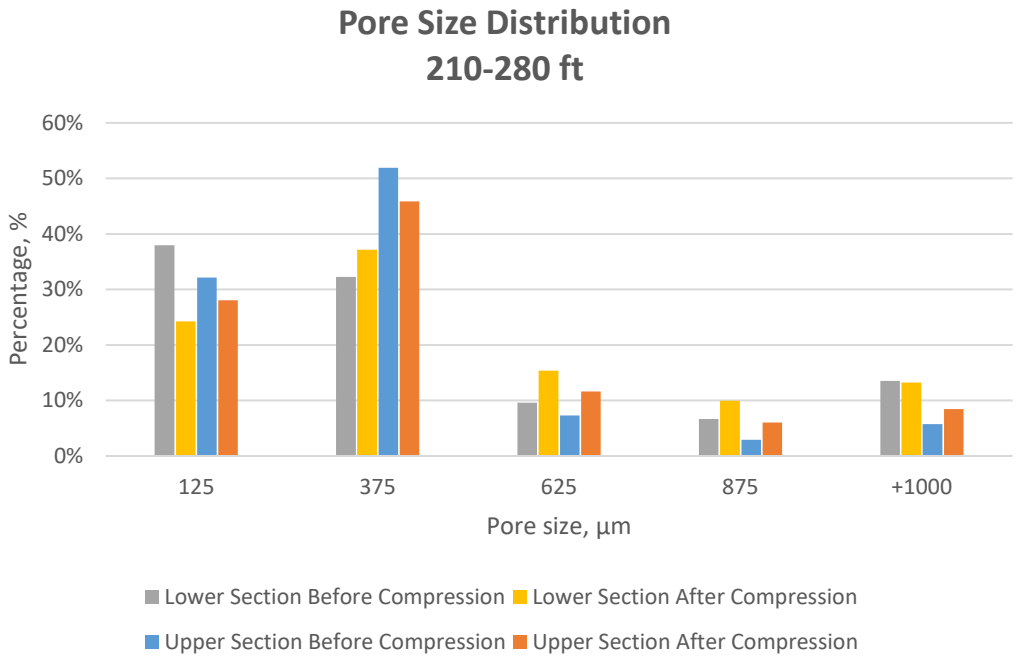

Figure 8: Pore size distribution 210–280 ft interval

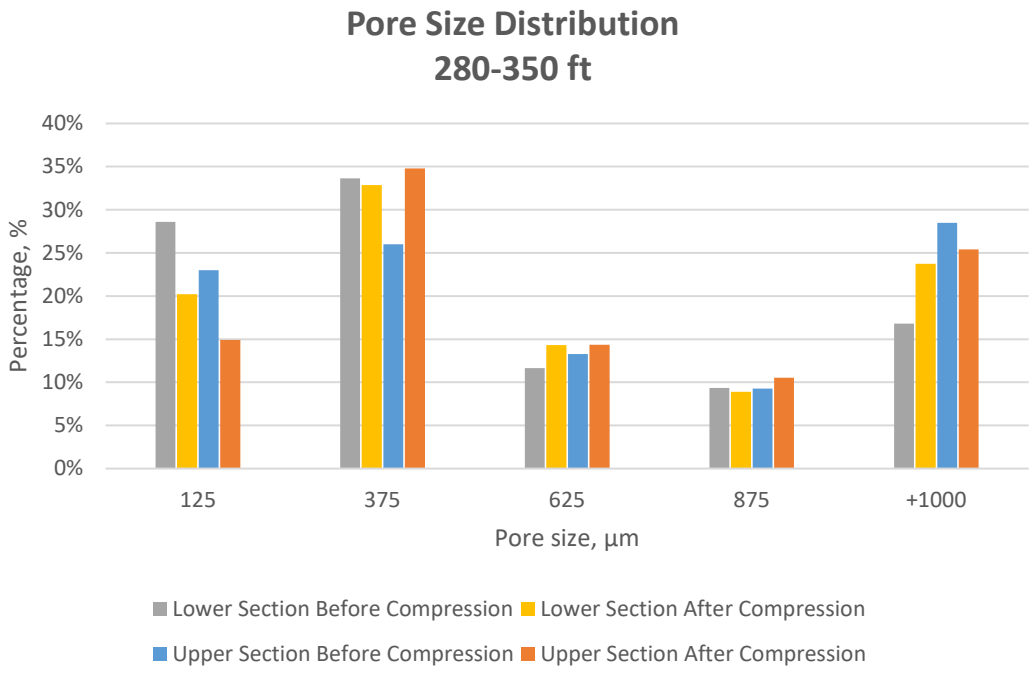

Figure 9: Pore size distribution 280–350 ft interval

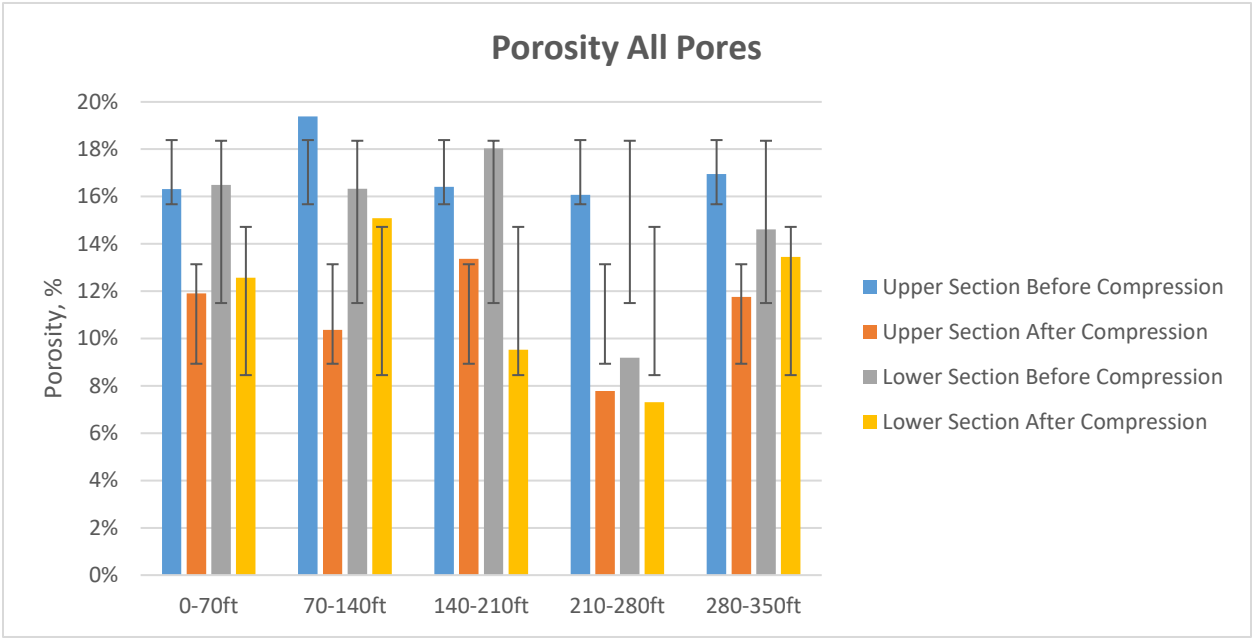

Figure 10: Porosity of all pores, including connected pores between particles, isolated pores because of limited voxel resolution, and isolated pores in particles. Bars show standard deviation

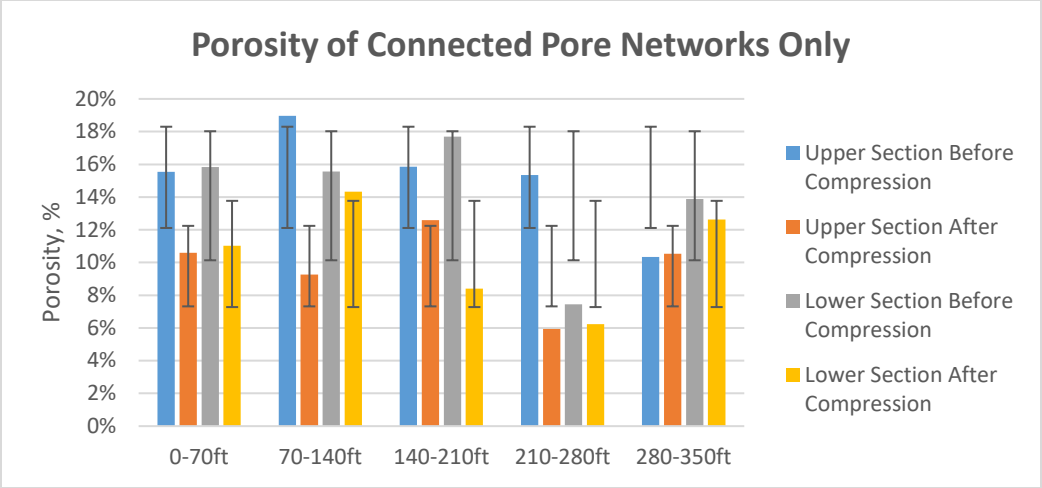

Figure 11: Porosity of connected pore networks, only pores
(Porosity of connected pores between particles. Isolated pores, because of limited voxel resolution, and isolated pores in particles were removed. Bars show standard deviation.)

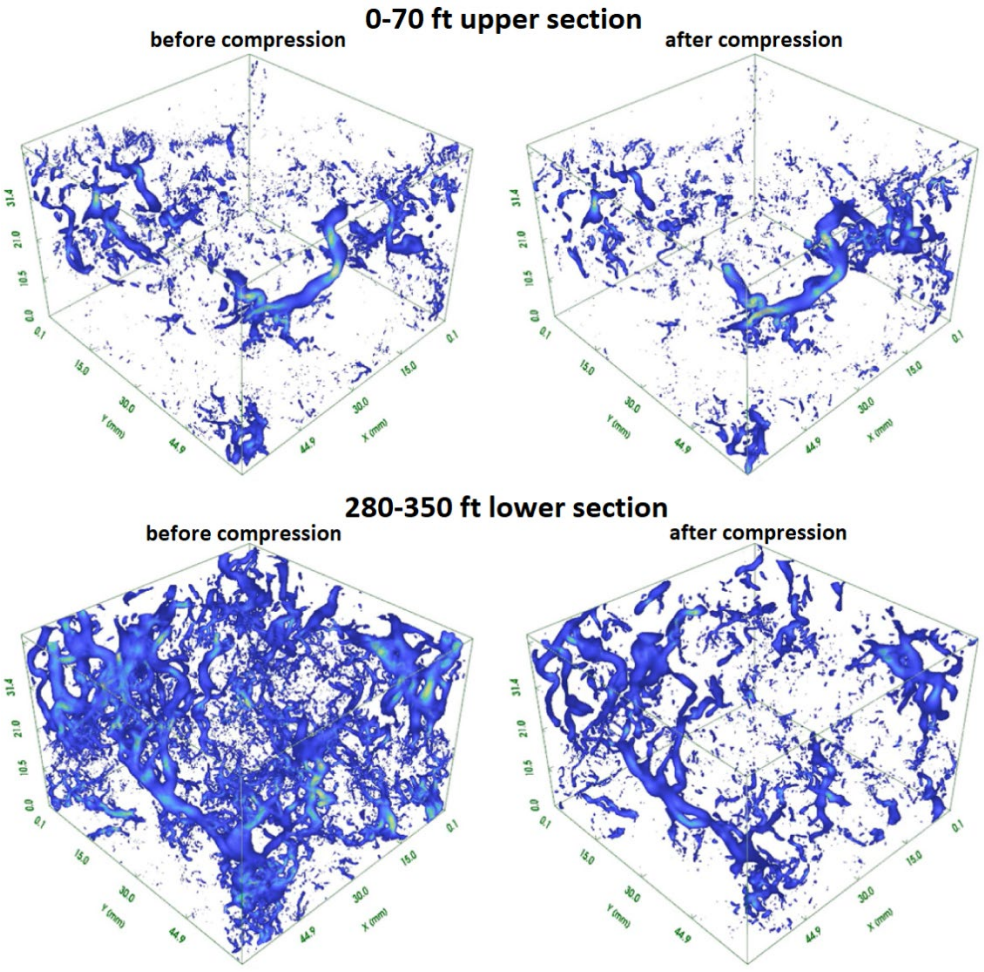

Figure 12: Flow channel of two sections (6 cm x 5 cm x 4.2 cm)
as examples for before and after compression

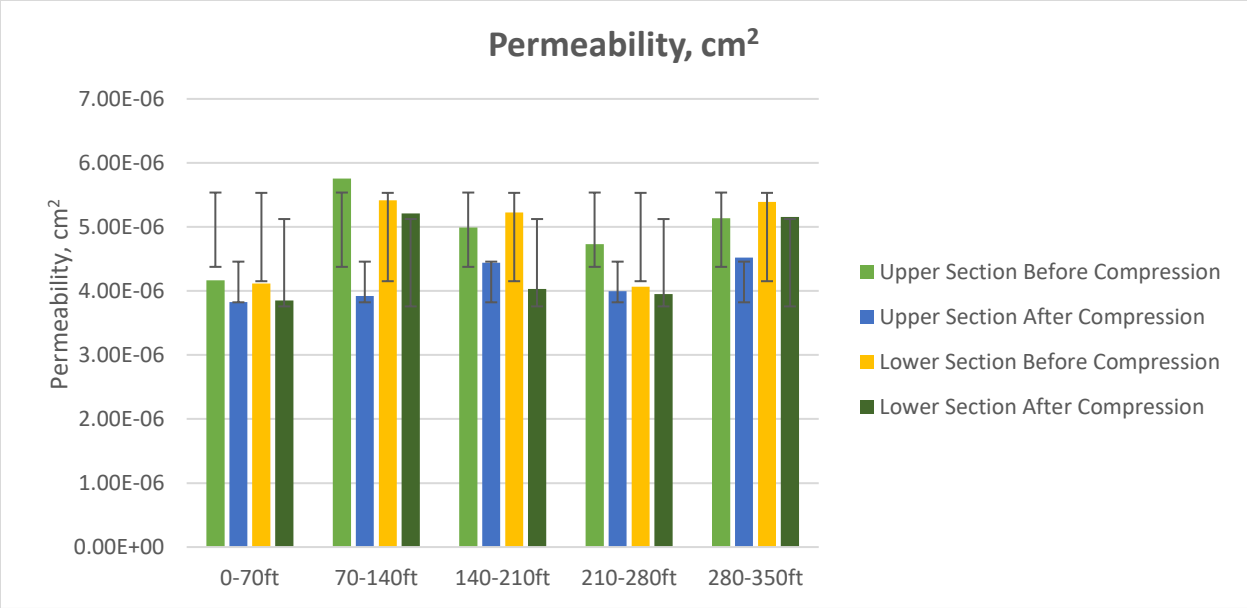

Figure 13: Permeability (cm², bars show standard deviation)

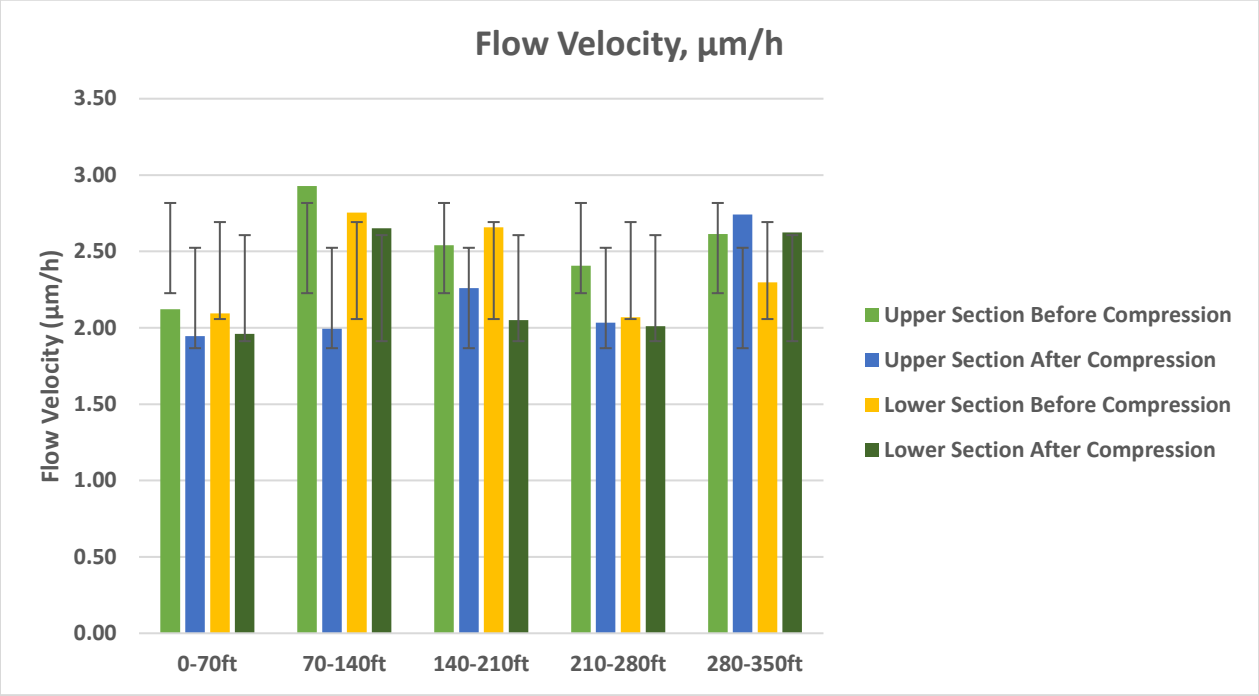

Figure 14: Flow velocity (µm/h, bars show standard deviation)

Taken together with the particle size and compression results, the porosity and permeability data show that material evolution with depth is not monotonic. The heap tightens up down to about 250 ft, then particle breakage and micro-fracturing begin to reopen flow channels near the base.

Discussion

The laboratory approach offers insight into compressibility and pore evolution in ROM leach pads; however, its relevance to full-scale heap leach facilities (HLFs) requires careful consideration. Most commercial operations use crushed heaps, which typically differ in PSD, permeability, and fines management. By focusing on ROM dump leach material, this study examines one of the most heterogeneous and challenging cases. Nevertheless, the finding that fines content, rather than stress alone, controls compressibility may be transferable to crushed heap systems where fines segregation also affects solution flow.

Results indicate a non-monotonic evolution of material properties with depth, suggesting a complex interplay between compaction and particle breakage processes. This dynamic behavior is particularly evident in the porosity and permeability data, which indicate a tightening of the heap structure down to approximately 250 ft, followed by a reopening of flow channels near the base. The creation of new micro-voids during deep particle breakage appears to play a crucial role in maintaining flow pathways, even as the overall skeleton remains relatively stiff.

This observation challenges the conventional understanding of heap behavior, which often assumes a continuous decrease in porosity and permeability with depth. The reopening of flow channels at greater depths could have significant implications for leaching efficiency and overall heap performance. Further investigation into the mechanisms driving this non-monotonic evolution could lead to improved heap design and management strategies, potentially optimizing metal recovery in heap leaching operations.

Furthermore, these findings also suggest that large decreases in porosity and permeability might likewise be found closer to the surface of heap leach pads than has been previously assumed. The motive of which could be due to the high responsiveness of the material that is being subjected to the variabilities in compaction or heap construction methods that cause higher than desired stress.

The leach pad material evaluated in this study was sourced from a ROM dump leach facility constructed in successive lifts during the mid-2010s. The ore placed on this pad was designated primarily as “oxide” or “low-grade” material in mine production records. Mineralogy studies were not performed on the material. The bulk ROM ore fragments placed in this facility generally exceeded several inches in nominal particle size, and the pad was constructed by end-dumping successive truckloads, resulting in lift-scale and truckload-scale textural heterogeneity. This depositional style can promote segregation of fines and preferential flow paths, which must be considered when interpreting laboratory column behavior relative to in-situ leach conditions. While 70 ft composites average the stratigraphical variability of the study area, local segregation during placement and lift construction may still govern preferential flow at smaller scales. Future studies should evaluate how lift-scale heterogeneity influences the representativeness of laboratory-prepared columns.

Segregation of particle sizes and ore types is a recognized feature of HLFs, particularly ROM dumps constructed by end-dumping in successive truckloads, where heterogeneities may develop at the scale of individual lifts or even individual shovel loads (Young & Rogers, 2021). These heterogeneities can strongly influence preferential flow in the field, and we acknowledge that a laboratory column cannot fully reproduce these depositional complexities. In the present study, sampling was performed on homogenized bulk material from designated pad intervals rather than on discrete shovel loads, and column specimens were prepared by representative splitting and compaction to approximate average conditions over the sampled interval. As such, the columns are intended to capture bulk-scale hydraulic and porosity characteristics rather than fine-scale heterogeneities. We note that the 4-inch laboratory columns necessarily smooth out short-interval segregation effects, but the intent here is to establish a baseline relationship between compression, pore structure, and fluid flow under controlled conditions. Future work could more directly address segregation effects by either sampling at higher spatial resolution within lifts, or by using larger-diameter columns and/or multiple replicate columns to evaluate heterogeneity at the scale of shovel loads.

Future Work

Future research will focus on developing a diffusion model that integrates these laboratory findings. Such a model could potentially incorporate the various factors that influence channel formation, including material properties, construction methods, and leaching parameters.

Developing a better heap leaching diffusion model involves several strategic approaches highlighted in existing research:

1. Comprehensive Process Understanding:

A good starting point is gaining a thorough understanding of the current heap leaching processes and their limitations. The process involves complex interactions, including rock leaching kinetics, solution flow, and oxygen transport mechanisms. Understanding these elements allows for precise adjustments that can enhance leaching efficiency (Bartlett 1997, 2013).

2. Mathematical Modeling:

Utilizing a dimensionless mathematical model can help interpret data from column and heap leaching tests. Such models should consider particle-scale kinetic factors and heap-scale operating variables. An approach that leverages the concept of a heap effectiveness factor can offer insights into the operational modes of heaps, enabling the prediction and optimization of leaching processes (Dixon & Hendrix, 1993; Dixon, 2003).

3. Uncertainty and Sensitivity Analysis:

Incorporating uncertainty quantification techniques helps in understanding the variability of input variables and their effect on the model's output. Global Sensitivity Analysis (GSA) can be particularly useful in evaluating model parameters, ensuring that the model is not over-parameterized and can effectively predict recovery behavior under a range of conditions (Mellado et al., 2018).

5. Hydrodynamics and Mass Transfer Modeling:

Advanced mathematical models that simulate solute transport through both flowing and stagnant pore spaces are crucial. These models can help predict advection and diffusion processes within the heap, particularly considering factors such as particle size, solution flow rate, and bed height. By honing these variables, a more efficient leaching system can be developed (Bouffard & Dixon, 2001).

6. Gangue Mineral Interactions:

Understanding the interactions between gangue minerals and acids is vital. This involves studying mineralogical characteristics and their effects on leach performance at different stages of the process. Techniques like X-ray diffraction and electron microscopy can offer insights into textural relationships and reactivity of gangue minerals, allowing for predictive adjustments to the leaching process (Chetty, 2018).

Implementing these strategies provides a coherent path towards improving heap leaching diffusion models, optimizing metal recovery rates, and increasing overall process efficiency. By incorporating fines-controlled compressibility into heap-scale simulations, it may be possible to improve predictive accuracy for leaching performance. Additionally, expanded field sampling and scale-up studies are planned to validate laboratory observations across full-scale heap operations.

By accurately simulating the evolution of flow patterns over time, this model could aid in optimizing heap design and operational strategies to minimize short-circuiting and maximize ore contact with leaching solutions. This could lead to significant improvements in overall heap leaching efficiency and metal recovery rates. This preferential flow bypasses much of the ore and short-circuits the leaching process, which results in production loss. Every step in the construction of a heap, from blasting, loading, hauling, dumping, to crushing, conveying, and stacking of the material, influences the solution flow and material transport patterns that will develop over time. Material pretreatment, leach solution composition, and application rates are also known to be influential in the formation of preferential flow channels (Orr, 2002).

Conclusion

This study demonstrates that high-resolution XCT imaging combined with controlled uniaxial compression provides valuable insights into the evolution of pore networks within ROM heap leach material. The results

reveal a non-monotonic relationship between depth and hydraulic properties: in the case of the heap studied, initial compaction tightens the pore system to ~250 ft equivalent depth, after which particle breakage and micro-fracturing reopen conductive pathways. This behavior highlights the dual role of compaction and comminution in controlling permeability and flow distribution within dump leach facilities.

In conclusion, fines generation and redistribution, rather than applied stress alone, govern the magnitude of porosity loss under loading. This finding has broader implications for both ROM and crushed heap leach facilities, where segregation of fines is a persistent driver of preferential flow and recovery variability. Although the laboratory columns necessarily smooth out localized heterogeneities, the experiments provide a reproducible framework for quantifying the coupled mechanical and hydraulic response of leach pad materials as well as a path forward for calibrating computational diffusion models.

References

Al Mahbub, A., & Haque, A. (2016). X-ray computed tomography imaging of the microstructure of sand particles subjected to high pressure one-dimensional compression. *Materials, 9*(11), 890. https://doi.org/10.3390/ma9110890

Bartlett, R. (2013). *Solution mining: Leaching and fluid recovery of materials*. Routledge.

Bartlett, R. W. (1997). Metal extraction from ores by heap leaching. *Metallurgical and Materials Transactions B, 28*(4), 529–545.

Bouffard, S. C., & Dixon, D. G. (2001). Investigative study into the hydrodynamics of heap leaching processes. *Metallurgical and Materials Transactions B, 32*(4), 763–776.

Butler, I., Fusseis, F., Cartwright-Taylor, A., & Flynn, M. (2020). Mjölnir: A miniature triaxial rock deformation apparatus for 4D synchrotron X-ray microtomography. *Journal of Synchrotron Radiation, 27*(5), 1480–1487.

Cheng, Z., & Wang, J. (2021). An investigation of the breakage behaviour of a pre-crushed carbonate sand under shear using X-ray micro-tomography. *Engineering Geology, 293,* 106286. https://doi.org/10.1016/j.enggeo.2021.106286

Chetty, D. (2018). Acid-gangue interactions in heap leach operations: A review of the role of mineralogy for predicting ore behaviour. *Minerals, 8*(2), 47. https://doi.org/10.3390/min8020047

Dixon, D. (2003). Heap leach modeling—The current state of the art. In *Proceedings of the TMS Fall Extraction and Processing Conference* (Vol. 1, pp. 289–314). TMS.

Dixon, D. G., & Hendrix, J. L. (1993). A mathematical model for heap leaching of one or more solid reactants from porous ore pellets. *Metallurgical Transactions B, 24*(6), 1087–1102.

Erskine, A. N., Jin, J., Lin, C.-L., Miller, J. D., & Wang, S. (2024). 3D imaging of leach columns from Rochester mine for pore network characteristics and permeability simulated by the Lattice Boltzmann Method. *Hydrometallurgy, 228,* 106365. https://doi.org/10.1016/j.hydromet.2024.106365

Fala, O., Molson, J., Aubertin, M., & Bussière, B. (2005). Numerical modelling of flow and capillary barrier effects in unsaturated waste rock piles. *Mine Water and the Environment, 24*(4), 172–185.

Gbor, P. K., & Jia, C. Q. (2004). Critical evaluation of coupling particle size distribution with the shrinking core model. *Chemical Engineering Science, 59*(10), 1979–1987.

Gerke, H. H. (2006). Preferential flow descriptions for structured soils. *Journal of Plant Nutrition and Soil Science, 169*(3), 382–400. https://doi.org/10.1002/jpln.200521955

Mellado, M. E., Cisternas, L. A., Sepúlveda, F. D., Lucay, F. A., & Gálvez, E. D. (2018). A posteriori analysis of analytical models for heap leaching using uncertainty and global sensitivity analyses. *Minerals, 8*(2), 44. https://doi.org/10.3390/min8020044

Miller, J. D., & Lin, C. L. (2004). Three-dimensional analysis of particulates in mineral processing systems by cone beam X-ray microtomography. *Mining, Metallurgy & Exploration, 21*(3), 113–124.

Orr, S. (2002). Enhanced heap leaching—I. Insights. *Mining Engineering, 54*(9), 25–31.

Renard, F., Cordonnier, B., Dysthe, D. K., Boller, E., Tafforeau, P., & Rack, A. (2016). A deformation rig for synchrotron microtomography studies of geomaterials under conditions down to 10 km depth in the Earth. *Journal of Synchrotron Radiation, 23*(4), 1030–1034.

van Staden, P. J., & Petersen, J. (2021). Towards fundamentally based heap leaching scale-up. *Minerals Engineering, 168,* 106915. https://doi.org/10.1016/j.mineng.2021.106915

Young, A., & Rogers, W. P. (2021). Modelling large heaped fill stockpiles using FMS data. *Minerals, 11*(6), 636. https://doi.org/10.3390/min11060636

Young, A., & Rogers, W. P. (2022). A high-fidelity modelling method for mine haul truck dumping process. *Mining, 2*(1), 86–102. https://doi.org/10.3390/mining2010006

Zhao, B., Wang, J., Andò, E., Viggiani, G., & Coop, M. R. (2019). Investigation of particle breakage under one-dimensional compression of sand using X-ray microtomography. *Canadian Geotechnical Journal, 57*(5), 754–762.

Towards an Advanced Monitoring System for Leaching Heaps Based on Muon Radiography

Tancredi Botto, Muon Vision Inc., USA
Adrian Casais Vidal, Muon Vision SpA, Chile
Samridha Kunwar, Muon Vision Inc., Canada
Ricardo Repenning, Muon Vision SpA, Chile
Tomas Salvadores, Muon Vision SpA, Chile
Rob Stephens, Muon Vision Inc., Canada

Abstract

In this paper, we discuss potential use cases for muon radiography, an emerging technology for the mining industry, to deliver a step change for leaching operations.

Muon radiography is a well-established technique for characterizing and digitally mapping large objects located above or below the surface. Muon radiography and/or tomography has already been successfully utilized for cavity detection and exploration activities in mining. Muon radiographic measurements are close analogues of medical or industrial X-rays. However, in place of a conventional radionuclide source or X-ray tube, muon radiography utilizes the naturally occurring flux of so-called cosmic ray particles (aka muons) originating in the Earth's upper atmosphere. This benign background radiation is available for free everywhere on Earth and is intrinsically safe.

The muon flux is highly penetrating (up to several hundred meters), extends over a very broad angular range (+-70 degrees from the vertical), and maintains excellent directionality even in the subsurface. In the case of leaching heaps, 2D (radiographic) or 3D (tomographic) density profiles can be reconstructed with high precision (~0.02 g/cc relative) and good spatial resolution (a few m^2), a few days to a few weeks of observation time, depending on the heap height and sensor location.

Muon radiography can enable operators to maintain, over time, a precise, quantitative 3D map of the actual volumetric fluid and air content (saturation) in the pore space of a leaching heap, i.e., the fractional fluid-filled and air-filled porosity. Both of these parameters are challenging to obtain at scale in the field, yet remain primary drivers of ultimate metal yields, operational costs, financial, and geotechnical risk.

Introduction

Muon density radiography, also known as muography, is a well-established technique for characterizing and digitally mapping bulk density across large objects in near real-time.

Muon bulk density measurements are close analogues to the better-known medical or industrial X-ray. The key difference is that in place of a conventional nuclear source or X-ray tube, muon radiography utilizes the naturally occurring flux of so-called secondary cosmic ray particles (aka muons) originating in the earth's upper atmosphere. As such, it is entirely passive. This benign background radiation source is not only free and intrinsically safe, but also continuously available everywhere and at any time on Earth. Muon particles are also highly penetrating and maintain directionality even in the subsurface. This enables muon radiography to analyze and map the interior of dense structures up to thicknesses of at least a few hundred meters.

Indeed, so-called muon radiography has been utilized for looking inside of ancient pyramids (Alvarez et al., 1970), volcanoes (Lesparre et al., 2012), inspecting nuclear fuel casks (Gilboy et al., 2007), tunnels (Guardincerri et al., 2017), and in mine exploration (Schouten & Ledru, 2018). Generally, muon radiography services are most efficiently delivered using either vertical or horizontal boreholes. One of the authors of this paper was the first to build and field test a modern borehole detector for muon density measurement in an oil & gas application operating on a wireline in an actual oil well (Botto et al., 2014).

In Figure 1, we show how the muography concept applies to a single lift leaching operation.

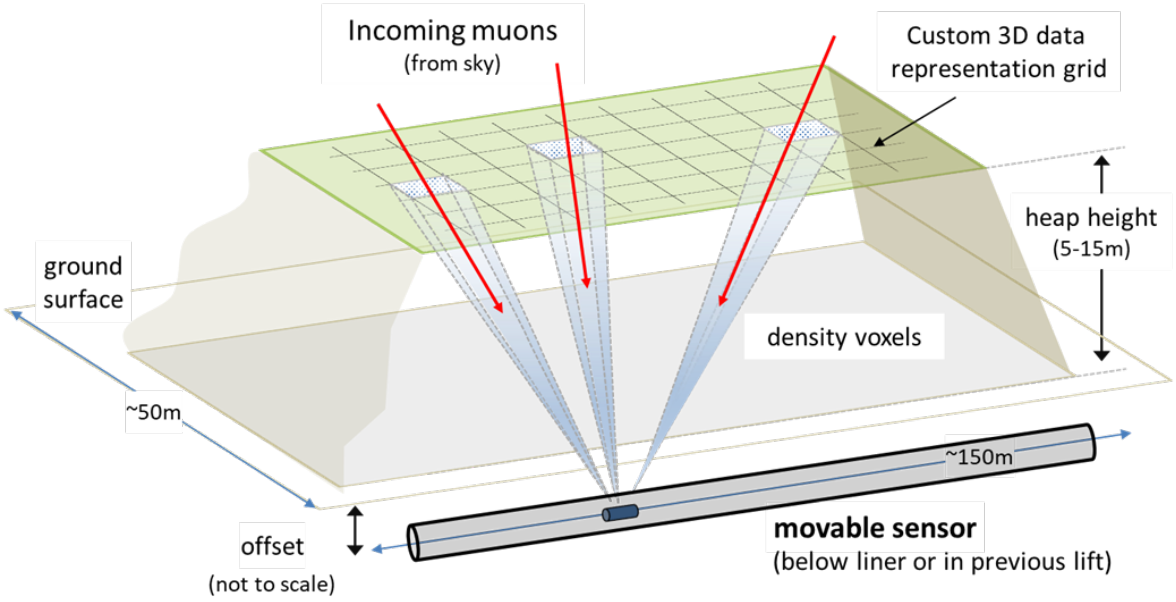

Figure 1: Muon radiography concept applied to a leaching heap, with a muon borehole imaging detector inserted and moving within a HDPE pipe buried under the heap. Muon borehole sensors are also compatible for operation and movement in vertical or slanted wells

In the example above, as the detector advances along its installation pipe, it counts and determines the arrival direction for each of the individual muon particles that are naturally traversing the heap over a wide range of angles. Once sufficient statistical precision is accumulated over time, this allows for an accurate reconstruction of the bulk density of the asset, independently for each voxel within a customizable 3D grid.

Like other well-known nuclear density probes (i.e., γ–γ density loggers or X-ray scanners), muography measures the aggregate bulk density for all materials in the heap, directly in g/cc, by determining the relative attenuation of the muon flux traversing the same. From this, one can extract valuable information. In fact, the basic volumetric equation for the bulk density of any porous material can be written as

$$\rho_{bulk} = (1 - \Phi)\rho_{matrix} = \rho_{dry} \quad (1)$$

where ρ_{matrix} is the matrix density, i.e., the average grain density of the crushed ore, and Φ the average porosity of the heap. When fluid is added to the system, the aggregate bulk density picks up an additional contribution and can be written as

$$\rho_{bulk} = \rho_{dry} + \Phi S \rho_{fluid} \quad (2)$$

where ρ_{fluid} is the fluid density and S is the fluid saturation or fluid-filled fractional porosity.

Thus, given an average value of ρ_{matrix} for the material at hand (which can be estimated in several ways), one can determine the total air-filled porosity from an initial scan of the heap in its dry or initial state (via Eq. 1) and—knowing that—determine the volumetric fluid content S or fluid-filled porosity in subsequent scan of the heap in its wet or final state (via Eq. 2). Clearly natural compaction phenomena will tend to reduce the heap porosity between the initial and final state, but this effect can be corrected for using the volumetric information from simple drone-based topographic surveys, under the benign assumption that the shrinkage of the heap primarily pushes the air out of the heap, and not its liquid and solids.

In this way, muography can robustly and continuously quantify both air-filled and fluid-filled porosity, two key drivers of the efficiency and safety of any leaching operation. Generally, muography can reconstruct 2D or 3D bulk density with a high precision (~0.02 g/cc relative, <0.1 g/cc absolute), good spatial resolution (a few m^2) and high reliability (2σ confidence level) within time intervals typically ranging from a few days to a few weeks. For typical porosities (i.e., 30–40%), a 0.02 g/cc uncertainty on the bulk density translates to a precision of ~5% in terms of fluid and air saturation content (2σ confidence level).

As the muon flux is essentially constant all over the surface of the earth (with the notable exception of high elevations, where it can be substantially higher than at sea level) the necessary measurement time

for a successful scan is primarily driven by the required precision on density, the size and number of the detectors used to catch the muon flux, and the depth at which they are positioned. In Figure 2, we show the effect of longer measurement or exposure times on the sensitivity to density changes (Δρ) for a ~8" diameter, 1 m long cylindrical borehole detector placed under a 15 m tall lift with ρ_{dry} = 1.66 g/cc.

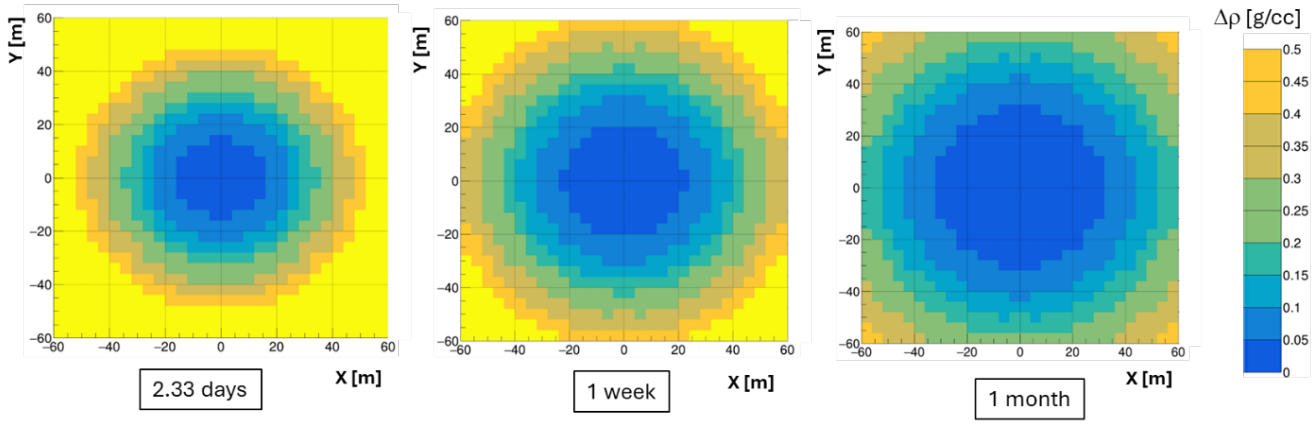

Figure 2: Expected sensitivity or precision to bulk density changes (Δρ) for a ~8" diameter, 1-m-long cylindrical borehole detector placed at (0, 0) under a 15 m tall lift with ρ_{dry} = 1.66 g/cc

Other important features of muon measurements are that they are independent of the chemical state (i.e., solid, fluid, gas), temperature, salinity, or pH of the materials within the object under study. To a large extent, they are also insensitive to their chemical composition, as Z/A = 0.5 is a good approximation for most of the periodic table elements within soils, which, on the other hand, is also precisely calculable.

Thus, muon radiography is a promising diagnostic tool for the quantitative characterization of leaching heaps and other partially saturated media, including stockpiles and tailing dams. This is expected to bring about significant value.

Problem Statement and Value Proposition

Leaching operations at scale, while less energy and water-intensive than conventional concentrator processing, remain challenging to accurately model and their outcomes difficult to forecast.

Key drivers of recovery efficiency during field operations are: i) the presence of clays in the heterogenous material; ii) the emergence of preferential channels and local voids, possibly due to non-uniform particle size distributions; iii) the migration of fines and precipitates, and, particularly for sulfide leaching, iv) insufficient air-filled porosity and circulation, due to excessive compaction. These effects are due to hard-to-predict characteristics of the operation and the ore, such as the ore's wettability and propensity for capillary flow. Together, they affect the permeability of the stacked ore differently in various

zones, and thus the distribution of fluid content within the heap itself, ultimately leading to uneven and/or substandard recovery, longer production cycles, and an increased risk of slope instability.

In many cases, leaching parameters and ore properties are determined based on laboratory column tests, which can then be interpreted and scaled within sophisticated modelling frameworks. Nonetheless, these tests, by their very nature, significantly under-sample the ore at play and are not necessarily representative of full assets at scale over time. Consider that a single 20-cm-diameter, 2-m-tall column represents just 0.0065% (65 parts per million) of the total volume of ore for even a small test leaching pad ($100 \times 100 \times 10\ m^3$). It is intrinsically difficult (and expensive) to capture all process variability with a test-only approach. The net result of this is that yields from the field are typically lower than column leach performance and take more time, as reported by many studies (van Staden & Petersen, 2021; Jansen & Taylor, 2002; John, 2011; Scheffel, 2002; Scheffel et al., 2016) and summarized in Figure 3. While heterogenous conditions are often inevitable, their effects can be managed via selective irrigation, targeted injections, and optimized leaching strategies once that information is available. Today, gathering such information typically requires heap access and sampling, which involves exposure to personnel risk. This approach remains labor-intensive, costly, and incomplete.

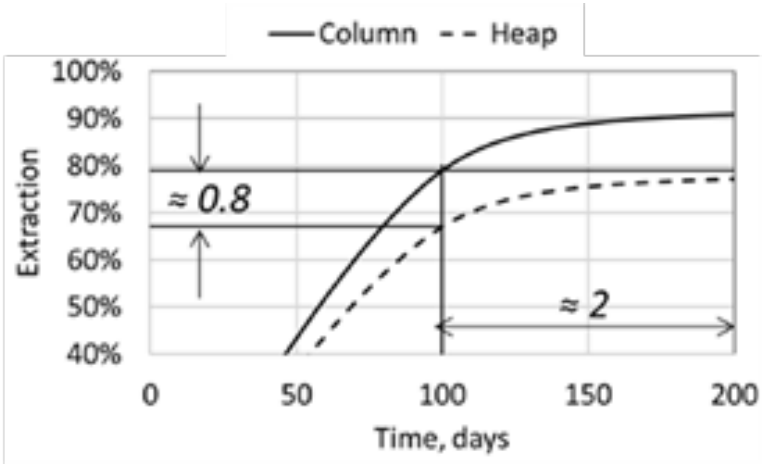

Figure 3: Typical comparison of laboratory and heap scale recovery curves (van Staden and Petersen, 2021)

Given that average recovery yields are only 30–60% across the industry (BHP, 2023; Freeport, 2022), any loss of recovery from ideal column or bottle roll leach performance is material to any operation. This calls for a novel approach, wherein rather than extrapolating from a few sparse samples or column tests, actual heap performance and stability are continuously measured in situ and without personnel exposure.

As the copper industry moves towards leaching an increasing fraction of transition and sulfide ores, we believe that having the right reagent chemistry (e.g., Nuton, Jetti, Ceibo, etc.) is a necessary but not sufficient condition for increased leaching yields. Similarly, we believe that existing secondary leaching

approaches based on re-injecting lixiviant into heaps could be improved, as current methods are currently unable to determine in advance precisely where and how much fluid to add.

At the same time, we believe that secondary leaching or injection leaching campaigns, while not an industry standard, can generate significant value. In Lizama (2023), a dedicated geophysical campaign showed that ~15% additional copper could be recovered from both transition sulfide and oxide leaches at scale, by addressing select dry volumes with a tailored irrigation/re-leaching strategy. This allowed the leaching operation to continue past its expected end of life and to bridge mine operations over to sulfide ore leaching (without loss of mining license). Similarly, in (9), a thermal camera system demonstrated that irrigation adjustments based solely on surface data resulted in ~10-20% higher Cu recovery curves. Ultimately, it is hoped that muography applied to leaching heaps can bring about the following benefits:

Table 1: Summary of Potential Benefits of Radiographically Assisted Leaching Operations

Benefit	Comment
Increased metal recoveries	Up to +10-20%, depending on operation
Additional recoverable reserves	From increased yields and reduced costs for lower-grade materials
Reduced water and reagent consumption during operations	Via selective irrigation strategies, to avoid wasting fluid in non-productive zones and dangerously over-wetting others
Optimized leach cycle times and planning	Via improved predictions based on actual flow percolation data zone by zone, accounting for ore and deposition variability
Reduced geotechnical risk	By determining actual fluid content & over-wet volumes
Reduced personnel and contractor exposure and costs	By reducing/replacing the need for manual inspections and test work
Improved metal reconciliation	Reduced uncertainty about leaching recoveries
Deferral of closure activities and costs	Up to $100's M deferred, by extending asset profitability until new projects are approved

Validation of Muography for Operation in Leaching Heaps

Muon Vision is a young service company dedicated to developing advanced muography solutions for leaching and other mining applications. In 2025, Muon Vision inaugurated its one-of-a-kind underground Demo and Calibration Facility located ~45 minutes outside of Las Condes, Santiago (Chile).

This was designed to resemble a scaled down version of an actual test leaching heap, with the dual goals of i) providing a reliable density standard for the calibration and validation of Muon Vision sensors and reconstruction algorithms against clearly defined density contrasts and controlled experiments; ii) performing ore characterization studies such as the measurement of water saturation curves; and iii) promoting collaboration with potential customers. The general layout of the facility is shown in Figure 4.

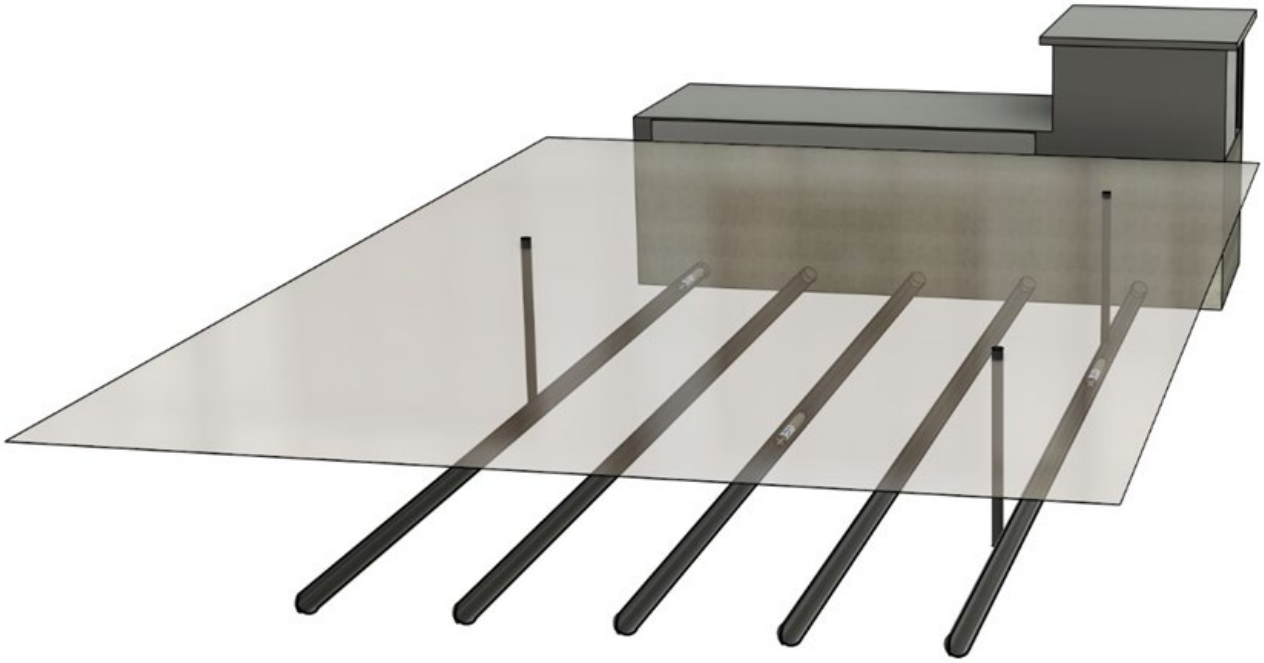

Figure 4: Layout of Muon Vision's demo and calibration facility. Five HDPE pipes and three vertical wells are buried at 3 m depth

The facility features five HDPE horizontal pipes at ~5 m spacing and buried at a depth of 3.5 m in dry soil. Additionally, three vertical wells were drilled to an initial depth of 3 meters, with the potential to be extended to greater depths. This can also be used to support Muon Vision's technology roadmap, which includes full remote control of sensor operation and positioning in either vertical or horizontal configurations.

As shown in Figure 6, the above surface portion of the facility can be flexibly configured to offer different density problems or "phantoms" for the validation of Muon Vision service by using simple tote bins, stackable up to a maximum 3 m height, thus enabling the realization of mock-up heap geometries up to 5 m tall over a ~10 × 20 m^2 area.

Figure 5: Overview of Muon Vision's demo facility, as built

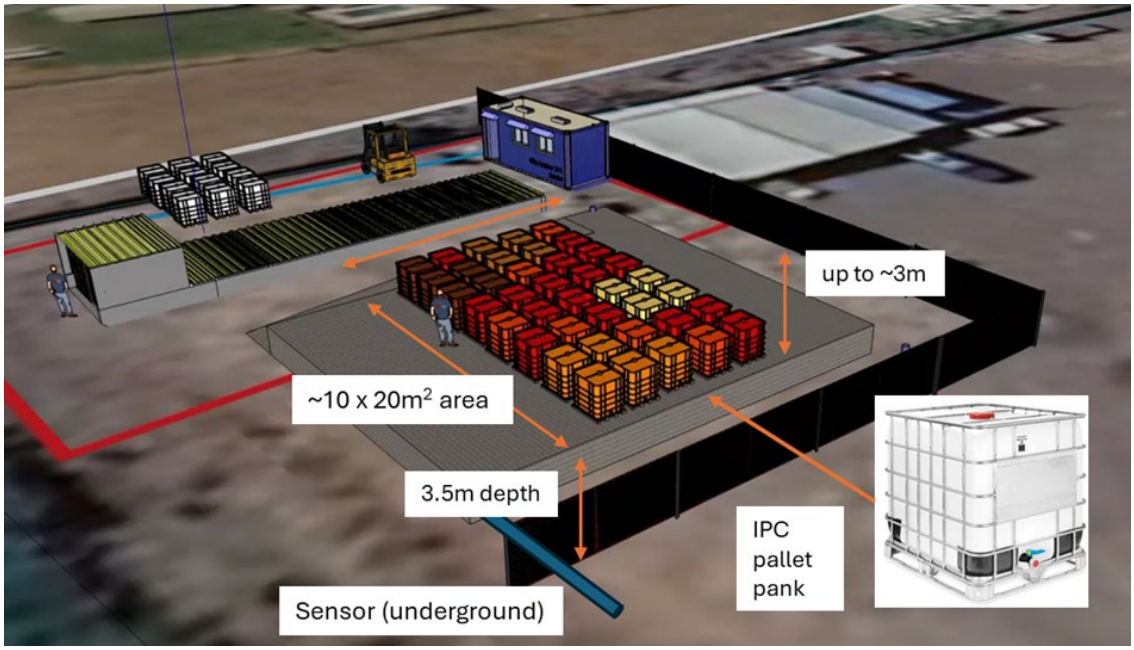

Figure 6: Using tote bins, partially or completely filled with soils and/or liquids, an arbitrary number of density configurations can be quickly realized and test with muon radiography

Initial Scan Data and Validation Results

Data taking has just started at our Demo Facility as we submit this paper. Therefore, we are only able to report initial results in this section. In contrast, the next section will discuss the expected performance for reconstructing 3D density using simulated data from our forward model.

As with any instrumentation, the first task is to demonstrate that the system is stable. Below, we show the relative performance of different sensors (MV8_B4_1,2 & 3) when performing multiple passes along a given scan line, as indicated by the advancing position. The three sensors will therefore detect three different opacities, as the thickness and bulk density of the soil above each scan line vary.

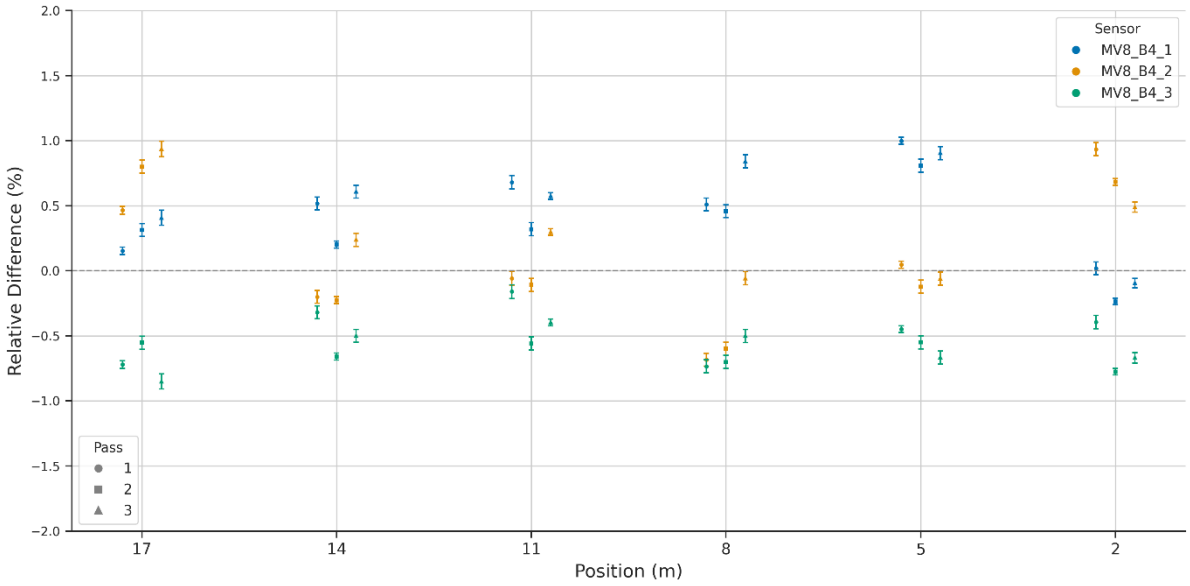

Figure 7: Relative difference across repeat muon density measurements for the 3 MV8 sensors as a function of position along their individual scan lines at the MV Demo Facility

In Figure 7, each repeat pass is represented by a different style symbol, and data from each sensor is associated with a given color. Generally, we find that system repeatability is of the order of ~0.5%, which is a good initial result for data collected over a period of ~2 weeks, without applying any corrections or external controls, such as the normalization to a reference muon flux. This type of precision is generally unattainable in a laboratory setting, where the observed apparent muon flux is dominated by a low-energy component with relatively high variability, as well as by unavoidable environmental EM noise (especially in an urban environment). These effects quickly disappear the moment the muon sensors are placed at some appreciable depth (in this case, a nominal depth of 3 m in soil).

Next, we utilized the above measured muon flux to infer the depth of the sensors and compare it to the expected depth profile of the HDPE pipes. This was done for sensor MV8_B4_1, assuming our best determination of the absolute detector efficiency. The best match to the data is when we assume an average

bulk density of 1.7 g/cc for the material above pipe #2, which is not far off expectations, given the compacted nature of our soil. Note that if we have assumed a lower efficiency, then the best fit to the data would have been with a bulk density.

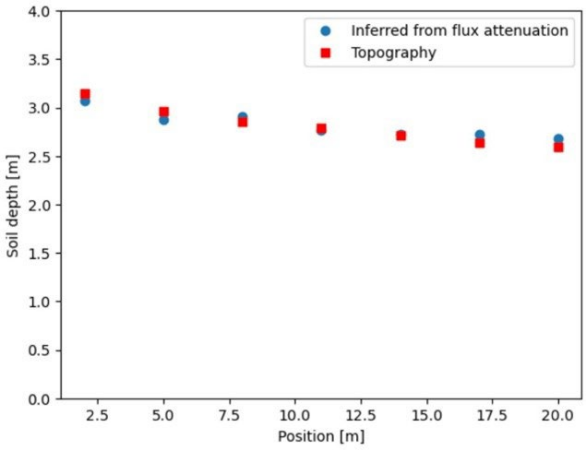

Figure 8: Preliminary best fit to the apparent soil density at the demo facility, utilizing known depth data for the sensor

3D Validation

To validate the feasibility of performing density reconstruction from sensor data, we plan to initially set up 8 IPC pallet tanks, with a capacity to hold 1 m^3 of water each, to build a density anomaly on top of the soil. In this case, the density anomaly would consist of an 8m^3 cube filled with water, against a nominally uniform background of 3 m of soil. The idea is to compare results with or without the tank. Data is being acquired in August 2025 and hopefully will be presented at the conference and in the final version of this paper. Below, we will show how we have validated our reconstruction procedure using simulated data.

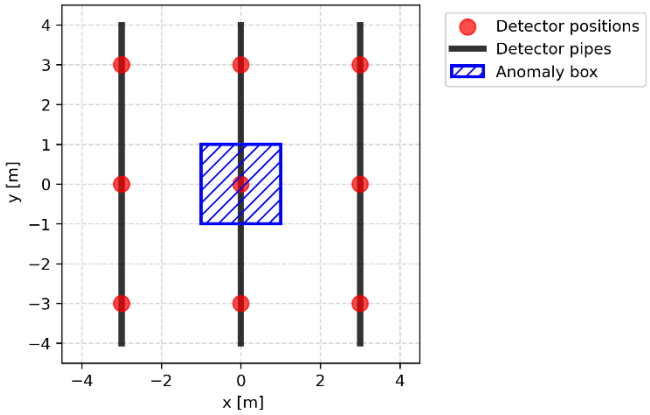

Figure 9: Left: arrangement of sensor measurement positions (top view) for the first 3D validation experiment with a 2 × 2 × 2 m^3 density anomaly. Right: implementation at the Demo Facility

Simulation Method

To validate and benchmark our expected sensitivity, we have developed a fast simulation tool that allows us to develop and validate our 3D reconstruction tool. With this tool, we generate muon trajectories following realistic angular and energy distributions. For this, we use the measurement positions and the synthetic distribution of material densities shown in Figure 9.

Our simulation is a conventional nuclear transport calculation. These types of transport simulations are commonly used in applications such as oil and gas (O&G) and cancer therapy. In our simulation, we use a standard parametrization of the muon flux (Gaisser, 1990), which models the energy distribution as a function of the muon arrival angle with respect to the vertical direction. We model the density in the soil and ad-hoc anomaly using a simple voxelization of the geometry, and then calculate the muon energy loss and thus flux attenuation using standard energy loss tables. In Figure 10, we show the relative attenuation of muon tracks at each detector location due to the presence of the water-filled pallet tanks.

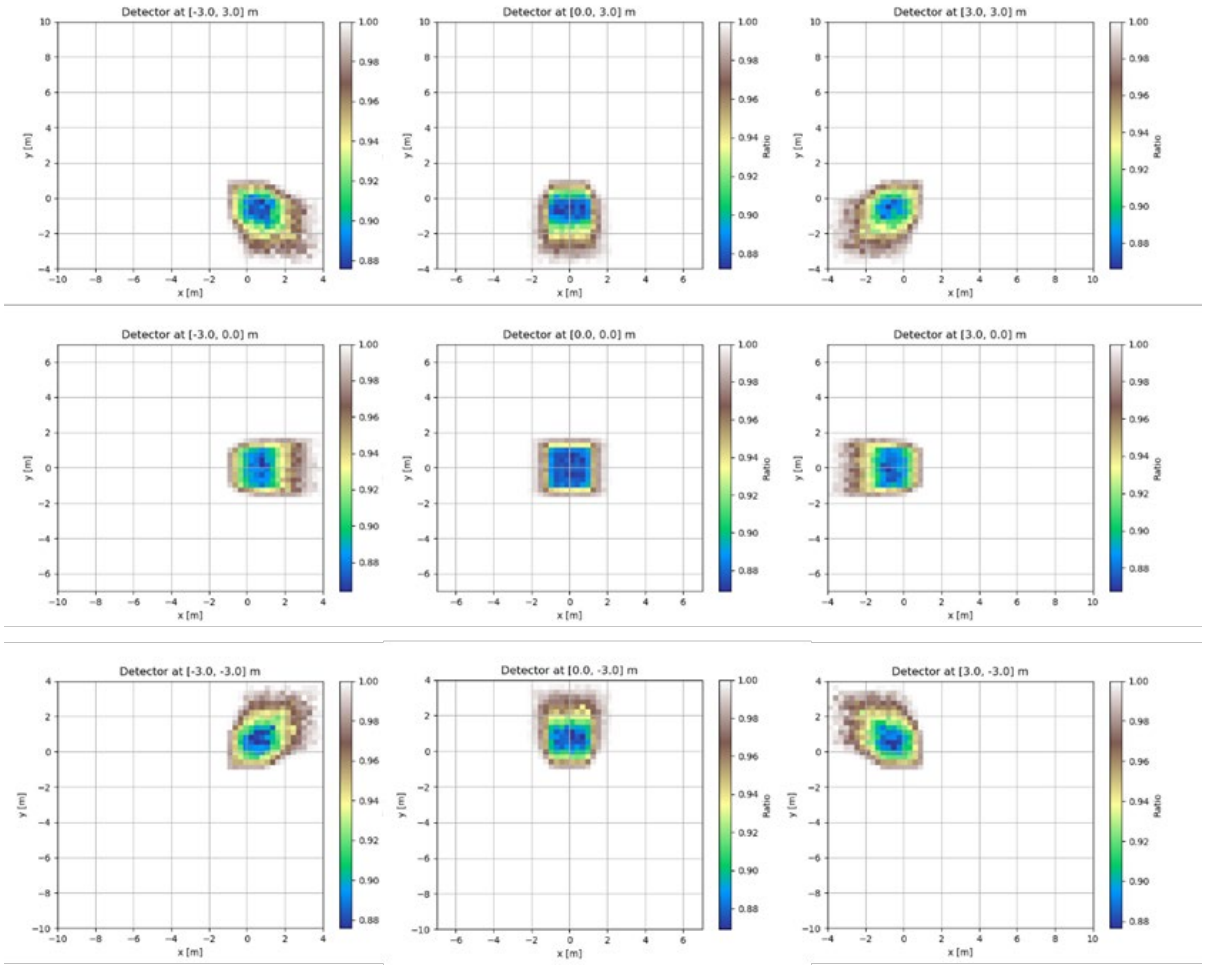

Figure 10: Simulation of the box shadow visualized through the relative count-rate at different detector positions

Reconstruction Method

Our 3D reconstruction method relies on the relation between the number of muons detected along a direction, or a solid angle, over an observation interval, and the integrated density along the direction of that solid angle, which we call opacity. Once the opacities are estimated from data, across the multiple directions seen by the detectors at different positions around the anomaly, a tomographic algorithm reconstructs the density of the heap.

The directions of arrival of the detected muons are binned into a prescribed number of directions. The opacity along each direction can then be estimated from the detected number of muons using the expression (cf. Guardincerri et al., 2017):

$$\frac{N_I}{N_D} = \int_{E_0}^{\infty} f(E,\Omega)\ dEd\Omega = A(E_0,\Omega)$$

where N_I_ is the reconstructed muon tracks and N_D is the reference number of muons that would be reconstructed in the absence of the material to be studied. The energy threshold E_0 depends non-linearly on the opacity, with larger opacities yielding a larger energy threshold, which in turn lowers the ratio of detected muons. We note that good angular resolution propagates back to the quality of the inferred opacity, since the energy distribution changes for each illumination angle. In reality, some uncertainty will be unavoidable because of the finite size of the detector.

Similar to many other so-called inverse problems in geophysics (e.g., electrical resistivity), our tomographic algorithm is challenged by the fact that only the opacities over a limited number of directions are known. Consequently, there is (in principle) an infinite number of possible densities that are compatible with the measured set. To mitigate this, we perform a constrained inversion, in the form of solving a variational problem, in which we promote features that we know must be present in the underlying density distribution.

For the current experimental setup, we promote a density distribution that is likely to be piecewise constant. This reflects the stark differences in density between rock, water, and air. To validate these assumptions, we first perform a constrained inversion from opacities computed analytically under the assumption of a homogeneous rock, air, and water distribution. The reconstruction can be seen in Figure 11. When the opacities are estimated, our constrained inversion can be modified to account for the uncertainty in the opacities. In this case, the reconstruction can be seen in Figure 12. These numerical experiments validate our choice of constrained inversion for the experimental setup at the Demo Facility and can be adapted to other features and experimental setups as needed.

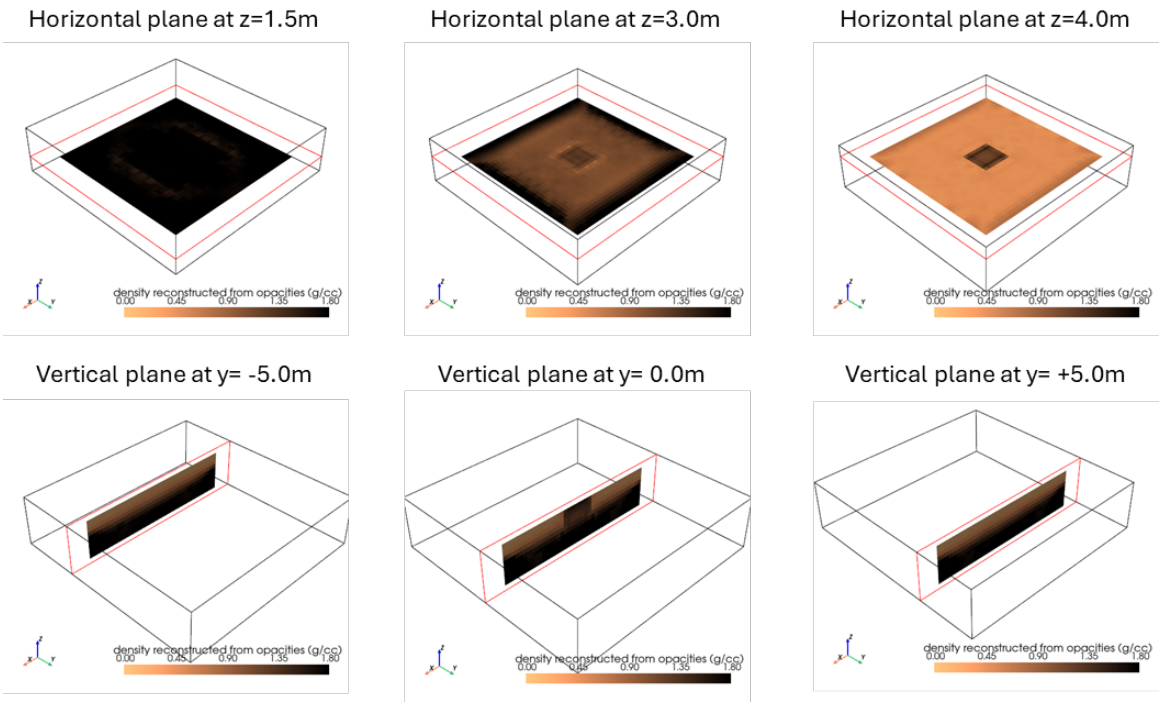

Figure 11: Density distribution reconstructed from simulated opacities. The density scale goes from 0.0 to 1.8 g/cc

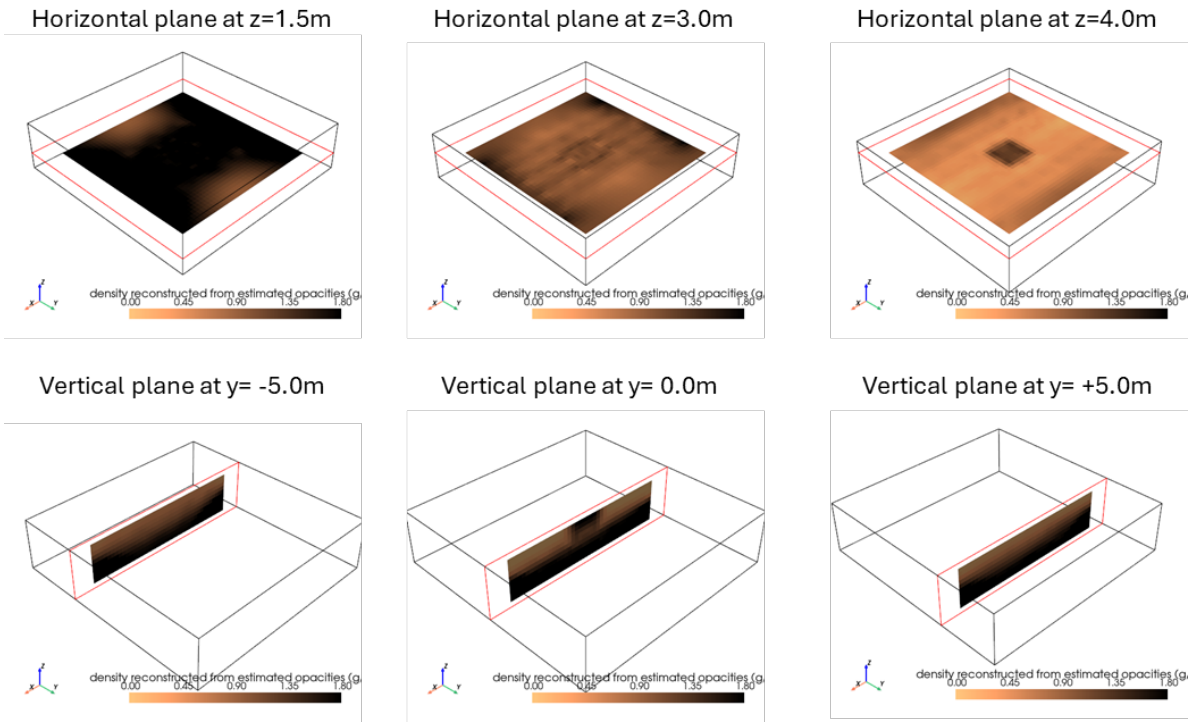

Figure 12: Density distribution reconstructed from opacities estimated via the detector response. The density scale goes from 0.0 to 1.8 g/cc

Conclusion

In this paper, we made a case for why 3D muon bulk density radiography holds great potential for enabling a quantitively precise characterization of a full-volume leaching asset in near-real time. Several potential benefits were highlighted, which hold promise for a significant increase in leaching yields as well as a much-improved stability analysis for leaching operations.

We then discussed steps being taken to validate this novel radiographic technique, presenting preliminary data and expected 3D results from the Muon Vision Demo Facility in Santiago. At the conference, we hope to have the full results on the first 3D validation of muon radiography for leaching operations.

References

Alvarez, L. W., et al. (1970). Search for hidden chambers in the pyramids. *Science, 167*(3919), 832–839.

Aplik. (2023). *Leach heap monitoring system.* https://www.aplik.cl/riego-en-pilas-lix-2

BHP. (2023). *Annual report 2023* (p. 226). https://www.bhp.com/investors/annual-reporting/annual-report-2023

Botto, T., et al. (2014). Reservoir saturation monitoring with cosmic rays. In *Proceedings of the World Heavy Oil Congress* (Paper WHOC14-296). New Orleans, LA.

Freeport. (2022). *Sustainability report 2022* (p. 84). https://www.fcx.com/sustainability/reports-and-documents

Gaisser, T. K. (1990). *Cosmic rays and particle physics*. Cambridge University Press.

Gilboy, W. B., Durham, J. M., Guardincerri, E., Morris, C. L., Bacon, J. D., Fabritius, J., Fellows, S., Plaud-Ramos, K., Poulson, D., & Renshaw, J. (2007). Industrial radiography with cosmic-ray muons: A progress report. *Nuclear Instruments and Methods in Physics Research Section A,* 580(1), 785–787. https://doi.org/10.1016/j.nima.2007.05.191

Guardincerri, E., Rowe, C. A., Schultz-Fellenz, E. S., Roy, M., George, N., Morris, C., Bacon, J. D., Durham, J. M., Morley, D. J., Plaud-Ramos, K. O., Poulson, D. C., Baker, D., Bonneville, A., & Kouzes, R. (2017). 3D cosmic ray muon tomography from an underground tunnel. *Pure and Applied Geophysics, 174*(5), 2133–2141. https://doi.org/10.1007/s00024-017-1526-x

Jansen, M., & Taylor, A. (2002). A new approach to heap leach modelling and scale-up. In *Proceedings of the ALTA Conference*. Perth, Australia.

John, L. W. (2011). The art of heap leaching: The fundamentals. In *International Conference on Percolation Leaching* (pp. 17–42). Southern African Institute of Mining and Metallurgy, Misty Hills, Muldersdrift, South Africa.

Lesparre, N., et al. (2012). Density muon radiography of La Soufrière of Guadeloupe volcano: Comparison with geological, electrical resistivity and gravity data. *Geophysical Journal International, 190*(2), 1008–1019.

Lizama, H. M. (2023). In-situ leaching of copper from spent heaps. *Hydrometallurgy, 215*, 105997. https://doi.org/10.1016/j.hydromet.2022.105997

Scheffel, R. E. (2002). Copper heap leach design and practice. In A. L. Mular, D. N. Halbe, & D. J. Barratt (Eds.), *Mineral processing plant design, practice and control* (pp. 1571–1605). Society for Mining, Metallurgy, and Exploration (SME). Vancouver, Canada.

Scheffel, R. E., Guzman, A., & Dreier, J. E. (2016). Development metallurgy guidelines for copper heap leach. *Minerals & Metallurgical Processing, 33*(4), 187–199.

Schouten, D., & Ledru, P. (2018). Muon tomography applied to a dense uranium deposit at the McArthur River Mine. *Journal of Geophysical Research: Solid Earth, 123*(10), 8637–8652.

van Staden, P. J., & Petersen, J. (2021). Towards fundamentally based heap leaching scale-up. *Minerals Engineering, 168*, 106915. https://doi.org/10.1016/j.mineng.2021.106915

Understanding and Addressing Low Permeability in Heap Leaching

S.W. Robertson, Mintek, South Africa
Jochen Petersen, University of Cape Town, South Africa

Abstract

Heap leaching has experienced substantial growth in recent decades, driven by various factors including declining grades, water supply issues, and stricter environmental regulations. Heap permeability often serves as the limiting factor, particularly in African ores characterized by high clay content. Laboratory test protocols have been established to assess the physical and hydraulic properties of crushed ores and agglomerates for heap leaching. Traditional capillary flow models such as Brooks-Corey (BC) or van Genuchten-Mualem (VGM) were used to describe unsaturated flow in ore beds. However, the hydraulic conductivity versus moisture content curves exhibit a discontinuity, with an inflection point corresponding to the air entry point. This suggests that at higher moisture contents, all pores connected to flow channels have been filled, leaving behind "disconnected pores" or "dead voids".

The moisture hold-up in the bed was found to increase with fines (<4 mm) content, whereas finer silt and clay material (-150 µm) do not contribute individually to the surface area exposed to the fluid but bind together as clay lumps or onto larger rocks. During irrigation, clay lumps tend to break apart and obstruct flow channels. Low permeability is also attributed to a high steady-state moisture hold-up, resulting in the bed operating close to saturation. Poor permeability was addressed in copper heap leaching (acid medium) by agglomeration with an acid-resistant cementitious binder. The binder formed stable bonds that endured prolonged exposure to sulfuric acid and reduced slumping in 1 m leach columns from 20% to zero. This allowed an increase in the irrigation rate from 1.4 L/m^2/h to the target of 6 L/m^2/h in a system where the leach rate was limited by the supply of acid from irrigation. To date, test work has been limited to laboratory scale (4 m tall, 320 mm ID leach columns). It is expected that agglomeration with the cementitious binder may provide a cost-effective method for whole-ore leaching of low-permeability ores.

Introduction

Although there has been a substantial increase in the number of heap leach operations over the past decades, low permeability remains a challenge in clay-containing ores. Several operations have reported problems with solution permeability, e.g., Benkala (Whiterow, 2013), Cerro Verde (Galdos et al., 2013), and Chuquicamata (Ramírez et al., 2019). It is therefore important to incorporate physical and hydraulic testing as part of a heap leach development program. This typically comprises uniaxial compression tests, as well as hydrodynamic column tests (Guzman et al., 2013; Milczarek et al., 2013; Robertson et al., 2013; Lupo, 2011; Afewu, 2009).

Over the past two decades, the lead author has conducted extensive physical and hydraulic characterization of a wide range of ore samples (e.g., Guzman et al., 2013; Robertson et al., 2013). An attempt was made to develop correlations between the hydraulic properties and the physical properties of the bed, such as bulk density, porosity, and surface area. Unsaturated flow is typically described by the hydraulic conductivity function (HCF) relating the relative hydraulic conductivity (K_r) to the dimensionless effective saturation (S_e). This function was modeled with traditional soil capillary models such as those by van Genuchten-Mualem (VGM) or Brooks Corey (BC). However, the data is generally discontinuous, with a point of inflection well below full saturation. Robertson et al. (2023a) showed that this point corresponds to the air entry point and concluded that below the point of inflection, the pores connected to flow channels are filled up so that only "poorly connected" pores remain.

Low permeability is attributed to a high steady-state moisture hold-up, resulting in the bed operating close to saturation. Agglomeration with cement is commonly applied in gold heap leaching (alkali medium) (Garcia and Jorgensen, 1997; Kappes, 2002; Bouffard, 2008) but there is currently no commercially available agglomeration binder for copper heap leaching (acid medium), except that sulfuric acid is commonly added in the agglomeration step (Lewandowski and Kawatra, 2009; Chen et al., 2020). It has recently been shown that stable agglomerates can be produced by agglomeration with modified Ordinary Portland Cement (OPC), which are acid-resistant even after prolonged exposure in dilute sulfuric acid when applied to a micaceous copper stockpile with low permeability (Robertson et al., 2023b). This resulted in reduced slumping and enhanced permeability, which resulted in final copper dissolutions of approximately 90% in leach columns.

Methodology

Agglomeration

A micaceous copper stockpile material (100% -40 mm, 62% -212 μm, and 42% -75 μm) was scrubbed in a 1 m diameter, 0.26 m long trommel scrubber for 10 minutes at 50% solids. The wet slurry was deslimed

over a vibratory screen to generate two feed materials at +212 µm and +75 µm, respectively. The coarse fraction was dried and agglomerated with tap water and 98% H_2SO_4 (14.3 kg/t). Alternatively, whole ore samples were agglomerated by adding modified OPC (dry) to the ore (1 to 10 kg/t) and agglomerated with tap water on a plastic sheet or in a cement mixer. Agglomerates were cured for 28 days in an enclosed plastic bag or in a leach column.

Compression Tests

Uniaxial compression tests were performed by loading approximately 10 kg of agglomerates into an 8" diameter steel pot (Figure 1). The sample was pre-wetted by irrigating at 6 L/m^2/h for 24 hours with 5 g/L H_2SO_4 and then allowed to drain for an additional 24 hours before applying the mechanical load. An incremental mechanical load was then applied between 3 kPa to a maximum of 400 kPa, representing the weight of the heap overburden. The bulk density and porosity profiles were generated. Finally, the saturated hydraulic conductivity was measured by passing a solution (in this case, 5 g/L H_2SO_4 in tap water) through the bed from a constant head reservoir. Experience has shown that the bed should maintain at least 30% porosity and a saturated hydraulic conductivity of at least 100 × the target application rate (e.g., 1000 L/m^2/h for a target irrigation rate of 10 L/m^2/h) (Robertson et al., 2013).

Hydrodynamic Column Tests

Hydrodynamic column tests were performed by loading approximately 25 kg of agglomerates in a 6" column or approximately 40 kg of agglomerates in an 8" column (Figure 1). The columns were loaded at a uniform bulk density and irrigated at incremental rates from a central dripper point. A moisture balance was performed in order to calculate the moisture hold-up and degree of saturation profiles. Finally, the columns were saturated, and the saturated hydraulic conductivity was measured by passing a solution through the column from a constant head reservoir.

In the case of the low-permeability ore sample, the feed material was a micaceous copper oxide stockpile material, agglomerated with cement, versus a control sample with no cement. Additional samples tested covered a wide range of mineralogies as described by Robertson et al. (2022 and 2023a). A drain-down curve was then generated, and the ratio between drained and residual moisture was measured. It is recommended that the degree of saturation should not exceed 65% for aerated heaps and 85% for non-aerated heaps (Robertson et al., 2013).

Metallurgical Leach Column Tests

Leach tests were conducted in water-jacketed columns (160 mm, 200 mm, and 320 mm ID) at 25ºC. Columns were irrigated with 8 g/L H_2SO_4 in tap water from a central dripper point. Parameters recorded daily were: (a) feed and drainage pH, (b) feed and drainage solution potential, (c) mass, volume,

temperature and specific gravity (SG) of feed solution, (d) mass, volume, temperature and SG of drainage, (e) daily pregnant leach solution (PLS) (Cu) and (Fe) by AAS (atomic absorption spectroscopy), (Fe^{2+}) and (H_2SO_4) by titration. Dissolution profiles and acid consumption profiles were generated. Final solid residues were removed from the columns, dried, pulverized and analyzed by multi-element Inductively Coupled Plasma-Optical Emission Spectrometry (ICP-OES). Mass balances were performed for copper and iron based on the dry feed solids and residue masses removed from the columns and the head and residue solid assays, as well as the daily solution Cu and Fe AAS analyses.

Figure 1: Compression test (a) and hydrodynamic column test (b) apparatus

Figure 2: Short (1 m, left) and tall (6 m, right) leach column facilities

Results and Discussion

Modeling Unsaturated Flow

In a previous study (Robertson et al., 2023a), data from the hydrodynamic column tests were processed to generate hydraulic conductivity functions (HCFs) and air conductivity functions (ACFs). These functions are plotted for three examples in Figures 3 and 4, where K_r is the relative hydraulic conductivity (Equation 4), S_e is the effective saturation (Equation 3), $S_{e\,max}$ is the effective saturation at the point of inflection, θ (m^3/m^3) is the soil water content, θ_s and θ_r are the soil saturated and residual volumetric contents, respectively, and m and γ are constants. The samples shown are KC2RS and KC2H (Congolese sedimentary dolomite hosted copper oxides, -25 mm) and EB (Namibian uranium ore, -9 mm) agglomerated with synthetic raffinate and sulfuric acid only. A detailed list of samples are provided in Robertson et al. 2022 and 2023a).

The HCFs are discontinuous, for which a modified form of the VGM model (Equation 1) was developed. Above the inflection point, ($S_{e\,max}$), K_r remains equal to 1 (Figure 3). The modified VGM model (Equation 2) was used to fit the ACF, where K_g (cm/s) is the air conductivity, $K_{g\,max}$ (cm/s) is the air conductivity when only residual moisture is present), θ_{aep} (m^3/m^3) is the air entry point), and S_g is the relative degree of gaseous saturation (Equation 5). The point of inflection was found to correspond with the air entry point, suggesting that above this point, the moisture content keeps on increasing as it fills up "disconnected pores" or "dead voids" without generating new flow channels. This is a departure from earlier investigators (Mohanty et al., 1997; Luckner et al., 1989) who propose that the discontinuity is a result of a change from capillary to gravity-controlled flow. The air entry point is the moisture content above which the air permeability falls off completely.

$$K_r = \left(\frac{S_e}{S_{e\,max}}\right)^{\Upsilon}\left[1-\left(1-\left(\frac{S_e}{S_{e\,max}}\right)^{\frac{1}{m}}\right)^{m}\right]^2,\ S_e < S_{e\,max} \qquad K_r = 1,\ S_e \geq S_{e\,max} \quad (1)$$

$$K_g = K_{g\,max}\left(1-S_g\right)^{\Upsilon}\left[1-S_g^{\frac{1}{m}}\right]^{2m} \quad (2)$$

$$S_e = \left(\frac{\theta-\theta_r}{\theta_s-\theta_r}\right) \quad (3)$$

$$K_r = \frac{K_w}{K_s} \quad (4)$$

$$S_g = \left(\frac{\theta-\theta_r}{\theta_{aep}-\theta_r}\right) \quad (5)$$

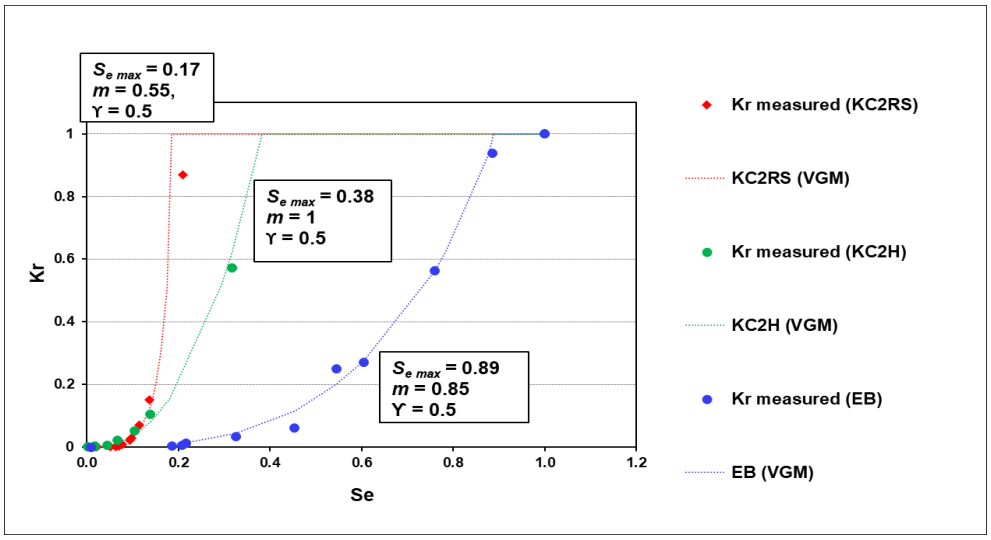

Figure 3: HCF for 3 selected materials (KC2RS, KC2H, EB) (Robertson et al., 2023a)

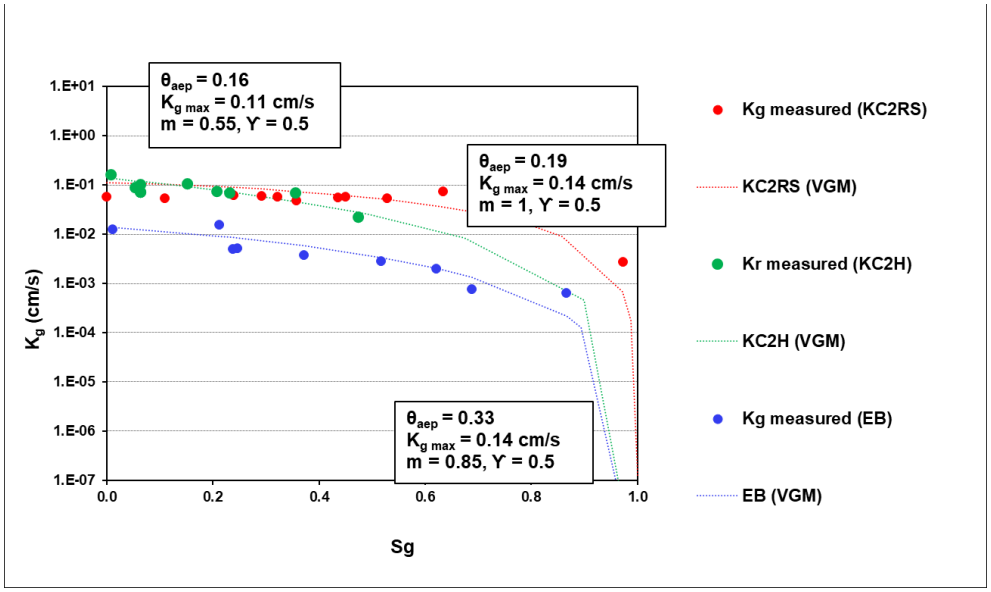

Figure 4: ACF for 3 selected materials (KC2RS, KC2H, EB) (Robertson et al., 2023a)

The distribution of volumetric void fractions in the hydrodynamic column tests is plotted in Figures 5 and 6 in order of increasing fines (-4.75 mm) content over the x-axis. The bed volume θ (m^3/m^3) is divided into residual moisture (θ_r), mobile moisture (θ_{max} - θ_r), "dead voids" (θ_s - θ_{max}), and solids (1 - θ_s). The close agreement between the air entry point (θ_{aep}) and the point of inflection (θ_{max}) suggests that the air entry point occurs close to or at the point of discontinuity in the HCF. θ_{max} is defined as the moisture content corresponding to $S_{e\ max}$. Air flow channels are converted to solution flow channels as the moisture increases and once all flow channels are filled, air permeability correspondingly drops off. Sandy materials to the right of Figure 5 had little or no dead voids, indicating that all the void space is connected to pore channels.

Normalized void fractions (e.g., excluding the fraction occupied by solids) are plotted in Figure 6. The average air entry point occurs at a saturation of 66%, which agrees with the 65% saturation rule proposed by Robertson et al. (2013). In other words, 65% void saturation provides, on average, a good estimate of the air entry point (θ_{aep}) above which gas does not pass through the bed and above which the heap cannot be aerated. Coarser samples (to the left, Figure 6) generally have a lower air entry point and a larger proportion of "dead voids" (θ_s -θ_{max}).

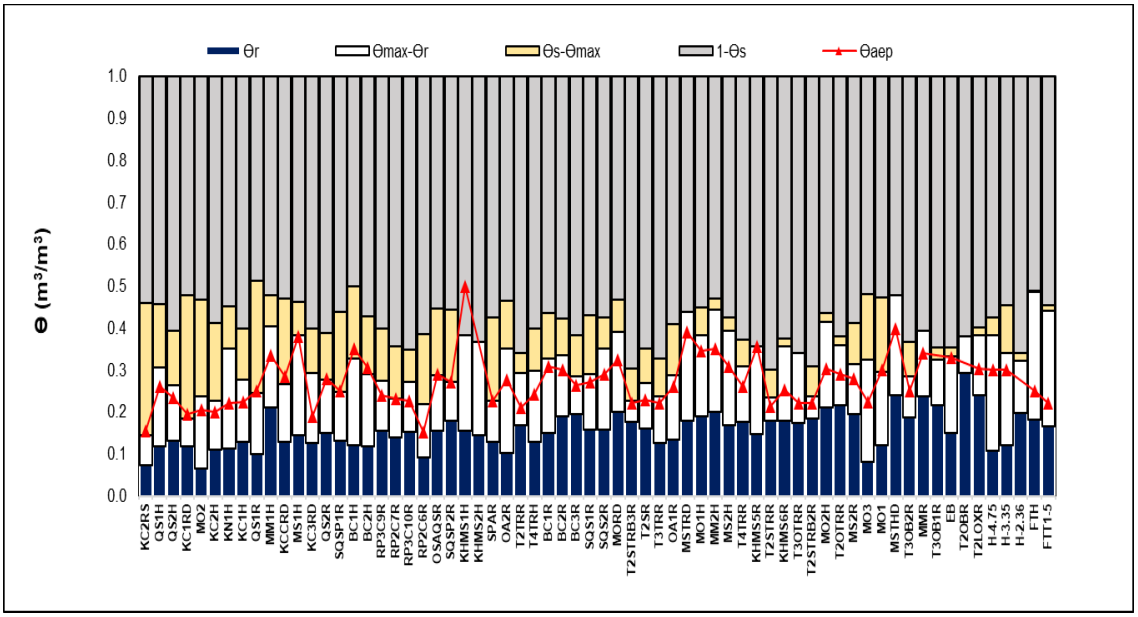

Figure 5: Volumetric void fractions and air entry point (Robertson et al., 2023a)

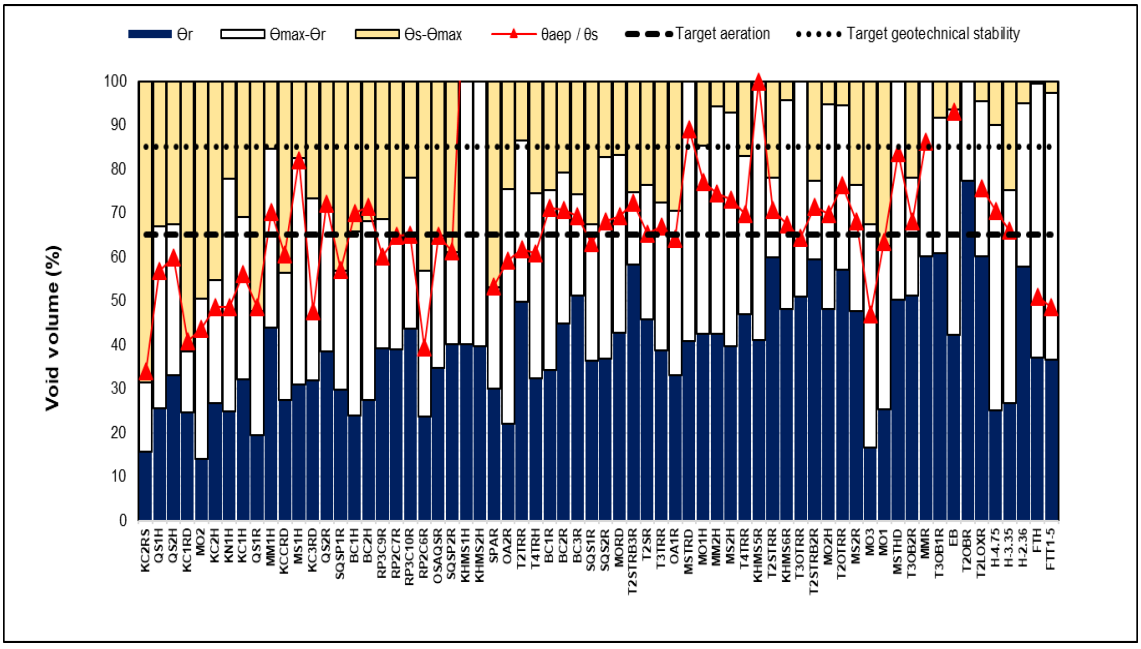

Figure 6: Normalized void fractions (Robertson et al., 2023a)

Low-Permeability Ores

Figure 7 shows the effects of binder addition on the compressibility curves of the micaceous ore type. Agglomeration with cement resulted in lower compressibility as the cement dosage increased. At the highest cement addition (10 kg/t), no slumping occurred after initial pre-wetting. Only the samples with 3 kg/t and 10 kg/t binder were able to conduct solution during the saturated flow (K_s) measurement, which was performed at the maximum compression of 5-5.5 m. Although conduction may occur at lower compressions, K_s was only measured at maximum compression.

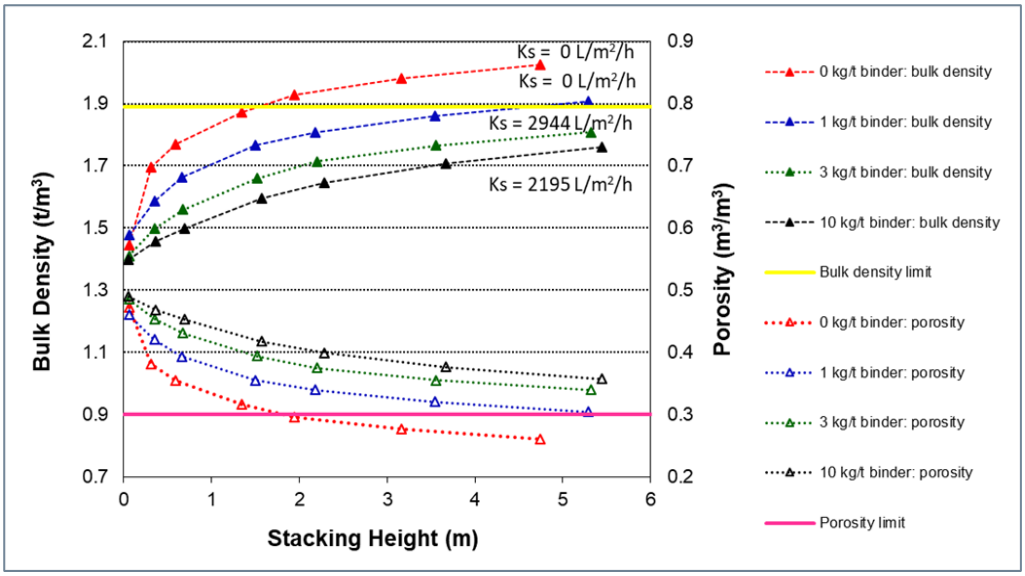

Figure 7: Effect of binder on compressibility

Leach column test results are presented in Table 1 and Figures 8 to 12. Copper dissolution profiles are presented in Figure 8. Where fines removal was applied (T6 and T7) a target application rate of 6 L/m²/h could be applied and copper dissolutions of above 80% were achieved after 140 days. The addition of curing acid increased the initial copper dissolution rates. However, based on the original ore mass before desliming, the actual copper recoveries are only 27.2% and 16.9%, respectively, due to the loss of copper to the fines.

T1 was performed on the whole ore in a 1 m column without a binder. The sample was agglomerated only with water. Upon wetting, the sample slumped by 20% and could only be irrigated at 1.4 L/m²/h before ponding occurred. As a result, the copper extraction was slower as it was limited by the supply of acid. A final copper dissolution of 43.7% was achieved after 162 days, at which point the column was stopped. Agglomeration with binder (T2, T3, and T4) resulted in almost no slumping (<1%). Irrigation could be performed at 6 L/m²/h, and final copper dissolutions of above 80% were achieved after 141 days.

Table 1: Summary of Column Test Results

Test	Pre-treatment	Column	Binder	Dosage (kg/t)	Head Assay CuT (%)	Dissolution CuT (%)	NAC (kg/t)	TAC (kg/t)
T1	Whole ore (-40 mm)	1 m tall, 160 mm ID	None	0	1.05	43.7	23.4	30.0
T2	Whole ore (-40 mm)	1 m tall, 160 mm ID	Cement A	10	1.05	87.7	91.1	105
T3	Whole ore (-40 mm)	1 m tall, 160 mm ID	Cement B	10	1.05	86.6	89.1	102
T4	Whole ore (-40 mm)	1 m tall, 160 mm ID	Cement C	10	1.05	88.1	93.3	107
T5	Whole ore (-40 mm)	4 m tall, 320 mm ID	Cement C	10	1.05	90.0	131	145
T6	Deslimed (+75 µm)	4 m tall, 160 mm ID	H_2SO_4	14.3	0.68	83.4	30	40
T7	Deslimed (+212 µm)	4 m tall, 160 mm ID	H_2SO_4	14.3	0.65	82.0	27	36

Cement A (64% OPC, 36% fly ash)
Cement B (38% OPC, 31% fly ash, 31% slag)
Cement C (50% OPC, 25% fly ash, 25% slag)
NAC – net acid consumption
TAC – total acid consumption

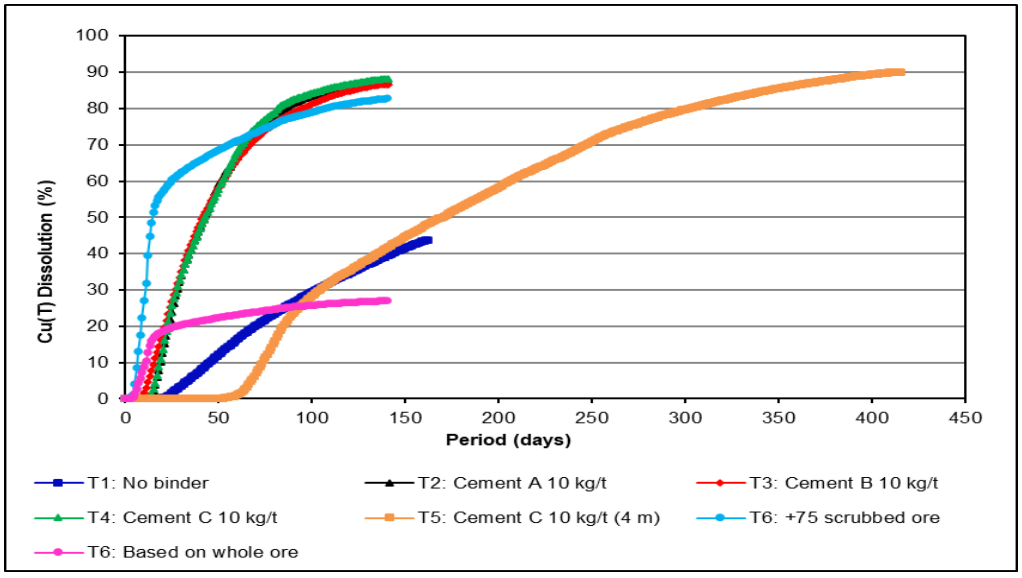

Figure 8: Cu dissolution profiles

Drainage pH profiles are presented in Figure 9. These show that T5, conducted with a binder at a lift of 4 m, initially experienced a high drainage pH. As a result, copper only appeared in the PLS after 50 days. The feed acid concentration for this column was also increased to 15 g/L after 53 days, whereas all the other columns were irrigated at 8 g/L throughout the duration of the tests. The copper recovery was 90% after 415 days, with <5% slumping. This shows one of the disadvantages of the agglomeration process. Since acid is not added in agglomeration, the benefit of the initial high copper dissolution rate generated by the curing acid is not achieved.

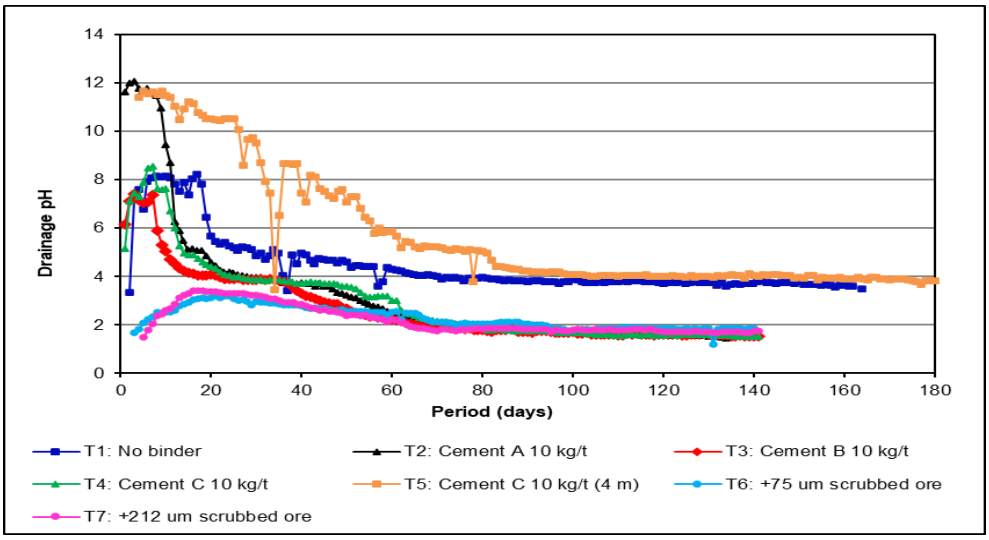

Figure 9: Drainage pH profiles

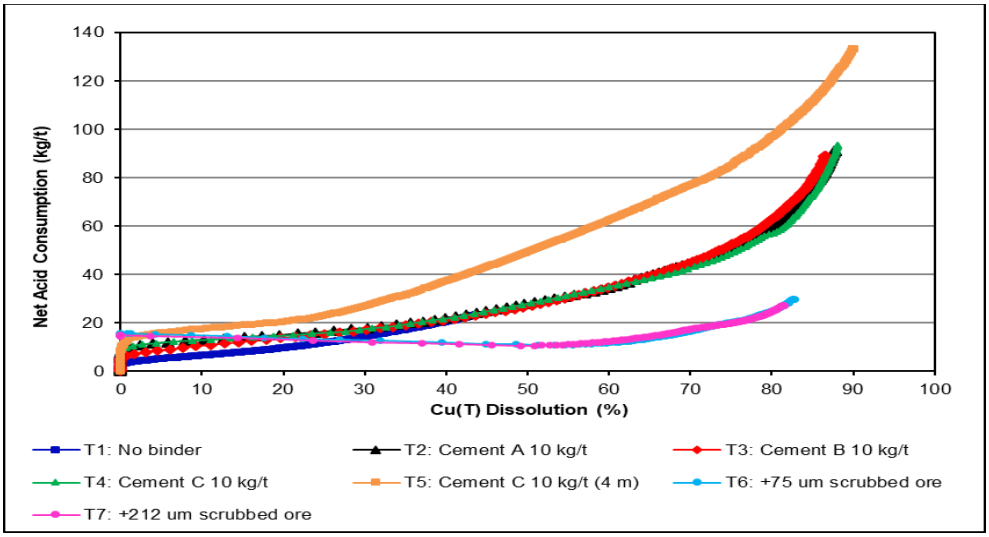

Figure 10: Net acid consumption versus copper dissolution

Figure 10 shows the net acid consumption (NAC) versus copper dissolution profiles. Acid consumptions were lower in columns T6 and T7 since less surface area was available for reaction due to fines removal. The acid consumption for T5 (4 m, 10 kg/t Cement C) was higher since the feed acid concentration was increased to 15 g/L after 53 days on account of the high drainage pH. T1 (no binder) had a net acid consumption of close to 20 kg/t, which was similar to T2, T3, and T4 at the point of 43.7% copper extraction, at which point T1 was stopped, and the acid consumptions for T2, T3, and T4 increased further. This seems to indicate that the binder does not increase the acid consumption significantly.

Theoretical acid consumptions due to the binder of 7.07 kg/t (T2), 4.2 kg/t T3), and 5.5 kg/t (T4), respectively, were calculated assuming an OPC content of 63% CaO and Equation 6. An estimate of the

cost of the binder is 1 USD per tonne of ore, assuming a binder dosage of 10 kg/t and a 100 USD/tonne cost of cement, excluding transport costs. If the ore contains 0.8% soluble copper at a price of 9600 USD per tonne of copper (Ycharts, May, 2025), the ore has a recoverable copper value of approximately 76.8 USD per tonne of ore. Hence, the cost of the binder is relatively low compared to the recoverable metal value.

$$CaO + H_2SO_4 \rightleftharpoons CaSO_4 + H_2O \quad (6)$$

The distribution of voids in the leach columns is presented in Figure 11. The sample without a binder (T1) operated close to saturation due to the high moisture content as well as high slump (20%), which further reduced the porosity. The moisture hold-up for the columns with a binder (T2-T5), although still high at around 30%, was not close to saturation since the bed porosity remained high due to the limited slumping. This aspect needs to be tested in the field, since the leach columns are expected to provide support and maintain a higher bulk density than in the field.

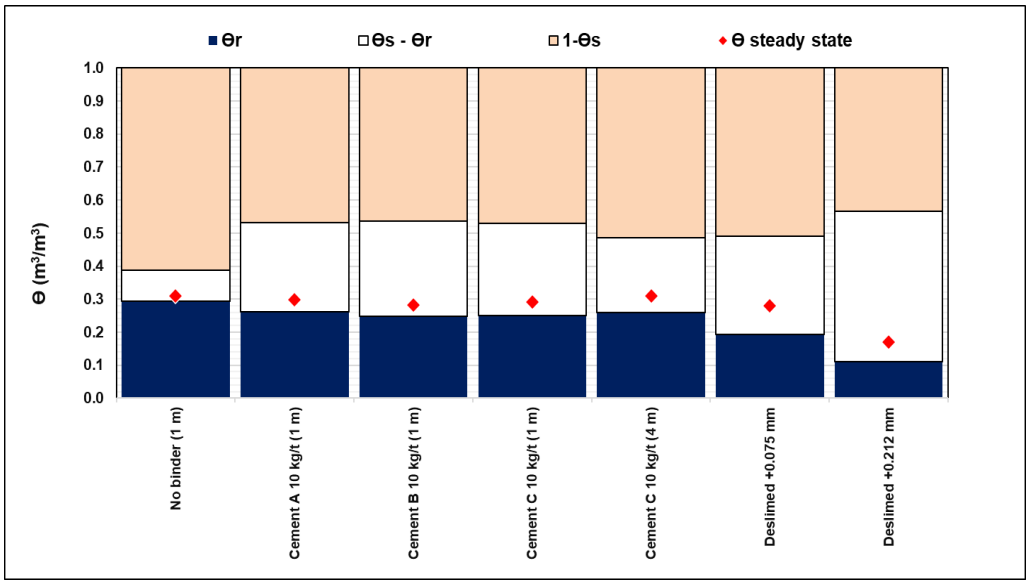

Figure 11: Void fractions versus steady state moisture hold-up

Figure 12 shows the agglomerates (>1 mm in diameter) and rim agglomerates generated with the cement binder. The binding agent appears to be a fine clay, which may have originated from kaolinite in the original ore. Phases identified were quartz, feldspar, mica (Mg-rich and Mg-poor), and clay -Mg-deficient and Mg-hosting. Ca components from the original cement were not detected, whereas Al, Si, O (kaolinitic components) and up to 4% Mg were detected. Ca-, Al- and Si-bonds form bonds during agglomeration with water and these harden during curing. The bonds remain firm after prolonged exposure to sulfuric acid and prevent slumping in the leach columns.

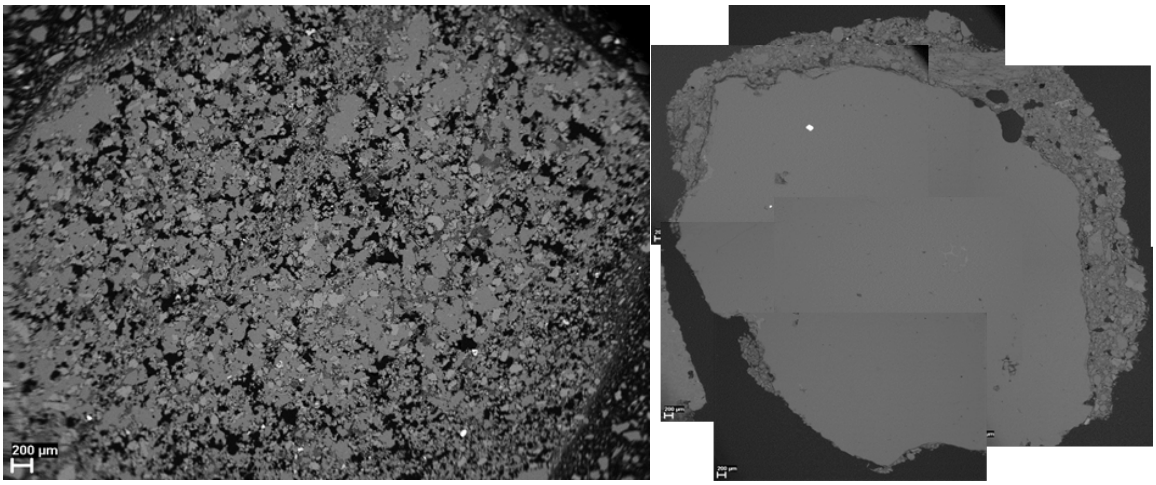

(a) (b)

Figure 12: Agglomeration of fines into lumps (a) and onto rocks (b)(Robertson et al., 2024)

Conclusion

Unsaturated flow below the air entry point can be modeled by traditional capillary models, such as BC and VGM. The point of discontinuity in the HCF corresponds with the air entry point. Below the air entry point, "connected pores" fill up, whereas above the air entry point, "unconnected" pores fill up without creating additional flow channels. The heuristic of <65% saturation required for forced aeration to permeate the heap agrees on average with the data. Coarser samples had a larger percentage of "unconnected pores".

Low permeability was correlated with a high steady-state moisture hold-up, which, combined with slumping, makes the bed operate closer to saturation. In order to maintain permeability, it is only necessary to remove the silt + clay (<75 µm) fraction. However, in practice, this is difficult, and dry screening is typically performed at a higher screen size (e.g., 1 mm). Both desliming and agglomeration with a modified cementitious binder were successful in improving permeability. However, a large loss of the target metal to the fines fraction makes desliming unattractive.

Agglomeration with acid-resistant cement reduced slumping significantly, hence maintaining a higher porosity available for solution flow. The agglomerated sample maintained low slumping (<5%) over the entire leach cycle. The improved porosity needs to be confirmed in test heaps, as it is expected that the columns benefited from wall support. Although the binder may enable whole ore heap leaching, acid cannot be introduced during the cement curing step. As a result, the process cannot take advantage of the initially high dissolution rates typically achieved by acid curing.

Acknowledgements

I wish to thank my supervisors, Prof. Jochen Petersen and Dr. Petrus van Staden, for their guidance

throughout the PhD studies

I wish to thank my former manager, Petrus Basson for his encouragement, ideas and mentorship in the field of heap leaching and tank bioleaching over more than a decade.

I wish to thank the current CEO of Mintek, Dr Molefi Motuku, who encouraged me to start the PhD and for Mintek to provide funding, in line with a broader policy of encouraging post-graduate study of Mintek employees.

I wish to thank Amado Guzman and HydroGeoSense for introducing me to the field of geomechanical laboratory testing.

I wish to acknowledge Sibabalwe Mxinwa for the execution of experimental work.

References

Afewu, K. I. (2009). Development and testing of a 2D axisymmetric water flow and solute transport model for heap leaching (PhD thesis). The University of British Columbia.

Basov, V. (2015). Heap leach: Mining's breakthrough technology. Mining.com. https://www.mining.com/heap-leach-minings-breakthrough-technology

Bouffard, S. C. (2008). Agglomeration for heap leaching: Equipment design, agglomerate quality control, and impact on the heap leach process. *Minerals Engineering, 21*(15), 1115–1125.

Chahua, L., Barreda, G., Satelo, G., & Narva, M. (2016, October). Study of the behavior of materials with fines content in heap leaching processes. In *Heap Leach Solutions 2016*. Lima, Peru.

Chen, K., Yin, W., Rao, F., Wu, J., Zhu, Z., & Tang, Y. (2020). Agglomeration of fine-sized copper ore in heap leaching through geopolymerization process. *Minerals Engineering,* 159, 106649.

Galdos, H., Guevara, J., & Saavedra, A. (2013). Geotechnical lessons learned from the operation of Cerro Verde's crush leach pad 4-A. In 5th International Seminar on Process Hydrometallurgy. Santiago, Chile.

Garcia, A., & Jorgensen, M. (1997). Agglomeration and heap leach testing requirements for high clay ores. In Randol Gold Forum (pp. 143–146).

Guzman, A., Robertson, S. W., & Calienes, B. (2013). Constitutive relationships for the representation of a heap leach process. In the International Heap Leach Conference. Vancouver, Canada.

Kappes, D. W. (2002). Precious metalheap leach design and practice. In *Mineral processing plant design, practice, and control* 1606–1630.

Lewandowski, K. A., & Kawatra, S. K. (2009). Binders for heap leaching agglomeration. *Minerals & Metallurgical Processing, 26*(1), 1–7.

Lupo, J. F. (2011). Sustainability issues related to heap leaching operations. In *Percolation leaching: The status globally and in Southern Africa*. The Southern African Institute of Mining and Metallurgy, Misty Hills, Muldersdrift, South Africa.

Luckner, L., Van Genuchten, M. T., & Nielsen, D. R. (1989). A consistent set of parametric models for the two-phase flow of immiscible fluids in the subsurface. *Water Resources Research, 25*(10), 2187–2193.

Milczarek, M., Yao, T., Banerjee, M., & Keller, J. (2013). Ore permeability methods of evaluation and application to heap leach optimisation. In the International Heap Leach Conference. Vancouver, Canada.

Mohanty, M. P., Bowman, R. S., Hendricks, J. M. H., & Van Genuchten, M. T. (1997). New piecewise-continuous hydraulic functions for modelling preferential flow in an intermittent-flood-irrigation field. *Water Resources Research, 33*(9), 2049–2063.

Ramírez, L., Font, J., & Saldaña, M. (2019). Chuquicamata improvements for low permeability heap leaching dump. In *Proceedings of the 11th International Seminar on Process Hydrometallurgy*. Santiago, Chile.

Robertson, S. W., Guzman, A., & Miller, G. (2013). Implications of hydraulic behaviour testing for heap leach modelling. In *Hydroprocess: 5th International Seminar on Process Hydrometallurgy*. Santiago, Chile.

Robertson, S. W., Basson, P., Van Staden, P. J., Chaerkaev, A., & Petersen, J. (2022). Properties governing flow of solution through crushed ore for heap leaching. *Hydrometallurgy,* 208, 105811.

Robertson, S. W., Basson, P., Van Staden, P. J., & Petersen, J. (2023a). Properties governing flow of solution and air through crushed ore for heap leaching: Part II unsaturated dual-phase flow. *Hydrometallurgy,* 215, 105990.

Robertson, S. W., Mxinwa, S., Basson, P., Ndhlalose, M. S., & Nxumalo, D. N. (2023b). Binder for an agglomeration process. Namibian Patent NA/P/2023/0001.

Robertson, S. W., Basson, P., Brill, S., Van Staden, P. J., & Petersen, J. (2024). Properties governing flow of solution through crushed ore for heap leaching: Part III – Low permeability ores. *Hydrometallurgy,* 224, 106247.

Whiterow, P. (2013). Update – Frontier Mining says Benkala now generating cash for the first time in its history. Proactive Investors. https://www.proactiveinvestors.com.au/companies/news/54061/update-frontier-mining-says-benkala-now-generating-cash-for-first-time-in-its-history-64083.html

YCharts. (2025). Copper price. https://ycharts.com/indicators/copper_price

Optimizing Heap Leach Performance through an Integrated Characterization Approach

Amado Guzman, HydroGeoSense, Inc., USA

Abstract

Heap leaching is a complex, multi-variable hydrometallurgical process whose success depends not only on chemical reactivity, but also on the ore's geological, physical, hydraulic, and mechanical properties. Traditional metallurgical testing—while useful—often fails to capture these critical factors, limiting its predictive power and increasing the risk of underperformance or failure. This paper presents a decision-oriented framework built on HydroGeoSense's Integrated Characterization Approach (ICA), which incorporates geotechnical, metallurgical, hydraulic, and chemical data into a cohesive design methodology. The ICA systematically selects optimal conditions for the five key design elements—particle size distribution, ore conditioning, stacking geometry, reagent delivery, and liquid saturation—ensuring that ore-specific data support each design decision. Applications to copper, gold, nickel, rare earths, and bio-assisted leaching systems have demonstrated ICA's ability to improve metal recovery, reduce leach cycle duration, and optimize reagent utilization and solution inventory. By aligning characterization with operational realities, the ICA provides a robust pathway for technically sound and economically viable heap leach designs.

Introduction

Heap leaching is a complex hydrometallurgical process that depends not only on the chemical reactivity of the ore but also on its geological, physical, hydraulic, and mechanical properties. While standard metallurgical testing offers valuable insights into chemical extraction potential, it often overlooks critical variables such as solution transport mechanisms, ore structure stability, and reagent distribution efficiency—all of which are essential to predicting and achieving economic performance.

A properly designed heap leach facility must address a number of key elements to ensure that the selected process can be implemented efficiently and at scale. These elements include ore preparation, agglomeration, stacking geometry, solution application, and air or reagent delivery systems. Each of these components must be calibrated to the specific characteristics of the ore to maximize metal recovery, minimize reagent consumption, and maintain long-term heap stability.

It can be argued that each ore body is geologically unique—controlled by its mineralization, alteration history, and structural evolution. Therefore, leach process design must go beyond standardized templates and pursue tailor-made solutions that reflect the peculiarities of the deposit. The proposed Integrated Characterization Approach (ICA) provides the technical foundation for such customized designs, enabling a structured decision-making process supported by relevant and ore-specific data.

Key Elements in a Heap Leach Design

Designing a heap leach facility requires addressing a series of interdependent technical elements that directly impact the efficiency, stability, and economic viability of the leaching process. These elements—ranging from particle size distribution and ore conditioning to stacking geometry, reagent delivery, and degree of liquid saturation—must be carefully evaluated and selected based on a rigorous understanding of the ore's physical, hydraulic, geochemical, and mechanical behavior under operational conditions. Each decision creates a cascading effect that influences downstream parameters, reinforcing the need for a systematic and integrated design approach. Failure to address these interactions holistically, particularly when relying on conventional metallurgical testing alone, can lead to suboptimal metal recovery, inefficient reagent use, elevated solution inventories, or even structural instability. The following paragraphs outline the five core design factors that must be addressed through an integrated characterization framework to ensure successful heap leach performance.

1. **Particle Size Distribution (PSD):** The PSD of the ore is a critical parameter that governs both the liberation of target minerals and the percolation capacity (hydraulic conductivity) of the ore mass. A finer PSD can improve mineral exposure and enhance leach kinetics, but it may also compromise permeability, leading to percolation capacity and increased risk of compaction. The crushing method and degree of comminution directly influence the PSD, especially if fine particles (<74 μm) are liberated, which can significantly affect heap performance if not properly managed. The selected PSD must ensure the ore maintains adequate hydraulic conductivity to support the selected irrigation rate, maintain a safe moisture content, and promote thorough solution-to-ore contact for optimal metal recovery, and drainage to facilitate ore removal in the case of a static heap or to minimize solution inventory in the case of a permanent heap.
2. **Ore Conditioning:** Proper agglomeration, typically achieved through controlled moisture and acid addition, is essential for building a stable porous structure and achieving a uniform leach response. In many cases, effective agglomeration has rendered difficult ores leachable by enhancing particle cohesion and facilitating reagent distribution throughout the ore mass. Additional benefits include reduced particle size segregation during stacking, increased overall porosity, and improved

partitioning between micro- and macro-porosity. This last aspect is particularly critical in bioleaching processes, where adequate macro-porosity supports air and solution flow, while microporosity ensures close contact between the ore and the microbial community. A well-designed cure stage can further initiate beneficial early-stage chemical reactions, suppress undesirable gangue reactions, and stabilize the ore matrix—ultimately leading to higher metal recovery and improved operational stability.

3. **Stacking Geometry:** The choice of heap geometry must be guided by the ore's mechanical properties —particularly its strength, compressibility, and ability to maintain percolation capacity under increasing overburden stress. A key decision is the selection of lift height (for dynamic heaps) or total heap height (for permanent pads), which directly impacts operational feasibility and metallurgical performance. In bioleaching systems, lift height also strongly influences the heap's thermal regime: greater lift heights help retain the exothermal energy generated by microbial activity, thereby accelerating reaction kinetics and improving metal recovery. However, excessive lift heights can compromise reagent delivery, aeration, and drainage—especially if the ore's hydrodynamic characteristics are not adequately accounted for. As such, stacking geometry must be tailored to the ore's specific physical and hydraulic behavior to ensure a stable structure, sufficient percolation capacity, and, where applicable, effective thermal management.
4. **Reagent Delivery:** The selection of irrigation rate, dosing schedule, and distribution method is critical to achieving uniform reagent contact, minimizing consumption, and promoting efficient leaching. Extensive operational experience has shown that reagent delivery is highly sensitive to timing and dosage —even when the total reagent addition over the leach cycle remains constant. Variations in the delivery schedule can significantly affect reaction kinetics, leach uniformity, and overall metal recovery. A key design decision is whether to introduce reagents—such as acid or inoculum—during the ore conditioning phase (e.g., curing or agglomeration) or during active heap irrigation. This decision influences the early-stage chemical environment and can impact the success of both chemical and bio-assisted leaching processes. Furthermore, the rate of solution (and, where applicable, air) delivery must be aligned with the hydrodynamic properties of the ore to ensure an appropriate degree of liquid saturation and maintain adequate air permeability. These parameters are especially critical in bioleaching operations, where microbial activity depends on oxygen availability and suitable moisture contents.
5. **Liquid Saturation:** The degree of liquid saturation within the ore pile is one of the most critical yet least understood parameters in heap leach design among the metallurgical community. It has profound implications for both heap performance and operational safety. Excessive saturation can lead to mechanical instability, increased risk of slope failure, compromised structural integrity, and

reduce the effectiveness of forced aeration, which is particularly critical in bio-assisted leaching operations. Conversely, insufficient saturation can limit solution-to-ore contact, reducing leaching effectiveness. Maintaining saturation below 85% is generally recommended to preserve heap stability, while levels below 65% are essential to enable effective air permeability and oxygen transfer in bioleaching systems.

The selected irrigation rate must be compatible with the ore's hydrodynamic properties —namely, its hydraulic conductivity, porosity, and compressibility—which vary with depth (overburden stress). These properties influence how saturation changes with increasing heap height, particularly in permanent multi-lift systems where mechanical compaction and chemical decrepitation (caused by repeated leach cycles) can alter pore structure over time. Furthermore, the degree of saturation directly impacts the volume of solution retained within the heap and therefore determines the amount of metal inventory tied up in the process. Accurate control and monitoring of saturation are essential for optimizing metal recovery, minimizing operational risks, and managing working capital effectively.

Each design decision on these five key elements must be grounded in a comprehensive dataset that captures the ore's behavior under realistic operational conditions. The impacts of these decisions are not isolated; they can be thought of as a cascading sequence, where each choice influences and constrains the next. For example, the selected particle size affects agglomeration performance, which in turn impacts stacking structure and percolation capacity—ultimately controlling how reagents and fluids interact with the ore. Relying solely on conventional metallurgical testing overlooks these interdependencies and increases the risk of suboptimal design outcomes. Poorly informed decisions can lead to reduced metal recovery, inefficient reagent utilization, excessive solution inventory, compromised aeration, or even geotechnical instability and structural failure. An integrated characterization approach is therefore essential to ensure a technically sound, operationally viable, and economically optimized heap leach facility.

Limitations of Standard Metallurgical Testing

Conventional metallurgical testing remains a cornerstone of leach process design, typically focusing on the chemical extraction potential of a given ore under fixed laboratory conditions. These tests are useful for understanding solubility and extraction kinetics but are fundamentally limited in their ability to predict full-scale heap behavior. Specifically, standard column and bottle roll tests do **not** evaluate key physical and hydraulic mechanisms that directly affect solution inventory, metal recovery, operational efficiency, and structural stability.

Critical limitations include the lack of information on:

1. **Solution-to-ore contact efficiency**—Standard tests used by metallurgical practitioners often rely on measurements of percolation capacity under full liquid saturation. While these measurements provide a general idea of the ability of the ore to support solution movement, they ignore the fact that a functional heap requires partial liquid saturation to be stable. The surface contact area between the leaching solution and the ore is typically not quantified or considered in the calculation of metal recovery.
2. **Moisture retention and transport under varying saturation**—Liquid saturation levels are critical to leach kinetics, aeration potential, and heap stability. Yet, conventional tests do not collect the necessary data to determine real-world saturation profiles or drainage behavior.
3. **Air and liquid conductivity under compaction**—Full-scale heaps undergo mechanical consolidation due to self-weight. Standard tests ignore permeability losses due to ore compressibility or the impact of changing solution saturation along the heap profile on the air conductivity. The lack of this information is the cause behind the failure of a large number of forced aeriation systems.
4. **Reagent breakthrough timing and residence time distribution**—The timing of reagent arrival and its residence in the ore volume govern the reaction efficiency, yet are rarely captured in traditional leach tests, which are not designed to track moisture or reagent fronts or potential flow heterogeneity.
5. **Mechanical deformation under stacking loads**—The geomechanical response of the ore mass—including settlement, porosity reduction, or failure planes—is rarely assessed, despite being critical to stability, percolation, and long-term performance.

The recent events at the Çöpler Gold Mine in Turkey and the Eagle Gold Mine in Yukon, Canada (both in 2024) underscore the increasing complexity of modern heap leach operations and the critical need to broaden the scope of design considerations. In both cases, conventional characterization methods did not fully capture the hydromechanical behavior of the ore under operational conditions. These incidents highlight the importance of moving beyond traditional testing protocols and adopting an integrated, data-driven approach—such as the one proposed in this paper—that unifies geotechnical, hydraulic, mineralogical, and chemical information within a cohesive design framework.

Without addressing these limitations, even well-intentioned heap designs are vulnerable to poor metallurgical performance, excessive solution inventories, inefficient reagent usage, and, in extreme cases, structural failure. To effectively manage these technical and operational risks, a modern heap leach design must be grounded in site-specific, multidisciplinary characterization. This integrated approach is essential not only for ensuring technical soundness but also for maximizing long-term economic returns.

Integrated Characterization Approach (ICA)

HydroGeoSense's Integrated Characterization Approach (ICA) provides a comprehensive, decision-oriented framework that integrates geological, mineralogical, geotechnical, hydrodynamic, and metallurgical parameters into a unified workflow. Its primary objective is to generate actionable, site-specific data to answer the key design questions outlined in the section above, "Key Elements in a Heap Leach Design," enabling robust and predictive heap leach facility design.

The ICA workflow consists of five sequential and interdependent steps:

1. **Analytical Characterization**

   Assess the ore's chemical and mineralogical composition, including head grade, mineral deportment, and the presence of impurities. This step is conducted on the as-mined particle size distribution (PSD) to preserve representativeness. Quantification of key deleterious elements is also performed to anticipate potential impacts on processing efficiency and downstream recovery.

2. **Ore Preparation**

   Determine the optimal crushing method and degree of comminution required to produce a PSD that supports the selected maximum heap height and desired permeability. The target PSD must balance mineral liberation with percolation capacity. Final heap height is dictated by the type of facility (dynamic vs. permanent) and the mechanical and hydraulic behavior of the ore mass under compaction.

3. **Ore Conditioning**

   Evaluate the need for agglomeration and define optimal reagent addition (moisture, acid, or additives) in terms of dosage, method, and timing. Effective agglomeration improves particle cohesion, enhances permeability, promotes solution-to-ore contact, and reduces solution and metal inventory. Additionally, a well-designed cure stage can trigger early-stage beneficial reactions in the early stages and suppress unwanted interactions with gangue. For bioleaching applications, a proper balance of micro- and macro-porosity is essential to ensure aeration and microbial activity. Optimal agglomeration improves the solution to ore contact, minimizes the solution and metal inventory, and promotes proper drainage.

4. **Leaching Process Design**

   Design the irrigation scheme—including application rate, cycle schedule, and reagent concentration—to ensure the desired degree of liquid saturation and reagent contact throughout the heap's operational life. Liquid saturation must remain below 85% to ensure geotechnical stability, or below 65% when natural or forced aeration is required (e.g., in bioleaching). The leach design must demonstrate the ability to maintain these saturation thresholds across the full heap height and over multiple leaching cycles in permanent facilities.

5. **Process Optimization**

   Use laboratory data and techno-economic analysis to determine optimal operating parameters—such as leach cycle duration, irrigation rate, leach-to-rinse ratio, reagent consumption, and recovery targets. These variables are evaluated through trade-off analyses to identify the operational envelope that maximizes economic performance while minimizing risk.

Importantly, this approach emphasizes a *tailor-made* design based on ore-specific behaviors—not assumptions or industry templates. The process design resulting from this approach, in combination with real-time monitoring, can significantly reduce operational uncertainty and risk, providing a strong foundation for successful decision-making.

Applications and Benefits

The Integrated Characterization Approach (ICA) has been successfully applied across a diverse range of projects, including:

- **Copper (oxide, sulfide, and mixed ores):** Enabled hybrid chemical/bioleaching strategies and stable multi-lift heap designs.
- **Refractory Gold:** Improved pore structure and permeability, enhancing liberation and gold recovery.
- **Rare Earth Elements (REEs):** Supported both ionic clay and hard rock systems through tailored leach chemistry control.
- **Nickel Laterites:** Addressed mineralogical variability and optimized moisture distribution.
- **Bio-assisted Leaching:** Enhanced microbial performance and redox control via optimized irrigation and aeration regimes.

Table 1 (adapted from the supporting publication: *Integrated Characterization for Improved Leach Design and Performance [Guzman, 2025])* summarizes the results from two copper and one Rare Earths projects:

- Metal/Element recovery increases up to +9%
- Leach cycle durations reduced by up to 35%
- Water consumption reduced by up to 38%
- Decreased acid consumption by up to 63%
- Decrease solution inventory by up to 36.3%
- Improved pad efficiency with higher maximum lift heights and larger ore mass per unit area or smaller operational footprints.

Table 1: Integrated Characterization Approach—Examples

	Max heap height (m)	Extraction (%)	Solution Inventory (L/t)	Leach Cycle (Days)	Leach Ratio (m^3/t)	Acid Consumption (kg/t)
Mixed Cu Ore, active multi-lift heap						
Original Design	<8	60.3	242	360	2.9	10.9
Integrated Design	>30	66.4	200	300	2.0	10.7
Exotic Cu Ore, multi-lift heap project						
Original Design	<8	70.6	157	120	2.1	23.5
Integrated Design	>50	79.6	100	85	1.7	21.7
TREEs+Y, multi-lift heap project						
Original Design	90	80.0	145	60	13.3	117.5
Integrated Design	90	80.0	175	45	5.0	74.3

These improvements underscore ICA's potential to enhance metallurgical performance, reduce operating costs, and manage risk. While instrumentation is not the focus of this report, properly monitored heaps (e.g., temperature, pH, ORP, and saturation sensors) can provide real-time data to support continuous process optimization.

Conclusion

Heap leach design is a complex engineering challenge involving multiple interrelated variables. Achieving technical and economic success requires more than conventional laboratory testing—it calls for a deliberate, data-driven strategy rooted in multidisciplinary characterization.

Optimizing heap leach performance demands that we move beyond legacy testing routines and embrace a decision-oriented framework. The design process must be guided by a clear understanding of how the ore behaves under operational conditions—chemically, physically, hydraulically, and mechanically. Each decision—from particle size distribution and agglomeration to stacking geometry, reagent delivery, and target saturation—carries downstream implications that affect recovery, stability, and process efficiency.

HydroGeoSense's Integrated Characterization Approach (ICA) provides a structured, predictive pathway for making these critical design decisions. By aligning characterization tasks with key design milestones, ICA facilitates the development of heap leach systems that are not only technically robust but also scalable, resilient, and economically optimized.

As both laboratory studies and operational failures have shown, integrated, site-specific design is no longer optional; it is essential. Facilities that rely solely on conventional testing risk suboptimal

performance, excessive solution inventories, and, in extreme cases, structural failure. In contrast, ICA offers a forward-looking methodology that minimizes risk and maximizes value across the life of the heap.

References

Guzman, A. (2025). Integrated characterization for improved leach design and performance. *Mining Engineering Magazine,* Fine Grind Series, March 2025. Society for Mining, Metallurgy & Exploration (SME).

Chapter Three

Modeling

Innovative Draindown Modeling for Heap Leach Systems Using Hydrus 1D and Python

I.J. Vega, Geotechnical Engineering, SRK Consulting, Buenos Aires, Argentina
L. Carrizo, Geotechnical Engineering, SRK Consulting, Buenos Aires, Argentina
A.G. Terlisky, Geotechnical Engineering, SRK Consulting, Buenos Aires, Argentina
J. Parshley, Geoenvironmental Engineering & Mine Closure, SRK Consulting, Nevada, USA
M. Noël, Mine Waste Management & Geoenvironmental Engineering, SRK Consulting, Montreal, Canada

Abstract

Accurate draindown modeling is essential for the design, operation, and closure of heap leach facilities, particularly in scenarios involving complex geometries or challenging operational conditions. Traditional 2D and 3D numerical models, while robust, often require significant computational resources and time, limiting their practicality for iterative design processes or real-time decision-making. To address these challenges, we present an innovative tool that integrates Hydrus 1D with Python to enable automated, large-scale iterative simulations for a pseudo-3D modeling approach.

This tool combines the computational efficiency of Hydrus 1D, a widely used software for simulating water flow and solute transport in variably saturated media, with Python scripting to automate the execution of multiple 1D simulations. By discretizing in time, the heap leach facility into a network of vertical 1D columns, the tool captures the time-dependent spatial variability in material properties, stacking sequences, and geometries, providing a comprehensive time-dependent 3D representation of the system without the computational burden of full 2D or 3D models.

The methodology is demonstrated through two case studies. The first case study focuses on a conceptual heap leach design with simplified geometry but a challenging stacking sequence. The objective is to predict heap leach outflow rates during operation and closure to support leachate management decisions. The second case study involves an operational heap leach facility situated in mountainous terrain with highly complex geometry. Here, the tool is used to predict the draindown time required for the outflow rate post-closure to reach the evaporation rate of the outflow pond.

The results from both case studies highlight the tool's ability to provide actionable insights for both operational and closure planning. Key advantages of this time-dependent pseudo-3D approach include reduced modeling time, enhanced flexibility in scenario analysis, and the ability to incorporate site-specific

complexities. Additionally, the integration of Python scripting facilitates seamless model running, data processing, visualization, and sensitivity analysis, further enhancing the tool's utility for practitioners.

This novel approach bridges the gap between the simplicity of 1D modeling and the complexity of higher-dimensional models, in particular in 3D. It offers a practical and efficient solution for draindown modeling in heap leach systems. This tool has the potential to streamline design and operational workflows by reducing reliance on resource-intensive modeling techniques.

Introduction

Heap leach pads are engineered structures widely used in the mining industry to extract valuable metals, such as gold, copper, and silver, through the application of chemical solutions. While effective during operations, the closure of these facilities presents interesting challenges, particularly in managing the fluid inventory within the heap. Accurate draindown prediction is critical for ensuring a safe and sustainable closure process, as it informs strategies for managing excess fluid and seepage while mitigating environmental risks.

The duration and intensity of the draindown depend on factors such as the volume of fluid stored in the heap, the capacity to manage collected seepage, and the potential impacts on the receiving environment. Once irrigation ceases, excess fluid within the heap will gradually seep out, requiring a well-defined fluid management strategy. Initial efforts often involve reducing the fluid inventory through treatment, evaporation, consumption, or storage, with recirculation employed to achieve target flow rates or volumes.

This paper presents two case studies that demonstrate the application of an innovative pseudo-3D time-dependent modeling tool for draindown prediction. The tool integrates Hydrus 1D with Python scripting to automate large-scale simulations, capturing time-dependent spatial variability in material properties, stacking sequences, and geometries. The first case study focuses on a conceptual heap leach design with simplified geometry, while the second examines an operational facility in mountainous terrain with complex geometry. These case studies highlight the tool's ability to provide actionable insights for both operational and closure planning, offering a practical and efficient alternative to traditional 2D and 3D numerical models.

Case Study 1

This heap leach pad (HLP) is designed to process sulfide ore through a series of stacked lifts, each 10 meters in height, culminating in a total height of 90 meters. The HLP is divided into three groups (layers) of lifts, each separated by intermediate linear low-density polyethylene (LLDPE) liners. The primary objective of this study was to estimate the probable operational and drain-down flows from the HLP. These results are

intended to support water chemistry and oxidation models, as well as support leachate management planning.

The analyses presented in this paper correspond to a conceptual design stage, and the modeling approach incorporates approximations aligned with this phase. The study integrates the physical properties of the heap material, the leakage through the liners, construction and irrigation processes, and one-dimensional unsaturated water transport modeling. The results were combined to represent the overall construction sequence of the HLP. While the findings are indicative, they provide valuable insights into the seepage behavior of the HLP during operation and post-closure.

Heap Geometry and Construction Sequence

The HLP consists of nine 10-meter lifts, divided into three groups (layers) of 30 meters each. Each group is separated by an LLDPE liner, with drainage systems installed above the liners to collect seepage. The construction sequence follows a symmetrical progression, with each lift subdivided into irrigation cells (see Figure 1).

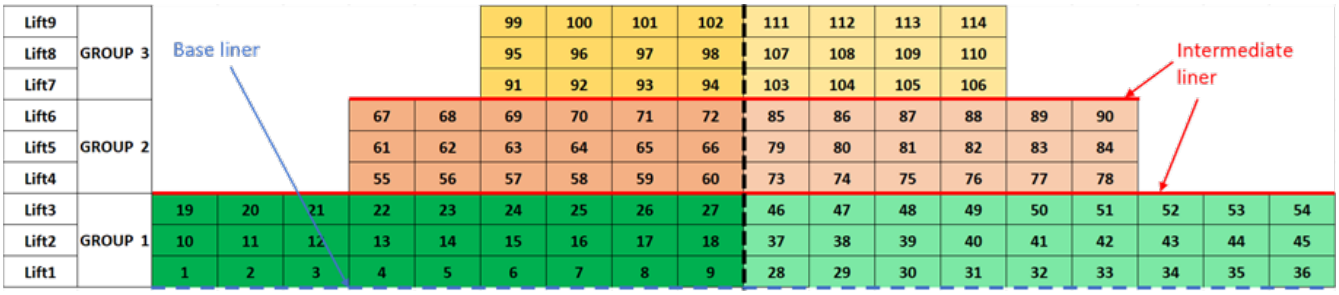

Figure 1: Modeled geometry, with construction sequence order number

The total construction time for the heap is estimated at approximately 12 years, with 40 days allocated for constructing each cell and 200 days for irrigation. The average footprint area of Group 1 is 1,486,100 m^2.

Symmetry was assumed for the heap geometry, and average footprint areas were used for each group. Leakage through the intermediate liners was incorporated into the model. The construction and irrigation sequence were integrated into the modeling to account for the timing and spatial distribution of seepage.

Material Properties

Given the early design stage of the project, most of the hydraulic properties of the heap material needed to be estimated. The saturated hydraulic conductivity (Ksat) was estimated based on the irrigation rate, with values ranging from 10 to 100 times the irrigation rate (6 liters per square meter per hour) to ensure sufficient residence time for leaching efficiency while preventing saturation. Sensitivity analyses were conducted to evaluate the impact of varying Ksat values on seepage behavior.

The Soil-Water Characteristic Curve (SWCC) was estimated using the particle size distributions (PSDs) of the heap material and the HYDRUS pedotransfer function Rosetta. The Rosetta model uses PSD data (percentages of sand, silt, and clay) and bulk density to predict SWCC parameters. Due to the significant proportion of gravel in the samples, the gravel percentage was combined with the sand percentage for input into the prediction tool. The SWCC was then adjusted to reflect the heap material's porosity of 0.38, which was derived from the bulk dry density (1.8 t/m³) and specific gravity (2.9). The Rosetta function predicted a residual volumetric water content of 0.04 for the heap material using PSDs and bulk dry density. Column laboratory tests measured a post-drain-down gravimetric moisture content of 7.7% (dry basis), corresponding to a volumetric water content of 0.14. However, these tests were conducted at a lower bulk density than the design and under insufficient suction conditions to define residual water content per the SWCC. Considering the Rosetta prediction and the higher laboratory values, a residual volumetric water content of 0.08 was adopted for SWCC modeling, representing the upper bound of typical values for gold heap leach materials. These approximations were necessary due to the lack of site-specific laboratory data at this stage. The predicted SWCC utilized in the models is illustrated in Figure 2.

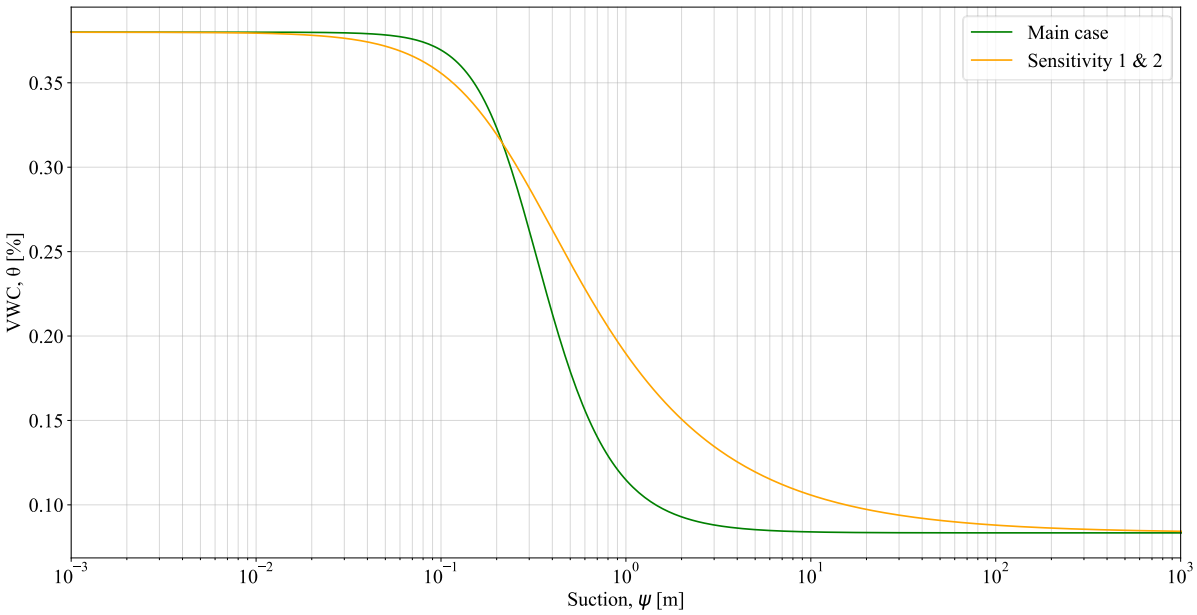

Figure 2: Adopted SWCC for the main case and sensitivities cases

Numerical Model

The automatic time-dependent stacking modeling was performed using HYDRUS-1D as presented in Noël et al. (2023). A Python script was developed to integrate the results of multiple 1D simulations into a simplified 3D representation of the HLP. The top boundary conditions included irrigation rates, temporary covers, and inter-lift liner leakage. The bottom boundary was set as a drainage system open to atmospheric

pressure. Closure conditions incorporated net percolation rates based on climatic data and cover performance.

Three scenarios were modeled: a base case and two sensitivity analyses with varying hydraulic properties. These scenarios evaluated the impact of material properties on seepage and saturation profiles. The sensitivity analyses incorporated adjustments to Ksat values and particle size distributions to address uncertainties in the hydraulic properties of the heap material.

Results

As an initial step, single 1D column models were simulated in HYDRUS-1D for each group, representing one irrigation cell and its subsequent lifts. These models calculated seepage per square meter over time, accounting for construction, irrigation, temporary cover stages, and leakage flux from the group above.

After running the single 1D column model for each group, the seepage curves were scaled and coupled in time to represent the overall seepage behavior for each group. The pink curves in Figure 3 illustrate the scaled seepage curves of Group 1. To scale these curves, the cumulative volumes obtained from the 1D column models were multiplied by the average footprint area for each group and divided by the number of irrigation cells within each group. For instance, Group 1 has an average footprint area of 1,486,100 m² and consists of 18 irrigation cells; thus, the 1D seepage curves were scaled by dividing 1,486,100 m² by 18, resulting in a scaling factor of 82,561 m². The scaled seepage curves were subsequently coupled in time based on the construction sequence and summed to produce the overall cumulative bottom volume curve for Group 1, shown in green in Figure 3.

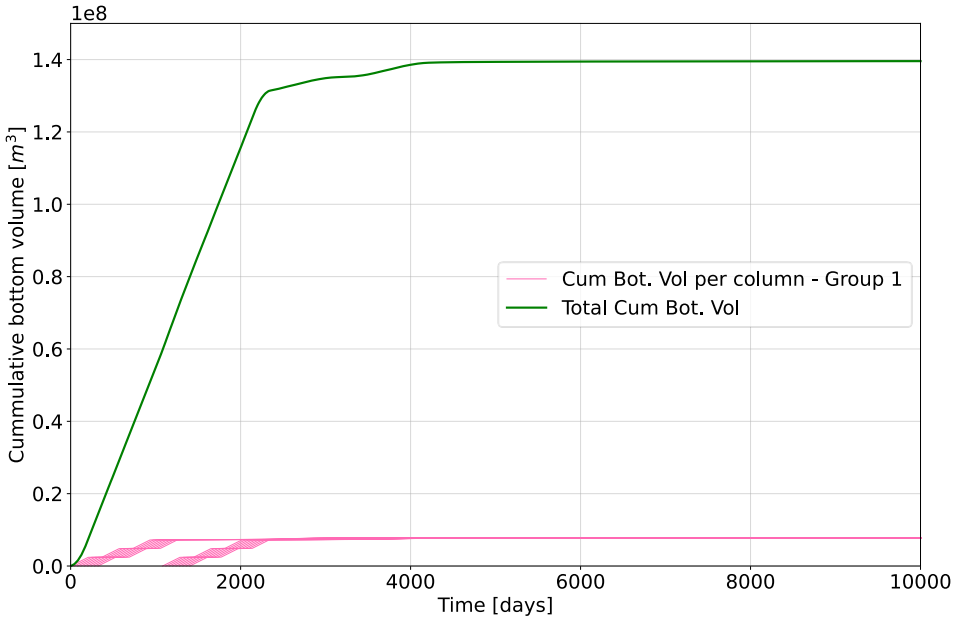

Figure 3: Cumulative bottom flux for all cells—Group 1—main case model

A time lag between individual curves reflects the symmetrical construction and irrigation sequence. Finally, the cumulative bottom flux curves for all three groups were combined to generate the overall cumulative bottom flux curve for the heap leach, presented in Figure 4.

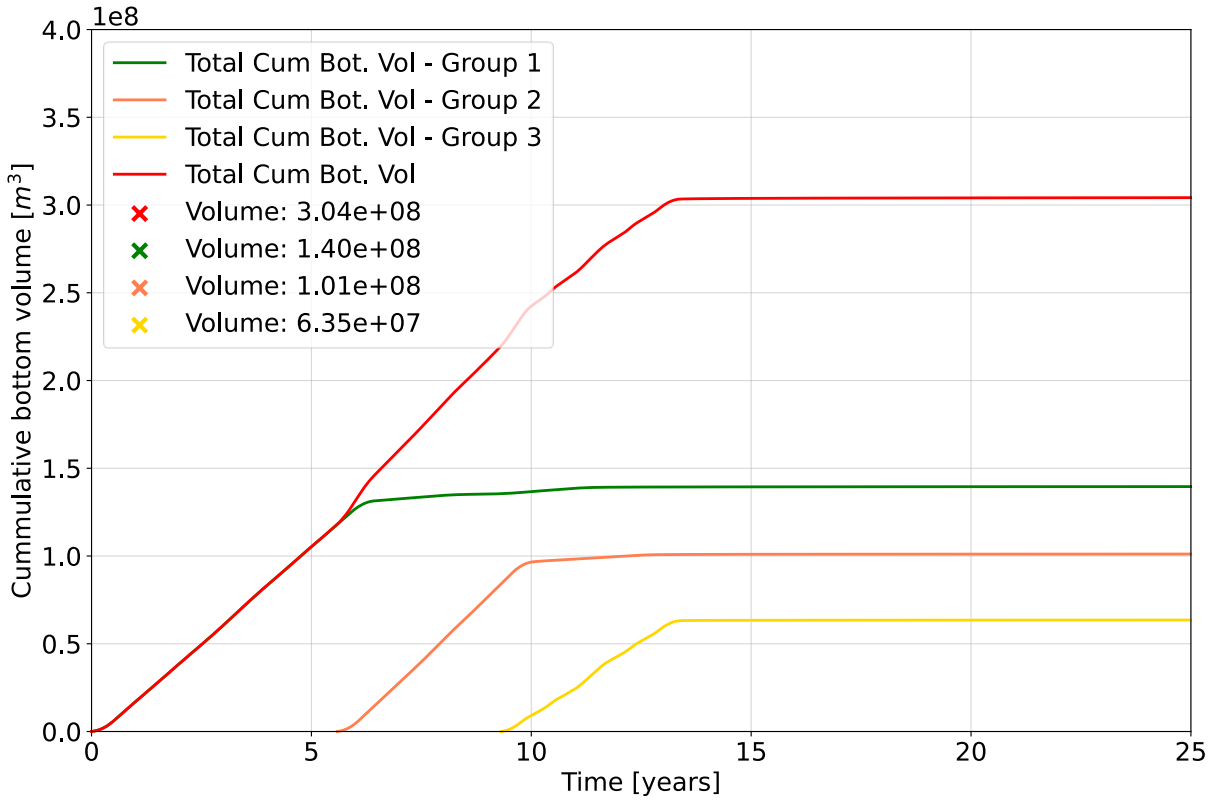

Figure 4: Cumulative bottom flux for all cells—Groups 1, 2, 3, and total—main case model

Outflow rates were calculated using the same method as the cumulative bottom volumes, first for each group individually and then combined to represent the total outflow rates for all three groups. Figures 5 and 6 show the total outflow rates for the base model and sensitivity analyses, with several peaks observed due to overlapping outflow rates from Groups 1, 2, and 3. The final irrigation event occurs around day 4720, marking the beginning of the drain-down phase. The cumulative bottom flux graphs (Figures 3 and 4) do not account for the effect of net percolation resulting from climatic conditions.

However, in Figure 5, a net percolation flux rate of 218 m³/day was added to the draindown curve following the placement of the final cover. As part of the irrigation system, a temporary cover is installed to minimize evaporation and divert precipitation during operation. Consequently, climatic factors have no significant influence on the bottom fluxes of the heap leach pad until the temporary cover is removed, which coincides with the construction of the final cover. The observed increase in the outflow rate after the construction of the final cover reflects the impact of climatic conditions, as net percolation occurs through the final cover.

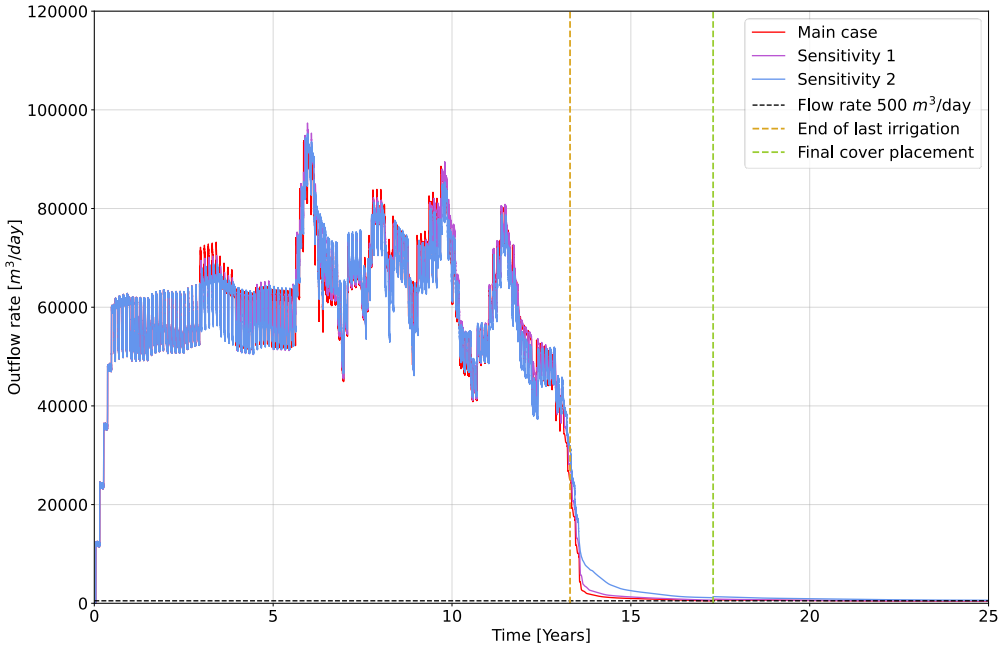

Figure 5: Total outflow rate for the entire heap leach—main and sensitivities models

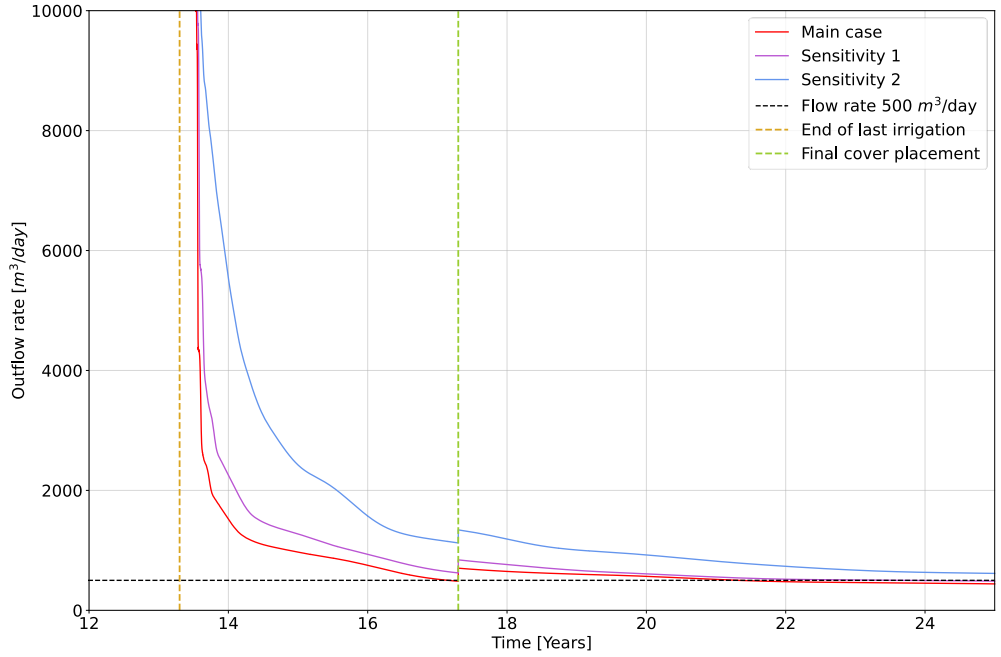

Figure 6: Total outflow rate for the entire heap leach—main and sensitivities models

The results in this case study are preliminary and based on approximations suitable for the current design stage of the HLF. The outflow rates over time were determined, with maximum values occurring during overlaps of irrigation groups. Post-closure, drain-down will eventually stabilize and be governed by net percolation through the top cover once equilibrium is reached.

Case Study 2

This case study focuses on a gold-producing mine situated in a high-altitude and arid region. The operation employs a heap leaching process for gold extraction, with the heap leach pad located on mountainous terrain. Following the completion of pit exploitation, the mine will transition to a secondary leaching phase. This phase, projected to span five years, is designed to maximize recovery of the remaining gold inventory from the heap by recirculating a cyanide solution. The process will conclude with solution exhaustion through recirculation, promoting evaporation.

A critical aspect of this study is determining the time frame required for the complete depletion of the cyanide solution from the leaching heap and identifying viable alternatives to accelerate this process. Accurate modeling of drain-down volumes is essential to achieving these objectives, as it provides a detailed understanding of how solution flows and accumulates within the heap.

The study focuses on modeling drain-down volumes by discretizing the heap into geometric domains, enabling a more precise analysis of solution behavior. By integrating drain-down modeling into the process, this comprehensive approach aims to deliver actionable insights for efficient solution management during the mine's closure stage.

Heap Geometry and Areas Discretization

Geomembrane liners and 3D elements of the heap leach surfaces were assembled to create a comprehensive map of thicknesses across the entire domain of the heap leach pad (see Figure 7). The analysis revealed that the maximum thickness point of the heap is approximately 120 meters.

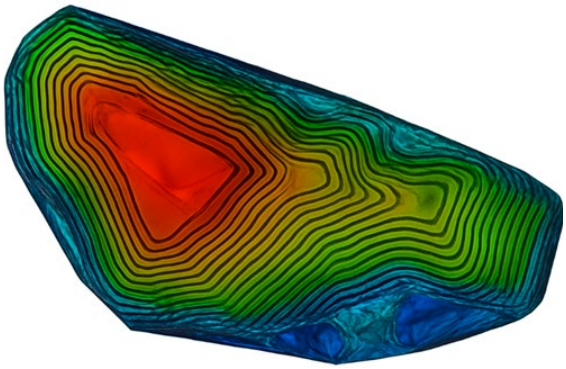

Figure 7: Thickness color map of the heap leach pad

The domain was subsequently divided into distinct secondary irrigation areas, based on the secondary irrigation schedule proposed by the mine.

The thickness, or height, of the heap is a critical input for drain-down modeling, as it directly influences the volume of solution retained within the heap and the rate at which it drains over time. Thicker sections of the heap retain more solution, leading to longer drain-down periods, while thinner sections drain

more quickly. By accurately mapping the thicknesses, the model can better predict the flow behavior and timing of solution depletion across different areas of the heap.

Operational leaching volumes are not a concern in this project, as the focus is specifically on closure drain-down flows. Consequently, the construction sequence of the heap leach pad is not a required input for this case. Instead, one key input is the last secondary irrigation rate applied to each domain within the heap, as this will serve as the starting point for developing the drain-down curves for the secondary leaching areas.

Material Properties

The material properties of the heap leach pad were characterized using various parameters derived from in-situ testing and laboratory analyses.

Saturated hydraulic conductivity (Ksat) values based on in situ Le Franc permeability tests performed at various depths ranged from 4.5 E-06 to 7.0 E-05 m/s, with values of 5.00 E-05 and 1.50 E-05 m/s used in the modeling.

Laboratory testing was also conducted to determine the SWCC parameters for the heap leach material. The laboratory-derived SWCC data were validated using the HYDRUS pedotransfer Rosetta function to ensure the reliability of these parameters. This validation incorporated PSD data collected from samples distributed across the entire domain of the heap leach pad. The comparison yielded consistent curves, demonstrating good agreement between the laboratory results and the Rosetta function predictions, as illustrated in Figure 8.

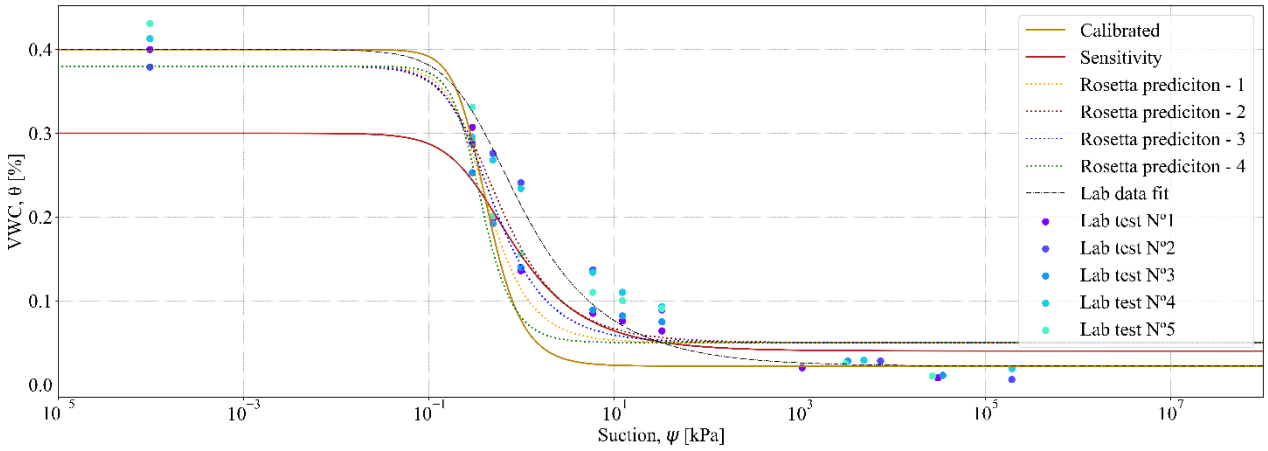

Figure 8: Adopted SWCC

Additionally, the porosity values in the SWCC curves were adjusted to reflect in-situ density measurements obtained throughout the heap leach pad. This adjustment ensured that the SWCC parameters accurately represented the field conditions.

The van Genuchten relationship between saturated hydraulic conductivity and water content was applied to calibrate the SWCC parameters to ensure the numerical model accurately reflects the operational moisture content determined through laboratory testing. In the test, the metallurgical team irrigated a sample at 5 L/m²/hr until steady-state conditions were reached, where the bottom outflow equaled the top inflow. The humidity measured at this point, defined as the operational moisture content, was used as the initial water content in the drain-down model. To achieve alignment with the observed behavior, the Ksat value was adjusted from 1.58e-05 m/s to 5e-05 m/s, and the slope of the SWCC was modified, resulting in a volumetric water content of 0.21 corresponding to the irrigation rate of 5 L/m²/hr. The calibrated SWCC curve, used as the main case set of properties, is shown in gold in Figure 8.

As detailed in the previous paragraph, the calibration process involved adjustments to the measured Ksat and the measured slope of the SWCC. A sensitivity analysis of these properties was performed to address potential variability. The sensitivity analysis included a modified slope of the SWCC consistent with laboratory measurements, a lower porosity to account for in situ variability across the full depth of the pad, and a reduced Ksat (1.58e-05 m/s) to reflect the assumption of a denser material. Furthermore, the residual water content was increased to better reflect typical heap leach pad materials. The residual water content of 0.022, measured in the SWCC lab tests and used in the main case, appears to represent a lower bound. The alternative SWCC curve, used as the sensitivity set of properties, is shown in red in Figure 8.

Numerical Model

The modeling approach utilized the operational volumetric water content as the initial condition, allowing the model to simulate drainage over time. A zero-flux boundary condition was applied at the top, while a free-drainage boundary condition was set at the bottom to represent a drainage system exposed to atmospheric pressure. The precipitation into the heap leach was neglected in the drain-down model due to the site's very arid climate, where the potential evaporation rate is an order of magnitude higher than the precipitation rate. This significant disparity indicates that any precipitation that does occur is likely to be rapidly evaporated, minimizing its contribution to the overall water balance of the heap leach. Consequently, the impact of precipitation on the drain-down process is considered negligible in this specific context.

Drain-down phenomena exhibit non-linear behavior with respect to height, and the heap leach pad consists of numerous slopes with varying elevations. To accurately capture this complex geometry, it is essential to generate a sufficient number of unit-dimensional drain-down curves.

Approximately 120 unit-dimensional column models, each representing varying heights, were created using HYDRUS 1D to produce corresponding drain-down curves, as illustrated schematically in Figure 9.

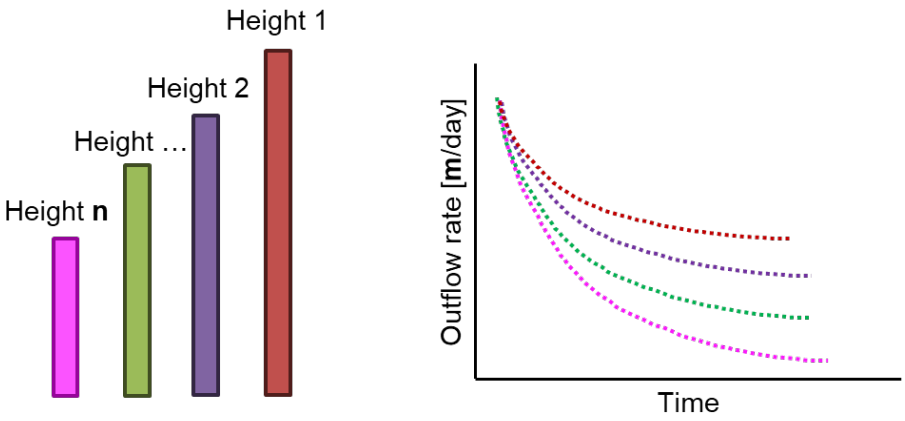

Figure 9: Fundamental unit-dimensional draindown curves for various heights

These curves were generated at 1-meter height intervals to best capture the thickness variation of the heap leach pad. By leveraging Python programming, the process was streamlined, ensuring efficiency and minimizing workload.

After generating the fundamental drain-down curves using HYDRUS 1D models, the heap leach pad domain was discretized into secondary irrigation areas. These areas were further subdivided based on thickness, using 1-meter height intervals for greater precision as depicted in Figure 10.

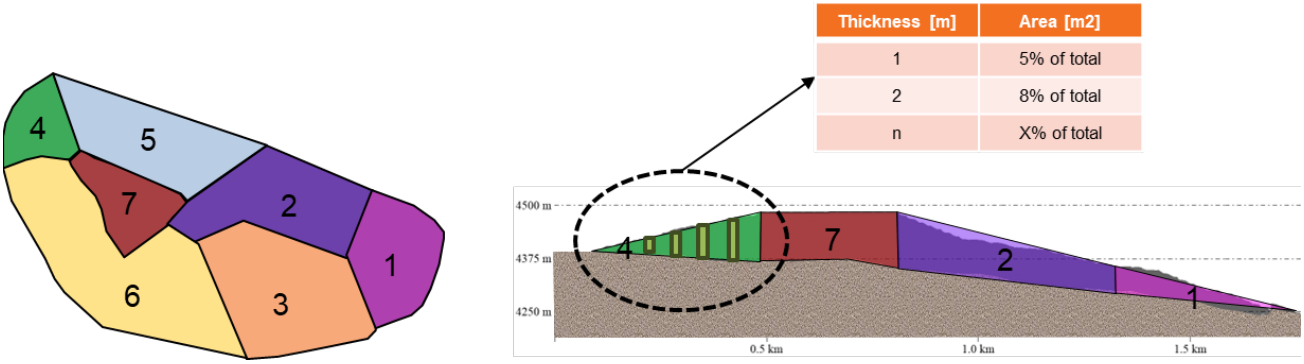

Figure 10: Irrigation areas discretization

The next step involves calculating the total drain-down curve for each secondary irrigation area. This is achieved by scaling the fundamental drain-down curves by their corresponding surface areas and aligning them in time relative to the last irrigation end date. The overall drain-down curve for the entire heap leach pad is generated by integrating the drain-down curves of all discretized areas following the closure date.

Results

The dates of the last secondary irrigation for each discretized area were incorporated into the overall drain-down curve to provide the mine with insights into how the secondary leaching schedule influences the drain-down behavior of the heap leach facility. This analysis aims to assist the mine in understanding the

potential impacts on closure costs and balancing these costs against the average closure expenses and the additional gold recovery achieved through secondary leaching.

The mine's proposed secondary leaching schedule involves irrigating different areas at intervals distributed over the final five years before closure. Greater spacing between the last irrigation dates of different areas is expected to reduce the overall drain-down time, as the earlier irrigated areas will begin draining well before the closure date. By comparing various scheduling scenarios, the mine can evaluate the trade-offs between secondary gold recovery and the associated closure costs. However, this paper focuses on a single secondary irrigation schedule.

Using the closure layout provided by the mine, which includes plans to repurpose the pregnant solution pond and the event pond as evaporation ponds, the evaporation rates of these ponds were calculated. The analysis accounted for their respective sizes and the site's climate data, where potential evaporation exceeds precipitation by an order of magnitude. The calculated evaporation rate for the ponds is approximately 163 cubic meters per day. The point at which the drain-down curve intersects the ponds' evaporation capacity marks the transition to passive evaporation.

Two scenarios were modeled using different sets of hydraulic properties: the calibrated set of parameters (main case) and a sensitivity set to account for potential variability in material properties across the facility. Figure 11 illustrates the overall drain-down curve for the main case, shown in blue. Each colored drain-down curve represents a different secondary irrigation area, with varying starting dates prior to year 0 (the closure start date), as determined by the secondary irrigation schedule proposed by the mine. The intersection with the ponds' evaporation capacity occurs approximately 7.5 years after the last irrigation date.

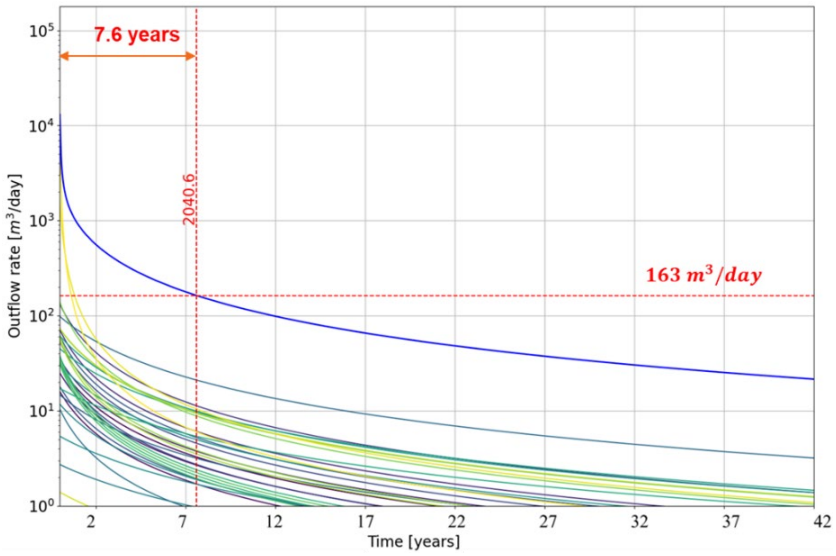

Figure 11: Overall heap leach draindown curve—calibrated set of parameters

Figure 12 presents the overall drain-down curve for the sensitivity analysis, also depicted in blue. In this case, the intersection with the ponds' evaporation capacity occurs later compared to the main case. This delay is primarily attributed to lower saturated hydraulic conductivity and a reduced slope of the SWCC, which together prolong the drain-down process.

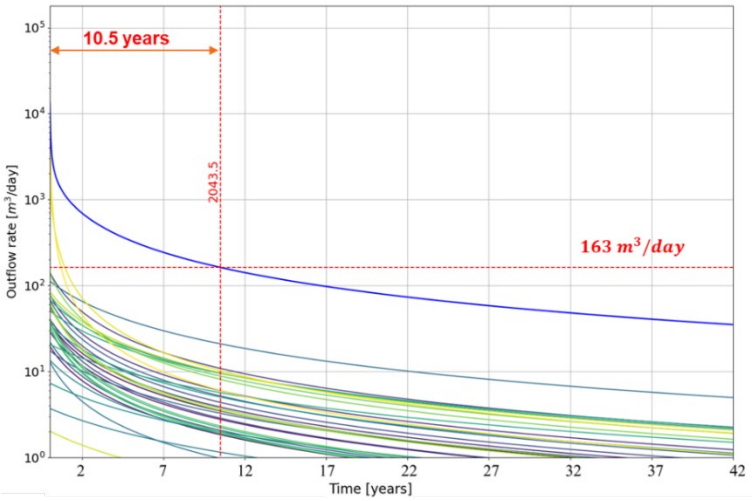

Figure 12: Overall heap leach draindown curve—sensitivity set of parameters

The drain-down curves for the entire heap leach pad were generated by integrating various irrigation areas, accounting for significant height variations across the geometry of the pad. The modeling process incorporated the secondary leaching schedule and included a sensitivity analysis of material properties. These variables were all considered in the prediction of the drain-down curves without relying on complex 2D or 3D models. Instead, the analysis utilized HYDRUS-1D simulations, coupled with Python programming to discretize the domain, execute the simulations, and post-process the outputs from the HYDRUS-1D models.

The modeling presented in this report did not evaluate the water balance analysis with consideration for recirculation as a strategy for excess fluid depletion. Instead, it focused solely on outlining the drain-down results, which serve as inputs for the water balance. However, adopting a recirculation-based strategy could potentially extend the drain-down curve over a longer period, as it depends on ongoing irrigation activities.

Conclusion

This study introduces an innovative tool that combines Hydrus 1D and Python scripting to efficiently model time-dependent drain-down behavior in heap leach systems. By discretizing heap leach facilities into vertical 1D columns as a function of time, the tool captures critical factors such as construction sequences, geometry variations, and irrigation scheduling. This pseudo-3D modeling approach bridges the simplicity

of 1D models with the complexity of higher-dimensional simulations, offering actionable insights for operational and closure planning.

The integration of Python scripting enhances the tool's flexibility, enabling automated simulations, data processing, and sensitivity analyses. This allows practitioners to explore multiple scenarios and adapt to site-specific challenges. The case studies demonstrate the tool's ability to predict drain-down behavior under diverse conditions, from conceptual designs to operational facilities with complex geometries. Its versatility ensures applicability to almost any heap leach pad, regardless of geometry, complex deposition schemes, or irrigation sequences, making it a universal solution for drain-down prediction.

Key advantages include reduced computational time, scalability, and the ability to account for spatial variability, making it a practical alternative to resource-intensive 2D and 3D models. This methodology streamlines workflows, enhances decision-making, and establishes a robust framework for addressing the complexities of heap leach systems, promoting more efficient and sustainable mining practices.

Next Steps and Future Enhancements

While the innovative tool presented in this study has demonstrated significant potential for modeling drain-down behavior in heap leach systems, there are several opportunities for further development. The following features are being targeted for future enhancements of this modeling tool:

- Incorporating consolidation phenomena and dynamically adjusting hydraulic properties, such as saturated hydraulic conductivity and the SWCC, as a function of void ratio variations over time.
- Modeling material heterogeneity across depth by assigning depth-dependent hydraulic properties would improve accuracy, especially for heaps with complex stacking sequences.
- Integrating geochemical processes, such as solute transport and chemical reactions, would enhance predictions of leachate quality and environmental impacts during closure.

References

Noël, M., Vega, I., Terlisky, A., Rivarola, F., & Ezama, I. (2023). Coupling tailings deposition modelling with Hydrus-1D and Python for pseudo-3D seepage predictions. *Tailings & Mine Waste 2023*.

Simunek, J., & van Genuchten, M. T. (2018). HYDRUS-1D, version 4.17.0140: Code for simulating the one-dimensional movement of water, heat, and multiple solutes in variably saturated porous media. Department of Environmental Sciences, University of California, Riverside.

van Genuchten, M. T. (1980). A closed-form equation for predicting the hydraulic conductivity of unsaturated soils. *Soil Science Society of America Journal*, *44*(5), 892–898. https://doi.org/10.2136/sssaj1980.03615995004400050002x X-Mo

Criticality of 3D Numerical Modeling for Assessing Heap Leach Pad Stability and Integration with Monitoring Data, Including InSAR

Neil Bar, Gecko Geotechnics, Saint Vincent and the Grenadines
Alison McQuillan, Gecko Geotechnics, Saint Vincent and the Grenadines
German Zlobin, KAZ Minerals, Kazakhstan
Francesco Meloni, TRE ALTAMIRA, Italy

Abstract

Geotechnical analysis is a crucial aspect of heap leach site design and management, ensuring stability and safety throughout the operational lifespan and beyond. In this study, a comprehensive approach was undertaken, utilizing and comparing both Limit Equilibrium Method and Finite Element Method modeling techniques in 2D and 3D to assess the stability of the heap leach slopes.

The 3D modeling results provided a more nuanced and detailed understanding of the deformation mechanisms at play within the heap leach structure compared to the 2D model. This enhanced insight revealed potential failure modes that were not apparent in the 2D analysis, and it also highlighted areas of lower safety factors. These findings underscore the importance of 3D modeling in geotechnical analysis, especially for complex structures like heap leach pads, where the geometry and stress distribution can vary significantly in three dimensions.

Furthermore, the stability of the slopes was evaluated considering the steepness of the foundation, which is a critical factor in slope stability analysis. Steeper foundations generally result in higher stresses and greater potential for instability. Therefore, a thorough assessment of the foundation's geometry and geotechnical properties is essential for ensuring the overall stability of the heap leach pad.

Satellite InSAR monitoring was employed to track slope stability over time. This remote sensing technique allows for continuous monitoring of surface deformations, providing early warning signs of potential slope instability. By integrating satellite InSAR monitoring with geotechnical modeling, engineers can proactively manage heap leach slope stability and mitigate risks associated with slope failure.

Overall, this study highlights the importance of a multi-faceted approach to geotechnical analysis in heap leach site design and management. By combining advanced modeling techniques, consideration of

key geotechnical parameters, and continuous monitoring, engineers can ensure the long-term stability and safety of heap leach operations.

Introduction

Waste dumps, ore stockpiles, and heap leach pads (HLPs) are engineered rock fill structures for various purposes. However, all facilities are subject to common requirements in terms of slope stability, operational safety, compliance with environmental and regulatory requirements, and ensuring economic compliance with the mining project (Sharma & Roy, 2015; Trevithick et al., 2004).

The short-term and long-term stability of the slopes of these structures depends on the features of the relief and structure of the foundation, the characteristics of the backfill material, the size and geometry of the structure, as well as regional conditions of the site, including seismicity and the amount of precipitation (Hawley & Cunning, 2017; Bar et al., 2020). Heap leaching is widely used in modern large mines, since it allows you to obtain ore concentrate at lower costs compared to traditional processing methods (Petersen & Dixon, 2002; Trujillo et al., 2011). The use of heap leaching determines the economic feasibility of the mining process (Bouffard & Dixon, 2001). Typically, copper is extracted from low-grade ores using this method. The process includes filtering a leaching solution (e.g., sulfuric acid) through a layer of ore to extract target metals. The bed of ore (or heap) is built from blasted or crushed material and is designed to allow percolation of the leach solution into all areas of the structure. The solution reacts with the solids to extract the target minerals, and the dissolved particles are transported from the heap for subsequent extraction (McBride et al., 2018). Bartlett (1998) describes this process in detail.

Figure 1: Construction of the Aktogay Copper Mine HLP Stage 1 during winter, Kazakhstan

In addition to the slope stability requirements imposed on the pads, the integrity of the impermeable plastic or clay liner is important for the recycling of the solution and the prevention of damage to the environment. This, in turn, requires consideration of differential settlements and may limit the load on the pad or its maximum height or size (Reyes & van Zyl, 2015).

Heap Leach Pad Expansion at Aktogay Copper Mine

The Aktogay copper mine is located in south-eastern Kazakhstan, 470 km north-east of Almaty and 250 km west of the border with China. Ore mining began in 2015; the expected life of the quarry is at least 25 years. The average annual precipitation in Aktogay is less than 200 mm, with a maximum of 297 mm recorded in 1957 (Sagintayev et al., 2015). Snow cover typically lasts for about five months from November to March, with an average annual snowfall of 268 mm. Temperature ranges can be extreme, exceeding +40 °C in summer and -40 °C in winter. According to the general seismic zoning map, peak ground acceleration (PGA) at Aktogay is 0.05 g with a probability of exceeding 10% over 50 years (Silacheva et al., 2018).

The Aktogay Heap Leach Pad (HLP) was initially designed with 5 lifts, each 13 m high, with a resulting slope angle of 23°. The HLP is operated year-round using a heated solution, which is delivered through a network of insulated pipes to the active cells (Figure 1).

Stage 1 of HLP construction was completed with excellent slope performance and minimal settlement of the placed rock fill (Figure 2). This paper presents the results of the surveys and geotechnical assessment carried out for the HLP expansion project (Stage 2) with an additional two tiers and a total slope height of 91 m with an overall HLP slope angle of 20°.

Figure 2: Completed HLP Stage 1: 65 m high (5 lifts)

Site Investigations

At the Aktogay copper mine, the HLP foundation is relatively uniform and nearly flat, sloping at approximately 7 degrees to the south. Initial site investigations for the HLP foundation identified the following ground conditions (from the most recent deposition):

- 0.1 – 0.2 m topsoil: a mixture of clays and silts.
- 1.0 – 2.0 m gravelly & sandy clay with traces of silt.
- 1.0 – 2.0 m sandy gravel with traces of clay & silt.
- 3.0 – 10.0 m highly to moderately weathered rock.
- 7.0 – 10.0 m slightly weathered to fresh rock.

Based on Bar & Teleu (2023), HLP foundation preparation and construction comprised:

- Engineered fill to create a base with required planarity and ≥1% sloping gradient using a mixture of 20–50% fine gravel (<25 mm particle size), 20–70% sand, and 10–30% fines with plasticity index <10.
- Clay underliner with low hydraulic conductivity: plasticity index <10 and a minimum thickness of 150 mm compacted to 95% maximum dry density based on the Modified Proctor Test.
- LLDPE (liner low-density polyethylene): 1.5 mm thick, single-sided, geotextile with textured side facing down to improve shear strength between LLDPE & clay underliner.
- Coarse overliner (protection against punctures from subsequent rock fill comprising 60–85% gravel up to 50 mm particle size, 15–35% sand, and <5% fines).
- Rock fill (oxide ore with a target of 80% of particles ranging from 1 to 200 mm, <10% cobbles or larger fragments, and fines <3–5%) end-tipped from up to 13 m high lifts as shown in Figure 4.

Figure 3: HLP construction sequence. 1: Engineered fill base and clay underliner with ≥1% gradient. 2: LLDPE installed on clay under-linear. 3: Coarse overliner and initial oxide ore lift

Figure 4: Haul truck end-tipping typical oxide ore (rock fill) on 13 m high lift. Rock fill angle of repose ranging from 37 to 39°

Slope Performance—Stage 1

Slope performance on HLP Stage 1 has been very good with only a few localized crest instabilities during construction. Leaching solution recycling and recirculation have not identified any losses, nor has downstream groundwater quality monitoring identified adverse changes in water chemistry, suggesting the clay underliner and LLDPE textured geotextile performance has also been satisfactory thus far.

Survey prisms have observed minimal slope deformation during initial construction stages and subsequent, seasonal InSAR (interferometric synthetic aperture radar) monitoring. Both systems indicated deformation rates over the heap leach pad are either low-velocity and constant (creep) or decelerating, which are analogous to stable conditions and low risk.

InSAR images were processed by TRE Altamira using their SqueeSAR® algorithm to calculate vertical and east-west horizontal vector components (Ferretti, 2014; Bischoff et al., 2020). SAR image stacks were obtained from two different satellites:

- Sentinel-1 (C-band) of the European Space Agency in ascending geometry (flying south to north, eastward looking) with a medium spatial resolution of 5 × 25 m.
- TerraSAR-X (X-band) of the Deutsches Zentrum für Luft- und Raumfahrt (German Aerospace Center) in descending geometry (flying north to south, westward looking) with a high spatial resolution of 3 × 3 m.

Maximum vertical displacements (settlement) of up to 175 mm/year were observed on the northern side of the HLP. The vertical component of the displacements is significantly greater with respect to the east-west component, as shown in Figure 5. Both vertical and east-west components indicate linear and decelerating trends, i.e. no accelerating trends have been observed.

Vertical displacement was expected as the rock fill undergoes compaction with loading over time. Vertical displacements are significantly more prominent near the top of the HLP compared with its lower lifts, validating in conjunction with displacement trends that the observed displacements are settlements due to compaction, i.e., not a sign of larger-scale instability.

East-west displacements generally did not exceed 30 mm/year (i.e., <0.1 mm/day). Displacement monitoring using InSAR was not effective on the active parts on the western side of the HLP at this time due to ground disturbance and active heap leach cells. However, as lifts are progressively constructed, monitoring displacements on the slopes of the lower lifts will sequentially become possible.

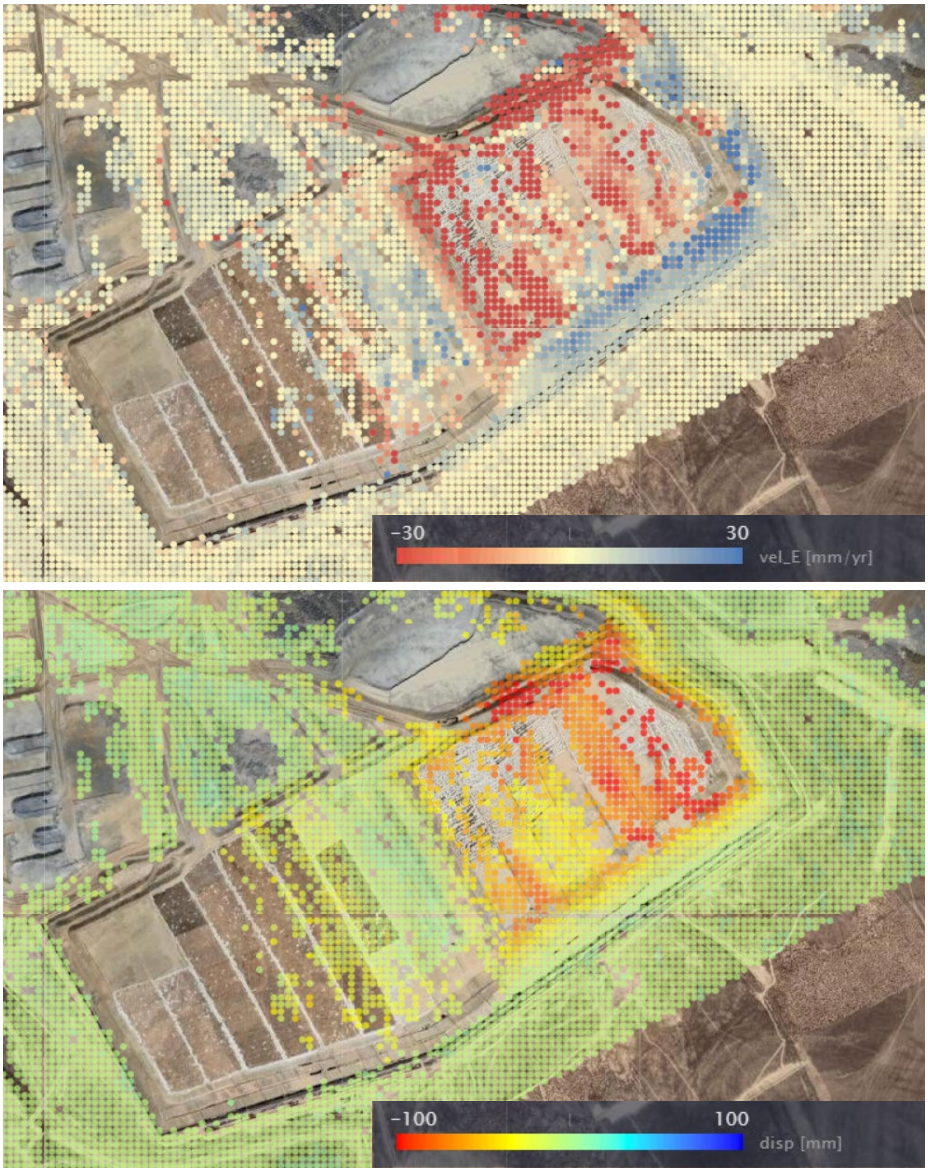

Figure 5: Heap leach pad InSAR data after completion of five lifts on the eastern end. Top: East-West Horizontal Deformation (positive values indicate eastward movement). Bottom: Vertical Deformation (negative values indicate downward movement or settlement)

Material and Liner Characteristics

A series of test pits was used to collect bulk samples of underliner and overliner materials for shear testing of liner interface materials. Samples were transported using air freight to Anddes Laboratorio Geotécnico in Peru for testing under different normal stresses commensurate with future loading conditions using a large-scale (300 mm) direct shearing frame (Figure 6). The lowest shear strength results for the interface between the liner and clay underliner (mixture of clays and silts) were:

- Peak strength: effective cohesion (c') = 0 kPa; effective friction angle (ϕ') = 19°.
- Residual strength: c' = 18 kPa; ϕ' = 11°.

Figure 6: Large-scale direct shear frame

Material density and strength properties in Table 1 were derived from information in earlier site investigations and studies, and material testing. Rock fill shear strength was simplified and reduced (conservative) from estimation-based approaches by Leps (1970) and Barton & Kjærnsli (1981).

Table 1: Physical and Mechanical Material Properties

Material (in Order of Deposition)	Unit Weight, γ (kN/m³)	Effective Cohesion, c' (kPa)	Effective Friction Angle, ϕ' (degree)
Fresh rock	26	515	44
Weathered rock	26	160	26
Residual soils	20	0	28
Engineered fill	20	0	35
Clay underliner	18	2	20
LLDPE interface	10	0	19
Gravel overliner	20	0	35
Rock fill (oxide ore)	20	0	37

Slope Stability Modeling

Three-dimensional (3D) slope stability models were developed using 3D LEM (Limit Equilibrium Method) and 3D FEM (Finite Element Method) modeling software packages, Slide3 and RS3 of Rocscience Inc, respectively. Two-dimensional (2D) LEM and FEM models in Slide2 and RS2 software can be directly derived from the 3D models for comparative purposes (Cobián et al., 2022).

The model geometry shown in Figure 7 was based on the ground conditions and foundation preparation described earlier. The 3D model developed is 2.8 km long (NE-SW), 2.0 km wide (NW-SE), and approximately 0.3 km deep to accommodate the heap leach pad footprint of 2.0 by 0.9 km.

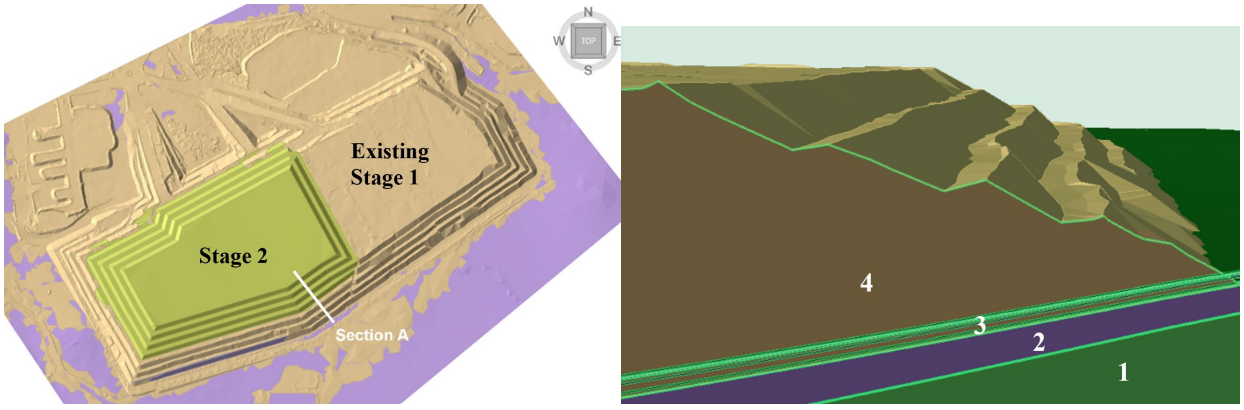

Figure 7: 3D LEM model in Plan View with existing HLP Stage 1 and planned Stage 2 lifts with an overall slope angle of 20° under evaluation. Section A through 3D LEM model of the existing Stage 1—1: Fresh rock. 2: Weathered rock. 3: Weak layers (interfaces). 4: Existing rock fill

Isotropic material properties from Table 1 were applied. Weak layers (i.e., interfaces) were used to simulate the residual soils, engineered fill, clay underliner, LLDPE, and gravel overliner. As a conservative

approach, an elevated groundwater table was assumed to be 0.5 m above the LLDPE rather than at the base of the weathered rock.

LEM analyses utilized ellipsoidal (3D) and non-circular (2D) slip surfaces to calculate Factor of Safety (FoS) using methods of columns and slices, respectively. The lowest FoS slip surfaces were further adjusted or optimized to find the lowest FoS. This methodology within the Slide3 and Slide2 software enabled the generation of complex slip surfaces that combine near-circular shearing through the rock fill with sliding along a discrete plane (i.e., LLDPE interface), as shown in Table 2. Both 2D and 3D LEM analysis results indicate stable conditions with FoS exceeding 2.00 for the overall HLP slope.

Based on the LEM analyses for overall HLP slopes, 2D LEM analysis results *overestimated FoS by >10%* compared to the 3D LEM model. 3D LEM was able to identify a lower FoS associated with a mildly convex slope profile (bullnose shape), which could not be assessed using 2D analysis. Similar results were found for a pit slope failure (non-daylighting wedge) at Pueblo Viejo gold mine, where 2D LEM results overestimated FoS by approximately 10% compared to 3D LEM (Bar et al., 2022).

Table 2: Comparison of 2D and 3D LEM Analysis of HLP Stage 2 at Aktogay Copper Mine. Note: Foundation Angle is Approximately 7°; Overall HLP Slope Angle: 20°

Analysis Method	Failure Mechanism and Analysis Results	
2D Limit Equilibrium Method	**FoS=2.22 (overall)** FoS=1.41 (double lift) Sliding on the liner and shearing through the HL material	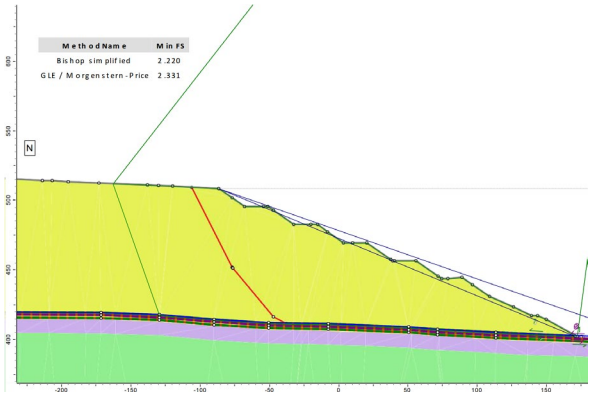
3D Limit Equilibrium Method	**FoS=2.01 (overall)** FoS=1.67 (multi-bench) FoS=1.18 (double lift) Note: mildly convex slope profile Sliding on the liner and shearing through the HL material	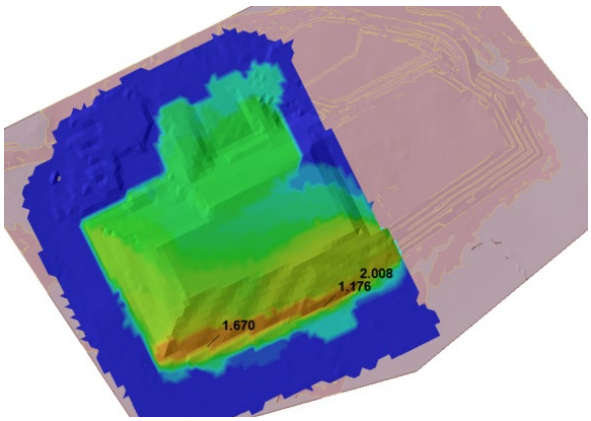

The LEM models were compared against stress-strain analysis with the FEM method, assuming elastic, perfectly plastic conditions with equal peak and residual strength inputs. 2D FEM models were developed with a 6-noded triangle mesh formed by approximately 20,000 elements. A 3D FE model was also developed with only a single interface layer (i.e., the weakest: clay underliner and LLDPE). However, even with this geometric simplification, a 4-noded tetrahedral mesh was formed by over one million elements. Material stiffness properties were estimated from previous work and have not been calibrated against observed surface displacements since the focus of the evaluation was global stability.

The finite element method uses SSR (shear strength reduction) to systematically reduce the shear strength envelope of materials by a factor of safety or strength reduction factor (SRF) and compute results (Griffiths & Lane, 1999; Diederichs et al., 2007). The process of SSR and computing is repeated until deformations are unacceptably large or solutions do not converge (Hammah et al., 2005). The SRF at which this occurs is termed the critical strength reduction factor ($SRF_{critical}$), which is equivalent to FoS.

Table 3: Comparison of 2D and 3D FEM analysis of HLP Stage 2 at Aktogay Copper Mine. Note: Foundation Angle is Approximately 7°; Overall HLP Slope Angle: 20°

Analysis Method	Failure Mechanism and Analysis Results	
2D Finite Element Method	**$SRF_{critical}$=1.90** Active-passive blocks sliding along a liner	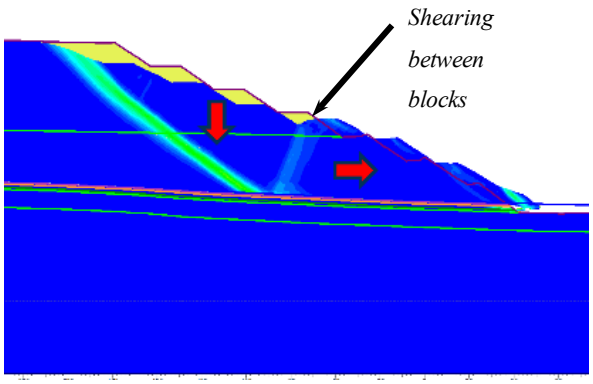
3D Finite Element Method	**$SRF_{critical}$=1.63** Note: mildly convex slope profile Active-passive blocks sliding along a liner	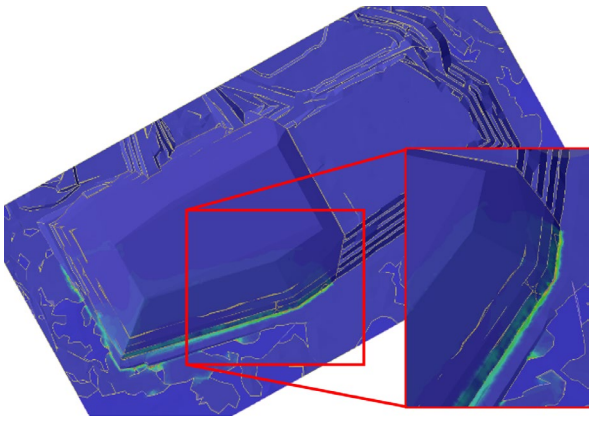

Table 3 summarizes the 2D and 3D FEM analysis results, which identified a more complex failure mechanism. An active-passive block failure mechanism was identified, with the active block being formed by the rock fill lifts driving a wedge downward to mobilize the passive block to slide along the interface of the clay underliner and LLDPE. For FEM analysis identifying active-passive blocks, $SRF_{critical}$ (i.e. FoS) was up to 23% less than the LEM results, which are unable to model the complex failure mechanism.

Based on the FEM analyses for overall HLP slopes, the 2D FEM analysis results *overestimated FoS by >15%* compared to the 3D FEM model. The 3D FEM was able to identify a lower FoS associated with a mildly convex slope profile (bullnose shape), which could not be assessed using 2D analysis.

Both 2D and 3D FEM analysis results indicate stable conditions with FoS exceeding 1.50 for the overall HLP slope due to the shallower dip of the HLP foundation.

All methods indicate stable conditions for additional planned lifts. Notably, modeled FoS for future lifts is higher than that for existing, constructed lifts, which are stable with excellent slope performance. This is commensurate with a lower overall HLP slope angle used for the expansion. Based on the analyses for overall HLP slopes, 2D LEM analysis results (i.e. FoS=2.22) using Slide2 *overestimated FoS by over 35%* compared to the 3D FEM model (i.e. $SRF_{critical}$=1.63) using RS3. This is caused by LEM's inability to model complex failure mechanisms such as active-passive blocks, and the presence of a mildly convex slope profile (bullnose shape), which could not be assessed using 2D analysis.

Effect of Foundation Angle on Conceptual HLP Failure Mechanisms

A brief review of conceptual failure mechanism development was undertaken using 2D FEM analysis by considering different foundation angles.

Foundation angles for a conceptual HLP with simplified geometry (90 m high with an overall HLP slope angle of 24 degrees and a perfectly planar foundation) were varied from horizontal (0 degrees) to 20 degrees, as shown in Table 4.

As the foundation angle is increased, the Critical Strength Reduction Factor reduces significantly, and as the foundation angle increases above 5 degrees, the failure mechanism changes from sliding along the linear and shearing through the Heap Leach (rock fill ore) to an active-passive block failure mechanism.

The reader is reminded that 2D analysis can overestimate FoS and $SRF_{critical}$ compared to 3D analysis, i.e. the actual $SRF_{critical}$ in Table 4 could be substantially lower if a convex slope profile were present, and/or if the foundation was located on a convex profile or if the foundation angle varied, e.g. increased near the base of the HLP.

Table 4: Comparison of Conceptual 2D FEM Models to Assess the Effect of the Foundation Angle on HLP Failure Mechanisms and Stability

Foundation Angle	Failure Mechanism and Analysis Results (Contours Represent Dimensionless Maximum Shear Strain: 0 in Blue to 0.001 in Red)	
Horizontal (0 degrees)	$SRF_{critical}$=1.58 Sliding on the liner and shearing through the HL material	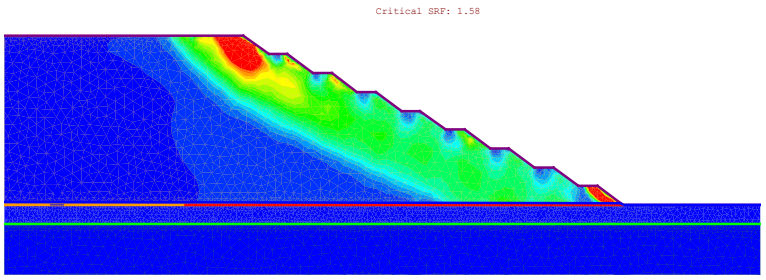
Inclined to 5 degrees	$SRF_{critical}$=1.56 Sliding on the liner and shearing through HL material	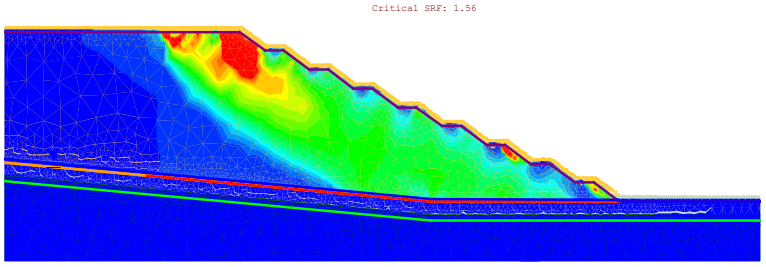
Inclined to 10 degrees	$SRF_{critical}$=1.50 Active-passive blocks sliding along the liner. Signs of shearing between blocks	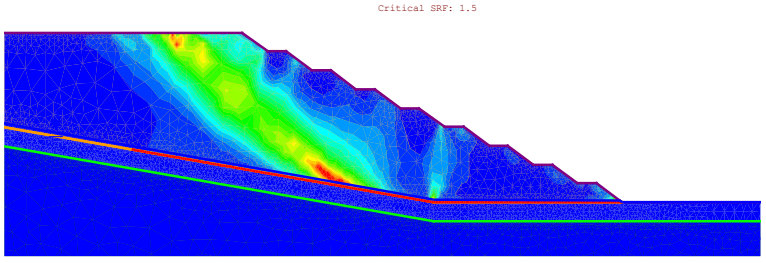
Inclined to 15 degrees	$SRF_{critical}$=1.40 Active-passive blocks sliding along the liner. Distinct shearing between blocks.	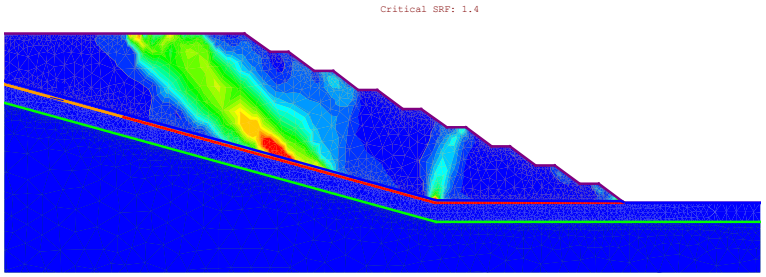
Inclined to 20 degrees (approx. equal to the friction angle of the liner)	$SRF_{critical}$=1.31 Active-passive blocks sliding along the liner. Distinct shearing between blocks.	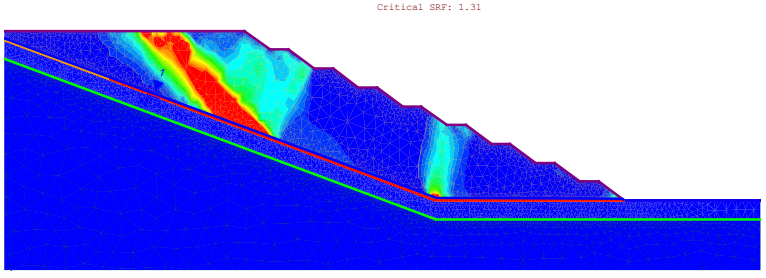

Conclusion

The Aktogay Heap Leach Pad has been designed and is being constructed in a very favourable geotechnical setting with a flat foundation, good quality rock fill (ore) and a dry environment. Based on the geotechnical evaluation performed, the HLP expansion involving two additional lifts is feasible and further expansions could be considered (subject to further investigations).

Different slope stability modeling approaches can identify different failure mechanisms in two and three dimensions. These modeling approaches yield vastly different results that even for an HLP designed on a simple, uniform foundation. The two-dimensional Limit Equilibrium Method (2D LEM) remains the most commonly utilized analysis method for assessing slope stability in the mining industry. 2D LEM analysis results *overestimated FoS by over 35% compared to the 3D FEM model due to the inability of LEM to model complex failure mechanisms such as active-passive blocks, and the presence of a mildly convex slope profile (bullnose shape),* which could not be assessed using any form of 2D analysis. The significance of this potential FoS overestimation using 2D LEM is profound, to say the least. By way of example, if a Design Acceptance Criteria required a minimum FoS of 1.30 to permit HLP construction and 2D LEM was used to assess stability, the actual FoS could be more than 35% less, i.e. FoS could be below 1.00 (unstable).

For more complex 3D HLP slope and/or foundation geometry, 3D analysis results could yield even lower FoS compared to 2D results. Based on the observations in this case study, limitations of 2D slope stability analysis that are well documented for open pit and natural slopes (Bahsan & Fakhriyyanti, 2018; Chakraborty & Goswami, 2021; McQuillan & Bar, 2023) are also applicable to rock fill structures, including Heap Leach Facilities. Most notably, these include non-linear slope geometry and curvature, and spatially or laterally varying geological (foundation) conditions.

According to the conceptual review of failure mechanisms on simplified foundations, it appears that any Heap Leach Facility constructed on a foundation angle exceeding 5 degrees may develop an active-passive block failure mechanism. For active-passive blocks, FEM modeling is required, i.e. LEM analysis is only able to simulate sliding on the liner and shearing through the Heap Leach (rock fill ore) material.

It is strongly recommended that any Heap Leach Facility that is being designed, under construction, or is in operation be assessed considering the risk of active-passive block failure in a three-dimensional setting. That is, 3D FEM analysis (or 3D finite difference analysis) should be mandatory.

Irrespective of any slope stability modeling results, the construction of a Heap Leach Facility on a foundation angle equal to or exceeding the friction angle of any element within the foundation or liner is not advised due to uncertainty in material characterization and numerical modeling limitations.

A comprehensive surface and sub-surface slope monitoring plan with a trigger-action-response plan is required for strategic and tactical objectives, including but not limited to:

- Strategic: early identification of deformations and hazards with sufficient time to respond with slope stabilization or unloading.
- Tactical: identification of an imminent slope collapse with sufficient time to evacuate personnel and/or the public from at-risk areas.

Acknowledgements

The authors sincerely thank Nurkhair Teleu and Philipp Mohr from KAZ Minerals for their initial inputs to this work. Anddes Laboratorio Geotécnico is thanked and acknowledged for their laboratory testing.

References

Bahsan, E., & Fakhriyyanti, R. (2018). Comparison of 2D and 3D stability analyses for natural slope. *International Journal of Engineering & Technology, 7*(4.35), 662–667.

Bar, N., Mojica, B., Cobián, J. C., Bautista, M. M., Hammah, R., McQuillan, A., Yacoub, T., Gaich, A., Pötsch, M., Coli, N., & Preston, C. (2022). Cumba slope failure: A technical review. *Proceedings of Slope Stability 2022*, Tucson, 12 pages.

Bar, N., Semi, J., Koek, M., Owusu-Bempah, G., Day, A., Nicoll, S., & Bu, J. (2020). Practical waste rock dump and stockpile management in high rainfall and seismic regions of Papua New Guinea. *Proceedings of Slope Stability 2020*, Perth, 117–128.

Bar, N., & Teleu, N. (2023). Geotechnical evaluation of heap leach pad design. *Proceedings of the 14th Australia and New Zealand Conference on Geomechanics (ANZ2023)*, Cairns, 6 pages.

Bartlett, R. W. (1998). *Solution mining*. Amsterdam: Gordon & Breach Science Publishers.

Barton, N. R., & Kjærnsli, B. (1981). Shear strength of rockfill. *Journal of Geotechnical Engineering Division, 107*(7), 873–891.

Bischoff, C. A., Ferretti, A., Novali, F., Uttini, A., Giannico, C., & Meloni, F. (2020). Nationwide deformation monitoring with SqueeSAR® using Sentinel-1 data. *Proceedings of IAHS, 382*, 31–37.

Bouffard, S. C., & Dixon, D. G. (2001). Investigative study into the hydrodynamics of heap leaching processes. *Metallurgical and Materials Transactions B, 32*, 763–776.

Chakraborty, A., & Goswami, D. (2021). Three-dimensional slope stability analysis using stability charts. *International Journal of Geotechnical Engineering, 15*(6), 624–649.

Cobián, J. C., Bautista, M. M., Bar, N., & Hammah, R. (2022). 3D limit equilibrium analysis and risk appraisal of Hondo waste rock stockpile designs. *Proceedings of Rocscience International Conference*, Accra, 10 pages.

Diederichs, M. S., Lato, M., Quinn, P., & Hammah, R. (2007). Shear strength reduction approach for slope stability analyses. *Proceedings of 1st Canada-US Rock Mechanics Symposium*, Vancouver.

Ferretti, A. (2014). *Satellite InSAR data – Reservoir monitoring from space*. EAGE Publications.

Griffiths, D. V., & Lane, P. A. (1999). Slope stability analysis by finite elements. *Géotechnique, 49*(3), 387–403.

Hammah, R., Yacoub, T. E., Corkum, B. C., & Curran, J. H. (2005). The shear strength reduction method for the generalized Hoek-Brown criterion. *Proceedings of the 40th US Symposium on Rock Mechanics*, Anchorage, 6 pages.

Hawley, M., & Cunning, J. (2017). *Guidelines for mine waste dump and stockpile design*. Clayton: CSIRO Publishing.

Leps, T. M. (1970). Review of the shearing strength of rock fill. *Journal of Soil Mechanics & Foundations Division, ASCE, 96*(SM4), 1159–1170.

McBride, D., Gebhardt, J., Croft, N., & Cross, M. (2018). Heap leaching: Modelling & forecasting using CFD technology. *Minerals, 8*(1), 9.

McQuillan, A., & Bar, N. (2023). The necessity of 3D analysis for open-pit rock slope stability studies: Theory and practice. *Journal of the Southern African Institute of Mining & Metallurgy, 123*(2), 63–70.

Petersen, J., & Dixon, D. G. (2002). Thermophilic heap leaching of a chalcopyrite concentrate. *Minerals Engineering, 15*(11), 777–785.

Reyes, A., & van Zyl, D. (2015). Consolidation and deformation analysis for the stability assessment of a heap leach pad. *Proceedings of Heap Leach Solutions 2015*, Reno, 135–148.

Sagintayev, Z., Yerikuly, Z., Zhaparkhanov, S., Panichkin, V., Miroshnichenko, O., & Mashtayeva, S. (2015). Groundwater inflow modelling for a Kazakhstan copper ore deposit. *Journal of Environmental Hydrology, 23*, 1–13.

Sharma, S., & Roy, I. (2015). Slope failure of waste rock dump at Jayant open cast mine, India: A case study. *International Journal of Applied Engineering Research, 10*(13), 33006–33012.

Silacheva, N. V., Kulbayeva, U. K., & Kravchenko, N. A. (2018). Probabilistic seismic hazard assessment of Kazakhstan and Almaty city in peak ground accelerations. *Geodesy & Geodynamics, 9*, 131–141.

Trevithick, R. S., Loch, R. J., Roseby, S. J., & Vacher, C. A. (2004). The application of digital photogrammetry to assess long-term stability of mine site waste rock dumps. *Proceedings of the 13th Soil Conservation Organization Conference*, Brisbane, 5 pages.

Trujillo, J. Y., Mellado, M. E., Galvez, E. D., & Cisternas, L. A. (2001). A method for the design and planning operations of heap leaching circuits. *Computer Aided Chemical Engineering, 29*, 306–310.

Steady-State Infiltration Analysis in Dump Leach under Saturated Conditions Using Finite Element Modeling

Andres León, Axios Engineering, Chile
Ehiner Montiel, Axios Engineering, Colombia
Daniel Zúñiga, Axios Engineering, Chile

Abstract

The safe design and operation of a dump leach facility depends, among other factors, on understanding the hydraulic behavior of the leached ore, specifically under the influence of surface irrigation-induced infiltration. This study evaluates the impact of the irrigation on pore water pressure generation and phreatic level depth in a dump leach deposit, based on numerical modeling using a saturated steady-state groundwater flow approach.

The main objective was to determine how flow distribution varies across representative cross-sections of the dump under different irrigation scenarios. The sections were modeled under the assumption that the system has reached hydraulic equilibrium, representing prolonged irrigation conditions that enable the assumption of internal saturation. This assumption supports the application of a steady-state analysis, which, although it does not consider the transient nature of the process, provides a representative condition for evaluating stabilized pore pressures.

Results indicate that while flow tends to concentrate in localized areas within the dump, there is no significant accumulation that would compromise overall slope stability. The location of the phreatic level varies across sections, primarily influenced by internal topography and the type of surface irrigation applied. However, in all scenarios, flow lines remain confined and do not reach critical zones near the slope base. Pore water pressures remain within acceptable ranges, consistent with previous stability analyses.

This analysis provides a valuable tool to complement stability assessments in leached ore dumps, enabling the visualization of how irrigation water redistributes internally through the ore, as well as guiding decisions in the optimization of high-permeability overliner materials and the implementation of efficient drainage systems.

Introduction

Dump leach facilities are widely used in mining operations for the extraction of metals through the

percolation of leaching solutions over ore piles. The safe design and long-term operation of these structures depend not only on geotechnical stability, but also on a comprehensive understanding of their internal hydraulic behavior under irrigation conditions.

In particular, the accumulation of infiltrated water within the dump may lead to elevated pore water pressures and rising phreatic levels, which in turn can reduce effective stress and potentially impact slope stability. Understanding how water redistributes internally under operational irrigation conditions is critical for the proper design of drainage systems and the optimization of construction materials.

This study focuses on a practical design challenge in the Phase IX expansion of the leached ore dump leach at the Radomiro Tomic Division in Chile. Due to the limited availability of high-permeability cover material (Cover Type A), the project required a hydraulic assessment to determine whether its use could be optimized without compromising system performance.

To support this goal, finite element analyses were performed using SEEP/W software to simulate saturated steady-state conditions representing prolonged irrigation. The analyses focused on evaluating the distribution of pore pressures and phreatic surfaces across representative cross-sections of the dump.

The results of this study offer insights into internal water flow patterns and provide technical justification for material use optimization, contributing to the development of more efficient and cost-effective dump leach designs.

Project Context and Design Background

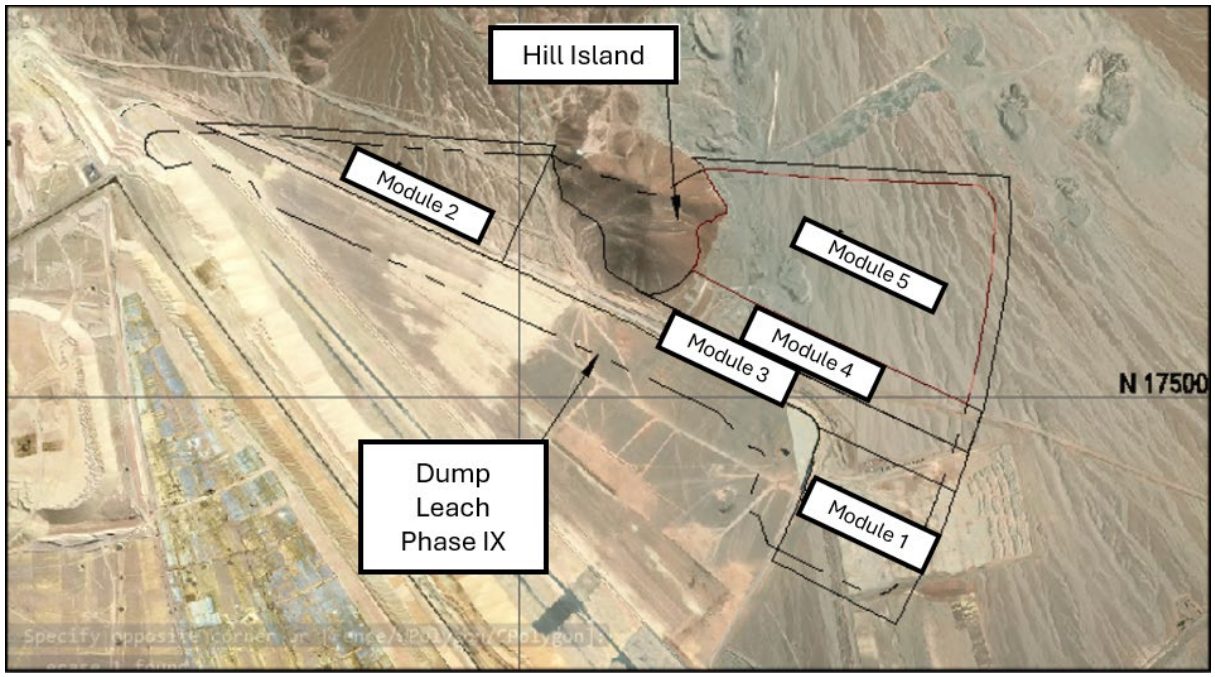

Figure 1: Phase IX configuration of the DRT dump leach

Phase IX of the Radomiro Tomic dump leach includes six operational modules developed over an existing lined foundation. Five of the modules are located over relatively flat terrain, while one module, known as "Hill Island," is situated on a natural slope with steeper geometry. The design incorporates a geomembrane liner system and a granular cover layer intended to protect the liner and facilitate the collection of leachate into drainage pipes. Figure 1 shows a plan view of the Phase IX configuration.

Two types of cover materials were defined: Cover Type A, a high-permeability gravel layer used primarily over flat terrain, and Cover Type B, a lower-permeability granular material intended for use in areas with reduced hydraulic demand, such as interior zones or slopes with lower irrigation exposure. Due to the limited availability of Cover Type A, a technical evaluation was required to assess whether its use could be optimized, especially in the Hill Island area, without compromising hydraulic performance.

To investigate this, the project team selected four radial cross-sections that traverse representative areas of the dump, including Hill Island. Each section was analyzed under different irrigation patterns based on the expected operating configurations. These analyses informed decisions regarding the possible replacement of Cover Type A with Cover Type B and the need for drainage piping in certain zones. Figure 2 shows the radial sections for infiltration analysis.

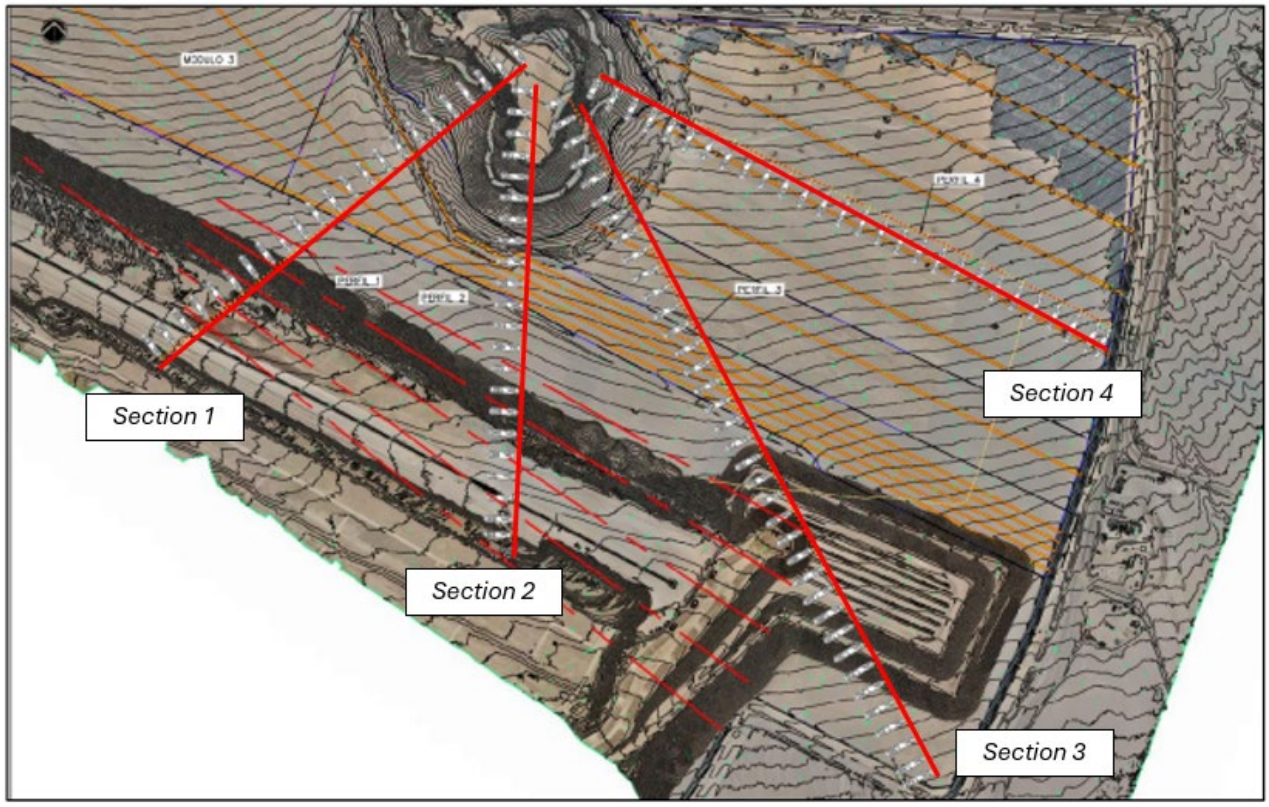

Figure 2: Radial sections for infiltration analysis

Methodology

The hydraulic behavior of the dump leach was analyzed using SEEP/W, a finite element software developed by GeoStudio for simulating saturated and unsaturated groundwater flow in geotechnical systems. The modeling approach adopted in this study was steady-state saturated flow, representing a scenario in which the dump has reached hydraulic equilibrium after prolonged irrigation.

The steady-state assumption was adopted as a conservative representation of hydraulic equilibrium under prolonged irrigation. Long-term piezometer monitoring at the site has indicated that pore water pressures tend to stabilize after sustained irrigation cycles, qualitatively supporting the use of a steady-state approach. Although the model does not reproduce transient fluctuations, it provides a practical upper-bound scenario for assessing potential pore pressure accumulation.

This assumption is justified by the continuous application of irrigation over time, which—combined with the low evapotranspiration and the retention properties of the ore material—leads to the development of near-saturated conditions in specific zones of the dump. By modeling this stabilized scenario, the objective was to evaluate the distribution of internal pore pressures and phreatic levels under operationally realistic, but conservative, conditions.

The materials present in the analysis were modeled as “saturated” due to the long-term continuity of irrigation and the water absorption capacity of the ore matrix. The continuous irrigation considered in the model represents a secondary leaching process applied to ripios previously leached, aimed at recovering residual metal content. This condition is supported by SEEP/W for flow modeling in granular media. A steady-state analysis was executed, representing a non-transient condition beyond a single day of irrigation.

Although the saturated steady-state scenario is conservative and allows assessing maximum pore pressures, it should be noted that such conditions might reduce the shear strength of the ripios and potentially affect stability. This aspect is beyond the scope of the present hydraulic analysis but is recommended for future geotechnical assessments.

Saturated Condition

The analysis assumed that seepage velocities are laminar and that flow rates are proportional to the permeability of the materials, following Darcy’s Law, expressed in Equation 1:

$$v = K \cdot i \qquad \text{Eq. 1}$$

Where:

- v: flow velocity through the pore space (m/s)
- k: hydraulic conductivity (m/s)
- i: hydraulic gradient (m/m)

Assuming steady flow through porous media, the infiltration is governed by the continuity equation (Equation 2):

$$\frac{\partial}{\partial x}\left(k_x \frac{\partial h}{\partial x}\right) + \frac{\partial}{\partial y}\left(k_y \frac{\partial h}{\partial y}\right) + \frac{\partial}{\partial z}\left(k_z \frac{\partial h}{\partial z}\right) = 0 \qquad \text{Eq. 2}$$

Where:

- h: hydraulic head (m)
- x, y, z: principal coordinate axes (-)

This equation is solved analytically for multiple layers, materials, and boundary conditions.

Modeling Considerations

- All materials were considered isotropic with a vertical-to-horizontal hydraulic conductivity ratio of 1:1.
- The foundation soil was excluded from the model, as the entire dump is lined with an intact geomembrane that prevents infiltration into the subgrade. This assumption is conservative for estimating internal phreatic levels.
- The geomembrane element was modeled using SEEP/W's "impermeable barrier" boundary condition.
- Phase IX includes a total of 82 irrigation plots. The worst-case scenario modeled corresponds to simultaneous irrigation of 66 plots during the final stage prior to Phase X, involving all eight irrigation sub-matrices. This scenario produced two irrigation conditions for Sections 3 and 4, which are discussed in the results.

Boundary Conditions

- Drainage zones (P=0): Points where collector channels are located, assumed to convey flow out of the system.
- Potential seepage face: Applied to downstream slopes, assumed inactive unless hydraulic conditions generate outflow.
- Irrigation rate: Maximum operating rate of 4 L/h·m² applied to the dump crest according to plot layout.
- Impermeable barrier: Defined at the interface between cover and foundation soils, preventing flow toward the foundation.

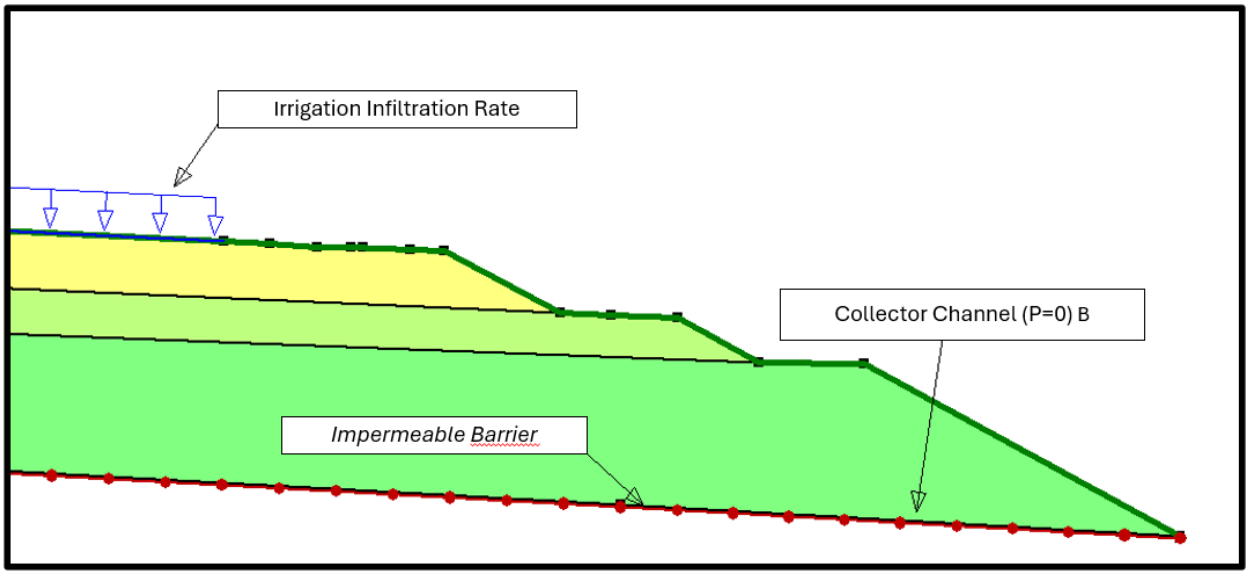

Figure 3: Boundary conditions used in modeling

Hydraulic Conductivity

Hydraulic conductivity and saturation properties were defined from laboratory data and past project experience. Table 1 summarizes the saturated hydraulic conductivity and volumetric water content used for the different dump terrace materials and cover layers:

Table 1: Hydraulic Parameters of Dump Materials

Material	Layer	Saturated Hydraulic Conductivity (cm/s)	Saturated Volumetric Water Content, θ_{sat} (-)
Debris	Dump Terrace 3	$5{,}5 \times 10^{-3}$	**0,33**
	Dump Terrace 2	$1{,}3 \times 10^{-3}$	**0,29**
	Dump Terrace 1	$2{,}3 \times 10^{-4}$	**0,21**
Cover A		$1{,}0 \times 10^{-2}$	**0,20**
Cover B		**$6{,}0 \times 10^{-6}$**	**0,20**

Cover Type A exhibited the highest permeability (1.0×10^{-2} cm/s), while Cover Type B had significantly lower values (6.0×10^{-6} cm/s), corresponding to its role as a protective layer with minimal drainage function.

Cover B is a low-permeability layer (k=6.0 × 10−6 cm/s) designed to limit downward infiltration rather than to act as a drainage layer. This configuration intentionally promotes lateral flow towards collection systems while reducing percolation into the dump.

Although Cover Types A and B serve different hydraulic purposes, this study aimed to evaluate their performance in complementary use. Due to the limited availability of high-permeability material (Cover A), the analysis assessed scenarios where portions of the dump could be covered with Cover B while maintaining overall hydraulic performance. This trade-off analysis helps optimize resource allocation without compromising the system's operational objectives.

Four cross-sections were selected for analysis: Sections 1 through 4. Sections 3 and 4 were evaluated under two different irrigation scenarios (A and B) to simulate variations in irrigation distribution across the operational cycle. These configurations were designed to reflect the most demanding and representative conditions for assessing potential water accumulation and internal drainage performance.

Results and Discussion

The results showed varying patterns of water movement across the analyzed sections. In general, flow was observed to descend through the leached ore layers and accumulate above the liner, particularly where the hydraulic conductivity contrast was greatest. The following presents the results of the infiltration analyses for each section under operational irrigation flow.

Radial Section Analysis No. 1

The flow path from the Hill Island area (left side of Figure 4) gradually descends toward the central area of the section, where Cover Type A is projected. This configuration ensures that the high hydraulic conductivity of the material dissipates the entire infiltrated irrigation flow, even passing through the area of Cover Type B located over Hill Island. Consequently, no constant water columns are observed.

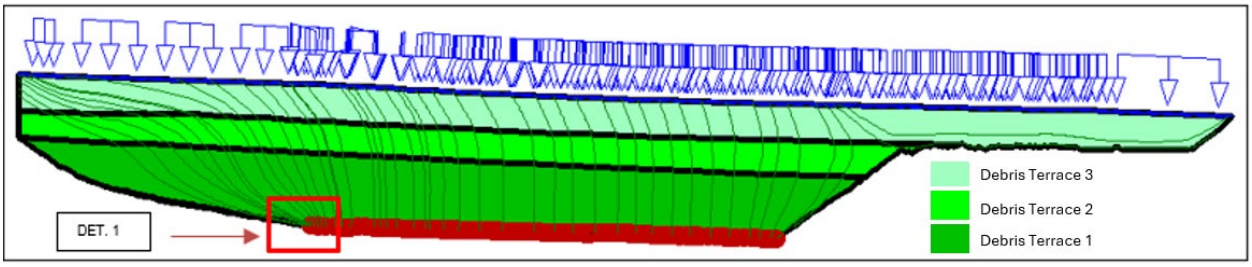

Figure 4: Infiltration conditions—Section No. 1, Phase IX modules

Regarding the phreatic level associated with operational irrigation, Detail 1 in Figure 4 (shown in Figure 5) indicates that the water table rises above the cover layer, though not to a height that would compromise the dump's global stability. Complementary slope stability analyses performed for the Phase IX expansion (not included in detail in this paper) confirmed that the observed phreatic rise does not compromise the dump's global stability under operational conditions.

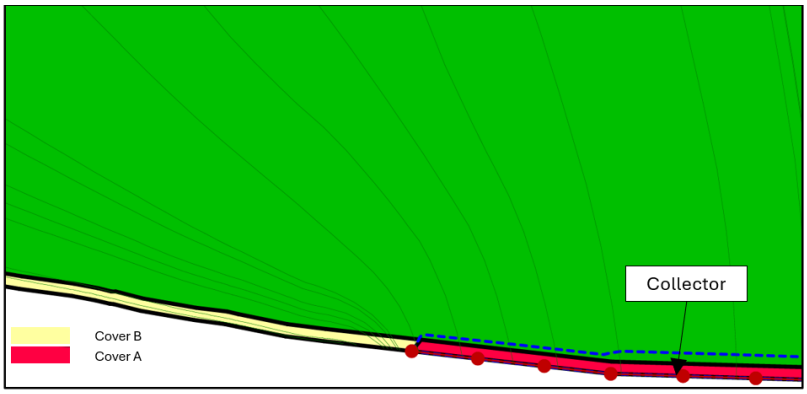

Figure 5: Detail 1—Section No. 1 analysis

Figure 6 shows the pore pressure generated inside the dump due to irrigation. In the central area, where Cover Type A is located, pore pressures remain relatively low, with higher pressures observed only in the Hill Island sector, where Cover Type B is used.

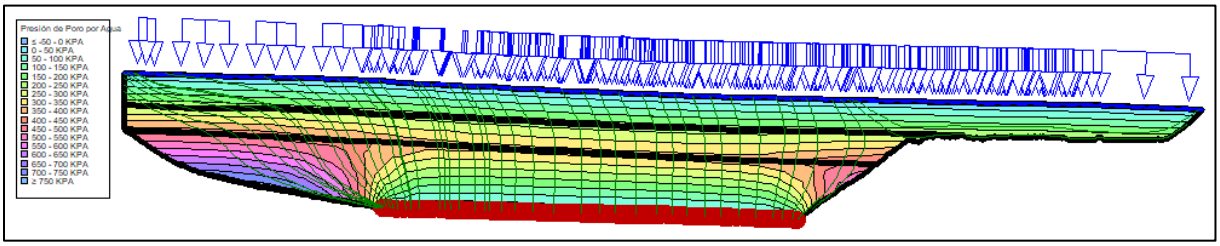

Figure 6: Pore pressure detail—Section No. 1

Radial Section Analysis No. 2

As in the previous case, the flow path gradually descends toward the central zone, where Cover Type A is projected. Results are shown in Figure 7, and a detail of the phreatic level height above the cover layer is shown in Figure 8.

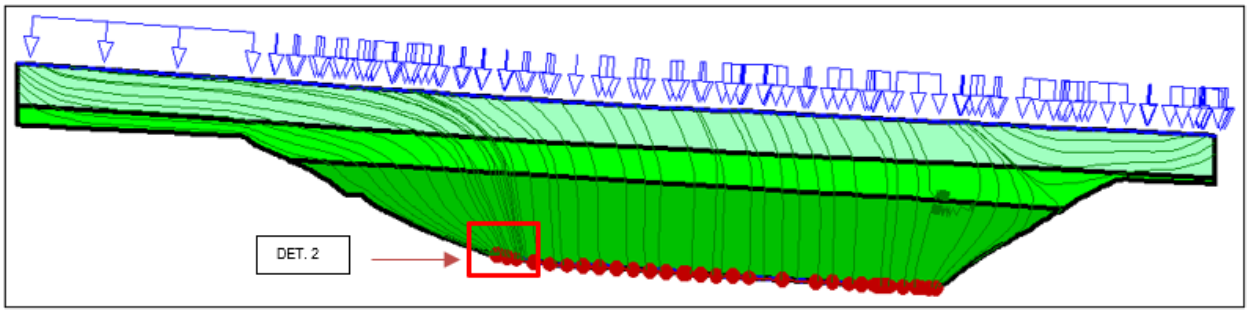

Figure 7: Infiltration conditions—Section No. 2, Phase IX modules

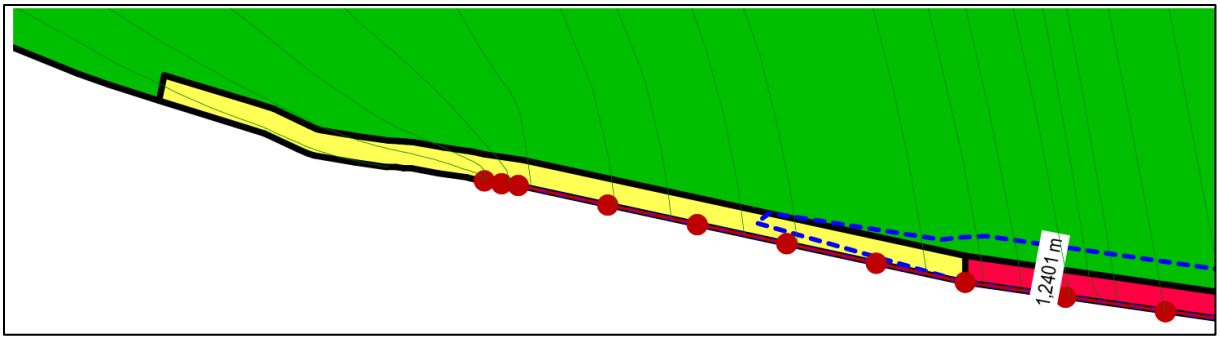

Figure 8: Detail 2—Section No. 2 analysis

Figure 9 presents the pore pressure distribution inside the dump. Lower pore pressures are observed in zones with Cover Type A, while higher pressures appear in zones with Cover Type B. In the upper areas, pore pressures are minor, suggesting that the water is progressively absorbed by the lower layers.

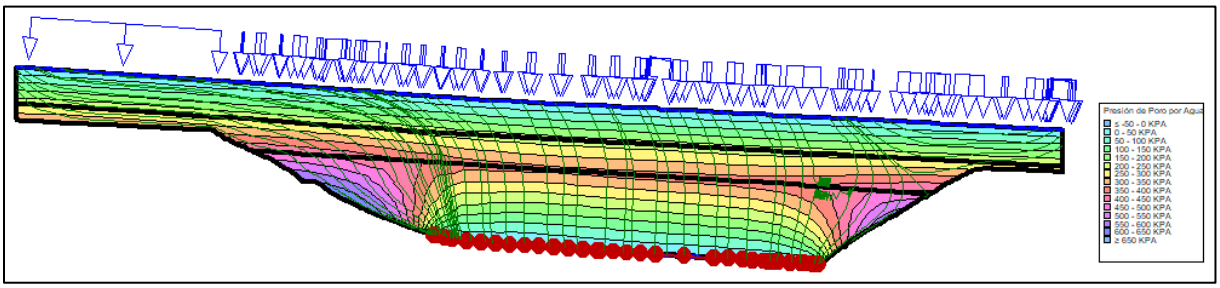

Figure 9: Pore pressure detail—Section No. 2

Radial Section Analysis No. 3

Infiltration conditions were analyzed for two radial sections: Section 3-A and Section 3-B, due to non-uniform irrigation over the section. Figures 10 and 11 present the results for Sections 3-A and 3-B, respectively.

In Section 3-A, water accumulates in the central area and other parts of the section, indicating non-uniform drainage and a significantly higher phreatic surface in the middle. In contrast, Section 3-B exhibits lower flow accumulation and a shallower water table.

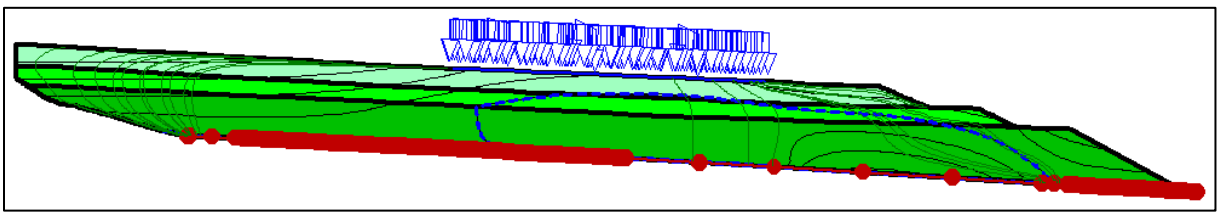

Figure 10: Infiltration conditions—Section No. 3-A, Phase IX modules

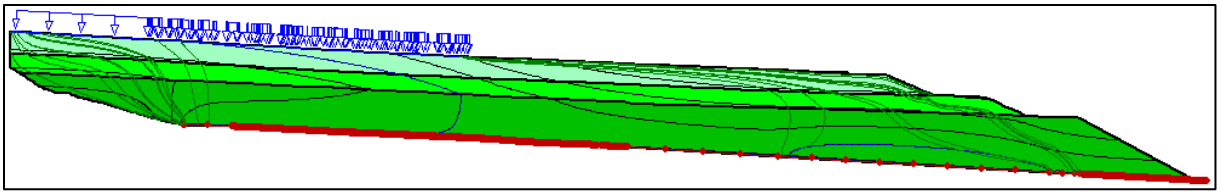

Figure 11: Infiltration conditions—Section No. 3-B, Phase IX modules

Figures 12 and 13 show pore pressure distributions for Sections 3-A and 3-B. Higher pore pressures are seen at the dump base, particularly in Section 3-A.

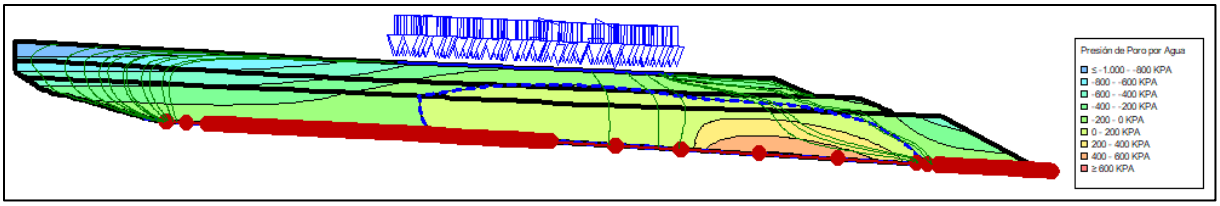

Figure 12: Pore pressure detail—Section No. 3-A

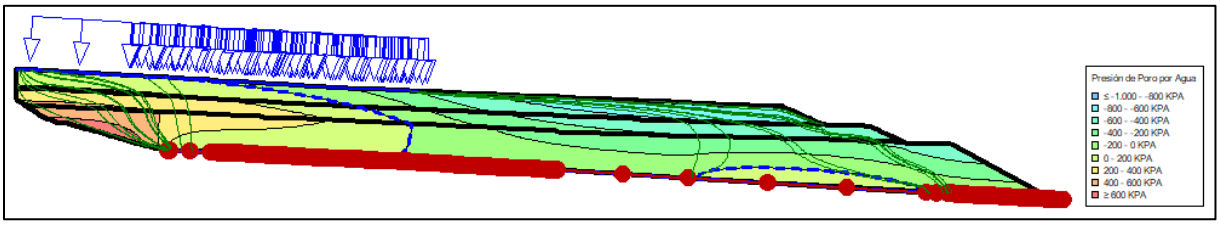

Figure 13: Pore Pressure Detail—Section No. 3-B

Radial Section Analysis No. 4

Similar to Section 3, two infiltration scenarios were analyzed: Section 4-A and Section 4-B. Figures 14 and 15 present the results for each case. Section 4-A shows a rising phreatic surface in the center, where irrigation accumulates, with a downward trend toward the edges, supporting overall dump stability. In Section 4-B, flow remains stable.

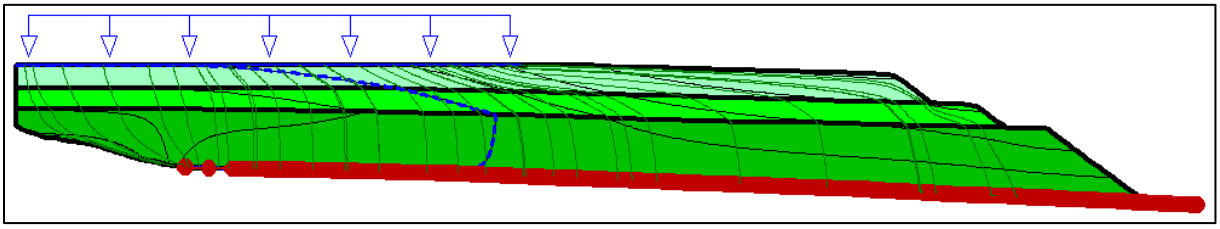

Figure 14: Infiltration conditions—Section No. 4-A, Phase IX modules

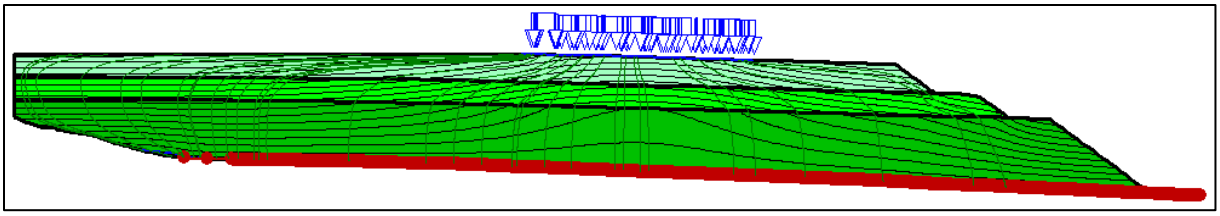

Figure 15: Infiltration conditions—Section No. 4-B, Phase IX modules

Figures 16 and 17 show the pore pressure distributions for Sections 4-A and 4-B. As in previous sections, the highest pore pressures accumulate toward the Hill Island area, avoiding stability concerns near the outer slopes of the dump.

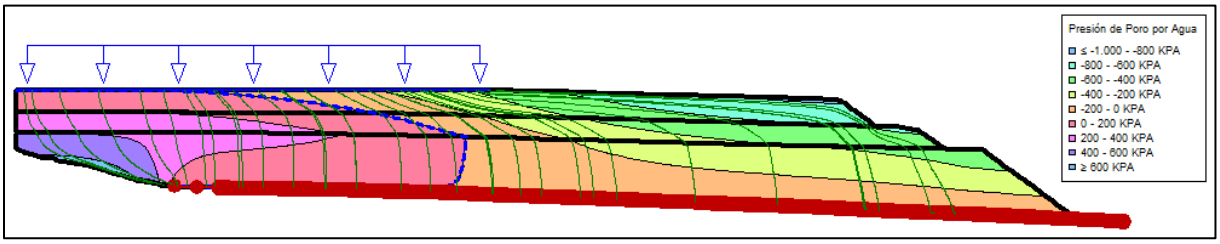

Figure 16: Pore pressure detail—Section No. 4-A

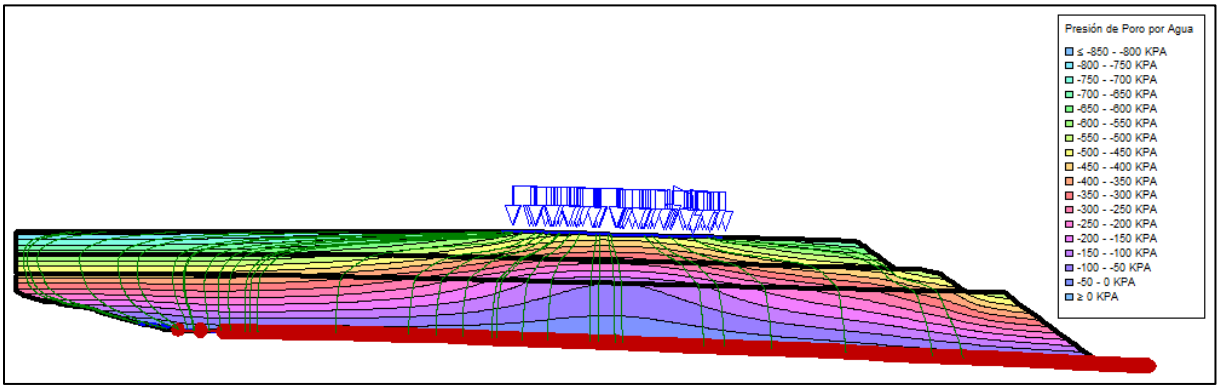

Figure 17: Pore pressure detail—Section No. 4-B

An important observation was that the use of Cover Type B in Hill Island did not generate hydraulic conditions requiring subsurface drainage piping, as long as the area remains within low irrigation intensity zones.

Conclusion

The steady-state infiltration analysis demonstrated that the internal water distribution in the dump leach varies significantly depending on irrigation configuration and local geometry. However, none of the scenarios evaluated presented conditions that would compromise the overall stability of the dump.

The results validate the potential to optimize the use of Cover Type A by selectively replacing it with Cover Type B in low-demand areas, especially over slopes such as Hill Island. This approach reduces the consumption of high-permeability materials without negatively impacting the hydraulic performance of the system.

Furthermore, the analysis confirms that under long-term irrigation conditions, pore pressures stabilize in a predictable manner, and the current drainage design is sufficient to manage the expected flow patterns. Continuous monitoring in critical areas is recommended to validate these findings in the field.

This study provides a practical framework for assessing internal hydraulic conditions in dump leach facilities and supports decision-making regarding material optimization and drainage system design.

References

Axios Engineering. (2024). *Informe de optimización del cover—Análisis de infiltración en botadero de ripios Fase IX, División Radomiro Tomic: Informe técnico*. Santiago, Chile.

Bouffard, S. (2005). The effect of mineralogy, particle size, and wetting on the hydraulic properties of heap leach materials. In *Proceedings of the SME Annual Meeting*. Salt Lake City, USA.

GeoSlope International Ltd. (2012). *SEEP/W 2007: Seepage modeling with GeoStudio*. Calgary, Alberta, Canada.

MEND Program. (2001). *Design, operation and closure of heap leach facilities* (MEND Report 1.61.5). Mining Environmental Neutral Drainage, Ottawa, Canada.

Smith, M., & Beckstead, G. (2010). Hydraulic behavior of heap leach pads under prolonged irrigation. In *Proceedings of the International Conference on Heap Leach Solutions*. Vancouver, Canada.

Determining the Interpretive Yield of Heap Leaching Technologies

Aaron Young, University of Utah, USA
Thom Seal, University of Nevada, Reno, USA

Abstract

Operational, geotechnical, and economic uncertainties plague the safe and efficient productivity of heap leach pads and rock dumps around the world. Root causes for these uncertainties stem from a myriad of origins, including market volatility, comminution and stacking methods, subsurface heterogeneity, traceability of mine and operational data, solution management, and limitations in traditional modeling approaches. This paper identifies the origins of these uncertainties, overviews heap leach failures, and proposes a novel systems integration framework—Interpretive Yield Theory (IYT)—to address them. Based on Industry 4.0 concepts, IYT evaluates the yield of interpretable output, not merely the data volume, produced by different methods having equivalent inputs. After defining IYT, this paper presents the Interpretive Yield Diffusion Model (IYDM), a novel model that incorporates IYT with numerical and computational models for heap leaching originally developed in the 1970s. The IYDM is then used to compare three heap leaching strategies: traditional irrigation leaching, gravity or deep raffinate leaching, and injection/extraction leaching, aka Hydro-Jex®. Results, although still preliminary, demonstrate distinct differences in interpretive yield between the three methods, offering a basis for selectivity. Future work will focus on site-specific model calibration and validation.

Introduction

Uncertainty is commonplace within the mining industry (Heuberger, 2005; Kuhn & Visser, 2014; Carlson, 2019). Various efforts have been devised to mitigate this risk from the earliest moments of exploration (Carlson, 2019) through continuous improvement initiatives during productive mining operations (Neves et al., 2019; Armstrong et al., 2021) to post-mining land use agreements. These efforts most commonly intersect with mine planning (Fu et al., 2015), which focuses primarily on optimizing the mining of the deposit and the predictable delivery of ore to downstream mineral processes (Das et al., 2023). Among these mineral processes is heap leaching, which accounts for a significant proportion of all copper produced.

Heap leaching is an extractive hydrometallurgical process that utilizes man-made rock piles located on the surface. Sufficient permeability of the rock mass must exist within the rock pile to permit solution flow. Over time, channeling of solution flow within the rock pile develops, which causes a short-circuit in ideal solution flow and lowers the sweep efficiency in unpredictable ways. The result of this uncertainty in sweep efficiency is an uncertainty in economic forecasting (Bartlett, 2013). The way heap leach piles are engineered, built, operated, and monitored is influenced greatly by previous decisions made throughout the entirety of the mining process. Furthermore, since heap leaching is often employed for lower quality ores, some of which are in the way of relatively rich and lucrative ores, it is frequently the case that they are transformations of waste dumps or low-grade stockpiles that were never originally designed for leaching.

Compared with the concept of defining the optimal pit, which dates back to the 1960s, given an existing orebody, the engineering of the resulting ideal rock pile that it could yield is a relatively new concept (Li et al., 2013; Saldaña et al., 2019; Kaykov & Koprev, 2020). It is fair to say that within the geoscientific context, the effort spent to understand how natural mineral deposits form has been far greater than the amount of effort spent towards understanding how man-made mineral piles deform, deteriorate, decrepitate, etc.. However, both processes share many things in common.

A holistic viewpoint can be used to ascertain how uncertainty is compounded along each step of the mining process (Young & Rogers, 2021). Table 1 catalogs origins of uncertainty related to the major process steps of mining that surround heap leaching. A systemic underutilization of operational data causes uncertainty to compound across process steps, whereas a data-driven approach reduces uncertainty (Young & Rogers, 2019). Perfect characterization and traceability of each blasted fragment of in situ material from the pit to the pile is not manageable or practical, given historical methods (Young & Rogers, 2022). Despite extensive efforts to understand the geology of the deposit and despite the tremendous amount of supervision, engineering, and manpower that goes into constructing the resulting leach piles, the characteristic distribution of leach piles remains an enigma to many key decision-makers and mining stakeholders (Young & Rogers, 2021, 2022).

Key decision-makers and mining stakeholders often rely on plans that were set long before they arrived on the scene, and they frequently leave before the decisions they make are implemented at the mine. Reserves must be accounted for (Gillis et al., 2024), tons must be made, and all the metal in the heap must "eventually" leach, right? In fact, misaligning priorities from the pit to the pad has dramatic economic consequences that are neither easy to identify nor easy to solve once identified. These consequences, coupled with uncertainty in economic forecasting, can lead to financial pressure, which in turn can result in corporate negligence or malpractice within an organization, ultimately culminating in failures.

This paper aims to provide an overview of heap leaching failures and proposes novel technical solutions for reducing uncertainty within heaps.

Table 1: Origins of Uncertainty in Heap Leaching

Process Step	Sources of Information	Origins of Uncertainty
Exploration & Mine Planning	Exploration drill hole data Sampling data Block model Ore characterization Life of Mine (LOM), long-range & short-range mine plans	Drilling & sampling bias, core recovery issues, structure interpretation, etc. Block size, nugget effect, interpolation method, model assumptions, etc. Recovery, minerology, deportment (Blannin et al., n.d.), pH & redox variability, etc. Commodity price volatility, infrastructure assumptions, timing & amount of Capex projects, etc.
Production Drilling & Ore Control	Production drill hole data Drilling performance & perforation rate data Ore control grade and volume modeling	Drill hole deviation, bit wear, drilling accuracy, etc. Sample representativeness, ore/waste boundary delineation, lag time, etc. Blasting variability, fragmentation, dilution, etc.
Mining Operation	Fleet Management System (FMS) data Vehicle performance & maintenance data Shift records	Equipment utilization & maintenance, operator differences, safety incidents, etc. Logistics, weather impacts, labor relations, etc. Reconciliation, change management, OPEX constraints, etc.
Heap Leach Construction	FMS dumping locations Dozer operations Shift reports Leach pad design & construction plan	Settling rate variability, heterogeneity in material, moisture content, etc. Agglomeration differences, clay/slime content, lift height/compaction variance, adequate ripping (Uhrie & Koons, 2000), etc. Liner integrity, safety incidents, stormwater management, etc.
Heap Leach Operation	Metallurgical testing Geotechnical monitoring data Heap leach pad model	Representative sampling for testing, Minerals affecting pH, Leach kinetics, evaporation/infiltration differences, flow variability, etc. Preferential flow, pad movement, detection & repair difficulties, etc.
Environmental Monitoring & Closure	Environmental monitoring data Sampling Environmental assessments	Sensitivity of monitoring equipment, residual solution drainage, changing oxidation/reduction conditions, etc. Wildlife interaction, land use conflicts, evolving standards, etc.

Overview of Heap Leach Failures

The Copler mine disaster occurred on February 13th of 2024 (McGee, 2024). Approximately 10 million cubic meters of material moved downslope 800 meters, trapping and killing nine workers (2024). In addition to landslide and erosion risks being mentioned in its Environmental Impact Assessment (EIA)

(2024), corruption (2024) and negligence (2024), as well as increasing the amount of solution introduced to the heap, were all major root causes for the tragedy (Türkçe, 2024).

Table 2 shows a summary of heap leaching incidents from the last 30 years.

Table 2: Summary of Heap Leaching Incidents from 1995 to 2025

Year	Mine Name	Location	Operator/ Company	Incident Summary
1997	Gold Quarry	Nevada, USA	Newmont	A heap leach pad structural failure released ~930 m^3 (245,000 gal) of cyanide solution into two creeks. Surface land neutralized, and Environmental fines imposed.
2001	Timbarra Gold Mine	New South Wales, Australia	Ross Mining	Two cyanide-bearing ponds overflowed during storms, releasing solution into nearby wetlands and the Clarence River.
2003	San Andrés	Copán, Honduras	Greenstone Resources	A pipeline or pad breach released cyanide solution into the Lara River, killing ~18,000 fish and affecting downstream communities.
2005	Marlin Mine	San Marcos, Guatemala	Goldcorp	Alleged cyanide leaks led to major community protests; while not a catastrophic failure, the issues raised concerns about leach containment and environmental risk.
2007	Bellavista	Puntarenas, Costa Rica	Glencairn Gold	A major landslide in the heap pad led to closure. Geotechnical instability from a reactivated ancient landslide base caused ore and solution release.
2012	Talvivaara Mine	Sotkamo, Finland	Talvivaara Mining Co.	Gypsum pond failure released ~1.2 million m^3 of acidic and metal-laden leach solution, contaminating streams and groundwater.
2014	Veladero (pre-major 2015)	San Juan, Argentina	Barrick Gold	A pipe rupture caused a smaller cyanide spill; site vulnerability later led to the major 2015 incident.
2015	Veladero Mine	San Juan, Argentina	Barrick Gold	A valve failure caused ~1,000 m^3 of cyanide solution to spill into the Potrerillos River, sparking national investigations and sanctions.
2020	Tujuh Bukit	East Java, Indonesia	PT Merdeka Copper Gold	Subsurface instability led to a slump on the heap face. No injuries or external spill reported; operations paused for assessment.
2024	Eagle Gold Mine	Yukon, Canada	Victoria Gold	Heap leach pad slope failure released ore beyond containment; no casualties. Emergency berms prevented widespread cyanide contamination.
2024	Çöpler Mine	Erzincan, Turkey	SSR Mining/ Anagold	Catastrophic heap collapse on Feb. 13 buried nine workers and released ~10 million tonnes of ore. Investigations cited issues with design and overloading of the heap, which caused shear strength failures.

Another recent failure was the Eagle Gold Mine heap leach incident that occurred on June 24, 2024. The facility, located near Mayo Yukon and operated by Victoria Gold Corporation, suffered a side-slope failure that released as much as 300,000 m^3 of cyanide-bearing solution at the time of failure (Greene, 2024). Investigation into the root cause of the landslide of ore stacked in the heap that spilled over the embankment is still underway at the time of this publication.

Framework for Evaluating the Operating Uncertainty of Heap Leaching Methods

To evaluate and compare the effectiveness of various heap leach methods, this study introduces a novel conceptual framework termed Interpretive Yield Theory (IYT). IYT is based on the premise that, given identical input conditions, the most effective analytical or operational method is the one that produces the highest volume of interpretable output data. This framework shifts the focus from purely recovery-based metrics to a broader assessment of a method's ability to generate meaningful, high-resolution insight into subsurface processes. In this context, interpretive yield refers not only to the volume of data produced but also to the quality, resolution, and relevance of that data for decision-making. By integrating IYT into the comparative modeling process, this study enables a standardized evaluation of leaching technologies based on their capacity to resolve internal heap dynamics, support model calibration, and inform operational strategies.

The Interpretive Yield Ratio (IYR) is defined as the ratio of the total number of interpretable output data points to the number of standardized input units used in a modeling or monitoring scenario. It quantifies a method's capacity to generate meaningful, decision-supporting information from a given input baseline.

Formally, it is expressed as:

$$IYR = \frac{D_{Out}}{D_{in}} \quad (1)$$

Where:

Dout is the total number of interpretable output data points, such as pressure-flow curves, concentration gradients, or sensor readings that meet resolution and reliability thresholds.

and

D_{in} is the number of input units, typically standardized by injection volume, time, or number of leach events (e.g., m^3 of solution applied or injected)

An IYR value greater than 1 indicates a method that amplifies interpretive information relative to its input footprint, while a value less than 1 suggests lower interpretive efficiency. This ratio serves as a central metric for comparing operational methods under the Interpretive Yield Theory (IYT) framework.

Heap Leaching Methods

As hydrometallurgical processes go, heap leaching is relatively cheap, but also relatively time-consuming (van Staden & Petersen, 2021). While reagents may be recycled in the heap leaching process, the thermodynamics of time are yet to be quenched (Sels & Wouters, 2015). This is to say that the long timeframe involved in heap leaching adds to the difficulty of understanding the process in unique and complex ways. While time itself cannot be manipulated, the rate of the leaching reaction can.

Manipulating reaction rates in heap leaching involves optimizing various parameters. A heap leaching method is, therefore, considered to be an operational process that employs various optimization mechanisms. Although there are many heap leaching methods, this paper investigates only three: traditional or surface irrigation, gravity or deep raffinate leaching, and the patented Hydro-Jex® method.

Traditional Irrigation

In traditional surface irrigation leaching, control of the leaching reaction rate is typically approached by:

1. solution management strategies and application rates that aim to control the chemistry, flow of solution within the heap, and the time solution is applied,
2. modification of the material to be leached through pre-treatment, crushing, agglomeration, etc., or
3. bulk manipulation of the heap leach pad from lift height design, inter-liners, cover systems, monitoring, etc.

Gravity/Deep Raffinate Wells

Figure 1: Gravity or deep raffinate well installed atop a heap leach pad

Gravity or deep raffinate leaching controls the leaching reaction rate through all the means of traditional leaching. It adds a mechanism to apply raffinate to the lower portions of the heap directly. Figure 1 shows a picture of a gravity well installed on top of a heap leach pad.

Patented Hydro-Jex® Leaching Technology

Hydro-Jex® enables the leaching reaction rate to be controlled through the combined means of both traditional surface irrigation and gravity/deep raffinate leaching, and in addition, offers:

1. hydro-geo-mechanical manipulation of internal heap characteristics,
2. direct application of the solution to essentially any location within the entire heap volume, and
3. delivery mechanisms for near-total bulk manipulation and solution management of a heap.

By selecting these three methods, a simple, comparative evaluation may be performed whereby the concept of interpretive yield can be easily showcased.

Heap Leaching Models

Computer models for leaching in copper oxide heaps were developed in the 1970s (Ronald et al., 1975). These models used the concepts of unit volume and unit heap. Figure 2 provides visual schematics of these unit variables from early computer models of diffusion within heaps. Several other efforts have been made to improve the predictability of scale-up from laboratory column leaching to pad performance (Jansen & Taylor, n.d.; Dixon, 2003; Silver, 2013).

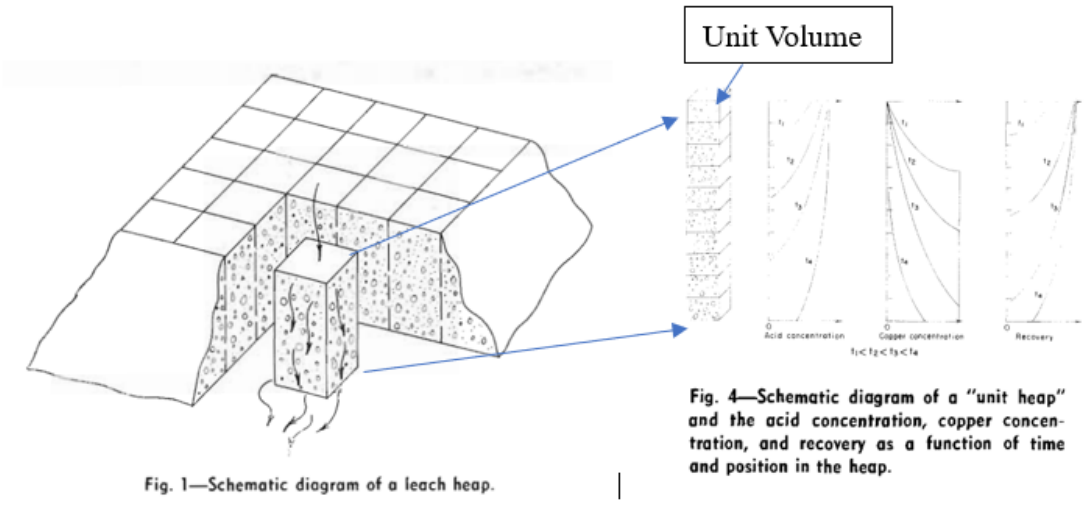

Fig. 1—Schematic diagram of a leach heap.

Fig. 4—Schematic diagram of a "unit heap" and the acid concentration, copper concentration, and recovery as a function of time and position in the heap.

Figure 2: Visual schematics from early computer model assumptions used to model heap leaching diffusion (adapted from Ronald et al., 1975)

While the assumptions of heap leach homogeneity match well with laboratory column testing, other efforts to model rock piles have demonstrated that heterogeneity exists within heaps (Young & Rogers, 2021). Figure 3 shows examples from rock pile modeling work available in the literature that inform how unit volumes and unit heaps can be modified to account for heterogeneity in computational modeling.

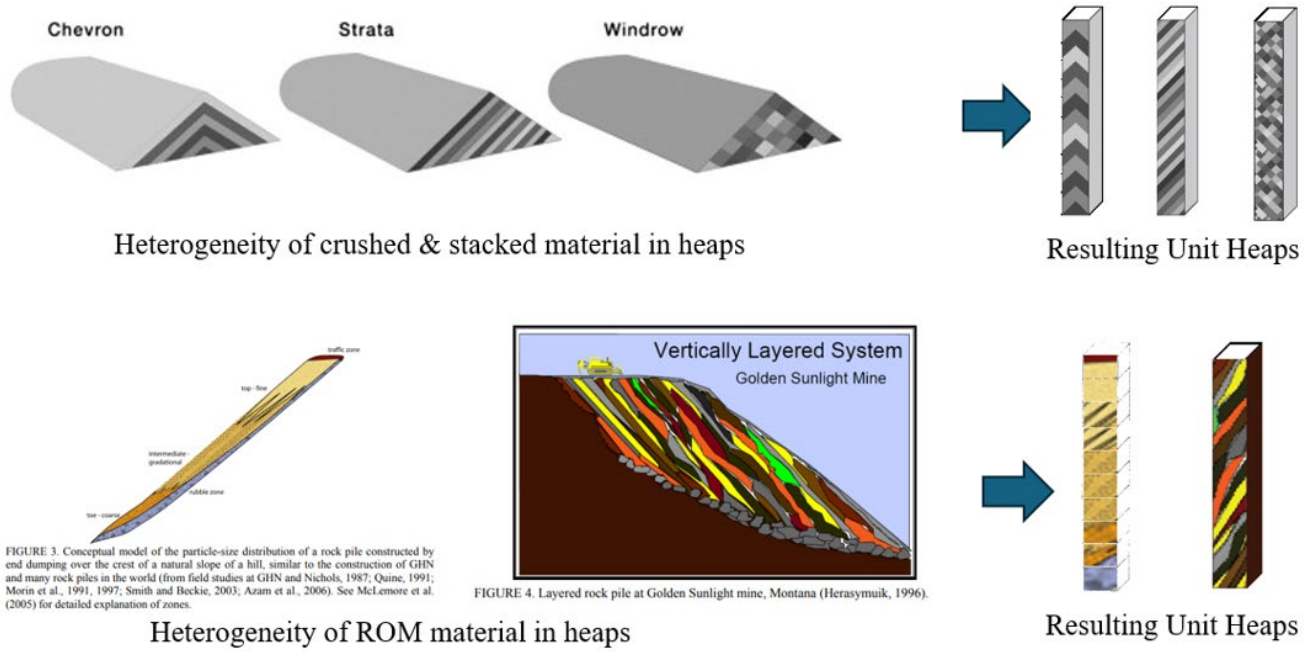

Figure 3: Examples of heterogeneity resulting in modified unit heaps (adapted from McLemore et al., 2009, and Zhao et al., 2013)

Another computer model for predicting heap leach behavior is shown in Figure 4 (McBride et al., 2012). In this model, columns are assumed homogeneous along their height. However, averages for fresh leaching sections are combined along their length and width based on the area that is put under leach simultaneously.

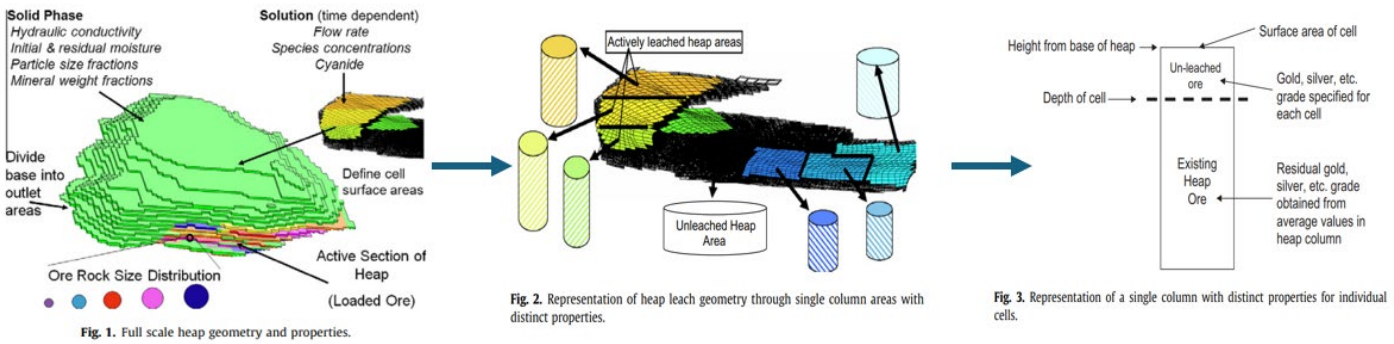

Figure 4: Example of a process heap model (adapted from McBride et al., 2012)

The input parameters to all diffusion models typically include physical characteristics of the heap, such as height, porosity, and particle size distribution. Additionally, chemical properties of the ore and leaching solution, like mineral composition and reagent concentrations, are crucial inputs. These models often incorporate kinetic factors, such as reaction rates and diffusion coefficients, to simulate the leaching process over time.

Evaluating Interpretive Yield

To evaluate the interpretive yield of the three heap leaching techniques mentioned (traditional irrigation, gravity/deep raffinate wells, and Hydro-Jex®), we can apply the Interpretive Yield Theory (IYT) framework and compare their Interpretive Yield Ratios (IYR).

Traditional Irrigation:

- Provides surface-level data on solution application and drainage
- Limited insight into internal heap dynamics
- Relatively low spatial resolution of data
- IYR is likely close to 1, as interpretable output closely matches input data

Gravity/Deep Raffinate Wells:

- Offers data from both surface and deeper sections of the heap
- Improved vertical resolution compared to traditional irrigation
- Provides some insight into solution flow paths and preferential channels
- IYR potentially >1, as it generates more interpretable data points per input unit

Hydro-Jex®:

- Enables data collection from multiple points within the heap volume
- Highest spatial resolution among the three methods
- Provides detailed information on internal heap characteristics and solution flow
- Allows for targeted application and extraction of solutions
- IYR likely significantly >1, offering the most interpretable data per input unit

Comparative Evaluation:

Table 3 lists some of the qualitative differences in IYT for each method, and Figure 5 displays a wiring diagram that maps which conceptual data are utilized by each method and how those streams overlap.

Table 3: Qualitative Input/Output Differences for IYT Evaluation

Method	Key Inputs	Representative Outputs
Traditional Irrigation	Raffinate flow & chemistry Weather (rain, evap) Stacking schedule & tonnage Periodic bottle-roll tests Monthly solution balance	Heap-wide recovery curve Daily PLS grade trend Pad water-balance status Spray uniformity heat map Annual recovery reconciliation
Gravity/Deep Raffinate	All Traditional inputs Well depth & screen logs Injection volumes & timing Down-hole permeability logs	Vertical breakthrough curves Sub-grade pore-pressure data IYR amplifier (ΔC/ΔV) 3-D early-recovery iso-surfaces
Hydro-Jex®	All Gravity inputs High-pressure injection schedule Extraction flow rates Real-time down-hole ORP & pH Micro-seismic monitoring Drone photogrammetry	Micro-seismic density map Real-time 3-D RTD Daily depth-specific forecast Heap deformation vectors Dynamic IYR dashboard

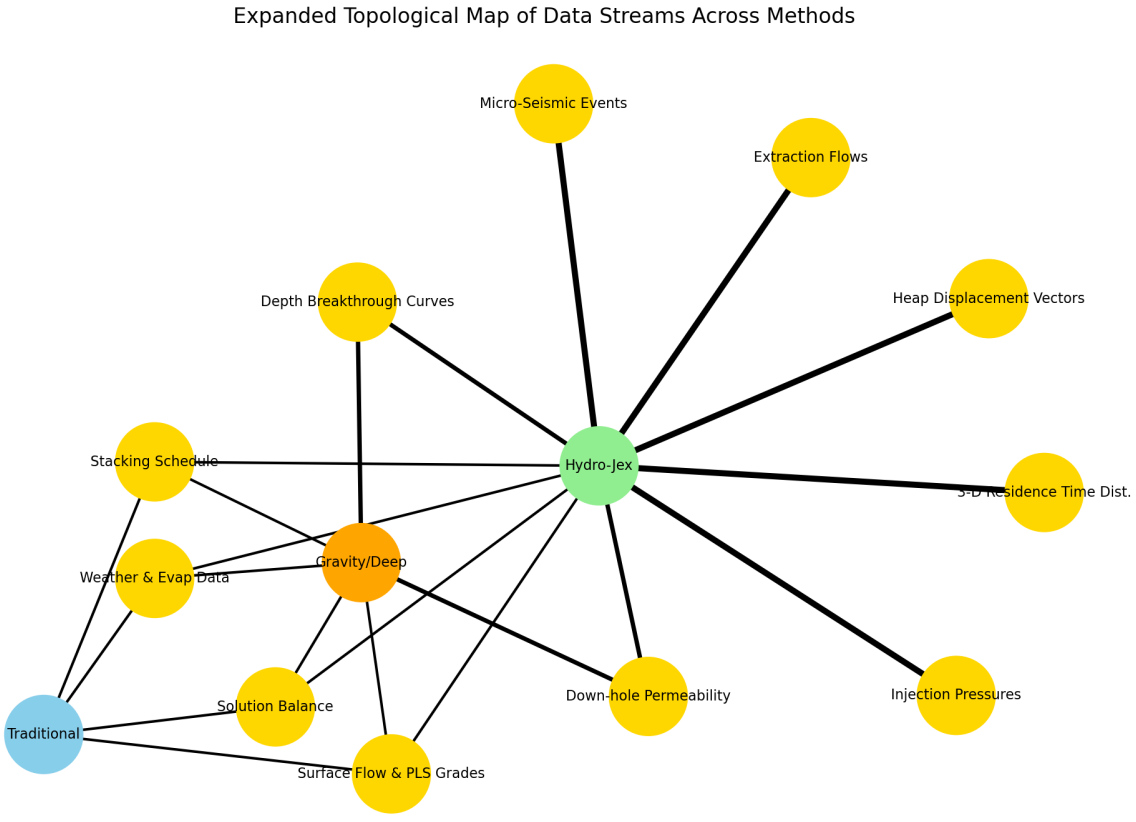

Figure 5: Topological map of data streams across leaching methods

Based on the IYT framework, Hydro-Jex® appears to offer the highest interpretive yield, followed by gravity/deep raffinate wells, with traditional irrigation providing the lowest interpretive yield. This

evaluation suggests that Hydro-Jex® would be most effective in reducing uncertainty and improving operational decision-making in heap leaching processes. The multiplicative lift in actionable insight is the core driver behind a higher interpretive yield.

Risk Assessment

By providing a framework for evaluating the information yield of different heap leaching methods, IYR offers a valuable tool for enhancing overall risk assessment and management in these operations. IYR can relate to risk assessments for heap leaching operations in several key areas, as outlined in Table 4.

Table 4: IYR-Based Risk Assessment Categories for Heap Leach Methods

Category	Description
Data Quality & Monitoring	Improved data resolution: A higher IYR indicates more interpretable data points are generated relative to inputs. This increased resolution enables more detailed mapping of internal heap dynamics, allowing for better identification and assessment of potential risks, such as solution channeling or uneven leaching.
Data Quality & Monitoring	Real-time monitoring: Technologies that yield higher IYR often provide more continuous and spatially diverse data streams. This enables real-time monitoring of heap conditions, allowing for faster detection and response to emerging risks.
Operational Control	Targeted risk mitigation: Higher IYR methods like Hydro-Jex® offer more precise control over solution application and extraction. This allows for targeted interventions to address specific risk areas within the heap, rather than relying on broad, less effective measures.
Operational Control	Failure prevention: The detailed insights provided by high IYR methods can help identify early warning signs of potential heap failures, such as excessive internal pressures or solution buildup, allowing for preventive actions.
Predictive Modeling	Enhanced predictive capability: Methods with higher IYR provide more comprehensive data on heap behavior, allowing for more accurate modeling and forecasting. This improves the ability to predict and mitigate potential risks before they manifest.
Predictive Modeling	Uncertainty reduction: By providing more interpretable data per input, high IYR methods reduce overall uncertainty in heap operations. This directly translates to lower operational risk and more confident decision-making.
Regulatory & Compliance	Enhanced regulatory compliance: More comprehensive data from high IYR methods can help demonstrate due diligence in risk management to regulatory bodies, potentially reducing compliance-related risks.
Strategic & Financial	Improved economic forecasting: Better understanding of internal heap dynamics through higher IYR methods can lead to more accurate predictions of metal recovery and operational costs, reducing financial risks.
Strategic & Financial	Optimized resource allocation: With more detailed data on heap performance, operators can better allocate resources to areas of highest risk or potential, improving overall risk management efficiency.
Strategic & Financial	Lifecycle risk assessment: The ability to gather more detailed data throughout the heap's lifecycle enables better long-term risk assessment and management, from initial stacking through to closure and remediation.

Case Study

Although previous sections in this paper were merely conceptual, this section examines two real case studies, one from the literature (Abbasi et al., 2020) and preliminary findings from another that is still underway. Figure 6, adapted from the study found in the literature, shows the initial conditions of a heap leach pad prior to utilizing Hydro-Jex®, but after using gravity/deep raffinate wells.

It is clear from Figure 6 that excessive application rates beyond the permeability of the pad material can create near-vertical channels to capture the excessive fluid, bypassing under-leached material, or causing pools of solution or phreatic ponding. This internal ponding will reduce the material's friction and cohesion factors. The formation of these vertical channels and internal ponding can significantly impact the stability and efficiency of the heap leach pad.

In geotechnical evaluation, wet rocks weigh more than dry rocks. Low-permeable material tends to retain solutions, causing an increase in weight on the material below. Friction between particles and the interface of particles and a liner goes to a minimum with saturation. The increased weight and reduced friction can lead to potential slope failures or slumping within the heap. These conditions may also result in preferential flow paths, causing uneven leaching and reduced metal recovery.

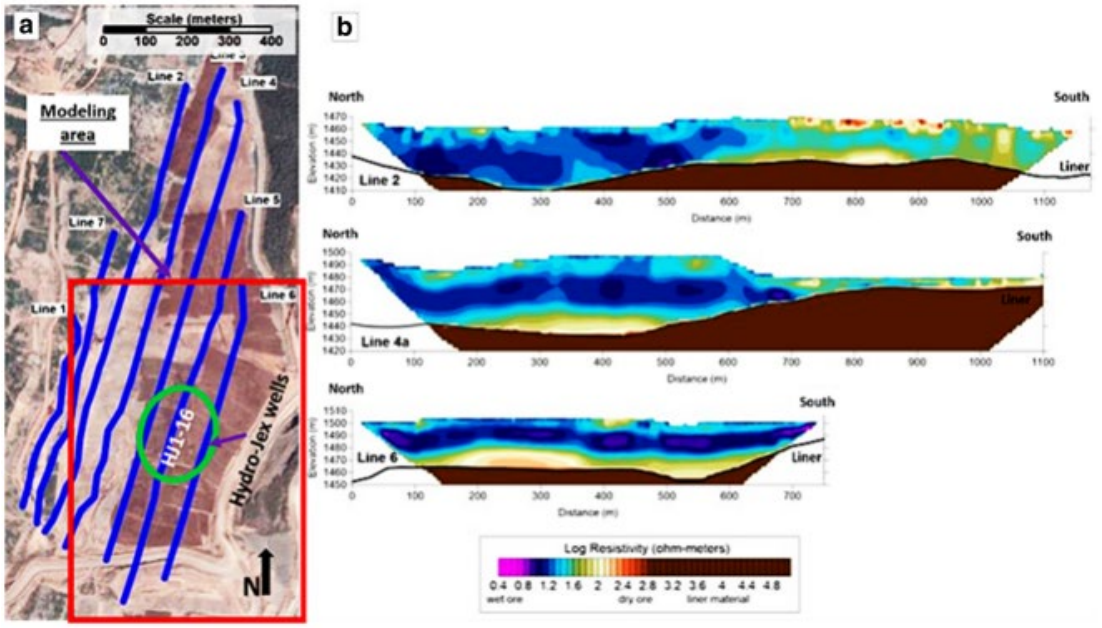

Fig. 3 Electrical resistivity survey across leach pad at Los Filos Mine used to build the phreatic surface and pore pressure in numerical modeling. **a** Survey line locations. **b** Results of three resistivity lines [22]

Figure 6: Case study of heap condition after deep raffinate gravity well leaching (adapted from Abbasi et al., 2020)

Regular monitoring and proper drainage systems are crucial to mitigate these risks and maintain optimal heap leach pad performance. Gravity or deep raffinate wells are relatively cheap and easy to

operate, but only achieve minimal horizontal wetting with very minimal sweep efficiency. They also do not provide enough *Interpretive Yield* to inform heap leach operators of the reality of the conditions within the heap. If left unchecked, there is insufficient data available to operate the heap efficiently or monitor the internal ponding.

Prolonged low flow decreases the hydraulic gradient, slowing down the movement of solution through the heap. Over time, fine particles can migrate and accumulate in certain areas, reducing permeability and creating localized zones of poor drainage. The weight of the ore and ongoing leaching processes can lead to compaction, particularly in lower layers, further impeding solution flow. Areas with reduced permeability tend to retain more solution, creating pockets of internal ponding, as illustrated by the case study in Figure 6. Saturated zones have lower internal friction, weakening the overall stability of the heap. The combination of increased weight and reduced friction can lead to localized slumping or larger-scale slope failures.

In the case study shown in Figure 6, it was determined that Hydro-Jex® improved the stability of the heap by 26%. The root of the instability prior to Hydro-Jex® operations was not based entirely on the gravity/deep raffinate leaching method itself, but also largely due to the reduced *Interpretive Yield* that method produces. Operators simply have less ability to know what effect gravity wells are having in their heaps, since gravity wells provide less operational insight.

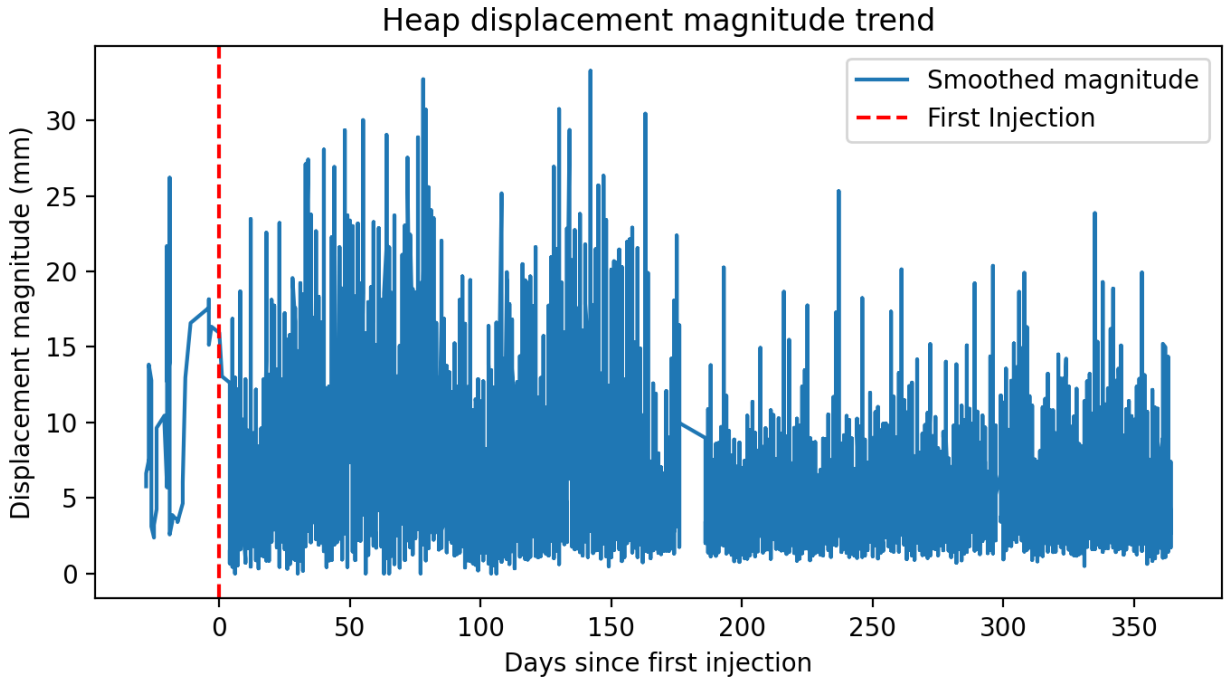

Figure 7: Displacement magnitude trend for a heap operating Hydro-Jex® over time

Preliminary findings from a current study confirm the positive effect of Hydro-Jex® on improving heap stability. GPS monitoring data from that ongoing case study is presented in Figure 7.

Figure 7 shows how the mean displacement magnitude decreases over time. Mean displacement magnitudes prior to the first injection were 11.4 mm, on average, over each sampling window prior to the first injection, and decreased to an average of 5.6 mm after the last injection finished. This is approximately a 50% decrease in displacement amplitude. Furthermore, GPS sensors typically recorded a noticeable calming of movements within just a few hours after a high-pressure injection, with 75 % of injections being followed by a reduction in displacement magnitude within three hours, thus reinforcing that the injections are stabilizing the heap.

Assuming small-strain stiffness is inversely related to displacement, the first-order approximation, albeit preliminary, of the improvement to the Factor of Safety (FOS) is roughly ~50%. Additional factors would need to be considered to calculate the actual FOS of the heap, but this relative increase in FOS correlates to the value determined by (Abbasi et al., 2020).

Conclusion

This study has introduced the novel concept of Interpretive Yield Theory (IYT) as a framework for evaluating and comparing different heap leaching technologies. By focusing on the interpretable data output rather than just recovery metrics, IYT provides a more comprehensive assessment of a method's ability to generate actionable insights into heap dynamics and support operational decision-making.

The comparative analysis of traditional irrigation, gravity/deep raffinate wells, and Hydro-Jex® technologies using the IYT framework revealed significant differences in their interpretive yields. Hydro-Jex® demonstrated the highest interpretive yield ratio, followed by gravity wells, with traditional irrigation providing the lowest yield. This suggests that Hydro-Jex® offers the greatest potential for reducing uncertainty and improving operational control of heap leaches.

The case study examining the impact of Hydro-Jex® on heap stability further validated the practical benefits of higher interpretive yield. GPS monitoring data showed approximately a 50% decrease in displacement amplitude after Hydro-Jex® implementation, with the overall decrease following a trend of discrete movement patterns congruent with operational events. Although preliminary, this suggested increase in FOS corroborates previous findings that Hydro-Jex® improves heap stability (Abbasi et al., 2020).

References

Abbasi, B., Azarfar, B., Ahmadvand, S., Seal, T., & Ulrich, B. (2020). The effect of Hydro-Jex operation on the stability of heap leach pads: A case study of a heap leach operation in central Mexico. *Mining, Metallurgy & Exploration, 37*(5), 1583–1592.

Anonymous. (2024a, February 28). EU Court confirms Hungary's daily fines in asylum case. Hungarian Official News Digest.

Anonymous. (2024b, March 5). Hungarian parliament adopts “Sovereignty Protection” law package. Hungarian Official News Digest.

Anonymous. (2024c, April 12). Hungary faces EU scrutiny over media freedom restrictions. Hungarian Official News Digest.

Anonymous. (2024d, May 20). Constitutional amendment sparks protests across Hungary. birgun.net.

Armstrong, M., Lagos, T., Emery, X., Homem-de-Mello, T., Lagos, G., & Sauré, D. (2021). Adaptive open-pit mining planning under geological uncertainty. *Resources Policy, 72,* 102086. https://doi.org/10.1016/j.resourpol.2021.102086

Bartlett, R. (2013). *Solution mining: Leaching and fluid recovery of materials*. Routledge.

Blannin, R., Tusa, L., Birtel, S., Gutzmer, J., Gilbricht, S., & Ivascanu, P. (n.d.). Metal deportment and ore variability of the Bolcana porphyry Au-Cu system (Apuseni Mts, Romania): Implications for ore processing. *Unpublished manuscript.*

Carlson, R. (2019). Understanding geologic uncertainty in mining studies. *SEG Discovery, 117,* 21–29.

Das, R., Topal, E., & Mardaneh, E. (2023). A review of open pit mine and waste dump schedule planning. *Resources Policy, 85,* 104064. https://doi.org/10.1016/j.resourpol.2023.104064

Dixon, D. (2003). Heap leach modeling—The current state of the art. In *Proceedings of the TMS Fall Extraction and Processing Conference* (Vol. 1, pp. 289–314).

Fu, Z., Li, Y., Topal, E., & Williams, D. J. (2015). A new tool for optimisation of mine waste management in potential acid forming conditions. In *Tailings and Mine Waste Management for the 21st Century Conference* (pp. 27–28). Sydney, Australia.

Gillis, A., Steen, J., Dunbar, W. S., & von Nordenflycht, A. (2024). What causes mining asset impairments? *Resources Policy, 90,* 104821. https://doi.org/10.1016/j.resourpol.2024.104821

Greene, J. (2024, February). “Every minute matters”: Experts with first-hand accounts at Victoria Gold mine disclose gravity of problems. *CBC News.*

Heuberger, R. (2005). Risk analysis in the mining industry. *Journal of the Southern African Institute of Mining and Metallurgy, 105*(2), 75–79.

Jansen, M., & Taylor, A. (n.d.). A new approach to heap leach modeling and scale-up. *Unpublished manuscript.*

Kaykov, D., & Koprev, I. (2020). Rationalising the location and design of the waste dump in the case of open-pit mining. *Sustainable Extraction and Processing of Raw Materials, 1,* 42–46.

Kuhn, C., & Visser, J. K. (2014). Managing uncertainty in typical mining project studies. *South African Journal of Industrial Engineering, 25*(2), 105–120.

Li, Y., Topal, E., & Williams, D. (2013). Waste rock dumping optimisation using mixed integer programming (MIP). *International Journal of Mining, Reclamation and Environment, 27*(6), 425–436.

McBride, D., Cross, M., & Gebhardt, J. E. (2012). Heap leach modeling employing CFD technology: A 'process' heap model. *Minerals Engineering, 33,* 72–79.

McGee, N. (2024, February). Turkey suspends search for mine workers; Government focuses on preventing environmental catastrophe after SSR Mining operation was hit by landslide. *Globe & Mail* (Toronto, Canada), p. B3.

McLemore, V. T., Fakhimi, A., van Zyl, D., Ayakwah, G. F., Anim, K., Boakye, K., Ennin, F., Felli, P., Fredlund, D., & Gutierrez, L. A. F. (2009). Literature review of other rock piles: Characterization, weathering, and stability. *Questa Rock Pile Weathering Stability Project.* New Mexico Bureau of Geology and Mineral Resources, New Mexico Tech, USA.

Neves, J., Pereira, M. J., Pacheco, N., & Soares, A. (2019). Updating mining resources with uncertain data. *Mathematical Geosciences, 51*(7), 905–924.

Ronald, J. R., George, W. B., & Blair, R. B. (1975). Diffusion model for heap leaching and its application to scale-up. *American Institute of Mining, Metallurgical, and Petroleum Engineers.*

Saldaña, M., Toro, N., Castillo, J., Hernández, P., & Navarra, A. (2019). Optimization of the heap leaching process through changes in modes of operation and discrete event simulation. *Minerals, 9*(7), 421. https://doi.org/10.3390/min9070421

Sels, D., & Wouters, M. (2015). The thermodynamics of time. *arXiv preprint,* arXiv:1501.05567.

Silver, R. (2013). Unsaturated flow analysis of heap leach soils. *Unpublished manuscript.*

Türkçe, B. N. (2024, February). Erzincan altın madeninde bilim insanlarından inceleme: Liç yığınının yüksekliği dünya standartlarının üstündeydi. *BBC News Türkçe.*

Uhrie, J. L., & Koons, G. J. (2000). The evaluation of deeply ripping truck-dumped copper leach stockpiles. Society for Mining, Metallurgy & Exploration.

van Staden, P. J., & Petersen, J. (2021). Towards fundamentally based heap leaching scale-up. *Minerals Engineering, 168,* 106915. https://doi.org/10.1016/j.mineng.2021.106915

Young, A., & Rogers, P. (2019). A review of digital transformation in mining. *Mining, Metallurgy & Exploration, 36*(4), 683–699.

Young, A., & Rogers, W. P. (2021). Modelling large heaped fill stockpiles using FMS data. *Minerals, 11*(6), 636. https://doi.org/10.3390/min11060636

Young, A., & Rogers, W. P. (2022). A high-fidelity modelling method for mine haul truck dumping process. *Mining, 2*(1), 86–102. https://doi.org/10.3390/mining2010006

Zhao, S., Lu, T.-F., Koch, B., & Hurdsman, A. (2013). Dynamic modelling of 3D stockpile for life-cycle management through sparse range point clouds. *International Journal of Mineral Processing, 125,* 61–77.

Unlocking Value: Economic Modeling and Optimization Strategies for Heap Leach Pads

W. Pratt Rogers, University of Utah, USA
Kirk Farrell, University of Utah, USA
Aaron Young, University of Utah, USA

Abstract

Heap leaching is a widely used hydrometallurgical technique for extracting metals from low-grade ores, yet conventional practices often leave significant metal unrecovered within the leach pads. This paper explores the potential for optimizing heap leach pad performance through technological, operational, and modeling improvements. The authors review both commercially implemented and emerging strategies—including enhanced irrigation systems, ore agglomeration, injection techniques, dynamic stacking based on ore geochemistry, and real-time monitoring tools—that aim to increase metal recovery and process efficiency. Additionally, gaps in current reporting frameworks that may underrepresent the value of recoverable metal in existing leach operations have been assessed. An economic modeling framework is proposed to evaluate the cost-benefit trade-offs of implementing such optimizations, accounting for productivity gains, operational complexity, environmental impacts, and potential returns on investment. Through a synthesis of best practices and new research directions, the authors have outlined a roadmap for advancing heap leach pad management. The findings support the broader goal of improving resource efficiency, maximizing metal recovery, and extending the economic life of mine operations through smarter, data-informed leaching strategies. This work provides a foundation for future innovations in heap leach optimization and more accurate valuation of metal assets across the mining industry.

Introduction

Heap leaching is a vital hydrometallurgical process used to extract metals such as copper, gold, and uranium from low-grade ores in large, stacked ore piles (heaps). This technique offers a low initial capital requirement and a relatively simple method for recovering metals by percolating leach solutions through crushed ore. However, conventional heap leaching often leaves a significant portion of metal value unrecovered in the heap. Industry estimates suggest that a considerable percentage of metal remains "stranded" in spent heaps even after standard leaching and rinsing are completed. As a result, there is

growing interest in technologies and methods that can improve leaching efficiency and metal recoverability. This review provides a comprehensive overview of emerging and established approaches to enhance heap leach pad performance across various metals (copper, gold, uranium, and more) and regions.

The authors have also examined how current reporting standards may underrepresent recoverable metal, leading to unrealized value in their economic modeling. The upside potential of current best practices in heap leach modeling, operation, and monitoring, serving as the framework for potential trade-offs (productivity, recovery, environmental, and economic), was examined. The strategy is to optimize a mining method that has not been properly addressed in the past, where simple changes could lead to significant improvements in metal recovery.

Challenges and Opportunities in Heap Leach Pad Efficiency

Heap leach operations face inherent challenges that limit metal recovery. In a typical heap leach, only a fraction of the metal value is recovered during the primary leaching cycle—the remainder is locked up due to factors like incomplete irrigation coverage, slow leaching kinetics, or solution channelling. For instance, heaps often develop preferential flow paths that leave portions of the ore under-leached. Fine particles can clog pores, preventing the leaching solution from contacting all the ore. Additionally, as heap height increases, the lower lifts become compacted, reducing permeability and slowing the leaching in deeper zones (Thiel & Smith, 2004). These issues mean that even "spent" heaps may contain substantial metal inventory that is written off as unrecoverable under traditional methods. This represents lost economic value and lends to the motivation for technological innovation (Guzmán-Guzmán et al., 2014).

At the same time, improving heap leach efficiency presents a significant opportunity. By recovering more metal from existing heaps, mines can increase output without mining additional ore, thereby potentially extending the life of reserves and reducing the need for new extraction with its associated costs and environmental impacts. Industry analysts estimate that hundreds of billions of tons of ore are currently under-leached globally (approximately 100 billion tons each of copper and gold ore), containing a $100+ billion worth of metal that is potentially recoverable with improved techniques. Unlocking even a fraction of this value through better heap leach technologies and methodologies can significantly boost mine profitability and metal supply. Furthermore, capturing more metal per ton of ore improves the overall resource efficiency and lowers the environmental footprint per unit of product (since more metal is produced without expanding mines or waste dumps) (Zaman et al., 2024). These drivers have spurred both commercial entities and research institutions to develop new methods for heap leach optimization.

Advances in Heap Leach Technologies and Methods

In response to the above challenges, a range of technologies and operational methods have emerged to

improve heap leach pad performance. These innovations span physical engineering solutions, chemical and biological enhancements, as well as digital monitoring and control systems (Guzmán-Guzmán et al., 2014; León et al., 2025). Some of these are already commercially applied at mine sites, while others are in pilot or research stages. Key developments—including notable examples like JEX Technologies' Hydro-Jex® process—and identified similar technologies aimed at increasing metal recovery and leach efficiency (Jex, 2025).

Enhanced Leaching Techniques (Injection and Secondary Recovery)

One prominent innovation is the use of in-heap injection systems to recover residual metal from heaps that have finished their primary leach cycle. JEX Technologies' Hydro-Jex® is a leading example: it employs injection wells to introduce leach solutions into the interior of the heap, in effect "micro-fracturing" the ore body to release trapped metals. This 3D leaching approach is analogous to the reservoir stimulation (fracking) used in oil and gas, but applied to ore heaps. By breaking up impervious zones and rewetting dry pockets, the technology can mobilize metal that standard top-down leaching has left behind.

Another method in this category is restacking or reprocessing of spent heaps. Rather than in-situ injection, some operations remove the spent ore and convey it to a new pad (or back through a mill) for a secondary leach. By crushing or agglomerating the reclaimed ore a second time, then re-leaching, additional recovery can be achieved. This approach was taken at certain gold heap leach sites where old heaps (sometimes decades old) were mined and re-processed when gold prices rose, yielding substantial ounces that had been left in the original leach. Such restacking is essentially a physical means to reintroduce fluid flow through ore that had become stagnant. Its feasibility depends on economics (rehandling costs) and geotechnical considerations, but it demonstrates that what is considered "spent" ore may still hold value recoverable with improved processing.

Improved Heap Construction and Material Handling

How a heap is built—from ore preparation to stacking methodology—has a profound impact on leach efficiency. Several best practices and technologies have emerged to optimize heap construction (Barbouchi et al., 2024; León et al., 2025; Thiel & Smith, 2004).

Agglomeration of Ore Fines

The inclusion of agglomeration drums in heap leach circuits has become standard in many gold and copper operations to deal with fine particles (Bouffard, 2019). In an agglomeration drum, ore fines are tumbled with water and binders (like cement) to form coarse pellets, which are then placed on the heap. This process greatly improves the permeability and uniformity of the heap. Figure 1 illustrates this effect: before

agglomeration, fine particles can clog pore spaces (left), whereas agglomerated ore forms more uniform, porous aggregates (right), allowing leach solution to percolate uniformly. By ensuring better solution flow paths, agglomeration increases the overall metal recovery and leaching rate. It also allows an initial "wetting" of the ore with the leach solution in the drum itself, essentially jump-starting the leaching process before the heap is even stacked. This technique has been a notable improvement, especially for gold heaps and copper oxide heaps with high fines content, resulting in higher recovery percentages than non-agglomerated heaps.

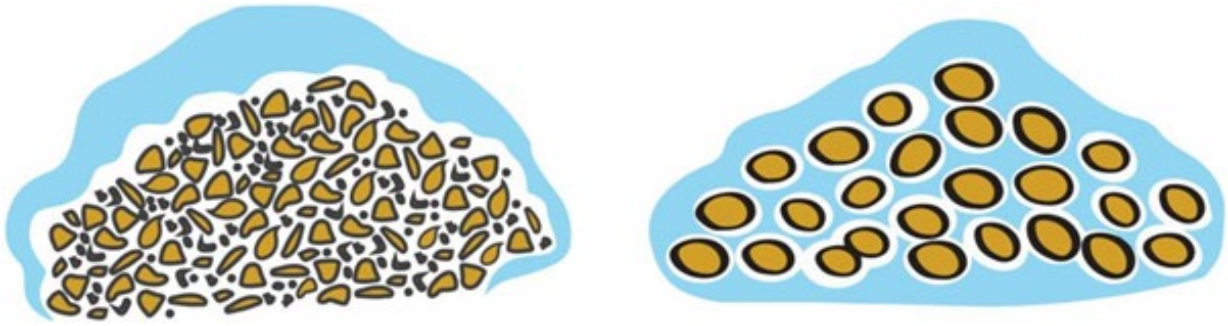

Figure 1: Conceptual illustration of the effect of agglomeration on heap leach percolation. Left: Before agglomeration, the ore fines and irregular particles can clog channels, trap solution (blue) and limiting flow. Right: Agglomerated ore (forming larger, uniform pellets) permits more uniform solution distribution around particles, improving metal leaching and recovery

Optimized Heap Stacking and Lift Configuration

The method of stacking the ore (height of each lift, compaction, layering) is crucial for maintaining permeability over the life of a heap. Best practices include stacking in relatively thin lifts and minimizing heavy equipment traffic on the heap to avoid over-compaction. Research shows a clear relationship between heap height and ore bulk density, and between density and percolation capacity (Lupo, 2010; Thiel & Smith, 2004). In practice, many mines limit individual heap lifts to a certain thickness (e.g., 6–8 meters) and allow a resting period for initial leaching before placing the next lift. This helps ensure that the lower layers don't become prematurely saturated or compacted by the weight of overlying ore. Some operations have also experimented with using conveyor stacking systems that spread ore in a more controlled manner (using mobile conveyors and stackers) instead of truck dumping. Conveyor stacking can reduce particle size segregation (coarse vs. fines) that often occurs with dumping and can result in a more homogeneous heap. By achieving an even heap density and avoiding zones of low permeability, the leach solution can uniformly irrigate the heap, thus improving overall metal recovery.

Intermediate Leach Enhancement Layers

An emerging practice is to incorporate special layers or features within the heap to aid leaching. For example, placing horizontal drainage/irrigation pipes at certain lift interfaces can allow better aeration or

solution recirculation in deeper parts of the heap. In bioleach heaps (common in copper sulfide operations), engineered air distribution systems (e.g. perforated pipes or injections at the heap base) are used to supply oxygen to the bacteria throughout the heap, accelerating the oxidation of sulfide minerals and improving copper extraction. Maintaining sufficient airflow in a tall sulfide heap is challenging, but modern large-scale operations in Chile and elsewhere have shown that forced aeration can markedly increase leach kinetics for secondary copper sulfides. Similarly, some operations insert monitoring and irrigation pipes during stacking, which later serve to both observe conditions (through sensors or sampling ports) and introduce reagents to deeper zones if needed. These engineered modifications to heap architecture are part of a shift to view the heap as a more actively managed "reactor" rather than a static pile.

Advanced Irrigation and Solution Application Strategies

The way the leach solution is applied to the heap has evolved to maximize contact with the ore and minimize inefficiencies.

Drip Irrigation over Sprinklers

Modern heap leach pads predominantly use drip irrigation tubing laid across the heap surface, as opposed to the sprinkler systems that were common in earlier years. Drip irrigation emits the leach solution at a slow, controlled rate directly onto the ore, leading to more uniform wetting and far less evaporation loss than sprinklers. Sprinkler spray can be uneven (due to wind drift, pooling in some areas) and can also cause evaporation of cyanide or acid, as well as precipitate salts on ore surfaces. Drip systems avoid these issues and are gentle on the heap surface, preventing erosion or physical disturbance of the top layer of ore. By maintaining an even distribution of solution, drip irrigation ensures that more of the heap participates in leaching, thus increasing overall metal recovery. One patent in the early 1990s described a controlled percolation system to improve irrigation uniformity—essentially preceding the broad adoption of drip emitters in heap leaching (Elena, 1994). Today, specialized drip emitters for mining (e.g., kink-resistant, acid-resistant tubing) are available from vendors and are considered a best practice technology for heap leach operations globally.

Pulsed and Multistage Leaching Cycles

Rather than maintaining a constant irrigation rate, many operations have found benefit in pulsing the application of the solution. For example, applying a leach solution for several days, then pausing to allow air to re-enter pores and heap chemistry to re-equilibrate, can enhance recovery. In gold heap leaching, intermittent drying periods allow oxygen to diffuse deeper to sustain the cyanide leaching of gold (since the dissolution of gold requires oxygen as well). In copper heaps, a rest period can enable ferric iron in the

solution to diffuse and react further before being flushed. Additionally, late in a leach cycle, some mines introduce a "rinsing" stage with higher-pH or fresh water solution to desorb residual metal values or re-leach areas that might have become acidic and unproductive. The timing and composition of leach solutions may be dynamically adjusted—for instance, initial leaching with higher acid strength for base metal ores, then lower strength later to wash and avoid waste of acid when grades decline. Such solution management strategies, when informed by monitoring, can improve the ultimate recovery while controlling reagent consumption.

Targeted Reagent Addition:

Emerging methods also include adding special reagents or catalysts through the irrigation system to boost the leaching of difficult minerals. In some gold heap operations with clays, surfactants or wetting agents are added to the leach solution to break surface tension and improve penetration into packed fine particles. For copper heaps with mixed oxide/sulfide ore, oxidizing agents like hydrogen peroxide or sodium chlorate might be intermittently added to rejuvenate the ferric/ferrous balance and leach copper sulfides faster. Nutrients (ammonium, phosphate) may be dosed in bio-leaching heaps to keep bacteria healthy. These chemical additions are usually done via the solution application system and require careful control, but they represent another lever to improve efficiency beyond just basic acid or cyanide leach liquor.

Dynamic Stacking and Ore Blending by Ore Characteristics

Large heap leach operations often deal with significant variability in the ore geology, grade, particle size distribution (PSD), clay content, acid consumption, etc., which can vary across a mine. Dynamic stacking refers to adapting how and where ore is placed on a heap based on these characteristics, aiming to optimize leach performance. In practice, this might involve blending ore types or sequencing the stacking in a manner that evens out extremes (León et al., 2025; Zaman et al., 2024). For example, if a particular ore type is known to have very low permeability (perhaps due to high clay content or fines), instead of stacking a huge segment of that ore all at once (which could create a waterlogged zone), an operation might mix it with coarser ore or stack it in thinner lifts with extra curing time. Alternatively, high-grade but refractory ore could be blended with lower-grade easily leachable ore, so that the overall heap section leaches more uniformly (the refractory portion can benefit from extended leaching time as the easier ore around it leaches out). Ore geochemistry can guide dynamic stacking as well. If one part of the orebody has high acid consumption (e.g., carbonate content from copper leach), it may be preferentially placed in a location where it can be pre-treated with acid (such as at the bottom of a new heap lift where it will get more concentrated acid early on). Mines also sometimes segregate by lift: the first lift on the liner might be higher permeability ore to act as a drainage layer, whereas subsequent lifts can include more fine-grained ore since solution will

have an easier time percolating once it hits the more porous bottom layer. All these approaches leverage knowledge of ore properties—geologists and metallurgists work together to create a stacking plan that maximizes recoveries. While historically heap stacking was relatively crude (ore was placed as it came, with minimal specialization), modern operations increasingly incorporate block models of geometallurgical data to inform how the heap will be built over months and years. This dynamic management can reduce the formation of problematic zones and ensure that each portion of the heap is leached under near-optimal conditions for that ore's characteristics.

Real-Time Monitoring and Heap Leach Modeling Tools

A major development in recent years is the application of advanced monitoring instruments and modeling software to heap leaching—effectively bringing a "digital twin" concept to what was once considered an unmonitorable black box of rock (Guzmán-Guzmán et al., 2014). Traditional heap leach management relied on external measurements (like solution flow rate, heap outlet solution grades, and periodic core drilling of heaps) to infer what was happening inside the heap. Now, new sensor technologies are being tested to directly observe heap conditions in real or near-real time, enabling better control and prediction of leach performance.

Instrumentation within Heaps

Researchers and innovative operations have started embedding sensors in heap leach pads to track parameters such as moisture content, solution composition, and even temperature. For instance, moisture probes (similar to those used in agriculture for soil) can be buried at different elevations in a heap to detect whether a zone is getting wet or remains dry. If a sensor indicates persistent dryness, operators can adjust irrigation or install supplemental drips/injection in that area. Another example is the use of electrical resistivity tomography (ERT)—effectively imaging the heap's moisture distribution by sending electrical currents through it. Wet ore is less resistive than dry ore, so periodic ERT surveys can create a three-dimensional (3D) map of where solution has penetrated. Such techniques were reported in a 2014 heap leach conference where integrated process control using real-time 3D monitoring significantly improved understanding of the heap's internal state (Guzmán-Guzmán et al., 2014). Similarly, some operations have used fiber optic cables to measure temperature profiles; this is particularly useful in bioleaching heaps, since active microbial oxidation releases heat. A rising temperature in a zone could indicate good bacterial activity (positive for copper recovery), whereas a cool zone might signal a slow or stalled leaching process. By mapping these conditions, the operation can target aeration or change irrigation to "wake up" that part of the heap.

Solution Monitoring and Control Systems

The output from a heap (the pregnant leach solution, PLS) is continuously monitored for flow rate, pH, metal grade, and other chemistry. Modern systems feed this data into software that can model the recovery curve and even predict when the leaching of a particular heap or lift is nearing completion (when the remaining grade in solution is trending to uneconomic levels (Bouffard & Dixon, 2001; Guzmán-Guzmán et al., 2014; Lupo, 2010; Thiel & Smith, 2004; Zaman et al., 2024)). If real-time data from the heap (via sensors or frequent sampling) is integrated with such models, the operation achieves closed-loop control—adjusting leach variables on the fly to optimize results. For example, if one section's PLS is dropping in copper grade faster than expected, it might indicate that part of the heap is leaching out; the model could suggest redirecting fresh leachate to a newer section and starting the rinse cycle on the depleted section (Barbouchi et al., 2024; Guzman et al., 2024; León et al., 2025). Conversely, if gold in solution is still high, the model would indicate it is worth continuing leaching longer. Some mines have implemented supervisory control and data acquisition (SCADA) systems to automate leach pad irrigation valves, enabling different areas of a pad to be irrigated according to a schedule that maximizes overall metallurgical efficiency. Integrated with weather data (rain, evaporation forecasts) and heap sensors, such systems embody the concept of the "smart heap leach pad."

Heap Leach Simulation Software

In parallel with physical monitoring, significant progress has been made in computational modeling of heap leaching. Early models treated heaps in a simplistic way, but newer models capture the multiphase flow and reaction kinetics in heaps with much greater fidelity. They consider the heap as a heterogeneous reactor, accounting for unsaturated flow of leachate, diffusion of reagents into ore particles, and leaching chemical reactions (often modeled via shrinking-core kinetics for each particle). These models are calibrated with laboratory column tests and then scaled to field dimensions with the help of field data. While challenges remain in scaling (due to the heterogeneity and dimensionality factors), modeling tools have improved to the point where they can suggest recovery predictions as a function of time, under various operating strategies. This allows for scenario analysis—e.g., "If we increase irrigation rate by 20% for the next month, how much faster will we reach 50% recovery? Will it plateau due to channeling?" or "What if we rest the heap for winter and resume in spring—how much do we lose or gain?"—all in silico, before making operational decisions. Mining companies have started to use these digital twins of heap leach pads to inform their practices, effectively bringing a level of optimization that was traditionally limited to more controllable processes like milling. The literature has reported cases that incorporate real-time data into heap models (so-called integrated process control), which have led to enhanced performance and fewer surprises in heap behaviour (Saldaña et al., 2022). In summary, monitoring and modeling innovations are

turning heap leaching from an art into more of a science, improving the predictability of recovery curves and enabling timely interventions to maximize metal extraction.

Weaknesses in Reporting Recoverable Metal—JORC, SEC and Beyond

Despite technological advances, there are gaps in how current mineral reporting standards capture heap leach recoveries and practices. Codes such as the Australasian Joint Ore Reserves Committee (JORC) (JORC, 2012), Canadian Securities Administrators National Instruments 43-101(NI 43-101) (NI-43101, 2023), and United States Securities and Exchange Commission Item 102 of Regulation S-K Subpart 1300 (SEC S-K 1300) (SEC, 2018) require mining companies to report mineral resources and reserves with "reasonable prospects for eventual economic extraction," which includes assumptions about metallurgical recovery. In heap leach projects, companies typically assume a certain recovery percentage based on laboratory tests or pilot trials, and this is used in reserve calculations. However, these reporting frameworks have limitations in reflecting the true recoverable metal from heap leach operations.

Static Recovery Factors

Reserve statements often use a single overall recovery factor for a given ore type (e.g., "70% recovery for oxide ore by heap leaching"). In reality, actual recoveries can vary depending on the pad stacking method, lift height, leach time, and whether secondary processes (such as injection or retreatment) are applied. Reporting standards do not usually account for the possibility of staged recovery—for example, an initial recovery of 70% in 90 days, plus an additional 10% over a year of secondary leaching. Unless a company explicitly plans and states an extended leaching program, that extra 10% may simply be excluded from reserves. This means reserves can be conservative, effectively under-reporting the metal that will eventually be recovered with a more optimized or prolonged leach.

Heap Inventory and Residuals

During operations, heap leach mines track the metal inventory in the heap (the difference between metal placed and metal recovered) as work-in-progress. This inventory can be substantial. However, reporting codes lack clear guidelines on how to treat remaining metal in heaps at the end of mine life. Often, companies will not count it as a reserve because it's not planned for extraction with certainty. As a result, there is a gray area in reporting—a mine might have, say, 100,000 ounces of gold sitting in its heaps that are not in the reserve statement because they were assumed unrecoverable with the base case method. If a new process (like Hydro-Jex® injection or reprocessing) is later developed, that metal suddenly becomes a target for recovery, effectively adding to the mine's yield beyond what was reported. This suggests that

current standards may undervalue mines that have large heap leach operations, as the potential upside of recovering residual metal is not fully transparent to investors or regulators.

Pad Design and Methodology Not Explicitly Reported

Resource and reserve reports typically provide some detail on planned processing methods (for example, that heap leaching will be used, with crushing to a certain size, maybe agglomeration, etc.), but they do not require a detailed breakdown of pad stacking methodology or leach cycle design. Thus, differences in approach—say, a company planning on deep lifts and quick turnover vs. another planning on on-off pads with aggressive re-leach—are not obvious in public reports. This lack of detail can mask how recoverable metal is accounted. A project might assume a higher cutoff grade or lower recovery if using a less efficient stacking method, whereas a more innovative approach could allow lower-grade material to be economically leached. Unless these nuances are captured in the study and clearly communicated, the standards don't force a discussion of how pad practices impact recoverable metal. In essence, the reporting frameworks treat heap leach recovery as a black-box percentage, without revealing the methodology of how that percentage could be improved or how much metal is left behind.

Regulatory Constraints on Claiming New Tech

Another gap is that reserves under JORC/NI 43-101/SEC rules must be based on demonstrated technology and reasonable assumptions. If a company wanted to include the benefits of a novel recovery technology (like a new bioleach process or injection method) in their official recovery assumption, they would need strong evidence from test work or industry precedent. Often, companies are conservative and use only well-proven methods in their reserve basis. This inherently discourages the inclusion of the upside of emerging technologies in official reports. The consequence is that even if engineering teams know there is a method to get more metal out, they might not bank that metal in the reserve until the method is proven. Thus, current reporting can lag behind technological capability—a source of "hidden" value that is not reported until later.

To improve this, some have suggested that companies should report the total metal in inventory in heaps and perhaps an estimated recoverable portion of that inventory under various scenarios. This would shine a light on the underreported value. As the industry adopts new standards (e.g., the SEC's S-K 1300 now encourages more disclosure of recovery assumptions and risks), more transparency may be observed. For now, analysts and engineers must read between the lines of technical reports to gauge if a heap leach operation has unrecognized upside (such as a large residual gold in a pad that could be recovered by retreatment). In summary, current codes ensure that declared reserves are achievable with proven methods, but they do not fully capture the spectrum of recoverable metal, especially where improvements in pad performance are possible. This is an area where better reporting guidelines could close the gap between what is ultimately extracted and what was initially projected.

Productivity, Recovery, Environmental, and Economic Trade-offs

Implementing heap leach pad improvements is not without its trade-offs. Each innovation or method must be evaluated in terms of its impact on metallurgical performance, throughput, cost, and environmental factors. Discussed below are some of the key considerations and potential downsides that accompany the heap leach optimization strategies reviewed earlier.

Metallurgical Gain vs. Time and Throughput

Many improvements (e.g. extended leach cycles, secondary injection) focus on squeezing more metal out of the same heap. This often means leaching for a longer time or diverting resources to older material, which can conflict with the goal of maintaining production throughput. There is a trade-off between achieving a higher ultimate recovery and the rate of recovery. For example, if a heap leach operation normally moves ore on and off pads in 150 days for a 70% recovery, but by leaching 300 days, it could get 80% recovery, the operation must decide if the extra 10% is worth doubling the leach time (and thus having fewer new heaps leached per year). In some cases, it may be more profitable to start leaching fresh ore than to continue leaching diminishing returns from spent ore. Advanced modeling helps identify the point of diminishing returns on the recovery curve so that operators can make this call. Technologies like Hydro-Jex® aim to accelerate the recovery of that last fraction, thus mitigating the time trade-off by recovering residual metal faster. Nonetheless, the overall balance between recovery percentage and processing rate is a primary trade-off.

Cost vs. Benefit

All enhancement technologies come with additional costs—whether capital costs (for new equipment like agglomeration drums, injection systems, sensors) or operating costs (additional reagents, power for pumps/blowers, labour, monitoring). The economic benefit of higher recovery or faster leach must outweigh these costs. For instance, drip irrigation has a moderate cost to install and maintain, but it usually pays back via higher recovery and reagent savings (due to reduced evaporation). Agglomeration adds cost (extra processing step, binder material), so it is justified mostly when the ore has a lot of fines that would otherwise cause low recovery. In the case of injection techniques, the cost of drilling, pumping and managing those systems must be weighed against the value of the extra metal recovered. If only marginal additional metal is present, the technology might not pay off. Therefore, many improvements are applied first to high-value scenarios (e.g., injecting heaps that still have relatively high soluble metal grade left). Economic analysis, as discussed in the next section, is crucial to navigate these cost-benefit trade-offs.

Operational Complexity and Risk

Introducing new processes can increase the complexity of heap leach operations, which have traditionally

been simple and robust. More equipment and steps mean more things that can go wrong. For example, an aeration system might lead to over-oxidation or drying out parts of the heap if not balanced correctly. Agglomeration could be done improperly and create cemented lumps that don't leach well if the moisture or binder is wrong. Injection wells, if not carefully engineered, could cause slope instability or preferential flow that actually bypasses some ore. There are also potential maintenance challenges—drip lines can clog, sensors can fail in the acidic, wet environment of a copper heap, etc. Each added layer of technology requires training operators, implementing monitoring, and sometimes adjusting the overall mining plan. Some mines may prefer a lower-tech operation for reliability, especially if remote or with limited skilled workers' availability. Thus, the risk profile of the operation may increase with certain optimizations, and mitigation measures must be in place (such as good monitoring of heap stability during injections or redundancy in critical sensors).

Environmental Considerations

Generally, improving recovery has positive environmental implications, since more metal is obtained per unit of ore, reducing waste (Zaman et al., 2024). For example, if injection allows an extra 5% copper recovery, that is 5% less copper that needs to be mined from new ore elsewhere. Additionally, some technologies reduce environmental impact directly—drip irrigation lowers evaporation and potential emissions of cyanide mist; better heap stability and monitoring reduce the risk of pad leakage or failure. However, some trade-offs exist. Using new chemicals (surfactants, oxidants) in heaps could introduce new reagents that need to be managed in the effluent or may have their own environmental risk if they seep away. Agglomeration may use binders like Portland cement, which has a CO_2 footprint to produce. Aeration systems that promote bacterial action might result in more sulfate generation in the heap drainage that must be treated. Also, extending leach cycles means the site may have leach solution in circulation for longer periods, which prolongs the time that active management (and potential environmental risk of solution handling) is present. Regulators will consider these factors—for instance, if a heap is kept "wet" for additional years of secondary leaching, there must be assurance that containment systems remain intact for that extended period. In summary, while most efficiency improvements are environmentally beneficial on net, they still must be evaluated for any localized or short-term environmental impacts.

Resource Reporting and Valuation

As discussed, current reporting might not immediately credit the extra recoveries from new techniques. This can be a trade-off in terms of corporate valuation or project finance—a company might have to invest in a new heap leach optimization without being able to count the benefits in official reserve numbers initially. There is a potential financial trade-off in how markets perceive the value: if not communicated well, an optimization project might be viewed simply as an added cost or experimental effort. Companies

mitigating this often publish the results of trials or include an "upside case" in technical reports to show the potential value of the improvements. Over time, as techniques become proven, the standards will catch up and allow those gains to be fully valued.

Overall, the decision to implement a heap leach improvement comes down to balancing these trade-offs in the context of a specific operation. A mature operation with a large inventory of residual metal and low remaining mine life might aggressively pursue optimizations to scavenge value from existing heaps. A new project, on the other hand, might incorporate only select proven enhancements at startup (like agglomeration, drip) and plan to phase in others after initial validation (e.g., only doing injection in later years if needed). Each site will weigh the productivity vs. recovery, cost vs. benefit, and risk vs. reward equations differently. The next section outlines how a formal economic modeling framework can be applied to support these decisions.

Economic Evaluation Framework for Heap Leach Optimization Investments

To determine whether and how to invest in heap leach pad optimizations, mining operations require a rigorous economic modeling approach. This is analogous to how companies evaluate capital investments in mill upgrades—by quantifying the expected increase in throughput or recovery, the cost, and the overall impact on project value. A similar framework can be applied to heap leach improvements:

1. Baseline Performance Model: First, establish a reliable model of the heap leach operation under the status quo. This includes the tonnage leached per year, the baseline recovery curve (metal percent vs. time) for each heap or ore type, the operating costs (reagents, pumping, etc.), and the resulting cash flow from metal production. This baseline is essentially the "do nothing new" scenario derived from the mine's feasibility study or current performance. For example, the model might show that for each 100,000 tonnes of ore placed, 70% of the recoverable metal is produced over 1 year, with diminishing recovery thereafter, and the heap then goes into closure.
2. Scenario Definition for Each Improvement: Define the changes expected with a given improvement. This could be higher ultimate recovery, faster recovery (shorter leach cycle), or cost savings (e.g., less reagent per ton due to better efficiency). It might also involve additional capital or operating costs. For instance, adding an agglomeration drum might increase recovery from 70% to 78% for clay-rich ore and reduce leach time by 15%, but cost $1 per ton in binder and require a $2 million capital investment. An injection system might recover an extra 5% copper from old heaps at a cost of $0.5 per pound of copper recovered. These inputs are obtained from pilot tests, vendor data, or comparable operations.

3. Cash Flow and Net Present Value (NPV) Analysis: For each scenario, project the cash flows over the mine life or heap life. This means integrating the changed recovery or cost profile into the mine's production schedule. Key outputs are: incremental metal produced (which yields incremental revenue), incremental costs, and any change in timing of production. Using discounted cash flow (DCF) analysis, calculate the NPV of the operation with and without the improvement. The difference gives the NPV attributable to the improvement. For a valid comparison, one must ensure that production schedules are adjusted—for example, if faster leaching frees up pad capacity sooner, that might allow processing more ore or accelerating mining, which has its own value. On the other hand, if extended leaching slows metal production, there is an opportunity cost for delaying revenue (which the DCF will account for via discounting).
4. Internal Rate of Return and Payback: Compute the Internal Rate of Return (IRR) for the incremental investment in the improvement. A high IRR (above the company's hurdle rate) indicates the improvement is financially attractive. Also, estimate the payback period—how long until the extra investment is paid back by additional net cash flow. For example, if installing heap monitoring sensors costs $500,000 and is projected to enable $5 million extra gold recovery, and if that extra gold is produced within 1 year of leaching, the payback might be just a few months. These metrics help translate technical benefits into business decisions, akin to how mill optimization projects are justified by improved recovery/throughput leading to strong IRRs.
5. Sensitivity and Risk Analysis: It's important to run sensitivities on key assumptions: metal prices (higher prices make recovery improvements more valuable), recovery uplift (what if the actual gain is only half of expected?), costs (what if operating the new system is more expensive than thought?), and failure risk (what if the system doesn't work as planned?). Techniques like Monte Carlo simulation can be used to assign probabilities to different outcomes, yielding a range of possible NPVs. This provides insight into the risk-adjusted benefit. For instance, if a novel reagent could give 15% more recovery but there's uncertainty, the analysis might show a high upside but also a chance it gives no benefit—management can then decide based on risk tolerance and optionally stage the investment (e.g., spend a smaller amount on further pilot tests first).
6. Integration into the Mining Plan: If the improvement is economically justified, the final step is to integrate it into the official mining plan and possibly into the reported reserves/resources if appropriate. For example, after successful pilot results, a company might update its technical report to include agglomeration and thereby lower the cutoff grade or increase recoverable ounces, formally adding value to the project. Likewise, once successful injection leaching has been demonstrated, the life-of-mine plan may be revised, thus showing improved economics to stakeholders.

This framework ensures that each potential heap leach optimization is evaluated on a consistent economic basis. It treats improvements not just as metallurgical tweaks but as business investments with capital and returns. Notably, some improvements may be hard to quantify fully (like the benefit of better monitoring may be avoiding losses rather than producing extra metal directly), but these can still be modeled as risk reductions or efficiency gains. In practice, operations often implement a suite of improvements in tandem, so attribution can be complex—a holistic model might be needed to capture interactions (for example, agglomeration might enable higher heap heights, which then work well with drip irrigation and monitoring to manage).

One real-world example is from a large copper mine that modeled the addition of a sulfide bioleaching phase to its existing oxide heap leach (Jia et al., 2024). The economic model showed that by installing blowers and nutrient systems to bioleach low-grade sulfide ore (previously considered waste), they could add tens of thousands of tonnes of copper production for a modest investment, with an IRR well above 30% (Jia et al., 2024; Petersen & Dixon, 2002). The mine proceeded with a pilot, and upon success, it incorporated this into the plan, effectively converting waste to ore—a clear increase in value (Bouffard, 2019). This kind of analysis—showing a strong business case—is essential to justify optimization of capital expenditures to management and investors.

In summary, the economic modeling of heap leach optimizations parallels that of other mine improvements: it should quantify how the change affects the bottom line. By utilizing tools such as NPV and IRR, and by framing the problem in terms of additional cash flow versus additional costs, mining companies can make informed decisions. This disciplined approach supports the justification for capital expenditures and operational changes in heap leaching, aligning with corporate objectives of maximizing asset value. It also demonstrates to stakeholders (including shareholders and regulators) that improvements are not just technically interesting but are also financially sound and aligned with maximizing resource utilization.

Conclusion

Heap leaching has become an indispensable technique for extracting metals from low-grade resources. However, it has historically left significant value on the table in the form of unrecovered soluble metal in spent heaps. Today, a convergence of innovative technologies and better scientific understanding is driving a new era of heap leach optimization. The authors have reviewed how physical interventions (like ore agglomeration, improved stacking methods, and engineered injection systems) can greatly enhance leach efficiency and metal recovery. Chemical and biological advances—from alternative leaching reagents to controlled bio-oxidation—further expand the envelope of treatable ores and improve yields. In parallel, real-time monitoring and modeling tools are transforming heap operations from a largely empirical practice

into one guided by data and predictive simulations. These developments enable mining operations to recover more metal faster and with potentially lower environmental impact than was possible with conventional practices.

Additionally, it has been shown that industry reporting standards have not yet fully caught up with these technological advancements. Current JORC/NI 43-101SEC reserve reporting can underestimate the recoverable metal in heap leach projects, as they seldom account for secondary recovery techniques or extended leaching beyond the base case. This underscores the importance of transparent reporting and perhaps future updates to codes to encourage disclosure of heap leach pad inventories and potential recovery improvements. Such clarity would highlight the latent value in many operations, where improved practices could unlock additional reserves from existing heaps.

Finally, the implementation of heap leach improvements must be guided by careful evaluation of trade-offs and economics. Not every technology will suit every site—factors like ore type, climate, mine life, and capital availability dictate which solutions are optimal. By applying rigorous economic modeling frameworks, mining companies can prioritize investments that yield the best return, much as they do for processing plant optimizations. Case studies and emerging operations show that when done properly, heap leach pad optimization can significantly boost projected NPV and IRR, turning marginal ounces or pounds into profitable production. Moreover, these optimizations contribute to sustainable mining: more metal from the same footprint means reduced waste and less new disturbance for equivalent output.

In conclusion, the landscape of heap leaching is being reshaped by technology and refined methodologies. Commercial successes like Hydro-Jex® demonstrate that even "old" heaps can become new opportunities for metal recovery. Ongoing research into leach dynamics, whether through better or novel reagents, promises to further improve recoveries for challenging ores (e.g., primary copper sulfides) that are increasingly part of the mining portfolio. The integration of these advancements will require collaboration between metallurgists, mining engineers, geotechnical engineers, hydrologists, and data scientists—reflecting the multidisciplinary nature of modern heap leaching as an engineered system. As the industry continues to adopt these best practices and emerging ideas, it is expected that heap leach operations will become more efficient, predictable, and valuable. In a time when maximizing resources and minimizing environmental impact is paramount, improving heap leach pad performance stands out as a high-impact lever for the mining industry's future.

References

Barbouchi, A., Louarrat, M., Mikali, M., Barfoud, L., El Alaoui-Chrifi, M. A., Faqir, H., Benzakour, I., Idouhli, R., Khadiri, M.-e., & Benzakour, J. (2024). Advancements in improving gold recovery from refractory gold

ores/concentrates: A review. *Canadian Metallurgical Quarterly*, 1–18. https://doi.org/10.1080/00084433.2024.2441548

Bouffard, S. C. (2019). *Agglomeration pretreatment*.

Bouffard, S. C., & Dixon, D. G. (2001). Investigative study into the hydrodynamics of heap leaching processes. *Metallurgical and Materials Transactions B, 32*(4), 763–776.

Elena, A. P. (1994). Subsurface irrigation system. In Google Patents. https://patents.google.com/patent/US5310281A/en

Guzmán-Guzmán, A., Hernández, O. Y. C., Srivastava, R., & Jones, J. W. (2014). Integrated process control to enhance heap leach performance. In *Proceedings of Heap Leach Solutions, 2014*. Lima, Peru.

Guzman, A., Korsikas, S. S., Olson, T., & Zepeda P, Y. O. (2024). Agglomeration scale: A method to improve leaching performance. *Mining, Metallurgy & Exploration, 41*(2), 501–514.

Jex. (2025). *Introducing Hydro-Jex®*. Jex Technologies Corporation. https://www.jextechnologies.com/thetechnology

Jia, Y., Ruan, R., Qu, J., Tan, Q., Sun, H., & Niu, X. (2024). Multi-scale and trans-disciplinary research and technology developments of heap bioleaching. *Minerals, 14*(8), 808. https://doi.org/10.3390/min14080808

JORC. (2012). The Australasian Code for Reporting of Exploration Results, Mineral Resources and Ore Reserves (The JORC Code).

León, F., Rojas, L., Bazán, V., Martínez, Y., Peña, A., & Garcia, J. (2025). A systematic review of copper heap leaching: Key operational variables, green reagents, and sustainable engineering strategies. *Processes, 13*(5), 1513.

Lupo, J. F. (2010). Liner system design for heap leach pads. *Geotextiles and Geomembranes, 28*(2), 163-173.

NI-43-101. (2023). National Instrument: NI-43-101—Standards of Disclosure for Mineral Projects.

Petersen, J., & Dixon, D. G. (2002). Thermophilic heap leaching of a chalcopyrite concentrate. *Minerals Engineering, 15*(11), 777–785.

Saldaña, M., Neira, P., Gallegos, S., Salinas-Rodríguez, E., Pérez-Rey, I., & Toro, N. (2022). Mineral leaching modeling through machine learning algorithms − a review. *Frontiers in Earth Science, 10*, 816751. https://doi.org/10.3389/feart.2022.816751

SEC. (2018). Modernization of property disclosures for mining registrants (Regulation S-K, Subpart 1300). In 17 C.F.R. § 229.1300 (2019): U.S. Securities and Exchange Commission.

Thiel, R., & Smith, M. E. (2004). State of the practice review of heap leach pad design issues. *Geotextiles and Geomembranes, 22*(6), 555-568. https://doi.org/10.1016/j.geotexmem.2004.05.002

Zaman, Q. U., Zhao, Y., Zaman, S., Batool, K., & Nasir, R. (2024). Reviewing energy efficiency and environmental consciousness in the minerals industry amidst digital transition: A comprehensive review. *Resources Policy, 91*, 104851.

Chapter Four

Operations

Decrepitation of Crushed Leach Copper Ore Under Sulfuric Acid Leaching Conditions—Part 1

Michael Grass, WSP USA Inc., USA
Christopher Jester, WSP USA Inc., USA
Vashish Taukoor, WSP USA Inc., USA
Lino Manjarrez, WSP USA Inc., USA
Salvador Ortiz, Freeport-McMoRan Inc., USA

Abstract

Historically, stockpiles constructed from crushed leach copper ore for the purpose of copper recovery through sulfuric acid leaching have been assumed to be freely draining throughout their lifetimes based on initial hydraulic conductivity tests completed using fresh or column test samples during the design stage. However, decrepitation of copper ore can produce fine-grained layers that significantly hinder vertical percolation of raffinate, redirecting flow laterally with a possible mound forming, and potentially creating seepage points. As a result, certain areas of a stockpile may experience partial and/or impeded drainage through time, necessitating the installation of additional collection systems to direct solution from within the stockpile into process ponds. These seepage challenges can also reduce copper recovery from deeper lifts during secondary leaching via surface irrigation. Sulfuric acid leaching on copper stockpiles thus requires careful management to maximize copper extraction before permeability limits copper recovery and potentially requires operational adjustments. Therefore, understanding the effects of decrepitation is essential for evaluating its impact on copper recovery, slope stability, and operational costs.

A review of technical literature revealed that geotechnical data aimed specifically at quantifying decrepitation of crushed leach copper ore is limited, mainly because the collection of such data involves significant resources associated with repeated drilling, sampling, and testing through the lifetime of the stockpile. Within this paper, we present laboratory geotechnical properties, including grain size distribution, Atterberg Limits, and in-situ measurements of hydraulic conductivity using two different methodologies collected at existing crushed leach copper stockpiles with various ages to quantify decrepitation of crushed leach copper ore under sulfuric acid leaching conditions. Using depth within a stockpile as a proxy for time under leach that ranges from 0 days to 25 years, we show that decrepitation of crushed leach copper ore as

a result of sulfuric acid leaching can result in an increase of fines content, an increase of liquid limit, and a decrease of hydraulic conductivity.

Introduction

For crushed leach ore to be considered free draining, a measured hydraulic conductivity is commonly assumed to be two orders of magnitude greater than the raffinate application rate and at least have a hydraulic conductivity of 1×10^{-3} cm/s (Duncan et al., 2014). Additionally, the ore should have a hydraulic conductivity between 10 times the solution application rate (Breitenbach and Thiel, 2005), if not 100 times, to maintain a low degree of saturation and air availability to allow for optimal ore recovery (Van Zyl et. al., 1988). However, sulfuric acid leaching tends to decrepitate crushed leach ore and leads to negative changes in geotechnical properties through time. Decrepitation of crushed leach copper ore under sulfuric acid leaching refers to the breakdown of the ore through mechanical and geochemical means. Mechanically, the process of stacking and burying via multiple lifts of ore will break down the ore over time. Geochemically, sulfuric acid solution leaching will break down the ore by reacting with a variety of gangue and ore minerals to generate new minerals that generally cause a volume change of those altered minerals and a subsequent decrease of overall grain size distribution.

Together, decrepitation of the crushed leach ore through these two processes fundamentally leads to a greater quantity of finer particles and a shift in the uniformity of the grain size distribution, resulting in a decrease in hydraulic conductivity and subsequent potential slope instability, as well as delayed copper recovery, leading to operational challenges. The greatest concern regarding the slope stability of a crushed ore heap leach facility (HLF) is the buildup of excess pore pressure within the heap, which could lead to lower effective stress and subsequent decrease of shear strength and may generate the potential for a static liquefaction event. With sufficiently low hydraulic conductivity, there is an expectation that undrained conditions will also be present within the heap, further decreasing the shear strength of the crushed leach ore.

Samples of crushed leach ore were taken from four HLFs directly from a conveyor belt, immediately after crushing, and before agglomeration with sulfuric acid, as well as within the HLF pads from various locations and depths using sonic drilling methods. The samples were laboratory tested for index properties (i.e., grain size distribution and Atterberg Limits). The sampling and testing program was conducted over multiple years to evaluate any changes in those properties over time, as summarized in Table 1.

Table 1: Number of Tests at the Four Heap Leach Facilities

Heap Leach Facility	In-situ Hydraulic Conductivity Tests	Hydraulic Profiling Tool	Cone Penetration Test		Laboratory Test			
			Test Locations	Zones of Interest	Samples	Atterberg Limits	Fines Content	Particle Size Distribution
HLF 1	3	–	4	9	9	9	9	9
HLF 2	2	–	5	13	13	13	13	13
HLF 3	24	8	30	77	58	35	58	58
HLF 4	–	–	6	6	6	6	6	6

A hydraulic conductivity testing campaign was completed using a hydraulic profiling tool (HPT) (ITRC, 2019), as part of a cone penetration test campaign from one HLF, to evaluate changes with depth and to compare with index properties and cone penetration test measurements. Additionally, falling head permeability tests were completed within selected boreholes on the same HLF as the HPT, as well as other HLFs, to measure the hydraulic conductivity within various lifts of the heap, where relatively low hydraulic conductivity was estimated to exist based on previous field geotechnical investigations, operational data, and field observations.

Comparison of Particle Size Distribution

Geotechnical index tests provide a reliable method for evaluating the changes in physical characteristics of crushed leach ore over time. Samples can reliably be taken from the same location at different times and directly measure changes in material properties. Samples of crushed ore were taken from a conveyor belt after the full crushing of the sample and before the material was agglomerated with sulfuric acid solution and stacked on the HLFs. During the life of the HLF, samples were also taken at various times and depths within the HLFs using sonic drilling methods to collect samples at depth that were submitted for geotechnical index tests. Tests were generally conducted on samples across all depths within the boreholes.

Figure 1 illustrates the laboratory test results, maximum and minimum, for grain size distribution comparing the results between the belt samples after crushing and the crushed leach ore materials collected from the HLFs during the various drilling campaigns for the life of the HLF. There is generally a decrease in particle size across all measured sieve sizes between the belt samples and the borehole samples. Of greatest concern is the increase in fines content (particles passing the #200 sieve size [75 microns]), which ranges from 1.1 to 12.2 percent passing for belt samples to 6.7 to 30.8 percent for the samples collected from the boreholes. In addition, the grain size diameter for material passing 60 percent (i.e., D_{60}) decreases from approximately 7 mm to approximately 1.5 mm. In addition, the coefficient of uniformity for the belt

samples is relatively consistent and increases across the range of borehole samples, such that the coefficient of uniformity increases and affects the pore space and thus hydraulic conductivity of the crushed leach ore.

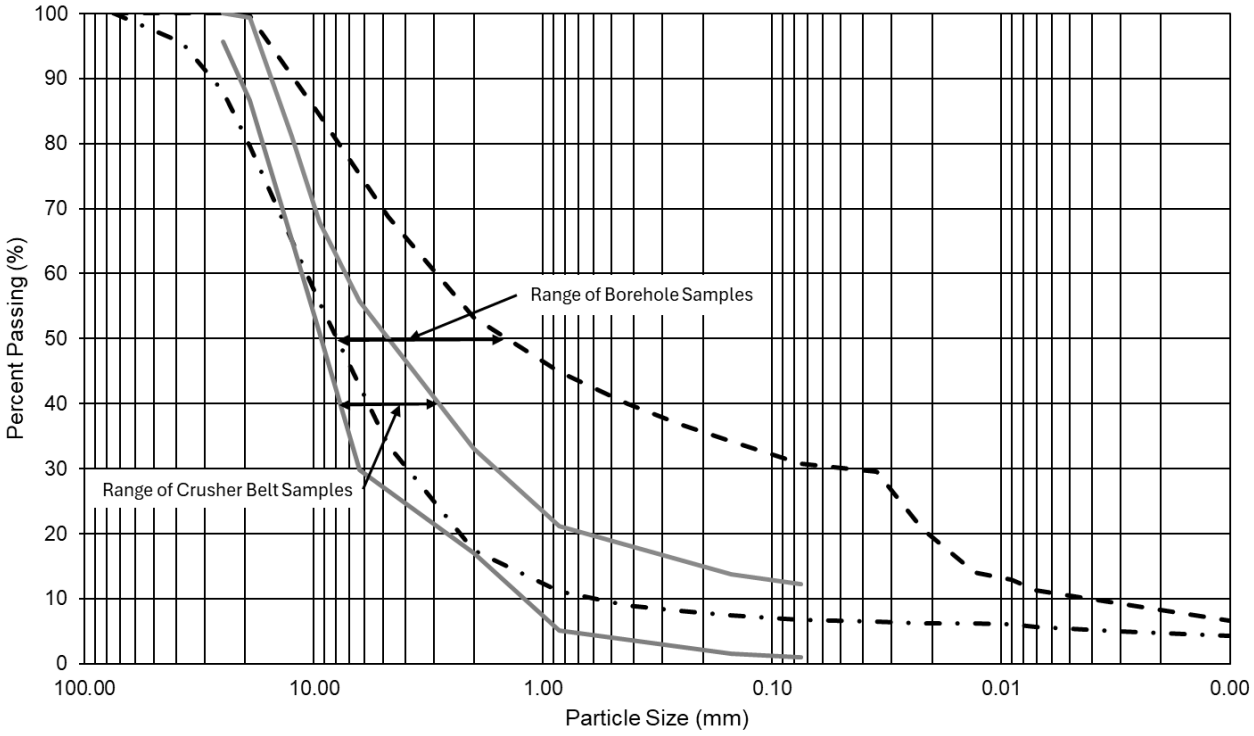

Figure 1: Comparison of grain size distribution between crusher belt and borehole samples

The noticeable and unusual drop along the particle size distribution amongst the fine particles range (less than 0.075 mm) for some of the borehole samples tested for hydrometer analysis could potentially be a result of a reaction between the dispersing agent and the calcium within the crushed leach copper ore minerals at one of the HLFs. A companion paper (Taukoor et al., 2025) discusses this in more detail.

Figure 2 presents a plot of the fines content with depth, which demonstrates a general trend towards increased fines content with depth for samples collected with the sonic core. It should be noted that the drilling method likely contributed to a small amount of the increase in fines content. Dashed lines provide boundaries for the general trend with data points, in which areas outside of those lines represent unusually high (plotting above the upper dashed line) or low fines content (plotting below the lower dashed line). The high fines content at shallow depths may represent rock types that are either very soft and therefore susceptible to mechanical decrepitation under light overburden pressures or have mineralogy that is susceptible to geochemical reactions. Those soils falling below the lower dashed line may have the opposite characteristics, with high rock strength and low susceptibility to geochemical reactions. There is also the possibility that these low-fines-content soils may have been protected from contact with sulfuric acid

leaching solutions due to overlying, low-permeability layers preventing solution vertical flow from interacting with these deeper ore layers.

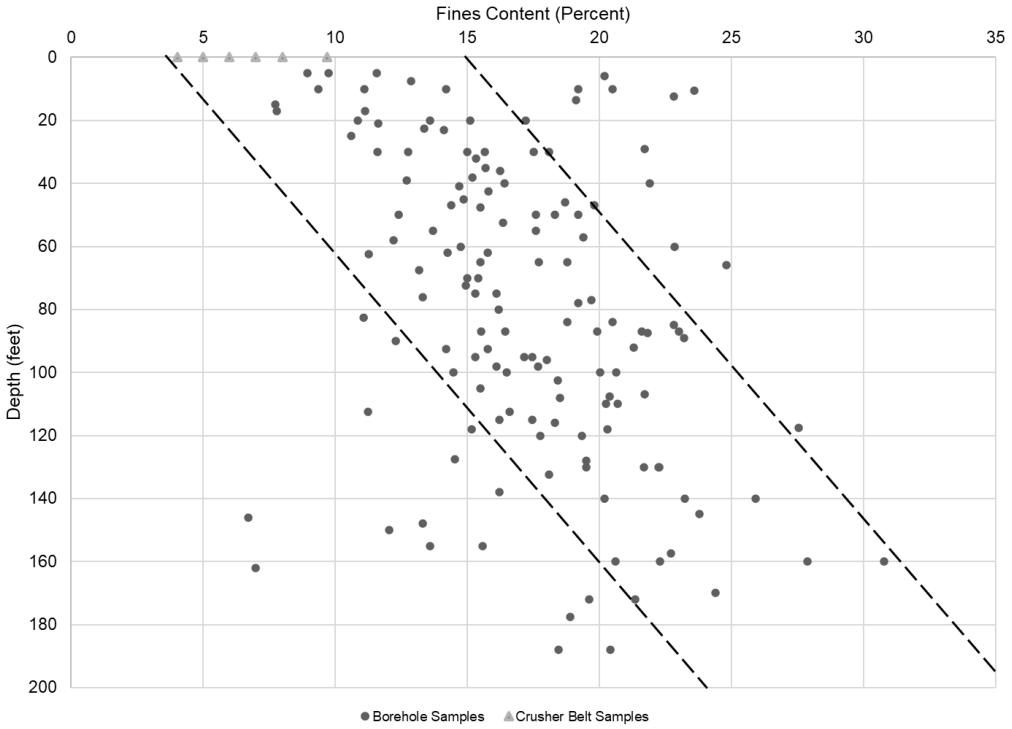

Figure 2: Fines content with depth from borehole samples

Comparison of Atterberg Limits

Atterberg Limit tests were completed on the same set of samples as those shown in Figure 1. Figure 3 presents the results of the laboratory tests using a Casagrande plasticity chart, which illustrates an increase in both Liquid Limit and Plasticity Index between the crusher belt samples and the HLF borehole samples. The crusher belt samples had Liquid Limits ranging from 14 to 25 percent and Plasticity Indices ranging from non-plastic to 10 percent. Borehole samples had Liquid Limits ranging from 20 to 36 percent and Plasticity Indices ranging from 5 to 19 percent.

Figure 4 presents the same data set comparing the Liquid Limit results with depth. The results generally depict a trend of increasing Liquid Limit with depth that is comparable to the results from the fines content (Figure 2). Similar to Figure 2, dashed lines provide boundaries for the general trend with data points. The increase in Liquid Limit is likely controlled primarily by the changes in fines content. This change cannot be directly related to any changes in the mineralogy, as the mineralogical tests required to make the assessment were not completed as part of this study. (i.e., percentage increase of clay mineral content).

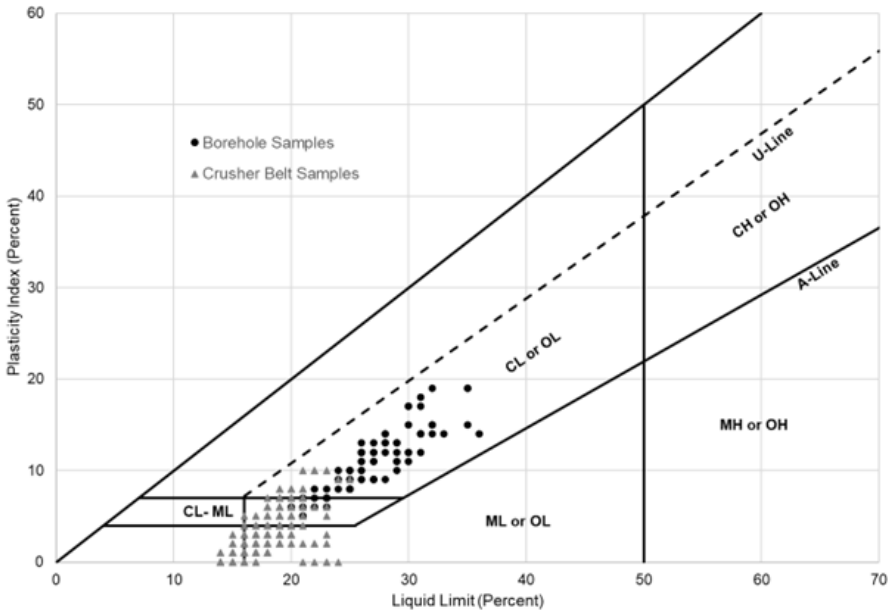

Figure 3: Casagrande plasticity chart comparing crusher belt to borehole samples

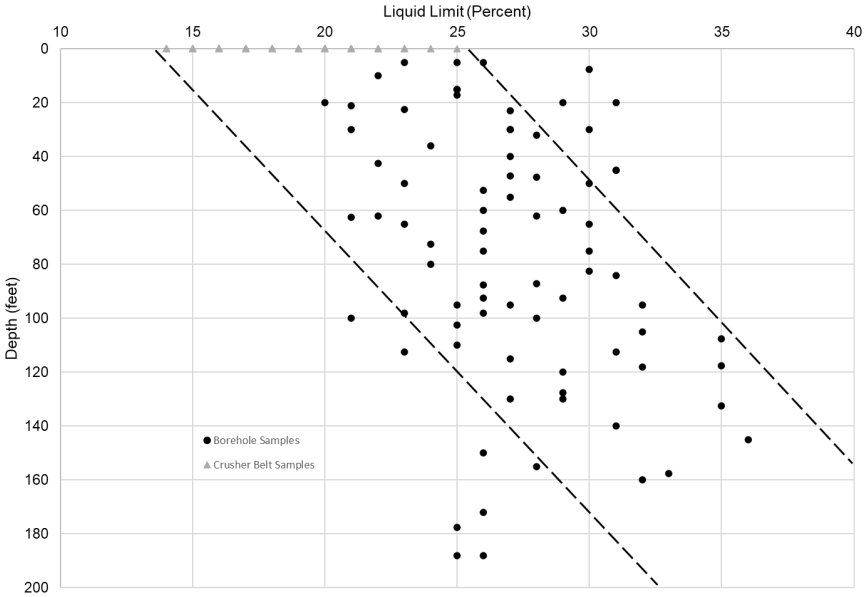

Figure 4: Liquid Limit with depth comparing crusher to borehole samples

Figure 5 presents the same comparison between samples but with respect to Plasticity Index. The data presents a similar trend of increased Plasticity Index with depth as seen with Liquid Limit.

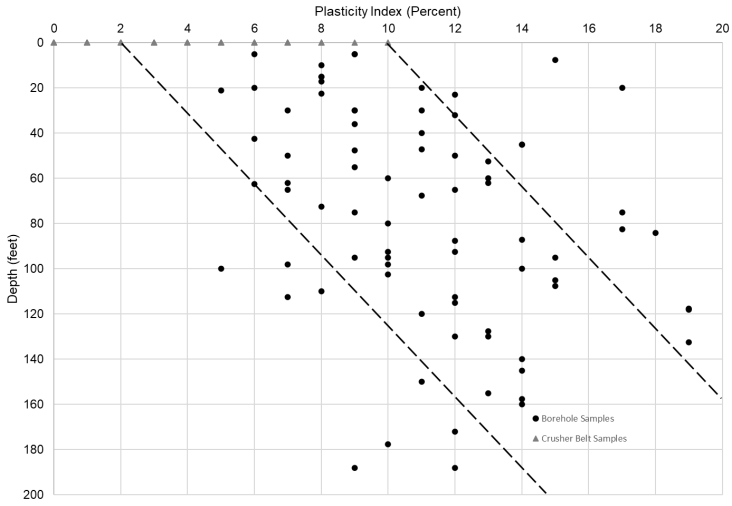

Figure 5: Plasticity Index with depth comparing crusher to borehole samples

Impact on hydraulic conductivity

The trend of increasing fines content and Liquid Limit with depth is expected to lead to a trend of decreasing hydraulic conductivity with depth. Additionally, this should be expected considering the self-weight consolidation of the crushed leach ore. As new lifts of crushed leach ore are stacked on the heap, consolidation should lead to decreased pore space and subsequently decreased hydraulic conductivity. HPT was used to estimate the hydraulic conductivity of crushed leach ore at eight locations within one of the crushed ore HLFs. The HPT has an upper measurement limit of approximately 1×10^{-1} centimeters per second (cm/s) (283 feet per day), where there is insufficient back pressure for the tool to measure the hydraulic conductivity, and a lower limit of 1×10^{-4} cm/s (0.28 feet per day), where the back pressure exceeds the measurement capacity of the tool. Figure 6 presents a typical HPT profile that was completed as part of this data set.

To complement and confirm the HPT rest results, the hydraulic conductivity of crushed leach ore was also assessed via 11 in-situ falling head hydraulic conductivity tests or a slug injection test, performed within 11 open standpipe piezometers that were specifically drilled and installed to measure hydraulic conductivity as part of this study. The setup included a 5-foot slotted screen installed at the bottom of a drill hole and within the targeted crushed leach ore zone, while the remaining portion of the hole was installed with solid casing. The test procedure consisted of positioning a pressure transducer at the bottom of the screened interval to measure changes of porewater pressure within the standpipe while slowly pouring a known volume of water down the standpipe (i.e., a slug of water) and monitoring the subsequent water level equilibration. The hydraulic response was then analyzed to estimate hydraulic conductivity, e.g., using the Bouwer-Rice method of estimating hydraulic conductivity of an unconfined aquifer from an

overdamped slug test (Bouwer & Rice, 1976). The locations and depths for the falling head tests were chosen in areas of known, low hydraulic conductivity and do not represent a random or even distribution (with depth), as was completed for the geotechnical index test results.

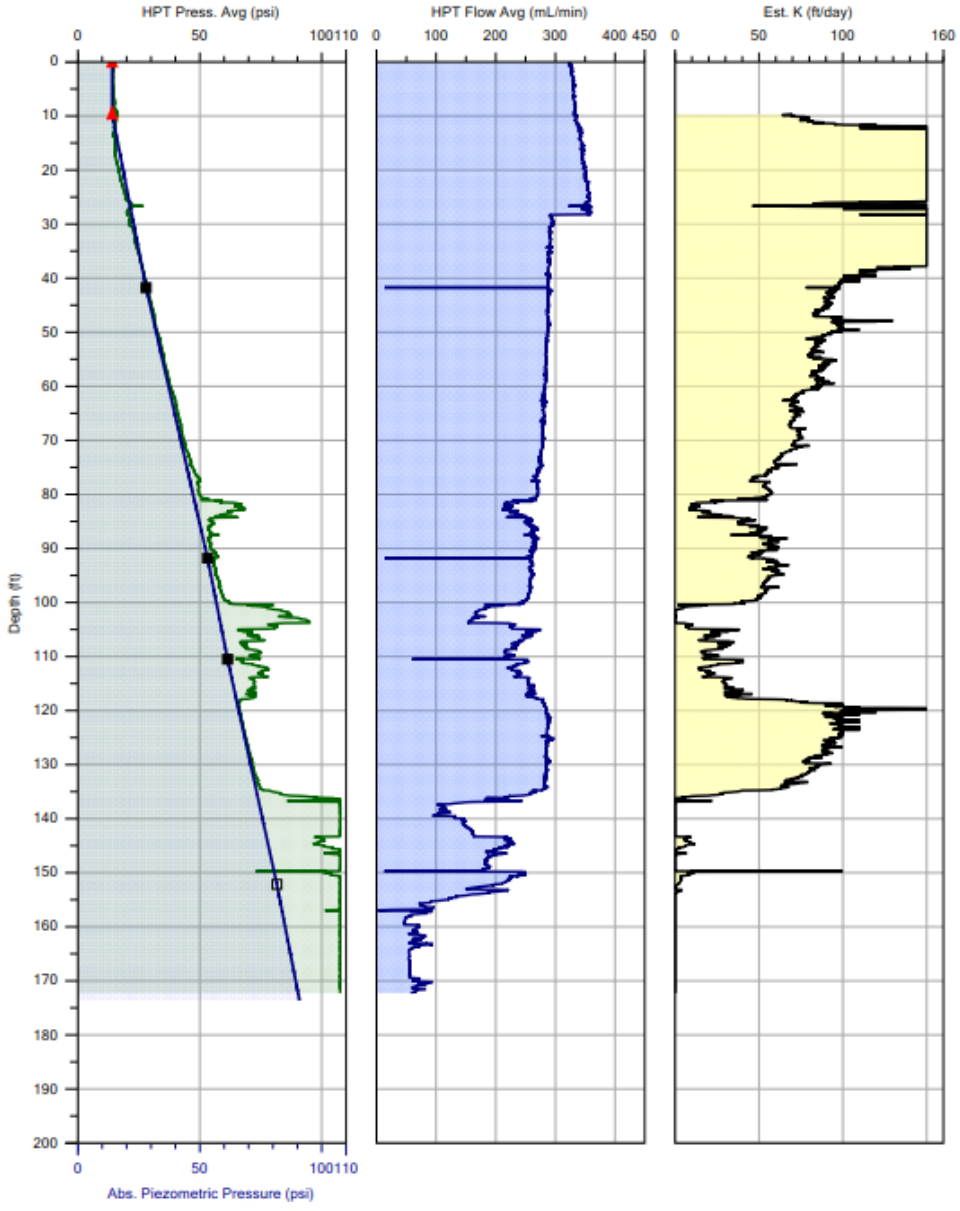

Figure 6: Typical HPT test result taken from a representative borehole

Figure 7 presents the arithmetic average HPT results from the eight individual test locations on one crushed, leach heap and the results of the 11 falling head permeability tests from the four crushed, leach heaps. The HPT tests generally measured a decrease of hydraulic conductivity with depth until a depth of approximately 135 feet, at which the measured hydraulic conductivity reaches the HPT measurement threshold of 1×10^{-4} cm/s.

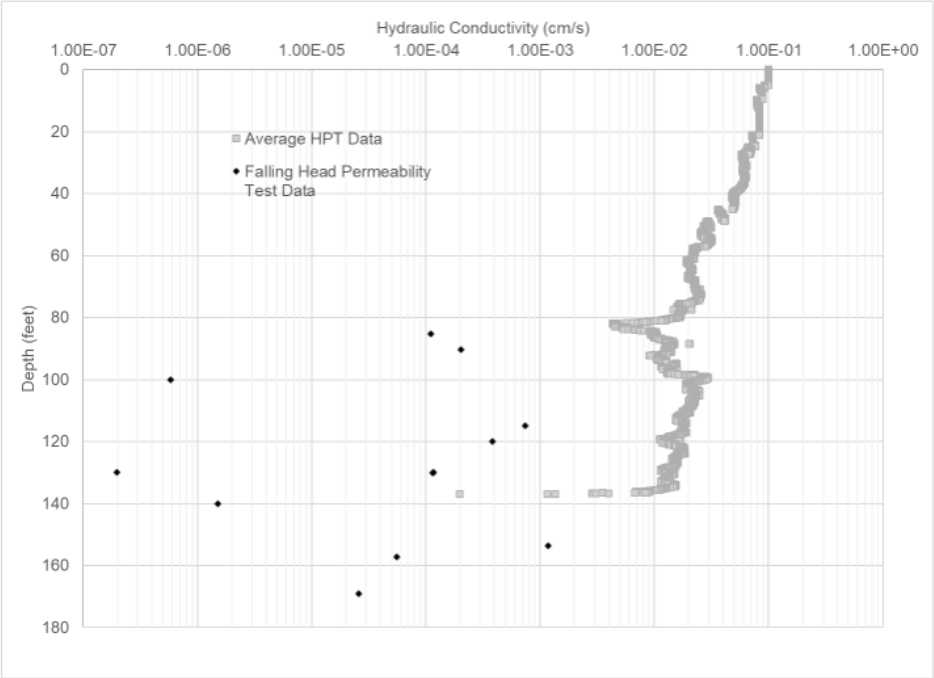

Figure 7: Comparison of hydraulic conductivity with depth

The falling head tests measured hydraulic conductivity ranged from 1×10^{-3} cm/s to nearly 1×10^{-7} cm/s. These results do not present the same trend as seen with fines content, Liquid Limit, or HPT test results as presented within Figures 8 and 9. Instead, individual layers at relatively shallow depths exhibit lower hydraulic conductivity than layers at greater depth. This likely indicates crushed leach ore that is either highly susceptible to geochemical decrepitation or potentially impacted by operational practices (i.e., compaction).

Figure 8 presents a graph of hydraulic conductivity from the falling head permeability tests compared to fines content of samples taken from each respective borehole at the same depth as the hydraulic conductivity test. There is no laboratory data to compare with the HPT test data as laboratory data was correlated with previously located CPT locations; however, HPT tests were completed on one of the four crushed leach HLFs.

In general, there is agreement between an increase in fines content and a subsequent decrease in hydraulic conductivity. For low hydraulic conductivity values (i.e., below 1×10^{-5} cm/s), fines content alone does not account for the orders of magnitude change with hydraulic conductivity. To get to this low hydraulic conductivity likely requires a change of mineralogy through geochemical decrepitation. Furthermore, there is a potential that the shape of the grain size distribution curve may provide an answer to the decrease of hydraulic conductivity. It may be that the coefficient of uniformity (i.e., the ratio of D_{60} to D_{10} particle sizes) might be more indicative of the impacts from decrepitation on hydraulic conductivity as compared to fines content.

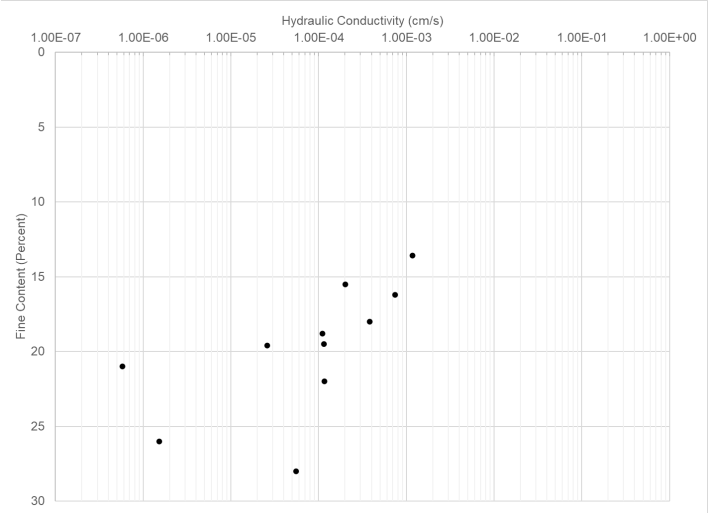

Figure 8: Comparison of hydraulic conductivity with fines content for a subset of the dataset

A comparison of the hydraulic conductivity with Liquid Limit presents a slight correspondence, as presented in Figure 9, but does not explain the very low hydraulic conductivity measured via the falling head tests.

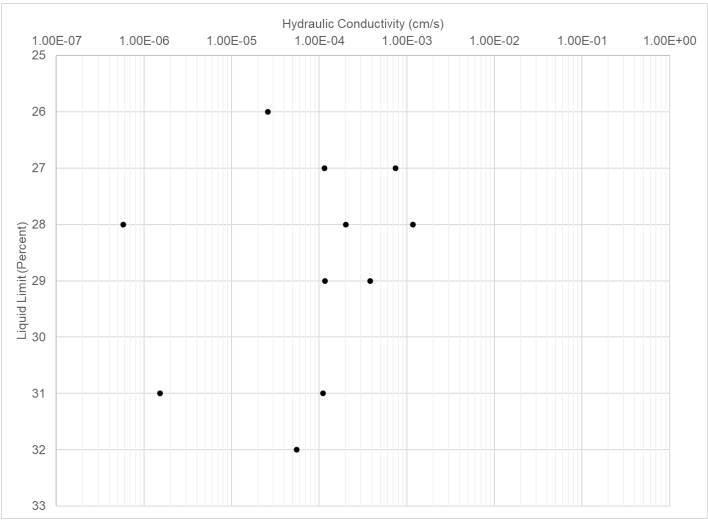

Figure 9: Comparison of hydraulic conductivity with Liquid Limit

Importance of Active Facility Management

As demonstrated above, the geotechnical material properties of crushed ore HLFs vary and change with time, which requires an active management plan to maintain slope stability and operational efficiency. The Observational Method, utilizing a robust investigation and monitoring program, is required to provide sufficiently reliable data to evaluate changes and the subsequent performance of the HLF during the life of mine with stacking and leaching processes (e.g., Grass et al., 2022). Site geotechnical and operational teams, in conjunction with an Engineer of Record (EOR) as well as a third-party reviewer, should utilize a

program of overlapping data sources and collection methods, which generally consist of, but are not limited to, geotechnical investigations (i.e., sample collection and laboratory and field tests), visual inspections, pore pressure monitoring (i.e., piezometers), and deformation monitoring (i.e., InSAR, prisms, shape arrays). Monitoring should be performed on a regular schedule, dependent on the data collection method, even if slope instability is not indicated, so that baseline data, rate of change measurements, and early slope instability data are collected to detect evidence for this change of material geotechnical characterization.

The operational team should also consider evaluating the geotechnical properties of the crushed leach ore coming from the mine to the crusher to determine if there are pre-existing conditions (i.e., high fines content or high clay mineralogy) that could lead to poor geotechnical conditions after stacking and leaching processes. Rates of acid consumption, particularly when evaluating gangue minerals, may provide estimates of future geochemical decrepitation of the ore. Relatively soft rocks can also contribute to high fines content after crushing and subsequent mechanical decrepitation of the crushed leach ore through time. Blending strategies can be developed to support improving copper recovery and geotechnical properties via mixing weaker or high clay content ores with stronger and low clay content ores to limit the impacts on future decrepitation.

Conclusion

A decrease in hydraulic conductivity for crushed leach ore due to self-weight consolidation is to be expected for any HLF. However, the impacts of decrepitation, both mechanical and geochemical, within sulfuric acid leaching environments produce lower hydraulic conductivity as discussed within this paper and a companion paper (Taukoor et al., 2025) than previously industry-anticipated during geotechnical tests for the initial design of a crushed leach ore HLF (Van Zyl, 1988).

Historically, stockpiles constructed from crushed leach copper ore for the purpose of copper recovery through sulfuric acid leaching have been assumed to be freely draining throughout their lifetimes based on initial hydraulic conductivity tests completed on fresh or column test samples that were subjected to a limited leach cycles during the design stage.

A typical application rate for sulfuric acid leaching within the copper industry is approximately 0.0025 gallons per minute per square foot (or approximately 6 liters per hour per square meter), which represents an equivalent hydraulic conductivity of approximately 1.7×10^{-3} cm/s. This would require that the crushed leach ore maintains a hydraulic conductivity of at least 1.7×10^{-1} cm/s. The results of the hydraulic conductivity measurements presented herein demonstrate that the potential for saturated conditions and development of undrained shear strength within an HLF are higher than what is typically assumed or measured within the design stages for an HLF.

If the results presented within this paper hold true for other sulfuric acid, crushed leach ore HLFs, then HLF operators should assume that saturated conditions and the build-up of pore pressure within these HLFs are likely to exist. These conditions may not be visible on the surface of the HLF and are likely to be identified only through subsurface investigations, such as cone penetration tests and vibrating wire piezometers. Furthermore, low ore hydraulic conductivity may lead to the development of undrained behavior under load. A simple methodology to identify and quantify these conditions is presented within a companion paper (Taukoor et al., 2025).

Periodic geotechnical investigations are required to identify these conditions and may consist of electrical resistivity geophysical surveys, cone penetration tests, borehole drilling, and subsequent laboratory tests of collected samples, and in-situ measurement of hydraulic conductivity. A robust application of the Observational Method can provide a framework for the active management of these HLFs to provide for the safe operation, where the geotechnical properties of the crushed leach ore should be expected to change through time.

Acknowledgements

The authors would like to thank Freeport-McMoRan Inc. for its support and time in developing this paper. The sharing of useful data, ideas, and insights by Teresa Speigl, Georgia Lysay, Kanyembo Katapa, Salvador Ortiz, John Lupo, ConeTec, and others has been helpful and is greatly appreciated.

References

Bouwer, H., & Rice, R. C. (1976). A slug test method for determining hydraulic conductivity of unconfined aquifers with completely or partially penetrating wells. *Water Resources Research, 12*(3), 423–428.

Breitenbach, A. J., & Thiel, R. S. (2005, December). A tale of two conditions: Heap leach pad versus landfill liner strengths. In *North American Geosynthetics Society / Geosynthetics Research Institute 19 Conference*. Las Vegas, NV.

Duncan, J. M., Wright, S. G., & Brandon, T. L. (2014). *Soil strength and slope stability* (336 pp.). John Wiley & Sons.

Grass, M. J., Nketia, P., & Jester, C. D. (2022, October). Geotechnical engineering: The observational method applied to monitoring of slopes during operational activities for heap leach pad facilities. In *Heap Leach Solutions 2022*. Sparks, NV.

Interstate Technology and Regulatory Council. (2019). *Implementing advanced site characterization tools*. https://asct-1.itrcweb.org/

Taukoor, V., Jester, C. D., Grass, M. J., Manjarrez, L., & Bagley, Z. (2025). Decrepitation of crushed leached copper ore under sulfuric acid leaching conditions—Part 2. In *Heap Leach Solutions 2025*. Sparks, NV. (Accepted for presentation)

Van Zyl, D., Hutchison, I., & Kiel, J. (1988). *Introduction to evaluation, design and operation of precious metal heap leaching projects* (372 pp.). Society of Mining Engineers, Inc.

Decrepitation of Crushed Leach Copper Ore Under Sulfuric Acid Leaching Conditions—Part 2

Vashish Taukoor, WSP USA, Inc., USA
Christopher Jester, WSP USA, Inc., USA
Michael Grass, WSP USA, Inc., USA
Lino Manjarrez, WSP USA, Inc., USA
Zumhin Bagley, WSP USA, Inc., USA

Abstract

Decrepitation of crushed leach copper ore under sulfuric acid leaching conditions refers to the mechanical and geochemical breakdown of the ore. Mechanically, the process of stacking and burying via multiple lifts of ore will break the ore down over time. Geochemically, sulfuric acid solution leaching will break down the ore by reacting with a variety of gangue and ore minerals to generate new minerals. Together, these two processes fundamentally lead to a greater quantity of finer particles, shifting the uniformity of the grain size distribution, reducing the hydraulic conductivity, and potentially leading to the generation of excess pore pressure when sheared, all of which are potential precursors to undrained behavior of ore during loading or shearing.

Historically, leached copper ore stockpiles have been assumed to remain freely draining during their lifetimes, mobilizing drained shear strengths. However, decrepitation can create low-permeability, fine-grained layers that force parts of a stockpile to mobilize undrained shear strengths, reducing the overall shear strength or generating the potential for a static liquefaction event. Sulfuric acid leaching on copper ore stockpiles thus necessitates careful management to monitor for evidence of decrepitation, potentially leading to low permeability that limits copper recovery, as well as a potential reduction of shear strength that may require implementation of stability management practices.

A reliable and reproducible methodology to identify and quantify the onset of decrepitation is essential for evaluating its overall impact on a copper ore crushed leach stockpile. Within this paper, we present a methodology based on a study conducted at four existing crushed leach copper stockpiles with various ages under sulfuric acid leaching to investigate the relationship between the cone penetration test (CPT) response, hydraulic conductivity, and laboratory geotechnical properties of crushed leach copper ore. We identify two different and distinct trends for crushed leach copper ore exhibiting drained behavior versus

undrained behavior, signaling the onset of decrepitation, and quantify the transition point between these two behaviors with regards to CPT-based criteria, hydraulic conductivity, and laboratory geotechnical properties for which the shear behavior fundamentally changes.

Introduction

Heap leach facilities (HLFs), constructed from crushed leach copper ore for the purpose of copper recovery through sulfuric acid leaching, have historically been designed as, and are commonly assumed to remain freely draining throughout their lifetimes, such that slope stability evaluations conducted as part of their design typically assume drained shear strength conditions (Van Zyl, 1988). However, as demonstrated within a companion paper (Grass et al., 2025), decrepitation of crushed leach copper ore can lead to fine-grained layers within a stockpile, forcing a portion of the stockpile to mobilize an undrained shear strength, thus resulting in a reduction of its overall shear strength or possible static liquefaction event. Additionally, these fine-grained layers have the potential to limit the flow of solution within a stockpile, further limiting copper recovery. Therefore, a reliable and reproducible methodology to identify as well as quantify the onset of decrepitation of crushed leach copper ore under sulfuric acid leaching conditions is essential for evaluating the impact of decrepitation on slope stability and efficient copper recovery.

The cone penetration test (CPT) is a routinely performed and widely available means of evaluating in-situ geotechnical profiles and properties. Within the context of crushed leach copper ore stockpiles under sulfuric acid leaching, it can allow for tracking both the mechanical and geochemical breakdown of copper ore over time. An estimate of the in-situ hydraulic conductivity of crushed leach copper ore measured through time is also a reasonable means to track the progress of decrepitation. Furthermore, routine laboratory geotechnical tests performed on samples of crushed leach copper ore collected as part of drilling programs, such as changes in fines and moisture contents, and particle size distributions, can also provide valuable insights into decrepitation through time. Therefore, it is informative to track the decrepitation of crushed leach copper ore through time using a suite of data associated with the CPT, in-situ hydraulic conductivity, and geotechnical laboratory data. However, a review of the technical literature revealed that an assessment of decrepitation using cross-correlation of CPT data, in-situ hydraulic conductivity, and laboratory-based geotechnical parameters of crushed leach copper ore is limited, mainly because collection of such data involves resources associated with repeated drilling, sampling, and testing through the lifetime of the stockpile (Breitenbach & Thiel, 2004; Saavedra, 2014; Chahua et al., 2016; Torres et al., 2022).

Within this paper, the authors present the data, analyses, and observations of a study conducted at four existing HLFs with various ages under sulfuric acid leaching conditions to investigate the relationship between the CPT response of crushed leach copper ore quantified with terms of the in-situ hydraulic

conductivity as well as laboratory-based geotechnical properties and two CPT-based criteria, namely Delta Q (Saye et al., 2007) and normalized friction ratio F_r (Robertson, 1990).

Geotechnical Data

General Terms and Definitions

Cone Penetration Test Response

The CPT involves pushing an instrumented cone vertically into the ground at a controlled rate of approximately 2 centimeters per second (cm/sec) and collecting a set of three main data: the cone tip stress corrected for porewater pressure effects (q_t) that measures the resistance of the ground to the cone's penetration; the sleeve friction (f_s) that records the frictional resistance along the cone's sleeve; and the dynamic porewater pressure (u_2) that records the porewater pressure generated by the cone penetrating through the material.

Based on the data collected during a CPT push, the normalized friction ratio F_r is estimated as a percent using Equation 1 (Robertson, 1990), as the ratio of sleeve friction (f_s) to the corrected cone tip stress minus the total vertical stress ($q_t - \sigma_{v0}$).

$$F_r = \frac{f_s}{q_t - \sigma_{v0}} \quad \text{Equation 1}$$

In addition to normalized friction ratio, the authors also estimated the term Delta Q using Equation 2 (Saye et al., 2017) as the ratio of the normalized cone tip resistance Q_t given as $(q_t - \sigma_{v0})/\sigma'_{v0}$ to the sleeve friction normalized with in-situ effective vertical stress (f_s/σ'_{v0}) with an offset of (0.67, 10). Based on early works with CPT interpretations (e.g., Begemann, 1965) as well as newer ones (e.g., Schneider et al., 2008, 2012), Saye et al. (2017) proposed the Delta Q methodology for interpreting CPT data in soils where the traditional Robertson approach may be inaccurate, such as in overconsolidated soils. They introduced a new soil classification method based on a linear relationship between Q_t and the ratio (f_s/σ'_{v0}), where the slope Delta Q can be defined across a wide range of soil types, from coarse sands to highly plastic organic clays. Within this paper, the authors use both F_r and Delta Q as key parameters to characterize the CPT-based response of crushed leach copper ore.

$$Delta\ Q = \frac{(Q_t + 10)}{\left[\left(\frac{f_s}{\sigma'_{v0}}\right) + 0.67\right]} \quad \text{Equation 2}$$

Hydraulic Conductivity

The hydraulic conductivity of crushed leach copper ore within the context of heap leach engineering represents the ease with which raffinate solution and pregnant leach solution flow through an HLF,

assuming all void spaces (pores) are fully saturated. Higher hydraulic conductivity indicates easier solution flow due to factors such as greater pore distribution, interconnectivity of pore space, and larger pore sizes. By contrast, a low hydraulic conductivity is a result of a smaller pore distribution, low interconnectivity of pore space, and relatively smaller size of pore space that may lead to crushed leach copper ore having an undrained response to shearing.

The hydraulic conductivity of crushed leach ore can be assessed via an in-situ falling head hydraulic conductivity test or a slug injection test, typically performed within an open standpipe piezometer. The setup includes a 5-foot slotted screen installed at the bottom of a drill hole and within the targeted crushed leach ore zone, while the remaining portion of the hole is installed with solid casing. The test procedure consists of positioning a pressure transducer at the bottom of the screened interval to measure changes of water pressure within the standpipe via slowly pouring a known volume of water down the standpipe (i.e., a slug of water) and monitoring the subsequent water level equilibration. The hydraulic response is then analyzed to estimate hydraulic conductivity, e.g., using the Bouwer-Rice method of estimating hydraulic conductivity of an unconfined aquifer from an overdamped slug test (Bouwer & Rice, 1976).

Geotechnical Index Characteristics

Geotechnical Index characteristics of crushed leach copper ore, such as fines content (FC) and coefficient of uniformity (C_u) have a direct impact on pore distribution, connectivity, as well as size; and therefore, influence behavior type (i.e., drained behavior versus undrained behavior). Geotechnical index characteristics are quantified through laboratory-based geotechnical tests on samples of crushed leach copper ore collected as part of field investigation drill programs through time.

- Fines Content (FC), defined as the percentage of material by dry weight passing through the No. 200 sieve corresponding to an opening size of 0.075 millimeter (mm) or 75 microns, according to American Society for Testing and Materials (ASTM) D6913 and D7928 procedures.
- Coefficient of Uniformity (C_u) is defined as the ratio of particle size finer than 60 percent by dry weight (D_{60}) to a particle size finer than 10 percent by dry weight (D_{10}). Both D_{60} and D_{10} values were obtained or extrapolated from particle size distribution curves generated by sieve analysis tests conducted in accordance with ASTM D6913 and D7928 procedures.

Geotechnical Field Investigations

Data from four existing crushed leach copper stockpiles with various ages under sulfuric acid leaching conditions relating CPT responses, in-situ hydraulic conductivity, and laboratory-based geotechnical properties were considered. The dataset spans 10+ years of relevant field and laboratory data with co-located CPTs, drill holes for the purpose of well installation, and in-situ hydraulic conductivity tests at

targeted depths, and drill holes allowing for the sampling of crushed leach copper ore at targeted depths for the proposed laboratory tests. At the time of this writing, the dataset comprises 42 co-located CPTs, 30 field hydraulic tests, and 86 samples tested for geotechnical index characteristics (i.e., grain-size and coefficient of uniformity).

Based on the data from the four sites, the authors compiled a database containing 105 data points: 11 complete data points relating to CPT responses, in-situ hydraulic conductivity, and geotechnical index characteristics, and 94 partially complete data points relating to two of the three parameters. The authors intend to expand and refine the database over time by incorporating data from future field investigations and other comparable sites.

Data Analysis and Observations

Using the compiled database, the authors worked on relating CPT responses quantified with regard to normalized friction ratio (Fr) and Delta Q, in-situ hydraulic conductivity, and geotechnical index characteristics quantified in terms of fines content and coefficient of uniformity. These relationships are further discussed below.

Although noticeable scatter amongst the data exists, likely due to the inherent variability of the crushed leach copper ore and testing inaccuracy, the data indicates a typical trend generally characterized by a change of slope at the occurrence of a unique combination of CPT-based parameters, in-situ hydraulic conductivity, and/or geotechnical index characteristics interpreted by the authors to indicate a change of crushed leach copper ore from drained behavior to undrained behavior—referred to as a "transition point". The transition points illustrated within Figures 1 through 9 below are marked by a clear change of slopes, suggesting a fundamental behavioral shift of the crushed leach copper ore, i.e., from drained behavioral conditions to undrained behavioral conditions, once these parameter thresholds are crossed.

Falling Head and Cone Penetration Tests

Figures 1, 2, and 3 illustrate the relationships between in-situ hydraulic conductivity and the CPT-based parameters of normalized friction ratio, 1 / normalized friction ratio, and Delta Q, respectively.

The term "1 / normalized friction ratio" showed a trend with slightly less scatter than the normalized friction ratio when correlated with in-situ hydraulic conductivity. This is also evident for relationships with geotechnical index characteristics (described later within this paper).

Upon reviewing the data presented within Figure 1 through Figure 3, the observed transition points range approximately from 2×10^{-5} to 1×10^{-4} cm/sec for in-situ hydraulic conductivity, respectively, associated with 5.0 percent for normalized friction ratio (refer to Figure 1), 22 (4.5 percent for normalized

friction ratio) for 1 / normalized friction ratio (refer to Figure 2), and approximately 18.5 for Delta Q (refer to Fig. 3).

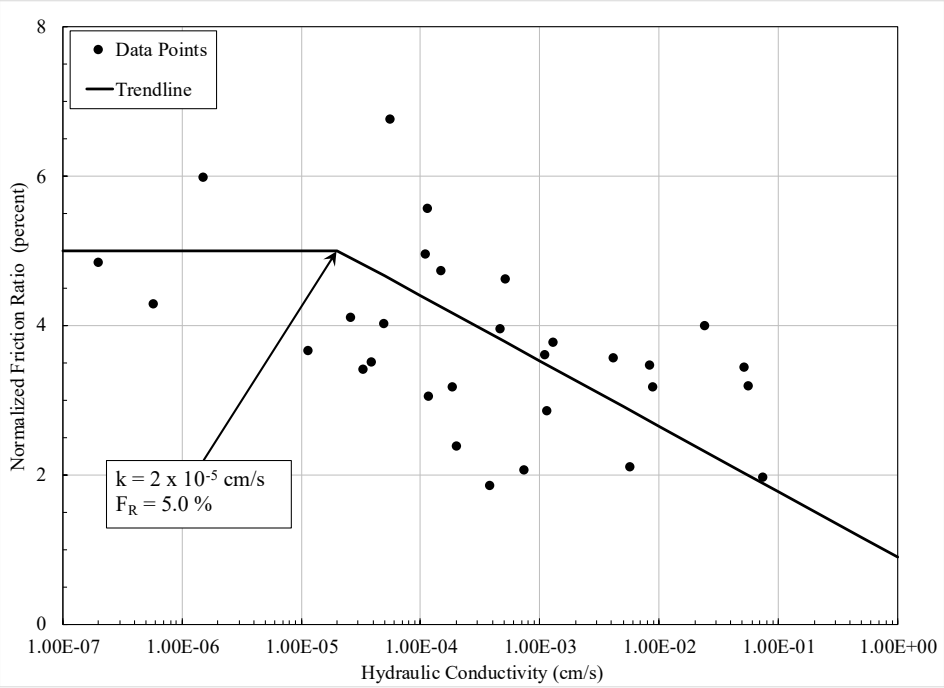

Figure 1: Relationship between hydraulic conductivity and normalized friction ratio

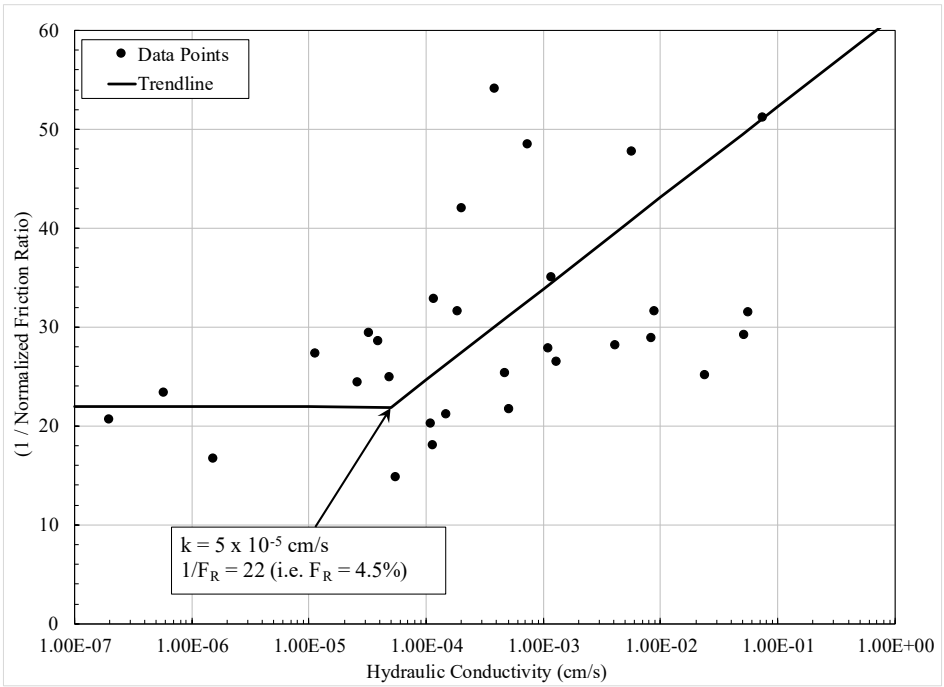

Figure 2: Relationship between hydraulic conductivity and (1 / normalized friction ratio)

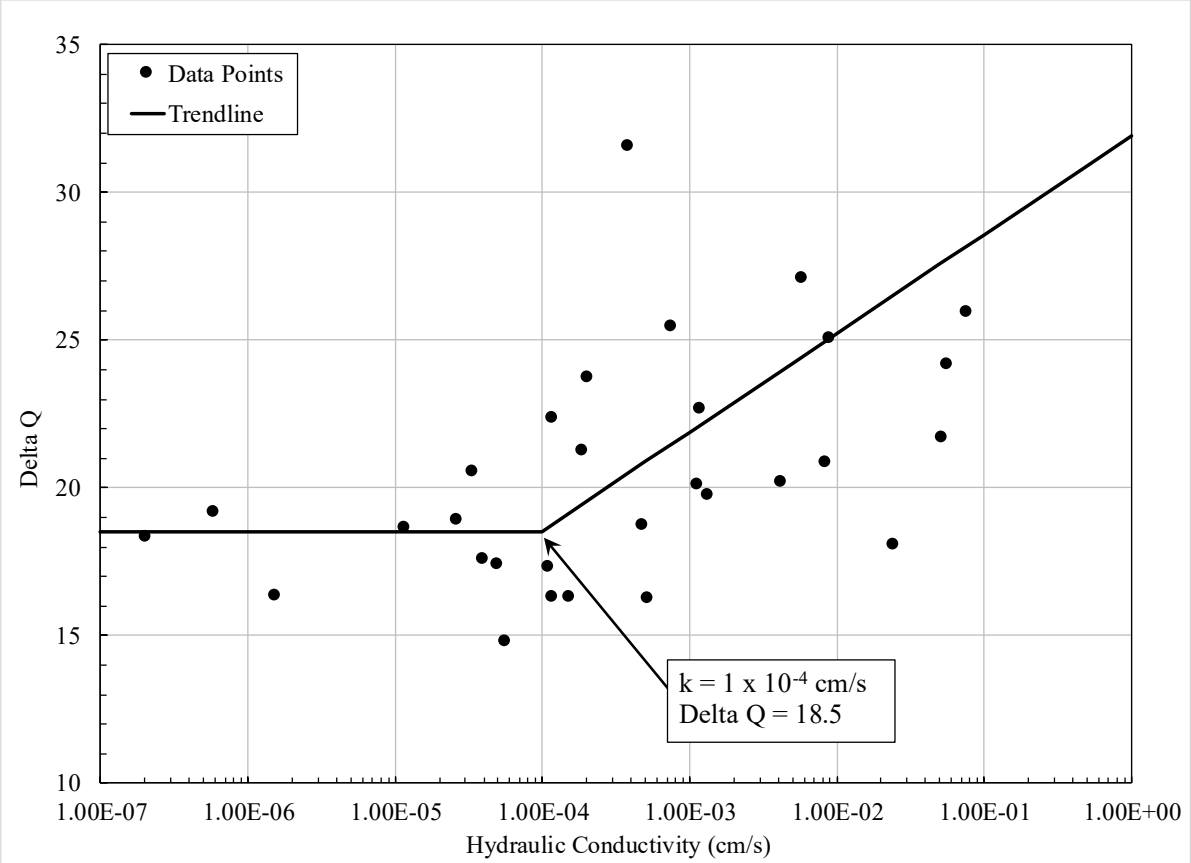

Figure 3: Relationship between hydraulic conductivity and Delta Q

Falling Head and Laboratory Tests

Figures 4 and 5 illustrate the relationship between in-situ hydraulic conductivity and geotechnical index characteristics, fines content, and coefficient of uniformity, respectively.

Of the 11 samples tested for hydrometer analysis, three exhibited a noticeable and unusual drop along the particle size distribution in the fine particle range (less than 0.075 mm). The discrepancy of the laboratory-determined D10 led to a significant underestimate of the coefficient of uniformity despite having relatively high fines content, respectively, of 21 percent, 26 percent, and 28 percent. This anomaly could potentially be a result of a reaction between the dispersing agent used during the hydrometer analysis test, sodium hexametaphosphate, and the calcium within the calcium-rich crushed leach copper ore at one of the HLFs. Therefore, we reviewed the data and calculated an estimate by shifting the unusual drop upward to meet the laboratory value for fines content passing the #200 sieve (75 microns) to augment the laboratory D_{10} values for these samples of 0.006 mm, 0.004 mm, and 0.001 mm, respectively.

Upon reviewing the data presented within Figures 4 and 5, the observed transition points are approximately 2×10^{-5} to 3×10^{-5} cm/sec for in-situ hydraulic conductivity, 23 percent for fines content, and 1,500 for coefficient of uniformity.

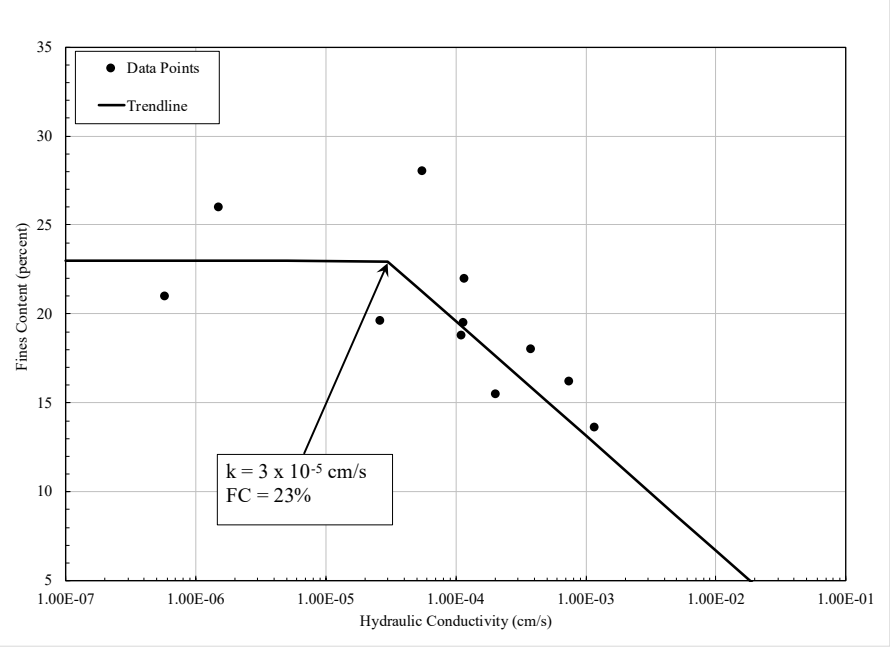

Figure 4: Relationship between hydraulic conductivity and fines content

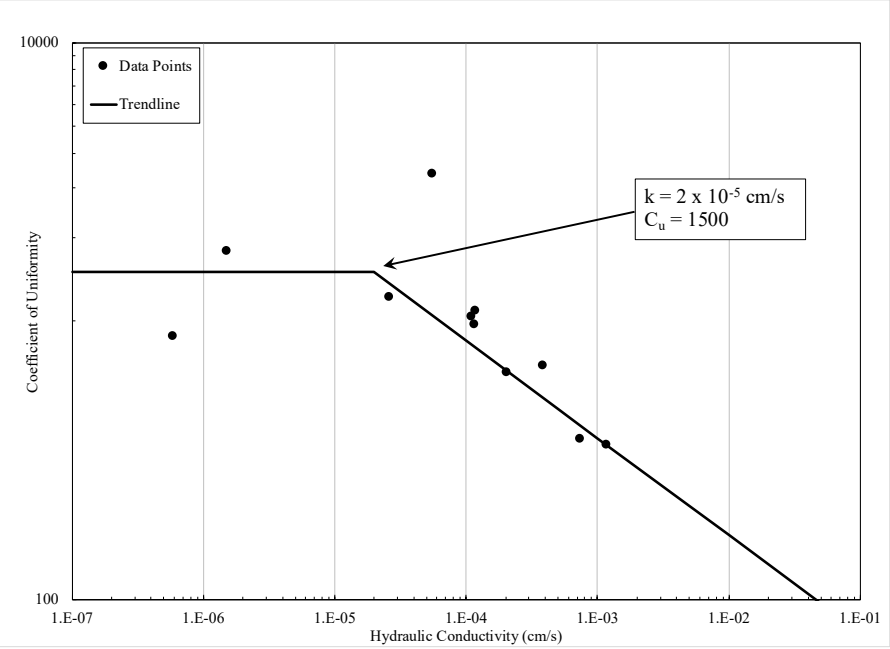

Figure 5: Relationship between hydraulic conductivity and coefficient of uniformity

Cone Penetration and Laboratory Tests

Figures 6 and 7 illustrate the relationship between the CPT-based parameter 1 / normalized friction ratio and geotechnical index characteristics, fines content, and coefficient of uniformity, respectively. Figures 8 and 9 illustrate the relationship between the CPT-based parameter Delta Q and geotechnical index characteristics, fines content, and coefficient of uniformity, respectively.

Upon reviewing the data presented within Figures 6 through 9, the observed transition points are approximately 23 to 24 for 1 / normalized friction ratio (4.2 percent to 4.4 percent for normalized friction ratio), approximately 20 for Delta Q, approximately 19 percent to 20 percent for fines content, and 650 to 700 for coefficient of uniformity.

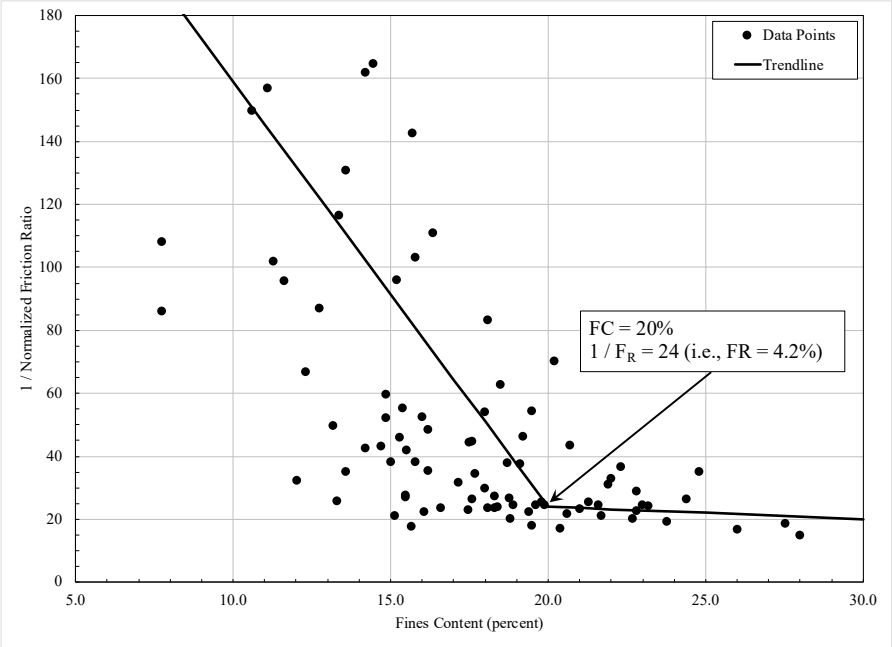

Figure 6: Relationship between 1 / normalized friction ratio and fines content

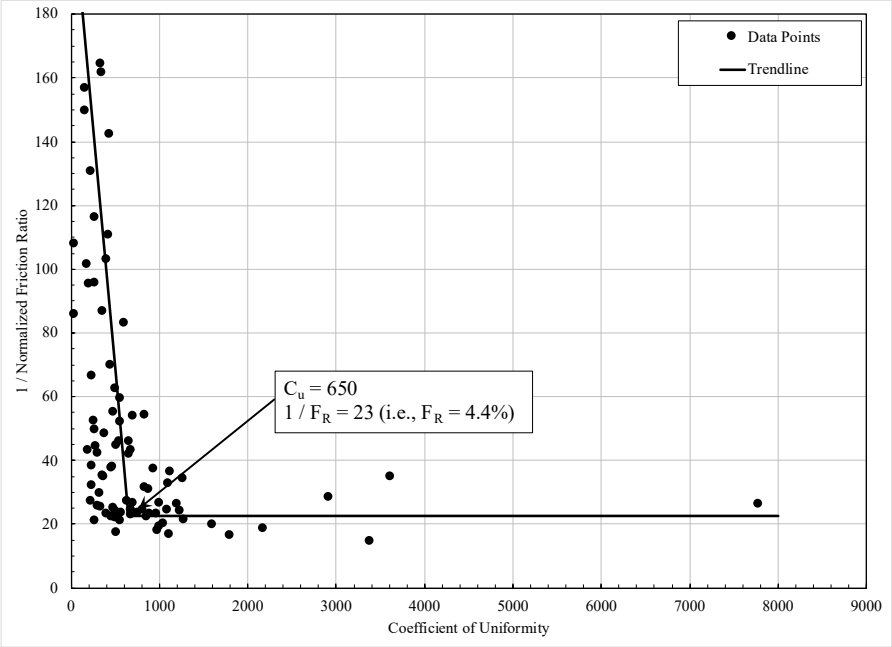

Figure 7: Relationship between 1 / normalized friction ratio and coefficient of uniformity

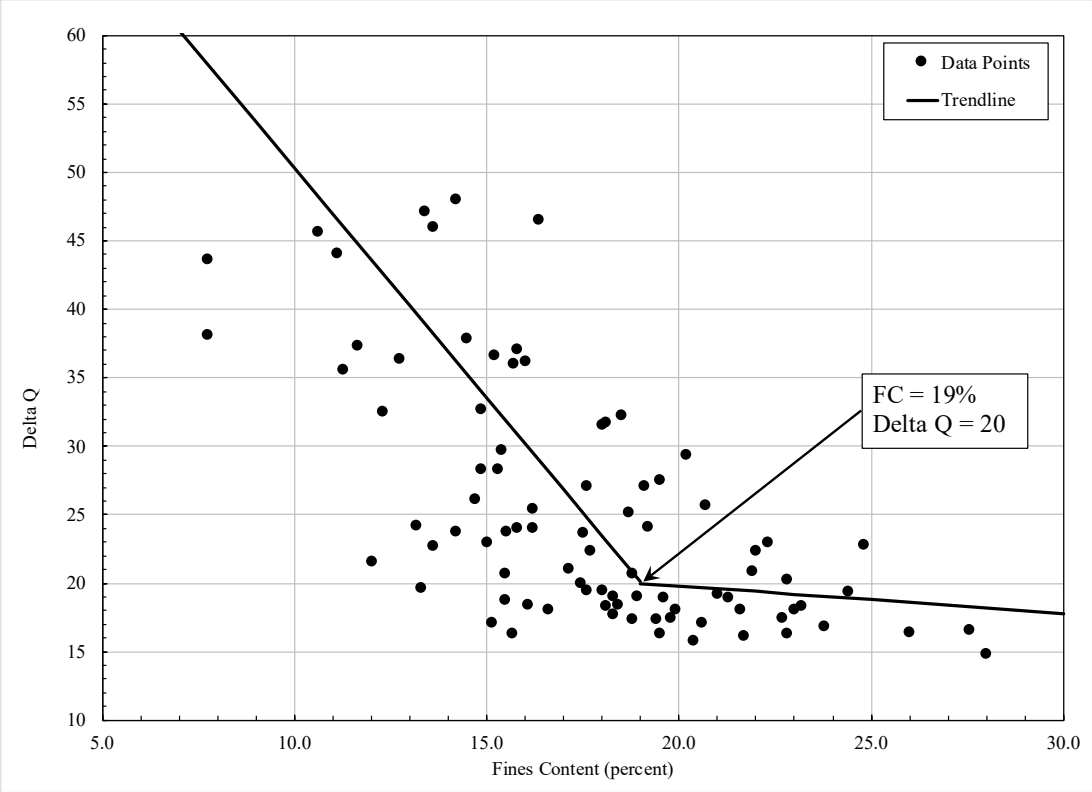

Figure 8: Relationship between Delta Q and fines content

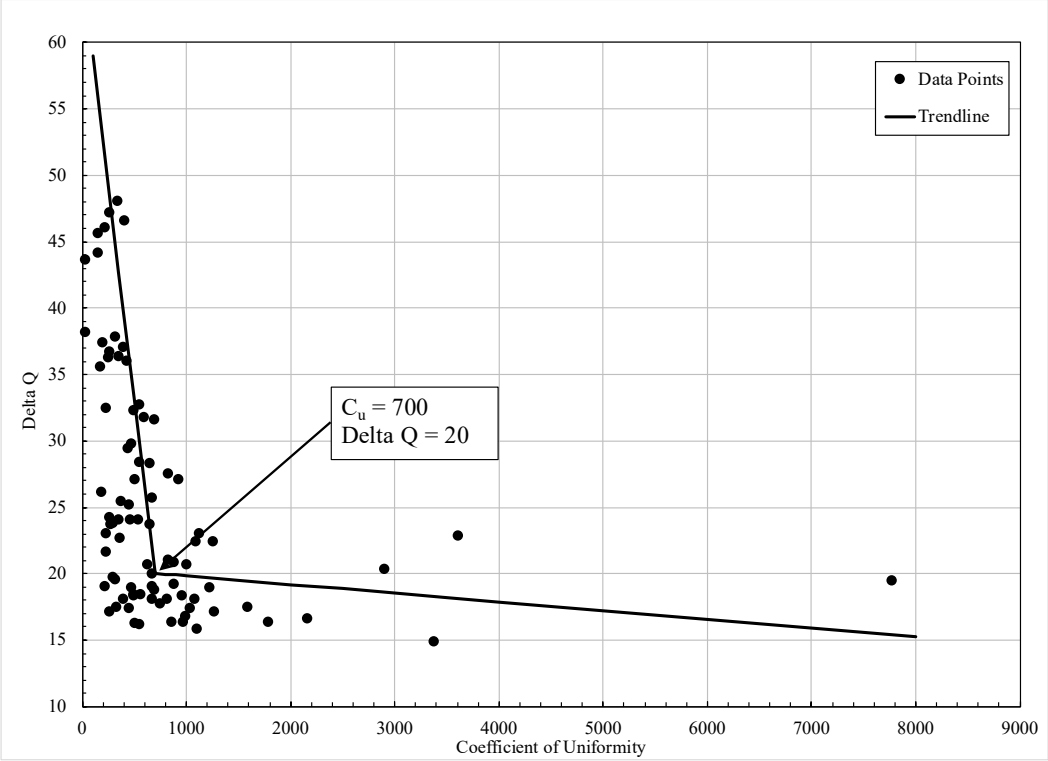

Figure 9: Relationship between Delta Q and coefficient of uniformity

Summary and Conclusion

Data from four existing crushed leach copper ore stockpiles (Grass et al., 2025) with various ages under sulfuric acid leaching conditions were reviewed and analyzed with the purpose of identifying key parameters signaling the onset of decrepitation with a simple, reliable, and reproducible methodology. The data included CPT response, in-situ hydraulic conductivity, and geotechnical index characteristics.

Although a noticeable scatter of the data exists for the relationships presented within Figures 1 through 9, the authors identified a general trend among the data, signaling that predominantly drained crushed leach copper ore has a different slope than predominantly undrained crushed leach copper ore. The intersection between the trends or lines for the two different behaviors, referred to as the "transition point", represents a unique combination of values of CPT-based parameters, field hydraulic conductivity, and grain size characteristics for which crushed leach ore behavior fundamentally changes. The transition points as shown within Figure 1 through Figure 9 are summarized within Table 1, and are interpreted by the authors to indicate that heavily-decrepitated crushed leach copper ore is likely to have an in-situ hydraulic conductivity less than 10^{-5} cm/sec, 1 / normalized friction ratio less than 22, Delta Q less than 20, fines content greater than 21 percent and coefficient of uniformity greater than 1,000.

Table 1: Summary of Observed Transition Points Describing the Onset of Decrepitation for Crushed Leach Copper Ore under Sulfuric Acid Leaching Conditions

Relationship Investigated		Transition Points Observed				
Parameter 1	Parameter 2	k (cm/s)	F_r (%)	Delta Q	FC (%)	C_u
Hydraulic Conductivity	Normalized Friction Ratio	2×10^{-5}	5.0	–	–	–
Hydraulic Conductivity	1 / Normalized Friction Ratio	5×10^{-5}	4.5	–	–	–
Hydraulic Conductivity	Delta Q	1×10^{-4}	–	18.5	–	–
Hydraulic Conductivity	Fines Content	3×10^{-5}	–	–	23	–
Hydraulic Conductivity	Coefficient of Uniformity	2×10^{-5}	–	–	–	1,500
1 / Normalized Friction Ratio	Fines Content	–	4.2	–	20	–
1 / Normalized Friction Ratio	Coefficient of Uniformity	–	4.3	–	–	650
Delta Q	Fines Content	–	–	20	19	–
Delta Q	Coefficient of Uniformity	–	–	20	–	700

Future work on the topic of decrepitation includes expanding the existing database to include CPT, hydraulic conductivity, and laboratory-based data from other crushed leach copper ore stockpiles under sulfuric acid leaching conditions, as well as including at least mineralogy-based parameter(s) to the list of transition points. The overarching objective of this paper along with the companion paper (Grass et al., 2025) and forthcoming studies based on the future work, in conjunction with the site geotechnical and

operational teams as well as a third-party reviewer, is to identify, limit, and/or mitigate the impact of decrepitation on slope stability and operational efficiency of copper ore HLFs subjected to sulfuric acid leaching to improve copper recovery through new design parameters.

Acknowledgements

This work could not have been completed without the support, encouragement, and input from Freeport-McMoRan Inc. The sharing of useful data, ideas, and insights by Teresa Speigl, Georgia Lysay, Kanyembo Katapa, Salvador Ortiz, John Lupo and others has been helpful and is greatly appreciated.

References

Begemann, H. K. S. (1965). The friction jacket cone as an aid in determining the soil profile. *Proceedings of the 6th International Conference on Soil Mechanics and Foundation Engineering (ICSMFE)*, Montreal, Canada, 2, 17–20.

Bouwer, H., & Rice, R. C. (1976). A slug test method for determining hydraulic conductivity of unconfined aquifers with completely or partially penetrating wells. *Water Resources Research, 12*(3), 423–428.

Breitenbach, A. J., & Thiel, R. S. (2005). A tale of two conditions: Heap leach pad versus landfill liner strengths. *North American Geosynthetics Society / Geosynthetics Research Institute 19 Conference*, Las Vegas, NV, December 2005.

Chahua, L., Barreda, G., Satelo, G., & Narva, M. (2016). Study of the behavior of materials with fines content in heap leaching processes. *Heap Leach Solutions 2016*, Lima, Peru, October 2016.

Grass, M. J., Jester, C. D., Taukoor, V., Manjarrez, L., & Ortiz, S. (2025). Decrepitation of crushed leach copper ore under sulfuric acid leaching conditions – Part 1. *Heap Leach Solutions 2025*, Sparks, NV. (Accepted for presentation).

Robertson, P. K. (1990). Soil classification using the cone penetration test. *Canadian Geotechnical Journal, 27*(1), 151–158.

Saavedra, A. (2014). Permanent heap leach phreatic level characterization with the aid of CPTu soundings. *Heap Leach Solutions 2014*, Lima, Peru, November 2014.

Saye, S. R., Santos, J., Olson, S. M., & Leigh, R. D. (2017). Linear trendlines to assess soil classification from cone penetration test data. *Journal of Geotechnical and Geoenvironmental Engineering, 143*(9), 04017060.

Schneider, J. A., Hotstream, J. N., Mayne, P. W., & Randolph, M. F. (2012). Comparing CPTu Q–F and Q–$\Delta u2/\sigma'v0$ soil classification charts. *Géotechnique Letters, 2*(4), 209–215.

Schneider, J. A., Randolph, M. F., Mayne, P. W., & Ramsey, N. R. (2008). Analysis of factors influencing soil classification using normalized piezocone tip resistance and pore pressure parameters. *Journal of Geotechnical and Geoenvironmental Engineering, 134*(11), 1569–1586.

Torres, G., Pinos, S., Soto, C., & Moffat, R. (2022). Geotechnical evaluation of properties and liquefaction potential using CPTu for heap and ROM leaching facilities. *Heap Leach Solutions 2022*, Sparks, NV, October 2022.

Van Zyl, D., Hutchison, I., & Kiel, J. (1988). *Introduction to evaluation, design and operation of precious metal heap leaching projects.* Society of Mining Engineers Inc.

Consequence Classification Approach for Heap Leach Pad Design

Franco Sánchez, Anddes, Peru
Jesus Negrón, Anddes, Peru
Denys Parra, Anddes, Peru
Romy Valdivia, Anddes, Mexico

Abstract

Heap leach pads are structures used in mining for the extraction of metals such as gold, copper, nickel, and uranium. While heap leach pad failures have been very rare throughout history and have typically generated minor impacts compared to tailings dams, they can shut down mining production, significantly affecting the profitability of the operation. Therefore, it is crucial to implement design procedures that minimize the risks associated with these facilities.

This paper proposes applying a similar approach used for tailings dam classification to heap leach pad projects, based on the consequences of a potential failure. This approach is based on the recommendations of international guidelines such as the Canadian Dam Association (CDA, 2019) and the Global Industry Standard on Tailings Management (ICMM, 2020), which establish categories of failure consequences for tailings dams ranging from low to extreme. This involves a detailed analysis of aspects such as the proximity of operating personnel and populations, the vulnerability of nearby ecosystems, the infrastructure that could be affected, and the economic, social, and cultural repercussions of a potential heap leach pad collapse.

This classification will enable the determination of return periods for seismic and flood events that must be considered in the design of these facilities, thereby reducing the risk of failure. Due to the limited impacted areas, high return periods are not expected to be used, at least during the operational phase.

Implementing this procedure involves quantifying the magnitude of potential impacts to support classification. Adopting this methodology not only seeks to improve the safety and efficiency of leach pads but also ensures operational continuity of mining operations, avoiding costly interruptions and promoting more responsible and sustainable mining practices.

Introduction

Heap leach pads are designed to ensure physical stability and operational efficiency during the operation,

closure, and post-closure phases of mining projects. Despite their widespread use, there is currently no specific international guide that consolidates the technical criteria required for their design. For this reason, engineers rely on best practices and adapt regulatory guidelines for other structures such as water dams, waste rock dams, or tailings dams.

A key aspect of the design of this type of facility is assessing the level of consequences that a potential failure could generate. This determines not only the required factors of safety but also the return periods that must be considered for seismic and hydrological events. Guidelines such as those from the Canadian Dam Association (CDA, 2019) and the Global Industry Standard on Tailings Management or GISTM (ICMM, 2020) present consequence classification procedures for tailings dams ranging from Low to Extreme, and which can be extended to heap leach pads, due to the operational and environmental risks they entail.

This article argues that incorporating consequence classification criteria into heap leach pad design is not only feasible but necessary. It proposes adapting methodologies used in tailings dams, integrating rigorous analyses of credible failure mechanisms, environmental and social exposure, and quantification of downstream impacts.

As a practical demonstration, a case study of a leach pad in southern Peru is presented, where this methodology was applied. The assessment included stability analyses with minimum credible parameters and simulations of failure and its runout distance, which allowed for quantifying the impacts and assigning a technical classification supported by objective data. This approach seeks to contribute to more rigorous risk management aligned with international standards, promoting more responsible and sustainable practices in the operation of heap leach pads.

Criteria for Heap Leach Pad Design

Heap leach pad projects are designed to guarantee their physical stability and ensure adequate performance during their operation, closure, and post-closure phases. The criteria used to evaluate physical stability are based on factors of safety and the magnitude of the displacement that the structure can tolerate.

Currently, there is no specific guide that groups together all the criteria necessary for the design of heap leach pads. Therefore, the design criteria are defined by taking into account good engineering practices and the recommendations of guides developed for other earth structures such as water dams, tailings dams, and waste dumps. These criteria are based on the exposure time, the reliability of the available information, and the level of consequence that a potential failure of these facilities could generate. Hawley and Cunning (2017) developed a guide for the design of waste rock dumps and proposed factors of safety for static (FS of 1.3 to 1.5) and pseudostatic (FS of 1.05 to 1.10) loads, which depend on the reliability of the available information and the level of consequence, but they do not indicate the return periods for seismic events and

flooding that should be considered in the design. This guide defines three levels of consequence: low, moderate, and high, which are determined by considering the slope angle and height, potential environmental impact, the presence of nearby critical infrastructure, and the intensity and frequency of annual rainfall.

International guides such as the Canadian Dam Association (CDA, 2019) and the Global Industry Standard on Tailings Management (GISTM, 2020) are used to design tailings dams. These guides propose the minimum factors of safety to be considered in the design for static loads (FS from 1.2 to 1.5) and pseudo-static loads (minimum FS 1.0), which depend on the exposure time (temporary or permanent) and the different phases of the structure's life cycle (construction, operation, closure, and post-closure). In addition, they recommend using a return period for the earthquake and the design flood according to the consequence classification level. These guides define up to five consequence levels: low, significant, high, very high, and extreme, which are determined considering the possible impacts of a tailings dam failure on the potential population at risk, potential loss of life, impacts on the environment, social, cultural, infrastructure, and economy.

According to the guide proposed by Hawley and Cunning (2017), the consequence level of a waste rock dump is determined qualitatively, taking into account the dump's geometry. The consequence classification proposed in the CDA and GISTM guides is more rigorous because it considers the potential loss of life and the economic impact of repairing potential damage, among other factors. To quantify the impacts, the CDA and GISTM guides recommend performing a dam break analysis, simulating a credible failure mechanism.

With the goal of achieving a robust design that integrates the current knowledge base and minimizes the risk of failure that could affect people and the environment, while also considering the social context, the authors propose that heap leach pads be designed with consequence levels in mind. To do this, credible failure mechanisms must be determined, considering all available geotechnical information, and then performing a runout analysis to determine the impacts downstream of the heap.

Criteria for Determining the Level of Classification by Consequence

To determine the level of consequences of a heap leach pad failure, credible failure mechanisms must be defined taking into account all available geotechnical information and external agents that could generate a possible failure of the structure, which may be associated with a seismic event, loss of strength of the materials due to lack of control during construction and operation, saturation due to irrigation effects, among others. With the credible failure mechanism and the strength properties of the material, the shape of the failure surface is defined, for which a factor of safety of less than 1.0 is obtained, which indicates that

the structure will fail. A runout analysis can then be performed to determine the impacts downstream of the leach pad.

Geotechnical Evaluation

In heap leach pad projects, rotational and block-type faults can occur, as shown in Figure 1. Generally, rotational fault mechanisms develop along the heap ore at the bench and interbench levels, and in some cases, they reach global failures, while block-type faults are generated by the interface zone, that is, at the contact of the foundation soil with the geosynthetic that makes up the heap liner system. The failure mechanisms in heap leach pads depend on the shear strength properties and hydraulic conductivity of the stacked mineral and the shear strength of the interface system. As shown in Figure 1, during the operation stage, in some cases of heap leach pads with ore that have a high fines content, which is increasingly common, saturated or near-saturation zones can be generated by irrigation, and therefore, excess pore pressures will be generated because of the undrained conditions. These conditions cause the ore to behave differently in each sector of a heap leach pad.

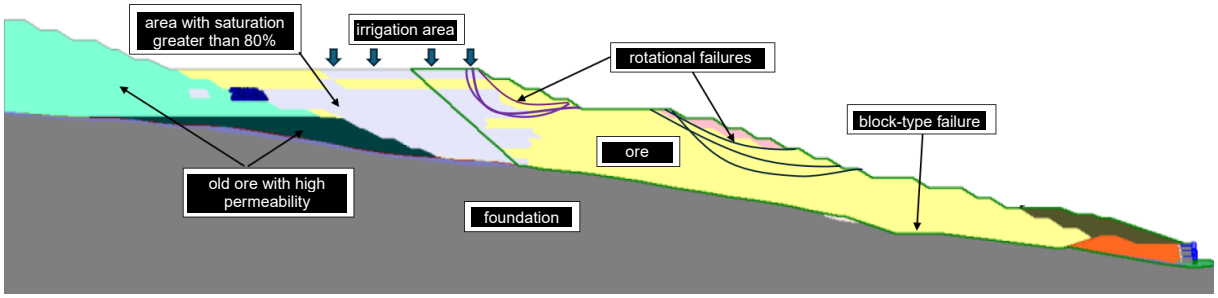

Figure 1: Failure mechanisms in heap leach pads

To define the consequence classification level, the GISTM establishes that the most credible failure mechanism must be determined. Therefore, in heap leach projects, a slope stability analysis must be performed with reliable geotechnical information to define the minimum credible material parameters and potential external agents that could cause a heap failure.

Figure 2 shows a gold heap leach pad located in southern Peru. The part shown in this figure, which controls the stability of the leach pad, has been built on a rock foundation and has a reinforced soil wall and buttress at its base to ensure its physical stability. The design was carried out considering the consequence classification proposal, following the general guidelines of the CDA and GISTM guides.

Figure 2: General layout of the heap leach pad

The leach pad shown in Figure 2 is supported by geotechnical information obtained during the design, construction, and operational stages. During the design stage, geotechnical field investigations, such as test pits, drill holes, geophysical, sampling, and laboratory testing, were conducted to characterize the foundation soil and the materials to be used in the leach pad construction. Subsequently, during the construction stage, the use of appropriate construction materials was verified during the quality control and quality assurance; also, laboratory tests were performed to characterize the strength properties of the materials that control the leach pad stability (fill and liner materials); the laboratory tests were performed with samples of the same materials used in the leach pad construction. As part of the mine's best practices, the stacked ore is sampled and tested frequently to determine its geotechnical characteristics. Records indicate that the stacked ore has not exceeded the design parameter associated with the maximum possible fine content. During the operational phase, sonic drilling and CPTU testing were also performed to determine the undrained residual strength, a parameter used in stability analyses in areas with saturation greater than 80% due to the ore with high fines content placed in the earlier stages of the operation with no rigorous control. These best practices in data management allow us to conclude that the geotechnical information available on the leach pad is robust and reliable.

Based on the existing information, it was determined that two credible failure mechanisms could occur in the leach pad. The first corresponds to failures through the ore due to the material being discharged by dumping and then moistened by irrigation. In some previously identified older areas where adequate fine control was not maintained, irrigation has produced saturation, but the pore water pressure generated is

dissipated after irrigation stops. The second mechanism corresponds to failure at the interface zone because it presents the lowest shear strength. To determine the shape and extent of the possible failures, the strength properties of the materials that make up the leach pad were interpreted. Figure 3 shows the interface strength parameters defined during the design and construction stages. As seen in this graph, the strength is homogeneous and does not have much variability; therefore, the lowest strength value can be considered the minimum credible strength.

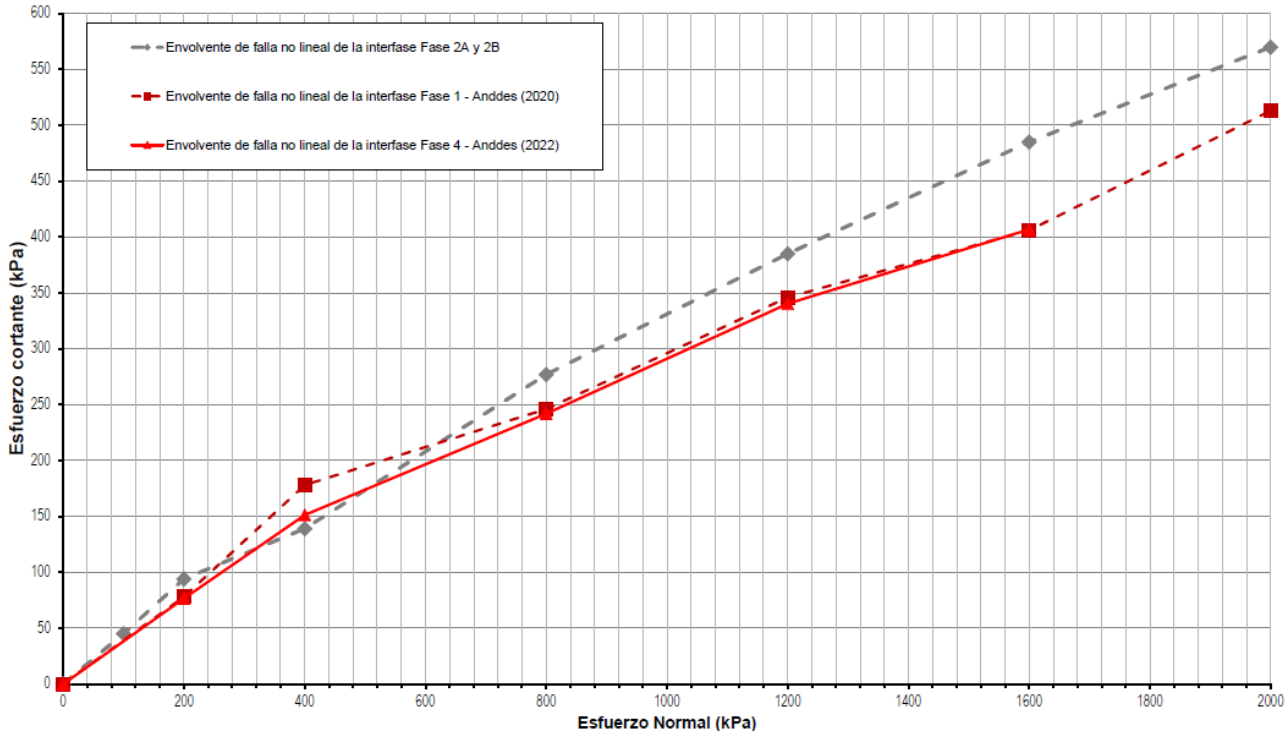

Figure 3: Shear strength of the leach pad interface system

Figure 4 shows the variation in the drained ore angle of friction according to the confinement level and for different percentages of fines. This information has been placed on the well-known graph proposed by Leps (1970). As seen in this figure, the drained friction angle is greater than 36° for any confinement level, so this value can be considered the minimum credible strength.

Furthermore, due to continuous irrigation in the leach heap, the ore moisture content during the operating stage can vary from dry to saturated in some zones. To determine the ore strength properties under these conditions, CPTu tests were performed in different areas of the heap. Figure 5 shows the variation in the internal angle of friction with depth obtained in all the CPTu conducted in the heap. According to this Figure, the ore with low moisture could have a minimum friction angle of 32.5° according to the correlation proposed by Kullhavy and Mayne (1990), while the saturated ore could have an undrained friction angle of the order of 5° according to Olson and Stark (2003).

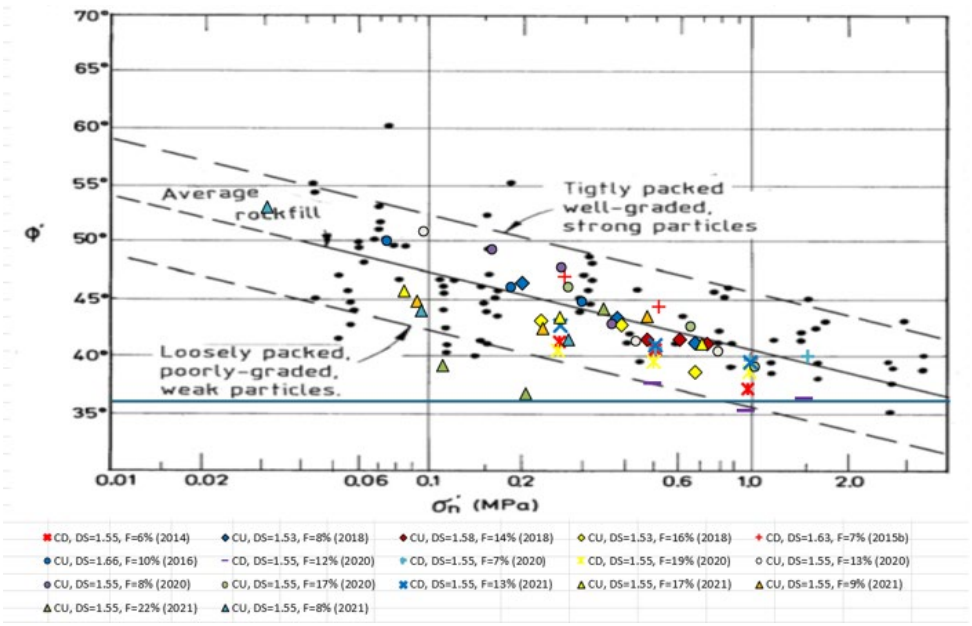

Figure 4: Drained strength of stacked ore

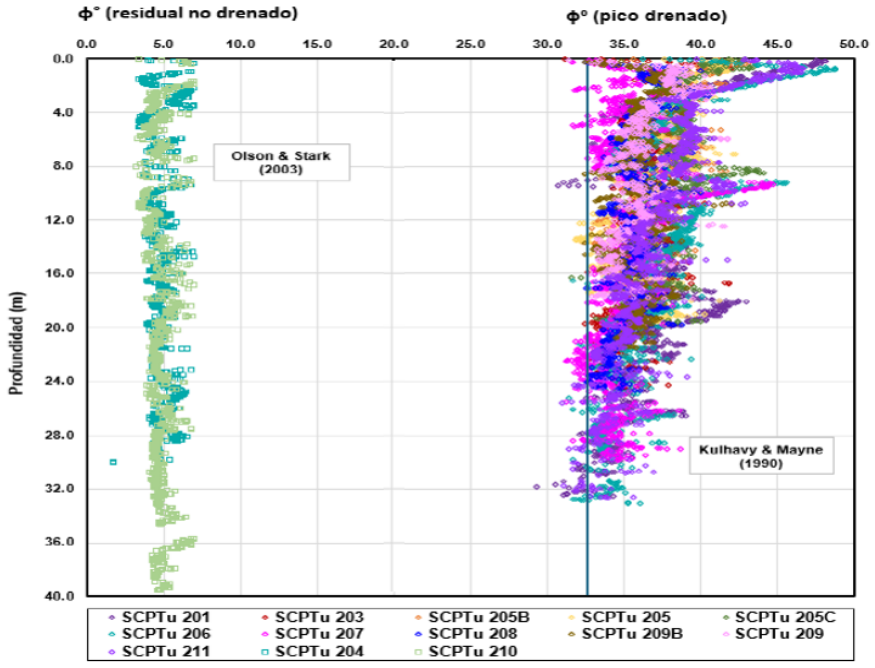

Figure 5: Undrained residual strength and peak strength of the ore

To determine the shape and extent of potential failure surfaces, geotechnical stability analyses were performed considering the minimum credible parameters, maintaining the irrigation sequence and the presence of potential credible external agents such as earthquakes or saturation of certain zones of the heap. Figure 6 shows that the failure surface passing through the interface shows the lowest safety factor for static conditions and is also very similar to the failure surface under pseudostatic conditions, considering the

maximum credible earthquake (MCE). Therefore, this failure surface must be used to determine the classification level.

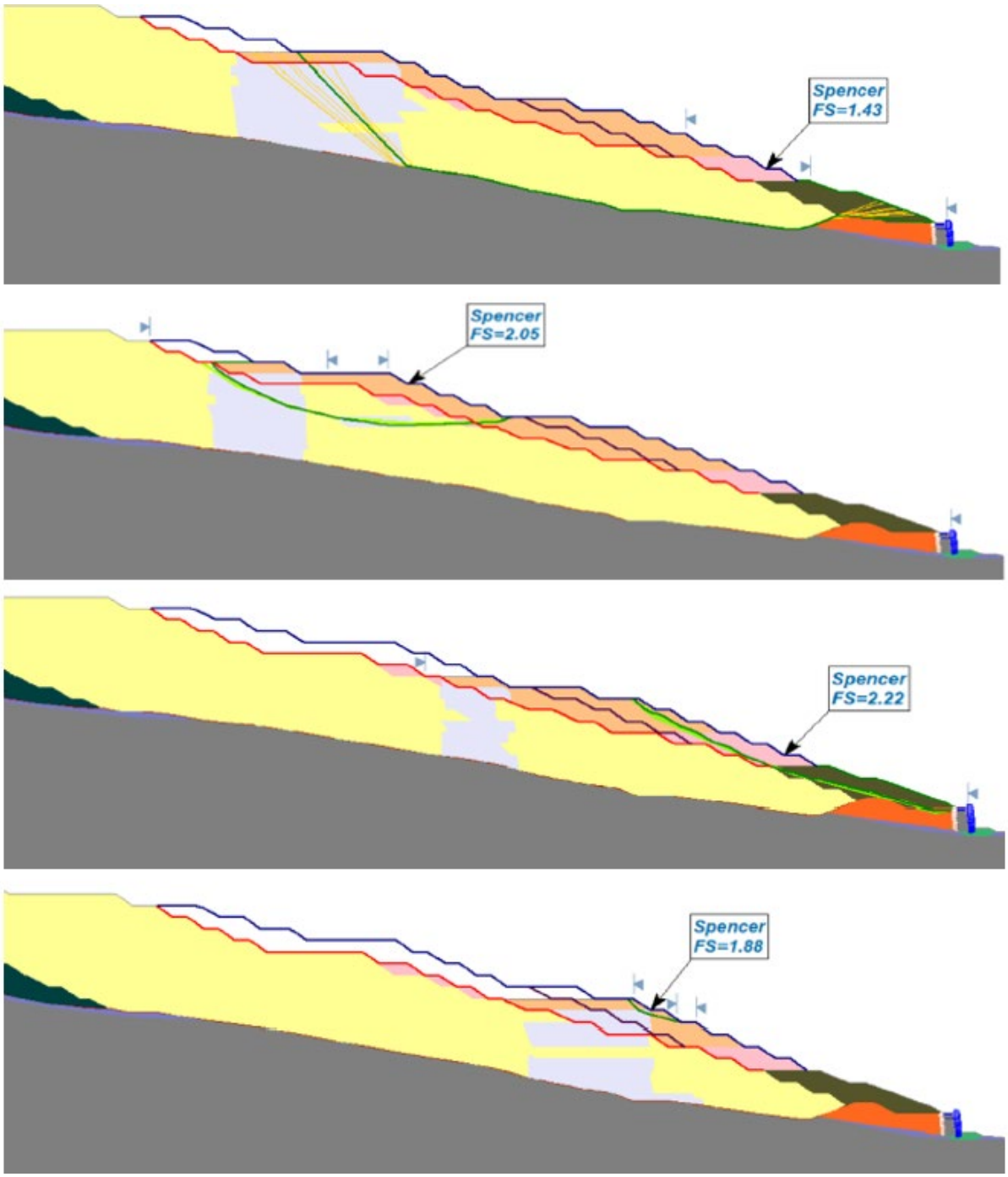

Figure 6: Failure surfaces for static loads

After defining the credible failure surface, a runout analysis was performed to determine the potential impacts downstream of the heap leach pad. For the runout simulation, a two-dimensional model

implemented in RiverFlow2D software was used, capable of simulating the flow of non-Newtonian fluids, as described in the document "RiverFlow2D Two-Dimensional Flood and River Dynamics Model" developed by Hydronia (2025). The Mud and Tailings Flow module is capable of simulating the flow of hyperconcentrated sediment flows, mudflows, torrential avalanches, and runouts or landslides.

The model requires input data such as the digital elevation of the existing terrain, the failure surface, and the ore stacking in the runout area, terrain roughness, and geotechnical material parameters such as density and angle of friction. Since the runout analysis performed by Riverflow2D does not allow the inclusion of external forces and a single material with its properties can be entered, stability simulations were performed in the Slide program until an equivalent angle of friction was found that represents the strength of the ore that generates a failure condition similar to the critical surface obtained in the pseudostatic analysis and that this strength is consistent with the properties of the ore, which could have an angle of friction between 5° and 36° depending on the ore moisture content. The analyses indicate that with an equivalent friction angle of 20°, a very similar failure mechanism would occur in the event of a seismic event. The failure surface considered in the runout analysis is shown in Figure 7.

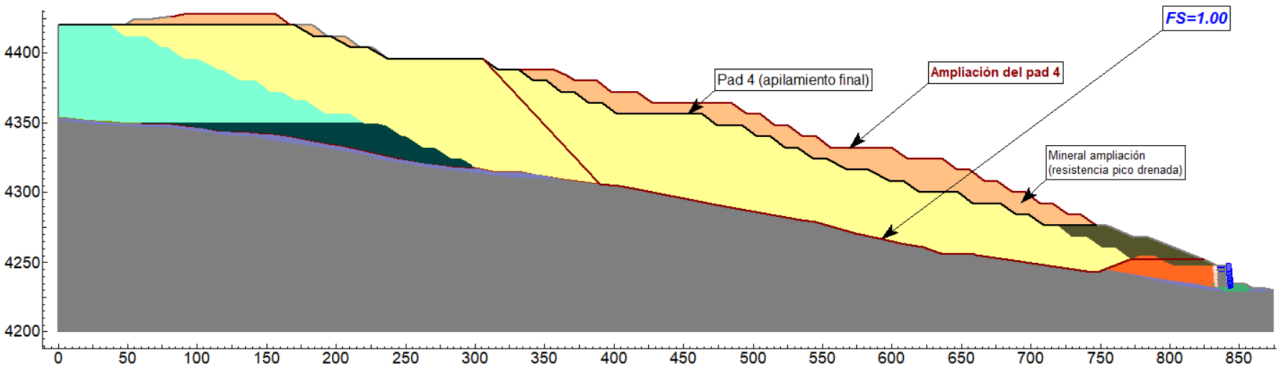

Figure 7: Failure surface in seismic conditions considering the maximum credible earthquake

The results of the runout analysis are shown in Figures 8 and 9. According to the impact footprint, presented in Figure 8, in the event of a hypothetical failure of the leach pad, the displaced material would be contained within the operational area of the pad and would not impact the reinforced soil wall, the operating accesses, or the process plant area. The hypothetical failure would generate local landslides at the bench and inter-bench levels, and the upper part of the heap would have a vertical and horizontal displacement of 4.0 m and 13.2 m, respectively. In the lower part, an accumulation of 10.2 m of ore was determined, which will be retained in the buttress bench, and a horizontal displacement of up to 77 m, which will be retained on the crest and slope of the buttress. With this magnitude of displacement of the heap, significant damage to the liner system would be expected, which was considered to determine the classification level accordingly.

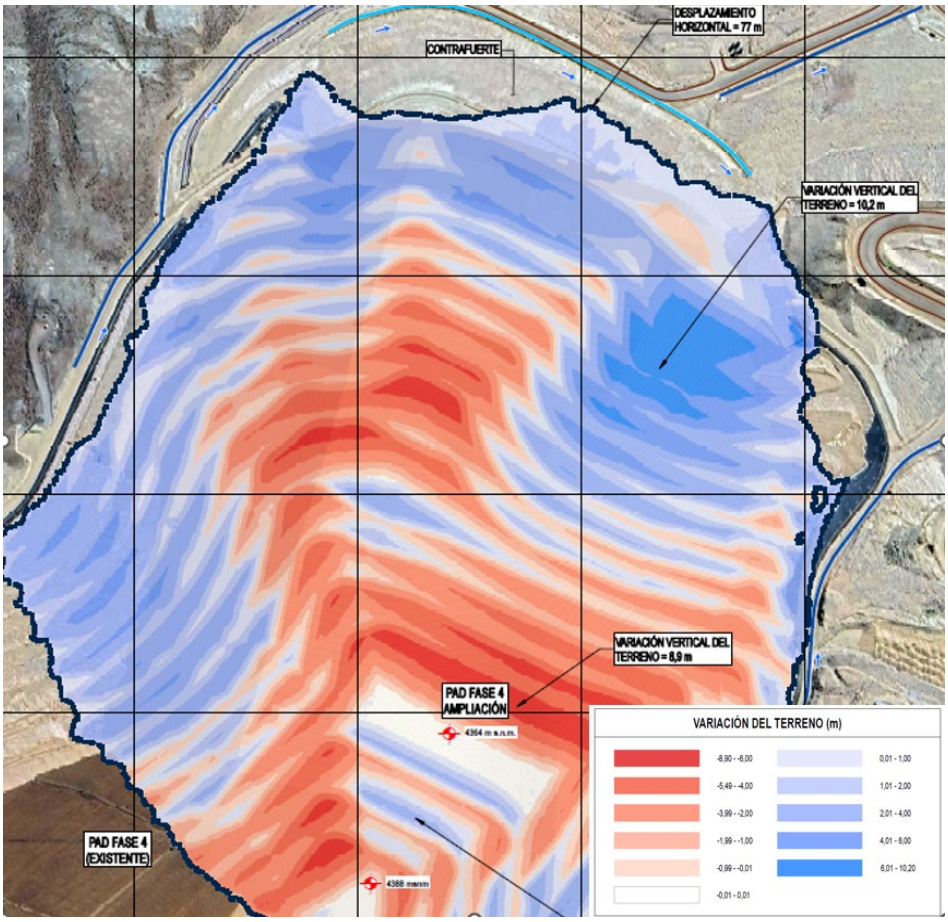

Figure 8: Displacements obtained from the runout analysis—plan view

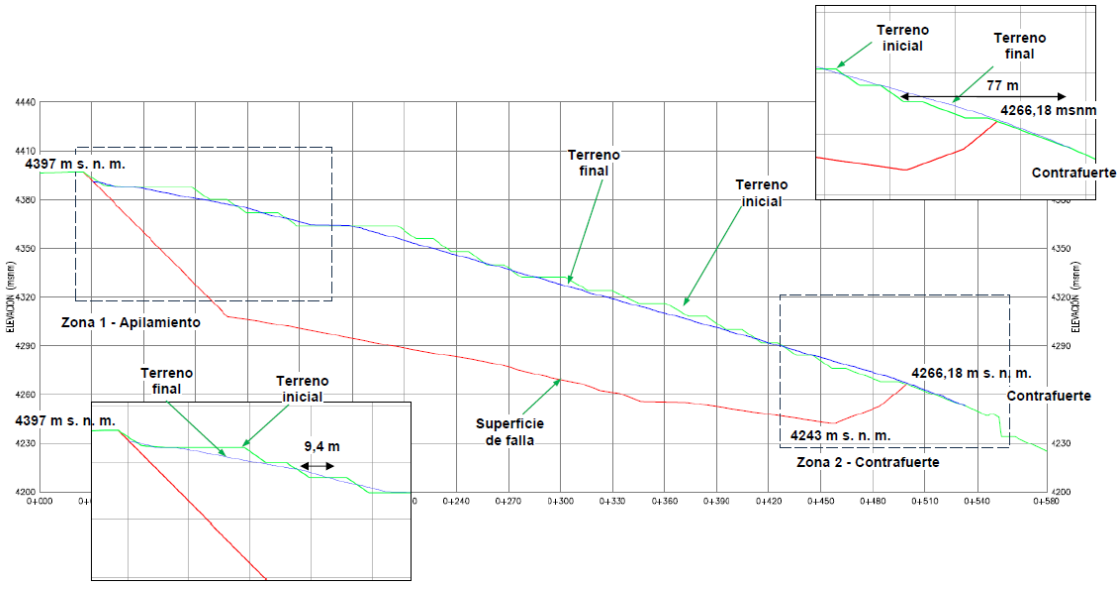

Figure 9: Displacements obtained from the runout analysis—section

Classification Criteria

GISTM Criteria

The GISTM establishes, as part of the requirements for the design, construction, operation, and monitoring of tailings facilities, that the classification of tailings facilities by failure consequences based on credible failure modes must be determined.

The classification scheme considers consequences affecting: potential population at risk, potential loss of life, environment, health, cultural and social aspects, and infrastructure and economy losses. The GISTM criteria to be considered are presented in Table 1.

Table 1: GISTM Criteria

Classifi-cation	Potential Population at Risk	Potential Loss of Life	Environment	Health, Social, and Cultural	Infrastructure and Economics
Low	None	None expected	Minimal short-term loss or deterioration of habitat or rare and endangered species.	Minimal effects and disruption of business and livelihoods. No measurable effect on human health. No disruption of heritage, recreation, community, or cultural assets.	Low economic losses: area contains limited infrastructure or services. <US$1M.
Significant	1–10	Unspecified	No significant loss or deterioration of habitat. Potential contamination of livestock/fauna water supply with no health effects. Process water with low potential toxicity. Tailings are not potentially acid-generating and have low neutral leaching potential. Restoration is possible within 1 to 5 years.	Significant disruption of business, service, or social dislocation. Low likelihood of loss of regional heritage, recreation, community, or cultural assets. Low likelihood of health effects.	Losses to recreational facilities, seasonal workplaces, and infrequently used transportation routes. <US$10M.
High	10–100	Possible (1 – 10)	Significant loss or deterioration of critical habitat or rare and endangered species. Potential contamination of livestock/ fauna water supply with no health effects. Process water is moderately toxic. Low potential for acid rock drainage or metal leaching effects of released tailings. Potential area of impact 10 km^2 – 20 km^2. Restoration is possible but difficult and could take > 5 years.	500-1,000 people affected by the disruption of business, services, or social dislocation. Disruption of regional heritage, recreation, community, or cultural assets. Potential for short-term human health effects.	High economic losses affecting infrastructure, public transportation, commercial facilities, or employment. Moderate relocation/compensation to communities. <US$100M.
Very High	100 – 1,000	Likely (10 – 100)	Major loss or deterioration of critical habitat or rare and endangered species. Process water is highly toxic. High potential for acid rock drainage or metal leaching effects from released tailings. Potential area of impact > 20 km^2. Restoration or	1,000 people affected by the disruption of business, services, or social dislocation for more than one year. Significant loss of national heritage, community, or cultural assets. Potential for	Very high economic losses affecting important infrastructure or services (e.g., highway, industrial facility, storage facilities for dangerous substances), or employment. High

Classifi-cation	Potential Population at Risk	Potential Loss of Life	Environment	Health, Social, and Cultural	Infrastructure and Economics
			compensation is possible, but very difficult and requires a long time (5 years to 20 years).	significant long-term human health effects.	relocation/compensation to communities. < US$1B.
Extreme	> 1,000	Many (> 100)	Catastrophic loss of critical habitat or rare and endangered species. Process water is highly toxic. Very high potential for acid rock drainage or metal leaching effects from released tailings. Potential area of impact > 20 km^2. Restoration or compensation in kind is either impossible or requires a very long time (>20 years).	5,000 people have been affected by the disruption of business, services, or social dislocation for years. Significant National heritage or community facilities, or cultural assets destroyed. Potential for severe and/or long-term human health effects.	Extreme economic losses affecting critical infrastructure or services (e.g., hospital, major industrial complex, major storage facilities for dangerous substances) or employment. Very high relocation/compensation costs to communities, as well as very high social readjustment costs. >US$1B.

CDA Criteria

The technical bulletin Application of Dam Safety Guidelines to Mining Dams (CDA, 2019) classifies mining dams according to the consequences of a likely dam failure and the displacement of tailings and water resulting from the failure.

The classification scheme considers the following consequences: population at risk, loss of life, loss of environmental and cultural values, and economic and infrastructure losses. The CDA criteria to be considered are presented in Table 2.

Table 2: CDA Criteria

Dam Class	Population at Risk	Loss of Life	Environmental and Cultural Values	Infrastructure and Economics
Low	None	0	Minimal short-term loss No long-term loss	Low economic losses; area contains limited infrastructure or services
Significant	Temporary only	Unspecified	No significant loss or deterioration of fish or wildlife habitat Loss of marginal habitat only Restoration or compensation in kind is highly possible	Losses to recreational facilities, seasonal workplaces, and infrequently used transportation routes
High	Permanent	10 or fewer	Significant loss or deterioration of important fish or wildlife habitat Restoration or compensation in kind is highly possible	High economic losses affecting infrastructure, public transportation, and commercial facilities
Very high	Permanent	100 or fewer	Significant loss or deterioration of critical fish or wildlife habitat Restoration or compensation in kind is possible but impractical	Very high economic losses affecting important infrastructure or services (e.g., highway, industrial facility, storage facilities for dangerous substances)
Extreme	Permanent	More than 100	Major loss of critical fish or wildlife habitat Restoration or compensation in kind is impossible	Extreme losses affecting critical infrastructure or services (e.g., hospital, major industrial complex, major storage facilities for dangerous substances)

Consequence Analysis

Sectors 1 and 4 of the leach pad, as presented in this study, were evaluated independently based on their unique characteristics. This paper summarizes the current conditions and consequences for each sector.

Impact on Infrastructure and Economy

To estimate the impact on infrastructure and the economy, the cost of damage, remediation, and corresponding sanctions in the event of a failure event for each sector has been estimated. It is shown in Tables 3 and 4.

Table 3: Costs of Damage to Infrastructure—Sector 1

Description	Unit	Quantity	Unit cost (US$/unit)	Cost (US$)
1 Infrastructure repair				
1.1 Interlift area to implement	m²	82,550	53	4,375,150
2 Environmental remediation				
2.1 Hydrogen peroxide treatment	m³	137	3	411
2.2 Soil removal	m³	274	16	4,384
3 Social compensation				
3.1 Affected population	Pop.	10	10,000	100,000
3.2 Fatalities	Pop.	0	10,000,000	0
4 Economic sanctions				
4.1 Fines	gbl	1	230,000	230,000
Total				**4,709,945**

Regarding the repair of the damaged infrastructure, specifically the rupture of the geomembrane due to the failure, thus preventing the solution from leaking and allowing the continued ore stacking on the leach pad, the following options were considered for the continuity of operations:

- Removal of material displaced during the failure.
- Repair of the geomembrane.
- Use of other non-toxic leaching agents.
- Placement of leached ore and termination of irrigation.
- Installation of an intermediate liner or interlift system.

Among these options, the installation of an interlift proved to be the most cost-effective. The costs of the interlift area to be implemented were estimated for Sectors 1 and 4, considering an area of 187,000 m² and 478,000 m², respectively.

Table 4: Costs of Damage to Infrastructure—Sector 4

Description	Unit	Quantity	Unit Cost (US$/Unit)	Cost (US$)
1 Infrastructure repair				
1.1 Interlift area to implement	m^2	45,000	53	2,385,000
2 Environmental remediation				
2.1 Hydrogen peroxide treatment	m^3	137	3	411
2.2 Soil removal	m^3	274	16	4,384
3 Social compensation				
3.1 Affected population	hab	10	10,000	100,000
3.2 Fatalities	hab	0	10,000 000	0
4 Economic sanctions				
4.1 Fines	gbl	1	115,000	115,000
Total		**45,000**	**53**	**2,385,000**

As indicated above, the sliding of the overall slope of the leach pad would generate contaminant seepage due to rupture of the geomembrane. To remediate this contamination, a seepage rate of 1,000 L/day was considered, with 1 year of discharge into the environment 365 days a year, and 37.5% of the solution being released into the environment, resulting in a discharge of 137 m^3. The impacted soil, which would have a volume equivalent to twice the volume of the solution leak, would be treated with hydrogen peroxide and then removed. A direct cost of US$ 0.91/m^2 was considered for the hydrogen peroxide treatment item, as shown in Table 5.

Table 5: Unit Cost of Hydrogen Peroxide Treatment

Item—Description	Unit	Total Reagent Consumed	Cost by Unit (US$/kg)	Total Cost of the Reagent (US$/kg)	Unit Cost (US$/$m^3$)
Total treated flow rate	7,150 m^3				
H_2O_2 consumption	kg	6,370.50	0.63	4,013.42	0.56
$CuSO_4$ consumption	kg	358.00	2.20	787.60	0.11
NaOH consumption	kg	227.00	0.87	197.49	0.03
NaSH consumption	kg	515.05	0.74	381.14	0.053
Coagulant CT-3160 consumption	kg	752.82	1.50	1,129.23	0.16
Floculant CT. 3560 consumption	kg	4.46	4.50	20.07	0.003
Total cost	**(US$/kg)**			**6,528.94**	
Total cost of treated flow	**(US$/$m^3$)**			**0**	**0.91**

A direct cost of US$6.36/m^3 was considered for the soil removal item according to the unit price analysis shown in Table 6.

Table 6: Unit Cost of Removing Contaminated Soil

Description	Unit	Resources	Quantity	Cost	Subtotal
1 Labor					2.79
1.1 Foreman	hours	0.10	0.0075	18.75	0.14
1.2 Journeyman	hours	0.50	0.0375	14.26	0.53
1.3 Laborer	hours	2.00	0.1500	14.11	2.12
2 Equipment					3.57
2.1 Tools			5.0000	2.79	0.14
2.2 Wheeled backhoe (60-80 HP)	machine hours	1.00	0.0750	45.74	3.43
Total cost					**6.36**

A direct cost of US$22.00/m^2 was considered for the interlift area to be implemented, considering the construction costs of leach pads with similar characteristics from projects in the Anddes database. Table 7 shows the costs per unit of measurement for hydrogen peroxide treatment, soil removal, and the interlift area (m^2).

Table 7: Cost of Items

Description	Percentages	Hydrogen Peroxide Treatment	Soil Removal (US$/m^3)	Interlift Area (US$/m^2)
Direct Construction Cost (CD)		0.91	6.36	22.00
Overhead expenses (GG)	35 %	0.32	2.23	7.70
Profit, (U), 10 %CD	10 %	0.09	0.64	2.20
Construction budget (PC), CD+GG+U		1.32	9.22	31.90
Equipment fuel cost (% = fuel / CD)	20 %	0.18	1.27	4.40
Supervision (S)	10 %	0.15	1.05	3.63
Owner Cost (CP)	6 %	0.10	0.69	2.40
Contingency (CO)	25 %	0.44	3.06	10.58
Cost (PC+COMB+S+CP+CO)		2.19	15.30	52.91
Rounded cost		3.00	16.00	53.00

To estimate the cost of a lost life, the U.S. Department of Transportation (DOT) guidelines, which quantify the value of a statistical life at $10.5 million, were used as a reference. A figure of $10 million was

used as a reference. For the affected population, compensation of $10,000 is also considered, a figure derived from the same guidelines.

Likewise, based on the workshops held, it was concluded that fines or sanctions should be considered. The Peruvian government's Supreme Decree 016-93-EM of January 5, 2009, which regulates environmental protection in mining and metallurgical activities, was considered. Article 47 of the aforementioned document details that there is a fine for noncompliance with the rules established by the regulation, which ranges from US$600 to US$575,000. Therefore, due to the severity of the environmental impact explained above, US$230,000 was considered for the estimation of fines due to pollution in Sector 1 and US$115,000 in Sector 4.

Finally, in both sectors of the leach pad, according to Tables 3 and 4, the economic impact ranges between US$1 million and US$10 million. Therefore, the CDA and GISTM classification in terms of economic impact will be Significant in both sectors.

Impact on Potential Population at Risk

In the analysis of the potential population at risk, fewer than 10 people were considered affected by the presence of the access ramp for Sectors 1 and 4 of the leach pad, where trucks with drivers could pass through, i.e., temporary personnel who would work around the landslide zones of the leach pad. Therefore, the impact on the potential population at risk is classified as Significant in both sectors.

Impact on the Potential Loss of Life

The results of the runout analyses for Sectors 1 and 4 do not exceed 2 m of displacement, so they would not affect any infrastructure downstream of the leach pad where permanent personnel are working. However, as explained in the previous item, truck traffic could occur on the ramp to the leach pad, so there is some possibility of a failure occurring when a truck is traveling on the ramp. Therefore, the classification for potential loss of life impact according to the CDA and GISTM is Significant in both sectors.

Impact on the Environment

To analyze the environmental impacts, the solution leak in the pads due to the geomembrane rupture caused by the failure of the leach pad's overall slope was taken into account. In Sector 1, the potential impact is the water source for animals, with minimal, short-term, and insignificant habitat deterioration. Therefore, the CDA and GISTM classification is considered Significant. In Sector 4, no areas of potential impact on water sources for animals or people have been identified, so the CDA and GISTM classification is Low.

Impact on Health, Cultural, and Social Spheres

The health, cultural, and social analysis concluded that there are no impacts due to the lack of populations living near the mine site. Therefore, the GISTM classification is Low, while the CDA does not establish a classification for this aspect.

Global Classification

Based on the above, Table 8 presents a summary of the impacts assessed in the two sectors analyzed of the leach pad. According to this table, the highest classification across all impact types and in both sectors is "Significant"; therefore, this classification is used as the overall classification for both sectors for the leach pad operating conditions.

Table 8: Global CDA and GISTM Classification

Tipo de Impacto	CDA		GISTM	
	Sector 1	Sector 4	Sector 1	Sector 4
Infrastructure and economy	Significant	Significant	Significant	Significant
Potential population at risk	Significant	Significant	Significant	Significant
Potential loss of life	Significant	Significant	Significant	Significant
Environment	Significant	Low	Significant	Low
Health, cultural, and social spheres	N/A	N/A	Low	Low
Global classification	Significant	Significant	Significant	Significant

Conclusion

The following conclusions are presented.

The proposed consequence classification approach is applicable and necessary for the design of heap leach pads, as it enables the incorporation of risk criteria similar to those used in tailings dams and other critical facilities, thereby improving overall safety management.

The presented methodology enables the systematic identification of the most credible failure mechanisms through physical stability analysis and geotechnical characterization, utilizing minimum credible parameters, thereby strengthening the technical basis of the designs.

The use of failure and runout simulation models allows for the quantification of the downstream impact of a potential failure, facilitating the objective classification of the facility based on technical, economic, environmental, and social criteria.

In the case study presented, the only credible exposure is less than 10 temporary personnel (truck drivers, workers) on the access ramp; consequently, the potential population at risk and potential loss of life are both classified as "Significant".

The simulated failure runout remains fully contained within the operational area, with no impact to the reinforced soil wall, operating accesses, or process plant. Expected deformation includes about 4.0 m vertical and 13.2 m horizontal displacement at the upper heap; about 10.2 m more accumulation downslope retained on the buttress bench; and up to 77 m horizontal displacement retained on the buttress crest/slope, which implies significant damage to the liner system.

Considering potential solution leakage from geomembrane rupture: Sector 1, possible short-term impact at an animal water source, classifying as "Significant"; Sector 4, no identified receptors, classifying as "Low". Health/social/cultural impacts are "Low" (no nearby populations).

Using itemized costs (infrastructure repair, environmental remediation, social compensation, and regulatory fines), the credible failure yields a total economic impact between US $2.3 – 4.7 million, which corresponds to "Significant" classification under CDA/GISTM.

It was determined that both analyzed sectors have a "Significant" consequence classification according to the CDA and GISTM guidelines, due to the estimated runout displacements, the potential economic impact, including potential pollution due to the liner rupture, and the potential presence of temporary personnel in access areas. Incorporating this type of classification in the early design stages and during heap modifications or expansions enables the definition of design criteria more closely aligned with the actual risk level, such as earthquake and flooding return periods and differentiated factors of safety.

The classification obtained in this study according to the CDA and GISTM criteria is the same, meaning that for the operating condition, the annual probability of exceedance and the return periods for flooding and earthquakes are very similar in both cases. However, the greatest differences are found in the classification for leach pad closure conditions, in which the GISTM criteria are much more rigorous, since they consider that, for any classification, the recurrence is extreme; for example, the design earthquake must, in all cases, be the 10,000-year return period or the maximum credible earthquake (MCE).

This approach contributes to operational continuity, informed decision-making, and compliance with international standards, promoting more responsible and sustainable mining in the face of current social, regulatory, and environmental expectations.

References

Aydemer, A., & Güven, A. (2020). *Risk assessment of dams*. Cham: Springer.

Canadian Dam Association (CDA). (2019). *Technical bulletin: Application of dam safety guidelines to mining dams*.

Hawley, M., & Cunning, J. (2017). *Mine waste dump and stockpile design*. CSIRO Publishing / CRC Press.

Hydronia. (2025). *RiverFlow2D two-dimensional flood and river dynamics model*.

International Council on Mining & Metals (ICMM). (2020). *Global industry standard on tailings management*.

ISO. (2018). *ISO 31000:2018*.

Kulhawy, F. H., & Mayne, P. (1990). *Manual on estimating soil properties for foundation design*. Prepared by Cornell University, Geotechnical Engineering Group, Hollister Hall, Ithaca, New York.

Leps, T. M. (1970). Review of shearing strength of rockfill. *Journal of the Soil Mechanics and Foundations Division, ASCE, 96*(SM4), 1159–1170.

Olson, S. M., & Stark, T. (2003). Yield strength ratio and liquefaction analysis of slopes and embankments. *Journal of Geotechnical and Geoenvironmental Engineering, 129*(8), 727–737.

U.S. Department of the Interior Bureau of Reclamation, & U.S. Army Corps of Engineers. (2019). *Best practices in dam and levee safety risk analysis*.

Wyllie, D. C. (2024). *Risk management for geotechnical engineering: Hazard, risks and consequences*. Boca Raton: CRC Press.

Xiao, F., Chong-Shi, G., Huai-Z., S., & Xiang-Nan, Q. (2018). Risk analysis of earth-rock dam failures based on fuzzy event tree method. *International Journal of Environmental Research and Public Health, 15*(5), 886.

Opportunities to Improve Heap Leaching Operations

Percy Mayta, PM&H Consulting SAC, Peru
Rosario Mayta, PM&H Consulting SAC, Peru

Abstract

Over the past 40 years, heap leaching operations have evolved significantly, both in terms of operational practices and technological implementation. Despite this evolution, metal recoveries—particularly for gold and copper—often fall short of design expectations and project targets due to a variety of operational challenges. This paper aims to present real-world case studies where substantial improvements in metal recovery were achieved in both large-scale and small-scale heap leaching operations across Chile, Peru, and Argentina. Key operational parameters that were optimized include application rate, irrigation network design, surface preparation, and chart organization. The objective is to share practical insights and strategies that have proven effective in enhancing recovery rates in diverse operational contexts.

Introduction

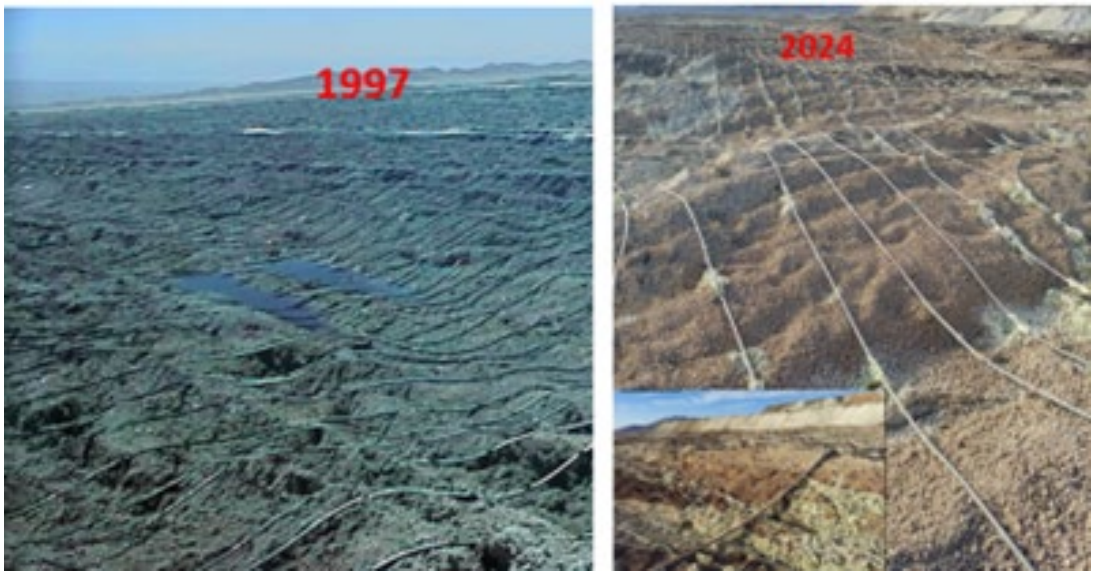

Figure 1: Heap leaching operations evolution?

Throughout the years, we have gained valuable insights into the management of leaching operations, and various new technologies have become available. However, many operational challenges persist, often due

to the lack of consistent attention to fundamental practices.

Figure 1 shows photographs from both a significant mining operation and a smaller-scale facility. It reveals similar patterns in operational behavior, suggesting that the two face comparable challenges in achieving optimal metal recovery.

Opportunities to improve

From my perspective, enhancing the performance of heap leaching operations depends on addressing several key factors, including:

Leaching Chart Organization

The effectiveness of heap leaching operations often depends on the company's operational focus. Below are my suggestions:

- Assign a Superintendent or Supervisor with exclusive responsibility for the leaching area.
- Designate personnel focused solely on irrigation efficiency monitoring and improvement.
- Have a dedicated team responsible for the assembly and maintenance of the irrigation network.
- Provide metallurgical support directly to the leaching operation. This support should be field-based, emphasizing operational improvement rather than being limited to generating historical reports.

Irrigation Network Design

The design of the irrigation network is a critical factor in achieving efficient heap leaching. A well-designed system ensures uniform irrigation, reduces the risk of emitter clogging, and maximizes the leaching coverage area. The following recommendations are based on field experience:

- Use low-capacity drip emitters, 1 lph.
- Apply lower application rates to maximize the area under leaching.
- Maintain square separation between drip emitters.
- Design emitter operation at higher pressure, 25 PSI.
- Ensure homogeneous cell dimensions across the leaching area.
- Utilize appropriately sized solution distribution pipes.
- Use basic tools to monitor leaching performance, for example: pressure indicators and/or flowmeters.

Maximize the Area under Leaching

Irrigation design should address not only freshly prepared flat surfaces but also sloped areas within the

leach pad. Effective slope leaching requires tailored irrigation network designs, and in certain cases, adjusting the original slope angle can significantly enhance irrigation efficiency and overall leaching performance.

Use of Technology to Follow Leaching Efficiency

IOn the field, there are several alternative technologies that monitor leaching efficiency:

- Geophysics: using these tools to monitor irrigation efficiency is crucial for the optimization of heap leaching operations. An example is illustrated in Figure 2:

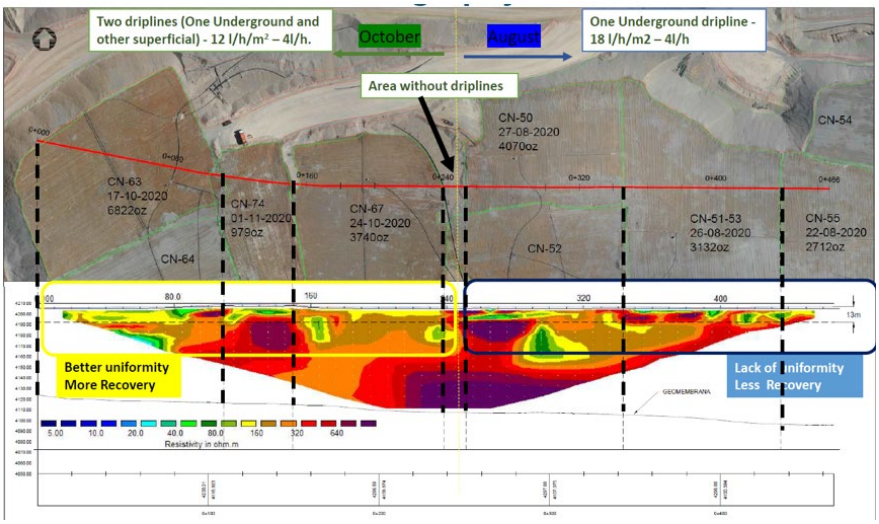

Figure 2: Geophysics results

- Basic automatic control system: efficient leaching performance can be monitored effectively using online pressure indicators alone. The basics of leaching KPI need to be defined. In my opinion, two are crucial:
    - KPI Efficiency LX = (Instantaneous Watering Rate)/(Design Watering Rate) and
    - KPI Op. Modules = Standard deviation pressure irrigation modules. It is relevant to know: Total area under irrigation (cells in operation × area each module).
- Usage of drones: for large irrigation areas, high-resolution video technology can be employed to carry out continuous inspections of leaching operations.

Practical Cases of Leaching Operations Improved

Case 1: Chilean Copper Mine with 225,000 TPY Cathode Production

Figure 3 illustrates the discrepancy between targeted and actual total copper (TCu) recovery. Prior to 2002,

we consistently fell short of the recovery targets. However, beginning in 2002, actual TCu recovery surpassed the objectives. This improvement can be attributed to several key areas of focus:

- Hire a Leaching Superintendent.
- Reduce the application rate from 15 l/h/m^2 to 8 l/h/m^2.
- Design a new irrigation network. Change drip emitter capacity from 4 lph to 1 lph.
- Extend the leaching cycle to increase the lift height, maximize the area under leaching, and reduce the application rate.
- Coordinate leveling of the stacking surface prior to irrigation, using dozers.
- Manage slope irrigation.

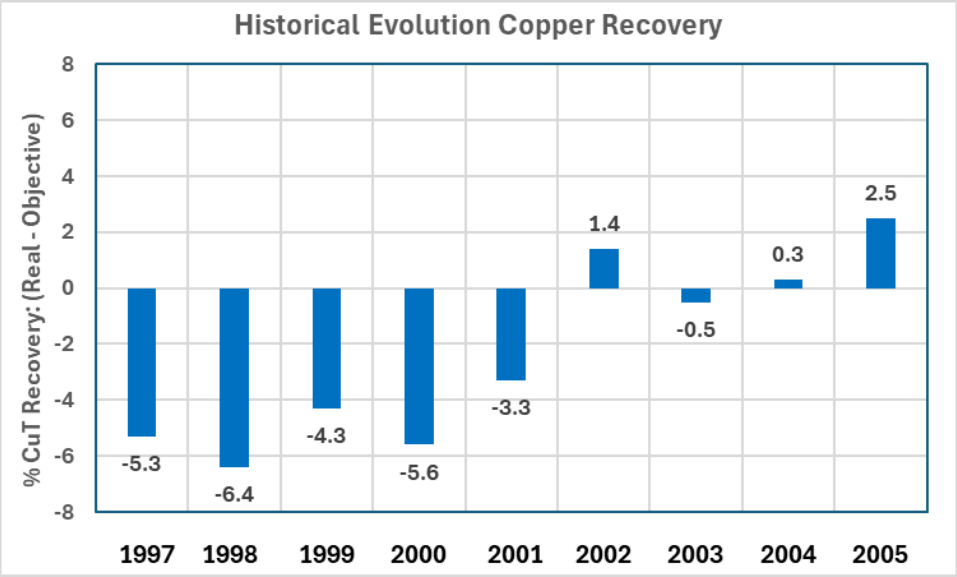

Figure 3: Historical TCu recovery, Chilean Copper Mine

Case 2: Chilean Copper Mine with 125,000 TPY Cathode Production

Figure 4 shows the discrepancy between targeted and actual total copper (TCu) recovery. Prior to 2011, we consistently fell short of the recovery targets. Nevertheless, after 2011, actual TCu recovery surpassed the objectives. This improvement can be attributed to several key areas of focus:

- Hire a Leaching Superintendent.
- Reduce the application rate from 12 l/h/m^2 to 8 l/h/m^2.
- Design a new irrigation network. A change of drip emitter capacity from 2 lph to 1 lph. Moreover, no drip lines are recycled.
- Extend the leaching cycle to maximize the area under leaching and reduce the application rate.
- Coordinate leveling of the stacking surface prior to irrigation, using dozers.
- Manage slope irrigation.

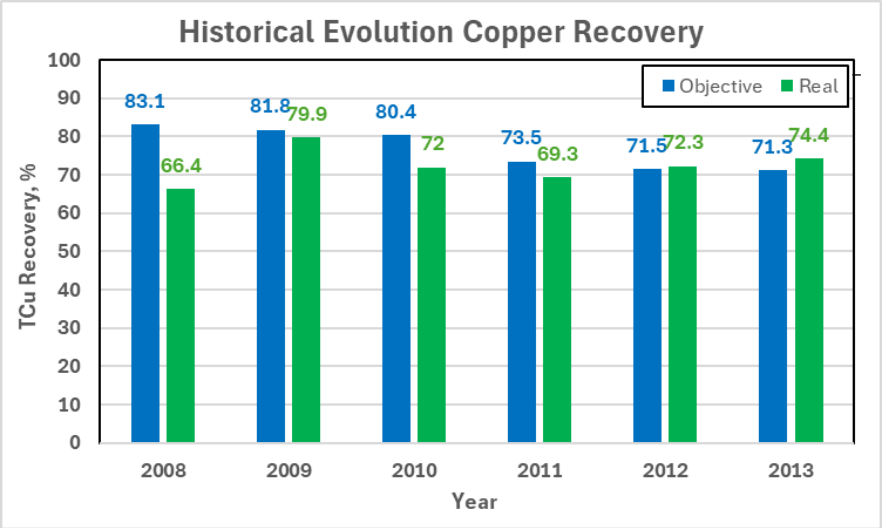

Figure 4: Historical TCu recovery, Chilean copper mine

Case 3: Peruvian Gold Mine with 240,000 Oz/Year Gold Production

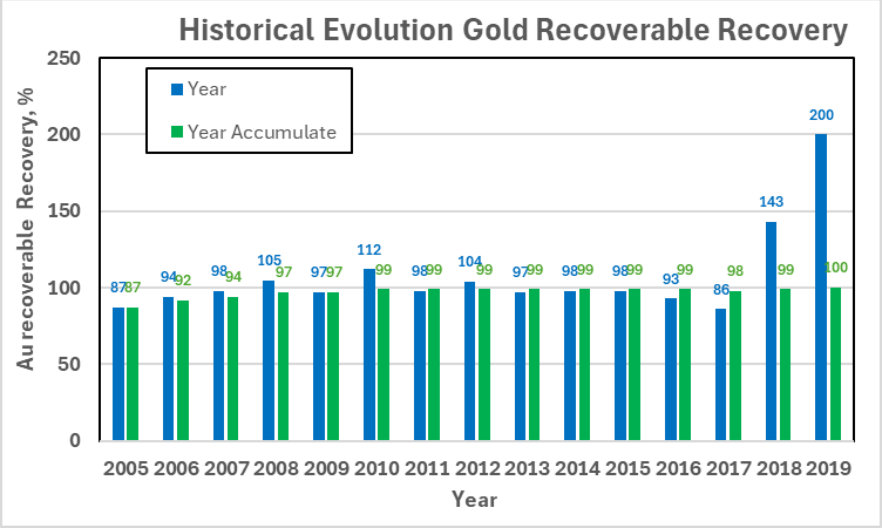

Figure 5: Historical Au recovery, Peruvian gold mine

Figure 5 shows the historical recoverable gold recovery and its annual accumulation. Until 2016, the cumulative recovery remained around 99%. However, during 2016 and 2017, gold recovery rates declined. In 2018, significant changes were implemented in operational practices, resulting in an improvement in gold recovery. As a result, in 2019, the cumulative annual recovery reached 100%, primarily due to increased gold recovery from the historical inventory. This improvement can be attributed to several key areas of focus:

- Reduce the application rate from 20 l/h/m^2 to 8 l/h/m^2.
- Design a new irrigation network. A change of drip emitter capacity from 4 lph to 2 lph.

- Extend the leaching cycle to maximize the area under leaching and reduce the application rate.
- Coordinate leveling of the stacking surface prior to irrigation, using dozers.
- Manage slope irrigation with a new slope profile.

Case 4: Argentinian Gold Mine Producing Gold from Historical Inventory

Figure 6 shows the daily gold production from January 2024. In February 2024, the gold production was around 60 oz/day. In 2024, significant changes were implemented in operational practices, resulting in an improvement in gold recovery. As a result, in December 2024, the gold production was increased to 150 oz/day. This improvement can be attributed to several key areas of focus:

- Reduce the application rate from 8 l/h/m^2 to 4 l/h/m^2; and 2 l/h/m^2 for slopes.
- Design a new irrigation network. A change of drip emitter capacity from 4 lph to 1 lph. Eliminate drip line recycle.
- Extend the leaching cycle to maximize the area under leaching and reduce of application rate.
- Coordinate leveling of stacking surface prior to irrigation, using dozers, and underground installation of drip lines with calcium hydroxide precipitation on the surface.
- Manage slope irrigation with a new slope profile. The new slope angle was considered during the closure plan.

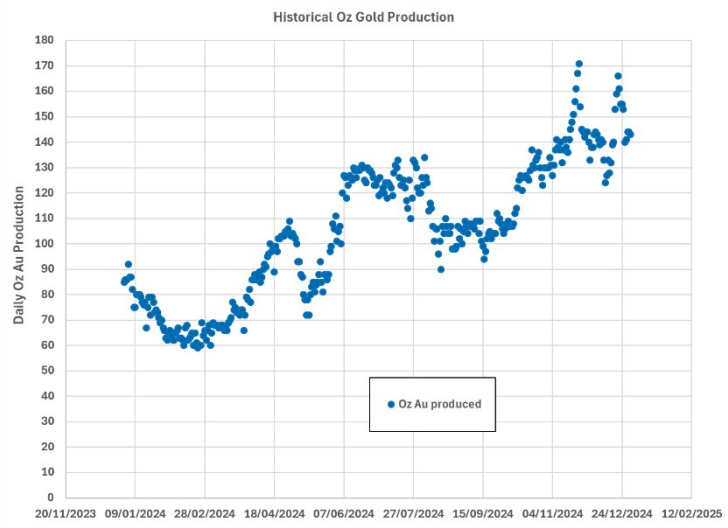

Figure 6: Au recovery improvement, Argentina gold mine

Case 5: Argentinian Gold Mine with 10,000 TPD of Ore

Figure 7 shows the daily gold production from July 2024. In July 2024, the gold production was around 30 oz/day. From then on, significant changes were implemented in operational practices, resulting in an improvement in gold recovery. As a result, in April 2025, gold production was increased to 100 oz/day. This

improvement can be attributed to several key areas of focus:

- Permanent support of a Supervisor with exclusive dedication to leaching.
- Reduce the application rate from 8 l/h/m^2 to 3 l/h/m^2; and 1.5 l/h/m^2 for slopes.
- Design a new irrigation network. A change of drip emitter capacity from 4 lph to 2 lph. Eliminate drip line recycle. Work with the drip emitter at 25 PSI of pressure.
- Extend the leaching cycle to maximize the area under leaching, reduce of application rate, and improve lime addition.
- Coordinate leveling of the stacking surface prior to irrigation, using an excavator.
- Manage slope irrigation at a lower application rate.

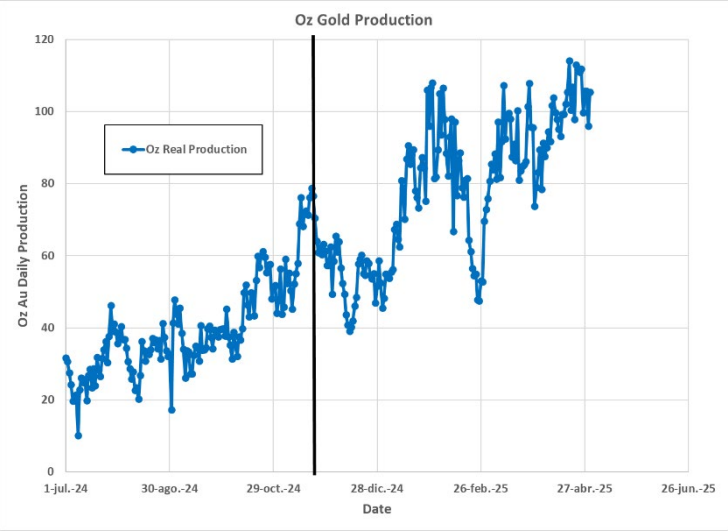

Figure 7: Au recovery improvement, Argentina gold mine

Case 6: Chilean Copper Mine with 4,000 TPY Cathode Production Capacity

Figure 8 shows the monthly SCu recovery accumulated in 2024 from a Chilean dynamic leach pad. Until September 2024, the SCu recovery had higher variation. In January 2024, the recovery was 87.5% and, in March, it was only 63.9%. In August 2024, significant changes were implemented in operational practices, resulting in an improvement in SCu recovery. As a result, the SCu recovery increased to an average of 90% during Q4 of 2024. The improvement was primarily due to these changes:

- Assign two supervisors, exclusively dedicated to supporting the leaching operation.
- Reduce the application rate from 8 l/h/m^2 to 4 l/h/m^2.
- Design a new irrigation network for surface and slopes. A change of drip emitter capacity from 4 lph to 1 lph. Eliminate drip line recycle. Work with the drip emitter at 25 PSI of pressure.
- Extend the leaching cycle to maximize area under leaching, reduce application rate, and increase the irrigation rate and lift height.

- Focus on operator training to improve the leveling of the stacking surface after previous irrigation with the excavator.
- Start slope irrigation at a lower application rate.

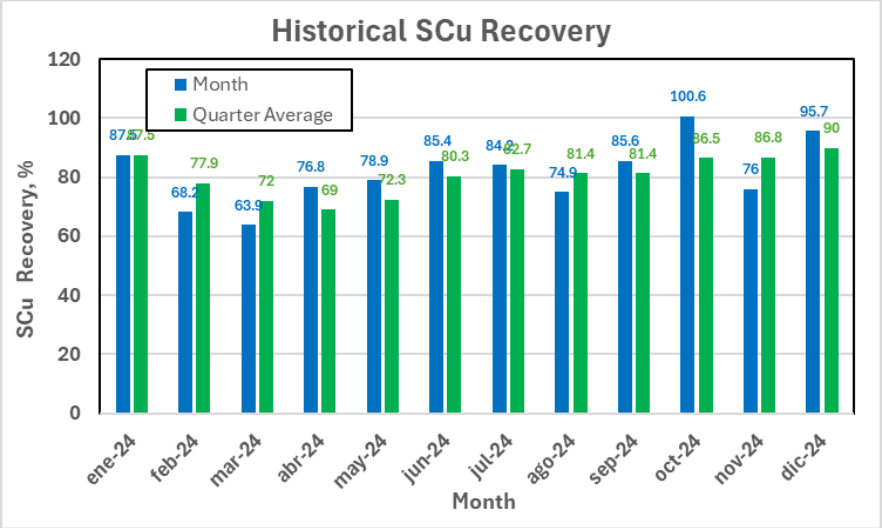

Figure 8: SCu recovery improvement, Chilean Copper Mine

Conclusion

To continue improving our current heap leaching operation in terms of *recovery* and *productivity*, we must maintain a strong focus on *executing the basics during daily operations*.

Shaping the Future of Heap Leach Facility Management: Closing the Governance Gap

Marvin Silva, AECOM, USA
Francisco Barrios, Tierra Group International Ltd, USA

Abstract

Heap leach facilities (HLFs) are essential to the economic viability of modern gold, silver, and copper mining, yet they operate in a regulatory and governance vacuum. While tailings storage facilities (TSFs) have come under increased global scrutiny following catastrophic failures, HLFs remain largely unaddressed in global risk management frameworks. This oversight is not only technically unjustified, but it is also ethically indefensible.

Despite processing billions of tons of ore globally, heap leach facilities operate without a unified international safety standard. This governance gap, rooted in the misconception that "dry" processing is inherently safer, has led to inconsistent practices, variable oversight, limited disclosure, and inadequate emergency planning. Recent incidents serve as urgent wake-up calls that a comprehensive global standard is overdue.

This paper issues a call to action: it is time to bring HLFs out of the regulatory blind spot and into the light of global standards. Building on the principles of the Global Industry Standard on Tailings Management (GISTM), we propose a comprehensive governance framework tailored to HLFs that centers values such as zero harm, lifecycle accountability, independent technical oversight, and public transparency. More than just technical structures, HLFs must be managed as ethical commitments, requiring executive-level accountability and trust-based stakeholder engagement.

The message is clear: if the mining sector is serious about responsible and sustainable practices, governance of HLFs can no longer be optional. It must be global, enforceable, and built on the same moral foundation that is now shaping the future of tailings management. The time to act is now.

Introduction

Heap leach facilities (HLFs) represent one of the mining industry's primary methods for extracting valuable metals such as gold, copper, and silver from low-grade ores. Utilizing a chemical leaching process, large volumes of ore are stacked on lined pads and treated with chemical solutions to extract metals. Despite their

widespread use and crucial economic role, HLFs remain notably absent from the robust global governance frameworks recently developed for tailings storage facilities (TSFs).

The establishment of the Global Industry Standard on Tailings Management (GISTM, 2020), following catastrophic events such as the 2015 Samarco disaster in Brazil and the devastating 2019 Brumadinho dam collapse, marked a turning point in industry governance. The GISTM introduced an ethical and values-driven approach to managing TSFs, emphasizing transparency, accountability, zero-harm objectives, and proactive stakeholder engagement. Yet, heap leach facilities, though different technically, share many critical risks, making the absence of similar governance structures ethically and operationally indefensible.

Recent failures underline this urgent governance gap:

- Çöpler Gold Mine, Turkey (February 13, 2024): A massive landslide at the heap leach pad resulted in nine fatalities and extensive environmental damage (Mining.com, 2024).
- Eagle Gold Mine, Yukon, Canada (June 24, 2024): A rotational slope failure released cyanide-laden ore at the Eagle Gold Mine (Mining News North, 2024). This incident illustrated that heap leach facility risks transcend geographic boundaries and regulatory jurisdictions, highlighting the need for comprehensive governance standards.
- Metcalf Dump Leach, Morenci, Arizona (early 1960s): A historically significant dump leach failure occurred when excessive solution application led to elevated pore pressures and subsequent slope collapse. The incident destroyed ore haulage infrastructure and resulted in multiple fatalities, providing an early documented example of heap-related geotechnical risk. This failure is cited in technical reviews of early dump leach practices as an example of the dangers associated with unmanaged saturation and lack of drainage control (Thiel & Smith, 2004; Breitenbach & Dolezal, 2015).

Recent Events: When Warnings Become Wake-Up Calls

Despite processing a large amount of global mineral production, heap leach facilities operate without unified international safety standards. This governance gap stems from a persistent misconception that HLFs present lower risks than tailings storage facilities.

The assumption that “dry” ore processing is inherently safer has led to:

- inconsistent safety practices across jurisdictions
- variable oversight mechanisms between companies
- limited public disclosure of operational risks
- inadequate emergency response planning

These incidents highlight the severe consequences when governance lags behind the technology and operational complexities inherent to HLFs. Unlike TSFs, heap leach facilities have received comparatively less scrutiny and fewer stringent international governance guidelines, despite their substantial potential for environmental harm and community disruption.

The mining industry is at a crossroads: continue to underestimate the risks and governance needs of heap leach facilities or proactively adopt a comprehensive governance framework. Such a framework must encompass lifecycle oversight, transparent risk management, stakeholder engagement, and strong accountability mechanisms inspired by the ethical standards set forth in the GISTM.

This paper argues that heap leach governance is not merely an operational necessity but a moral imperative. By proactively addressing these gaps now, the industry can avoid future disasters, enhance its social license to operate, and demonstrate leadership in sustainable and responsible resource management.

Why GISTM is a Governance Milestone for TSFs and Why HLFs Need the Same Attention

The Global Industry Standard on Tailings Management (GISTM) closed a critical safety gap for TSFs; heap leach facilities deserve a comparable standard to eliminate today's governance blind spot. Key pillars of GISTM include:

- **Ethical Commitment**: Clearly establishing the duty of care to protect human lives and the environment as paramount.
- **Transparency and Accountability**: Mandating public disclosure of risk assessments, design parameters, monitoring results, and incident reports.
- **Zero-Harm Objective**: Setting an explicit goal of preventing failures, thus prioritizing comprehensive risk management and proactive mitigation strategies.
- **Stakeholder Engagement**: Ensuring that affected communities and external stakeholders are actively engaged and informed throughout the facility's lifecycle.

Despite the obvious technical differences between TSFs and HLFs, both facility types share critical characteristics, such as potential for severe environmental impacts, long-term management challenges, and significant community and social license considerations. Yet, HLFs have historically attracted significantly less global scrutiny. Factors contributing to this oversight include perceptions of lower risk, regulatory complexities, and the limited public visibility of HLF risks compared to tailings dams.

However, the recent catastrophic incidents clearly illustrate that HLF risks can have consequences comparable to TSFs. Ignoring these risks contradicts the ethical and strategic intentions articulated within GISTM. It is imperative to recognize that the foundational governance principles underpinning the GISTM,

ethical responsibility, proactive risk management, accountability, and stakeholder transparency, apply equally to HLFs. Extending these principles into a tailored governance framework for HLFs is both a logical and ethical progression for the mining industry.

Key Differences and Similarities between TSFs and HLFs

Before designing an appropriate governance framework for HLFs, it is essential to examine how they compare to TSFs in terms of technical characteristics, failure mechanisms, and environmental risk. While HLFs are often perceived as lower-risk due to their relatively dry nature, their operational and structural complexity pose long-term challenges that are often underestimated. This section provides a comparative analysis to highlight the shared need for robust, values-based governance.

Technical and Operational Distinctions

TSFs primarily manage finely ground solids suspended in water, creating a structure often referred to as a slurry impoundment. The risk profile is often dominated by overtopping, seepage, and static/dynamic stability challenges.

Heap leach facilities, by contrast, handle coarse ore placed on impervious liners where chemical solutions percolate through ore heaps to dissolve target metals. The unique failure modes for HLFs primarily involve slope stability, liner breaches, leakage of chemical solutions, and long-term management of residual leachate following facility closure.

Shared Risks and Consequences

Despite these differences, TSFs and HLFs share significant overlapping risks:

- **Environmental contamination**: Both facilities pose risks of chemical leakage and environmental degradation, impacting water quality and ecosystems.
- **Community and social impacts**: Failure events at either type of facility can severely affect nearby communities, eroding trust and damaging the social license to operate.
- **Long-term liability**: Both facility types require extensive closure planning and post-closure monitoring, with potential liabilities extending decades beyond operational lifespans.

Given these shared characteristics and consequences, robust and ethical governance frameworks are equally critical for both TSFs and HLFs, reinforcing the need for urgent and comprehensive governance standards.

Proposed Governance Framework for HLFs

Building on the foundation of ethical responsibility and lessons learned from TSF failures, this section outlines a proposed governance framework tailored specifically for HLFs. While inspired by the GISTM,

the framework addresses the distinct operational, environmental, and societal risks associated with HLFs. The goal is to elevate HLF management to the same ethical and technical standards expected for other high-consequence extractive waste facilities.

Governance Philosophy and Ethical Foundation

HLFs must be managed not only as operational structures but as long-term ethical responsibilities. Governance frameworks should reflect values of zero harm, informed consent, and precautionary management throughout the facility lifecycle, reinforcing moral obligations toward future generations and affected communities. The proposed core governance principles for modern HLF management are:

- **Zero-Harm Commitment:** Establishing the highest operational priority for human life and environmental protection over operational convenience or cost considerations.
- **Executive Accountability:** Requiring board-level oversight and designated responsible individuals with clear authority and accountability for facility safety**.**
- **Transparent Risk Communication:** Mandating public disclosure of risk assessments, monitoring data, design parameters, and incident reports.
- **Continuous Stakeholder Engagement:** Ensuring affected communities have meaningful input throughout facility lifecycles, from planning through post-closure monitoring**.**

Executive Accountability and Governance Structure

- **Board-Level Oversight**: Mandate mining company boards to formally assume responsibility for HLF safety and environmental performance.
- **Appointment of a Responsible Individual**: Assign qualified, accountable personnel empowered to manage and oversee facility, integrity, and compliance.
- **Separation of Technical and Governance Roles:** Clearly differentiate the responsibilities of design, operation, independent review, and decision-making roles to avoid conflicts of interest.

Risk-Based Facility Classification

- Facility size and ore tonnage
- Chemical inventory and toxicity levels
- Proximity to communities and water sources
- Environmental sensitivity of location
- Geological and seismic conditions
- Climate and weather patterns

- Implement consequence-based categorization, dynamically reassessed according to changing conditions or evolving operational factors.
- Ensure transparency in classification criteria and results, providing stakeholders with clear insight into the risk profiles of HLFs.

Independent Review and Technical Oversight

- Conduct regular independent technical reviews at critical lifecycle stages.
- Establish independent technical review panels or boards for high-consequence HLFs, clearly defining reviewer qualifications and independence criteria.

Monitoring, Data Transparency, and Public Reporting

- Employ continuous monitoring systems for key performance indicators.
- Publicly disclose risk assessments, operational data, monitoring results, and incidents transparently and promptly.

Lifecycle Management and Closure Planning

- Integrate closure and post-closure considerations from initial design through operational phases.
- Provide for long-term stewardship, including funding and clear delineation of post-closure responsibilities.
- Encourage progressive rehabilitation to minimize long-term risks and environmental liabilities.

Community Engagement and Social License

- Implement community consent and involvement processes aligned with international human rights standards.
- Establish effective grievance mechanisms to address community concerns promptly.
- Involve community representatives in oversight and independent reviews, where appropriate.

Integration with Global ESG Standards

Align heap leach governance frameworks with recognized ESG reporting frameworks, such as the Global Reporting Initiative (GRI), Sustainability Accounting Standards Board (SASB), and International Council on Mining and Metals (ICMM) standards, ensuring consistent and auditable ESG disclosures.

Building Industry-Wide Collaboration for Safety Excellence

Translating governance principles into operational practice requires more than technical standards; it requires cultural change, corporate leadership, and sector-wide collaboration. This section outlines a

pragmatic path forward, including steps mining companies, regulators, investors, and industry bodies can take to implement and promote the proposed governance framework for HLFs. The roadmap emphasizes voluntary leadership, multi-stakeholder engagement, and integration with global ESG expectations.

Immediate Actions for Mining Companies

Governance Infrastructure Development

- Conduct comprehensive HLF governance audits
- Establish board-level safety oversight committees
- Appoint qualified responsible individuals
- Implement transparent reporting systems

Technical Upgrades and Monitoring

- Install continuous monitoring systems
- Upgrade drainage and containment infrastructure
- Develop comprehensive emergency response plans
- Engage independent technical review panels

Stakeholder Engagement Enhancement

- Establish community liaison programs
- Implement grievance mechanisms
- Provide regular public updates on facility status
- Support community capacity building initiatives

Industry Collaboration and Standards Development

- Facilitate multi-stakeholder workshops and dialogues involving industry bodies, mining companies, investors, and regulators.
- Develop voluntary industry guidelines and pilot governance frameworks inspired by the GISTM principles.
- Engage international organizations (e.g., ICMM, GRI, SASB) to integrate and standardize reporting and governance practices.

Regulatory Engagement Strategy

Proactive Policy Development: Mining Companies Should Lead Regulatory Engagement by:

- Sharing technical expertise with regulatory bodies
- Supporting evidence-based policy development
- Advocating for consistent international standards
- Facilitating knowledge transfer between jurisdictions

Capacity Building Support

- Provide training for regulatory personnel
- Share best practices and lessons learned
- Support development of technical guidelines
- Facilitate international regulatory cooperation

ESG integration and investor engagement

Aligning with Global Standards

- Integrate HLF governance with ESG reporting frameworks Align with Global Reporting Initiative (GRI) standards
- Meet Sustainability Accounting Standards Board (SASB) requirements
- Comply with International Council on Mining and Metals (ICMM) principles

Investor Communication:

- Provide clear disclosure of HLF risks and mitigation measures
- Report on governance improvements and safety investments
- Demonstrate commitment to international best practices
- Engage proactively with ESG-focused investors

The Business Case for Proactive HLF Governance

The mining industry is facing a pivotal moment. Recent heap leach incidents have underscored the consequences of governance gaps, challenging public confidence and prompting a call for proactive leadership.

The core message of this paper is clear: beyond moral imperatives, robust heap leach facility governance delivers tangible business benefits that strengthen long-term competitiveness.

Risk Mitigation Benefits

Financial Risk Reduction

- Lower insurance premiums through demonstrated risk management
- Reduced potential liability from environmental incidents
- Protection against operational disruptions
- Preservation of asset values through proper maintenance

Operational Advantages

- Improved operational efficiency through better monitoring
- Extended facility life through proper management
- Enhanced predictability of closure costs
- Reduced regulatory compliance costs

Competitive Advantages

Market Position Enhancement

- Stronger social license to operate
- Preferred partner status with responsible investors
- Enhanced access to capital markets
- Improved stakeholder relationships

Reputation Management:

- Proactive risk management demonstrates industry leadership
- Transparent reporting builds stakeholder trust
- Consistent safety performance attracts top talent
- Positive community relationships support expansion opportunities

Creating a Global Framework: The Path Forward

The mining industry stands at a critical decision point. Recent disasters have demonstrated the consequences of inadequate heap leach facility governance, while growing stakeholder expectations demand immediate action.

Multi-Stakeholder Collaboration Requirements

Industry Leadership

- Major mining companies must champion governance improvements
- Industry associations should develop voluntary guidelines
- Technical experts must share knowledge and best practices
- Equipment suppliers should support safety innovations

Regulatory Support

- Governments must update regulations based on current understanding
- International bodies should promote harmonization
- Regulatory agencies need adequate resources and expertise
- Cross-border cooperation should address transboundary risks

Community and Civil Society Engagement:

- Affected communities must have meaningful participation opportunities
- Environmental organizations should provide technical oversight
- Academic institutions should support research and training
- Media should maintain focus on safety and accountability issues

Conclusion: Leadership Opportunity in Crisis

The mining industry has reached a defining moment. Recent incidents have revealed the significant consequences of HLF failures, including environmental impacts, community disruption, and operational failures that have challenged public confidence and the industry's social license to operate.

These events underscore that a fundamental shift is needed in how the industry approaches heap leach facility management. The principles that have proven successful in tailings management—proactive oversight, rigorous operational standards, and comprehensive stakeholder engagement as embodied in the GISTM—present a proven pathway forward for heap leach operations.

Industry leaders, investors, and stakeholders have an opportunity to address the governance gap for heap leach facilities through collaborative action. A comprehensive industry framework incorporating independent verification, transparent reporting, robust operational standards, and meaningful community engagement would demonstrate the sector's commitment to operational excellence and sustainable development.

Acknowledgements

The authors gratefully acknowledge the support of AECOM and Tierra Group International Ltd in providing technical resources and encouragement during the preparation of this paper. Any views expressed remain those of the authors and do not necessarily reflect the positions of AECOM or Tierra Group International Ltd.

References

Breitenbach, A. J., & Dolezal, A. L. (2015). Impact of shallow and deep injection well leach solutions with respect to ore heap slope stability. In *Proceedings of Heap Leach Solutions, 2015* (September 14–14, Reno, Nevada, USA). Infomine.

Global Industry Standard on Tailings Management (GISTM). (2020). *Global industry standard on tailings management*. International Council on Mining and Metals, United Nations Environment Programme, and Principles for Responsible Investment.

Mining News North. (2024). Eagle Gold Mine heap leach pad collapse. https://www.miningnewsnorth.com

Mining.com. (2024). Çöpler Gold Mine landslide incident. https://www.mining.com

Mining.com. (2025, February 27). SSR review of Çöpler mine incident points to third-party design flaw. https://www.mining.com/ssr-review-of-copler-mine-incident-points-to-third-party-design-flaw/

Thiel, R., & Smith, M. E. (2004). State-of-the-practice review of heap leach pad design issues. *Geotextiles and Geomembranes, 22*(6), 555–568.

Chapter Five

Project Development

HEAP LEACH

SOLUTIONS 2025

Integrating the Risk Management of TSFs, WRFs, and HLFs

Álvaro Gutiérrez, Capstone Copper, Chile
Emilio López, Nava Consulting, Chile
Nicolás Villanueva, Nava Consulting, Chile
Ignacio Pizarro, Nava Consulting, Chile
Javier Ubilla, Nava Consulting, Chile
Gail Riddell, Nava Consulting, Chile

Abstract

An essential aspect of effective mine waste management is the integration of best practices, risk management principles, and lessons learned from tailings storage facilities (TSFs) case histories. While TSF governance has evolved significantly in recent years, with global mining companies aligning their practices with international standards such as the Global Industry Standard on Tailings Management (GISTM), similar efforts are needed for heap leach facilities (HLFs) and waste rock facilities (WRFs)—facilities that can pose comparable risks in certain contexts. Under these circumstances, the consequence classification for HLFs and WRFs remains a significant challenge.

Developed collaboratively by Capstone Copper and Nava Consulting, this paper presents a comprehensive approach to leaching ore and waste management, emphasizing a standardized consequence classification system that integrates HLFs and WRFs alongside TSFs. Establishing a consistent classification framework is fundamental to improving risk management and operational safety for all types of ore mining and waste storage facilities.

Furthermore, the paper proposes the development of a standard for the design, operation, and closure of HLFs and WRFs. By establishing a clear and structured standard, mining companies can ensure consistency across projects and operations, integrating risk management practices at every stage of a facility's life cycle. This approach is critical to minimize environmental and social impacts while enhancing safety, operational efficiency, and long-term sustainability in mine waste management. Also, this paper establishes the key pillars for the safe and responsible management of HLFs and WRFs, ensuring a comprehensive and structured approach to their governance.

Finally, a consequence-based risk framework is proposed that evaluates the potential impacts of failure across all leaching ore and waste storage facilities. An integrated consequence classification system

coupled with risk management processes ensures that mine waste risks are systematically incorporated into corporate risk management strategies. This allows for more effective prioritization of mitigation efforts and improved safety and environmental performance.

Introduction

In recent years, the mining industry has made significant progress in the governance and management of tailings storage facilities (TSFs), motivated by high-impact events such as the catastrophic failures at Mount Polley (2014), Samarco (2015), and Brumadinho (2019). These events drove the development of international standards such as the Global Industry Standard on Tailings Management (GISTM) (ICMM et al., 2020), promoting more robust governance and greater corporate responsibility. However, these advances have not yet extended with the same force to facilities such as heap leach facilities (HLFs) and waste rock facilities (WRFs), although these can also present significant risks to people, the environment, and operational continuity. According to Capstone Copper's definition, HLFs include: permanent leach pads, dynamic (on-off) leach pads, spent ore dumps or designated areas resulting from dynamic (on-off) leach pads, spent ore dumps resulting from permanent leach pads whose operation has ceased, and facilities undergoing secondary leaching. On the other hand, WRFs include: mineral stockpiles, waste rock stockpiles, and waste rock dumps.

In 2024, two significant failures occurred in HLFs: one at the Çöpler mine in Turkey and another at the Eagle Gold mine in Canada. The Çöpler failure consisted of a slide of approximately 10 Mm^3 along a 200-metre slope, trapping and causing the death of nine workers on site (Chen, 2025). In the Eagle Gold case, the slide covered approximately 1.4 km. While no fatalities were recorded, the potential environmental impact of the event is under investigation (Petley, 2024). In the case of WRFs, there have also been historical failures with high impact. Notable is the Bellavista failure that occurred in 2007 (Braun, 2024). Although this event did not cause fatalities, injuries, or environmental damage, it generated significant economic losses and led to the definitive closure of the mine after only two years of operation. This evidence and gap in risk management reflect the need to advance towards an integrated and rigorous approach that allows for the systematic evaluation and mitigation of risks associated with all types of mining facilities.

Capstone Copper currently manages five mining units: four in operation and one in the design phase, which together include more than 25 WRFs and more than 10 HLFs. Given the absence of specific regulatory frameworks for these facilities, the company has driven a process of progressive strengthening of its management, aiming to achieve levels of standardization and control similar to those existing for TSFs. This work has included the development of a dedicated governance structure, the preparation of specific technical processes and documentation, along with the implementation of risk analyses aimed at the systematic identification and mitigation of risks.

This paper, developed jointly by Capstone Copper and Nava Consulting, presents the work carried out to advance towards systematic management of HLFs and WRFs, integrating these facilities into a risk management approach comparable to that used for TSFs. In particular, a standardized consequence classification system is proposed as a basis for strengthening traceability, prioritization, and decision-making regarding the safety of these facilities. This work also proposes the fundamental pillars for safe and responsible management of these facilities, including clear governance, public disclosure, integrated monitoring, risk-based design and operation, reviews, and training. Finally, the need to advance towards the development of a technical standard is raised that would allow for the consistent integration of safety and sustainability principles throughout the entire life cycle of HLFs and WRFs.

Tailings Experience Applied to HLFs and WRFs

In response to catastrophic failures of tailings storage facilities (see Fig. 1), the International Council on Mining and Metals (ICMM), United Nations Environment Programme (UNEP), and Principles for Responsible Investment (PRI) developed the GISTM, which has as its main objective achieving zero harm to people and the environment, and zero tolerance for human fatalities.

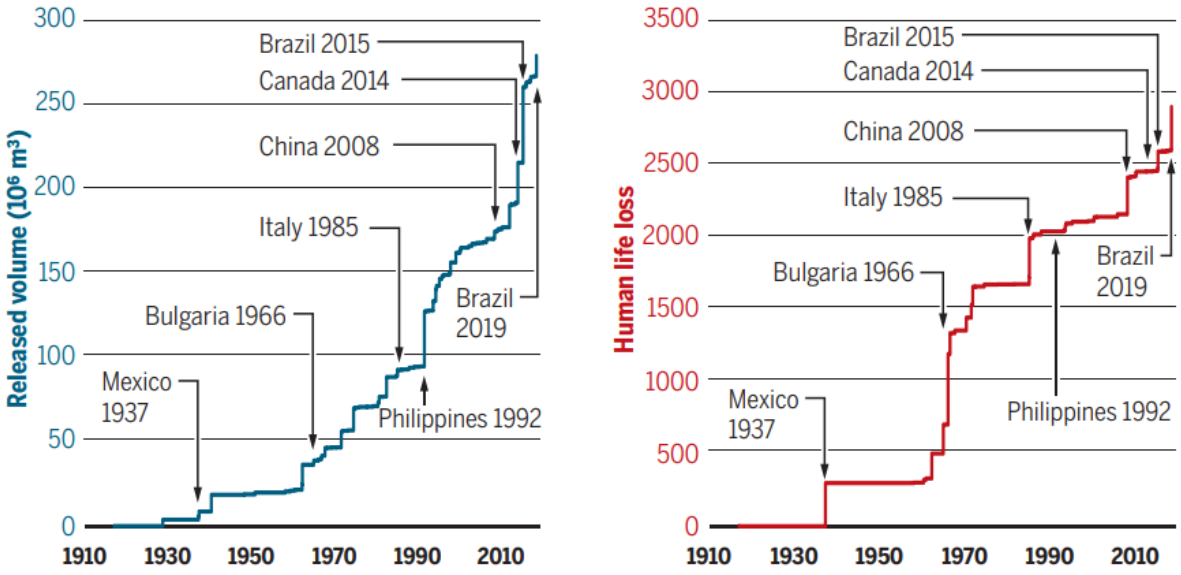

Figure 1: Losses from tailings dam failures, showing cumulative released volume and resulting loss of life (Santamarina et al., 2019)

Given that HLFs and WRFs share multiple characteristics with TSFs, such as their function of storing massive materials and their interaction with variable hydrogeotechnical conditions, it is possible to apply GISTM principles to these facilities. Documents such as the Emergency Preparedness and Response Plan (EPRP) or the Construction Record Report (CRR), used in TSFs, can be adapted to HLFs and WRFs to

strengthen their technical traceability. Likewise, critical roles such as the Engineer of Record (EoR) and the Independent Tailings Review Board (ITRB) can be extended, with appropriate adjustments, to these other facilities. Since the implementation of the GISTM, significant advances have been made in the industry, including greater emphasis on risk management, clearer definition of responsibilities, adoption of consequence classification systems, and greater transparency in communicating results and progress. These advances, although born reactively in response to tragic events, offer an opportunity for HLFs and WRFs to adopt a proactive and rigorous approach.

By applying lessons learned in tailings management to other mine waste and leached ore facilities, the overall governance of waste management at mine sites is strengthened. The maturity process achieved in TSFs can serve as a guide to avoid similar errors in facilities that until now have had less visibility. This implies not only transferring tools and roles, but also developing a risk management culture that comprehensively encompasses all types of mine waste and leached ore storage facilities.

Differences in Failures Between TSFs, HLFs, and WRFs

TSFs, HLFs, and WRFs are facilities with distinct functions and characteristics, which leads to relevant differences in their failure mechanisms, associated consequences, and risk management strategies. In general, TSFs present the greatest destructive potential in case of failure, as they can release large volumes of material in the form of rapid flow, affecting extensive areas downstream. Common failure modes in TSFs include overtopping, liquefaction, and containment failures, all of which can generate catastrophic impacts. In contrast, failures in HLFs and WRFs usually manifest through mechanisms such as slow slides or loss of stability under specific conditions, such as extreme rainfall, prolonged seepage, or geometric modifications without technical justification. While these events do not always involve destructive flows comparable to those of a TSF, they can generate severe consequences, including fatalities, environmental impacts, or significant operational interruptions, depending on the local context and the magnitude of the event.

A key aspect is that the perception of lower risk in HLFs and WRFs can lead to lower investment in specific studies, monitoring, or controls. This underestimation can result in gaps in geotechnical and hydrogeological characterization, structural design and verification, or in the absence of adequate response plans. For example, the presence of acid-generating materials in WRFs or unmonitored internal pressures in HLFs can evolve into failures whose late detection aggravates their consequences. Figure 2 illustrates a conceptual scheme of the expected consequence classification for TSFs, HLFs, and WRFs, showing that while TSFs tend to present higher consequences on average, there are cases where HLFs and WRFs can exceed the impact levels attributable to TSFs. This approach reinforces that the type of facility does not by

itself determine its level of criticality; it is essential to consider factors such as location, stored volume, processes involved, and geotechnical and hydrogeological conditions.

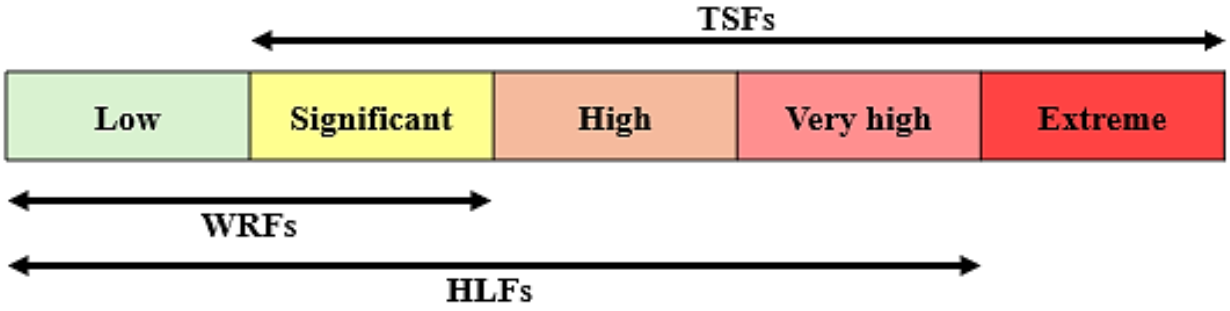

Figure 2: Expected lowest and highest consequence classification for TSFs, HLFs, and WRFs

These technical differences reinforce the need to adopt a risk-based approach that allows for adequate characterization of each facility, prioritization of resources according to their consequence level, and definition of strategies proportional to the identified failure scenarios. In this regard, integrated and structured management allows addressing the specific conditions of each type of facility without losing sight of the common principles of safety and sustainability that should govern all of them.

Integrated Management and Technical Governance of HLFs and WRFs: Capstone Copper's Experience

Capstone Copper, in collaboration with Nava Consulting, has developed standards aimed at strengthening integrated management and technical governance of HLFs and WRFs, responding to the need for robust guidelines that systematically address all aspects of these facilities' life cycle. These standards establish minimum requirements for the planning, design, construction, operation, closure, and post-closure phases. The objective is to ensure these facilities are safe enough to prevent harm to people and the environment.

The standards incorporate recognized best practices, national and international regulatory frameworks, and GISTM principles, adapted to the specific context of HLFs and WRFs. This allows for raising technical requirements and aligning their management with international-level references, promoting safer, more efficient, and responsible operation.

As part of this process, Capstone Copper has strengthened its technical governance structure, establishing clear roles, responsibilities, and communication channels at both corporate and operational levels (see Fig. 3). Key figures have been defined such as the Accountable Executive Officer (AEO), General Manager (GM), Responsible Facility Engineer (RFE), Engineer of Record (EoR), and the Independent Review Board (IRB), who fulfill specific functions aimed at ensuring technical quality, traceability, and independent review at each stage of the HLFs' and WRFs' life cycle.

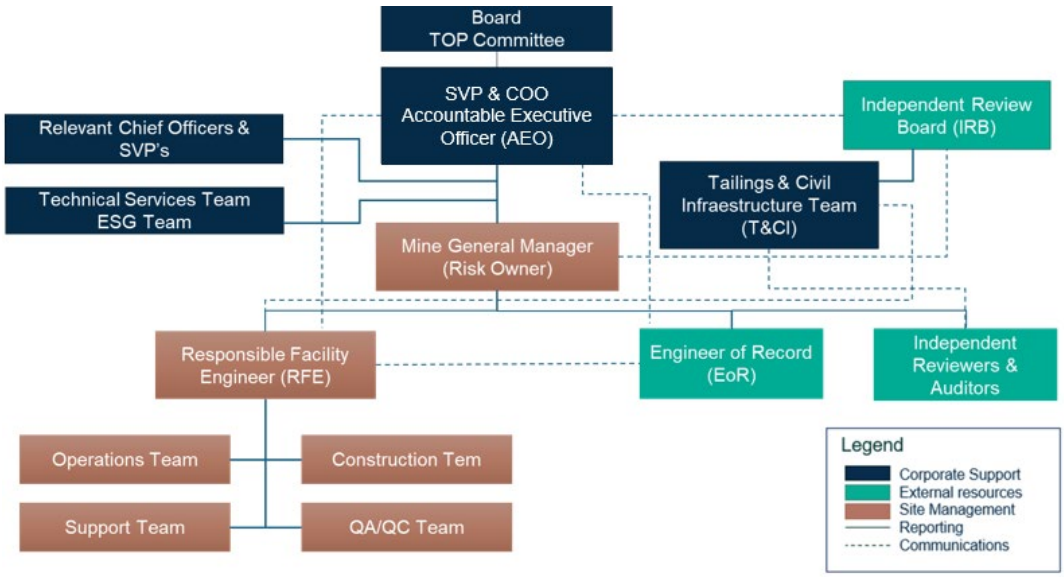

Figure 3: Proposed minimum governance structure for HLFs and WRFs

In addition to defining roles, the standard establishes a set of technical documents that must be prepared and kept updated for each facility. These include, among others, the CRR, which describes all as-built aspects of the facilities; and the EPRP, which defines emergency preparedness and response protocols. The existence and systematic updating of these documents reinforces technical traceability and accountability at all stages of the HLFs' and WRFs' life cycle.

This organizational structure is complemented by formal requirements related to technical expertise, official designations, allocated resources, and communication protocols, ensuring robust and transparent management. This foundation allows Capstone to advance towards a more mature operation, where the experience and learnings from TSF management are applied to other critical facilities, consolidating a comprehensive corporate approach to risk management at mine sites.

These elements, together, establish a solid foundation for the effective integration of risk management in HLF and WRF management, ensuring that operational decisions are based on robust, traceable technical criteria aligned with industry best practices.

Pillars for Responsible Management

The responsible management of HLFs and WRFs requires the implementation of a structured management system aligned with the principles defined in the standards for managing these facilities. As part of the standards and efforts that Capstone Copper has been undertaking, the company has committed to creating a system that ensures the implementation of the standards and thus ensures compliance with the

requirements established therein. The following describes the key elements that form the pillars of this comprehensive management system:

Corporate Governance, Planning and Design

A clear and robust governance structure forms the foundation of the system. A defense model has been established, where responsibilities are clearly distributed among operational, technical, and assurance areas. The implementation of internal policies, standards, and guides, along with formal change management and quality control processes, ensures technical consistency and traceability in decisions throughout each facility's life cycle. Likewise, strategic facility planning and risk-based design are essential for preventing failures and optimizing performance.

Records, Reports and Public Disclosure

The system includes recommendation tracking tools, with traceability from identification to closure, as well as real-time monitoring of key variables when applicable. An updated registry of all facilities is maintained, with their consequence classification to be included. In line with best practices, progress has been made in public disclosure mechanisms for relevant information, and development continues on an internal tool for verifying standard compliance.

OMS and EPRP: Operation, Maintenance and Surveillance/Emergency Preparedness and Response Plan

Safe operation requires a system of performance indicators, monitoring programs, periodic inspections, and defined critical controls. Each facility must have an Operation, Maintenance and Surveillance (OMS) plan and an EPRP. These include Trigger Action Response Plans (TARPs). The progressive implementation of these elements has strengthened the capacity for anticipation and response to potential scenarios.

Risk Management

A Risk Management Plan has been adopted that integrates operational, construction, and strategic risks, framed within the corporate Enterprise Risk Management (ERM) model. Methodologies such as FMEA and Bow Tie Analysis are used, and mitigation actions are prioritized based on consequence classification. This approach allows aligning the management of HLFs and WRFs with the corporate risk strategy historically applied to TSFs.

Review and Assurance

An Independent Review Board (IRB) has been established that covers HLF and WRF facilities with the highest consequence classification. Additionally, internal and external audits are conducted to verify technical and regulatory compliance and foster continuous improvement of the system.

Training and Expertise

The system includes periodic technical training plans, focusing on critical roles such as the Responsible Facility Engineer (RFE) and operations teams. A succession plan has also been developed to ensure the availability of trained professionals for long-term system continuity.

These pillars not only establish a structured foundation for HLF and WRF management but also serve as key enablers for the safe and sustainable management of these facilities. Their consistent and progressive implementation significantly improves risk identification, evaluation, and control, strengthening the capacity to anticipate and respond to potential critical scenarios. Together, these elements enable integrated risk management aligned with international standards and ensure that operational and strategic decisions are based on robust technical criteria and a long-term vision focused on safety, social responsibility, and environmental performance.

Risk Management

Mining companies typically have risk matrices that define the level of risk they are willing to accept given the specific characteristics of their facilities. It is essential that companies establish this definition themselves rather than relying exclusively on the criteria of consultants who develop the analyses.

Capstone Copper has developed a corporate guide for managing risks at its TSFs. This guide establishes clear directives on how to perform analyses based on the facility's development level, along with three levels of analysis: qualitative, semi-quantitative, and quantitative. While quantitative analyses may be perceived as more comprehensive, tools such as FMEA (Failure Mode and Effects Analysis), PFMA (Potential Failure Mode Analysis), and SQRA (Semi-Quantitative Risk Assessment), included in the semi-quantitative approach, are widely recognized for their utility, robustness, and applicability in the mining industry.

Currently, Capstone Copper seeks to implement the consequence classification system proposed by the GISTM not only for its TSFs but also for its HLFs and WRFs. For these facilities, this system is complemented by the hazard classification (instability hazard) system developed by Hawley & Cunning (2017), which is primarily used to determine the required monitoring levels. Unlike the GISTM approach, the Hawley & Cunning system does not consider the consequences of a potential failure but instead focuses on design and location aspects, such as geology and climatic conditions.

The integration of both systems provides a more comprehensive view of each facility's status. This combination facilitates the identification of information gaps or characterization weaknesses, which can be proactively addressed to strengthen risk management. Given the wide range of potential consequences from HLF failures (see Fig. 2), it is advisable to conduct risk analyses on all facilities, regardless of their

consequence or hazard classifications. For WRFs, it is recommended to adopt a decision matrix that helps determine when a risk analysis is essential (see Fig. 4). This matrix is interpreted as follows:

- **Red zone**: A risk analysis is required.
- **Orange zone (***)**: A risk analysis is recommended. Alternatively, if there are information gaps affecting the hazard classification, addressing these gaps may allow reclassification to "Very Low" hazard.
- **Yellow zone (**)**: A risk analysis is not required if the EoR can demonstrate that the WRF/HLF has no credible failure modes with "High", "Very High" or "Extreme" consequences. If this is demonstrated, the consequence classification shall be revised accordingly.
- **Yellow zone (*)**: A risk analysis is not required if the EoR and AEO jointly justify it as unnecessary, or if they demonstrate that the risks are sufficiently low based on the likelihood criteria of the mine
- **Green zone**: No risk analysis required.

Very High Hazard	(*)	(*)	Required	Required	Required
High Hazard	(*)	(*)	Required	Required	Required
Moderate Hazard	(*)	(*)	Required	Required	Required
Low Hazard	Not required	Not required	(***)	(***)	(***)
Very Low Hazard	Not required	Not required	(**)	(**)	(**)
Instability hazard/Consequence classification criteria	Low	Significant	High	Very High	Extreme

Figure 4: Decision matrix to determine when risk analysis is required for WRFs

Conclusion

The responsible management of HLFs and WRFs requires not only robust standards but also dedicated and trained teams that actively lead implementation throughout the facilities' life cycle. Having a clear organizational structure with defined roles, supported by specific technical documentation, has been key to advancing effective governance aligned with Capstone Copper's corporate commitments.

This work represents a first step toward standardizing facilities that historically have not been managed with the same rigor as TSFs, despite presenting similar operational, environmental, and safety

challenges. The consolidation of this approach seeks not only to improve facility performance but also to contribute to a culture of continuous improvement and impact prevention throughout the mining industry.

Consequence classification enables understanding of the repercussions that structural failures can generate, whether for TSFs, HLFs, or WRFs. By complementing it with systems such as that proposed by Hawley and Cunning, which provides guidance on required monitoring levels, a more comprehensive vision is achieved that facilitates informed decision-making and enables anticipation of potential gaps.

Combining different classification methodologies allows consideration of both the intrinsic characteristics of facilities and their surrounding environment. This is key to a solid risk control approach aligned with the principles of prevention, continuous improvement, and long-term sustainability. This approach not only strengthens technical traceability and accountability but also enables effective integration of risk management into corporate strategy. This approach not only raises Capstone Copper's technical standard but also establishes a replicable foundation for other mining companies seeking to strengthen the comprehensive management of their storage facilities.

References

Braun, T. (2024). Geotechnical failure of a waste rock and heap leach facility at the Bellavista gold project. *Proceedings of Tailings and Mine Waste 2024.* https://www.srk.com/en/events/geotechnical-failure-waste-rock-heap-leach-facility-bellavista-gold-project

Chen, J. (2025). SSR review of Çöpler mine incident points to third-party design flaw. *Mining.com.* https://www.mining.com/ssr-review-of-copler-mine-incident-points-to-third-party-design-flaw/

Hawley, M., & Cunning, J. (Eds.). (2017). *Guidelines for mine waste dump and stockpile design.* CSIRO Publishing.

International Council on Mining and Metals, United Nations Environment Programme, & Principles for Responsible Investment. (2020, August). *Global industry standard on tailings management.* https://www.unep.org/resources/report/global-industry-standard-tailings-management

Petley, D. (2024). A major landslide at a heap leach pad at Eagle Gold Mine in the Yukon, Canada. *Eos.* https://eos.org/thelandslideblog/eagle-gold-mine-1

Santamarina, J. C., Torres-Cruz, L., & Bachus, R. (2019). Why coal ash and tailings dam disasters occur. *Science.* https://doi.org/10.1126/science.aax1927

Consideration of Shear Strains in Design and Construction of Heap Leach Facilities

Peter H. Yuan, SRK Consulting (U.S.) Inc., USA
Omar De Santiago, SRK Consulting (U.S.) Inc., USA
Joshua Sames, SRK Consulting (U.S.) Inc., USA
Tarik Hadj-Hamou, SRK Consulting (U.S.) Inc., USA

Abstract

The development of heap leach facilities in some project settings can be very challenging. Currently, the standard of practice for heap leach facility slope designs is the use of the limit equilibrium analysis method, which does not consider strain development in geomaterials, specifically the heap leach material and the interface between the geomembrane liner system and the heap leach material. Using finite-element-method modeling, this paper considers multiple engineering applications in the design and construction of heap leach facilities where consideration of shear strains within the geomaterials is crucial for the overall performance of the facilities during operations and into closure. The engineering issues considered in the paper include 1) downdrag stress and strain development over liner slopes with varying subgrade gradients, 2) impacts on a liner system due to different overliner placement and ore stacking practices, and 3) risks of strain softening and slope instability when stacking fresh (unleached) heap leach material over saturated previously leached lifts under significant vertical stresses. The results of the analyses presented in this paper demonstrate that stress and strain development in geomaterials should be considered. The recent failures of leach pads around the world reinforce this assertion.

Introduction

Heap leach facilities (HLFs) are used in the mining industry to extract precious metals, copper, uranium, and other compounds from ore using a series of chemical reactions. HLFs generally require a containment area with a solution collection system that recovers leach solution and routes it to a process plant for metal extraction. Challenges in developing these facilities vary from site to site. Geotechnical issues in the design and construction of HLFs must be carefully addressed to ensure successful project development in a safe and environmentally responsible way.

The authors have worked on multiple HLF projects across various environments and jurisdictions. While each project is unique, this paper highlights several common applications in HLF development where considering shear strains becomes especially important. These applications are categorized into three groups as follows:

- HLF Application 1: Liner interface strength
- HLF Application 2: Loading overliner systems
- HLF Application 3: Stacking over a saturated lift surface

For each of the above application categories, a finite-element method (FEM) program has been used to model the development of stress and strain. Considering shear strain development in geomaterials (ore and ore-liner interfaces) allows for a more accurate assessment of their behaviors to address geotechnical risks, as geomaterials display nonlinear relationships between stress and strain. It is noted that the limit equilibrium method (LEM), which is currently used for HLF stability evaluations as the standard practice, cannot model strain.

Shear Strain and Modeling Tool

Stress-Strain Relationship

Soils and some other geomaterials demonstrate nonlinear relationships between strain and stress. One behavior, specifically strain softening, has received much attention recently due to several failures in tailings dams and heap leach facilities around the world. Under strain softening (Fig. 1), the increase in strain (i.e., deformation) results in a reduction in strength. When the strain exceeds the magnitude corresponding to the peak strength, it may result in a flow failure or a catastrophic failure that can happen without significant early warning. This makes understanding strain in design models extremely important for some engineering applications.

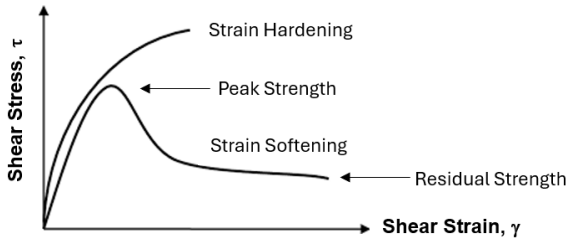

Figure 1: Strain softening versus strain hardening

Shear strain (γ) is defined by the deformation of an object where parallel internal surfaces slide past each other due to shear stress (τ), as illustrated in Figure 2 and calculated by Equation 1. The shear strain

is a unitless value and commonly presented in percentage or decimal values. The shear stress-strain relationship is expressed in Equation 2, where G is the shear modulus.

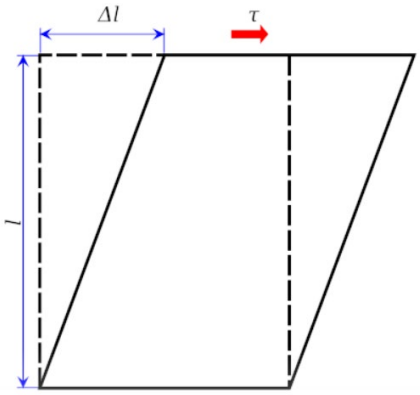

Figure 2: Definite of shear strain

$$\gamma = \frac{\Delta l}{l} \quad (1)$$

$$\tau = G \times \gamma \quad (2)$$

Numerical analyses also use bulk modulus (K) and Young's (elastic) modulus (E), in addition to G and Poisson's ratio (v). K and E are calculated through Equations 3 and 4:

$$K = \frac{2G(1+v)}{3(1-2v)} \quad (3)$$

$$E = 2G(1+v) \quad (4)$$

Modeling Tool

The stability of the HLF slope is commonly evaluated using the limit equilibrium method and using commercially available software. Advances in computing technology have enabled the use of complex numerical modeling methods in recent years as a powerful and viable alternative to traditional limit equilibrium methods. Finite element software is now comparable in ease of use to limit equilibrium software for many applications. Still, it does not relieve the user of the responsibility for selecting input parameters intelligently. One significant advantage of numerical modeling methods is their capability to model relationships between stress, strain, and time, enabling simulation of more complex conditions, including staged construction, deformation calculation, soil-fluid interaction, and time-dependent strength response (Major et al., 2009). Modeling tools include fine element programs such as RS2™ (by Rocscience Inc) and Plaxis™ (by Bentley Systems), finite difference programs such as FLAC™ (by ITASCA

Software), and discrete block models such as UDEC™ (by ITASCA Software). Numerical modeling methods generally calculate a Strength Reduction Factor (SRF), as described by Dawson and Roth (1999), by which the soil shear strength is divided to bring the slope to the verge of failure, instead of the traditional Factor of Safety (FOS) calculated from the limit equilibrium method. Major et al. (2009) provide additional discussions regarding the SRF and FOS.

The two-dimensional (2D) geotechnical finite-element-method (FEM) software RS2 by Rocscience Inc. (2025) for civil and mining applications was used to perform the analyses presented in this paper. Applicable for both rock and soil, RS2 is a general-purpose finite element analysis program that enables modeling stress and strain development under miscellaneous project applications, including heap leach development.

It is noted that both FEM and finite difference programs model materials as a continuum. The liner interface evaluated in this paper was modeled as a 0.3-meter-thick assembly that includes a geomembrane liner and a low hydraulic conductivity layer (LHCL), as shown in Figure 3. Although shearing along the interface usually behaves as discrete units against each other along a thin and distinct layer, shear strain and displacement are modeled as the performance of the 0.3 m assembly in this paper. The LHCL can be a soil material or geosynthetic clay liner (GCL), as both are used in HLF projects worldwide.

Figure 3: Liner interface assembly modeled

HLF Application 1: Liner Interface Strength

The first group of applications presented in this section addresses the strain development along the Liner Interface due to additions of stacking loads, and strain variation due to changing liner subgrade slopes. Deformations of the fill will be essentially vertical (i.e., settlement) with some outward sliding generating shear strain in the liner system, which may result in a reduction in the strength of the Liner Interface.

Model Inputs

In addition to the Liner Interface discussed in Section 2.2, other units modeled included a Foundation unit below the Liner Interface, an Overliner layer above the liner for liner protection and solution collection, and Heap Ore for leaching. Unless otherwise noted in the paper, all of the FEM models presented herein follow the configuration listed below and shown in Figure 4.

- Liner Interface assembly: 0.3 m

- Overliner thickness: 0.9 m
- Height of each stacking lift: 10 m (maximum)
- Overall stacking slope: 2.5H (horizontal): 1V (vertical)
- Angle-of-repose slope (lift slope): 1.33H:1V or about 37 degrees
- Subgrade (foundation) slope varies

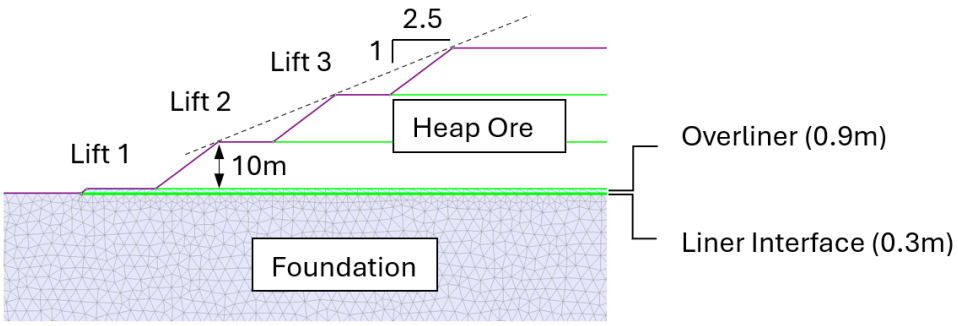

Figure 4: Model geometry used for modeling

The material properties assigned are summarized in Table 1. These are typical values for materials of a similar type and are consistent with the experience of the authors from relevant projects. All materials are modeled as elasto-plastic materials.

Table 1: Material Properties Used in RS2 Models

Material	Foundation	Liner Interface	Overliner	Heap Ore
Strength Parameters (Mohr-coulomb Criterion)				
Cohesion (kPa)	0	0	0	0
Friction Angle (°)	38	15	36	36
Deformation Parameters (Elasto-plastic Model)				
Young's Modulus (MPa)	200	14	50	50
Poisson's Ratio	0.3	0.3	0.3	0.3
Density (kN/m³)	19.6	15.7	19.6	19.6

Figure 5 shows the RS2 model setup for HLF Application 1. Under this group of applications, the HLF foundation (denoted as the Liner Subgrade Gradient) is assumed to be flat (inclination of 0%), and at inclinations of 2%, 5%, 10%, and 20%, and additions of ore lifts are modeled as staged loadings. The following two scenarios were evaluated and discussed as follows:

- Strain development under stacking loads of the first three lifts over a flat HLF foundation, i.e., HLF liner subgrades of 0%.

- Comparison of maximum shear strains under the first lift (Lift 1) stacking over varying HLF liner subgrades of 0%, 2%, 5%, 10%, and 20%.

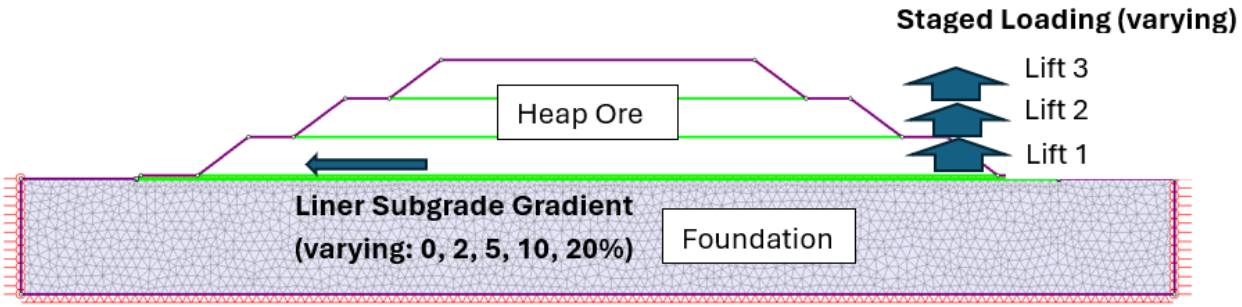

Figure 5: Model setup—HLP Application 1

Strain Development under Stacking

Figure 6 shows the development of maximum shear strain under stacking loadings. The HLF foundation in this case is assumed to be flat, and the initial three lifts (referred to as Lifts 1-3) are added as staged loadings to the model. After each staged loading, maximum shear strain along the Liner Interface is observed and tracked for changes. Figure 6 summarizes the development of maximum shear strain and changes versus loading.

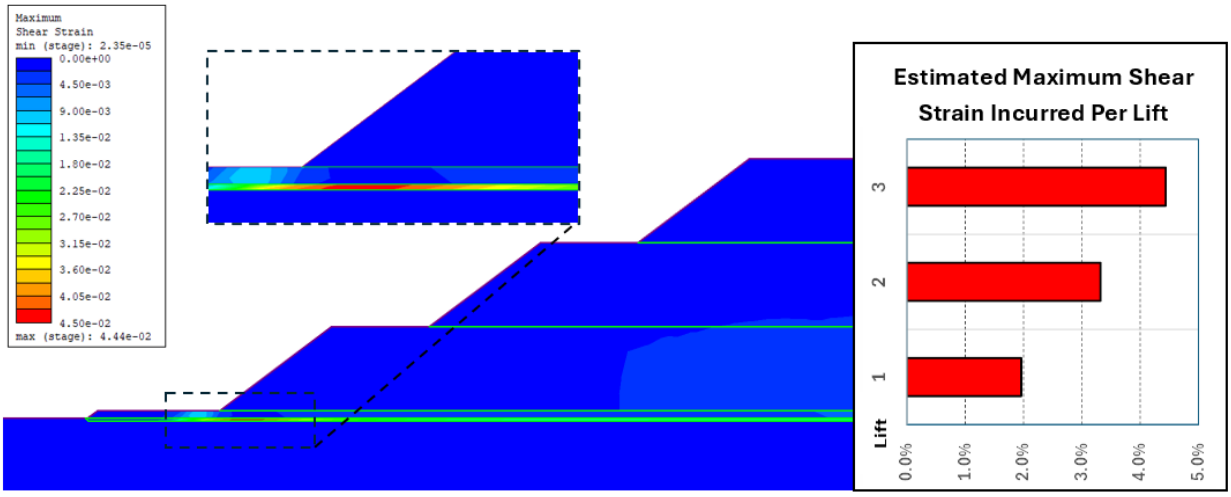

Figure 6: Shear strain development under stacking loads of lifts 1 to 3

Review of Figure 6 indicates the following:

- Under stacking loads, zones of high shear strain develop along the Liner Interface, as shown in the models (denoted in Figure 6 in warm colors as "hot" zones). As stacking progresses, the zone of high shear strain extends across the majority of the lined area.
- Development of shear strain continues throughout the placement of all three lifts modeled. A

maximum shear strain of 4 to 5% is indicated in the model after placement of Lifts 1-3, which corresponds to shear displacements up to 1.3 centimeters (cm), following Equation 1. It is noted that interface shear displacements of this scale could be enough to mobilize the interface shear strength past peak strength. The Liner Interface tends to involve strain softening material with residual strengths lower than the peak strengths (Figure 1). This is the case when a Geosynthetic Clay Liner or compacted clay layer is used as the LHCL. Seed et al. (1988) presented a case history where a landfill failure was governed by the Liner Interfaces and stated: "…the minimum ultimate or residual frictional resistance is fully mobilized at very small deformation levels which are likely to be exceeded by deformations occurring during construction and fill placement operations…". Seo et al. (2007) also reported that millimeter-scale shear displacements led to strengths past the peak values in multiple interface strength tests involving GCLs and geomembranes.

- It is critical to use residual strengths for Liner Interface in stability models instead of peak strengths.

It is noted that strength softening is irreversible in many cases. That said, a mobilized interface may lead to a reduced strength, which could be present for a facility's life of service and beyond. Any good practice that could be brought to the design and operation of a project to reduce the development of shear strain along the interfaces will significantly benefit the project moving forward.

Strain Variation with Liner Subgrades

Figure 7 shows the variation of maximum strain along the liner interface for different liner subgrade slopes. The FEM model developed in Section 3.2 was modified to incorporate varying liner subgrade slope gradients ranging from 0% (a flat lined subgrade as discussed in Section 3.2) to a sloped liner subgrade at inclinations of 2%, 5%, 10%, and 20%. The maximum shear strain under Lift 1 stacking is computed for each liner subgrade inclination and reported in Figure 7. From the figure, the following is observed:

- Maximum shear strain (SS) developed after Lift 1 stacking varies with liner subgrade (LS) slopes. While the maximum SS is generally around 2% after Lift 1 placement when the overall liner subgrade slope is flatter than 5%, the calculated SS significantly increases for LS slopes exceeding 5%. The upward non-linear trend shown in Figure 7 appears to be strong.
- The calculated SS after Lift 1 placement with the LS slope at 20% is even higher than the other four cases (as high as 50%). This model predicts slope instability with a plastic slip surface, as shown in Figure 7.
- It is important to consider instability potential governed by liner interface strengths and design a grading plan for each project that addresses risks associated with project settings and geotechnical constraints.

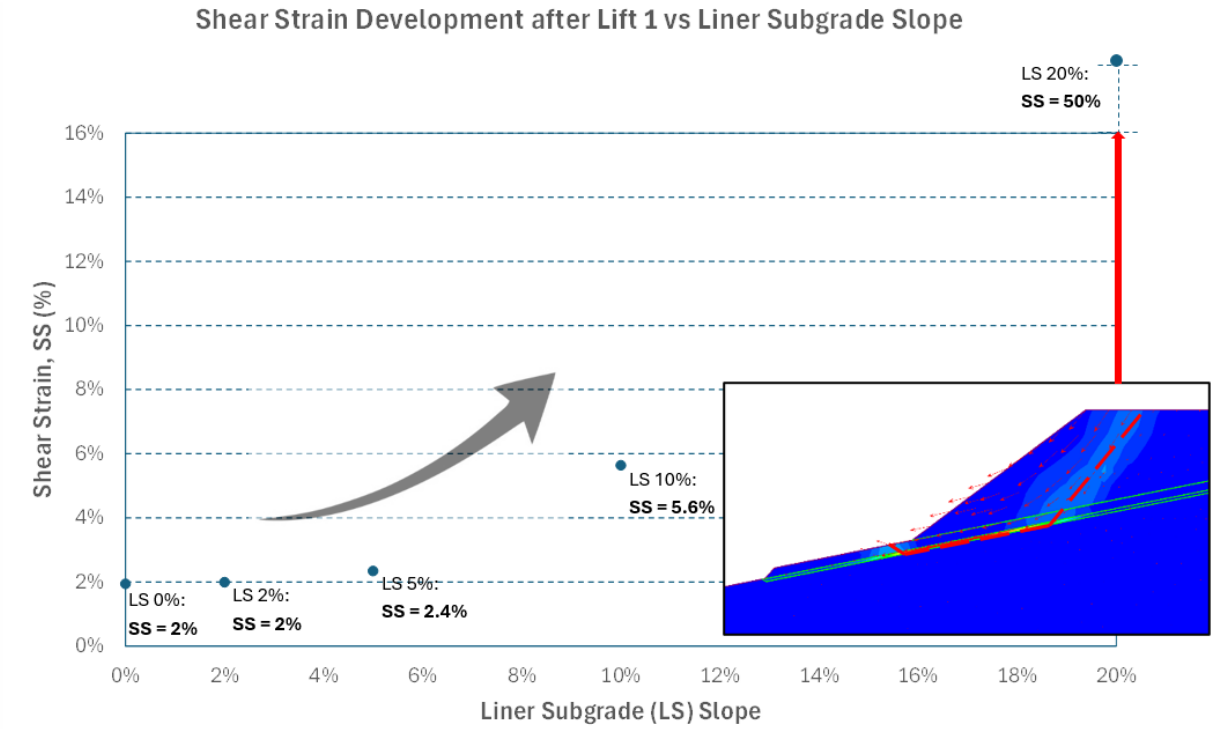

Figure 7: Shear strain development under Lift 1 stacking with varying liner subgrade

HLF Application 2: Loading Overliner System

Section 3 addresses strain development under stacking loads, which concludes that shear strain development under ore stacking is inevitable. Reduction in shear strain development under construction and stacking can be achieved by design optimization and will benefit a project as it progresses. In this section, two case scenarios are evaluated, which demonstrate that there are more ways during the construction and operation of a heap leach pad to reduce strain development and protect the Liner Interface. The use of residual strengths in the design process may not be sufficiently conservative for slope design, as further development of shear strain may reduce material strengths lower than measured residual strengths due to the limitations of laboratory test methods and the nature of geomaterials. Therefore, it is crucial to implement good practices and minimize strain development throughout the construction and operation of the HLFs to protect material strengths and ensure long-term stability.

Stacking Direction

In many cases, after a leach pad is constructed and delivered to the owner, it is up to the owner to use the facility and load the leach ore onto the pad. While the engineer provides general stacking guidance as part of the design process, it is important to keep the engineer involved during pad stacking and operations for

compliance with the design and to implement good practices to guide critical stages of facility development and mitigate geotechnical risks.

Experienced HLF engineers and mining operators understand the importance of constructing and stacking from downhill to uphill to protect the geomembrane liner and mitigate geotechnical risks. The application modeled herein addresses the reasons for doing so. To provide an illustration and comparison of the effects of uphill vs. downhill stacking, Figure 8 was prepared to summarize the predicted shear strain for modeled scenarios where ore stacking occurs uphill (Scenario 1) and downhill (Scenario 2).

The same physical model shown in Figure 5 was used for the evaluation of this application, with the Liner Subgrade slope modeled at 5%. In this particular application, the ore stacking is modeled as a newly placed wedge of ore being extended from a 10m-high stacking front on Lift 1 under both uphill and downhill scenarios. The results are summarized in Figure 8 and show significant differences in shear strain development. Scenario 1 (stacking uphill) incurs a maximum shear strain of about 1.6%, which is about 60% less than the 4.1% shear strain predicted for Scenario 2 (stacking downhill).

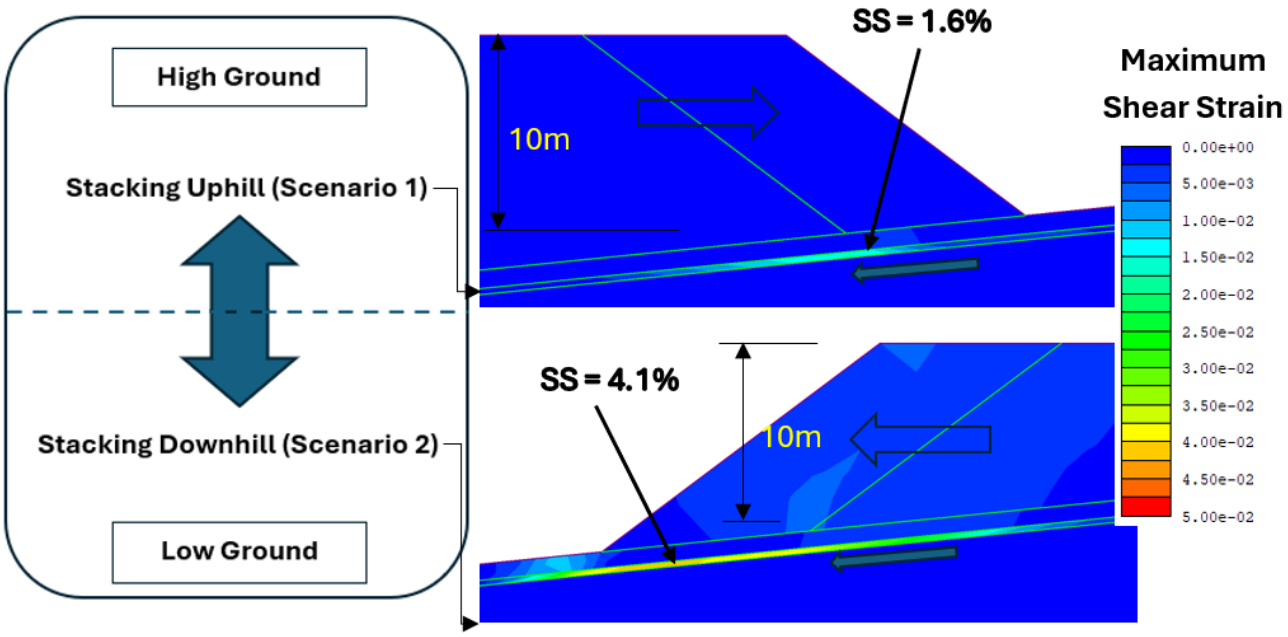

Figure 8: Shear strain development with ore stacking downhill versus uphill

Overliner Placement

The same conclusion is also applicable for overliner placement directions, i.e., placing overliner uphill results in lower shear strain development and thereby less geotechnical risk compared with downhill placement. There have been multiple cases of liner tears that occurred during overliner placement when

overliner materials were pushed in the downhill direction. While this is not elaborated on in this paper, the application is generally similar to that presented in Section 4.1.

On many projects, contractors must transport overliner materials onto the geomembrane-lined pad area using haul trucks. Typically, an extra-thick layer of overliner material is placed along hauling corridors to distribute the tire pressure load over a larger area, ensuring the load on the geomembrane remains within allowable limits based on protrusion size and geomembrane thickness. Moreover, this approach results in reduced shear strain along the Liner Interface.

To support this contention, another FEM model was developed assuming a loaded Caterpillar haul truck over the HLF pad area. A loaded Caterpillar 740 GC applies a tire pressure of 60 psi or a weight of about 70 metric tons. Figure 9 shows the results of two scenarios where Scenario 1 is Haul Truck Loading over an Overliner layer plus an additional 0.9 m of material (with a total thickness of 1.8 m), and Scenario 2 is Haul Truck Loading over an Overliner layer without the additional 0.9 m of material (i.e., without additional protection).

Figure 9 shows that in Scenario 2 (without the additional protective material), the shear strain in the liner interface is 50% larger than the shear strain in Scenario 1 (with protective material). Consideration of the effect of increased shear strain when no or insufficient protective material is placed over the liner interface is important because, typically, the designer will focus on the risk of perforation from the applied load on the geomembrane and not on other considerations.

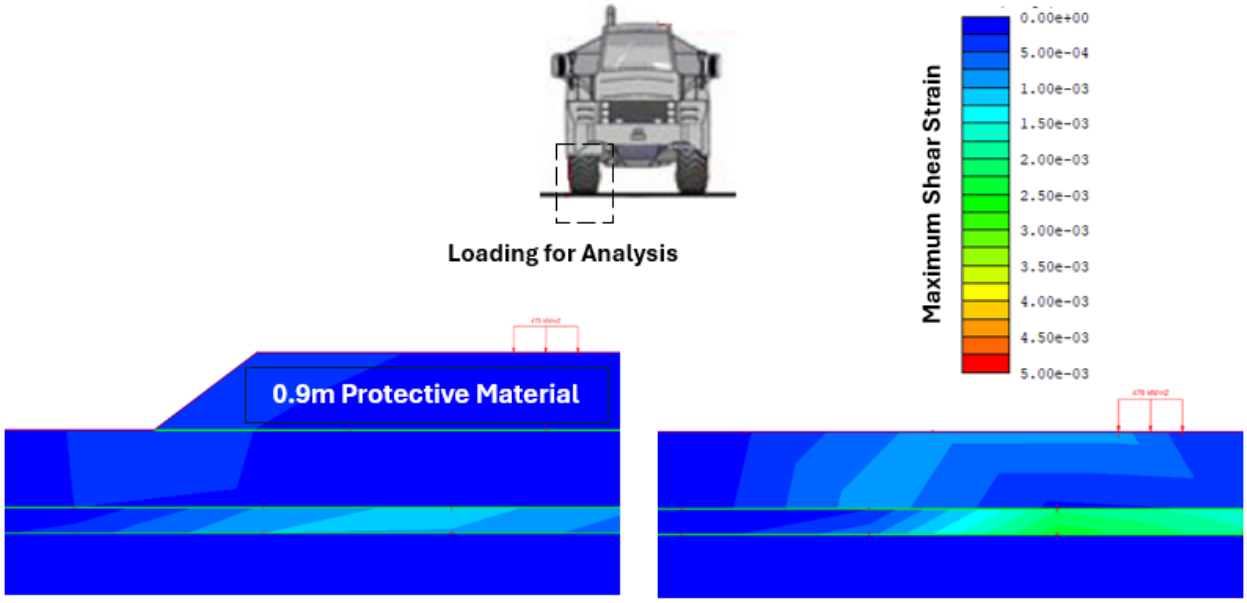

Scenario 1: with protective material **Scenario 2: without protective material**

Figure 9: Shear strain development with haul truck loading

HLF Application 3: Stacking Over Saturated Lift Surface

This paper has discussed strain development along the Liner Interface under different scenarios. The last application addressed in this paper involves stacking of new leach ore over previously deposited lifts of spent ore saturated by the leaching process; this can be the case where ore exhibits a low hydraulic conductivity. The model presented in Figure 5 was used to support this evaluation, with the focus on strain development within the ore instead of along the Liner Interface. In this example, it is assumed that the subgrade is horizontal.

As shown in Figure 10a, on a flat-lying subsurface, ore stacking alone will not result in significant shear strain development within the ore, compared with that along the Liner Interface discussed in the previous cases. However, ore stacking may result in the development of volumetric strain (Figure 10b), which can cause contraction of material and strength loss due to pore pressure development (another example of strain softening). This may happen under loading of new ore over a saturated spent ore platform if the ore behaves as a contractive and liquefiable material, similar to that of mill tailings, as reported by Oldecop et al. (2015).

Figure 11 shows the development of shear strain under undrained conditions, where the shear strength of the saturated and compressed ore is changed from drained strength (with effective-stress strength, as shown in Table 1 and Figure 10a) to a post-liquefaction strength represented by zero cohesion and a friction angle of 10 degrees. Figure 11 also shows the calculated Strength Reduction Factor (SRF) under post-liquefaction conditions, indicating a global slope instability. It is noted that stacking over contractive and saturated heap ore may lead to progressive flow failures that happen rapidly and with little to no early warning, similar to tailings static liquefaction failures.

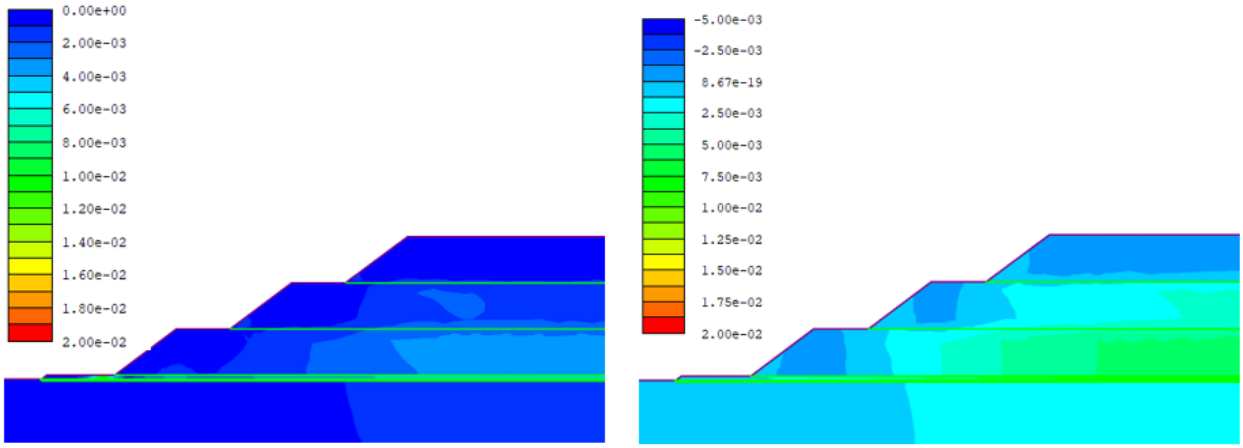

(a) Shear Strain (b) Volumetric Strain

Figure 10: Shear strain and volumetric strain development under ore stacking

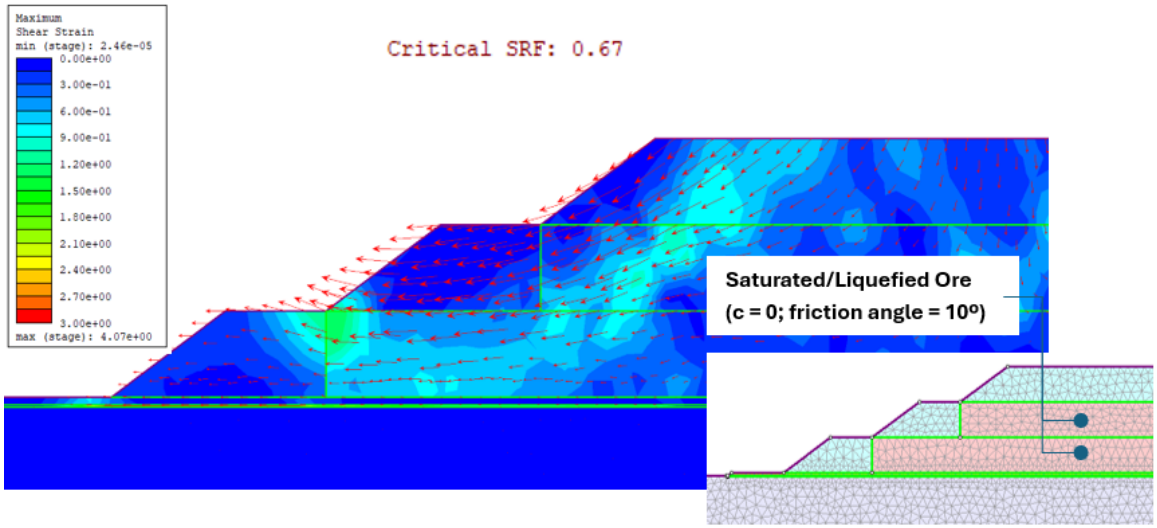

Figure 11: Shear strain development under undrained and liquefied conditions

Conclusion and Future Considerations

Discussion and evaluation of shear strain development are often ignored in the design of heap leach facilities. Through several case applications of HLF design and construction, this paper demonstrates the importance of considering shear strain development to guide engineering design and decision-making. With advancing computer technology and software development, FEM and other advanced analytical tools should be considered for design support in addition to the current standard-of-practice methods, particularly under challenging project development environments where strain considerations become even more important. The following conclusions are drawn from the analyses presented in this paper:

- It is important to use residual strengths instead of peak strengths for Liner Interfaces in leach pad designs on slopes.
- There are many ways to reduce shear strain and protect the strengths of the Liner Interface, such as developing appropriate grading plans and guiding contractors and operators to place materials on the leach pad in appropriate ways.
- Instability risks for HLFs are also possible if heap ore becomes contractive and liquefies. This may happen under certain conditions when ore stacking occurs over saturated spent ore platforms from previous lifts.
- Minimizing and mitigating geotechnical risks in HLF design and operation is a collaborative effort among engineers, contractors, and mine operators. It is vital to seek an engineer's input throughout the development and closure of HLF facilities, and an engineer's role in HLF projects should extend beyond just the initial preparation of design reports and drawings.

Simplifications and assumptions are made for the FEM models and HLF applications discussed here. While the limitations of numerical modeling are recognized, the results in this paper can serve as references when designing and operating HLFs. It is important to note that each project is unique, and inputs for advanced analytical models should be specific to the project, supported by appropriate characterization data and sound geotechnical engineering judgment.

Acknowledgements

Throughout the paper preparation, the author team has received close support from Gary Hurban and Breese Burnley of SRK. Their help with this paper is sincerely appreciated.

References

Dawson, E. M., & Roth, W. H. (1999). Slope stability analysis with FLAC. In *Proceedings of the International FLAC Symposium on Numerical Modeling in Geomechanics*, Minneapolis, MN, United States, September 1–3, 1999.

Major, G., Yuan, P., & Sharon, R. (2009). Optimizing design of high slopes in transported materials and residual soils. In *Proceedings of the International Conference on Rock Slope Stability 2009*, Santiago, Chile, November 2009.

Oldecop, L. A., Rodari, R., & Zabala, F. (2015). Shear strength parameters of a heap leach material. In *Proceedings of the XV Panamerican Conference on Soil Mechanics and Geotechnical Engineering*, Buenos Aires, Argentina, November 2015.

Rocscience, Inc. (2025). *RS2 2D finite element analysis computer program* (Version 11.026). Toronto, Ontario, Canada.

Rocscience, Inc. (2025). *Slide2 2D limit equilibrium slope stability computer program* (Version 9.038). Toronto, Ontario, Canada.

Seed, R. B., Mitchell, J. K., & Seed, H. B. (1988). Slope stability failure investigation: Landfill unit B-19, Phase I-A, Chemical Waste Management Inc., facility Kettleman Hills, California, Volume I: Report of investigation, June 29, 1988.

Seo, M. W., Park, J. B., & Park, I. J. (2007). Evaluation of interface shear strength between geosynthetics under wet conditions. *Soils and Foundations, 47*(5), 845–856.

Design and Installation of Liner Systems for Heap Leach Facilities with Steep Slopes

Andres León, Axios Engineering, Chile
Felipe Cornejo, Axios Engineering, Chile
Daniel Zúñiga, Axios Engineering, Chile

Abstract

The heap leach expansion project, Phase IX, aimed to ensure the operational continuity of the hydrometallurgical process at Codelco Chile's Radomiro Tomic Operation, extending the mine life from 2024 to 2028 for stacking and secondary leaching of 200 million tons of ore. The project required a redesign of the construction plan and a detailed evaluation of heap stability due to the steep slope conditions of the ground. This paper presents the results of using geosynthetics for protection and stability enhancement in topographically irregular areas.

As part of the liner system, 5 mm thickness geonets, 400 g/m² geotextiles, and 2 mm thickness LLDPE single-side textured geomembrane were installed on 50% maximum slope gradients. The selection of these materials was based on their capacity to improve interface shear resistance and protect the integrity of the liner system against concentrated high loads and differential settlements. Laboratory testing and numerical modeling demonstrated that the combination of these geosynthetics provides effective shear stress dissipation and stable performance of the lining system even under non-uniform loading conditions.

In addition, the use of high-strength geotextiles contributed significantly to the mechanical protection of the geomembrane during operation and for the long term. The hydraulic performance of the system was also evaluated, showing efficient leached flow toward collection pipes, avoiding localized high phreatic levels that could compromise slope stability. Field installation was carried out under strict quality assurance protocols, providing proper continuity between panels and adequate anchoring at the trenches upside and drainage ditches.

Introduction

Heap leach facilities are widely used in the copper mining industry for the treatment of low-grade ores by stacking and irrigating material with chemical solutions to recover metals. The design of these facilities typically considers relatively flat or gently sloping terrain to ensure the stability and effectiveness of the

liner and drainage systems. However, in mining areas with complex topography and limited available space, such as in the highland areas of northern Chile, new leach pad expansions often face challenging geometric and geotechnical constraints.

This paper discusses the engineering approach adopted for the design and installation of a liner system over steep slopes, specifically in the area known as Hill Island, as part of the expansion of a debris heap leach facility. Unlike traditional valley fill configurations, the area presented active slopes, high surface gradients, and restricted access for construction. This required the use of reinforced geosynthetics and careful installation planning to ensure the long-term performance of the liner system.

The work focuses on the integration of geosynthetics—namely GCLs, geonets, and LLDPE geomembranes—to mitigate erosion, enhance interface stability, and protect the system against concentrated loads and differential settlements. The paper outlines the criteria adopted, validation methods used, and performance observed, offering valuable lessons for the design of heap leach infrastructure in similar steep-slope environments.

Project Context and Challenges

The heap leach expansion project, known as Phase IX, was developed to extend the operational life of the hydrometallurgical line at the Radomiro Tomic Division of Codelco Chile. The project involved the stacking and secondary leaching of approximately 200 million tons of debris, with operations scheduled between 2024 and 2028. The expansion required the development of new stacking areas, including the integration of previously unused sectors with complex topography—most notably, the sector referred to as Hill Island. Figure 1 shows a plan view of the site where Phase IX is located.

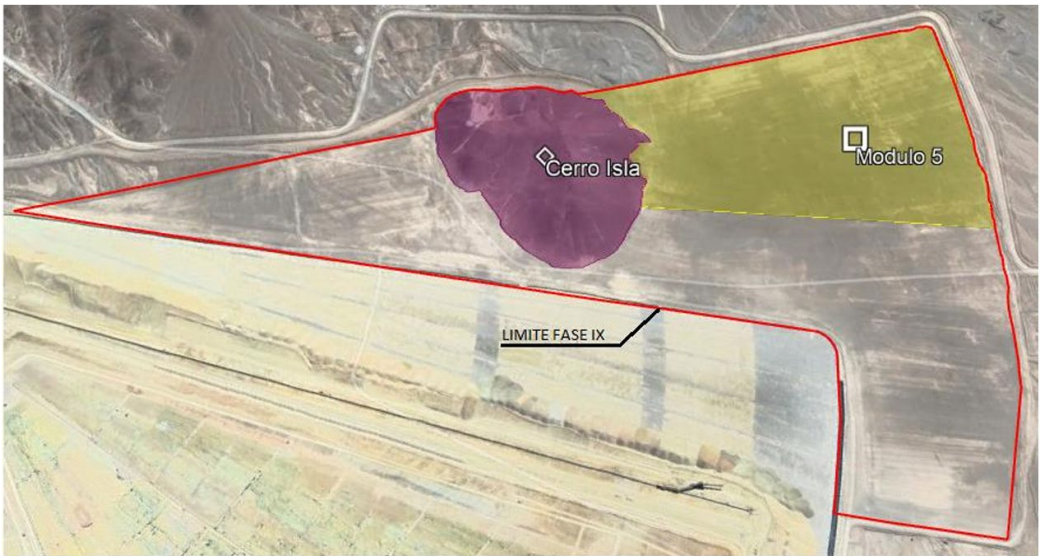

Figure 1: Plan view of Phase IX at DRT

Hill Island is characterized by its steep, rugged terrain, with continuous natural slopes exceeding 30% and localized sectors approaching or surpassing 50%. These conditions presented a series of challenges uncommon in conventional leach pad designs:

- Limited accessibility for heavy equipment and liner deployment.
- Increased risk of liner slippage and interface failure under operational loads.
- Difficulties in controlling surface water flow and erosion during both construction and operation.
- Complex anchoring and detailing required for liner stability in transition zones and crests.

In addition, the absence of a valley-fill configuration meant that the containment and confinement of the stacked material would rely heavily on slope geometry and liner performance, rather than on natural topographic boundaries.

Given these constraints, it became essential to adopt an engineered approach that prioritized mechanical stability, hydraulic efficiency, and practicality of construction under constrained field conditions. This required the definition of specific geometric criteria, the selection of reinforced geosynthetics, and fostering a close integration between geotechnical, hydraulic, and process design teams.

Methodology

The design methodology was based on an iterative process of engineering validation involving three key components: (1) definition of geometric and operational criteria, (2) material evaluation, and (3) numerical modeling to simulate liner system performance.

First, slope geometry and layout were defined based on topographic constraints, planned stacking configuration, and accessibility. Specific zones were delineated where geosynthetics would require enhanced shear strength and protection due to slope angle or loading conditions.

The selection of geosynthetics was supported by available manufacturer data and experience from similar applications. Published values of interface shear strength were considered in assessing the mechanical compatibility of GCLs, geonets, and geomembranes under steep slope conditions.

Stability analyses were carried out at the global scale of the heap, focusing on intermediate stacking stages and slope behavior. While these were not specific to the liner system, the findings supported the need for high interface shear resistance and drainage capacity in steep slope areas.

For material selection, geosynthetics were shortlisted based on mechanical properties, field performance in steep slope conditions, and compatibility with operational loads. Manufacturer data and prior project experience guided the selection.

Numerical modeling and shear interface testing (from analogous projects) were used to confirm the system's stability under design loads.

The selected system combined a textured 2 mm LLDPE geomembrane, a 5 mm-thick geonet, a 400 g/m² geotextile, and a GCL in areas with limited subgrade preparation. This configuration struck a balance between mechanical stability, hydraulic efficiency, and constructability.

Design and Implementation

The implemented design adapted the liner system to match the natural slope of Hill Island while providing continuity with the main heap leach operation. Construction sequencing was carefully planned to allow phased installation and tie-ins across the upper and lower portions of the slope.

The liner system in the area corresponding to Modules 5 and 6 (Hill Island) of Phase IX consisted of a 2.0 mm-thick LLDPE textured geomembrane. In the drainage zones (evacuator drains), a 400 g/m² nonwoven geotextile was added beneath the geomembrane to prevent puncture damage caused by contact with irregular excavation surfaces.

On steep slopes at Hill Island, a 5 mm-thick geonet was incorporated as a support layer beneath the geomembrane to enhance interface stability and allow subsurface drainage. Additionally, in areas where subgrade preparation was limited or irregular, a Geosynthetic Clay Liner (GCL) was used as a protective base layer under the geomembrane.

The geomembrane itself was composed of virgin-grade LLDPE and HDPE resin, supplied in rolls and free of blisters, voids, or perforations. Table 1 outlines the minimum performance requirements for this liner.

Table 1: Minimum Requirements for Textured LLDPE Geomembrane

Property	Unit	Value
Minimum thickness	mm	2
Minimum density	g/cc	0.939
Texturing thickness	mm	0.4
Tear resistance	kN/m	60
Elongation at break	%	250
Puncture resistance	N	400
Tensile strength	N	200
Asymmetric tensile resistance	kN/m	60
Oxidative Induction Time (OIT), Standard	minutes	100
Oxidative Induction Time (OIT), High Pressure	minutes	400

The geotextile was manufactured from synthetic fibers forming a needle-punched nonwoven fabric. These fibers consisted of at least 85% by weight of polyolefins, polyesters, or polyamides, and the geotextile was required to be free of defects that could significantly affect its mechanical properties. Specification limits are detailed in Table 2.

Table 2: Properties of Nonwoven Geotextile

Property	Unit	Value
Mass per unit area	g/m²	405
Tensile strength	N	1,420
Elongation at break	%	50
Puncture resistance	N	835
Trapezoidal tear resistance	N	555
Apparent opening size (AOS)	mm	0.150
UV resistance (% retained at 500 h)	–	70

The geonet was manufactured from virgin high-density polyethylene (HDPE), with a diamond-shaped mesh formed by two intersecting layers of parallel strands. These strands provided continuous deep flow channels. The geonet was supplied in rolls and required to be free from lumps, unmixed material, cuts, wrinkles, or any foreign matter, in accordance with the technical specifications listed in Table 3.

Table 3: Properties of Geonet

Property	Unit	Value
Thickness	mm	5
Minimum density	g/m²	790
Tensile strength	N/mm	7
Carbon black content	%	2 to 3
Polymer density	g/cm³	0.932
Melt flow index	g/10 min	1.0
Transmissivity	cm²/s	1×10^{-3}

All geosynthetic materials were installed in accordance with strict quality control protocols. Geomembrane panels were aligned downslope, welded or sealed as per manufacturer standards, and anchored using trenching at crest and toe areas. The integration of these materials allowed for mechanical

protection, efficient drainage, and enhanced interface stability, even under concentrated loads and slope deformations during operation.

In field practice, the geonet layer facilitated subsurface drainage while also serving as a separator between materials. The high-strength geotextile provided cushioning and reduced mechanical damage to the geomembrane during debris placement. In specific zones with irregular foundations or steep inclines, the GCL provided a redundant barrier layer with self-healing capabilities in case of minor punctures.

Performance Evaluation

Performance evaluation combined results from numerical simulations, laboratory data, and field observations. The interface shear strength values obtained in the laboratory confirmed that the selected configuration could maintain stability under critical loading conditions, even in slopes up to 50%.

The geosynthetic system showed excellent hydraulic performance, allowing controlled movement of solutions toward collection channels without accumulation or ponding. This minimized the hydrostatic pressure behind the liner and reduced the risk of localized uplift or slope instability.

In operational conditions, no significant liner displacement or erosion issues were observed during early stacking activities, validating the chosen material configuration and construction techniques. Hydraulic performance ensured uniform solution flow toward the collection channels, thereby avoiding hydrostatic buildup. Observations indicate that the geonet provided adequate drainage while protecting the geomembrane from stress concentrations.

Conclusion

The main conclusions of this study are the following:

- Geosynthetic combinations can be successfully applied in steep-slope leach facilities with proper material selection and interface evaluation.
- GCLs provide a reliable secondary barrier in complex terrain where subgrade preparation is limited.
- Project-specific anchoring and installation details are critical in non-valley fill configurations.
- Lessons learned from this project support the feasibility of expanding heap leach operations in topographically constrained environments, while maintaining structural and hydraulic integrity.

GCL-LLDPE Geomembrane Interface Friction Angle Evaluation and Stability Analysis of a Valley Fill Leach Pad Project

Daniel Zúñiga, Axios Engineering, Chile
Andres León, Axios Engineering, Chile

Abstract

The Los Chancas mining project, initiated in 1998, is a copper mine focused on extracting copper sulfides and oxides. In 2020, a mine plan update required a review of the constructability design and an evaluation of the Permanent Leach Pad and Filtered Waste/Rock Dump's physical stability. This paper presents results from an evaluation study regarding friction angles at the liner interface and stability analysis in the VLF pad. Previously, an internal friction angle of 23° was established for the basal liner interface (LLDPE-GCL) to meet stability requirements. However, due to the high required friction angle, the pad design was updated with lower slopes. The study evaluated various GCL materials from two suppliers using direct shear tests, revealing that the GCL from the second supplier achieved a high friction angle of 22.3° at the interface. Stability analysis considered two critical sections, examining three types of failure under both static and pseudo-static conditions. Results showed a need for a minimum friction angle of 16° in static conditions and 20.5° in pseudo-static conditions to ensure compliance. These results suggest the potential use of high strength geosynthetic materials in the studied areas, with a preference for the GCL material offering the highest friction angle.

Introduction

The management of tailings and ore leaching is critical in the mining industry, and the stability of the structures designed for these purposes is of crucial significance.

Within the framework of the Los Chancas mining project, initiated in 1998 and developed by Southern Peru Copper Corporation (SPCC) in the districts of Tapairihua and Pocohuanca, in the province of Aymaraes, Apurímac, Peru, an open-pit mine is operated to extract copper sulfides and oxides, processed through flotation and leaching. In 2020, the mine plan was updated, which required a review of the constructability design and an evaluation of the physical stability of the Permanent Leaching Heap and Filtered Tailings Deposit.

This paper focuses on the evaluation of friction angles at the interface of the leach pad liner and reviews the physical stability conditions in a high seismic risk mining environment, considering the final configuration of the leaching heap installation. Through detailed research and geotechnical analysis, solutions are explored to ensure the integrity and safety of this essential infrastructure in the Los Chancas project. The analysis includes the verification of Safety Factors in compliance with regulations for both static and operational seismic scenarios for two critical sections of the heap leach.

Structure Modeling

Heap Leach Geometry

The installation of the permanent heap leach was designed with a valley fill configuration, growing through the upstream construction method within the valley, completing its construction before the end of the filtered tailings and waste rock deposit construction.

To assess the stability of the heap leach, two sections were analyzed, considered as critical due to their geographical conditions. One is located in the central area of the heap leach, featuring higher slopes. The location of the sections in relation to the original design is shown in Figure 1.

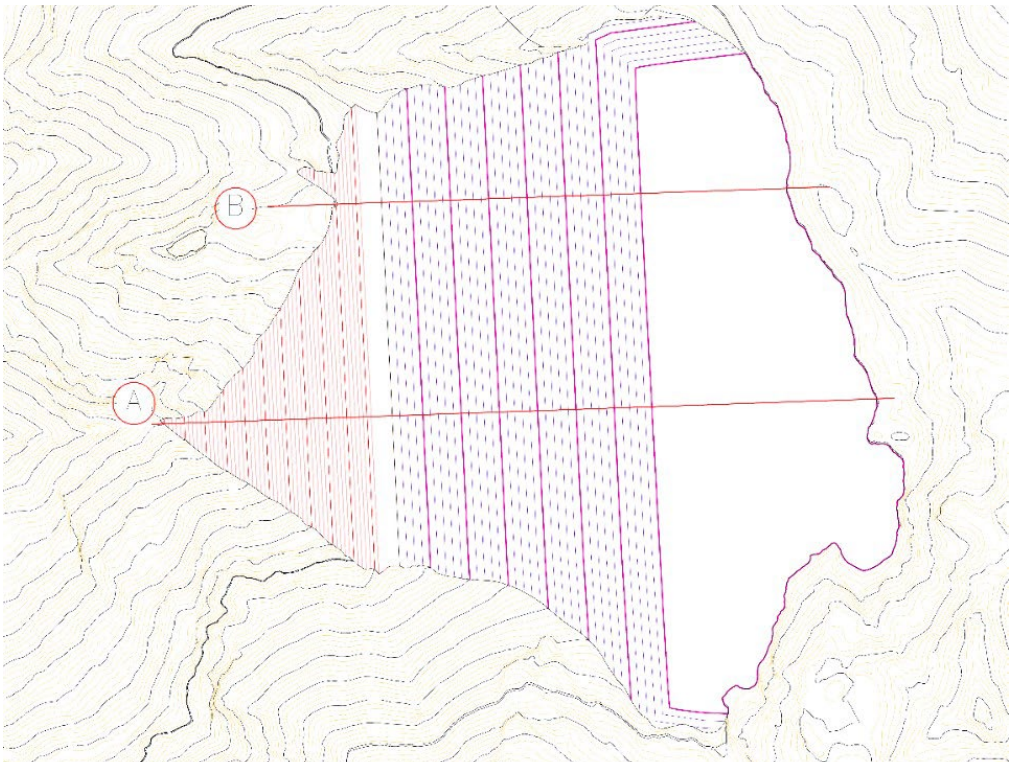

Figure 1: Site plan view—location of the analyzed sections of the permanent heap leach

Properties of the Materials in the Permanent Heap Leach

The permanent heap leach will consist of leaching ore and a liner system made up of 1.5 mm LLDPE

geomembrane and a GCL. In addition, at the base downstream, a containment embankment is designed, which will be composed of rockfill material.

The geotechnical properties of the materials that compose the heap leach are shown in Table 1.

Table 1: Geotechnical Properties of the Heap Leach Materials

Material	Density (kN/m³)	Cohesion (kPa)	Friction Angles (°)
Leaching ore	19	38	34
Rockfill Embankment	22	0	45
Foundation Soil	20	0	34
Bedrock	20	0	50
GCL	20	0	13,5
			16
			18
			20,5

Evaluation of Friction Angles at the Liner Interface

The results of the friction angle between LLDPE geomembranes and GCL obtained through direct shear stress testing on materials from two different suppliers were evaluated, as shown in Table 2. The maximum normal stress reached for the first supplier was 1,200 kPa, and for the second supplier, it was 800 kPa. The results obtained show a significant decrease in the residual internal friction angle compared to the peak friction angle.

It is important to note that material strength is degraded as the normal stress increases, and the tension in the proposed permanent heap leach is up to 1,800 kPa, which is higher than the values achieved in the presented tests.

Table 2: Internal Friction Angle of GCL from Two Analyzed Suppliers

Supplier	Material 1 (GCL)	Material 2	Maximum Vertical Stress (kPa)	Peak Angle (°)	Residual Angle (°)
1	Alvatech LLDPE 2FIX	Geotextile NW—HT 600 gr/m2	1200	29,7	13,5
		Geotextile NW—HT 800 gr/m2		27,4	12,9
2	Tektoseal 400	Geomembrane LLDPE SST 2mm	800	23,3	13,7
	NaBento 4500			22,9	22,3
	Tektoseal 4500			21,9	13

For a high friction angle at the interface, it is concluded that one specific type of GCL from the second supplier would be appropriate, which provides a residual value of 22.3° for 800 kPa of vertical load.

Seismic Coefficients

The method of Limit Equilibrium was used to simulate seismic loads through a pseudo-static analysis. In this way, horizontal and vertical forces equal to the weight of the sliding mass were incorporated into the model, multiplied by their respective acceleration coefficients, corresponding to the pseudo-static acceleration coefficients (kh and kv).

The pseudo-static acceleration coefficients were defined based on the site's seismicity. Table 3 shows the values for the event associated with the structure's operational scenario.

Table 3: Internal Friction Angle of GCL from Two Analyzed Suppliers

Scenario	Description	Value
Operational Seismic Event	Horizontal Seismic Coefficient, k_h	0,135
	Vertical Seismic Coefficient, k_v	0,0675

Phreatic Level

The phreatic level location was calculated using the Moore and Hooghoudt methods, considering the base with and without slope, respectively.

The model for the stability analysis considered a slope of the terrain only of 100 m from the base of the wall (upstream), while between 0 and 100 m, a horizontal base was considered to impose an unfavorable condition on the stability of the leach pad. Table 4 shows the phreatic level heights from the base of the leach pad.

Table 4: Phreatic Level Height

Distance from the Base of the Wall (Upstream)	Phreatic Level Height (m)
<100 m	2,28
>100 m	1,53

Acceptance Criteria

The acceptance criteria used for the stability analysis of the leach pad correspond to those established by the Ministry of Energy and Mines of Peru, as shown in Table 5.

Table 5: Acceptance Criteria for Stability Analysis

Case	Safety Factor (SF)
Static along the geomembrane interface	1,3
Static Earth-fill structures	1,5
Pseudo-static	1,0

Modeling

The stability analysis was conducted based on the conventional method of limit equilibrium (MLE), which determines the minimum safety factor for a potential failure surface and a predetermined geometry. The safety factor (SF) is defined as the ratio between the available shear strength and the mobilized shear strength, which depends on the properties of the materials involved and boundary conditions (foundation soil, drained or undrained condition, pore pressures, overloading, and seismic forces).

Stability analysis calculations were performed using the Bishop Simplified method, Spencer method, Morgenstern-Price method, and Corrected Janbu method. The critical Safety Factor is the lowest value obtained from all the methods. Using 2D modeling software, the method of discrete sections is applied, considering the limit equilibrium approach, and safety factors are established for block or circular failure surfaces. Figures 2 and 3 show the analyzed sections.

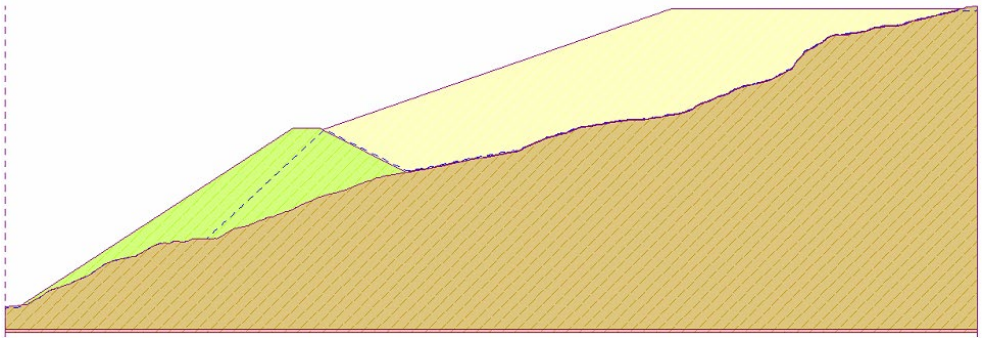

Figure 2: Analysis section A

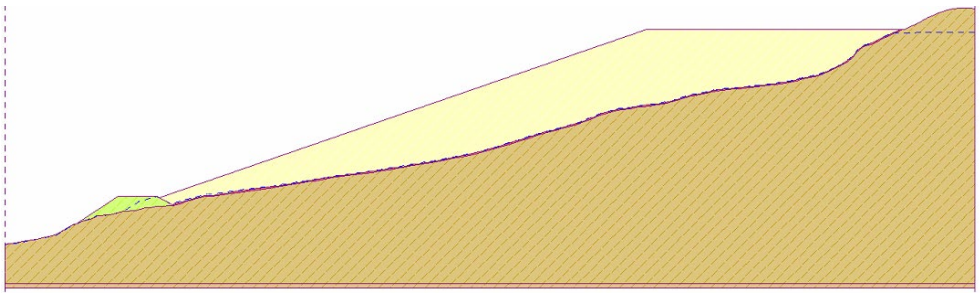

Figure 3: Analysis section B

Result Analysis

Base Case: Friction angle of 13.5° at LLDPE—GCL interface

Table 6 presents the safety factors obtained from stability analyses considering an internal friction angle at the LLDPE—GCL interface of 13.5°, which corresponds to the base case of a conventional GCL with a single textured LLDPE geomembrane on its lower side in contact.

Table 6: Stability Analysis Results for the Interface with a Friction Angle of 13.5°

Section	Condition	Zone	Surface Type	Safety Factor	Acceptance Criterion	Verification
A	Static	Wall	Circular	1,54	1,5	Meets
		Heap	Circular	2,27	1,5	Meets
		Interface	Block	1,54	1,3	Meets
	Pseudo-static	Wall	Circular	1,14	1,0	Meets
		Heap	Circular	1,54	1,0	Meets
		Interface	Block	1,01	1,0	Meets
B	Static	Wall	Circular	1,56	1,5	Meets
		Heap	Circular	1,97	1,5	Meets
		Interface	Block	1,10	1,3	Does not meet
	Pseudo-static	Wall	Circular	1,14	1,0	Meets
		Heap	Circular	1,35	1,0	Meets
		Interface	Block	0,68	1,0	Does not meet

The results obtained indicate a failure to meet the minimum safety factors for the interface of the heap leach in section B, both in static and pseudo-static conditions. Therefore, it is necessary to perform a sensitivity analysis for the internal friction angle of the interface in section B to establish the material requirements that meet the criteria for physical stability acceptability.

Sensitivity Analysis of the Friction Angle at the Interface

Based on the obtained results and the available background information on GCL-Geomembrane shear strength tests, a sensitivity analysis of the friction angle at the interface was performed, evaluating angles of 13.5°, 16°, 18°, and 20.5°, obtaining the results shown in Table 7.

From the results obtained, it is concluded that an interface with a friction angle of 20.5° meets the established acceptance criteria.

Table 7: Results for Sensitivity Analysis of the Angle at the Interface in Section B

Condition	Interface Angle	Safety Factor	Acceptance Criterion	Verification
Static	13,5°	1,10	1,3	Does not meet
	16°	1,30	1,3	Meets
	18°	1,47	1,3	Meets
	20,5°	1,69	1,3	Meets
Pseudo-static	13,5°	0,68	1,0	Does not meet
	16°	0,79	1,0	Does not meet
	18°	0,89	1,0	Does not meet
	20,5°	1,02	1,0	Meets

Analysis with a Friction Angle of 20.5° at the LLDPE—GCL Interface

Taking into consideration the results from the sensitivity analysis of the friction angle at the interface for section B, a comprehensive stability analysis is conducted with an angle of 20.5°. The safety factors obtained from the analyses are presented in Table 8, confirming that all of them meet the acceptance criteria.

Table 8: Stability Analysis Results for the Interface with a Friction Angle of 20.5°

Section	Condition	Zone	Surface Type	Safety Factor	Acceptance Criterion	Verification
A	Static	Wall	Circular	1,54	1,5	Meets
		Heap	Circular	2,27	1,5	Meets
		Interface	Block	2,05	1,3	Meets
	Pseudo-static	Wall	Circular	1,14	1,0	Meets
		Heap	Circular	1,54	1,0	Meets
		Interface	Block	1,29	1,0	Meets
B	Static	Wall	Circular	1,56	1,5	Meets
		Heap	Circular	2,07	1,5	Meets
		Interface	Block	1,67	1,3	Meets
	Pseudo-static	Wall	Circular	1,14	1,0	Meets
		Heap	Circular	1,40	1,0	Meets
		Interface	Block	1,01	1,0	Meets

Conclusion

In this study, three scenarios were analyzed for each section under both static and pseudo-static conditions: Circular failure in the embankment (platform), circular failure in the heap leach, and block-type failure through the interface (LLDPE-GCL). For section A, this was the critical section in terms of maximum height of the deposit and location, since it is where most of the infiltration will occur. On the other hand, section B was considered critical due to the increased slope of the existing ground with a smaller embankment, where the leached ore height generates a significant volume in this section, with a higher risk to fail due to sliding in the GCL base interface.

For section A, the most critical case is the circular failure scenario in the embankment of the platform, both in static and pseudo-static conditions. This corresponds to a surface failure, typical of non-cohesive materials, and does not compromise its overall stability.

For section B in the analysis carried out considering a friction angle of 13.5° at the interface of the base case, section B does not meet the acceptability criteria, with the most critical scenario being the block-type failure through that interface (GCL).

Through sensitivity analysis, material requirements were established to meet the minimum safety factors. The results indicated that to achieve the minimum safety factor, an interface friction angle of 16° is required for the static case, and 20.5° in pseudo-static conditions. Furthermore, it was verified that by considering a 20.5° interface angle, the acceptability criteria were met in all the studied scenarios.

Based on the results obtained, it was concluded that it is possible to use high-strength geosynthetic materials in areas that require it, particularly in the case of GCL material, where there is a type of high-friction product that could meet this requirement.

As final recommendations from the study, it is suggested to conduct direct shear tests to obtain representative parameters for the GCL and geomembrane. Additionally, measurements of the phreatic level within the permanent heap leach can be carried out by implementing a piezometric level system to validate the analyses conducted.

References

Huesker. (2016). *Direct shear test interface LLDPE—GCL Tektoseal and NaBento.*

Sotrafa Geosynthetics Division. (2016). *Alvatech fix textured—structured geomembranes.*

Changes in Gold Heap Leach Fluid Chemistry after 30 Years of Closure

Glenn C. Miller, University of Nevada, USA
Iain Dover, University of Nevada, USA

Abstract

Since the 1960s, mining for gold and silver using heap leach cyanide processes has been a major industry in the western United States. This has proven to be a cost-effective method for processing low-grade gold and silver ore. Following months to years of leaching, the heaps and associated ponds that collect the water are reclaimed. However, it is not well understood how various chemical constituents observed in the heap effluent change as closure is completed and as water is released from these facilities. The water quality of the released effluent is of concern. Even though the flow rates decrease/stabilize over time, the contaminant load in the released water can be high. This contaminant load depends on the extent of rinsing, either by recirculation or by the flow of meteoric water (rain and snow). Over time, as meteoric water rinses the heap, the concentrations of the easily soluble contaminants will decrease. As closure continues, specific constituents, including cyanide and mercury, will decrease. Nitrate concentrations will initially increase and then ultimately rinse out. Alternatively, the more tightly held constituents, particularly arsenic, will take longer to elute, and potentially can increase in concentration, depending on changes in pH or continuing reactions in the heap material, which can release arsenic. Understanding how the contaminant load changes over time will assist in the proper management of these facilities

Introduction

When economic extraction of gold from a precious metals heap leach reaches the point that further leaching is no longer profitable, closure of that heap begins. Cyanide additions are discontinued, and the remaining large volumes of water are generally evaporated by recirculation of the water to the top of the heaps until the amount of water being managed is sufficiently low that recirculation can be discontinued and the collected water can be managed separately or land applied. Meteoric water (rain and snow) will further rinse through the heaps over time, depending on the method used during closure, and this water collected from the heap is collected for management. Evaporation of the water using open ponds is commonly used to manage the excess and meteoric water. The rate of rinsing of the heaps will depend on the closure

methods, the type of heap construction, the temperature, and the quantity of meteoric water (U.S. EPA, 1994; Flynn & Haslem, 1995). Ultimately, the time frame for complete meteoric water rinsing of the heaps under Nevada conditions can be on the order of decades. This monitoring/sampling is performed under authority from the Nevada Division of Environmental Protection using certified testing laboratories.

During the closure period, the drainage water quality from the heaps is monitored at least quarterly. Direct discharge of the water into surface water rarely occurs, particularly in well-regulated regions, since the salt content of the water alone will generally not allow discharge of that water into surface water (U.S. EPA, 1994).

This study is designed to describe how specific chemical concentrations change during 30 years of closure of a heap leach operation at the Toiyabe mine. The data that is used in this study is from the Nevada Division of Environmental Protection, which has retained the long-term drainage data from both operating and closed mines for over 40 years.

Heaps that utilize cyanide are operated at a high pH (> 10.5) and dissolve carbon dioxide into the water. Various metals can complex with the carbonates and precipitate, particularly as calcium carbonate, since lime (CaO) is commonly used to maintain the pH above 10.5 during operation. During closure, the pH is reduced, but is expected to remain basic and stabilize around pH 8.3, since that is the pH that solid calcium carbonate will establish in the water via dissolution and hydrolysis (U.S. EPA, 1994). Alternatively, if the heap ore contains sufficient sulfides that oxidize to sulfuric acid, the heap drainage can become acidic and consume the available calcium carbonate. This situation will entirely change the evolution of the heap drainage water quality, since if the pH drops below 4, a variety of metals will dissolve in the water, resulting in severely degraded water. This situation is highly problematic, but will not be considered in this study, although examples of heaps in Nevada exist where the heap drainage has become acidic (see, for example, the Sleeper Mine, NDEP, personal communication).

The construction of the heaps is designed to create a heap that is homogeneous, both laterally and vertically, so that percolation of the cyanide-containing fluids can effectively occur uniformly (Kappes, 2005; Kowalski, 1999). Because the heap material is often heterogeneous, preferential pathways can be created that allow the fluids to drain through pathways and reduce the ability to rinse the entire heap in a well-controlled manner (O'Kane Consultants, 2000). These preferential pathways generally consist of larger pore spaces and allow for rapid fluid movement, and will allow some surfaces to be rinsed rapidly, while other areas will be rinsed more slowly. These heterogeneities will be expected to slow the complete rinsing of the heap and extend the time for improvements of the water quality being eluted from the heap.

Over the past 30 years, the management of heaps during closure has focused on reducing the volume of drainage from the heaps, in order to reduce the management of the contaminated initial drainage. The state and federal regulatory agencies in Nevada now effectively require a cap to be placed on heaps to

control the amount of meteoric water infiltration into the heaps. These "store and release" caps are made of growth media that reflect the native environment/parent material (Kowalski, 1999). During the seasons when rain or snow falls on the heaps, the soils can retain the water, which plants can then utilize for growth and the removal of that water. These caps are commonly also designed to have shrink and swell properties to ensure that (depending on the season) they do not crack and allow a greater amount of water infiltration. Even though a cap is placed on a heap during closure, the heaps are rarely completely sealed, except in very arid conditions. Because they are not completely sealed, some water can still pass through the heap, particularly in very wet years, and the resulting drainage water quality will likely be degraded for a longer period of time (Decker & Tyler, 1999). In arid areas that have higher temperatures and lower precipitation, less water will generally be introduced to the heap, resulting in less water released. While it will increase the time for meteoric rinsing of the heaps, it will also reduce the water management costs during the initial decades of closure. However, in areas that contain higher amounts of snowpack/rainfall, drainage is likely to be higher (Kampf et al., 2002).

Data Source

During mine closure, mining companies working under regulations of the Nevada Division of Environmental Protection use certified analytical laboratories to confirm water quality regulation and proper closure practices. As discussed previously, these practices range from placing caps on heaps to monitoring and management of chemical drain-down and meteoric water infiltration/flow. The chemical drain-down for the heap operation discussed below was monitored quarterly over the course of many years. Companies closing heaps sampled the drainage for various constituents, and submitted these water samples to testing laboratories, which report the concentrations draining from the heaps to the mining company, and ultimately to the regulatory agencies, particularly the NDEP, which maintains a record of these water quality measurements. These testing results have generally been available for the previous 30-40 years for heaps and consist of a large variety of water quality parameters, including many metals, WAD (weak acid dissociable) cyanide, mercury, arsenic, chloride, sulfate, TDS, and pH. The trends of these constituents would help understand how heap chemistry changes over time.

As can be observed from the figures, some breaks are shown where the data could not be found, although the trends of water quality are generally quite apparent. When cyanide was stopped from being added in approximately 1992, water was recirculated for 7 years, and some changes (i.e., pH) were observed. During the period from 2001, when meteoric water was the only source of new water, the concentration of constituents was dependent in part on the meteoric precipitation, with generally higher flow (and lower concentrations) following seasonal trends and various meteoric events.

Results and Discussion: The Toiyabe Mine

The Toiyabe mine is a decommissioned heap leach mine in central northern Nevada (Western Mining History, n.d.; McCrea, 2017). This mine is located approximately 10 miles southwest of Elko at an elevation of 7,200 feet above sea level, at the north end of the Toiyabe Range. It contains two closed heaps, together covering approximately 31 acres. This property was originally mined by Inland Gold, and was purchased by Placer Dome Gold, and was acquired by Barrick Mining, when Barrick purchased the Placer Dome company. The Toiyabe mine was a relatively small mining operation, and primarily produced gold and silver. Precious metals were discovered at this property by Homestake Mining in 1966, with exploration and drilling taking place in 1969. This property was in production from 1987 to 1991 by the then-current owner, Inland Resources, and produced around 89,000 ounces of gold. The Toiyabe mine operated using two heap leach pads during production.

Closure of the heaps requires reduction of water volume in the heaps and is usually done by evaporation and recirculation of the water over the heaps. Following reduction (and land application of excess water), meteoric water continues to rinse the heaps. These current heap drain-down flow rates vary between 0 to 12 gallons per minute (gpm), with a yearly average of 1.4 gpm (approximately 750,000 gal/year). The average precipitation ranges from 14.7 to 17.6 in/year, occurring mostly as snowfall. Since the closure of the Toiyabe mine, the site has been monitored by the environmental department of Placer Dome and by Barrick, under regulatory authority of the NDEP. The drainage water from the heaps, and surface and ground water have been monitored for specific chemical constituents by commercial certified laboratories quarterly and yearly, since closure (except where noted). The results of these tests have been held by the NDEP as indicators of the water quality throughout the site and potential changes in water quality over the closure period. The mine halted production in 1992, and drainage water from the heaps was recirculated and evaporated over several years until final closure allowed land application of approximately 4 million gallons in 1999–2001.

For this facility, we have examined how various constituents (W.A.D. cyanide, nitrate, mercury, arsenic, pH, TDS, chloride, and sulfate) change. Figures 1 to 10 display specific draindown from the closed Toiyabe facility over time (closure monitoring beginning in early 1992).

30 Years of Drainage

The literature of heap leach hydrology is extensive, but primarily appears to be on active gold mines. The draindown rates of several closed heaps have been considered by Kampf and co-workers (2002) over a period of approximately 4 years. They report that, following cessation of rinsing, the draindown rates appeared to stabilize in about 1 year, although it was noted that there was uncertainty if rates would slow further in later years. The Toiyabe data is for a period of 30 years, but 22 years following cessation of

rinsing/evaporation. From quarterly data on flows from the heap, drainage flows vary considerably, in general relation to precipitation patterns. Highest flows occurred in winter to early summer, although high flows were also measured even in late summer, presumably in relation to meteoric events. While it would be helpful to have flow data monitored more frequently, this was not available, in part due to the inability to access the site during winter. Because of high elevation and the inability to access the site, measurements and sample collection were not possible from December to March. The water quality and flow data were from the Heap Leach Pad Distribution Box 1 (HLPDB1).

The pH of the meteoric drainage is expected to decrease in the heap drainage water as carbon dioxide dissolves in the high pH recirculating water. Carbon dioxide is converted to carbonic acid, which releases a proton and decreases the pH of the drainage water to the carbonate equilibrium pH. The change in pH due to carbon dioxide is expected to affect other pH-dependent chemistry in the heap and drainage water.

The change in pH is shown in Figure 1.

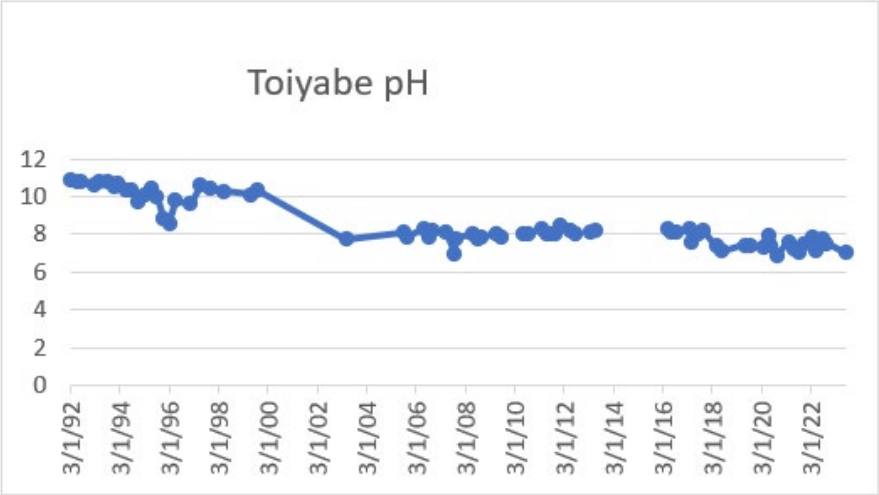

Figure 1

Following closure, no additional cyanide or lime is added to the circulating solution, and carbon dioxide is introduced into the heap, simply because the calcium present will form calcium carbonate and precipitate. If calcium carbonate were the only constituent to affect pH, the pH should stabilize at around 8.3. However, oxidation of sulfides will continue until those materials are depleted.

At the beginning of closure, after cyanide addition was discontinued and the pH allowed to drop, the cyanide concentration (as WAD CN) decreased over time (Fig. 2) as the water was recirculated to reduce the volume of water and allow meteoric water rinsing. Cyanide was likely lost both by oxidation and volatilization, although the relative contribution of each process is difficult to estimate. The WAD cyanide concentration dropped by over a factor of 100 within 2 years. WAD cyanide continued to be present, although at much lower levels (Fig. 3).

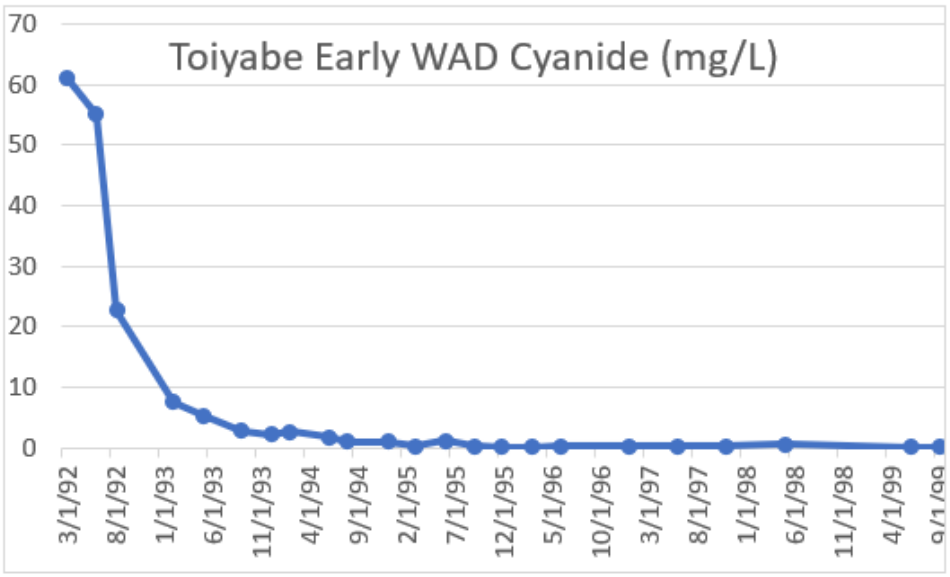

Figure 2

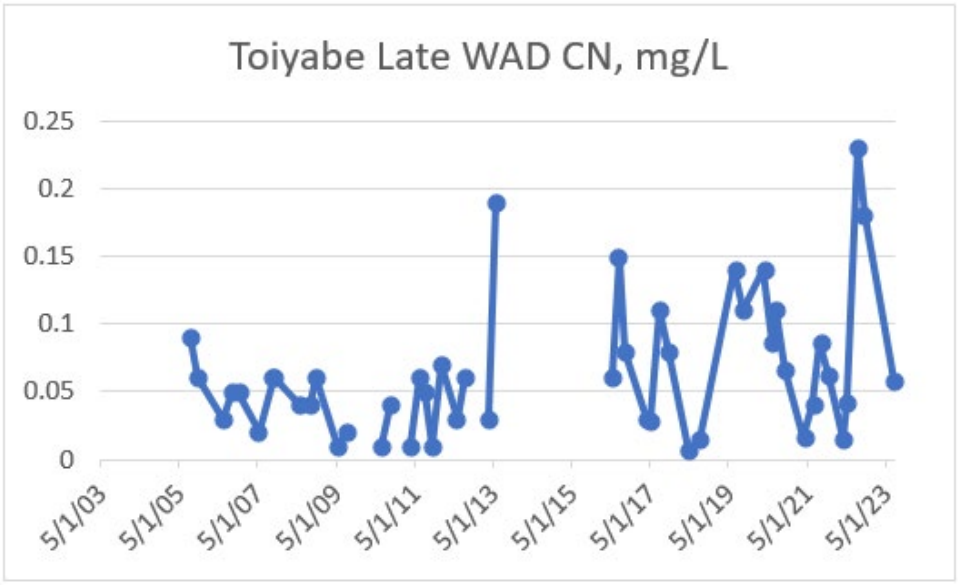

Figure 3

The mercury concentrations are also typically reduced (Fig. 4 and Fig. 5), following loss of cyanide, since mercury is mobilized by reaction with cyanide to form soluble mercury cyanide complexes. These complexes have been reported as "strong" (Flynn & Haslem, 1995), although in the days and weeks that cyanide is lost from fluids, mercury is also lost from the solution. The retained mercury is still sorbed onto the heap material, but not discharged. Both mercury and WAD cyanide are still present in the fluids during meteoric rinsing, and in many cases are above drinking water standards, but are dramatically reduced compared to active leaching concentrations.

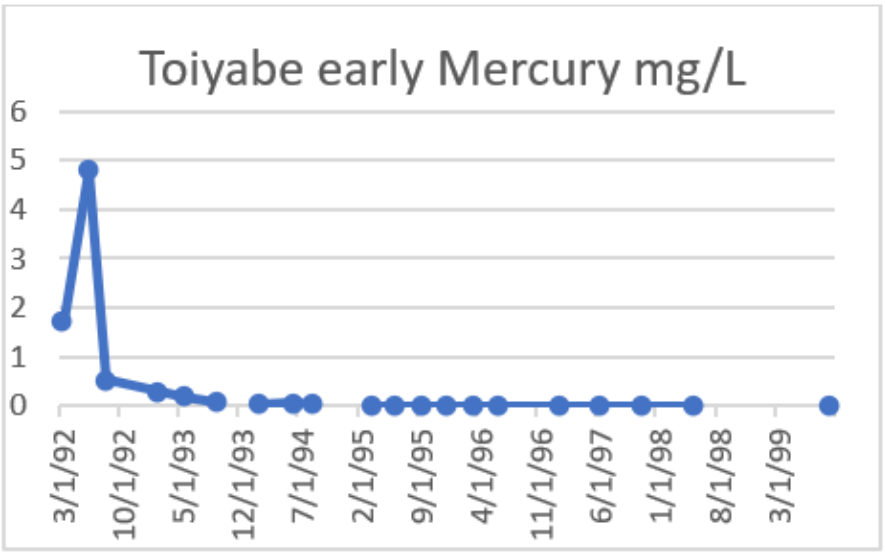

Figure 4

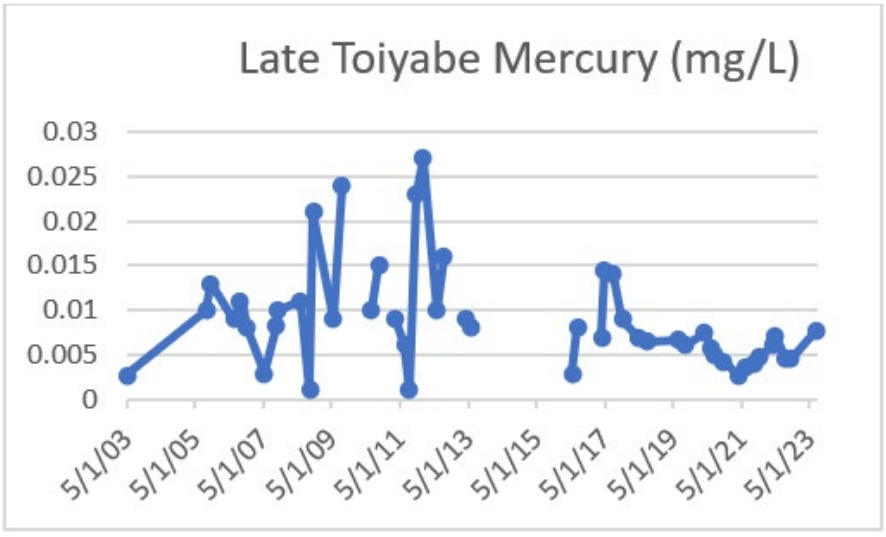

Figure 5

Arsenic is a naturally occurring element that is commonly present in gold ore in Nevada (SME). Arsenic is released into the environment through weathering, erosion, and oxidation of arsenic-containing rock, particularly the arsenic/sulfur-containing minerals (Decker et al., 2006), including arsenopyrite. Arsenic is an element of particular concern, since it is classified as a human carcinogen and will act as a soil sterilant when applied to soils at high concentrations (SME). At the beginning of closure, arsenic concentrations were relatively steady (0.5 to 1.5 mg/l). However, within 11 years, the arsenic levels have continued to slightly rise (Fig. 6), which was unexpected, since arsenic is known to sorb more strongly to surfaces as the pH drops from 10 to around 8 (Langmuir, 1997).

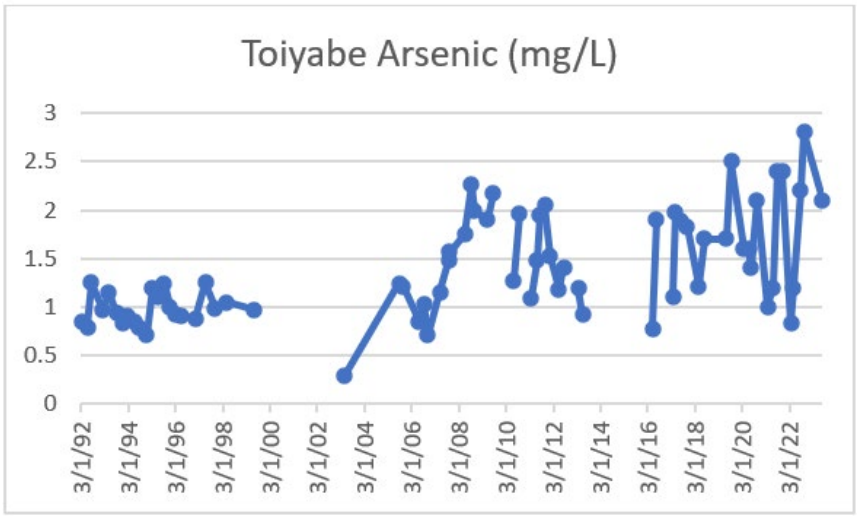

Figure 6

The slight rise in arsenic concentrations is supportive of the continued oxidation of arsenic sulfides, since this reaction is indeed slow, and it is difficult to predict how those concentrations will change over the long term (decades and beyond).

Sulfate is a common anion associated with mining, and if concentrations are sufficiently high, gypsum ($CaSO_4$) will precipitate. However, the sulfate and calcium (not shown) concentrations in the fluids are well below gypsum precipitation, and sulfate is expected to be rinsed out in a manner close to chloride, if oxidations did not continue to produce sulfate. Sulfides are a primary source of sulfate and are also naturally occurring constituents occurring as galena, pyrite, chalcopyrite, sphalerite, and arsenopyrite (Langmuir, 1997). Oxidation of sulfides creates sulfuric acid and is partially responsible for reducing the pH below 8.3.

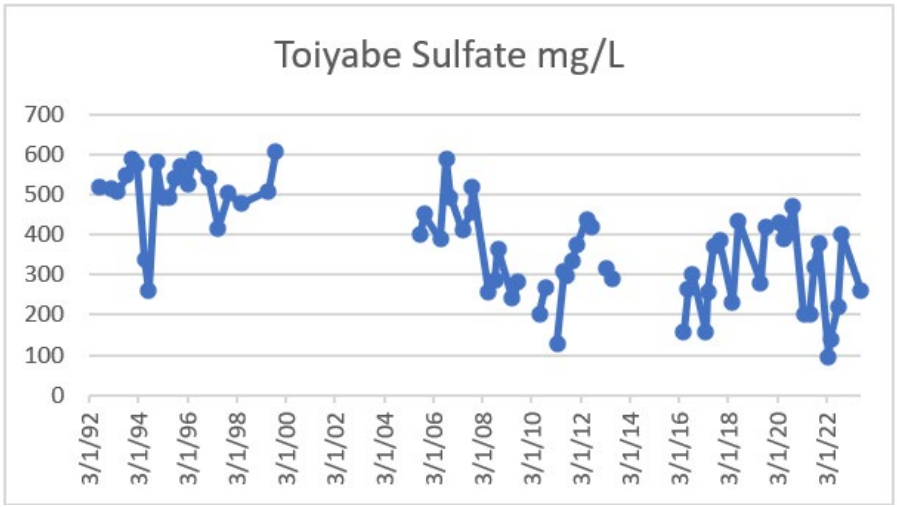

Figure 7

Sulfate is being rinsed out of the heap, although slowly. At the beginning of site closure, the sulfate concentration was a bit over 600 mg/l, and over the course of 30 years, the concentration fell to around 250 mg/l, approximately a 50 to 60% decrease.

Nitrate is common in cyanide heap fluids and originates from nitrate-containing explosives and, perhaps more likely, from oxidation of cyanide, first to cyanate or thiocyanate and then to ammonia and finally oxidation to nitrate (Watts et al., 2017; Johnson et al., 2000). As can be observed in Figure 8, nitrate concentrations rise to 90 mg/L and fall to 10 to 50 mg/L, consistent with metabolic production of nitrate, as the pH is lowered to below nine, and microorganisms can thrive in the absence of cyanide. While the highest concentrations exceed drinking water standards, if land-applied, it has fertilizer properties. Nitrate is highly soluble and does not bind to soil particles effectively. The increase in concentration early on (following reduction of the pH), followed by loss, suggests that it is being formed within the heap.

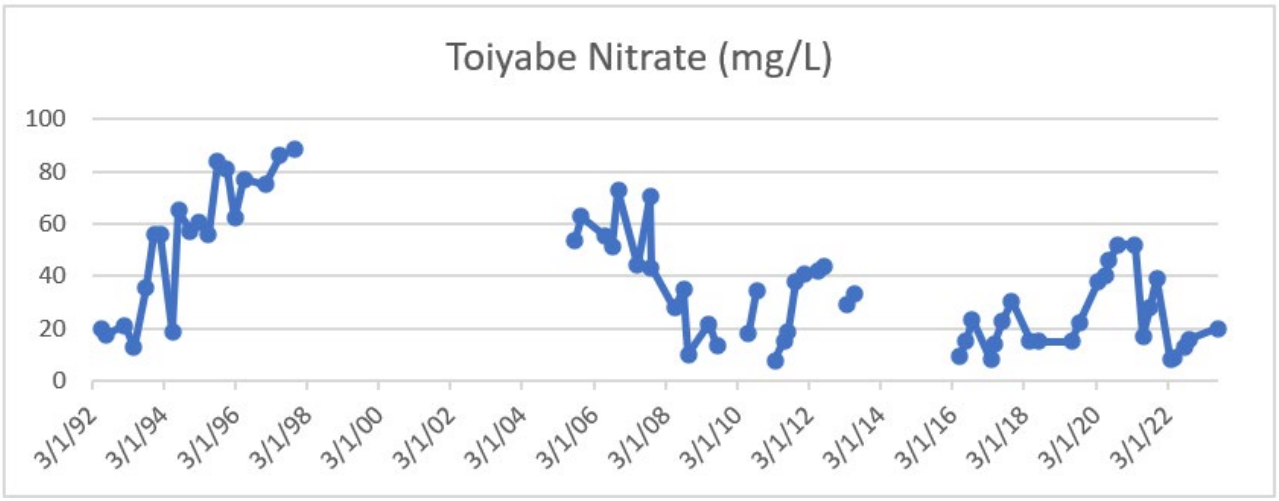

Figure 8

Chloride is water-soluble, and the decrease in concentrations occurs conservatively and indicates the amount of heap rinsing. Over the course of closure, the chloride concentrations have decreased by 75 to 80%. Chloride (Fig. 9) appears in heap leach probably as a concentrate during the recirculation closure. Background wells contain chloride from 7 to 60 mg/L, although the source of the water during operations was not indicated in the available documents.

Once closure is initiated and the heaps are rinsed with meteoric water, the chloride concentration is expected to decrease over time, since both are important constituents of the total dissolved solids (TDS) levels. Because chloride is observed in the drain-down water, these decreasing concentrations are a good indicator of meteoric water (rain and snow) rinsing through a heap.

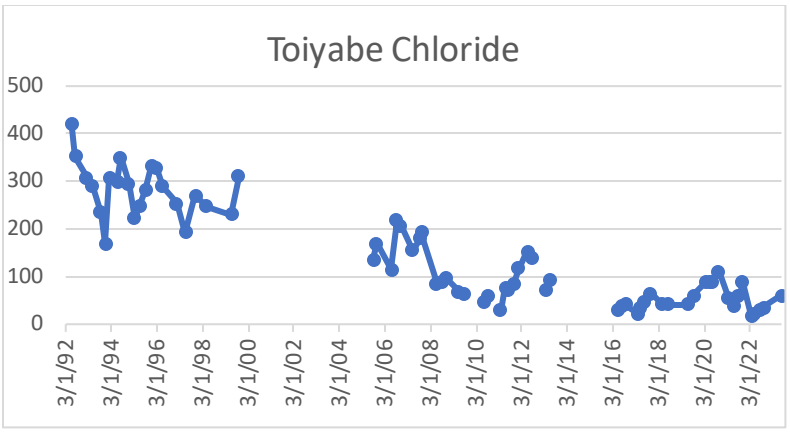

Figure 9

Finally, the total dissolved solids in effluent water (Fig. 10) are consistent with the reduction of the higher concentration constituents of the drainage. Some increases were observed during early recirculation of the drainage, but show a steady decrease in concentration over the last 20 years.

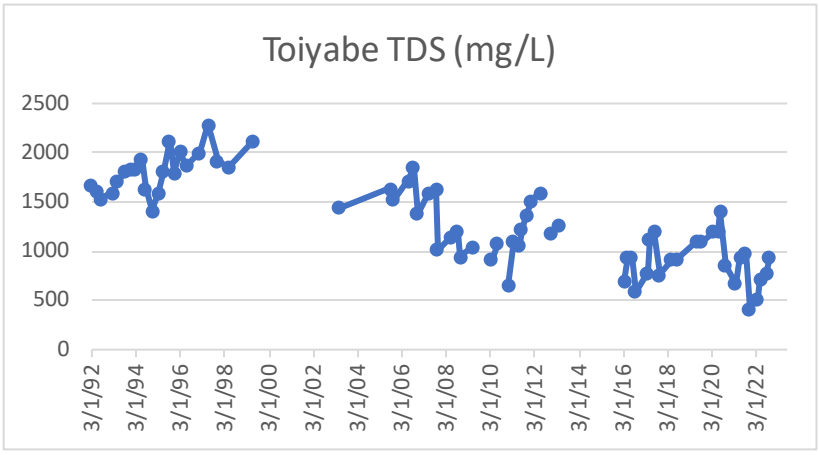

Figure 10

Conclusion

The 30 years of closure data for the Toiyabe heaps are illustrative of a low-sulfide, high-elevation, high-rainfall heap. As is the case for most mines, site-specific conditions need to be the primary consideration in how to relate the Toiyabe heap data to other heaps.

- Evidence from the 30 years of data suggests that reactions in the heap during meteoric rinsing still are occurring, although perhaps in a declining manner. WAD cyanide and mercury in drainage fluids over time are dramatically reduced.

- The appearance of increased arsenic concentrations raises some long-term concerns regarding the land application of draining fluids. It is difficult to predict how much arsenic will be released over the following decades.
- Nitrate increases throughout early closure and rinsing, very likely due to cyanide and iron cyanide complexes being microbially metabolized, yielding CO_2 and NH_3, and, ultimately, nitrate. Nitrate-based explosives are a contributing factor, although the substantial increase in nitrate indicates a source other than explosives for over 70% of the nitrate observed at the highest concentrations. The concentration is definitely decreasing, however.
- The pH decreased by over 1 pH unit, which suggests that sulfide oxidations are occurring, although sulfate concentrations are decreasing.
- Chloride is decreasing more rapidly than any other anions. Chloride is a conserved anion and is probably not a significant source in the heap material

Ackowledgements

The authors would like to thank the staff of the Nevada Division of Environmental Protection for assisting in the collection of this data, first from hard copy files, and later from downloaded files on the web. Karl McCrea was particularly helpful and explained some of the background on the Toiyabe Mine.

References

Decker, D. L., & Tyler, S. W. (1999). Evaluation of flow and solute transport parameters for heap leach recovery materials. *Journal of Environmental Quality, 28*(2), 543–544.

Decker, D. L., Šimůnek, J., Tyler, S. W., Papelis, C., & Logsdon, M. J. (2006). Variably saturated reactive transport of arsenic in heap-leach facilities. *Vadose Zone Journal, 5*(1). https://doi.org/10.2136/vzj2005.0039

Flynn, C. M., & Haslem, S. M. (1995). *Cyanide chemistry: Precious metals processing and waste treatment*. U.S. Department of the Interior, Bureau of Mines.

Johnson, C. A., Grimes, D. J., & Rye, R. O. (2000). Fate of process solution cyanide and nitrate at three Nevada gold mines inferred from stable carbon and nitrogen isotope measurements. *Transactions of the Institution of Mining and Metallurgy, Section C: Mineral Processing and Extractive Metallurgy, 109*(2), 68–78.

Kampf, S. K., Salazar, N., & Tyler, S. W. (2002). Preliminary investigations of effluent drainage from mining heap leach facilities. *Vadose Zone Journal, 1*(1), 186–196.

Kappes, D. W. (2005). Heap leaching of gold and silver ores. In M. E. Adams (Ed.), *Developments in Mineral Processing* (Vol. 15, pp. 456–478). Elsevier. https://doi.org/10.1016/S0167-4528(05)15019-4

Kowalski, P. (1999). Design and evaluation of engineered soil covers for infiltration control in heap leach closure. In D. Kosich & G. Miller (Eds.), *Closure, remediation & management of precious heap leach facilities* (pp. 1–12). University of Nevada, Reno: Center for Environmental Sciences and Engineering.

Langmuir, D. (1997). *Aqueous environmental geochemistry*. Upper Saddle River, NJ: Prentice Hall.

McCrea, K. (2017). *Cortez venture fact sheet: Barrick Cortez Inc., Toiyabe Mine Project*. Nevada Division of Environmental Protection.

O'Kane Consultants. (2000). *Demonstration of the application of unsaturated zone hydrology for heap leach optimization*.

Society for Mining, Metallurgy, and Exploration (SME). (n.d.). *The role of arsenic in the mining industry*. https://www.smenet.org/What-We-Do/Technical-Briefings/The-Role-of-Arsenic-in-the-Mining-Industry

U.S. EPA. (1994). *Treatment of cyanide heap leaches and tailings: Technical report*. Office of Solid Waste, U.S. Environmental Protection Agency, 1–40.

Watts, M. P., Gan, H. M., Peng, L. Y., Cao, K.-A. L., & Moreau, J. W. (2017). In situ stimulation of thiocyanate biodegradation through phosphate amendment in gold mine tailings water. *Environmental Science & Technology, 51*(22), 13127–13136.

Western Mining History. (n.d.). *Toiyabe-Saddle deposit*. https://westernmininghistory.com/mine_detail/10310330/

Young, C. A. (Ed.). (2001). *Cyanide: Social, industrial and economic aspects: Proceedings of a symposium held at the annual meeting of TMS (The Minerals, Metals & Materials Society), New Orleans, Louisiana, February 12–15, 2001*. Minerals, Metals & Materials Society (TMS).

Chapter Six

Author Index

Author Index